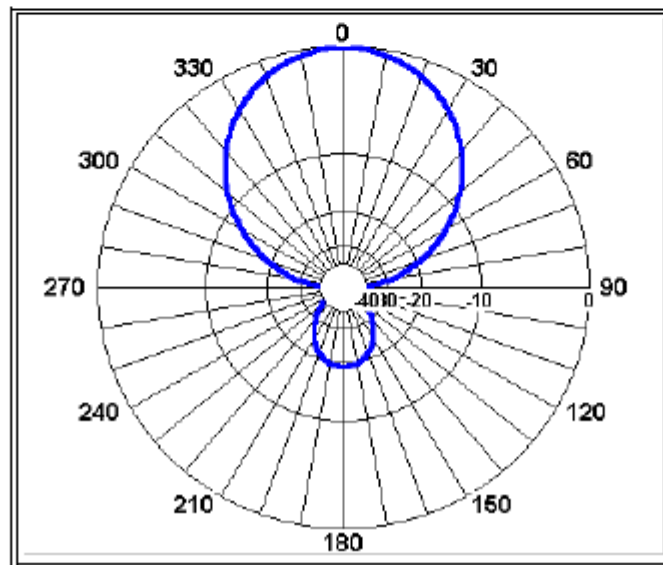


Basic Antenna Modeling A Hands-On Tutorial



L. B. Cebik



Basic Antenna Modeling A Hands-On Tutorial

L. B. Cebik

Published by
antenneX Online Magazine
<http://www.antennex.com/>
POB 271229
Corpus Christi, Texas 78427 USA

Copyright 1998, 1999, 2007 by **L. B. Cebik** jointly with ***antenneX Online Magazine***. All rights reserved.
No part of this book may be reproduced or transmitted in any form, by any means (electronic, photocopying, recording, or otherwise) without the prior written permission of the author and publisher jointly.

ISBN: 1-877992-03-8

Dedication

To my father, James S. Cebik, 1ATG, W1BUK
A designer of massive machine tools, a sharpshooter,
a pilot, a radio experimenter from the 1920s to the present day,
and the rarest of dads

Acknowledgments

The author would like to thank the following reviewers of a draft of this work. They have individually and collectively furthered my education on the workings of NEC-2 and on antenna modeling in general. Although they are responsible for innumerable improvements in the work, I alone am accountable for the remaining shortcomings.

- Richard W. Adler, Naval Postgraduate School
- Jim Breakall, WA3FET, Penn State University
- Gerald J. Burke, Lawrence Livermore National Laboratory
- Anthony Ferraro, Penn State University
- Keith A. Lysiak, Southwest Research Institute
- John Stanley, K4ERO, Broadcast Engineering Consultant

Table of Contents

<i>Chapter</i>	<i>Title</i>	<i>Page</i>
	Introduction	1
Part A	Basic Modeling and Model Testing	A-1
1	NEC-2 and NECWin Plus	1-1
2	Modeling Preparations	2-1
3	Basic Antenna Models	3-2
4	NEC Output Data	4-1
5	Careful Model Construction	5-1
6	Convergence Testing	6-1
7	Frequency Specification	7-1
Part B	Common Modeling Techniques, Limitations, and Work-Arounds	B-1
8	Source Types and Placement	8-1
9	Tapered-Diameter Elements	9-1
10	Geometry Limitations	10-1
11	Grounds and Applications	11-1
12	Resistive Loads	12-1
13	Reactive Loads	13-1
14	Transmission Lines	14-1
Part C	Practical Antenna Modeling	C-1
15	Monopoles and Ground Planes	15-1
16	Vertically Polarized Antennas and Arrays	16-1
17	Bi-directional Wire Arrays	17-1
18	Yagis	18-1
19	Horizontal Parasitic and Phased Arrays	19-1
20	VHF/UHF Antennas	20-1
21	Special Structures	21-1
Appendix	Some Useful Data for Antenna Modelers	App-1
Index		Ind-1

Important Update & Caveat

Since the initial writing of this book in 1997, the Windows OS has gone through several upgrades and thus, the reader should be made aware that any references to Nittany-Scientific, Inc.'s NECWin-Plus modeling software is known to work up to and including Windows 2000. However, it has issues running under any other new versions of Windows since that version.

Note the only reference in this book is to Windows 95 which was prevalent at that time.

It is emphasized that one does not need to use the above-mentioned software as there are other choices on the market.

The reader will find that this book is mainly about the use and application of NEC for antenna modeling and the software was used to produce examples.

This update is written in October 2007 and the plans for any further upgrades of the Nittany-Scientific, Inc.'s software mentioned here is unclear and doubtful.

The 330 exercise files that accompany this book are in “.nec” format and will run with any software that handles such files.

Moreover, the above files are also available in the “.ez” native format run by an alternative software by EZNEC. These files may be obtained at the *antennex* Software section of its Shopping Shack at:

<http://www.antennex.com/Sshack/model.htm>

Introduction

Objectives: *In these preliminary notes, you will become familiar with the basic purpose and design of this book on antenna modeling with NEC. You will come to understand why you should go through the exercises carefully with your software as well as reading the principles and techniques portions of each chapter. In addition, you will learn something about the author.*

Antenna modeling with NEC is both an art and a science--a craft that requires both a thorough understanding of what the computer programs make possible and ingenuity born of experience that permits you to overcome some of the program limitations. This guide is designed to start you down the road to using NEC effectively, whether your goal is to evaluate existing antennas or to design superior antennas.

At root, NEC employs mathematical algorithms to simulate as closely as possible the performance of antennas, that is, transducers of electrical energy into electromagnetic radiation. In all its forms, NEC is a calculating program using the method of moments supplemented by adjunct algorithms to handle special features of various antenna types. It treats all antenna elements and parts as thin wires subdivided into many segments. It calculates the mutual impedances among the wire segments, the current on each segment, and (upon call) the near and far fields developed. Source impedance, load loss, and other supplementary data are also generated by the program.

NEC contains four ground-description options. One is free space. Another is a perfectly reflecting ground. A third is a finitely conducting ground using Fresnel plane-wave coefficients: this method is fast, but grows inaccurate as an antenna is placed close to the ground. The final method--the Sommerfeld-Norton method--is more accurate but time consuming in the calculation process.

NEC has several incarnations. The most common public domain version is NEC-2, for which this guide is written. It replaced NEC-1 and has itself evolved into NEC-3 and NEC-4, both of which are proprietary programs. All forms of NEC were developed under the leadership of Jerry Burke of the Lawrence Livermore National Laboratory. A similarly named modeling program using different algorithms and initially designed for small desktop personal computers is MININEC, developed by Rockway and Logan.

NEC-2 remains a very competent program when used within its limits. However, as with all forms of NEC, it requires suitable input and output programs for effective use. The program accompanying this guide, NECWin Plus, is a highly effective Windows 95 implementation incorporating a version of NEC-2 specially modified for integration with

the input system and the collection of output facilities developed by Nittany Scientific.

To have a guide that is perfectly general and covers all implementations of NEC-2 is an ideal that must go unrealized. Different implementations of NEC-2 use varying techniques for inputting antenna model data and for displaying calculated output data. Therefore, practicality dictates that a guide to mastering the techniques of modeling antennas with NEC-2 must focus upon one program.

Nevertheless, the principles of antenna modeling successfully with NEC-2 that will appear in this guide are completely adaptable to all implementations of NEC-2 which utilize the same input possibilities. Most of the principles are also applicable to NEC-3 and NEC-4, although these improvements upon NEC-2 have overcome certain limitations and the need for some work-arounds. What you learn about using NEC-2 effectively will likely remain relevant, whatever the future evolution of NEC modeling may bring.

The Plan of This Guide

The goal of this guide is to introduce you to the art and craft of good antenna modeling using NEC-2. It is designed for use specifically with NECWin Plus, a user-friendly Windows 95 implementation of NEC-2. The program permits several forms of model data input and error checking. It also provides many forms of data output, both tabular and graphical, to enable the modeler to interpret his or her results more insightfully.

The art and craft of modeling requires initially only a broad general comprehension of antennas. NEC-2 may be used without an in-depth understanding of Maxwell's equations or even of the mathematical origins of method-of-moments techniques. However beneficial such knowledge may be ultimately, it is possible to master the rudiments of good antenna modeling with lesser tools.

The Overall Plan of the Guide

This guide presumes only the broadest understanding of antennas. Therefore, it is suited not only to formal introductory courses in college settings, but as well to self-study by individuals interested in developing modeling skills. To that end, it contains numerous useful features.

The guide is divided into three main parts:

- A. Basic Modeling and Model Testing
- B. Common Modeling Techniques, Limitations, and Work-Arounds
- C. Practical Antennas Modeling

Part A, on basic modeling and model testing, introduces both NEC-2 and the program that accompanies this guide. It then proceeds to pre-modeling preparations and from there to hands-on modeling of simple models in order to give the user a feel for the program and to introduce the processes of inputting and outputting data. Two exercise sets then follow on careful modeling and on convergence testing to assure the reliability of results. Part A concludes with exercises which focus upon frequency specifications for models, including various types of frequency sweeps and frequency scaling.

Part B covers common modeling techniques, limitations, and work-arounds, including exercises on source placement and alternatives. A crucial limitation and its work-around concern the use of tapered-diameter elements. One exercise set introduces the user to geometry limitations and potentials for NEC-2 modeling, while another exercise set involving the use of the ground systems built into NEC follow. Two exercise sets in this section introduce material (distributed) loads and reactive loads. The final series of exercises acquaints the user with procedures for implementing transmission lines in various functions.

The final part (C) introduces the modeler to techniques and cautions that apply to practical antenna work, beginning with vertical monopoles and ground planes. Other types of vertically polarized antennas and arrays--both parasitical and phased--appear in the follow chapter. A series of exercises is devoted to collinear, broadside, and end-fire bi-directional wire arrays. Because of their prevalent use in the HF (as well as VHF/UHF) range, Yagis receive extensive treatment, while horizontally polarized phased arrays receive a chapter of their own. Despite the similarity of VHF and UHF antenna types to HF counterparts, there are enough variations--especially for the modeler--to call for a series of exercises in upper frequency ranges. The exercises of Part C close with a potpourri of special structures, including helices, cages, and wire grid structures.

There are numerous advanced functions that this basic modeling tutorial must by-pass. Some have limited application; others are not available, either readily or at all, within the accompanying program. For example, we have omitted reference to catenary wires, symmetry, surface patches, and Green's functions: all of these input functions are best developed in advanced implementations of NEC. Some are available only in NEC-4. We shall limit the discussion of sources to voltage and current source, leaving the treatment of incident plane waves for more advanced handbooks. Likewise, we shall not work with near-field and other output data that are unavailable on the current version of NEC-Win Plus. Similarly, we have omitted discussion of networks, of which the transmission line facility is a special case. A more complete list of omissions appears at the end of Chapter 21.

It is the author's hope that an advanced handbook or tutorial on the many omitted techniques can be made available in the future. Indeed, one might write a significant applications treatise on each of the techniques that lie beyond the scope of our coverage.

The Plan of Each Chapter

As the outline of the parts of this guide indicates, each part is divided into 7 chapters, each focused on an interrelated cluster of basic or advanced techniques and concepts. Each chapter builds upon the preceding in a graded learning curve. Within the context of either a formal course or of individual study, each chapter might well be mastered within a week. The more extensive one's background, the faster the earlier chapters will go.

Each chapter is typically subdivided in the following manner (with exceptions for early background information and some late specialized chapters). After a statement of goals, the chapter provides background information on the focal subject. This information extends only to what the goals of the chapters require and is not a substitute for appropriate reading in other sources.

Key to the volume are extensive exercises that model actual antennas. Most of these antennas will be based on HF, VHF, and UHF antennas in common use in both amateur and commercial communications. All models (except where specifically noted for student development) are contained on a 1.44 MB floppy disk accompanying this guide. The guide user will be requested to open, possibly modify, run, and explore the output data for the models provided. For ease of location, all models are keyed to the chapters of the guide. For example, the models for chapter 6 have filenames of the form "6-x.NEC," where x is the sequential number of the model in the chapter progression.

For each exercise involving a model, the chapter will provide relevant commentary for both the input and output to which the user is directed. Because so many of the antennas are very common, not all will be pictured. The user may always employ the viewing function of the program (Necvu) to examine the configuration of any antenna used as in the exercises. Each chapter closes with a summary of the essential concepts and guidelines developed along the way.

A Note on the Antenna Models Used in this Guide

Most of the antenna models that appear in this guide are designed for one or another of the amateur radio bands. Besides that author's extensive experience with such antennas, there are several good reasons for this orientation. First, the amateur radio frequency allocations encompass a span of frequencies ranging from MF to well above UHF. Moreover, amateur radio communications situations encompass virtually all commercial and private types, as well as adding a few unique ones. Hence, radio amateurs work with directional and non-directional antennas, transmitting and receiving both very narrow-band and very wide-band emissions in simplex and duplex operations that involve almost all known methods of information encoding or modulation. They operate from fixed, portable, and mobile installations that employ vertical, horizontal, and circular polarization for local, long-distance, and even space communications.

In addition, unlike the structures of commercial antennas, which may be governed by proprietary and other protective measures, full fabrication details are available for most amateur antenna types, often with many variants of any given type. Therefore, the student of antennas has access to virtually unlimited information for practice in constructing models of both good and bad antennas. Compendiums of antenna designs for all frequencies, such as Rothammel's *Antennenbuch* and the ARRL *Antenna Book*, are readily available at reasonable prices. Finally, possession of an appropriate class of amateur radio license permits the modeler to build test versions of any of the antennas modeled in these exercises in order to correlate modeling outputs with real antenna performance.

Using This Guide

This tutorial is designed to be used either as a self-study guide or within a classroom context. Each context opens different possibilities and places different responsibilities on the user.

Using This Guide as a Self-Study Tutorial

The materials in this guide have been structured carefully to develop your skill in modeling. Proceeding step-by-step in order through the chapters and their exercises is essential to deriving maximum benefit from the work you put into this effort. Although it may be tempting to jump ahead to a problem area in which you may already have an interest, skipping the early chapters can lead to pitfalls, most notably, unreliable models that give misleading results.

A collateral temptation will be to skip one or more of the chapters in Part C, because you do not anticipate dealing with antennas of the sort covered by one or more of these sections. However, viewing these chapters as dealing with special modeling problems is not the only way to look at them. You can also see them as opening modeling possibilities. In this light, becoming familiar with the techniques involved in modeling antennas that are not of present interest can--either sooner or later--permit you to develop just the model you need for a particular task. Once you begin the progression through the exercises, commit yourself to working all the way through to the end.

This guide can help you develop a good understanding of modeling, but it is not itself a software instruction manual. If you are using NECWin Plus, you will want to have studied its user's manual before embarking on these exercises. Thoroughly familiarize yourself with how to implement each feature of the program. Keep the user's manual handy for reference along the way. Although the instruction sets for the exercises are keyed to NECWin Plus, they do not include detailed instructions regarding the necessary keyboard or mouse operations involved.

If you are using another software package, you will need to perform another set of tasks in addition to becoming acquainted with how to implement program features. First, you may need to rewrite the models provided on disk to suit the input requirements of your program. Most of the models on the disk are fairly simple and straightforward. You can read them with any ASCII viewing facility on your computer. Once you understand the fundamentals of the basic NEC input system, you can easily read the values and their meanings, which you can then translate into the keystroke entries for your own program.

Second, not every package implements all of the available features of NEC-2. For example, some software does not permit independent specification of the material for each element. In such cases, you will have to determine which material is best to use throughout the modeled structure to achieve the most accurate results. Additionally, different software packages may use slightly different values for various constants, including material conductivity and the exact speed of electro-magnetic radiation.

Third, not every feature is implemented in the same manner by various implementations of NEC-2. Therefore, you may wish to develop a small set of notes along the way that translate the instruction set given in specific exercises in this guide into the operative instructions for the software you are using. You can clip these notes to applicable pages or write them in the margins. The need to keep your software user's manual at hand is clearly evident.

One final word of caution. Different implementations of NEC-2 may yield slightly different numerical results than those you may find on these pages. Even software upgrades of NECWin Plus itself may yield slight numerical discrepancies from the version used in the development of these exercises. For identical models inputted to different packages, these numerical differences result from disparate rounding conventions used by the software author(s) and other factors that influence both the input and output sides of NEC. In all cases, you will have to determine whether the numerical variation is small enough to represent these minor programming differences or whether it is large enough to signal a possible error in your model construction.

Using This Guide in the Classroom

For ease of instruction, this guide is best studied in conjunction with the software used in its development, NECWin Plus. Although other software might be used, significant losses in classroom instruction time may occur, due to continuing questions concerning translating models and instruction sets into the operative procedures used with alternative software.

The chief goals of this volume include bringing together in one place a large, but certainly not exhaustive, collection of practical information on modeling with NEC-2. Moreover, the

volume aims to set forth the information and exercises in a progressive development of user understanding, both within chapters and within the guide as a whole. Within the compass of these goals, there remains yet a large potential for customizing the work of a course utilizing these materials. Minimally, any of the input, output, source, ground, or network techniques omitted from this manual make very important instructor-based additions to any course.

The 21 chapters comprising this guide offer considerable flexibility in the progression of an introductory course on antenna modeling. There are more chapters than would fit either a 10-week quarter or a 15-week semester, unless multiple classes occur each week. However, for more advanced classes, the early portions of this guide may be assigned in groups of chapters. For less advanced classes, the first two parts might comprise a normal progression of classroom effort, with elements from Part C assigned as outside or extra-credit study. More advanced or practical classes might use Parts A and B as universal preliminary assignments, with the chapters in Part C being assigned selectively and supplemented by the instructor. Variations on these themes are almost endless, according to the goals and level of the class.

The background material reported in each chapter by no means exhausts either the theoretical considerations underlying NEC-2 or the practical considerations affecting techniques of modeling. Instead, the background material is designed to focus the student's attention on the relevant considerations for the exercises. There is appreciable room for the instructor to bring additional information to the treatment, information that arises out of the specific goals of a course and out of the instructor's experiences.

Likewise, the graded exercises do not preclude the development of further modeling tasks designed to enlarge either the breadth or the depth of student understanding. Indeed, the assignment of additional variants on the exercises, including more advanced and complex problems of the types on which the chapters focus, is highly recommended. Such problems can minimally increase student abilities in modeling "from scratch," rather than simply modifying supplied models.

Use of this guide as a practice-intensive course text is only one of its possibilities. Another is letting it serve in conjunction with other texts on method-of-moments modeling so that the guide and NECWin Plus become an extended example of the real-world implementation of the fundamental principles and concepts. Alternatively, the guide and the software may be used as adjuncts to, or laboratory materials for, courses on basic antenna principles. The addition of instructor-supplied models to those in the guide is essential in either case.

Although variations on the application of this guide are nearly endless, the work itself may serve in a relatively self-sufficient way to guide students in developing their skills in mastering the craft of antenna modeling.

About the Author

L. B. Cebik

Dr. L. B. Cebik is professor of philosophy at the University of Tennessee, Knoxville, with special interests in formal logic. In addition, he has served the University in past years as Assistant Dean for Research and as Director of Research Compliances. His interests in radio frequency communications arose out of his amateur radio experiences as W1APS, W0JGG, and now W4RNL. He has been a student of electronics and antennas for some 45 years and a teacher for almost 35 years. His writings include 8 books and over 200 articles and reviews.

Dr. Cebik has tested and used almost all of the commercial implementations of NEC and MININEC over the past decade. In addition, he has written extensively about antennas and antenna modeling at both basic and more advanced levels for many U.S. amateur radio publications. His writings have included tutorial articles for electronics teachers and regular columns for several publications on various aspects of antenna fundamentals. He also maintains a web site with considerable material from his notebooks (URL: <http://web.utk.edu/~cebik/radio.html>).

The author would like to thank the staff, advisors, and beta testers of Nittany Scientific for their review of the initial draft of this tutorial. It is better for their efforts, although any remaining flaws belong exclusively to the author. Not every suggestion could be followed, often because the implementation of the requisite techniques would have required advanced program capabilities. Nonetheless, I am appreciative of all the illuminating remarks, recommendations, analyses, and explanations that were sent to me. Requests for the coverage of additional topics, on the one hand, and for a smaller book, on the other, indicate that this guide is far from perfect. I hope it will at least be useful.

1.

NEC-2 and NECWin Plus

Objectives: *This chapter will introduce antenna modeling and acquaint you with NEC-2 capabilities and limitations, as well as distinguishing NEC-2 from other NEC-type calculation cores. In addition, you will become familiar with the capabilities of NECWin Plus, the overall program which contains the NEC-2 core.*

"Antenna modeling" is a term used to express two different but related ideas. The first and more venerable meaning of the phrase is the technique of modeling antennas for use at low frequencies (LF) through high frequencies (HF) as very small ultra-high frequency (UHF) antennas. This process saves untold hours (if not days) of trying to erect large, expensive antennas and then to control the environmental variables that might affect performance and to sort them from the properties of the antenna itself. The small UHF antennas can be placed in chambers with well-known properties, thus permitting the derivation of properties associated solely with the antenna itself.

The second meaning attached to the phrase refers to the translation of physical properties of the antenna into mathematical equations (and arrays of equations), which permit the calculation of the antenna's essential properties. The idea is actually very old. For example, many antenna handbooks provide the following equation for the calculation of the length of a resonant 1/2 wavelength (λ) center-fed dipole composed of wire that is very thin relative to the length of the wave involved:

$$L_{(feet)} = \frac{468}{f_{(MHz)}} \quad 1$$

where L is the length of the dipole in feet and f is the frequency in MHz.

The equation, of course, is fraught with many limitations. First, the constant of 468 derives from an estimate of total end effects (k) affecting the antenna length. A generalized value of 0.95 is used for the most common wire sizes typically used for such antennas. Hence, a more accurate version of equation (1) should read as follows:

$$L_{(feet)} = \frac{k \ 491.7856}{f_{(MHz)}} \quad 2$$

The seeming precision of the new constant for a half wavelength is spurious, since k is quite imprecise. Moreover, the equation does not take into account the required changes in length for resonance (defined here as a feedpoint or source impedance that is purely resistive) as the antenna is varied in height above ground, especially at heights below 1.5λ .

Apart from the relative imprecision of our mathematical model of the center-fed $1/2\lambda$ thin-wire dipole, the model is extremely limited in the information it is capable of providing. In effect, it can provide only the length of the antenna at some approximation of resonance. A truly adequate model should provide a host of other information, such as the current magnitude and phase along the antenna wire, the source impedance, the antenna far field radiation pattern, the antenna near field electrical and magnetic field levels, and all of these figures both in free space and over grounds of varying types at any desired antenna height at any number of frequencies of operation. From these figures, it would be routine to calculate such additional useful information as the voltage, current, and power levels at the feedpoint (or anywhere else) for specified source conditions, voltage standing wave ratios (VSWR--or SWR, for short) relative to a given source impedance, and a myriad of radiation pattern shape relationships, such as front-to-back ratio, front-to-side ratio, -3 dB vertical and horizontal beamwidths, etc.

Until recent times (say, the last couple of decades) we lacked the two essential ingredients to make practical the mathematical modeling of antennas. We lacked the algorithms that would provide adequate models of actual antenna performance, and we lacked the means of solving those equations in a suitably efficient manner. To a great measure--but with limitations still to be overcome--the method-of-moments technique of antenna analysis (coupled with other mathematical methods, for example, of ground analysis) has resolved the first problem. The continuing development of faster, more capable computers for desk-top use has largely surmounted the second problem. Truly accurate and reliable (but not unlimited) antenna modeling is accessible and practical.

What is NEC?

The Numerical Electromagnetics Code (NEC) is an outgrowth of a program developed in the 1970s, called the Antenna Modeling Program (AMP). There are at least 4 versions of NEC, with NEC-2 emerging in 1981 and NEC-4 appearing in 1992. NEC-2 is the highest version of the code under public domain. NEC-4 remains proprietary with the Lawrence Livermore National Laboratory and the University of California. It requires a separate license for use, along with the cost of any user interface selected.

NEC in all its forms is a computer code for the analysis of the electromagnetic response of antennas and other metal structures that uses method-of-moments techniques for the numerical solution to integral equations for the currents induced on an antenna structure

by sources or by incident fields. The approach has no theoretical limit and may be used for very large arrays or for the very fine subdivision of smaller arrays. However, the matrices involved grows very large very fast, and thus may exceed the capabilities of a given computer.

In fact, NEC was originally developed in FORTRAN for use on large mainframe computers. An alternative method-of-moments program emerged called MININEC, of which version 3.13 is the latest public domain level. MININEC was developed specifically to run on small desk-top PCs and used compiled BASIC as its language. Limited by early memory constraints and by a slow running pace, the program placed many of the facets of NEC modeling in the hands of a wide range of both amateur and professional antenna designers and analysts.

The increased speed and memory of modern PCs, along with the development of FORTRAN compilers for the PC environment and the release of NEC-2 from security controls, made the higher capabilities of NEC-2 accessible to the desk-top computer. Because NEC-2 was itself limited to a rigorous FORTRAN-style input set of "cards," and because the outputs were wholly tabular, several software developers have incorporated NEC-2 (often modified) into a more complete computing environment. On the input side, developers created methods of easing the burden of entering the data for the antenna structure and other parameters of its operating environment. Fewer inputting errors produced more reliable models more quickly and also permitted more rapid model revision for antenna design development.

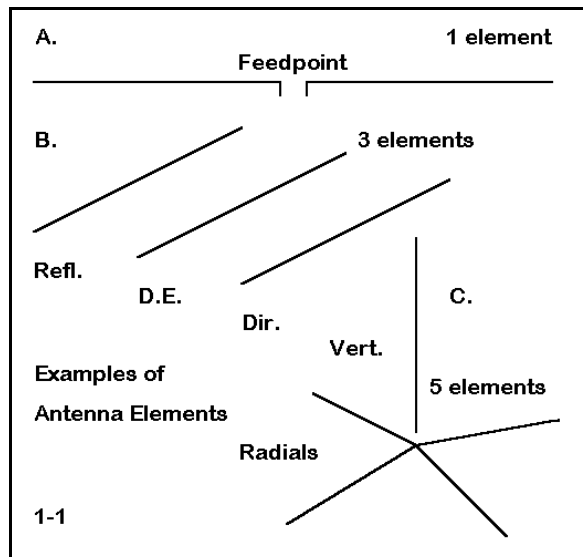
The output side saw the conversion of tabular data into a host of graphical outputs that enhanced the interpretation of results. These have included polar plots for far fields, as well as a number of rectangular plots that track such data as gain across a span of radial directions from the antenna or that chart source impedance or SWR across frequency spans. Antenna currents and other data that varies along the antenna structure can be plotted graphically on a representation of the antenna itself.

NECWin Plus, the program for which this guide is a tutorial, contains a highly competent modified version of NEC-2 along with extensive input and output facilities to allow both the beginning and advanced modeler to design and analyze a wide variety of antenna types with ease of construction and clarity of data interpretation.

NEC-2 Capabilities

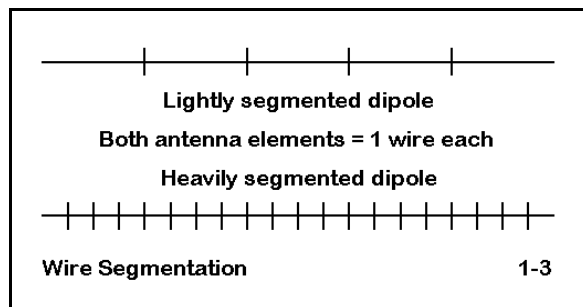
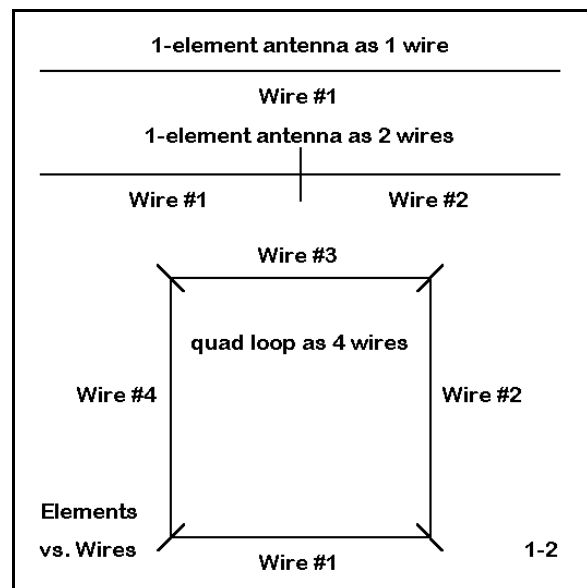
NEC-2 has proven capable of modeling accurately a wide variety of wire antenna geometries across a frequency span from VLF through UHF. Although NEC-2 is capable of modeling surfaces as well as wires, we shall focus mostly upon wire antennas, leaving surface modeling for lessons late in the volume.

The method of analysis used by NEC-2 requires that any antenna element be a collection of thin linear wires and that each be segmented within certain limits. Hence, the new modeler must make a threefold distinction:



Antenna or antenna element: the physical structure of the antenna or a subdivision of the physical structure of the antenna to be modeled. Examples of elements are (a.) a wire dipole antenna, (b.) the reflector (or other linear part) of a Yagi, and (c.) one radial of an antenna system consisting of a $1/4\lambda$ vertical and several radials. (Figure 1-1)

Wire: an element of the antenna model which may or may not be identical with an antenna element. With a simple center-fed dipole, the wire and the element may be the same, although the modeler may subdivide the antenna element into several wires for various purposes. With a quad loop antenna element, each element must be divided into four wires (minimally). (Figure 1-2)

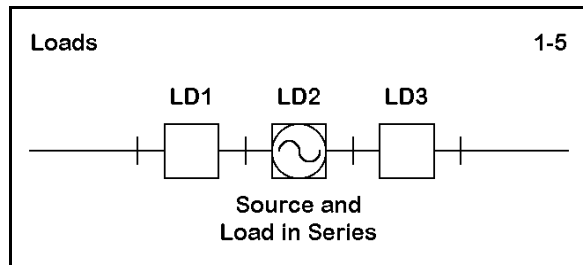
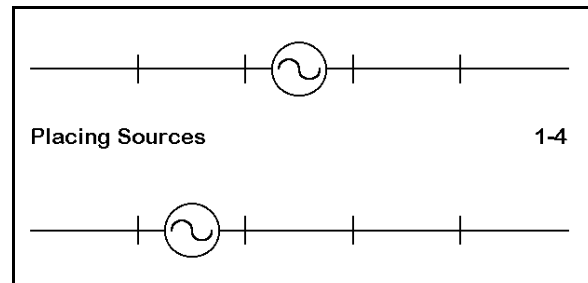


Segment: a subdivision of a wire, with the number of segments chosen to ensure modeling within program limitations. A dipole might have as few as 5 or as many as 100 or more segments, depending upon the purposes and required precision of the analysis. (Figure 1-3)

Some other key terms used with respect to

NEC models are these:

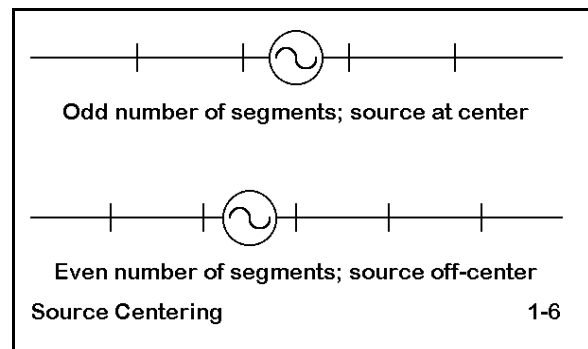
Source: every wire antenna has one or more sources, ordinarily a voltage (or current) source on the antenna itself. The modeler can place the source on any segment within the wire structure, and multiple sources are allowable. For example, a phased array of vertical antennas may have independent sources, each with its own voltage magnitude and phase. NEC sources are in series with the wire segment on which they appear, in the same way that one may properly view the circuit from an antenna feedpoint through the source and back to the antenna as a series circuit. (In fact, NEC-2 has provision for modeling lossless transmission lines for use with remote sources.) **(Figure 1-4)**



Load: a series R/X (resistance-reactance) or a series or parallel R/L/C (resistance-inductance-capacitance) circuit placed at a specified location on the antenna. Like sources, loads are in series with the wire segment on which they are placed. When combined with a source, as in an inductively center-loaded dipole, the load and the source

are in series with each other. **(Figure 1-5)** We shall look more thoroughly at loads in Chapter 14.

Since every antenna must have a source, its placement is important. Center-feeding of an antenna element is among the most common sourcing techniques. NEC-2 distributes the properties of each segment along its length, and hence, it is convenient for structural purposes to think of these properties as being centered on the segment's length. Consequently, true center-feeding of a single wire element requires an odd number of segments. Otherwise, the source point will be off-center. **(Figure 1-6)**



The number of segments you use for each wire is a function of the length of each segment relative to a wavelength. Segments should be under 0.1 wavelength long, with 0.05 wavelength preferred (about 10 segments per half-wavelength). Segments shorter than 0.001 wavelength should also be avoided. For reference, the following table

provides a U.S. amateur radio band list of the maximum and minimum recommended segment lengths. Values for other frequencies are easily extrapolated.

Frequency MHz	Segment length in inches/meters for 0.05λ segments	Shortest recommended segment length in inches/millimeters
1.8	327.9 / 8.329	6.657 / 169.1
3.5	168.6 / 4.282	3.372 / 85.6
7.0	84.3 / 2.141	1.686 / 42.8
10.1	58.4 / 1.483	1.169 / 29.7
14.0	42.2 / 1.072	0.843 / 21.4
18.068	32.7 / 0.831	0.653 / 16.6
21.0	28.1 / 0.714	0.562 / 14.3
24.89	23.7 / 0.602	0.474 / 12.0
28.0	21.1 / 0.536	0.422 / 10.7
50.0	11.8 / 0.300	0.236 / 6.0
144.0	4.1 / 0.104	0.082 / 2.1

Thin-wire segments yield the most accurate results. The wire circumference divided by the wavelength should be much less than 1 for accurate results. Moreover, the ratio of segment length to diameter should be greater than 4 for errors less than 1%. If the model demands a smaller ratio, it should be approached cautiously. Shorten segment lengths gradually, keeping an eye on results that may take off on a tangent.

Maintaining a larger segment length to diameter ratio at corners is also necessary to keep the center of one segment from falling within the radius of the other segment. Again, approaching this limit produces no sudden disastrous results, so you can press it cautiously.

Prevent wires from physically touching or coming in very close proximity when crossing. There is no hard and fast rule on where the proximity occurs, but several wire diameters separation is strongly recommended.

There is also a junction limitation. The number of wires joined at a single junction may be no more than 30. This limitation is especially applicable to models involving base-fed vertical antennas with radial systems modeled above ground. In some models, this

limitation may be accompanied by a further problem of the overlap of thick wires. The latter may be overcome by the use of thin wires, while the dimension limit itself should not be exceeded.

Most antennas that you model will fall well within the ranges specified as limits for the program. For example, a $1/2\lambda$ dipole will model well with only 11 segments, for a length of 0.0455λ /segment. Common HF Yagi design, whose elements are also about $1/2\lambda$ long, model very well with about 21 segments per $1/2\lambda$, for a segment length of about 0.024λ . Some irregular triangular shaped loop antennas may require as many as 50 segments per half wavelength, or a segment length of 0.01λ . All of these figures are distant from either the high or low segment length limits. We shall examine some further considerations applicable to segmentation in Chapter 5.

NEC-2 has provisions for a highly accurate ground effect calculation system variously called the Sommerfeld-Norton (S-N), SOMNEC, and other names. Although NEC-2 also has a "fast" ground calculation algorithm (somewhat faster in solutions than the S-N system), it is far more limited and less accurate than the S-N system, especially for antenna elements near the ground. Hence, wherever calculation of ground effects is critical to antenna design, only the more accurate system should be used. This applies to such modeling tasks as low dipoles (under 0.2 wavelengths up), elevated ground planes, and Beverage antennas.

The contrast between the results of the "fast" ground system and the S-N system are sufficiently vivid with low dipoles, that a small demonstration is in order. The following table compares NEC-2 S-N and fast data for a 3.5 MHz dipole (136.9 feet, #12 copper wire, resonated in free space) at heights from 0.05 to 0.30 wavelengths above medium or "average" earth (conductivity = 0.005 Siemens/meter; dielectric constant = 13).

Antenna λ	Height Feet	Fast Ground		S-N Ground	
		Gain Dbi	Source Z $R \pm jX \ \Omega$	Gain Dbi	Source Z $R \pm jX \ \Omega$
0.05	14.05	3.2	30.9 + j 21.5	1.2	48.7 + j 15.2
0.10	28.10	5.8	43.4 + j 23.0	5.1	49.8 + j 20.9
0.15	42.15	6.5	60.1 + j 28.7	6.4	62.5 + j 26.7
0.20	56.20	6.5	76.3 + j 26.7	6.5	76.9 + j 25.1
0.25	70.26	6.2	87.8 + j 18.1	6.2	87.7 + j 17.1
0.30	84.31	6.1	92.7 + j 6.4	6.1	92.3 + j 5.9

Above about 0.20λ , the gain and the source impedance figures are in reasonable and usable accord. Below that level, however, the fast ground overestimates both gain and source reactance, while increasingly underestimating the source resistance.

Despite the more reliable figures produced by the S-N ground calculations, the use of the S-N is not without some limitations. For example, NEC-2 is sometimes used to simulate surface ground radial systems with vertical antennas by placing the wires very close to the ground. One set of recommendations places the minimum height at 0.0001 wavelength, with segment-length tapering techniques applied below ground plane heights of 0.001 wavelength. For frequencies below the 80-meter ham band, some ground-wave measurements suggest that elevated radial models yield overly optimistic gain figures. Consequently, the limits of the S-N ground system should be approached cautiously. We shall attempt to master the fundamentals of using the ground systems in NEC-2 in Chapter 12.

NEC-2 also offers the modeler another useful provision: the introduction of transmission lines into the antenna structure. Transmission lines can be used to connect antenna elements, as in phased arrays or log periodics. They can also be added as feedlines to an antenna by the addition of a very short, remote wire to provide the line with a terminating point and for placement of the antenna source. Transmission lines can also be shorted or left open by various techniques and thus used as inductively or capacitively reactive stubs.

The transmission line models used in NEC-2 are mathematical, in contrast to the wire elements, which can be classified as "physical." Wire elements enter into the matrix calculations and contribute to the far field and other antenna performance specifications. However, transmission lines do not enter into those calculations. For example, providing a dipole with a transmission line will not yield results that show any radiation from the line.

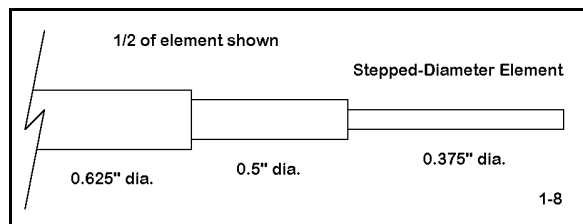
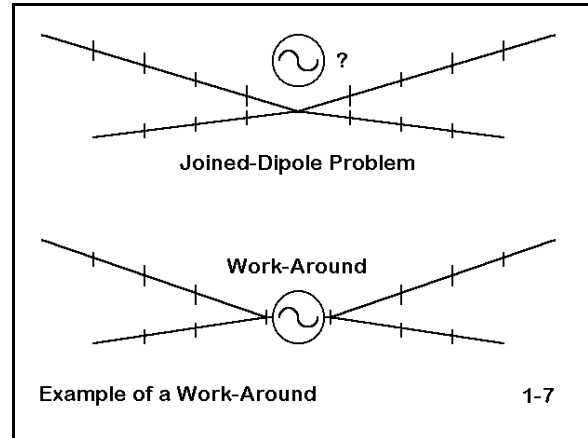
In addition, transmission lines in NEC-2 are lossless. Therefore, models using them will not reflect losses incurred in phasing lines, load lines, and the like. Calculation of those losses will have to be done by separate external means. We shall take a more extensive look at NEC and transmission lines in Chapter 15.

NEC-2 Weaknesses

NEC-2 operates most reliably within a set of limiting conditions that the modeler must observe. NEC-2 also exhibits a number of special limitations that fall within the range where the modeler expects good results. Some of these weaknesses have **work-arounds**, special substitute modeling techniques. A few of the substitute techniques are simple modifications of model construction. We shall pass along these techniques as we encounter the need for them. Other weaknesses require more complex methods of conquest, methods that are built into some program interfaces. Still other weaknesses

have no known solutions. These limit to a degree the modeling that you can successfully do with NEC-2.

An example of an easily overcome difficulty involves modeling multiple antennas with a common source at their center junction. See **Figure 1-7**. As modeled at the top, the source must be placed off center on one or the other dipole. The off-center placement yields inaccurate results for the other frequency band. The figure also hints at the work-around: the addition of a short wire at the antenna center, with the dipoles meeting at the ends of this wire, can resolve this difficulty. We shall find some other uses for this technique in Chapter 8.



An example of a more complex weakness inherent in NEC-2 involves the use of stepped-wire-diameter antenna elements. NEC-2 produces inaccurate results when an antenna element is composed of wires of differing diameters, as is commonly the case with HF Yagis using several sizes of

aluminum tubing. The basic situation is shown in **Figure 1-8**.

If an element is composed on each side of center of, say, only 2 wires of different diameters and the junction is past the mid-point on each side, results will be more accurate than elements having multiple diameter steps closer to the center. Large steps in diameter increase the accuracy problem.

Most commercial implementations of NEC-2 have incorporated a technique to overcome this problem effectively. Using equations developed by Dr. David Leeson, the programs calculate the antenna properties with substitute elements having a constant diameter. The resulting models have proven quite reliable. However, you must use caution in constructing the model to ensure that the stepped diameter element is continuous or collinear, with no bends or intervening geometric oddities along the way. For example, adding a mid-element capacity hat structure will disable the correction feature in some programs. Likewise, the source must be at the center of an element with open ends (such as a dipole), and loads must be symmetrically placed. Transmission line are sometimes disallowed. Moreover, the element may be required to be within a certain

percentage of resonance, which may complicate attempts to model in NEC-2 multi-band HF Yagis with stepped-diameter elements throughout. We shall construct a number of stepped-wire-diameter models in Chapter 9.

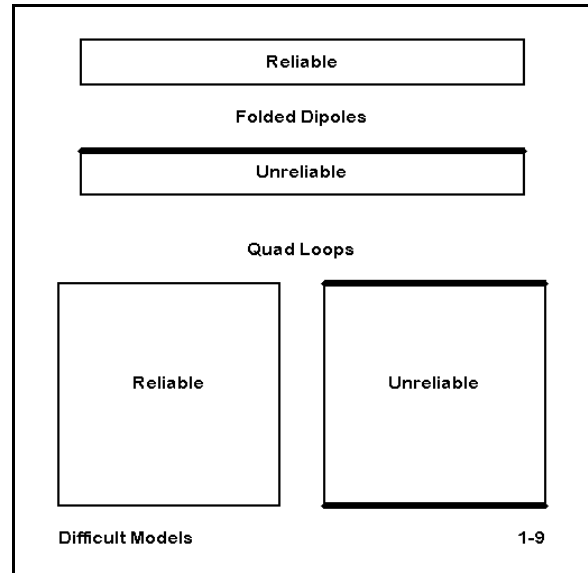
Although linear stepped-diameter elements are correctable, non-linear elements with changes of diameter are not. In many instances, NEC-2 will produce unusable results. Two such cases are the quad loop and the folded dipole, each with wires of unequal diameter. See **Figure 1-9**.

With the quad loop and the folded dipole which use a single diameter wire, the models yield quite reasonable results for both gain and source impedance data. However, when the antennas use wires of different diameters, the results become less reliable. A quad loop with "fat" horizontal members and "thin" vertical members presents different diameter wires at a corner junction, a situation for which the Leeson equations provide no solution.

In the case of the folded dipole, there are wires of different diameters in close proximity to each other, another case for which there is no present work-around. We shall look at these and similar cases in Chapter 10.

(Interestingly, although NEC-4 provides more reasonable output data for these cases, a result of overcoming the need for a stepped-diameter wire correction, the results are still less than satisfactory. NEC is a program whose evolution is far from complete.)

Despite its weaknesses and the need for some work-arounds, NEC-2 remains a highly competent calculational program that is capable of modeling a very large number of antenna types with great reliability. We have been surveying both the capabilities and the limitations in order to give you an introduction to some of the operative NEC-2 terminology, as well as something of a feel for working with antenna modeling programs. For more intensive study of NEC-2's stand-alone use, see G. J. Burke and A. J. Poggio, "Numerical Electromagnetic Code (NEC) Method of Moments," Vol. 2 (Part III: User's Guide), Tech. Doc. 116, Naval Ocean Systems Center, San Diego, 1982. Volume I contains two parts: "Part I: NEC Program Description--Theory" and "Part II: NEC Program Description--Code." Part I discusses the equations and numerical methods, while Part II provides a detailed description of the FORTRAN code.



What is NECWin Plus?

NECWin Plus is an antenna modeling program which uses a modified version of the NEC-2 core within an extensive array of input and output facilities. It has a twofold set of objectives. First, it is designed to allow the user to accurately and easily develop an antenna model in the format required for NEC-2 calculations. Second, it provides a large number of output data options to allow the user to examine the NEC-2 data both tabularly and graphically, in order to ensure the most correct and complete analysis and interpretation. NECWin Plus is written for the Windows 95/98 environment.

In this short introduction to the program for which this guide is written, we shall sample only some of the program features to acquaint you with them. In later chapters, we shall have occasion to develop some ideas on how to use these features most effectively in the modeling of the antennas in the assignments.

I recommend that you read the remainder of this chapter with the program in place and running. In this way, you can compare the text and the reference graphics to the screen. Also keep the NECWin Plus manual handy for detailed instructions on implementing features and functions. This guide will only instruct you to use them, but will not provide details of operation.

NECWin Plus Files

After installing the program on your computer, use your file facility to examine the subdirectory structure of the program. Most of the program files will be in a subdirector called \BIN. Another subdirectory called \EXAMPLES contains a number of standard antenna model files with the extension .NEC. Some of these files are keyed to the "Walk-Through" exercise in the "User's Manual" portion of the overall NECWin Plus manual. For practice and to familiarize yourself with the structure of the program, work through these exercises.

The models used in the exercises in this guide are contained on a 1.44 MB floppy disk attached to the guide. The files use a filename scheme that reflects their use within this guide. Hence, expect to see and open filenames such as 1-1.NEC, which is the first exercise example for the first chapter. 6-3.NEC is the third exercise file for Chapter 6.

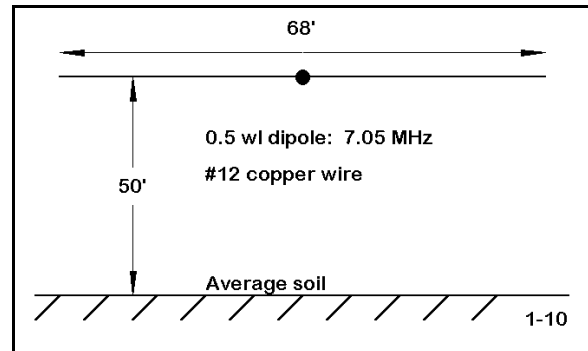
I recommend that you create a new subdirectory at the same level as \BIN and \EXAMPLES. You may call it anything you wish, but \GUIDE will do very nicely. Now copy the files from the floppy disk to this subdirectory. Alternatively, if you are equipped with a ZIP drive or its equivalent, you may copy the files to a directory within it.

If you examine the contents of the floppy disk for this guide, you will see that there is a large amount of unused space. The basic models are written as ASCII files that serve as the input for the NEC-2 core: they do not require much space. However, the files generated by NECWin Plus and NEC-2 require considerable storage space.

1-1.NEC

Every individual exercise will begin with the name of the file to be opened. Open file 1-1.NEC. You may run this file if you wish. However, the run, ground, and pattern plotting files for this example already exist on the floppy disk and should now be within the subdirectory you have created for exercise files.

The model consists of a #12 copper wire dipole for 40 meters (7.05 MHz) placed at a height of 50' above average soil (conductivity = 0.005 S/m; dielectric constant = 13), using the high accuracy Sommerfeld-Norton ground calculation system. See **Figure 1-10**. The file requests output in terms of two far field patterns, one an azimuth pattern taken at an elevation angle of 39° (or a zenith angle of 51°); the other an elevation pattern from horizon to horizon, taken along the azimuth angle of maximum gain. The data in the NEC screen for this file should be similar to that shown in **Figure 1-11**.



```

CM Program introduction model: 40-meter dipole
CM #12 copper wire, 50' over average soil, 7.05 MHz
CE
GW 1 15 -34 0 50 34 0 50 3.36778215223097E-03
GS 0 0 .3048
GE 1
GN 2 0 0 0 13 .005 0 0 0 0
EX 0 1 8 0 1 0
LD 5 1 1 15 5.8001E7
FR 0 1 0 0 7.05 1
RP 0 181 1 1000 -90 90 1 1
FR 0 1 0 0 7.05 1
RP 0 1 360 1000 51 0 1 1
EN

```

1-11

We shall explore the terms of this model construction in detail as we move through chapters of this guide. At this time, you may wish to verify your understanding of program functions by running the model and examining the plots as well as data about the source impedance. Once

you have done so, close the file and the program and examine all of the files in the \GUIDE subdirectory having the filename 1-1. You will discover four files:

1-1.NEC: this is the original input data file.

1-1.NOI: this file contains the NEC-2 data, both as received from the input file and structured for calculation and as calculated. File length is over 80 KB.

1-1.PLT: this file contains the values for the graphical plots of the polar azimuth and

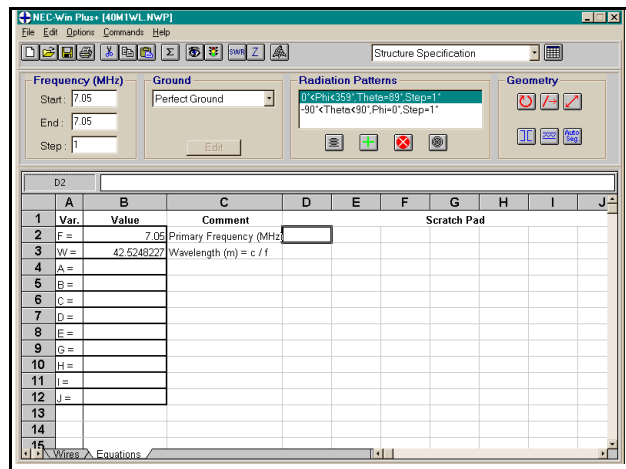


Figure 1-13 shows a further alternative available to the user. The generic name for the mode of data input for this screen is **symbolic entry**. For some geometries, modification of the antenna dimensions can be an arduous task. By specifying the antenna geometry in a sequence of equations for elements that may be varied, you can alter the wire sizes by changing only one or two entries in the list of equations. All the other values will follow according to the equations you enter. As a simple example, suppose you create a quad loop symmetrically around

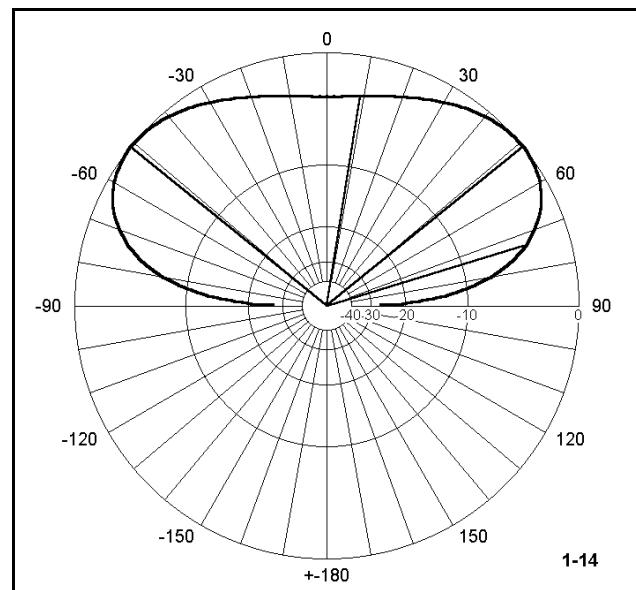
the X axis and at a height for the center point of 30 feet. By creating a value for A, and then defining the geometry points in terms of $\pm A$ and $30 \pm A$, you need only alter the value of A to change the wire lengths around the loop. The main screen will always show the resultant numerical values. We shall take a detailed look at model creation and entry in the next three chapters.

Other parameters of the antenna are accessible at the top of the main screen. Frequency (or frequencies) to be evaluated, ground specifications, and transmission line creation are among the features included for ready access.

NECWin Plus Outputs

NEC-2 produces its output data in a massive collection of ASCII tables in a single file. NECWin Plus permits you to examine the entire table or to view selected portions of the table. For example, you may look at just the currents along the wire elements or at the source impedance for each frequency checked.

In addition, the program offers a host of graphical data in both polar and rectangular formats, as appropriate. **Figure 1-14** to the right shows the elevation pattern of the antenna in 1-1.NEC, along with analytical lines indicating the angle of maximum gain and the -3 dB beamwidth angles. The pattern



is taken along the axis of maximum gain.

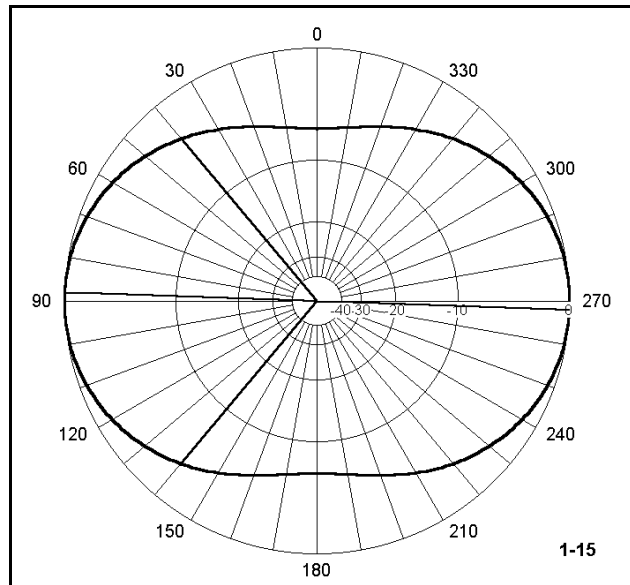
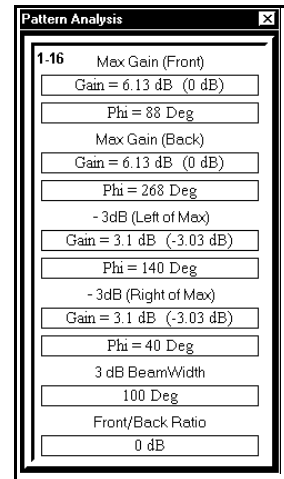


Figure 1-15, to the left, shows the equivalent azimuth pattern, taken at an elevation angle of 39° above the horizon. Once more, beamwidth angles and the angle of maximum radiation appear on the plot. These lines are a function of an analysis which



can appear on the screen with the plot. **Figure 1-16**, to the right, shows a sample for the azimuth pattern to the left.

Besides polar pattern plots, the program also offers numerous rectangular plot possibilities. For example, the same pattern data shown on the polar plot in **Figure 1-15** can also be represented on a rectangular graph.

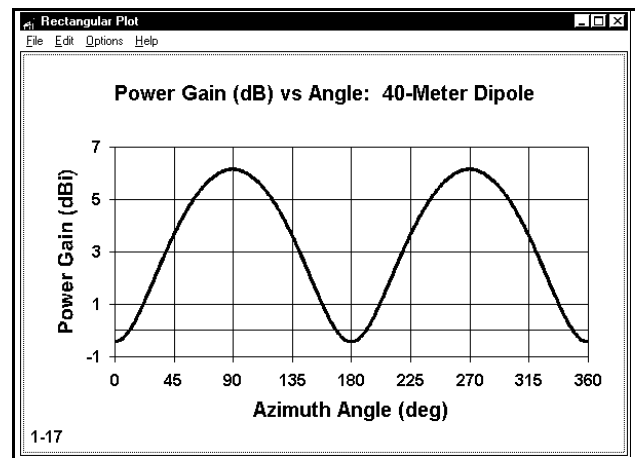
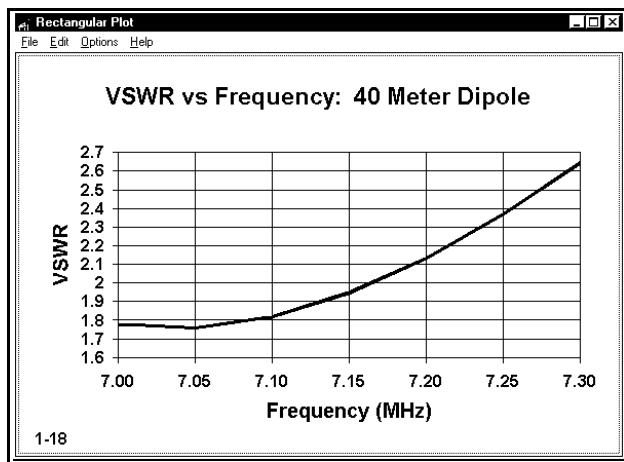


Figure 1-17 presents the total far-field radiation power data in terms of dBi for the dipole at 7.05 MHz at an angle of radiation that is 39° above the horizon. We may note in a preliminary way that the pattern does not dip much below 0 dBi off the ends of the antenna (0° and 180°), a fact also reflected by the lack of significant insets at these angles in **Figure 1-15**. This oval pattern is far different from the near-zero readings at these figures when modeling the antenna in free space. Nonetheless, while the azimuth pattern shows an oval, the rectangular graph more clearly shows the undulations of values. Had we overlaid the free-space pattern, the curves would have been had the same shape, differing only in maximum and minimum value. Using the graphical resources of the output can help us clarify the meaning of the data in the NEC-2 tables.

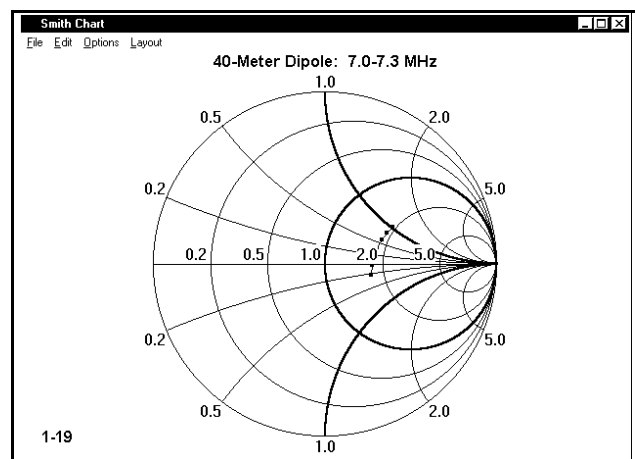


Since we can specify not just a single frequency for the calculation of data, but indeed an entire spectrum of frequencies, it is often useful to graph selected data for each frequency checked. **Figure 1-18** to the left is one example--a 50- Ω SWR curve for the 40-meter dipole over the entire amateur band from 7.0 to 7.3 MHz in 0.05 MHz steps. (Note: this requires a revision of the file 1-1.NEC. If you make this change, you should be aware that the file is no longer as it was--or you should save it at the prompt under another name, for example, 1-1A.NEC.) The graph

makes clear that the antenna was "cut" for about 7.05 MHz where its SWR is lowest. However, even at the frequency of lowest 50- Ω SWR, the lowest value is above 1.7:1. At a 50' height, the antenna is only about 3/8ths of a wavelength above ground. It might be interesting to compare curves for a range of heights, perhaps every eighth wavelength above ground up to about a 2-wavelength height.

The graphing program within NECWin Plus is quite powerful and allows a wide range of textual and layout editing. Should you wish to add further notes, arrows, or any other features to the graphs, you may screen capture them and then paste them into a graphical program of your choice. In this way, you may develop materials for reports and presentations, as well as for your own information files.

The SWR data which appeared in the rectangular graph in **Figure 1-19** might also be represented on a Smith chart. The row of dots represents the impedance data, normalized, for the 7.0 to 7.3 MHz limits of the run. This data may be used for designing matching networks for the antenna or for any other purpose to which the Smith Chart is suited.



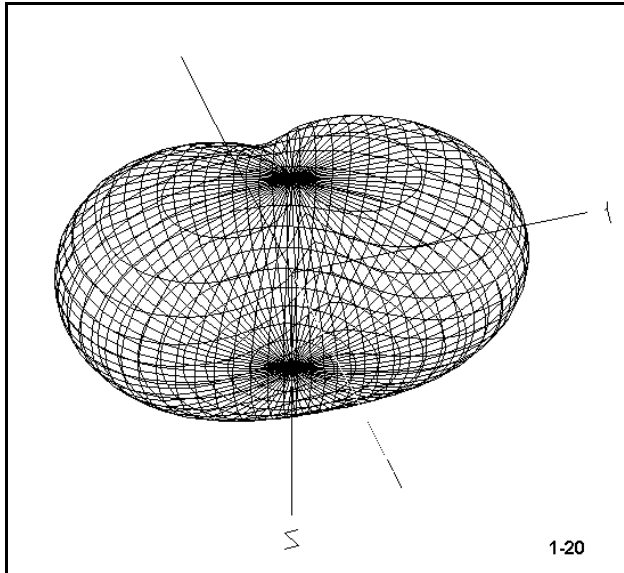


Figure 1-20, to the left, shows another graphical potential of the program: the 3-dimensional display of the far-field pattern. Although the 3-D pattern of our 40-meter dipole is not very interesting, the display can be very useful in discovering facets of complex patterns produced by complex antenna arrays. Indeed, the graphical portrayal often reveals pattern oddities that we may easily overlook while peering at the long tables of data.

We have sampled a number of NECWin Plus output potentials, but by no means all. In the course of the exercises to

follow, we shall call in both graphical and tabular outputs to interpret and clarify the performance of various antennas.

Summing Up

Antenna modeling via desk-top computer is a process of utilizing mathematical algorithms to replicate the performance of antenna structures. The development of the method-of-moments techniques used in the formulation of NEC-2 and the increased speed and memory capacity of modern PCs has converted antenna modeling from a main-frame activity to a personal enterprise open to anyone willing to master the program.

NEC-2 remains the primary calculating core for antenna modeling, since it resides in the public domain and is open to software developers who add both input and output facilities to the basic abilities of NEC-2. NECWin Plus, the program for which this guide has been written, offers a wide variety of capabilities on both ends of the calculating core to facilitate the development of accurate and error-free models and to aid the modeler in reading and interpreting the output data effectively.

Nonetheless, good modeling must be done within the constraints of the NEC-2 core, honoring the limits set for models that yield reliable results. The straight-wire requirements for model wires, the segmentation conditions, and the weaknesses remaining within the evolving NEC core development must be on the mind of every modeler who would use NEC-2 to design or analyze an antenna.

In many ways, the notes in this introduction to both NEC-2 and to NECWin Plus will make

better sense as the exercises roll by. Therefore, I recommend that you return periodically to this chapter for a rapid rereading. In addition, you will want to reread often both the instruction manual accompanying NECWin Plus and the fundamental source materials for NEC-2 itself. These materials and the exercises may also lead you to look into both the improvements and the remaining deficits of NEC-4, the latest stage in NEC evolution, and into MININEC.

However, for the moment, we shall turn our attention to mastering the NEC-2 program at hand and the fundamentals of good antenna modeling.

User Notes

2. Modeling Preparations

Objectives: *The exercises in this chapter introduce ways of preparing for a modeling run that go far to ensure sensible results. The use of simple paper forms help translate a physical antenna design into the data needed by the program for its calculations. The use of such forms is also the basis of good modeling records keeping.*

Constructing a model of an antenna within the context of NEC-2 requires three sets of considerations in addition to the calculating core:

1. The physical structure of the antenna;
2. The background parameters that define the antenna's environment; and
3. The desired data to be generated by NEC-2.

All three items must be adequately and correctly entered into any NEC program to generate usable and useful outputs.

We can identify these elements within even the simplest NEC input file, as in the following example:

```
CM 6-Meter 3 element wide-band Yagi
CE
GW 1, 31, -1.4835, -1.0334, 5.8, 1.4835, -1.0334, 5.8, .00635
GW 2, 31, -1.3729, 0., 5.8, 1.3729, 0., 5.8, .00635
GW 3, 31, -1.2206, .83206, 5.8, 1.2206, .83206, 5.8, .00635
GE 0
LD 5, 1, 0, 0, 2.5E+07, 1.
LD 5, 2, 0, 0, 2.5E+07, 1.
LD 5, 3, 0, 0, 2.5E+07, 1.
FR 0, 1, 0, 0, 52.
GN -1
EX 0, 2, 16, 0, 1.414214, 0.
RP 0, 1, 361, 1000, 90., 0., 0., 1., 0.
EN
```

We may call each line a **card**, each with its own 2-letter label. Many of the available cards are implemented in NECWin Plus, and we shall give some details on each as we work with them in this and later chapters. Only a few key cards appear here--but enough to make a good model of the antenna. I have widely separated the elements in each line,

but you will normally see the data compressed, with each entry on each line separated by either a single space or a punctuation mark.

1. The CM card is a comment card and consists of ASCII input that permits the modeler to make remarks that identify the model. You may have as many CM cards as you need, since you get 1 line of type per card. You can go back later and add performance data and other comments after you run the model so that they are permanently attached to the file. The CE card marks the end of comments: you need this card to tell NEC where to start inputting data.

2. The collection of GW cards define the antenna geometry. The 3 GW cards in this collection correspond to the 3 elements of the Yagi, telling us that we have used 1 wire per element. The first place in each line numbers the wire, while the second tells how many segments make up the wire (here 31 per wire). The next 6 elements define each wire's end point on an X, Y, and Z set of coordinates, one set for each end of each wire. At the far right in the line is the **radius** of the wire. Although we tend to think in terms of wire diameter, NEC uses the radius in its calculations. Program interfaces usually ask for the diameter and then halve that number in translating your input into the NEC card entry.

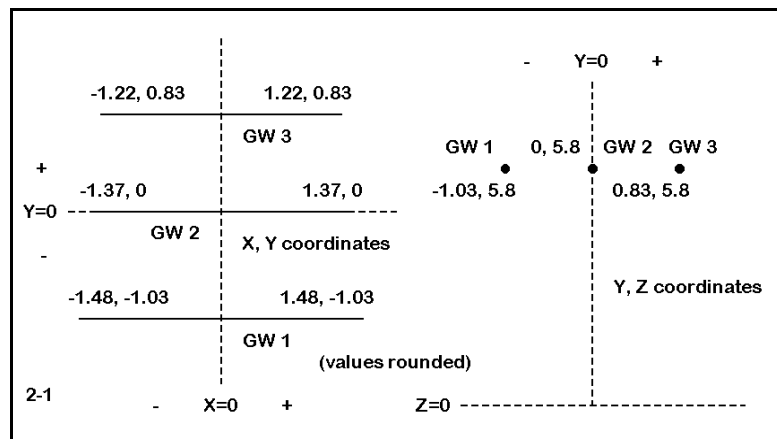
The basic unit of physical measure for NEC is the meter. In this example, all of the wire coordinates are listed in meters, as is the wire radius. (0.00635 meters is about 0.25 inches.) Program interfaces usually offer a variety of both metric and English units of measure for inputs. The interface can then convert the values to meters or it can order NEC to insert a GS card which contains the conversion factor for NEC to apply. The structure is closed by the GE (geometry end) card.

Let's take a closer look at the 3rd through 8th entries on each GW line. These define wire ends. Positions 3-5 define the X, Y, and Z coordinates of end 1 of each wire, while positions 6-8 define the X, Y, and Z coordinates of end 2 of each wire.

Note that the 3rd and 6th entries are numerically the same, but have different signs. This fact indicates that each antenna wire was constructed symmetrically around the X axis. The fact that each 3rd entry for the GW cards has a minus sign indicates that the modeler has adopted the convention of modeling straight wires from left to right or from - to +. We shall have more to say about adopting conventions as we look at different types of models.

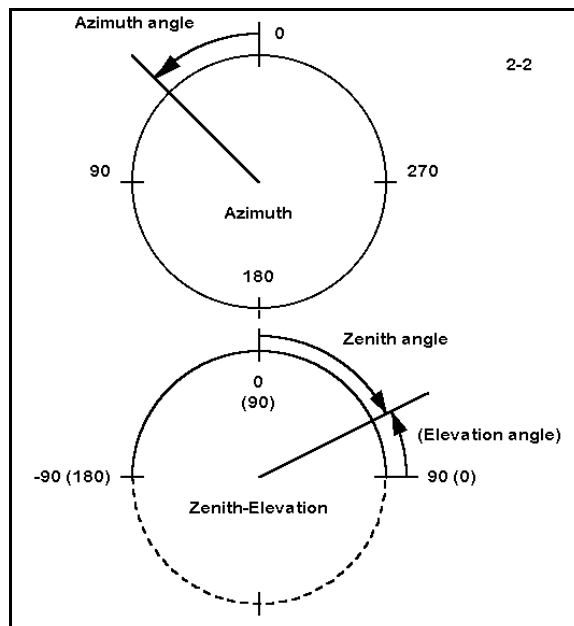
If we look at the 4th and 7th entries for each line, we see that they are the same within each line. The center (GW 2) wire has the coordinate $Y=0$, indicating that the modeler chose this wire as the baseline for the model. For Yagis, reflector elements normally have negative coordinates and directors positive coordinates, and we can detect this from the fact that the X-values for GW 1 are larger (reflector type) than those for GW 2, and those for GW 3 are shorter (director type).

Figure 2-1 represents the antenna in a pair of 2-dimensional sketches, one showing the X and Y coordinates, the other showing the Y and Z coordinates. NECWin Plus offers a three dimensional, rotatable sketch of all antennas, giving you more views than are possible with a single flat diagram.



3. Following the GW cards are three LD cards, indicating loads. For this model, these loads are (position 1) type 5, meaning distributed material loads. The right end of the line lists the conductivity of the material, which is the figure for aluminum. (Specifically, the figure is the conductivity of 6061-T6 alloy. See the appendix for a table of values for common antenna materials) These cards may be omitted for models using lossless wire.

4. The following cards set the parameters for the antenna's operation. The FR (frequency) card lists a single frequency, 52 MHz. The GN (ground parameter) card's value of -1 sets the antenna in free space. (Note that specifying free space sets the center of the antenna at Z=0, despite the listed value of 5.9 meters for the value of Z in the GW cards.)



The EX (excitation or source) card places a source on wire 2 at the 16th or center segment of the 31-segment wire. The source is a voltage source. (Note: NEC-2 uses peak values rather than r.m.s. values of voltage and current throughout.) Although other source types are available, we shall confine ourselves initially to voltage sources. The value in position 5 sets the excitation value at a peak voltage of 1.414. Together, the FR, GN, and EX cards define the minimal set of parameters necessary for any model whatsoever.

5. The RP card sets the output request of NEC. In this case, the card requests a 360-degree (0 to 360) azimuth table of field strength values in the plane of the antenna, as

indicated by the 90-degree value in position 5. Additional RP cards may be used for either azimuth or zenith (or elevation) plots. See **Figure 2-2**. We shall work more extensively with antenna plots and their conventions in Chapter 4.

Together, the cards following the GE (geometry end) card are called control cards. Finally, every NEC model ends with the EN (end) card. In effect, it tells the core to stop reading.

The best way to master these elements of NEC models is by constructing some models to see how the data input system works.

Exercise Preparation

In this set of exercises, you will construct a variety of antenna models of varying type and complexity. However, the process of constructing a model does not begin at the keyboard. Instead it begins with a piece of paper. The paper can be scratch paper or something more formal. For this exercise set, we have prepared a form that you may copy and use for each of the samples. It appears on the facing page with both front and reverse sides. For this set of exercises, only the face side should be needed.

Let's divide the form into 4 sections and see how it can help our model input work.

1. **The header:** The top lines of the form provide basic information about the model file and the background values within which the antenna will be modeled. The top line forces you to give the model a name--one that is either specific or generic--along with a file name and directory location. The last two items are important once you begin to develop collections of models. It is aggravating to lose ten minutes trying to remember where you stored a file.

The second line begins the modeling information. The band(s) entry allows you to specify one or more frequency or wavelength regions on which the antenna may be used, while the frequency entry is for either the antenna design center frequency or the upper and lower frequencies of a sweep you may intend to perform. The antenna height, even though it may be repeated in the wire table, is a reminder of the intended use of the antenna. Alternatively, if the model is preliminary, you may wish to enter "FS" for free space. Recording the number of elements is a check on the wire table entries below, which may consist of many wires. Recording the units of measure for the antenna elements can save you from trying to mix units later.

Recording the ground type and specifications (if other than free space) should be a standard part of your modeling practices. For horizontal antennas, such as dipoles and beams at HF, the use of a ground other than the usual program default may not make significant differences in the data produced by the program for the model. The default for

most implementations of NEC is "Good" or "Average" soil, with a conductivity of 0.005 S/m and a dielectric constant of 13. These values are taken ultimately from studies performed in the 1930s and often repeated in antenna handbooks. Other common ground condition values are listed in the Appendix.

As a modeler, you always have the choice to begin your modeling with zero-loss wire. However, it is usually good practice to specify the antenna wire material in terms of the actual material you intend to use (or are using) in order to take its distributed losses into account. In many cases, the differences between zero-loss wire and actual materials may make only insignificant differences in the output data. However, this fact will not be true for all antenna designs. In addition, some programs require a single material for the entire antenna, while others (including NECWin Plus) permit material or resistivity/conductivity specification on a wire-by-wire basis. If limited to a single material for some design combination of copper wire and aluminum tubing, you can choose the material that is quantitatively dominant in the design, the one most prominent near the high current regions of the antenna, or simply the one with the higher losses.

2. The antenna sketch: To get an understanding of the importance of sketching the antenna to be modeled, let's look at the form on the next page, a data sheet for a simple 10-meter aluminum dipole.

On this data sheet, the header is completely filled in with the basic and background data. Note that for this model, "Free Space" has been selected as the modeling medium. Note also that the material is 6063-T832 aluminum, whose conductivity value may differ from other types of aluminum that might have been used.

The sketch itself should be (and this one tries to be) as complete as possible. Not only does the drawing show the overall dimensions, but as well, it displays the lengths and diameters of the individual sections of the dipole elements. Since each change of diameter represents the stop/start point for a wire in the model, complete dimensional data is necessary in order to correctly enter the wire geometry.

Src #	Type (V/I)	Location (Wire #, Seg # or %)	Load #	Type (R/X, S/P R/L/C)	R/L/C or R/X Values	Location (Wire #, Seg # or %)
1	V	W 2, S 6 (Center)				

Although a CAD program has yielded a crisp graphic for the antenna sketch, a pencil sketch will normally suffice. However, strive to make it as clear and complete as possible. Remember that it is the fundamental reference for all other modeling work you do.

3. **The wire chart:** NEC and MININEC operate on the basis of wires that are segmented according to rules. A single antenna element may consist of more than one wire, if the diameter changes along the way. In our simple example, we have two 3/8" diameter end pieces and a 1/2" diameter center section.

In reality, the center section may consist of 2 pieces of aluminum, slightly separated at a center feedpoint. However, the source (the feedline) is considered to be in series with the segment to which it is connected, and therefore, the wire should be continuous. You can accomplish this by specifying a single 1/2" wire and placing the source at its center. In NEC, you will select an odd number of segments for this wire to ensure source placement at the exact center. Alternatively, you may choose to create two wires, one for each side of center. In NEC, this means of constructing the antenna wires requires selecting or creating a split feed to include the last segment of one wire and the first segment of the next.

In this model, I chose a symmetrical arrangement of the element, using the zero point as the center. I also chose to extend the element length along the Y-axis. Since the antenna has only length, the X-axis is always zero, and since it is in free space, the Z or height axis is also zero. (For dipoles intended to be vertically oriented over ground, the Z-axis may be used for the wires.)

It makes no difference to calculation speed whether the antenna element lengths appear in either the X-axis or the Y-axis. When surveying the wire length values of a very complex but linear antenna, it may be more visually convenient to scan the left-most X-axis to check for errors. In the end, however, try to adopt one consistent convention for

most--if not all--of your models. Swapping axes as you hop from model to model can be a source of unintended errors.

Among the most important conventions to adopt is to begin at one end of each antenna element and to proceed from that end to the other without changing directions in mid-stream. In the figure, note that the model proceeds from left to right along the sketch, symmetrically with respect to the zero-point of the Y-axis. Hence, a 16.78' antenna becomes +/-8.39' long.

Notice also that end 2 of the first wire becomes the starting point or end 1 of wire 2. For continuous antenna elements, be certain that the X, Y, and Z values of joined ends are the same. NEC connects wires that are within very tiny distances of each other, so also be certain that, if you do not want wires connected, they are far enough apart.

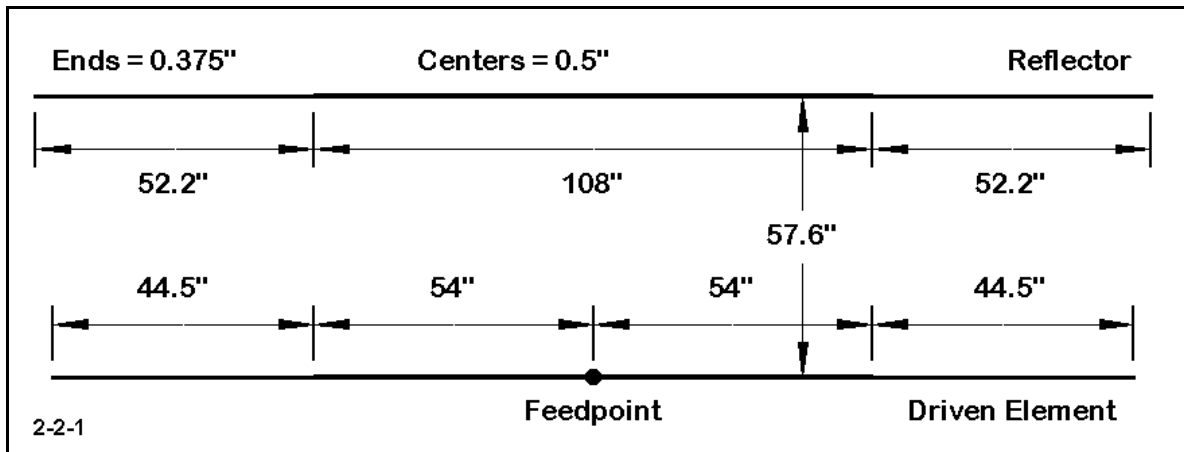
Wire entries also require that you specify the wire diameter **in the units of measure of the wire lengths**. You must convert the 3/8" and 1/2" diameters into 0.03125' and 0.04167' respectively. NECWin Plus also allows you to specify common American AWG wire gauges, which is useful for copper wire antennas. All diameters are converted in the wire's radius. The NEC input file will show the converted value of the diameter you entered in the input page or file. The Appendix contains charts with the diameters in inches and in millimeters for both AWG and BSWG wires in gauges from 1 to 40.

You must also specify how many segments the wires will have. In order to make the segments for each wire reasonably close in length, the end wires in our sample form have 5 segments (0.78' per segment) and the center wire has 11 (0.82' per segment).

4. Source and other data: The form has two places for the entry of source and load data. In the wires chart, you should note the location of sources (and loads). In the space at the bottom of the form, enter more detailed information. Enter not only the source location, but also the type (voltage or current, single or split) within the limits allowed by the program. We have already seen the utility of split sources. Single voltage sources are the native environment of most modeling programs. However, specifying a current source and giving it a value of 1 is often very useful for comparing current magnitude and phase output data for each segment along the antenna element(s).

This model is now ready for conversion into the appropriate program inputs. You will find this model on your disk listed as 2-1.NEC. Open the file and compare the data entry with the entries on the form. If you understand every corresponding element between the paper and the computer entries, you are ready to create some models for yourself.

2-2.NEC



In this exercise, we shall construct a model of a 2-element aluminum Yagi with a design center frequency of 28.5 MHz. The outlines of the antenna are shown in **Figure 2-2-1**.

In order to construct this model, we need further information. The units of measure, obviously, are in inches. The antenna material will be 6061-T6 aluminum, which has a conductivity from the table in the Appendix of about $2.50E7$ S/m. (Note that the conductivity figure need not be converted into S/inch.) The antenna will be at a height of 35' or 420" over average soil with a conductivity of 0.005 S/m and a dielectric constant of 13. We shall want a single azimuth pattern with a zenith angle of 76° (or elevation angle of 14°). We shall name the file 2-2A.NEC.

We can readily see that the antenna has elements composed of two different wire diameters (0.375" and 0.5"). Therefore each element must be broken into 3 wires. We shall specify (somewhat arbitrarily at this point in our work) that the total number of segments for each element is 21. Since the center section of each element is a little longer than twice as long as each element end section, we may assign 11 segments to each center section (0.5" diameter) wire and 5 segments to each end section (0.375" wire).

The diagram specifies a single feedpoint or source for the antenna: at the center of the driven element. Therefore, we shall place the source (a simple voltage source will do) at the center of the driven element 0.5" wire.

In this example, you have been guided through all the information needed to construct a form in preparation for data entry into NECWin Plus. The only missing data are the exact coordinates for the wire ends. Construct your own form before checking your work against the reference sample on the next page.

Comments: Consistent with the conventions used with preceding examples, the wire chart models elements as a sequence of wires from left to right and from the reflector forward.

Despite the detailed guidance presented in this exercise, there is still room for variation among perfectly comparable models. The reference form wire table adopts a convention of placing the wires ends in the X-axis (rather than in the Y-axis, as with the dipole example). You may compare the two entry forms and eventually settle upon the convention that best suits your way of working with models. The convention used in this example would make the most alterable dimensions (wire end positions, or element lengths) most visually evident, but it also positions azimuth patterns at 90° relative to the convention of placing wire ends in the Y-axis.

A second convention used in this model is to place the reflector or rearmost antenna element at "zero," with every other element of this type of antenna positioned forward with +Y values. Contrast this convention with the one noted in our very first example of setting the driven element at zero with other elements placed at -Y and +Y positions relative to the driver. Again, you should eventually adopt a convention for your own work that suits your way of working with models.

Src #	Type (V/I)	Location (Wire #, Seg # or %)	Load #	Type (R/X, S/P R/L/C)	R/L/C or R/X Values	Location (Wire #, Seg # or %)
1	V	W 5, S 6 (center)				

Once you have finished the paper version of the model, enter the data into a "New" model in NECWin Plus and save the model as 2-2A.NEC. Now open file 2-2.NEC and compare your work with it. As with the form, your work may vary from but must be compatible with the model in 2-2.NEC.

There are two items that might escape attention. First, in the GN card line, the specified ground type is 2, indicating selection of a Sommerfeld-Norton ground. You might well have selected the finite or "fast" ground, type 0. Second, notice the introduction of the GS or scaling factor card to convert the dimensions in inches into NEC-2's native environment of meters.

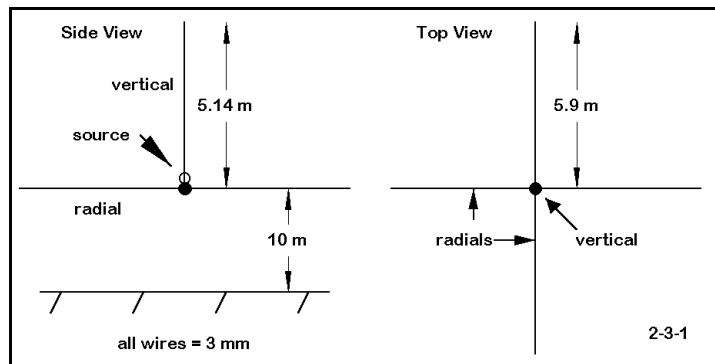
```

CM 2-2.NEC: 2-element 10-meter Yagi
CM 28.5 MHz; over average soil
CE
GW 1 5 -106.2 0 420 -54 0 420 .01565
GW 2 11 -54 0 420 54 0 420 .02085
GW 3 5 54 0 420 106.2 0 420 .01565
GW 4 5 -98.5 57.6 420 -54 57.6 420 .01565
GW 5 11 -54 57.6 420 54 57.6 420 .02085
GW 6 5 54 57.6 420 98.5 57.6 420 .01565
GS 0 0 .02540
GE 1
GN 2 0 0 0 13 .005 0 0 0 0
EX 0 5 6 0 1 0
LD 5 1 1 5 2.4938E7
LD 5 2 1 11 2.4938E7
LD 5 3 1 5 2.4938E7
LD 5 4 1 5 2.4938E7
LD 5 5 1 11 2.4938E7
LD 5 6 1 5 2.4938E7
FR 0 1 0 0 28.5 1
RP 0 1 360 1000 76 0 1 1
EN

```

2-2-2

Since you should be able to correlate your paper forms to entries in the .NEC files, no further reference forms will be shown in this chapter. However, continue to create, plan and refine your models on these or similar forms before creating model files.

2-3.NEC

Using the sketch to the left and the data to follow, create a model of a $1/4\lambda$ vertical antenna for 14.1 MHz with a ground plane of $4 \ 1/4\lambda$ radials. The antenna dimensions are in the sketch, and the base of the antenna is 10 meters above ground. Use 20 segments for each quarter-wavelength wire. Place the source on the last (lowest) segment of the vertical element wire (Wire 1,

Segment 20).

The material is copper wire 3 mm in diameter. Place the antenna over average soil using the S-N ground option. Request a single zenith (or theta) plot for -90 to +90 degrees. When you have finished your paper design work, create a new model file and save it as 2-3A.NEC.

Comments: Creation of a ground plane antenna model also requires that you adopt a convention of construction. In this case, it is useful to begin with the vertical element, placing the top end at end 1 of wire 1. End 2 of wire 1 becomes the junction for the radial system, as well as the lower terminus of the vertical element. Moreover, each radial must be a separate wire running from the junction outward. To give the model parts continuity, think of the antenna as starting at the top of the vertical and extending through the source to the end of each radial. Open model 2-3.NEC for reference.

Compare your work to the model description in **Figure 2-3-2**. Begin by checking the control cards, ensuring that the ground, frequency, and requested pattern cards are correct. Now recheck your wires. In the model as shown to the right, the radials make a clockwise pattern as viewed from above, each 5.9 meters long in either the X or the Y axis, as appropriate. The vertical element runs from 15.14 to 10 meters, for a net length of 5.14 meters. Note also that the wire radius should read 0.0015, the correct translation of the diameter in millimeters to the radius in meters. Finally note the location of the source on the EX card.

Although this model is simple in many respects, it displays a number of pitfalls into which a new modeler can fall, including failure to translate the wire diameter into the operative units of measure, careless handling of the radials, and misplacement of the source. Hopefully, your design on paper caught all of these potential difficulties before they occurred in the model entered into the program.

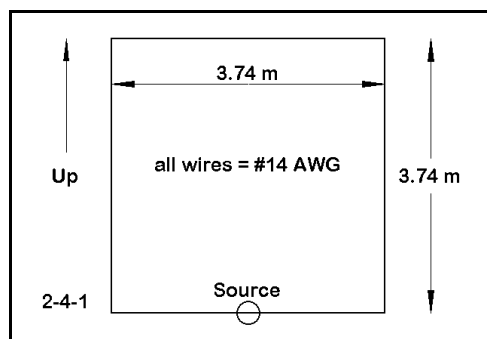
```

CM 2-3.NEC: 20-M ground plane
CM 14.1 MHz over average soil
CE
GW 1 20 0 0 15.14 0 0 10 .0015
GW 2 20 0 0 10 5.9 0 10 .0015
GW 3 20 0 0 10 0 5.9 10 .0015
GW 4 20 0 0 10 -5.9 0 10 .0015
GW 5 20 0 0 10 0 -5.9 10 .0015
GS 0 0 1
GE 1
GN 2 0 0 0 13 .005 0 0 0 0
EX 0 1 20 0 1 0
LD 5 1 1 20 5.8001E7
LD 5 2 1 20 5.8001E7
LD 5 3 1 20 5.8001E7
LD 5 4 1 20 5.8001E7
LD 5 5 1 20 5.8001E7
FR 0 1 0 0 14.1 0
RP 0 181 1 1000 -90 0 1 1
EN

```

2-3-2

2-4.NEC



For our next model, we shall look at a single quad loop set in the vertical plane for 21.15 MHz. The antenna will be in free space and use #14 AWG copper wire.

Each side of the quad loop is 3.74 meters long. When you model this antenna, place it symmetrically in the X-axis and symmetrically on the Z-axis. (If you later place this antenna over "real" ground, you will have to elevate all of the Z values by a like amount, since NEC-2 will not handle wires underground.) Use 21 segments per side for the loop. Place the source on the lowest horizontal element at its center. Save the file as 2-4A.NEC.

Comments: One of the easiest ways to construct squares, diamonds, and similar symmetrical shapes is to begin modeling at 0,0 (X, Z), using equal amounts of plus and minus length in each axis. First, this type of convention (which might also use the Y and Z axes) eases the process of model size revision, since each like value can be raised or lowered by an equal increment. Second, it also ensures that modeling additional quad loop elements--as in a multi-element quad beam--will be symmetrically larger or smaller than the first loop.

```

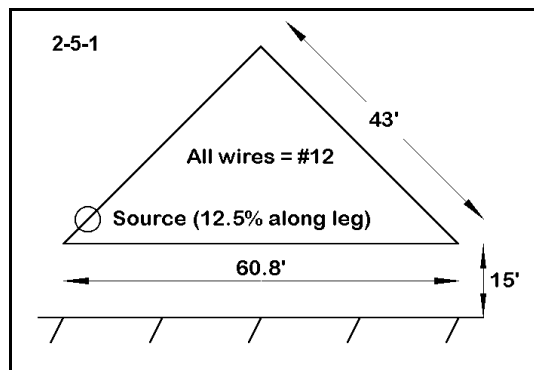
CM 2-4.NEC:  single quad loop
CM 21.15 MHz; Free Space
CE
GW 1,21,-1.87,0.,-1.87,1.87,0.,-1.87,.000814
GW 2,21,1.87,0.,-1.87,1.87,0.,1.87,.000814
GW 3,21,1.87,0.,1.87,-1.87,0.,1.87,.000814
GW 4,21,-1.87,0.,1.87,-1.87,0.,-1.87,.000814
GE 0
LD 5,1,0,0,5.7471E+7,1.
LD 5,2,0,0,5.7471E+7,1.
LD 5,3,0,0,5.7471E+7,1.
LD 5,4,0,0,5.7471E+7,1.
FR 0,1,0,0,21.15
GN -1
EX 0,1,11,0,1.414214,0.
RP 0,1,361,1000,90.,0.,0.,1.,0.
EN

```

2-4-2

Reference model 2-4.NEC, the description for which appears in **Figure 2-4-2**, provides clues to the conventions involved. Besides centering the loop, the model also approaches the wires systematically, beginning with the lowest horizontal wire and proceeding counterclockwise around the loop. Whether you prefer to move in one direction or the other, be consistent with all loops in a given antenna. At a minimum, having a convention speeds the work of revision and error detection.

2-5.NEC



The antenna in this exercise is a delta loop, placed in a vertical plane with the base at the lowest point (15' above average soil). The antenna base leg is 60.8' long and will have 47 segments. Each of the angular legs is 43' long and requires 33 segments (to keep each segment in the antenna about the same length). The antenna requires #12 AWG copper wire.

Since this particular design provides maximum vertically polarized radiation and minimum horizontally polarized radiation, it requires a feedpoint about $1/4\lambda$ from the upper apex--or about 12.5% up one of the two angular legs. This position is segment 5 of whichever wire extends upward from the antenna base wire.

Request a single theta plot, but be sure to specify an azimuth or phi angle of 90° if you place the longitudinal dimensions on the X-axis. Save your file as 2-5A.NEC.

Comments: This model intentionally threw a mild curve by not giving values for the dimensions that made the required coordinates obvious. However, the translation is not difficult to perform. Let the baseline extend from -30.4' to +30.4' on the X-axis. The apex will fall where X=0 and will be 30.4' above the baseline, since this is a right triangle. Since the baseline is 15' above ground, the z-coordinate of the apex is 45.4' up.

The antenna is easy to modify, while

retaining the right-triangle configuration, by changing both ends of the baseline and the apex by equal amounts. You can check the source point and other data against **Figure 2-5-2**, which is the model description for 2-5.NEC.

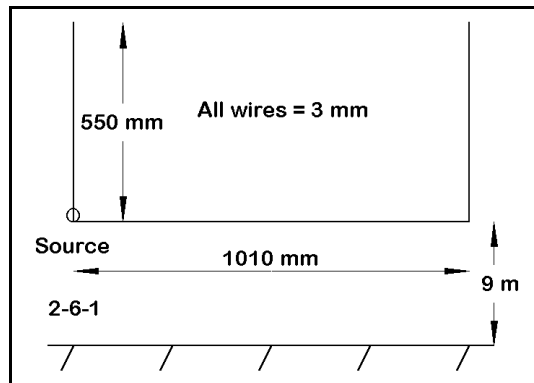
```

CM 2-5.NEC right-angle delta
CM 7.15 MHz; 15' over average soil
CE
GW 1 33 -30.4 0 15 0 0 45.4 3.36778215223097E-03
GW 2 33 0 0 45.4 30.4 0 15 3.36778215223097E-03
GW 3 47 30.4 0 15 -30.4 0 15 3.36778215223097E-03
GS 0 0 .3048
GE 1
GN 2 0 0 0 13 .005 0 0 0 0
EX 0 1 5 0 1.414214 0
LD 5 1 1 33 5.8001E7
LD 5 2 1 33 5.8001E7
LD 5 3 1 47 5.8001E7
FR 0 1 0 0 7.15 0
RP 0 181 1 1000 -90 90 1 1
EN

```

2-5-2

2-6.NEC



Our final exercise involves a half square antenna, which is essentially $2 \frac{1}{4}\lambda$ with a $\frac{1}{2}\lambda$ phasing line between them. The antenna provides a strong figure-8 radiation pattern, largely vertically polarized, broadside to the array. Often used on the lower HF bands with the horizontal wire and feedpoint high, the antenna offers good VHF service potential with the horizontal wire either high or low.

Although complex theoretically, the half square is physically simple, consisting perhaps of a single piece of wire with the ends bent up or down. Whatever the physical arrangement, we must model it as 3 wires, beginning at one end and proceeding to the other.

Use the dimensions in **Figure 2-6-1** to create a model of a half square for 146 MHz with the ends upward. The dimensions are given in millimeters, and the antenna is 9 meters above average soil. Select a single azimuth or phi pattern, using a zenith (theta) angle of 87° (or an elevation angle of 3° above the horizon). Use 3 mm 6061-T6 aluminum for the antenna material throughout. (You may also wish to survey the Appendix wire tables to familiarize yourself with AWG, BSWG, and wire diameter equivalencies.) Feed the antenna at one corner by placing a source on the last segment of a vertical wire, just as it joins the horizontal wire. Use 11 segments on the vertical wires and 21 segments on the horizontal wire. Save your file as 2-6A.NEC.

Comments: Of course, you remembered to translate the antenna baseline height from 9 meters into 9000 millimeters for determining the Z coordinates of the antenna. Note the GS card in the description, derived from reference file 2-6.NEC, to effect the translation of the millimeter dimensions into meters.

Millimeter dimensions are common at VHF and UHF frequencies, as are dimensions given in centimeters. As a supplementary exercise, convert the antenna dimensions to inches and the antenna height then to feet.

Becoming familiar and comfortable with both the metric and the English system is essential to good modeling.

```

CM 2-6.NEC 2-M halfsquare
CM 146 MHz; 9 meters over average soil
CE
GW 1 11 -505 0 9550 -505 0 9000 1.5
GW 2 21 -505 0 9000 505 0 9000 1.5
GW 3 11 505 0 9000 505 0 9550 1.5
GS 0 0 .001
GE 1
GN 2 0 0 0 13 .005 0 0 0 0
EX 0 1 11 0 1.414214 0
LD 5 1 1 11 2.4938E7
LD 5 2 1 21 2.4938E7
LD 5 3 1 11 2.4938E7
FR 0 1 0 0 146 0
RP 0 1 361 1000 87 0 1 1
EN

```

2-6-2

Summing Up

A good beginning is half the journey. Good modeling results emerge from the careful construction of good models. Two important components enter into this process.

First, we must understand the input system used by NEC calculations. To this end, we have looked at the basic data that NEC must have in order to perform. These data included the wire geometry as well as fundamental control information on the source placement, the frequency of operation, the type (or lack) of ground over which the antenna is used, the material conductivity, and the desired output information.

Second, we must convert physical antenna specifications into wire geometries that not only meet the minimal standards for NEC operation, but as well observe conventions that ease the process of model generation and revision. We have observed a number of conventions along the way in these exercises, and we shall encounter others in later chapters. The starting point for good model construction is a neat and orderly piece of paper that records in advance what we will then enter as our antenna model.

It is less important that you adopt either the forms used in this chapter or the conventions shown in the examples than it is that you adopt some structured paper form and some entry conventions that are suited to your own work. Together, the two practices will enhance your modeling skills.

User Notes

3.

Basic Antenna Models

Objectives: *In a series of simple models, this chapter will acquaint you with basic concepts used in modeling on both the input and output sides of the NEC-2 calculations. The exercises in this chapter will familiarize you with the process of modeling with NEC-2, including working with the input data, running models, and using fundamental output data.*

Having mastered some of the principles of model construction--at least for basic types of antennas used in the HF and VHF regions--we are now positioned to "operate" those antenna models. Operating an antenna in the real world involves providing the antenna with transmitters and receivers (and any necessary transmission line). We then perform either random tests with other stations or systematic range tests. Along the way, we make suitable antenna measurements, including the shape and strength of the antenna far field or surface wave pattern, the feedpoint (or source) impedance, and other derivative properties.

Antenna modeling with NEC-2 provides calculated equivalents of those tests. Since the calculational core of NEC-2 has been validated as reliable for a wide range of antenna models which adhere to the rules of construction, the results of the NEC-2 calculations provide a reliable representation of performance for a real antenna having the same properties as the model. Because making changes in the large and complex structure that comprises a real antenna is often difficult and always time consuming, modeling can speed the systematic variation of variables, either to check the performance of a given design or to perfect the performance of a prototype. Moreover, modeling permits us to vary the environmental variables surrounding an antenna, either in terms of modeled surrounding objects or in terms of the nature and quality of the ground beneath an antenna.

As with all mathematical models, reliable results depend upon honoring the limitations of the system of algorithms. In addition to restrictions on the model's geometry, there are also limitations on environmental variables. Even though we can easily vary the ground conditions beneath an antenna, we cannot track terrain variations that are present at a real antenna site. NEC-2 models antennas over level ground of a uniform composition. This constraint may leave some questions unanswered about the performance of a corresponding real antenna. Real ground is not uniform with respect either to surface area or with respect to depth. However, the use of uniform ground conditions is no hindrance to the comparison of antennas.

In these exercises, we shall look at the entire modeling process, from construction to evaluation, but over a limited set of parameters. The outputs of greatest interest in general modeling at HF and VHF include the far field patterns and the source impedance information at the design frequency and over a range of nearby frequencies. Although these data provide limited information about the antenna, they remain important first order data for the modeler.

Therefore, we shall examine only these data. However, we shall see how to maximize the information they give us as a collection of paradigm tests to be performed on almost all antenna models. By making a series of modifications to our model (including its control cards, such as ground and requests for patterns), we shall discover that even a few output items can provide a fairly complex and comprehensive data set.

We shall look at only three types of antennas in these exercises. All of the antennas are common types: a wire dipole, a vertical dipole, and a 3-element Yagi. Our object will be to discover the kinds of things we can learn about these antennas from even a limited data set.

Exercise Preparation I: The Wire Dipole

Although the simple wire dipole may seem less than exciting, it remains a worthy subject for modeling. Because it is simple, models run speedily in NEC-2, allowing us to do some very systematic data gathering. We shall begin with a wire dipole in free space, and then move to a copper wire dipole over real ground. By the time we finish with the dipole, you will have either confirmed much of the information you have learned from antenna theory or discovered a number of new things about dipoles--or a little of both.

3-1.NEC A dipole in free space

Open model file 3-1.NEC. Examine the model description. Notice that the 14.0 MHz center-fed dipole model is in free space (a default value, hence no GN entry) and that the wire is lossless (no LD card). Since the GS card has a value of 1, the dimensions are in meters.

Since we shall be interested in modifying the length of the dipole and there are no other requirements for our work to suggest a

symmetrical layout, we can let the antenna terminate (end 2) at 0,0,0, and place the positive dimension at end 1. We shall be making changes to this file. The program works

```

CM dipole: 14.0 MHz
CE
GW 1 21 10.42 0 0 0 0 0 .0005
GS 0 0 1
GE 0
EX 0 1 11 0 1 0
FR 0 1 0 0 14 0
RP 0 1 361 1000 90 0 1 1
EN

```

3-1-1

with temporary files so that, if you wish to save the file under its new configuration, you should go to the "File" and then the "Save" operations. To save both a modification and the original, you should alter the filename (for example, to 3-1A.NEC or 3-1B.NEC) to preserve the original file under its own name.

Exercise 1: Run the model with its lossless wire. Do not change the 10.42 m length or the 1 mm wire diameter. From the tabular data and/or from the pattern plot feature (under the "Analyze" option), determine the maximum free space gain. Note that the pattern requested is an azimuth pattern at a 90° theta or zenith angle (equal to a 0° elevation angle). Then modify the GW line to change the wire material, using the following 4 material conductivity values:

Material	Conductivity
Copper	5.80E7
6061-T6 Aluminum	2.49E7
Phosphor Bronze	9.09E6
Stainless Steel	1.39E6

Record your results in the following table:

3-1 Test Data Ex. 1			Reference	
Material	Gain (dBi)	Source Z (R±jX Ω)	Gain (dBi)	Source Z (R±jX Ω)
Lossless			2.14	72.1 + j 0.0
Copper			2.04	73.9 + j 1.6
6061 Al.			1.98	74.9 + j 2.4
Bronze			1.88	76.7 + j 4.0
St. Steel			1.47	84.8 + j10.0

Comments: The reduction in gain due to material losses is expected. However, note that increasing material losses also tend to make the antenna appear long (have inductive reactance at its source point). For each material of increasing loss, a resonant antenna would be shorter. This effect is in addition to the normal end effect, which is a function of wire size relative to a wavelength.

Exercise 2: Return to the original model using lossless wire. In successive steps increase the wire diameter by a factor of 4, moving from 1 mm through 4 mm and 16 mm to 64 mm. Record the gain and source impedance in the table below.

3-1 Test Data			Ex. 2 Reference	
Wire Diameter	Gain (dBi)	Source Z (R±jX Ω)	Gain (dBi)	Source Z (R±jX Ω)
1 mm			2.14	72.1 + j 0.0
4 mm			2.14	73.2 + j 7.7
16 mm			2.15	75.2 + j16.0
64 mm			2.16	79.3 + j25.7

Comments: If we do not change the dipole length from its original value (10.42 m), but increase the wire size, the source impedance increases, with most of the increase in the form of inductive reactance. The inductive reactance indicates that the dipole is long relative to a more precisely resonant length. Notice also that a dipole longer than resonant increases in gain (although very slightly) relative to a resonant length.

Exercise 3: Let's return the free space dipole to resonance for each wire size. Using the correct wire size, adjust the length (Wire 1, end 1) until the source reactance is less than $\pm 1\Omega$. Record both the gain and the source impedance for each test on the table below.

3-1 Test Data				Ex. 3
Dia. mm	Length m	Gain dBi	Source Z (R±jX Ω)	
1				
4				
16				
64				

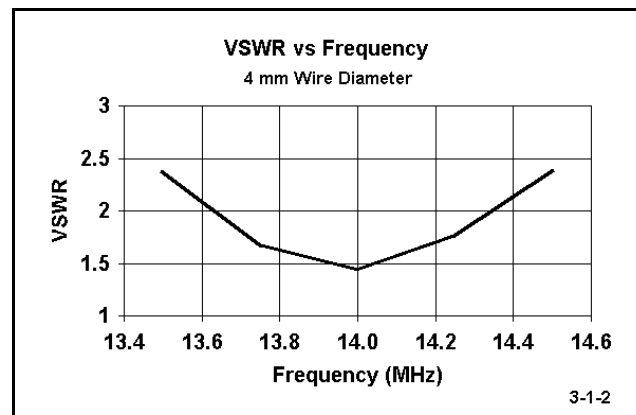
Comments: Compare your data with the reference data in the next table. Notice that as the antenna diameter increases, not only does the length decrease, but as well the source resistance at resonance also decreases, although only slightly. In addition, the gain decreases, indicating that to a small degree, the antenna gain is dependent upon its length. Although these very small changes in gain and source impedance that depend

upon wire diameter and length may make no operational difference in an actual wire dipole, they are real. In other antenna designs at other frequencies, these phenomena may take on some significance.

3-1	Reference Data		Ex. 3
Dia. mm	Length m	Gain dBi	Source Z ($R \pm jX \Omega$)
1	10.42	2.14	$72.1 + j 0.0$
4	10.36	2.14	$72.0 - j 0.1$
16	10.27	2.13	$71.9 + j 0.3$
64	10.10	2.13	$71.8 + j 0.1$

Exercise 4: Before we leave our free space model of a 14.0 MHz lossless wire dipole, let's perform one more set of runs. For each wire diameter and its associated resonant length, perform a frequency sweep. Open the frequency dialog box and set the start frequency at 13.5 MHz, use a step of 0.25 MHz, and specify 5 steps. For each of the four models, the program will calculate data for 13.5, 13.75, 14.0, 14.25, and 14.5 MHz. Since the antenna is resonant at the frequency in the middle of this range, it will have a 50- Ω SWR that is lowest at approximately 14.0 MHz. We shall be interested in the 50- Ω SWR at frequencies other than the design center frequency for the dipole.

To observe the SWR, you may examine the tabular data available or you may create a rectangular graph of the data. Open the rectangular graphing facility and specify a VSWR vs. Frequency graph. Specify a 50- Ω SWR curve. For each graph, adjust the X-axis to run from 13.4 to 14.6 MHz. Adjust the Y axis to run from 1 to 3. (Although some of the curves do not approach a 3:1 VSWR within the range of the sweep, the curves will be more readily comparable if each uses the same VSWR range.) You may print each chart for comparison with each other. **Figure 3-1-2** shows a sample of the VSWR vs. Frequency graphs.



Using each graph, estimate the highest SWR at each end of the frequency spread (or read the figure from the tabular data). In addition, estimate the frequency at which the

SWR curve crosses the line for a 2:1 SWR. Subtract the lower frequency of the 2:1 crossing from the higher frequency on the 2:1 crossing to obtain an estimated value in MHz for the 2:1 VSWR bandwidth. Record the data in the table below.

3-1		Test Data			Ex. 4	
Diameter	13.5 MHz SWR	2:1 SWR Low Freq.	2:1 SWR High Freq.	14.5 MHz SWR	2:1 SWR Bandwidth	
1 mm						
4 mm						
16 mm						
64 mm						

Comments: The curves establish the expected: the larger the wire diameter, the wider the operating bandwidth of a given linear antenna. Since many dipoles are operated with 50- Ω coaxial cable, establishing a 50- Ω 2:1 SWR operating bandwidth is a common practice. The procedure used here is essentially one way in which it is done. However, for greater precision, you may specify more steps and a smaller step size in the frequency sweep. In fact, you may wish to repeat this exercise using a step size of 0.1 MHz and 11 steps in order to check the accuracy of your estimates taken from the curves.

3-2.NEC A dipole over average soil

Open file 3-2.NEC. If you examine the model description, you will discover that it is the same dipole for 14.0 MHz, but this time made from copper wire and placed above a S-N ground using average soil, which is conventionally taken to have a conductivity (σ) of 0.005 S/m and a dielectric constant (ϵ) of 13. The initial height of the antenna (Z-axis) is 20 m.

In the RP card, we find a request for an elevation pattern, also called a "theta" pattern. The designation "theta" derives from the use of that

Greek letter to designate the zenith angle, the angle from directly overhead downward toward the horizon. The θ or zenith angle is the opposite of the common notion of an elevation angle, which counts upward from the horizon. Be certain that the Azimuth-Elevation vs. Theta-Phi option is set for Az-EI. This convention will coincide with common field engineering practice. The RP card will still show the theta angle.

```

CM dipole: 14 MHz, copper
CM over average soil
CE
GW 1 21 10.44 0 20 0 0 20 .0005
GS 0 0 1
GE 1
GN 2 0 0 0 13 .005 0 0 0 0
EX 0 1 11 0 1 0
LD 5 1 1 21 5.8001E7
FR 0 1 0 0 14 0
RP 0 181 1 1000 -90 90 1 1
EN

```

3-2-1

Exercise 5: In this exercise, we shall run the model at different heights above ground, working downward from 20 m in 2.5 m steps. The S-N ground system is capable of producing accurate results close to the ground, so it is the only ground system adequate to our task. Take data from the tabular information, but also be sure to examine closely the elevation patterns. In fact, you may wish to print out each pattern, along with its analysis box for reference. Record your data in the table below. In the box marked " λ Angle Degrees," record the angle of maximum radiation as given in the analysis that accompanies the elevation pattern. This elevation angle is also called the "take-off" or TO angle.

3-2		Test Data		Ex. 5
Height m	Gain dBi	θ Angle Degrees	Source Z (R±jX Ω)	
20				
17.5				
15				
12.5				
10				
7.5				
5				
2.5				

Comments: The height increments in the chart only roughly accord with $1/8\lambda$ points, since a λ is about 21.4 m long at 14.0 MHz. However, the markers are useful in recording some trends in the performance of simple dipoles with respect to their height above ground. Most obvious and consistent is the gradual increase in elevation angle (and decrease in theta angle) of maximum radiation. You can compare your test data with reference data on the next page.

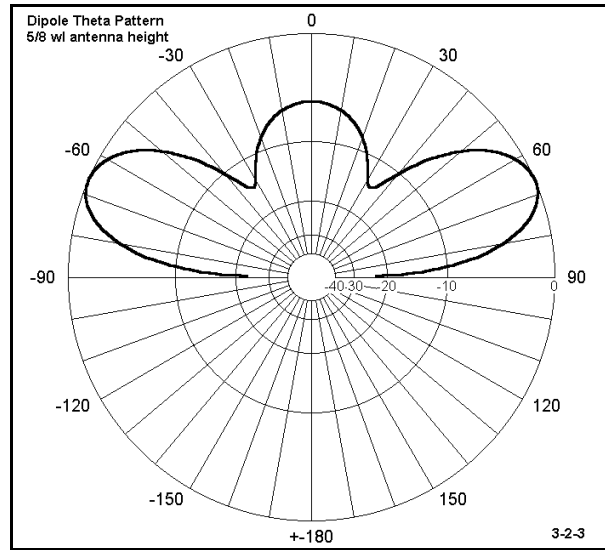
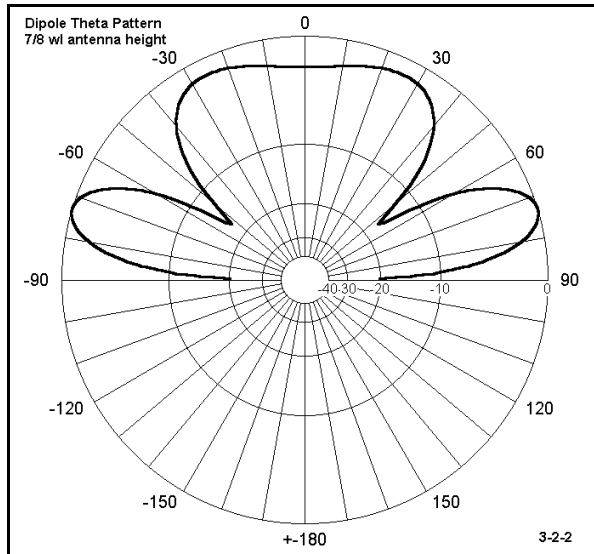
Less consistent is the variation in source impedance between $1/8\lambda$ and 1 wavelength height. You may wish to plot these numbers independently on a spreadsheet and graph them for reference. To construct a more sensitive curve, you may wish to rerun the exercise at 1 m intervals.

Equally inconsistent but more regular is the gain at the take-off (TO) angle for the variations in antenna height above ground. There is an approximate $1/4\lambda$ separation

between the maximum at $5/8\lambda$ up and the minimum at $7/8\lambda$ up. You may continue the test above 1λ to about 2λ to see if there are further maxima at $1\ 1/8\lambda$ and $1\ 5/8\lambda$, as well as minima at $1\ 3/8\lambda$ and $1\ 7/8\lambda$. This test is best conducted with more precise increments than used here. You will likely discover that the maxima and minima exist, but that as the antenna height is increased, the curve grows increasingly shallow.

3-2 Reference Data			Ex. 5
Height $m(\lambda)$	Gain dBi	θ/El Ang Degrees	Source Z ($R \pm jX \Omega$)
20.0 (1)	7.31	75/15	77.0 - j 0.6
17.5 (7/8)	7.06	73/17	80.7 - j 7.0
15.0 (3/4)	7.44	70/20	72.6 + j12.5
12.5 (5/8)	7.75	66/24	64.9 + j 4.0
10.0 (1/2)	6.95	60/30	74.1 - j 6.3
7.5 (3/8)	5.92	50/40	88.0 + j 2.0
5.0 (1/4)	5.77	20/70	81.7 + j21.5
2.5 (1/8)	4.53	02/88	58.5 + j20.1

Equally as interesting as the curve of gain is an explanation for it. A partial visual explanation can be gained by examining the theta patterns developed in the exercise. Compare, for example, the patterns for the $7/8\lambda$ and the $5/8\lambda$ heights, and notice the differential in energy at high angles above the main lobes of the pattern. At most, this is an indicator, since it does not account for all of the energy in the 3 dimensions of radiation, but it is suggestive for further modeling. For further investigation is this question: which types of antennas show similar variations with height and which do not--and, of course, why?



Exercise 6: Before leaving our copper wire dipole for 14.0 MHz at 20 m above ground, let's perform one more test. The variable this time will be the quality of the ground beneath the horizontal dipole. Using the data in the Appendix, we can define for our test 4 different soil quality levels:

Soil Description	Conductivity in S/m σ	Dielectric Constant ϵ
Salt Water	5	81
Very Good	0.0303	20
Average	0.005	13
Very Poor	0.001	5

Enter the "Ground" dialog box and successively change the S-N ground properties through these options, each time running the model. Record gain, TO angle, and the source impedance for each ground condition in the table below.

3-2		Test Data		Ex. 6
Soil Description	Gain dBi	TO angle degrees	Source Z (R±jX Ω)	
Salt Water				
Very Good				
Average				
Very Poor				

Comments: The chart, which you may compare with the reference data on the next page, should convince you that ground quality has little effect upon common horizontal antennas. The TO angle does not change at all, while the impedance changes only slightly. The resistive and reactive components each change by only about 4 Ω. The gain also changes only slightly: about 0.75 dB. (Do not make the mistake of thinking that the antenna has lost something like a tenth of its gain in the move from salt water to very poor ground. The gain figures are not measures of simple power in watts, but rather compare two power levels--in this case, the antenna field and the field of an isotropic source that radiates equally well in all directions. The relevant question would be something like this: what would it take to raise the quality of the very poor soil to at least the level of salt water? Every possible answer turns out to be more expensive and impractical than simply moving to an antenna with a higher gain in the desired direction.)

3-2		Reference Data		Ex. 6
Soil Description	Gain dBi	TO angle degrees	Source Z (R±jX Ω)	
Salt Water	7.68	15	80.0 - j 3.2	
Very Good	7.55	15	77.8 - j 2.3	
Average	7.31	15	77.0 - j 0.6	
Very Poor	6.93	15	76.0 + j 1.1	

Exercise Preparation II: The Vertical Dipole

In free space, there is no difference between a horizontal and a vertical $1/2\lambda$ dipole--except, of course, the orientation of its pattern relative to some fixed grid system. Over earth, however, there are great differences that are intrinsically interesting. Therefore,

let's look at a vertical dipole. We shall start over earth, but if you wish, you may change the ground to free space and explore the properties of the antenna in that medium. As always, if you wish to preserve the original model description, save all variations under different but related filenames, such as 3-3A.NEC, etc.

3-3.NEC A vertical dipole

Open file 3-3.NEC. Examine the model description. The fact that the X and the Y axes are both zero at both wire ends is the instant give-away that this is a vertical dipole. The GS card conversion factor of 0.3048 tells you that the dimensions are in feet. The frequency is 24.95 MHz, which makes the wave about 39.42' long, which is convenient, since a quarter wave is about 10' long. The 0.02085 radius figure translates into a 0.5" diameter, while the LD card tells us that the antenna is 6061-T6 aluminum.

CM vertical dipole 24.95 MHz
CM .5" aluminum average soil
CE
GW 1 21 0 0 49.84 0 0 31 .02085
GS 0 0 .3048
GE 1
GN 2 0 0 0 13 .005 0 0 0 0
EX 0 1 11 0 1 0
LD 5 1 1 21 2.4938E7
FR 0 1 0 0 24.95 0
RP 0 181 1 1000 -90 0 1 1
EN

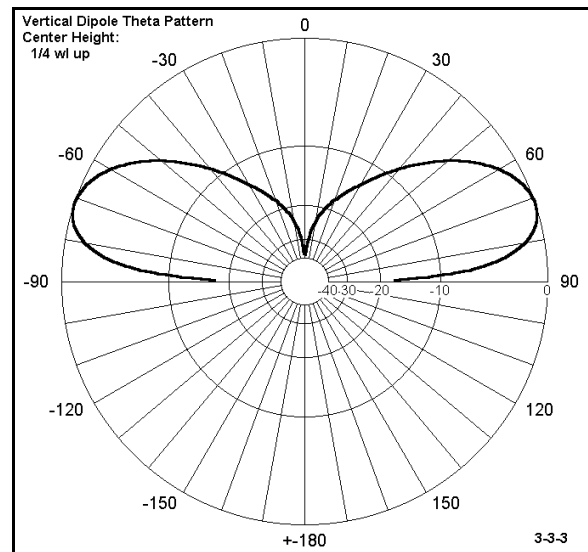
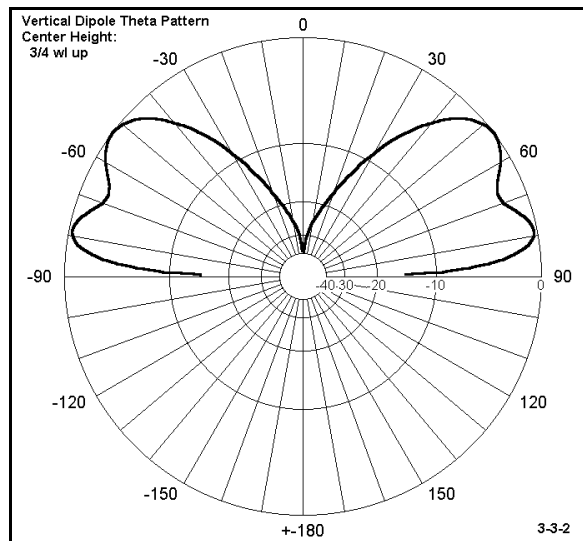
3-3-1

Subtracting the end 2 Z value from the end 1 Z value gives a length of 18.84' for the antenna, its resonant length in free space ($\pm 1\Omega$ reactance). Setting the antenna between 31 and 49.84 feet up places the source of the antenna (its center point) close to 1λ up. This is intentional, since we shall be dropping the antenna in 10' or approximate $1/4\lambda$ increments. The lowest point will place the antenna 1' off the ground.

Exercise 7: You are encouraged to repeat on your own some of the exercises performed on the horizontal dipole in free space. Our first formal exercise will be to examine the properties of the vertical dipole as we bring it closer to the ground. Using the pre-assigned average soil throughout, run the dipole at heights (relative to the low point) of 31, 21, 11, and 1 foot above ground. Using both tabular and theta pattern data, determine the maximum gain, TO angle, and source impedance of the antenna at these four heights, which correspond roughly to placing the feedpoint at 1, 3/4, 1/2, and 1/4 wavelength above ground. Enter your data in the following table.

3-3		Test Data		Ex. 7
Antenna Height feet (Center Height λ)	Gain dBi	TO angle degrees	Source Z ($R \pm jX \Omega$)	
31-49.84 (1)				
21-39.84 (3/4)				
11-29.84 (1/2)				
1-19.84 (1/4)				

Comments: The table of values that you created and may compare with the reference data on the next page shows that the source impedance is unaffected by the antenna height until the antenna is very close to the ground. Moreover, it shows a steady decrease in gain (almost linear) as the antenna is brought closer to the ground. However, the angle of maximum radiation recorded in the table can be misleading. Compare **Figure 3-3-2** and **3-3-3** (or your own saved elevation patterns) to see why.



The pattern in 3-3-2 is at an antenna center height of $3/4\lambda$ and is similar to the pattern for an antenna height of 1λ . The lobe of greatest radiation vertically is at a high angle, but the lower lobe at about 12 degrees is insignificantly weaker. The pattern in 3-3-3, at the lowest antenna height, shows only a single lobe.

3-3			Reference Data	Ex. 7
Antenna Height feet (Center Height λ)	Gain dBi	TO angle degrees	Source Z ($R \pm jX \Omega$)	
31-49.84 (1)	2.83	28 *	71.4 - j 0.3	
21-39.84 (3/4)	2.18	36 *	73.1 - j 0.4	
11-29.84 (1/2)	1.36	13	69.4 + j 1.1	
1-19.84 (1/4)	0.50	19	89.9 - j 1.1	

The patterns in this test are not inherently either good or bad, but can only acquire those labels when compared to some intended application. The pattern for the antenna when near ground does not respond well to high-angle radiation and therefore is naturally immune to interference and noise emerging from shorter skip angles. The patterns from the antenna when placed at a higher mounting point suggest greater sensitivity to higher angle radiation for applications needing communication at shorter skip distance.

Exercise 8: Just as we checked out the horizontal dipole over various types of ground quality, it makes sense to do the same with the vertical dipole. Let's begin by setting the height of the 24.95 MHz vertical dipole at its lowest point (1' to 19.84'). Retain all other properties of the original model except the ground quality variables. Vary the ground quality through the same four steps used earlier (Salt Water, Very Good, Average, and Very Poor), with the same sets of conductivity and dielectric constant values. Enter your values in the table below.

3-3			Test Data	Ex. 8
Soil Description	Gain dBi	TO angle degrees	Source Z ($R \pm jX \Omega$)	
Salt Water				
Very Good				
Average				
Very Poor				

Comments: Your data, which you may compare to the reference table, very quickly shows that the ground quality directly beneath the vertical dipole does not alter the source impedance by very much--less than 10Ω from the worst to the best ground conditions. Nor does the differential in ground quality introduce significant reactance to the antenna, which may be called "detuning" it. The TO angle rises in a uniform way from the salt water to the very poor soil value, while the gain decreases over the same range. However, with respect to gain, notice the very large jump from very good soil to salt water.

3-3		Reference Data		Ex. 8
Soil Description	Gain dBi	TO angle degrees	Source Z (R±jX Ω)	
Salt Water	5.69	08	96.1 + j 2.7	
Very Good	0.71	17	92.9 - j 1.1	
Average	0.50	19	89.9 - j 1.1	
Very Poor	0.10	21	85.4 - j 1.5	

Exercise 9: For our last vertical dipole exercise, let's elevate the antenna to the $3/4\lambda$ center point (Z equals 21' and 39.84'). We shall make the same modeling runs and enter the same data into the table below, but for the new antenna height.

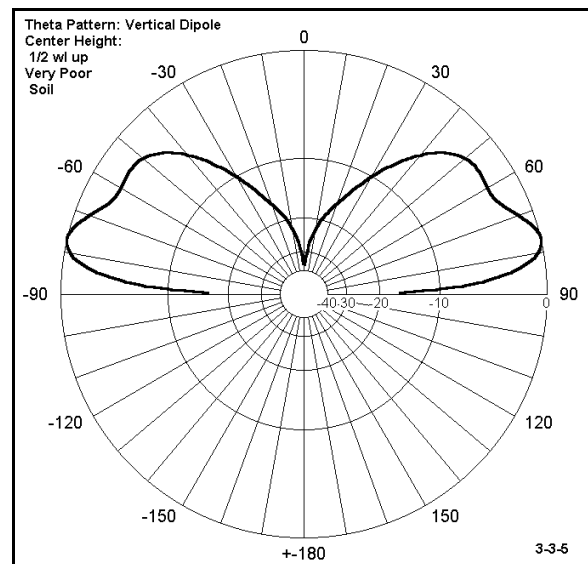
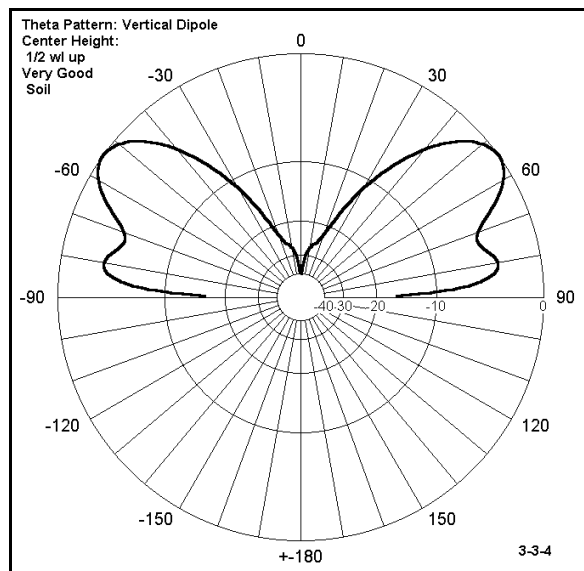
3-3		Test Data		Ex. 9
Soil Description	Gain dBi	TO angle degrees	Source Z (R±jX Ω)	
Salt Water				
Very Good				
Average				
Very Poor				

Comments: Once again, compare your data with the data in the reference table (as a check that you have performed the modeling correctly). As with the antenna at the lower height, the quality of the soil beneath the antenna had little affect upon the source impedance--even less effect with the antenna at some distance above the ground. However, there are major variations in the antenna gain, and the neat progression of values we saw when the antenna was next to the ground has disappeared. In its place

are seeming anomalies.

3-3		Reference Data	Ex. 9
Soil Description	Gain dBi	TO angle degrees	Source Z (R±jX Ω)
Salt Water	5.55	04	73.5 - j 0.4
Very Good	3.29	35	73.3 - j 0.5
Average	2.18	36	73.1 - j 0.4
Very Poor	3.09	13	72.9 - j 0.3

The variations in the angle of maximum radiation are a function of the double lobe present in the elevation patterns for this height. Over very good and average soil, the upper lobe dominates, as shown in **Figure 3-3-4**. **Figure 3-3-5**, the elevation pattern for very poor soil shows the lower lobe to dominate. The domination gives the antenna, when over very poor soil, a higher gain with a lower angle of maximum radiation.



The lesson in this pair of exercises is never to presume that a progression that appears across a set of variables in one set of model runs automatically carries over to seemingly comparable model runs. Always make the runs and see what the data yields.

If vertical antenna behavior holds interest for you, then you will wish to look into the complex relationship between vertically polarized radiation and the properties of ground

material that affect it. Standard references provide detailed information on pseudo-Brewster angles and their relationship to ground conductivity and dielectric constant, as well as to the frequency of operation.

Exercise Preparation III: Yagi Antenna Comparisons

One very useful function for NEC-2 is comparing the performance of competing antenna designs. So we shall compare two 3-element Yagis, both for the 6-meter amateur radio band (50-54 MHz). This time, however, we shall not copy down data, but study some graphics, first about each antenna individually, and then about the antennas side-by-side.

3-4.NEC: A Wide-Band Yagi

Open 3-4.NEC, the wide-band Yagi file. Notice that the GS card (0.0254) tells us that the dimensions are in inches, something we might intuitively know from the GW card entries once we have enough experience with antenna designs.

The wire entries use the convention of listing element lengths in the X-axis and element spacing in the Y-axis, with the driven element at Y=0. The Z-axis places the antenna at 30' up, but this is only for

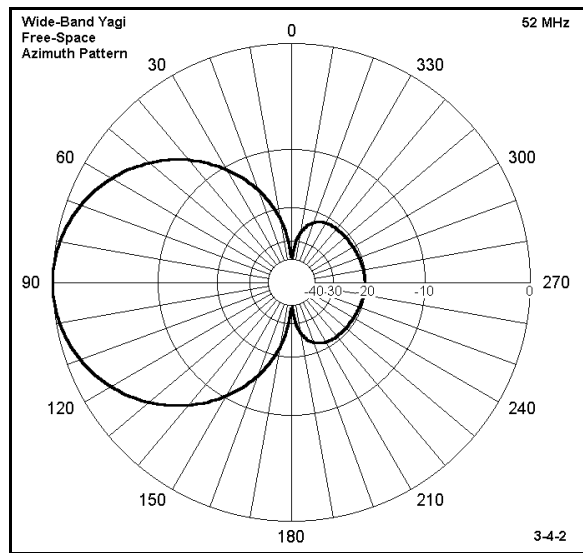
```

CM 6 meter wide band Yagi
CE
GW 1 31 -58.41 -40.69 360 58.41 -40.69 360 .25
GW 2 31 -54.05 0 360 54.05 0 360 .25
GW 3 31 -48.06 32.76 360 48.06 32.76 360 .25
GS 0 0 .02540
GE 0
EX 0 2 16 0 1 0
LD 5 1 1 31 2.4938E7
LD 5 2 1 31 2.4938E7
LD 5 3 1 31 2.4938E7
FR 0 9 0 0 50 .5
RP 0 1 361 1000 90 0 1 1
EN

```

3-4-1

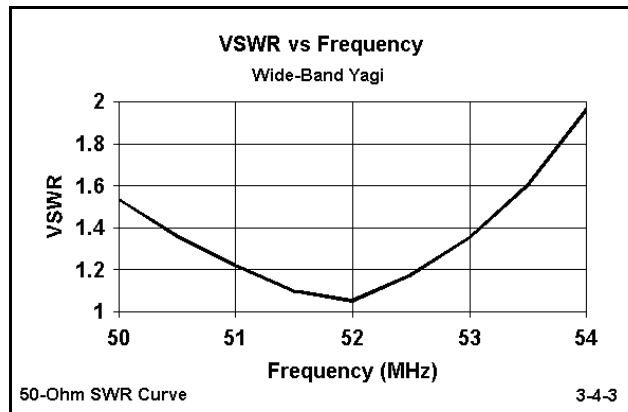
convenience should we wish to model its performance over ground. The absence of a GN card tells us that we shall initially model the antenna in free space. From the LD cards, we learn that the antenna is 6061-T6 aluminum, with half-inch elements indicated by the 0.25 radius entry on the wire lines of the model.



The FR (frequency) card tells us that we shall model the antenna in a frequency sweep from 50 to 54 MHz in 0.5 MHz steps, and we may assume that the design center frequency is 52 MHz. Run the model. Then examine the azimuth patterns for each frequency, using the "Analyze" option to determine the forward gain (in the favored direction) and the front-to-back ratio. Finally, construct a rectangular graph of the 50-Ω SWR for the antenna.

Comments: The azimuth patterns (only the one for the design center frequency is shown in **Figure 3-4-2**) for the antenna at each of the swept frequencies provide a portrait of

performance of this antenna across the amateur 6-meter band. The gain remains relatively consistent over a full 4 MHz, while the front-to-back ratio is reasonably good.



The chief merit of the antenna is its very wide 2:1 SWR operating bandwidth, which accompanies its useful gain and front-to-back ratio characteristics. **Figure 3-4-3** shows that the antenna will exhibit under 2:1 SWR with a 50-Ohm transmission line over the complete band and somewhat below the 50 MHz starting point for the curve. You can determine more exact numbers for the impedance in terms of resistance and reactance from the tabular data.

3-5.NEC: A high-gain Yagi

Before reaching any conclusions about the antenna we have just examined briefly, open file 3-5.NEC. If we examine the model description, we discover many features in common with 3-4.NEC. The antenna is 6061-T6 aluminum and uses 0.5" diameter elements. Like the wide-band model, the antenna has three elements and shares the conventions of placing the element lengths in

```

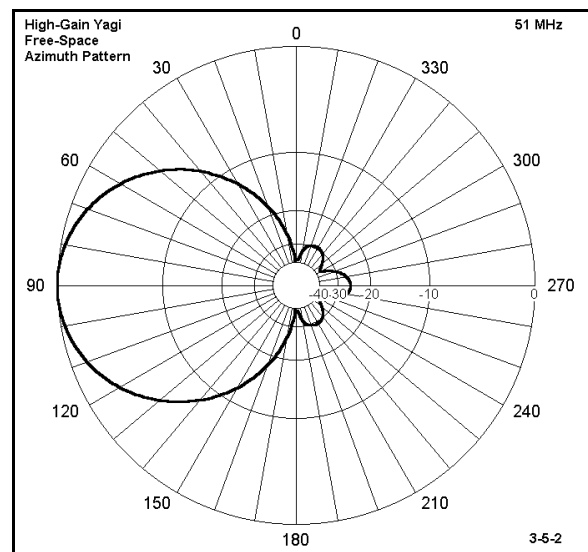
CM 6 meter high gain Yagi
CE
GW 1 31 -57.18 -37.8 360 57.18 -37.8 360 .25
GW 2 31 -54.48 0 360 54.48 0 360 .25
GW 3 31 -51.22 40.14 360 51.22 40.14 360 .25
GS 0 0 .02540
GE 0
EX 0 2 16 0 1 0
LD 5 1 1 31 2.4938E7
LD 5 2 1 31 2.4938E7
LD 5 3 1 31 2.4938E7
FR 0 9 0 0 50 .25
RP 0 1 361 1000 90 0 1 1
EN
    
```

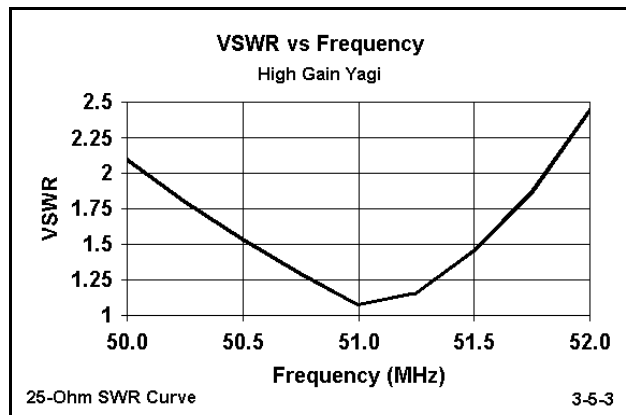
the X-axis, the element spacing in the Y-axis, and placing the driven element at $Y=0$. Also akin to the wide-band Yagi, this design sets the height at 30' (360"), which is not relevant to our immediate purposes, but provides an invitation to modifying the modeling parameters for checking the antenna over real ground.

Since the initial modeling is in free space, the azimuth patterns are at 0° elevation or a zenith angle of 90° . The FR card also indicates a sweep of 9 frequencies, but this time they cover only 50 to 52 MHz in 0.25 MHz steps. The span indicates a probable design center frequency of 51 MHz.

Run the model. Then examine the azimuth patterns for each frequency, using the "Analyze" option to determine the forward gain (in the favored direction) and the front-to-back ratio. Finally, construct a rectangular graph of the SWR for the antenna. However, in this case, first examine the feedpoint impedance data. You will discover that at the design center frequency, the impedance is very close to 25Ω . Therefore, be sure to specify a $25\text{-}\Omega$ VSWR graph.

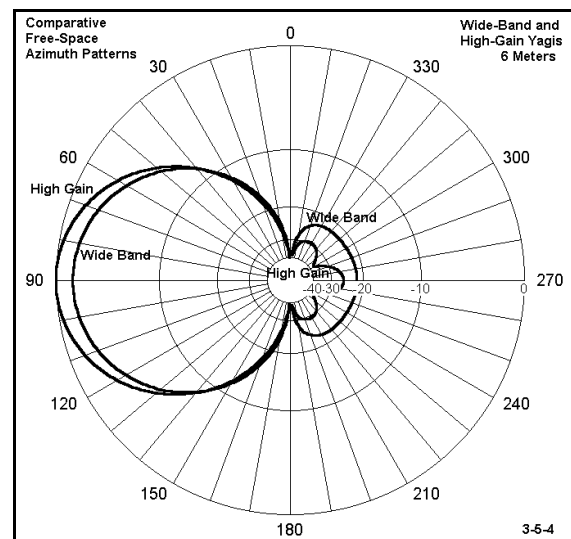
Comments: As shown in **Figure 3-5-2**, at the design center frequency (51 MHz), the high-gain Yagi shows an outstanding pattern for an antenna of its type. The rear lobe consists of three small lobes of very low gain, assuring a very high (>25 dB) front-to-back ratio. Of course, the performance falls off somewhat as one moves up or down from the design frequency. In one direction, gain and front-to-back ratio drop, while in the other, gain increases, but the front-to-back ratio decreases. If you are really curious, you may reset the frequency sweep to cover the entire 6-meter band in order to investigate further alterations in the antenna pattern.





However, for practical operation, this antenna promises less than 2 full MHz of 2:1 SWR operation. Even though the antenna will require a matching network for use with 50- Ω coaxial cable, running the 25- Ω SWR sweep provides an initial indication of the likely 2:1 SWR bandwidth that might be obtained. As shown in **Figure 3-5-3**, the curve exceeds an SWR of 2:1 at about 50.1 and 51.8 MHz.

Although the SWR curves for the two antennas are apt for direct comparison, the azimuth patterns—especially the one shown here without labels and normalized to the outer graphing ring—do not immediately lend themselves to comparison. However, you can import files from one model into another to develop composite patterns. In **Figure 3-5-4**, the azimuth patterns at design frequency are overlaid for a more direct comparison. The superiority in gain and front-to-back ratio of the high gain model at its design frequency are clearly apparent. However, do not hastily conclude that it is the better antenna.



What counts as a better or worse antenna is the match between the properties of the antenna and the function we need it to perform. The high-gain Yagi may be superior for communications work focused in a narrow portion of the band. However, for operations that encompass the entire band, the antenna is not satisfactory, given the degradation of pattern and the difficulty of matching it to common transmission lines across that frequency spread. On the other hand, with less gain, but stable properties, the wide-band Yagi may serve well this latter communications need.

A Special Note on Decimal Values

By this time, you cannot fail to have noticed a wide disparity in the number of decimal places used by various entries in the model descriptions and in the output data reported by the program. We should address two questions about these numbers that seem to violate our early training in "significant digits."

1. Where do the many-placed decimals come from? We often enter data in appropriate rounded numbers, using, for example, 0.5" or 32.0' for English system dimensions. These figures are converted by standard conversion factors within NEC, using the GS entry, to their equivalents in meters. The conversion factors may have more decimal places than are significant for the input data. Similarly, the program may use very long decimals as values for initial entries expressed as AWG wire sizes. Of course, whatever is accessible in a .NEC version of the file can be modified by any ASCII editor.

Output data may also show far more decimal places than will be significant, given a set of input data. Although some data may be displayed using appropriately truncated decimal values, the tabular data available within the NEC output file will show the maximum available number of decimal places. However, the question of how many decimal places may be significant in output data is not solely a function of the input data. It is also a function of the use to which the data will be put.

What good are the many placed decimals in the output data? The answer to this questions depends on the use to which we put the data. Let's contrast just two cases.

Antenna operation: In evaluating the operation of an antenna--or in comparing two competing designs--data requires only a couple of significant digits in most instances. Gain values beyond one decimal place are rarely useful, and the single decimal place may only be useful in sorting cases that might be obscured by excessive numerical rounding. An antenna with a gain of 6.6 dBi might be deemed inferior to one with a gain of 7.4 dBi, although both values would round to 7 dBi. However, it is dubious whether an antenna with a gain of 6.9 dBi is inferior to one with a gain of 7.0 dBi. Front-to-back comparisons are operationally satisfactory in most instances if they are recorded as integers. Source impedance figures recorded as integers (for example, $55 + j15 \Omega$) are as accurate as most operational purposes require. Two significant digits suffice for virtually all VSWR values.

Modeling trends: In some instances, the exploration of the properties of one or more antennas will require us to look systematically at performance trends as we vary one or more model inputs. Antenna dimensions, frequency of operation, height above ground, ground conductivity, and dielectric constant are common variables for these studies. In such cases, we may purposely use more decimal places in our results than are operationally significant. These numerical trends enable us to locate peaks, nulls, and sudden changes in the direction of performance curves more precisely with respect to the model under consideration. In turn, having this data can help us fine tune a design more readily.

Of course, we should not confuse data strings used for analytical purposes with operational expectations of a model converted into a real antenna. Too many variables intervene. Nonetheless, there are appropriate places in which to use operational levels

and numerical progression levels of significant digits. In the exercises in this guide, the recorded figures often exceed operational expectation precision by a wide margin. However, you may truncate these figures with ease. Had we reduced every value to a level appropriate to operational expectations, many curves we shall encounter along the way might well be obscured.

Summing Up

The simple models explored in this chapter have acquainted you with basic concepts and familiarized you with the process of modeling with NEC-2, including working with the input data, running models, and using fundamental output data. Even though you have only begun to explore what you can vary among the input data, you have discovered a wide range of conditions that you can simulate for NEC calculations. In addition, the output data is far richer than the numbers in the examples, but already NEC has yielded a plethora of data.

Throughout the exercises, the chapter has stressed both organized thinking about antennas and methodical modeling of them. Whether we systematically varied the antenna dimensions, materials, height, ground properties, or frequency, the variations multiplied the available output data. These data, in turn, both created patterns of performance and--in a few cases--disrupted patterns we might have presumed to exist. Both are valuable products of modeling exercises, whether guided by this volume, curiosity, or a professional goal.

NEC is not a substitute for a thorough grounding in antenna theory and practice. Rather, it is itself an outgrowth of those fundamentals. Its ability to generate a large body of data quickly and accurately, accompanied by the abilities of programs like NECWin Plus to display the data in a wide variety of tabular and graphical forms, make quick work of what were once days and weeks of tedious hand calculations. This combination makes NEC-2 more than just a tool for design and analysis; it is also a tool for learning more about antennas and deepening our understanding of them. I hope this chapter has uncovered for you at least one fact or idea about antennas with which you were not previously familiar. If not, we still have many chapters and exercises to go.

4. NEC Output Data

***Objectives:** NEC-2 provides a wealth of output data in tabular form which your program can display directly and also translate into other very useful forms. This chapter will acquaint you with the process of gathering and interpreting some of the most basic data involved in antenna evaluation.*

The control cards for NEC--those not involved in the setting of the antenna geometry and which follow the GE card--perform numerous functions. Although there is no strict requirement for the order of these cards, they generally fall into three types:

Type 1: FR GN KH LD

Type 2: EX NT TL

Type 3: CP EN NE NH NX PT RP WG XQ

You have already seen a number of these cards in our simple models. In the Type-1 group, FR is the frequency control card. GN specifies ground conditions. Type 1 cards should usually precede the other types. LD (load) cards will occupy an entire chapter of our work later. Type 2 cards generally come next. You will meet TL (transmission line) and NT (network) cards in their own chapters.

Finally come Type 3 cards. We shall discuss NE and NH (near field) cards in a separate chapter. The most familiar of the group is the RP (radiation pattern request) card. The others cards are sufficiently specialized in use that their application goes beyond our work. However, we can note that NE, NH, RP, and XQ all calculate currents in the antenna geometry, and we can do very little without those calculations.

RP cards fill the requirement for current calculations in NEC. We shall focus in this chapter on their use and what we can do with what they calculate for us. However, we should also warn you in advance that most of our applications are called RP(0): these are simple requests for azimuth and elevation plots of the far field. There are six other options available. RP(1), for example, combines far field and surface wave calculations, but uses a different specification of the pattern from RP(0).

For now, we may concentrate on RP(0) output cards, for there is much to become familiar with, both in setting up the card and in interpreting the output data. **Far fields** are essentially the sky wave fields of the antenna, the ones which, at HF, refract through the ionosphere to permit long-distance radio communications. RP(0) calculations do not

include **surface waves**, those waves traveling close to the surface of the earth. Moreover, only with some reservation can these far fields be interpreted as an accurate indication of the signals in point-to-point (line-of-sight, but without surface waves) communication, so common at VHF and UHF frequencies.

Nonetheless, for antennas used at HF through UHF, far field or sky wave patterns are used as one of the primary ways of characterizing the performance of antennas. Therefore, mastering all of the information these output cards give us, learning how best to implement them, and understanding the operative concepts used in interpreting this data is essential for effective antenna modeling.

Since RP cards produce the tabular data from which programs such as NECWin Plus produce polar plots of antenna patterns, our aim is also to glean the maximum information we can from these patterns--and to understand what that information means.

Exercise Preparation

In this series of exercises, we shall often have occasion to contrast antenna pattern data or plots in order to compare them. Therefore, we shall slightly alter our procedure to subdivide our work into a number of topics, each of which will use one or more of the antenna models on the disk accompanying this guide. Moreover, only some of our work will involve tabulating results. A good bit of it will demand that we carefully inspect and compare graphical representations of data. Therefore, you may wish to store printed patterns with the exercises in this chapter, clipping them to the relevant page, so that you may refer to them in the future.

As always, if the exercise requests that you modify a model and if you wish to save both the original and the modified model, be sure to give each new version a distinct filename.

Patterns and Tables

All of the data that appears in any rectangular or polar graphic produced by the program comes from tabular data produced by NEC-2 and subsequent calculations performed on that data. We have learned that it is possible to print the antenna model description, as well as the source impedance and VSWR information. NECWin Plus can dissect the total NEC output file, making it possible to print a number of useful tables. (At the end of each entry, the notation RG means that the data is also available in a rectangular graph, while the notation PG indicates that it is available in a polar plot.)

1. **The NEC output file:** this complete record of the antenna geometry, calculated

currents, far field data, and supplementary information can be very long, even for simple antennas.

2. **Power gains vs. angle:** This is the basic data for generating far field plots and also includes vertically and horizontally polarized components of the total far field data. (RG, PG)

3. **Electric field vs. angle:** Both magnitude (in Volts/m) and phase angle for electric fields are available for vertical (theta) and horizontal (phi) angles. (RG, PG) Note: In NECWin Plus, both power gain and electrical field data appear in a single Radiation Pattern table entry.

4. **Currents:** Current magnitudes and phase angles (or real and imaginary values) are available for each segment on an antenna. (RG)

4-1.NEC: A 40-meter wire dipole

In order to familiarize yourself with the tabular data and its correlation to graphical outputs, open file 4-1.NEC. This 40-meter (7.05 MHz) dipole has minimal construction (11 segments of #14 AWG copper wire) to minimize the segmentation and currents tables. It is over ground ("real" or reflection coefficient ground, GN(0)) and makes two radiation pattern (RP) requests, one for a theta or zenith pattern, the other for a phi or azimuth pattern. However, the theta pattern uses a step size of 10° and the phi pattern uses a step size of 30°. Both larger-than-normal steps are to reduce sizes of the respective pattern tables for this first intensive look.

```

CM 40-meter dipole: table test
CE
GW 1 11 -34 0 70 34 0 70 .00337
GS 0 0 .3048
GE 1
GN 0 0 0 0 13 .005
EX 0 1 6 0 1 0
LD 5 1 1 11 5.8001E7
FR 0 1 0 0 7.05 1
RP 0 19 1 1000 -90 90 10 1
RP 0 1 13 1000 62 0 1 30
EN

```

4-1-1

Run the file and examine the following tables: NEC output file, VSWR vs. frequency, Power gain vs. angle, Electric fields vs. angle, Input impedance, and Currents. In addition, call up each of the polar patterns and examine them. Compare the positions of points on the polar plots with entries in the Power gain columns in the Radiation Pattern table.

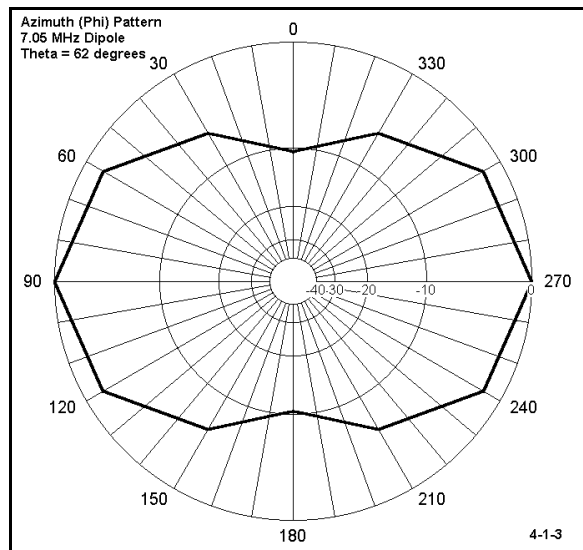
Comments: The NEC output file, although large for even this minimized example, provides a good view of the order of calculations performed by the core. Each calculation set is preceded by the identification of the cards used for the work, without repeating card identification for those previously recorded. Notice that there is data in this file no where

else identified, namely, the power budget, which also provides a measure of antenna efficiency in terms of power radiated vs. power lost as heat.

At this point in our work, the electric fields and the currents tables are largely matters of interest with respect to the form and the data they contain. If you have not previously been aware of the current magnitudes and phases along a linear antenna element, note especially the continuous change of current phase down the wire. The VSWR and Input impedance tables are short, but contain vital information for virtually all modeling efforts.

Before moving onward, you may wish to compare the sizes of these tables--especially the NEC output file--with those you might not yet have deleted for previous models. As a graphic illustration of the size that tables can reach, reopen and look at the NEC output files for models 3-4.NEC and 3-5.NEC from the last chapter.

The Power gain table actually offers two different tables, one for each radiation pattern. Only the phi or azimuth pattern appears in **Figure 4-1-2**. We shall look closely at both polar pattern plots.



4-1-2

- POWER GAINS -			
PHI DEGREES	VERT. DB	HOR. DB	TOTAL DB
0.00	-3.62	-999.99	-3.62
30.00	-4.47	-0.03	1.30
60.00	-8.45	5.53	5.70
90.00	-999.99	7.16	7.16
120.00	-8.45	5.53	5.70
150.00	-4.47	-0.03	1.30
180.00	-3.62	-999.99	-3.62
210.00	-4.47	-0.03	1.30
240.00	-8.45	5.53	5.70
270.00	-999.99	7.16	7.16
300.00	-8.45	5.53	5.70
330.00	-4.47	-0.03	1.30
360.00	-3.62	-999.99	-3.62

The polar plot of the phi pattern in **Figure 4-1-3** corresponds to the total field values in **4-1-2**. Remember that the shape is arbitrarily angular due to the 30° steps in the plot. (However, every smooth curve in polar plots of antenna models is illusory, since each data

point connects to the next with a straight line.) If you examine the theta plot, you will discover no line between the $\pm 80^\circ$ points and the base line. Now examine the tabular values for $\pm 90^\circ$: their values are too low to be recorded on the plot, and therefore, there can be no line to them. This fact will be true of every theta plot over real ground (either S-N or "fast"), although it may not be evident when the step is 1° or less.

Radiation Polarization

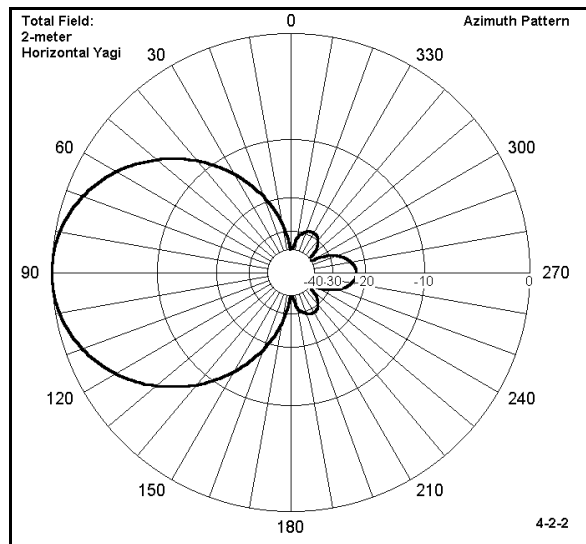
The table in **Figure 4-1-2** showed entries that we overlooked: the horizontal and vertical components of the total field pattern shown in **Figure 4-1-3**. In fact, we could have plotted them. However, since we know that we have a horizontally polarized dipole antenna, they would have added little, if anything, to our understanding of the antenna. This conclusion, however, is far from universal. Often, the tabular values and polar plots of these components provide important information. For example, suppose we wanted directional gain to receive vertically polarized signals over a modest beamwidth--say about 65° between -3 dB points. We shall examine 3 candidates for the task.

4-2.NEC: A 3-element 2-meter horizontal Yagi

Our first candidate is a horizontally oriented 3-element Yagi, as described in **Figure 4-2-1**. Like all the other antennas in this polarization exercise, the antenna is 30' over average soil, and the take-off angle is 3° above the horizon (and 87° zenith angle). Run this antenna and generate the indicated phi or azimuth pattern.

```

CM 2-m 3-element Yagi: horizontal
CE
GW 1 23 -19.86 0 360 19.86 0 360 .125
GW 2 23 -19.02 12.18 360 19.02 12.18 360 .125
GW 3 23 -17.94 26.256 360 17.94 26.256 360 .125
GS 0 0 .02540
GE 1
GN 2 0 0 0 13 .005 0 0 0 0
EX 0 2 12 0 1 0
LD 5 1 1 23 2.4938E7
LD 5 2 1 23 2.4938E7
LD 5 3 1 23 2.4938E7
FR 0 1 0 0 146 0
RP 0 1 361 1000 87 0 1 1
EN
    
```



Comments: The antenna shows a forward gain (as reported by the "Analysis" function available when viewing the pattern and also available in the tabular data) of over 14 dBi with a front-to-back ratio of over 22 dB, within a desirable 62° beamwidth. These properties show up in **Figure 4-2-2**. What does not show is the fact that virtually all of the radiation is horizontally polarized. If you generate the horizontal and vertical component patterns for this antenna, the horizontal will overlay the total field just about exactly, while the vertical will not show at all. Thus, the antenna will be cross-polarized,

with the signals to be received resulting in significant losses. You may use whatever sources you have to calculate or estimate the losses incurred due to cross-polarization. Perhaps we should examine another candidate.

4-3.NEC: A 3-element 2-meter vertical Yagi

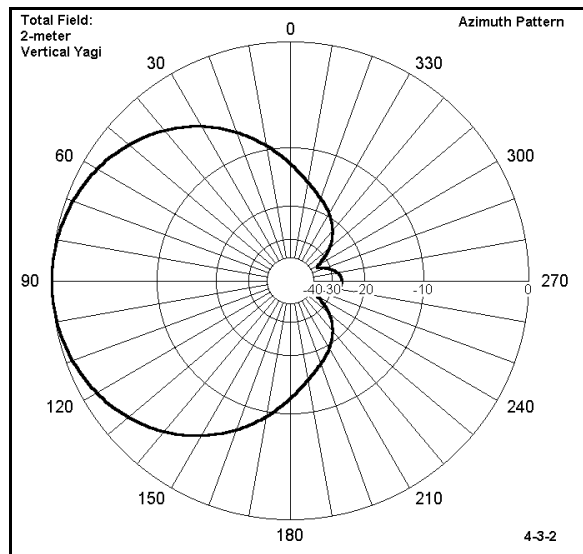
Open 4-3.NEC, which is essentially the same Yagi oriented vertically. The description appears on the next page in **Figure 4-3-1**. Like its horizontally oriented counterpart, the elements are 0.25" 6061-T6 aluminum, and the beam foot print is about 40" wide (element-tip-to-element-tip) by a little over 25" from front to back. Run this model and generate the indicated azimuth pattern, looking first only at the total pattern and then adding in the vertical and horizontal components.

```

CM 2-m 3-element Yagi: vertical
CE
GW 1 13 0 0 340.14 0 0 379.86 .125
GW 2 13 0 12.18 340.98 0 12.18 379.02 .125
GW 3 13 0 26.256 342.06 0 25.256 377.94 .125
GS 0 0 .02540
GE 1
GN 2 0 0 0 13 .005 0 0 0 0
EX 0 2 7 0 1 0
LD 5 1 1 13 2.4938E7
LD 5 2 1 13 2.4938E7
LD 5 3 1 13 2.4938E7
FR 0 1 0 0 146 0
RP 0 1 361 1000 87 0 1 1
EN

```

4-3-1



half square

Comments: As the pattern in **Figure 4-3-2** reveals, the antenna has a gain of nearly 13 dBi with a very high front-to-back ratio. (Consult either the "Analysis" function from the options on the pattern screen or the tabular data.) By generating the vertical and horizontal components to the pattern, we can discover that the antenna is vertically polarized, exactly what we wanted. Still, the -3 dB beamwidth is much wider than we specified, about 96° side-to-side. The results so far indicate that we may not be able to find what we have specified. However, we have one more candidate to check out.

4-4.NEC: A 2-element 2-meter parasitic

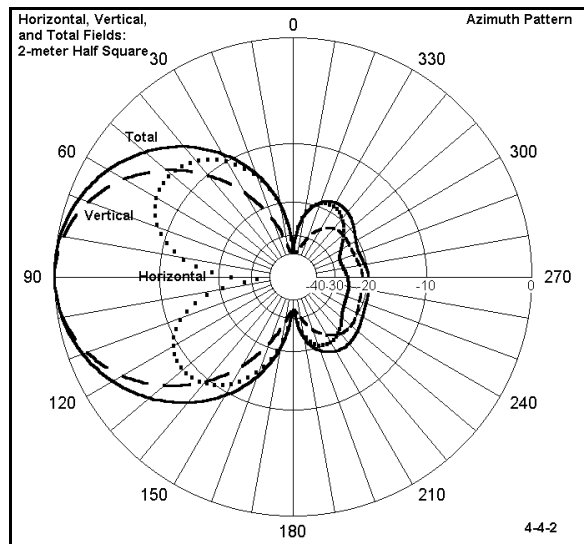
Open file 4-4.NEC. Our final test case is a 2-element half square. Each half square operates as a pair of phased verticals, with the horizontal member acting as the phasing line. By adjusting the lengths of the vertical portions of two half square elements and the spacing between the elements, one can obtain a directional beam. **Figure 4-4-1** describes the model, which you should view in Necvu. This model uses 0.25" 6061-T6 aluminum throughout. Note the feedpoint very near one corner of the driven element. The half square beam is 3-dimensional rather than planar. However, it only requires about 12.5" from back to front.

```

CM 2-m parasitic half square
CE
GW 1 11 -20 0 381.9 -20 0 360 .125
GW 2 22 -20 0 360 20 0 360 .125
GW 3 11 20 0 360 20 0 381.9 .125
GW 4 11 -20 12.5 380.3 -20 12.5 360 .125
GW 5 22 -20 12.5 360 20 12.5 360 .125
GW 6 11 20 12.5 360 20 12.5 380.3 .125
GS 0 0 .02540
GE 1
GN 2 0 0 0 13 .005 0 0 0 0
EX 0 4 11 0 1 0
LD 5 1 1 11 2.4938E7
LD 5 2 1 22 2.4938E7
LD 5 3 1 11 2.4938E7
LD 5 4 1 11 2.4938E7
LD 5 5 1 22 2.4938E7
LD 5 6 1 11 2.4938E7
FR 0 1 0 0 146 0
RP 0 1 361 1000 87 0 1 1
EN
    
```

4-4-1

Run this model and then initially generate only a total field azimuth pattern for it. After examining the total field and comparing it to the Yagi patterns, generate the azimuth pattern once more, this time adding the vertical and horizontal components.



Comments: You will note that the total-field pattern shape resembles that of the horizontally oriented Yagi and in fact has a -3 dB beamwidth of 70 degrees. Check its forward gain by the usual means. But, total field patterns do not tell everything.

Figure 4-4-2 shows the total field along with the vertical and horizontal components. Notice the relatively stronger vertically polarized field compared to the horizontal field. Also notice that the vertically polarized portion of the field has a narrower beamwidth than the total pattern. Although these facts alone do not make a final decision in antenna selection, it is clear that examining the total

field components has added to our understanding of the anticipated performance from the half square beam.

Take-Off and Other Angles of Interest

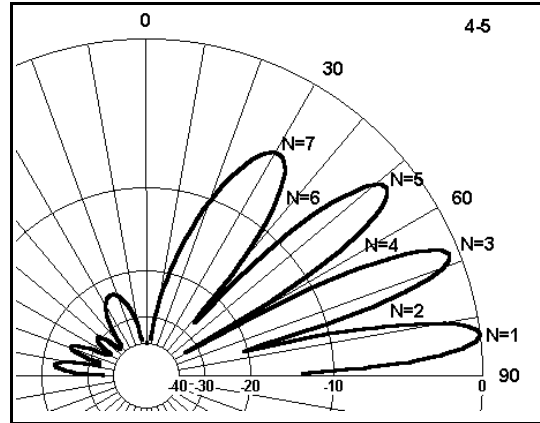
The vertical angle of maximum radiation, that is where the radiation is the strongest, has been dubbed the **Take-Off Angle (TO)**. It is a useful concept when no other overriding elevation angle is present. For example, the forward gain of many beam antennas is

specified relative to the take-off angle of the first (lowest) vertical lobe above ground, which over real ground is normally the strongest. However, the TO angle is sometimes used to mean simply the vertical angle of strongest radiation, regardless of the lobe count from the ground up.

The angle for any lobe of a horizontally-oriented antenna can be estimated from the simple equation

$$A_{LN} = \arcsin \frac{N}{4h} \quad 1$$

where A_{LN} is the angle of the lobe or null above the horizon and h is the antenna height in wavelengths or fractions thereof. As shown in **Figure 4-5**, odd values of N represent lobes (points of maximum radiation) while even values of N represent nulls (points of minimum radiation). Hence, if $N=3$, the lobe in question is the second above the horizon.



We may also define any vertical angle of interest in our modeling of particular antennas. If we have an application in mind that involves some particular angle for outgoing or incoming fields, then that angle of interest will override the TO angle. For example, some particular skip path on 80 meters might have an angle of 17° above the horizon. The task at hand may well be to evaluate the performance of antennas at this angle rather than with respect to their TO angles.

4-5.NEC: An 80-meter dipole

Open file 4-5.NEC. This common wire dipole is 15.25 m (about 50') above ground. Notice that there are 2 RP cards: one requests a theta plot along the azimuth axis of maximum gain; the second requests an azimuth pattern at a zenith angle of 73° (elevation angle of 17°). Note that even though we request an elevation angle of 17° , the .NEC file will show this as the corresponding theta angle. Run the model and produce the indicated patterns, printing copies for comparison with the next model.

```
CM 3.6 MHz dipole
CE
GW 1 37 -20.11 0 15.25 20.11 0 15.25 .0010265
GS 0 0 1
GE 1
GN 2 0 0 0 13 .005 0 0 0 0
EX 0 1 19 0 1 0
LD 5 1 1 37 5.8001E7
FR 0 1 0 0 3.6 0
RP 0 181 1 1000 -90 90 1 1
RP 0 1 360 1000 73 0 1 1
EN
```

4-5-1

Comments: The dipole shows above 6 dBi gain, but mainly at very high angles relative to the ground. At the angle of interest, the gain is about -1 dBi, or about 7 dB below maximum gain. If the desired signal arrives at an angle of 17° above the horizon, but

interfering signals and noise arrive at higher angles, the ability to communicate may well be seriously degraded.

4-6.NEC: A side-fed rectangle for 80 meters

```

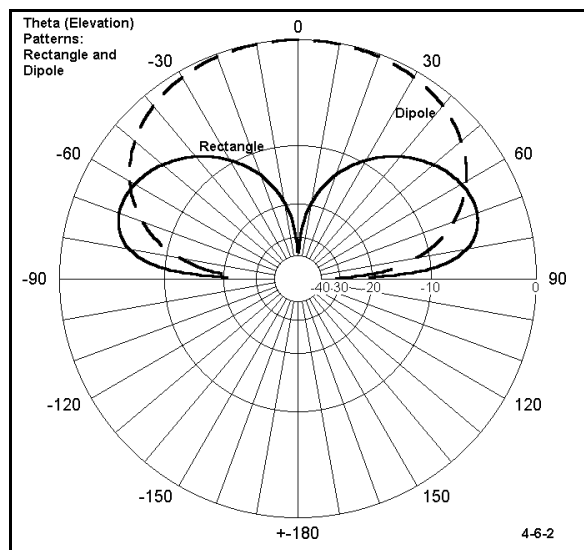
CM 3.6 MHz rectangular loop
CE
GW 1 31 -16.76 0 15.25 16.76 0 15.25 .0010265
GW 2 7 16.76 0 15.25 16.76 0 5.79 .0010265
GW 3 31 16.76 0 5.79 -16.76 0 5.79 .0010265
GW 4 7 -16.76 0 5.79 -16.76 0 15.25 .0010265
GS 0 0 1
GE 1
GN 2 0 0 0 13 .005 0 0 0 0
EX 0 2 4 0 1 0
LD 5 1 1 31 5.8001E7
LD 5 2 1 7 5.8001E7
LD 5 3 1 31 5.8001E7
LD 5 4 1 7 5.8001E7
FR 0 1 0 0 3.6 0
RP 0 181 1 1000 -90 90 1 1
RP 0 1 360 1000 73 0 1 1
EN
    
```

4-6-1

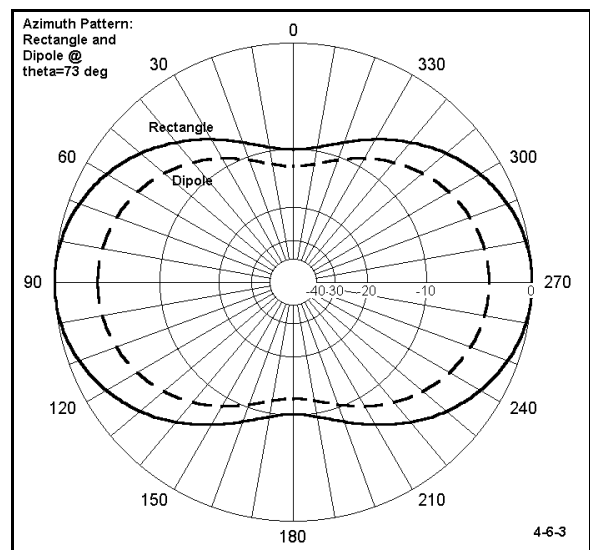
Now open file 4-6.NEC, a side-fed 80-meter rectangle. This particular antenna design produces mostly vertically polarized radiation in a pattern broadside to the antenna. Note the antenna dimensions: the top height is 15.25 m, about the same height as the dipole. The length is considerably less, since the antenna is roughly 1λ in its total perimeter measurement. One aim of the example was to create an antenna that might occupy a similar space to that reserved for the dipole above. If you check the source impedance of this antenna, you will discover it to be quite

low, but there are versions with more desirable source impedance levels. Run this model, producing the indicated patterns to determine the antenna's TO angle.

Comments: The maximum gain of the antenna is low compared to that of the dipole. However, the elevation pattern reveals a low TO angle and a greatly diminished response to high-angle fields. The antenna actually shows more gain than the dipole at the elevation angle of interest (17°). Using the pattern generating feature of NECWin Plus that permits us to combine patterns, we can display the data in the following two polar plots (**Figures 4-6-2 and 4-6-3**).



4-6-2



4-6-3

Despite its higher maximum gain at its TO

angle, the dipole is clearly inferior in performance (in several categories) to the rectangle at the angle of interest. This is but one of many kinds of instances in which an angle of interest will be more important in our analysis of NEC models than the take-off angle.

4-7.NEC: A 40-meter triangular loop at 18 MHz

For antennas operated at their fundamental frequencies, finding the TO angle is normally a simple matter of examining an elevation pattern taken along the horizontal axis of maximum radiation. However, when antennas are operated at other than fundamental frequencies, the problem of accurately locating the TO angle requires a systematic procedure. Open file 4-7.NEC. This is a vertically oriented square loop fed at one corner. The antenna was designed for 7.15 MHz, but is here used at 18.118 MHz. Note that there are two RP cards, one for a theta pattern at an initial phi angle of 90°; the other an azimuth pattern at an arbitrary low zenith angle of 88° (12° elevation). Run the model.

```

CM 1 wl vert loop side
CE
GW 1 17 0 0 10.67 0 0 21.69 .00103
GW 2 17 0 0 21.69 11.02 0 21.69 .00103
GW 3 17 11.02 0 21.69 11.02 0 10.67 .00103
GW 4 17 11.02 0 10.67 0 0 10.67 .00103
GS 0 0 1
GE 1
GN 2 0 0 0 13 .005 0 0 0 0
EX 0 1 1 0 1 0
LD 5 1 1 17 5.8001E7
LD 5 2 1 17 5.8001E7
LD 5 3 1 17 5.8001E7
LD 5 4 1 17 5.8001E7
FR 0 1 0 0 18.118 0
RP 0 181 1 1000 -90 90 1 1
FR 0 1 0 0 18.118 0
RP 0 1 360 1000 88 0 1 1
EN
    
```

4-7-1

Initially generate only the elevation pattern and use the "Analyze" option to determine the angle of maximum radiation in this azimuth heading. Then modify the azimuth pattern so that the elevation angle for it is the value just determined, rather than the initial value. Now generate the azimuth pattern, using the "Analyze" option to determine the azimuth angle of maximum radiation. Now, return to the model and modify the elevation pattern request to use the new azimuth angle of maximum radiation as the azimuth angle. Repeat this process in successive steps until the angles no longer change. Record your progress in the table below.

4-7 Test Data			Reference Data	
Pattern Type	Angle/Type	Max. Rad. Angle/Type	Angle/Type	Max. Rad. Angle/Type
Elevation	90 / Az	/ EI	90 / Az	13 / EI
Azimuth	/ EI	/ Az	13 / EI	62 / Az
Elevation	/ Az	/ EI	62 / Az	14 / EI *
Azimuth	/ EI	/ Az	14 / EI	62 / Az

Notice the repetition of the 62° azimuth angle of maximum radiation. This repetition indicates that the 14° elevation angle of maximum radiation will not change further and that it is the TO angle. (Remember that the tabulated data may show this angle in "zenith" terms as 76.) In case this example is too short and easy, use the same starting point in the chart (an elevation pattern at an azimuth angle of 90°), but change the frequency to 21 MHz.

Azimuth Angles and Ratios: Front, Side, and Back

When speaking about antennas without reference to a particular application, we ordinarily reference maximum gain of the antenna to the TO angle. Hence, a standard sort of azimuth pattern would use the elevation angle at which maximum gain occurs. In free space, of course, this is an elevation angle of 0° (a zenith angle of 90°).

Common HF and VHF antennas tend to be subdivided into three major (but not completely exhaustive) groups:

Omni-directional antennas, such as $1/4\lambda$ and longer verticals;

Bi-directional antennas and arrays, of which the common horizontal dipole is a paradigm; and

Directional antennas and arrays, for which the Yagi models we have used may serve as good examples.

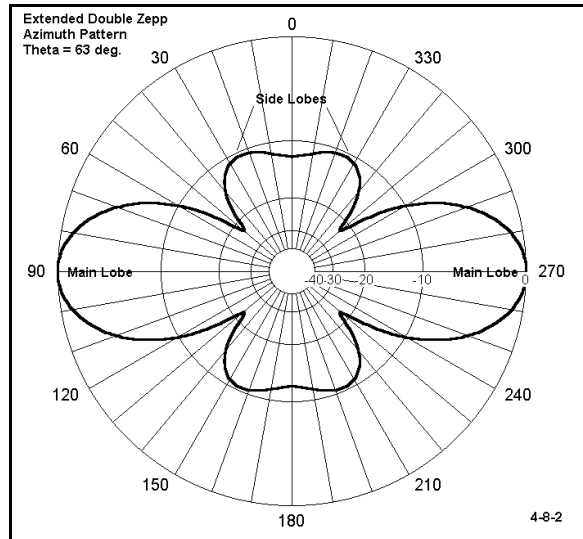
Bi-directional and directional antennas exhibit more gain in some direction or directions than others. Therefore, their standard azimuth patterns will have a **front** (or 2 fronts for a bi-directional antenna) and a **side**, where the side is roughly defined as the azimuth angle 90° from the azimuth or phi angle of maximum radiation (at the TO angle).

4-8.NEC: A 30-meter extended double Zepp

Open file 4-8.NEC. This #14 copper wire extended double Zepp is about 1.25λ at 10.125 MHz. The antenna is center-fed, and exhibits a very high capacitive reactance at the source. However, the antenna has several dB greater gain than a dipole at the same height (in this case, 50' over average soil). Run the model. Generate the maximum gain azimuth pattern (elevation = 27°). In addition, open the Radiation

```
CM Extended double Zepp: 10.125
CE
GW 1 31 -61 0 50 61 0 50 2.67E-03
GS 0 0 .3048
GE 1
GN 2 0 0 0 13 .005 0 0 0 0
EX 0 1 16 0 1 0
LD 5 1 1 31 5.8001E7
FR 0 1 0 0 10.125 0
RP 0 1 361 1000 63 0 1 1
EN
```

Pattern table for the antenna. Locate the total field gain for 0° and 180° (both 90° from the axis of maximum power). Calculate the **front-to-side ratio**. Locate the angle and total field gain of the secondary or **side lobes**. Calculate the **front-to-side-lobe ratio**.



Comments: The front-to-side ratio calculation is straightforward: it is simply the difference in the gains for the main lobe maximum gain figure and the gain figure for each of the two points separated by 90° from maximum gain point. Since either 90° or 270° may be used as the maximum gain point, then either 0° or 180° may be used as the side point. $10.69 \text{ dBi} - (-1.52) \text{ dBi} = 12.21 \text{ dB}$. This figure is the front-to-side ratio.

As roughly indicated in **Figure 4-8-2**, the 4 **side lobes** are located at 24° , 156° , 204° , and 336° . Note that we can classify these added gain maxima as side lobes only because this design features what we are

inclined to call a **main lobe**. Many multi-lobe antenna patterns have only a collection of lobes, with none being sufficiently larger than the others to be called a main lobe; hence, such antennas do not have side lobes.

The gain of each of the side lobes is 0.18 dBi . The front-to-side-lobe ratio is once more the difference between the gain of the main lobe and the maximum gain of the side lobe. $10.69 \text{ dBi} - 0.18 \text{ dBi} = 10.51 \text{ dB}$. The performance estimate of the antenna must take into account not only the existence of side lobes, but the consequences of their strength on how well the antenna will perform in its intended application.

4-9.NEC A 30-meter Moxon rectangle

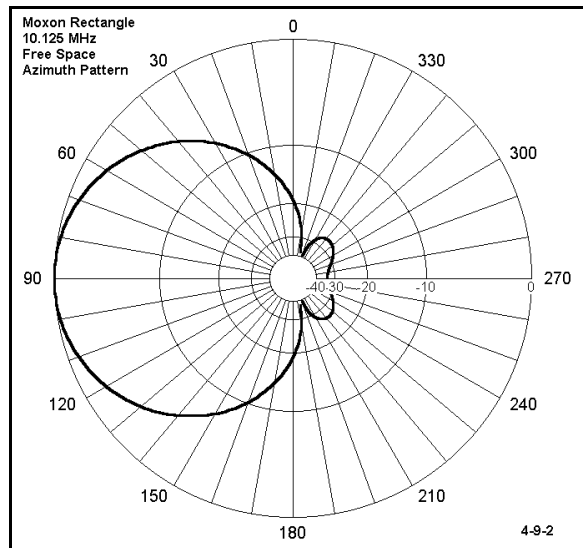
Open file 4-9.NEC. The #14 copper wire antenna is a Moxon rectangle, a parasitic 2-element directional antenna where the driven element and the reflector are folded back toward each other. The spacing between wire ends, the spacing between parallel wires, and the length of the main section all contribute to establishing the performance characteristics of the antenna. This version for 10.125 MHz has moderate gain, excellent front-to-back characteristics, and a source impedance that readily matches with common 50-Ω coaxial cable. (View on Necvu.)

```

CM 30-meter Moxon rectangle
CE
GW 1 9 -17.5 6.8 0 -17.5 0 0 2.67E-03
GW 2 45 -17.5 0 0 17.5 0 0 2.67E-03
GW 3 9 17.5 0 0 17.5 6.8 0 2.67E-03
GW 4 7 -17.5 7.8 0 -17.5 13.4 0 2.67E-03
GW 5 45 -17.5 13.4 0 17.5 13.4 0 2.67E-03
GW 6 7 17.5 13.4 0 17.5 7.8 0 2.67E-03
GS 0 0 .3048
GE 0
EX 0 5 23 0 1 0
LD 5 1 1 9 5.8001E7
LD 5 2 1 45 5.8001E7
LD 5 3 1 9 5.8001E7
LD 5 4 1 7 5.8001E7
LD 5 5 1 45 5.8001E7
LD 5 6 1 7 5.8001E7
FR 0 1 0 0 10.125 0
RP 0 1 361 1000 90 0 1 1
EN
    
```

4-9-1

The model for this antenna is in free space, so the pattern request is an azimuth pattern at an elevation angle of 0°. Run the model and generate the indicated azimuth pattern.



Comments: If you examine the pattern in **Figure 4-9-2** on the next page, you will discover a minor anomaly in our convention of taking front-to-side ratios. The antenna exhibits a very broad **forward lobe** (a term which we can use with directional antennas, but not with bi-directional or omni-directional antennas): about 80° wide between -3 dB points. It forms a cardioidal pattern which still has considerable gain at points 90° from the maximum gain point on the forward lobe. The side minimum gain points are 108° to the rear of the maximum gain point (at 198° and 342° on the azimuth plot).

Now examine the Radiation Pattern table. Locate the total gain figure for either 198° or 342° as well as the maximum gain figure. The difference is about 64 dB. If we use these modified locations as the side points, we see very deep nulls. This is common in free space models, and the nulls become shallower the closer we bring a horizontal antenna toward the ground.

While we have the Radiation Pattern table at hand, notice the region of the plot near the maximum gain point. The antenna shows its maximum gain figure of 5.79 dBi from 89° through 91° on the table. This fact will account for the tiny offset (usually no more than 1

to 2 degrees) in polar plots from the anticipated maximum gain heading. Plotting programs tend to identify the first occurrence of maximum gain as the maximum gain heading.

While we are here, let's use the Moxon rectangle to explore the idea of the **front-to-back ratio**. The rearward portion of the Moxon free space azimuth pattern is diminutive, indicating a high front-to-back ratio. But, how much?

Actually, there are three working notions of front-to-back ratio generally current in antenna work:

180-Degree front-to-back ratio: This ratio is simply the difference in gain between the maximum forward gain angle and another angle 180° opposite. Check the Moxon Radiation Pattern table for the gain at 270°. 5.79 dBi - (-27.57) dBi = 33.36 dB: this is the 180-degree front-to-back ratio. However, notice that the point used to derive this number is "dimpled" and there are places in the rear quadrant where the ratio is much less.

Worst-case front-to-back ratio: This ratio uses the maximum gain anywhere in the rear quadrant as the basis for establishing the ratio. In some circles, the side points, as defined by the 90° angle from the maximum forward gain heading, determine where the rear quadrant begins. Since the gain at these side points is -13.40 dBi, the worst-case front-to-back ratio would be 19.49 dB. If we use the modified rear quadrant--the area beyond the maximum side nulls--then the gain maxima occur at 224° and 342°: -20.35 dBi. 5.79 - (-20.35) dBi = 26.14 dB: this is our modified worst-case front-to-back ratio, which many automated graphing systems cannot identify. In such cases, we must rely upon tabular data.

Notice the difference between the two front-to-back figures: 7.22 dB. This is a significant differential in performance expectation from the antenna. (Very often, folks forget to specify how they derived their front-to-back figures, which can create some confusion.)

Front-to-rear ratio: To overcome misleading aspects of both 180-degree and worst-case front-to-back ratios, some engineers have adopted the front-to-rear ratio. This ratio is based on averaging the power gain of the antenna over the rear quadrant and using the resulting figure as the basis for a ratio with the forward gain. There is no general standard on exactly how many data points to use or where to locate them. However, let's calculate a sample front-to-rear ratio for the Moxon rectangle, beginning beyond the points of maximum null.

4-8 Test Data		Reference
Azimuth Angle	Gain dBi	Gain dBi
200		- 36.79
210		- 23.01
220		- 20.52
230		- 20.68
240		- 22.40
250		- 24.97
260		- 27.00
270		- 27.57
Total		-202.94
Average gain		- 25.37
Front-to-rear ratio (5.79 - average)		31.16 dB

The final figure would differ had we used more data points. Moreover, simple averaging over a single (modified) quadrant is not the only way to reach a usable mean value. However, it does illustrate the principle behind taking a front-to-rear ratio and the intermediate value that emerges. The Moxon rectangle's double rear lobe pattern is, of course, only one of many possible. We have already seen models of antennas displaying single rear lobes and others showing triple lobe rear areas. Incipient nulls may result in a bell-shaped rear lobe. Very long Yagis for VHF often show ragged edges (on the forward and the rear lobes, especially at angles approaching the side points).

Vertical Angle Resolution

It is easy to become comfortable using certain values within an antenna modeling program. If the results look plausible, then we presume they are correct. The end result can be a serious distortion of the actual situation with antennas. Proper interpretation of antenna behavior from models requires that we ask the right questions, including requesting the correct outputs. Therefore, it is unwise to simply use some standard values without some thought about whether you will in the end derive the right conclusions about the antenna in question.

One such arena is the resolution we choose for developing zenith patterns for antennas as we increase both frequency and height (or, more simply, height in terms of wavelengths). As we increase height, the number of vertical lobes will increase accordingly. At VHF and above, the standard resolution we use at HF may not catch them all.

4-10.NEC: A 2-meter 3-element Yagi

Open file 4-10.NEC. Examine certain aspects of the description, especially the antenna height and the resolution requested for the theta plot in the RP card. The initial height is 6 meters up. The resolution requested is 1 degree. (Of course, examine the other features of this 5 mm diameter 6061-T6 aluminum element antenna for 144.5 MHz, but do not lose sight of our focus.)

```

CM 2 meter high gain Yagi
CE
GW 1 31 -.5126 0 6 .5126 0 6 .0025
GW 2 31 -.4884 .38887 6 .4884 .38887 6 .0025
GW 3 31 -.4591 .69871 6 .45917 .69871 6 .0025
GS 0 0 1
GE 1
GN 2 0 0 0 13 .005 0 0 0 0
EX 0 2 16 0 1 0
LD 5 1 1 31 2.4938E7
LD 5 2 1 31 2.4938E7
LD 5 3 1 31 2.4938E7
FR 0 1 0 0 144.5 0
RP 0 181 1 1000 -90 90 1 1
EN

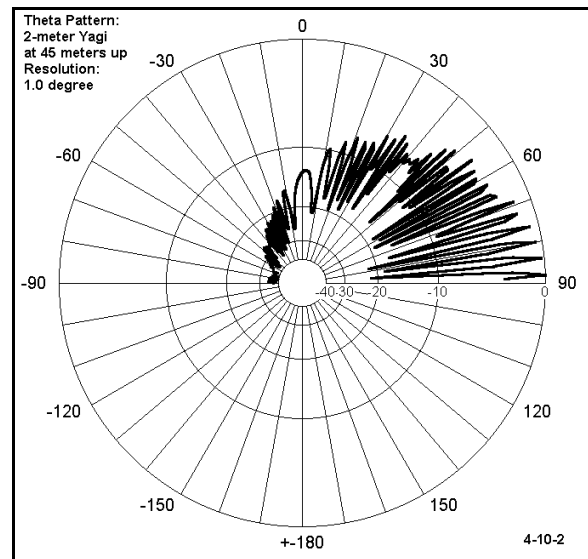
```

4-10-1

Run the model and examine the elevation plot. Notice the relatively smooth curves at the high-gain tips of the lobes, which you can confirm by examining the tabular data under Radiation Pattern. At a height of about 3λ , the resolution is adequate to portray accurately the antenna radiation field properties in the vertical plane.

Modification 1: Now revise the model (saving it under a modified name, if you wish to preserve the original model). Change the height or Z-axis settings to 45 meters. Now rerun the model.

Comments: The analysis that accompanies the graph seems plausible, identifying the lowest lobe at 2° elevation. The Radiation Pattern table seems to confirm the figures: 13.88 dBi gain at 88°. However, examine closely the tips of the lobes in **Figure 4-10-2** (on the next page), and compare them with the tabular data. The rate of change of the values yields sharply pointed graphical tips. This appearance should make us suspicious that we have not provided sufficient resolution to the data to let it tell a true story about the vertical lobe structure of the radiated field.



Modification 2: Revise the model once more by changing the step size for the output to 0.1°. Now rerun the model. Generate the indicated elevation plot and consult the Radiation Pattern table.

Comments: Notice immediately the increase in the number of lobes--too many for adequate reproduction here. At this point, return to the tabular data, looking at just the last 2 degrees (88-90). Of great interest is the fact that within these last 2 degrees are more than one lobe. The TO angle is 0.7° with a gain of 13.91 dBi.

Scan the values surrounding the TO angle. The gain figure for two readings each side of the main one go this way: 12.45, 13.46, 13.91, 13.87, 13.31. These values change slowly enough to give you confidence that you have captured the actual lobe structure and not a mathematical illusion. If you wish to see some consequences of such mathematical illusions, return the resolution to 1.0° and raise the antenna beyond 60 meters in height. Run the model, generate the elevation plot, and view the shrinkage of the lowest lobes from their actual values.

Although our modified model required 0.1° resolution for the elevation plot, 1.0° is sufficient for the azimuth plot. The antenna pattern in this dimension is quite smooth, and excessive resolution can be wasteful of time and computer memory resources. Nonetheless, be wary of all sharply pointed lobes on pattern plots. Examine the tabular data to ensure appropriate rates of value change. Whenever the issue is in doubt, try a finer resolution. Not all cases will require a 10:1 shift. Some doubts may be clear up by trying 0.5° to check the rate of change of the data.

Summing Up

Requesting, confirming, and interpreting NEC output data is the other side of the coin, relative to constructing good models from which to derive the data. Even the most fundamental of the output request cards, RP(0), provides a wealth of information about the antenna under test, if we know how to obtain the information and to translate it into a set of correctly formed statements and graphics. The radiation pattern request provides data on the total field and its polarized components as well as the vertical and horizontal angles of maximum and minimum radiation. From this basic data, we can derive measures of performance, such as gain, take-off angle, and a number of ratios relevant to bi-directional and directional arrays.

As with all antenna data, performance claims gain their sense only by reference to the intended application(s). Making those claims involves mastery of a number of parametric concepts commonly used in the study and evaluation of antennas. In short, antenna modeling does not take place in abstraction, but as one significant element in the overall study of antennas.

One last question deserves attention: why does antenna modeling use **dBi** rather than some other measure of power gain? Every measure in decibels, or dB, is ultimately a relative power measurement (with some defined relative voltage and current measures having been derived from the basic power measure). As a relative measure of power, the decibel is defined this way:

$$\text{Power Gain}_{ab} = 10 \log \frac{P_1}{P_2} \quad 2$$

where P_1 and P_2 are two power levels measured in the same units (e.g., watts). Since we may pick any two powers for P_1 and P_2 , power gain or loss is strictly relative.

However, we have found it useful to select--for specific purposes--certain baseline power levels. One such level is whatever power there might be in the far field of an isotropic radiator. An isotropic radiator is a lossless dimensionless point in free space that radiates (or receives radiation) equally well in all directions.

One of the chief advantages of the isotropic radiator is that its field never changes. Thus, it functions as an agreed upon constant against which every antenna may be measured in every direction. Every antenna measurement referenced to a P_2 that is the far field power from an isotropic radiator has a positive or negative gain in dBi. We can compare antenna gain figures from 2 or more antennas or at different points on the radiation pattern of a single antenna by citing the individual gain values in dBi and then comparing numbers.

Other standards exist and have their uses. Most apply to certain types of antennas or to certain types of antenna applications and testing procedures. However, dBi remains the

most universal of them--and the one in which all NEC gain figures are expressed.

User Notes

5. Careful Model Construction

Objectives: *Since hasty and careless modeling usually produces questionable output data, the exercises in this chapter will familiarize you with some basic guidelines for developing reliable models. It will also demonstrate some of the pitfalls of careless modeling in a series of comparative models.*

In our work to this point, we have surveyed two major perspectives on antenna modeling. First, we have developed our abilities to extract--from even the most fundamental forms and techniques of modeling--a wealth of information about the antennas in each exercise. In fact, going back to models in earlier exercises for which we produced only limited information, and running them through the range of possibilities in Chapter 3 and the range of available output data in Chapter 4, would be a worthy supplementary exercise set. Our sense of growing mastery of using NEC productively can, however, obscure the second perspective on antenna modeling.

The second perspective has been our insistence upon using very careful procedures in the construction of individual antenna models. We must ensure that they accurately reflect the physical structure of the antenna and that they meet the requirements and fall within the boundaries of the NEC-2 calculation core. Achieving this goal requires that we continually develop our understanding and appreciation of both antenna theory and how NEC-2 works.

In this guide, we shall not review the details either of antenna theory or of NEC-2 theory. Instead, we shall develop a series of modeling guidelines and suggestions that will permit you to avoid most of the common pitfalls in model construction. (Nonetheless, you are encouraged to develop your understanding of the theoretical foundations of NEC-2 in your extended reading.)

Whereas Chapter 2 concentrated on modeling correctly, this set of exercises will focus on modeling carefully. We need to use extra care only in those areas where we might be prone to carelessness. Since the tendency to carelessness has something of a random factor involved, our efforts here cannot be quite so orderly and progressive as it has been so far. Nonetheless, from the work of this chapter will emerge a number of practical precepts and practices that should have a permanent place in all future modeling efforts.

The guidelines correspond to snares into which almost all modelers have fallen at one

time or another. Common problems result from jumping to conclusions about a model in question; others arise from a desire for convenience of model structuring; still others spring from failures to observe details. Our sampling will not in any way be complete. However, the exercises should kindle two tendencies in your further work.

The first tendency is to learn from your mistakes--and you will make them in the same way that all modelers to this point in time have made them. Mistakes, errors, blunders, and howlers are all fields for interrogation. Ask yourself what is the source of the error and how may the error be prevented in further work. The second tendency you should develop is larger in scope. Develop reasonably reliable guidelines for modeling that do not let the errors arise in the first place.

In these exercises, we shall look at some common problems which past modelers have created for themselves and examine some guidelines that will help you avoid them. However, antenna modeling--in the contemporary sense of using massive mathematical programs to elicit a wide range of predictive performance characteristics of a large assortment of antenna types--is still in its youth. There is ample time for you to find brand new snarls and snares, and ample time as well for you to develop further guidelines or further refinements on existing guidelines.

Exercise Preparation

In these exercises, we shall do some extensive comparison of model pairs, one of which commits a modeling misdemeanor and the other of which displays the guideline which would have prevented the problem. Therefore, models will tend to have filenames slightly different than those used so far. Wherever we call for a matched pair of models, we shall name them "-1.NEC" and "-2.NEC." For example, our first pair will be 5-1-1.NEC and 5-1-2.NEC. If you save variants, alter the name without losing the ability to associate the variant with its origins.

In each case, we shall be looking for problems and guidelines to prevent problems. Be certain to commit to memory more of the solution than the problem. Throughout these exercises we shall make use of both tabular and graphical data outputs for problem detection and solution identification. In some cases, one form of output data will be superior to the other, while in other cases, either will do as well as the other. Part of the aim of these exercises, then, is to give you a sense of when it is profitable to use each kind of output report. Indeed, one of the hazards of highly graphical modeling programs is that they can lead us to forget the wealth of tabular information at our disposal.

We have already seen at the end of the last set of exercises an example involving a potential misidentification of a take-off angle, a difficulty that examination of tabular data allowed us to detect and correct. You may consider that exercise as the first one in this

set. Review the problem and its solution method before you undertake these new exercises.

5-1-1.NEC & 5-1-2.NEC: A multi-band doublet

A common antenna among amateur radio operators is a wire multi-band doublet. Open file 5-1-1.NEC, the description for which appears in **Figure 5-1-1**. Note the salient features of the model. The copper #14 wire is 134' long at a 60' height. The antenna is center-fed. The wire is about $1/2\lambda$ long and uses 11 segments in the model. The model requests a single elevation pattern with the azimuth angle set at 90° , the anticipated axis of maximum radiation. The ground is of the reflection coefficient or fast) type with a conductivity of 0.005 S/m and a dielectric constant of 13.

```

CM 134' multiband doublet
CE
GW 1 11 -67 0 60 67 0 60 .00267
GS 0 0 .3048
GE 1
GN 0 0 0 0 13 .005
EX 0 1 6 0 1 0
LD 5 1 1 11 5.8001E7
FR 0 1 0 0 3.7 1
RP 0 181 1 1000 -90 90 1 1
EN

```

5-1-1

In a moment, we shall want to run this model at the assigned frequency of 3.7 MHz. We shall be interested in the source impedance, to be read from the tabular data, and in the maximum gain, along with the elevation angle at which it occurs. However, we also want to operate the antenna at 28.0 MHz. Therefore, after you make the 3.7 MHz run, modify the model for a run at 28.0 MHz. Record your readings in the table below.

5-1-1 Test Data			
Frequency Mhz	Source Z (R±jX Ω)	Gain dBi	Elevation Angle
3.7			
28.0			

Comments: The most common practice, borne of haste, would be to change only the operating frequency of the antenna--from 3.7 to 28 MHz. Had you done only this, your data would look like the reference table below.

5-1-1 Reference Data			
Frequency Mhz	Source Z (R±jX Ω)	Gain dBi	Elevation Angle
3.7	91.9 + j 85.8	6.31	72
28.0	335.3 + j 964.0	-17.48	8

If your data looks like the reference table data, then you fell into at least two traps of hasty model revision.

Guideline 1: Use adequate segmentation for the frequency and element length.

The original model used 11 segments for a $1/2\lambda$ antenna at its approximate resonant frequency. For simple wire antennas, this degree of segmentation is considered adequate. (In the next set of exercises, we shall look more closely at the question of adequate segmentation and how to determine it.) When the frequency was raised by a factor of about 8 to 28 MHz, that antenna became about 8 half-wavelengths long. At 11 segments per half-wavelength, the required number would have been about 88. Since we wish to feed the antenna at the same center point, we should raise that number by 1 to 89.

Guideline 2: Ensure that the feedpoint is where you want it.

Had you raised the number of segments in the NECWin Plus model to somewhere near 89, your source would have remained on segment 6 (the center of the 11 segment model). This would have provided erroneous data relative to the model you intended to make. Hence, you should have revisited the source dialog box after resegmentation to move the source to the proper segment, in this case #45.

Guideline 3: Determine the correct azimuth angle for an elevation plot or the correct elevation angle for an azimuth plot.

The pattern for a 134' wire used at 28 MHz is nothing like the pattern at 3.7 MHz. It consists of many lobes, the strongest of which is not broadside to the wire. Therefore, obtaining a reliable set of values for maximum gain and the associated elevation angle requires location of the correct azimuth angle for the plot, using procedures outlined in the last set of exercises.

Open file 5-1-2.NEC and compare the model description to your own revision of 5-1-1.NEC. They should look very similar to each other. Among the items which might vary are these:

1. The segmentation might vary by ± 5 segments, so long as the 11 segments per $1/2\lambda$ rule for wire antennas is approximated.

```
CM 134' multiband doublet: 28 MHz
CE
GW 1 89 -67 0 60 67 0 60 .00267
GS 0 0 .3048
GE 1
GN 0 0 0 0 13 .005
EX 0 1 45 0 1 0
LD 5 1 1 89 5.8001E7
FR 0 1 0 0 28 1
RP 0 181 1 1000 -90 35 1 1
EN
```

5-1-2

2. The azimuth angle chosen for the elevation plot might actually be one of four angles, since the antenna produces 4 identical **major lobes** with the same maximum gain (along with some **minor lobes**, that is lobes of less strength). An elevation plot along any one of

the four lobes would yield the same data with respect to gain and elevation angle.

If you followed all of the guidelines, your data would look like the data for 5-1-2.NEC:

5-1-2 Reference Data			
Frequency Mhz	Source Z (R±jX Ω)	Gain dBi	Elevation Angle
3.7	93.0 + j 86.7	6.33	75
28.0	1127 + j 1243	11.02	8

Comparing the data sets between the worst case version of a revised 5-1-1.NEC and the better version in 5-1-2.NEC reveals the problems of not tending to all of the required model changes. The 3.7 MHz data changes very little between the models. However, the 28 MHz data changes drastically everywhere. The gain in the errant model was so implausible, that it would likely have spurred you into finding the appropriate azimuth angle to use. However, the source impedance data, without outside information, is not nearly so self-identifying. You might well have thought the bad data to be as close to correct as NEC could make it. Guidelines 1-3 should become a permanent part of your modeling practice.

5-2-1.NEC & 5-2-2.NEC: A folded dipole

Now that the first exercise may have caught you in one or more of its traps, you will undoubtedly be more wary with the instruction sets. Therefore, we shall have to ask you directly to make errors--and some big ones at that. The purpose of these errors will be to dramatize the consequences of careless modeling at the extremes. The errors that are more likely to occur will result in subtle differences in outcome that might easily be overlooked or taken to be adequately accurate.

Open file 5-2-1.NEC, a #14 copper wire folded dipole for 28.48 MHz. The antenna is 197.6"

long by 1" wide, roughly resonant at the designated frequency, in free space. The requested pattern is a standard azimuth pattern at a elevation angle of 0°. Run the model and determine its source impedance from the appropriate table and its maximum gain from either the polar plot or the power gain table. Record your values on the top line

```

CM Folded dipole: 28.48 MHz
CE
GW 1 11 -98.8 0 0 98.8 0 0 3.2E-02
GW 2 1 98.8 0 0 98.8 0 1 3.2E-02
GW 3 11 98.8 0 1 -98.8 0 1 3.2E-02
GW 4 1 -98.8 0 1 -98.8 0 0 3.2E-02
GS 0 0 .02540
GE 0
EX 0 1 6 0 1 0
LD 5 1 1 11 5.8001E7
LD 5 2 1 1 5.8001E7
LD 5 3 1 11 5.8001E7
LD 5 4 1 1 5.8001E7
FR 0 1 0 0 28.48 0
RP 0 1 361 1000 90 0 1 1
EN

```

5-2-1

below as indicated by the segmentation 11-1-11-1, corresponding to the 4 wires comprising the model.

5-2		Test Data		Reference Data	
Segments	Source Z ($R \pm jX \Omega$)	Gain dBi		Source Z ($R \pm jX \Omega$)	Gain dBi
11-1-11-1				287.3 + j 7.8	2.10
11-1-51-1				249.5 + j 8.3	1.44
21-1-51-1				265.2 + j 5.8	1.68
201-1-201-1				287.5 - j 0.3	2.11
201-1-101-1				287.1 + j 0.9	2.10

Comments: The values you obtained for the 11-1-11-1 version of the folded dipole present plausible gain and source impedance figures. A folded dipole with identical longitudinal wires multiplies the source impedance by 4. Since a single wire dipole in free space has an impedance of about 72Ω , the theoretical impedance for the folded dipole should approach 288Ω . There should be no significant difference in gain between the two types of antennas.

Now return to model 5-2-1.NEC. Make the following radical change in wire 3: change the number of segments to 51. Run the model and record the source impedance data on the line labeled 11-1-51-1. When complete, further alter the model to change the segmentation on wire 1 to 21. This move will require moving the source point to segment 11 on this wire in order to keep it centered. Run this new model and record the data on the line labeled 21-1-51-1.

It is clear that when parallel wires are closely spaced and the segments do not align with each other, erroneous values result for both the source impedance and the maximum gain. The assigned misalignments are very large. Even with lesser misalignments, some deviance will be noted.

However, notice the segment lengths in the model. With only 11 longitudinal segments, each is far longer than the single segments forming the ends. Now open file 5-2-2.NEC. The model is identical in dimension to the model in 5-2-1.NEC except for the segmentation. Here the

```

CM Folded dipole: 28.48 MHz
CE
GW 1 201 -98.8 0 0 98.8 0 0 3.2E-02
GW 2 1 98.8 0 0 98.8 0 1 3.2E-02
GW 3 201 98.8 0 1 -98.8 0 1 3.2E-02
GW 4 1 -98.8 0 1 -98.8 0 0 3.2E-02
GS 0 0 .02540
GE 0
EX 0 1 101 0 1.414214 0
LD 5 1 1 201 5.8001E7
LD 5 2 1 1 5.8001E7
LD 5 3 1 201 5.8001E7
LD 5 4 1 1 5.8001E7
FR 0 1 0 0 28.48 0
RP 0 1 361 1000 90 0 1 1
EN

```

5-2-2

number of longitudinal segments is 201 so that each is approximately 1" long to match the length of the end segments. Run the model, which will take a bit longer than the small original model. Record the results for source impedance and gain in the 201-1-201-1 line of the chart.

Staying with model 5-2-2.NEC, change the segmentation of wire 3 to 101. Run the model and record the data on the line labeled 201-1-101-1. The 2:1 ratio of segment lengths in this revised model creates far less deviance in the results than was the case were we used much longer segments. The overall body of data suggests the following good practice, not only for closely spaced parallel wires, but for all models.

Guideline 4: to the degree feasible, equalize all segment lengths within models.

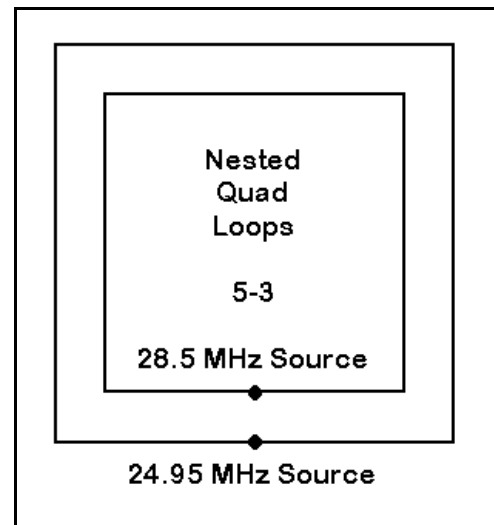
Although there are a few exceptions, which we shall encounter in later chapters, the guideline applies to all parallel wires, including those more widely spaced in parasitic beams, and to wires joining at their ends, for example in closed geometry structures.

As a practical note, the guideline may require judicious violation on occasion. In the case of model 5-2-2.NEC, the total number of segments is 402. If the folded dipole was a portion of a large array involving equally heavily segmented wires, the either time or computer resource limits might occasionally be overrun. Therefore, you may have to resort to using the less accurate but much smaller model. Every such decision should be made individually, with reference data on the divergence from a more ideal model and with reference to the project requirements for precision. You should never simply presume that a model is "good enough."

5-3-1.NEC & 5-3-2.NEC: Nested quad loops for 24.95 and 28.5 MHz

As an exercise to conduct on your own, open and run 5-3-1.NEC, which is a model of the nested quad loops pictured in **Figure 5-3**. The model appears at the top of the next page. Evaluate this model with respect to the adequacy of segmentation and the alignment of segments in wires of the two loops. In order to run the model at 28.5 MHz, you must change the location of the source from wire 1 to wire 5 (this applies to both 5-3-1.NEC and to 5-3-2.NEC.)

Before referring to the description of 5-3-2.NEC, to the right on the next page, develop your own conclusions about the adequacy of the data derived from the first model and make the changes that you believe will correct the situation. Then run model 5-3-2.NEC and compare the results of your correctives to those placed in this model.



```

CM Nested quad loops: 24.95/28.5 MHz
CE
GW 1 3 -1.5621 0 -1.5621 1.5621 0 -1.5621 .000814
GW 2 3 1.5621 0 -1.5621 1.5621 0 1.5621 .000814
GW 3 3 1.5621 0 1.5621 -1.5621 0 1.5621 .000814
GW 4 3 -1.5621 0 1.5621 -1.5621 0 -1.5621 .000814
GW 5 3 -1.3614 0 -1.3614 1.36144 0 -1.3614 .000814
GW 6 3 1.36144 0 -1.3614 1.36144 0 1.36144 .000814
GW 7 3 1.36144 0 1.36144 -1.3614 0 1.36144 .000814
GW 8 3 -1.3614 0 1.36144 -1.3614 0 -1.3614 .000814
GS 0 0 1
GE 0
EX 0 1 2 0 1 0
LD 5 1 1 3 5.8001E7
LD 5 2 1 3 5.8001E7
LD 5 3 1 3 5.8001E7
LD 5 4 1 3 5.8001E7
LD 5 5 1 3 5.8001E7
LD 5 6 1 3 5.8001E7
LD 5 7 1 3 5.8001E7
LD 5 8 1 3 5.8001E7
FR 0 1 0 0 24.95 0
RP 0 1 361 1000 90 0 1 1
EN

```

5-3-1

```

CM Nested quad loops: 24.95/28.5 MHz
CE
GW 1 11 -1.5621 0 -1.5621 1.5621 0 -1.5621 .000814
GW 2 11 1.5621 0 -1.5621 1.5621 0 1.5621 .000814
GW 3 11 1.5621 0 1.5621 -1.5621 0 1.5621 .000814
GW 4 11 -1.5621 0 1.5621 -1.5621 0 -1.5621 .000814
GW 5 9 -1.3614 0 -1.3614 1.36144 0 -1.3614 .000814
GW 6 9 1.36144 0 -1.3614 1.36144 0 1.36144 .000814
GW 7 9 1.36144 0 1.36144 -1.3614 0 1.36144 .000814
GW 8 9 -1.3614 0 1.36144 -1.3614 0 -1.3614 .000814
GS 0 0 1
GE 0
EX 0 1 6 0 1 0
LD 5 1 1 11 5.8001E7
LD 5 2 1 11 5.8001E7
LD 5 3 1 11 5.8001E7
LD 5 4 1 11 5.8001E7
LD 5 5 1 9 5.8001E7
LD 5 6 1 9 5.8001E7
LD 5 7 1 9 5.8001E7
LD 5 8 1 9 5.8001E7
FR 0 1 0 0 24.95 0
RP 0 1 361 1000 90 0 1 1
EN

```

5-3-2

Note especially the gain figures for the two loops. A gain value approaching 3.3 dBi is normal for thin (#14 in this case) copper wire quad loops in free space. The higher gain figures generated by the less adequate model, while not seriously erroneous for some purposes, will compound in multi-element quad arrays, leading to more seriously flawed estimates of array gain.

5-4-1.NEC & 5-4-2.NEC: A folded X-beam

There are occasions upon which the current table produced by NEC-2 becomes an important tool of analysis--not to mention error detection--with respect to antennas. Radical changes in current magnitude and phase often indicate that something is amiss in our model construction--unless we have intentionally modeled the antenna to produce those changes. In general, the best procedure is to avoid those abrupt changes when they are no more than careless modeling.

Often careless modeling will yield correct values for the source impedance, the gain and its direction and the magnitude of any major and minor lobes in the radiation pattern, and other pattern-related categories. If these data comprise our whole interest in the antenna, we are likely to be unaware of poor modeling practice. The awareness usually arises when we have occasion to examine the currents table. Sometimes the values do not tally with expectations. At other times, we simply cannot find our way about the table to track current level relative to positions on the antenna elements. Both are needless hindrances to efficient model analysis.

Reopen file 5-1-1.NEC. Run the model and open the Current and Location table. Look to the far right for the current magnitude and phase. Record the current magnitude and phase for each of the 11 segments of the model.

5-1-1			Test Data		Reference Data	
Segment	Current Magnitude (X E-03)	Current Phase		Current Magnitude (X E-03)	Current Phase	
1				1.26	-51.2	
2				3.48	-51.0	
3				5.30	-50.4	
4				6.64	-49.7	
5				7.40	-48.8	
6				7.57	-47.8	
7				7.40	-48.8	
8				6.64	-49.7	
9				5.30	-50.4	
10				3.48	-51.0	
11				1.26	-51.2	

Notice the pattern of values along this linear center-fed element. Such patterns are typical of common antenna elements, whether or not they are truly linear. Indeed, they may twist and bend. But with adjustment for altered interactions among the element wire segments, a similar pattern will emerge.

Open file 5-4-1.NEC, a folded X-beam for 28.5 MHz made from 12.5 mm 6061-T6 aluminum. Using the model description, attempt to sketch the antenna, identifying both the driven and director elements by reference to the source placement. The zero value in the Z-axis column and the absence of a ground description card together specify that this antenna will be

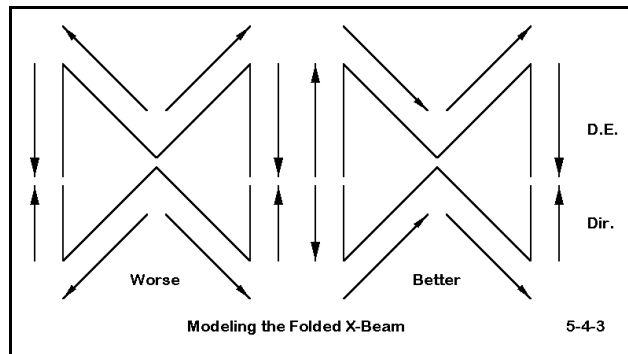
```

CM X-Beam: 28.5 MHz
CE
GW 1 19 -1.2561 -1.2561 0 -1.2561 .075 0 .00625
GW 2 25 -.0837 0 0 -1.2561 -1.2561 0 .00625
GW 3 3 -.0837 0 0 .08374 0 0 .00625
GW 4 25 .08374 0 0 1.2561 -1.2561 0 .00625
GW 5 19 1.2561 -1.2561 0 1.2561 .07537 0 .00625
GW 6 15 -1.2561 1.2561 0 -1.2561 .184 0 .00625
GW 7 25 -.0837 .02233 0 -1.2561 1.2561 0 .00625
GW 8 3 -.0837 .02233 0 .08374 .02233 0 .00625
GW 9 25 .08374 .02233 0 1.2561 1.2561 0 .00625
GW 10 15 1.2561 1.2561 0 1.2561 .18423 0 .00625
GS 0 0 1
GE 0
EX 0 3 2 0 1 0
LD 5 1 1 15 2.4938E7
LD 5 2 1 25 2.4938E7
LD 5 3 1 3 2.4938E7
LD 5 4 1 25 2.4938E7
LD 5 5 1 15 2.4938E7
LD 5 6 1 15 2.4938E7
LD 5 7 1 25 2.4938E7
LD 5 8 1 3 2.4938E7
LD 5 9 1 25 2.4938E7
LD 5 10 1 15 2.4938E7
FR 0 1 0 0 28.5 0
RP 0 1 361 1000 90 0 1 1
EN

```

modeled in free space. The antenna position will simplify your sketch.

Note that each element of the antenna is composed of 5 wires: 2 end "tails," 2 sloping wires, and 1 short center wire. The driven element source is placed at the midpoint of its short center wire.



Run the model. Our interests in it do not include the pattern and source impedance, although you should note key values for reference. More to our purpose is that you open the Currents table. Try to use that table to form a curve of current magnitude and phase along each of the two elements. The difficulty you encounter results from the beam elements having been modeled from the center element outward, as shown to the

left in **Figure 5-4-3**. The modeled ends do not correspond to the physical ends of the element as they connect, one with the next. We can avoid such difficulties by following a simple rule, derived from the dipole sample.

Guideline 5: Model each antenna element in a consistent pattern throughout the antenna from one end to the other.

This guideline directs the arrows of modeling direction to the right in **Figure 5-4-3**, which is reflected in 5-4-2.NEC, which you should now open. If you attempt to sketch this antenna, you will discover that it is the very same antenna, but modeled in an orderly manner.

Run the model and verify the equivalence of this model to the last by reference to the values of the source impedance and key pattern numbers. Open the Currents table and trace the values of current magnitude and phase at the far right of the table. You will discover that they form the relatively smooth curve from element end to element end that you found in the simpler dipole model.

```

CM X-Beam: 28.5 MHz
CE
GW 1 19 -1.2561 .07537 0 -1.2561 -1.2561 0 .00625
GW 2 25 -1.2561 -1.2561 0 -.0837 0 0 .00625
GW 3 3 -.0837 0 0 .08374 0 0 .00625
GW 4 25 .08374 0 0 1.2561 -1.2561 0 .00625
GW 5 19 1.2561 -1.2561 0 1.2561 .07537 0 .00625
GW 6 15 -1.2561 .18423 0 -1.2561 1.2561 0 .00625
GW 7 25 -1.2561 1.2561 0 -.0837 .02233 0 .00625
GW 8 3 -.0837 .02233 0 .08374 .02233 0 .00625
GW 9 25 .08374 .02233 0 1.2561 1.2561 0 .00625
GW 10 15 1.2561 1.2561 0 1.2561 .18423 0 .00625
GS 0 0 1
GE 0
EX 0 3 2 0 1 0
LD 5 1 1 19 2.4938E7
LD 5 2 1 25 2.4938E7
LD 5 3 1 3 2.4938E7
LD 5 4 1 25 2.4938E7
LD 5 5 1 19 2.4938E7
LD 5 6 1 15 2.4938E7
LD 5 7 1 25 2.4938E7
LD 5 8 1 3 2.4938E7
LD 5 9 1 25 2.4938E7
LD 5 10 1 15 2.4938E7
FR 0 1 0 0 28.5 0
RP 0 1 361 1000 90 0 1 1
EN
    
```

Notice another feature of the currents table. Although each wire is identified by a "tag" number, the segment numbers do not repeat with the beginning of each new tag. Rather, the numbering is continuous throughout the entire model. You may wish to go back to a number of other multi-element models we have used for practice in sorting out which currents belong to which element.

5-5-1.NEC & 5-5-2.NEC: A capacity-hat vertical

When you compared the current tables for 5-4-1.NEC and 5-4-2.NEC, you discovered that some of the wires in 5-4-1.NEC that were modeled "backwards" relative to the others had the correct magnitude, but were 180° out of phase with their counterpart wire positions at the other end of the elements. Correctly modeled, as in 5-4-2.NEC, the current phases at corresponding points along the element at equal distances from center were the same. For many applications, this correspondence may seem excessively fussy, since the correct phase value is readily deduced.

However, what may seem fussy is really a matter of using care that may lead to a better understanding of the antenna with which we are working. Open file 5-5-1.NEC. This is a model of a vertical antenna over perfect ground for 7.2 MHz. The 6061-T6 aluminum antenna uses 25 mm diameter elements. The antenna is short for the frequency and employs a capacity hat to bring it to resonance. The hat consists of 4 spokes symmetrically arranged at the vertical element top, plus a perimeter wire connecting the outer ends of the spokes. The dimensions (in meters) just happened to yield simple numbers for resonance at the desired frequency.

Note that the model lists as the first 4 wires the identical wires making up the perimeter, followed by the 4 identical wires making up the spokes, with the vertical element last. One might as easily have adopted the opposite convention, working up from the ground through the vertical element, then through the spokes, and finally to the perimeter wires.

```

CM Capacity-hat vertical: 7.2 MHz
CE
GW 1 6 1 1 5 1 -1 5 .0125
GW 2 6 1 -1 5 -1 -1 5 .0125
GW 3 6 -1 -1 5 -1 1 5 .0125
GW 4 6 -1 1 5 1 1 5 .0125
GW 5 4 1 1 5 0 0 5 .0125
GW 6 4 1 -1 5 0 0 5 .0125
GW 7 4 -1 -1 5 0 0 5 .0125
GW 8 4 -1 1 5 0 0 5 .0125
GW 9 10 0 0 5 0 0 0 .0125
GS 0 0 1
GE 1
GN 1
EX 0 9 10 0 1 0
LD 5 1 1 6 2.4938E7
LD 5 2 1 6 2.4938E7
LD 5 3 1 6 2.4938E7
LD 5 4 1 6 2.4938E7
LD 5 5 1 4 2.4938E7
LD 5 6 1 4 2.4938E7
LD 5 7 1 4 2.4938E7
LD 5 8 1 4 2.4938E7
LD 5 9 1 10 2.4938E7
FR 0 1 0 0 7.2 0
RP 0 181 1 1000 -90 0 1 1
EN

```

5-5-1

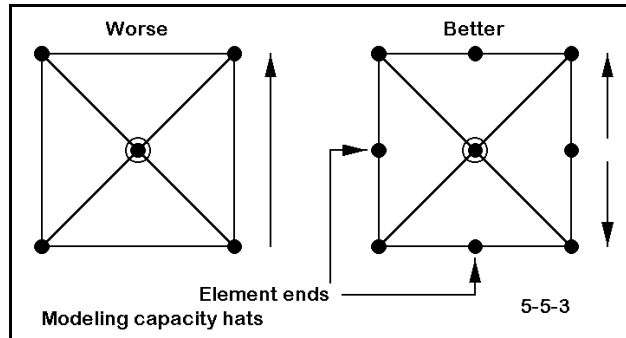
Run the antenna and record the values of source impedance and maximum gain for later reference. Open the Currents table. Begin at the bottom, looking at the current as you move up the vertical. At the point where the table moves into the first encountered spoke,

you will see a sudden decrease in current. However, if you multiply this value by 4, it again becomes reasonable in the progression. The current has simply been divided into the 4 spoke "branches." You will encounter a similar division, this time by a factor of 2, as you move from the end of the spoke into any of the perimeter wires.

The perimeter wires are of special interest to us. Record on the following table the current phases found for each of the segments along one perimeter wire (6 segments).

5-5-1		Test Data		Reference	
Segment	Phase		Phase		
1			-176.505		
2			-176.512		
3			-176.517		
4			3.483		
5			3.488		
6			3.495		

The sudden 180° shift in current at mid element indicates that something is amiss. The problem is simply identified by reference to the left portion of **Figure 5-5-3**. In the diagram, dots indicate where modeled wires end or join other wires.



```

CM Capacity-hat vertical: 7.2 MHz
CE
GW 1 3 1 0 5 1 1 5 .0125
GW 2 3 1 0 5 1 -1 5 .0125
GW 3 3 0 -1 5 1 -1 5 .0125
GW 4 3 0 -1 5 -1 -1 5 .0125
GW 5 3 -1 0 5 -1 -1 5 .0125
GW 6 3 -1 0 5 -1 1 5 .0125
GW 7 3 0 1 5 -1 1 5 .0125
GW 8 3 0 1 5 1 1 5 .0125
GW 9 4 1 1 5 0 0 5 .0125
GW 10 4 1 -1 5 0 0 5 .0125
GW 11 4 -1 -1 5 0 0 5 .0125
GW 12 4 -1 1 5 0 0 5 .0125
GW 13 10 0 0 5 0 0 0 .0125
GS 0 0 1
GE 1
GN 1
EX 0 13 10 0 1 0
LD 5 1 1 3 2.4938E7
LD 5 2 1 3 2.4938E7
LD 5 3 1 3 2.4938E7
LD 5 4 1 3 2.4938E7
LD 5 5 1 3 2.4938E7
LD 5 6 1 3 2.4938E7
LD 5 7 1 3 2.4938E7
LD 5 8 1 3 2.4938E7
LD 5 9 1 4 2.4938E7
LD 5 10 1 4 2.4938E7
LD 5 11 1 4 2.4938E7
LD 5 12 1 4 2.4938E7
LD 5 13 1 10 2.4938E7
FR 0 1 0 0 7.2 0
RP 0 181 1 1000 -90 0 1 1
EN

```

5-5-2

In fact, model 5-5-1.NEC misidentified the element ends. The elements do not correspond to the wire ends at the tips of the spokes. Rather, elements end where the current goes to zero. (This same fact allows us to identify correctly multi-wavelength long-wire antennas as collinear arrays.) Although the segmentation of the element does not reveal a "zero" current point, the magnitude of the currents sets that point at the junction of segments 3 and 4 on each of the perimeter wires.

The right portion of **Figure 5-5-3** correctly identifies the 4 points marking the element ends with dots showing a coincidence of element ends and wire ends. Open model 5-5-2.NEC, a corrected version of the original capacity hat model. Note that the perimeter wires are doubled in number. Run the model, verify the source impedance and gain figures to establish equivalency to model 5-5-1.NEC, and then examine the Currents and Location table. You will discover that there is no longer a 180° phase change in the middle of each perimeter element.

Guideline 6: Correctly establish all antenna element ends.

This guideline does not force the subdivision of wires in your models. However, it does focus your thinking upon the antenna structure in relationship to your model of it. If you take shortcuts, you should be aware of them and of their consequences.

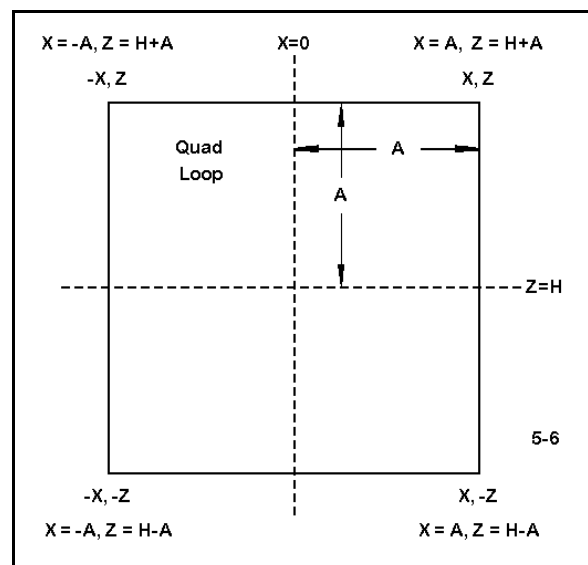
5-6.NEC - 5-8.NEC: Reader-created files

Maintaining precision while modifying model descriptions is not always easy. Many common human entry errors can occur, including modifying the wrong item, transposing numbers, and simply forgetting to change a value within a long list of needed changes. One technique that reduces the error rate in any of these tasks is the use of symbolic expressions for many of the antenna's X, Y, and Z geometry coordinates. NECWin Plus provides a spreadsheet environment for defining variables which may be used in the main geometry description. The following exercises are designed to acquaint you with the utility of using symbolic dimensions. However, you will need to consult your user's manual for the details of entering the appropriate model data and then executing the resultant model.

1. **Quad loop:** Modifying a quad loop, especially one symmetrically placed about either the X or the Y axis, requires the alteration of 8 values, each of which occurs twice (as end 1 of one wire and end 2 of another wire). If the antenna is at some assigned height, then the modification requires that we calculate the new Z-values above and below the centerline of the antenna.

Converting the numerical dimensions of the quad into symbolic values permits you to change antenna dimensions with the entry of a single number. Antenna height can be changed also by varying a single number.

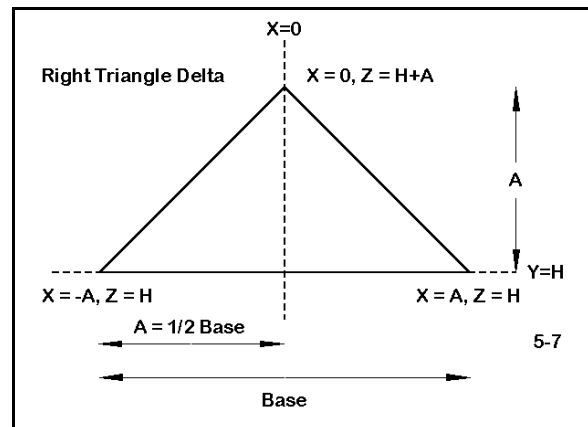
Figure 5-6 shows the applicable entries for a geometry description page. The equations page would simply need numerical values assigned to A and to H to complete the task. (Note: in all of the following sketches, variable selection is arbitrary. You should follow program rules for the order, selection, and naming of variables actually used in specific models.)



Using these clues, create a model for a single quad loop that is 9.36' per side and used

on a frequency of 28.5 MHz. Use #14 AWG copper wire, 11 segments per wire, and locate the source at the center of the lower horizontal wire. Place the antenna at 35' over reflection coefficient ground. Request a elevation pattern, using the axis broadside to the loop as the azimuth angle to determine the take-off angle. Next, revise the model to add a request for an azimuth pattern at the take-off angle. Then adjust the dimensions through a sequence of trial runs and new values for A until the antenna is resonant within $\pm 1\Omega$ reactance. Save the fully developed file as 5-6.NEC.

2. A right-triangle delta loop: Numerous equations exist that permit the modeler to describe almost any antenna structure in exquisite geometric detail. How complex we make our equations within an antenna model is to some degree a matter of choice. However, the modeling environment is not a theoretical treatise. Instead, it is a practical world where the use of equations is designed to ease problems of design and modification. Very often, the simplest and most transparent equations do the best work for us.

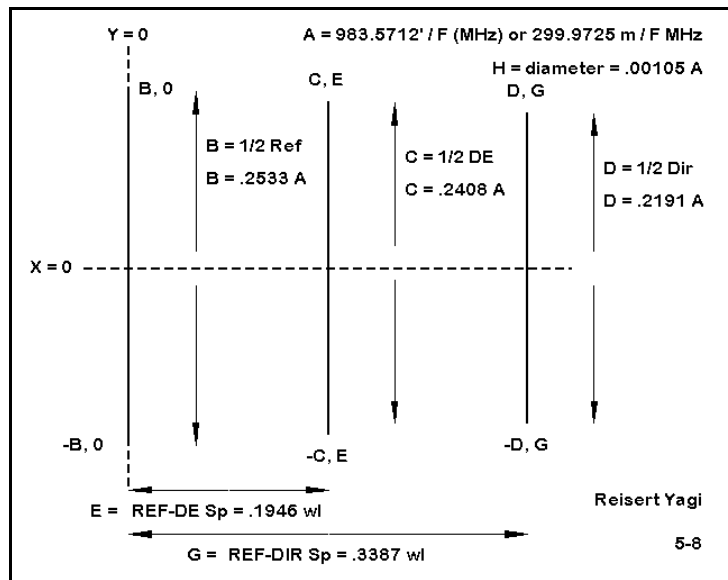


Consider the right-triangle delta loop antenna in **Figure 5-7**. The coordinates, symmetrically placed here around the X-axis, use the basic facts about the right triangle to establish equations that are the soul of simplicity. You can create this triangle as an antenna model using #12 copper wire for a frequency of 7.1 MHz, letting the baseline initially be 60' long. Set the antenna at any height. In fact, you can use this model to test patterns—especially their vertically and horizontally polarized components—by placing the source at either about 12.5% up one angular leg or centered on the baseline. Resonate the antenna for each configuration by adjusting the value of A.

You may discover several interesting facts about this triangle. Alternating the placement of the source can yield different dimensions for resonance. Optimal height will differ for use as a vertically or as a horizontally polarized antenna. In vertically polarized use, the right triangle provides a convenient match for $50\text{-}\Omega$ transmission lines. However, the "side-fed" triangular shape does not yield its highest gain as a right-triangle. You can alter the equation for the apex to produce different ratios of base to antenna height, working toward the maximum vertically polarized gain configuration. Save finished models as a sequence in the 5-7-x.NEC series.

3. **The Reisert Yagi:** It is possible to construct a symbolic model using equations directly related to wavelength. The model becomes self-scaling as one changes frequency for the model. To achieve this degree of completeness, all element lengths, diameters, and spacing must be expressed as functions of the wavelength.

Joseph Reisert has published a number of Yagi designs in this form, one of which appears in **Figure 5-8**. The figure adapts the original equations to the form needed for symmetrically placing the antenna around the Y-axis. Note that the work shown in the figure can be a paper exercise done apart from the modeling program.



Joseph Reisert has published a number of Yagi designs in this form, one of which appears in **Figure 5-8**. The figure adapts the original equations to the form needed for symmetrically placing the antenna around the Y-axis. Note that the work shown in the figure can be a paper exercise done apart from the modeling program.

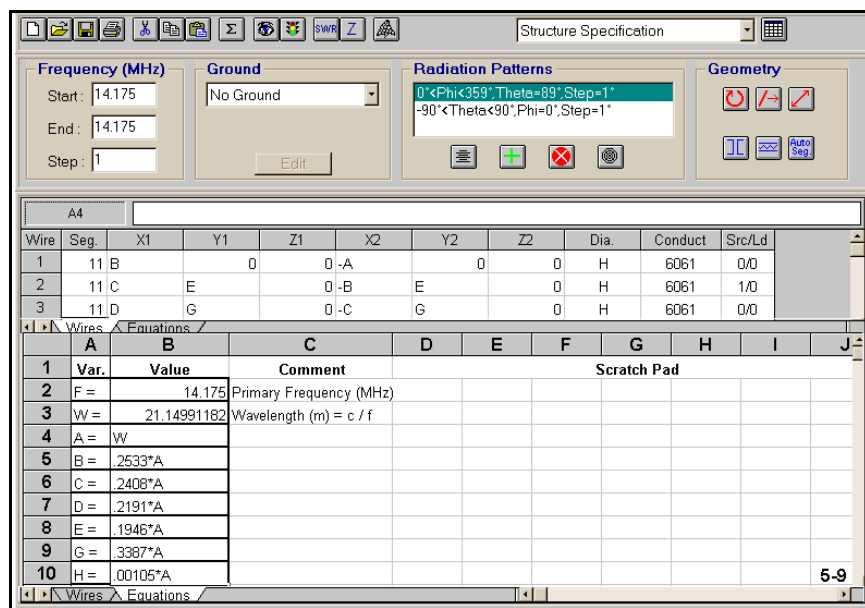


Figure 5-9 shows a composite of the "Wires" and the "Equations" pages of NECWin Plus. Since we had previously defined our equations and variables, "A" turns out to be equivalent to W, which has been automatically defined by the program. "A" has been left for clarity in correlating the two figures, but may be omitted simply by modifying the paper sketch. Add suitable notations to both the

paper sketch and the program "Scratchpad" for good record keeping.

One limitation of this style of model building is that the diameter variable (H) must come close to an existing material diameter if the antenna is to be built. Otherwise, the result will only be an approximation that requires further optimization for available materials.

This particular model is restricted to monotaper elements, that is, elements that have a uniform diameter throughout their length. Use this or other Yagi designs to develop auto-scaling designs, saving each in the 5-9-x.NEC series of model files.

Summing Up

Careful model construction is, in the end, a combination of three ingredients:

1. Developing good modeling practices, including making some of the guidelines noted in this set of exercises a fundamental and natural part of the modeling process;
2. Attending to details, such as the effect of a proposed model geometry on all parts of the output data; and
3. Utilizing every facility offered by a modeling program to ease the burden of tracking the maze of details within even straightforward antenna designs.

No set of exercises can be exhaustive in this regard. This chapter has only tried to make you aware of some of the dimensions of careful model construction and of some of the ways to achieve it. That awareness should follow you throughout the remaining exercise sets in this guide. Indeed, this may be a chapter you should periodically revisit just to renew your commitment to modeling care.

6. Convergence Testing

***Objectives:** In this set of exercises, you will become acquainted with convergence testing as one (but not the only) mark of a reliable antenna model. You will learn the rationale for convergence testing and then, through a series of hand-on exercises, learn to perform the test and to evaluate the results.*

The goal of antenna modeling with NEC is not just to produce any old model. Rather, we aim to produce reliable models, that is, models that accurately reflect the properties of corresponding real-world antennas. All forms of NEC are already limited in this capacity by being restricted to modeling with straight wires and to modeling over essentially flat terrain. However, we can produce reliable models of most antennas within these restrictions.

For most common types of antennas used in the HF and VHF region, there is a test of model reliability called the "**convergence test**." To understand the test, let's take note of certain features of NEC. First, as we noted in an early chapter of this volume, NEC has certain limits of wire segment length and diameter--and of the ratio of length to diameter. This sets certain limits to the lowest number of segments that should be used per half-wavelength for the antenna model. However, the lowest number of segments per half-wavelength is not always the correct number of segments to use.

Second, the outputs produced by NEC are the results of complex matrix calculations. Therefore, as we change the number of segments we use per half-wavelength (the segmentation density), without changing the dimensions of the antenna elements, the reported outputs will vary. This variation affects calculations of gain, front-to-back ratio, source impedance, and currents along the antenna model wires.

Variation among report outputs will ordinarily be greatest when the number of segments used per half-wavelength is small. The variation from one segmentation level to another will ordinarily decrease as the overall segmentation density increases. At a certain level of segmentation density, changes in reported outputs with further increases in segmentation density will be too small to be significant. At this level, the model is said to have reached convergence.

When none of the other program limits have been reached by a model, convergence becomes a good measure of model reliability. However, there are two important issues

that NEC itself cannot determine in advance.

1. Significance level of output differentials: Although we should always strive for the most highly converged models we can obtain, there are certain practical limits to the demands we can place on a model. Every increase in segmentation density increases the size of the matrices to be calculated, with increases in overall run time. (The time required to fill the matrix is a function of N^2 , to factor it a function of N^3 , and to compute currents for each excitation a function of N^2 , where N is the number of wire segments. Further details of run times appear in Section V of the NEC-2 Manual.)

2. Significance in relationship to tasks: The degree of precision demanded of a model depends in part on the objectives of the task of which modeling is a part. For some analytical tasks, small variations in reported outputs may make a significant difference in the analysis. In contrast to this are amateur radio antennas built by modelers after NEC design exercises. These are often subject to construction variables such that final adjustment must be an empirical procedure, no matter how precisely converged the original design model. Between these extremes are various manufacturing requirements, test unit requirements, etc., whose criteria of convergence may vary widely, sometimes depending upon whether an antenna is being designed for wide-band or frequency-specific use. In the end, only the user--with a solid grasp of task objectives--can decide how much convergence is enough.

Needless to say, a poorly converged antenna model that yields inflated performance figures when modeled with too little segmentation density should never be the basis for reporting the antenna, no matter how much vested interest the designer has in the model.

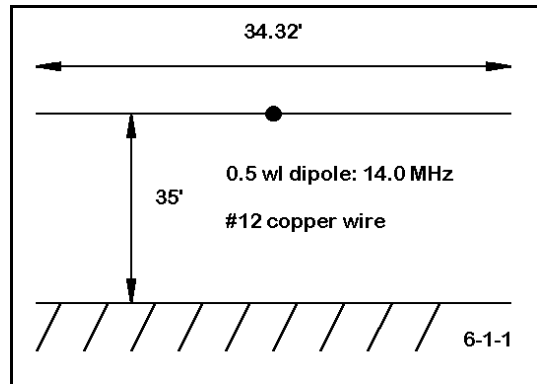
Exercise Preparation

In this set of exercises, you will test the convergence of a variety of antennas, each one of which is designed to give you a different perspective on convergence testing. The 7 models for this chapter appear on your floppy disk as 6-1.NEC through 6-7.NEC. Even though some of the antenna models are very simple antennas, please do not skip them. When modifying models with respect to the number of segments per wire, do not forget to verify that the source is located on the correct segment to maintain its physical position.

Most of the exercises in this chapter will make use of tabular data, rather than plots and graphs. Although plotted and graphical data are often the most attractive sorts, there are important conclusions that can only be drawn from a survey and comparison of numbers themselves. Throughout this exercise, we shall be interested in numerical differences in reported outputs, and we shall not presume in advance any particular level of precision that might be adequate to one or another task. Indeed, determining the level of necessary precision will become part of our task.

6-1.NEC: The half-wavelength dipole

The initial model is a single wire (#12 copper) half-wavelength dipole for 14.0 MHz. It is 34.32' long and is placed 35' above ground, as shown in the **Figure 6-1-1**. Open file 6-1.NEC and verify that your NEC screen has data identical to that in **Figure 6-1-2**.



```

CM Convergence test 1: 20-meter dipole
CE
GW 1 41 -17.16 0 35 17.16 0 35 3.36778215223097E-03
GS 0 0 .3048
GE 1
GN 2 0 0 0 13 .005 0 0 0 0
EX 0 1 21 00 1 0
LD 5 1 1 9 5.8001E7
FR 0 1 0 0 14 0
RP 0 181 1 1000 -90 90 1 1
FR 0 1 0 0 14 0
RP 0 1 360 1000 62 0 1 1
EN
    
```

6-1-2

Be certain to verify that the ground is "average" (Conductivity = 0.005 S/m; Dielectric Constant = 13), and the selected ground system is Sommerfeld-Norton.

Before running this model, notice that the number of segments assigned to this antenna is only 5. As part of our data gathering, we shall increase the segmentation for each run by 6 segments, making runs with 5, 11, 17, 23, 29, 35, and 41 segments. Be certain that, for each modification, you set the source on the correct segment. We shall collect data on the reported gain of the antenna in dBi and the reported source impedance ($R \pm jX$ in Ohms). You may fill in your output data in the table below.

6-1 Test Data			Reference	
No. of Segments	Gain dBi	Source Z ($R \pm jX$) Ohms	Gain dBi	Source Z ($R \pm jX$) Ohms
5			7.29	69.64 - j1.05
11			7.34	69.31 + j0.21
17			7.37	68.97 + j0.24
23			7.39	68.77 + j0.19
29			7.40	68.67 + j0.20
35			7.40	68.62 + j0.23
41			7.40	68.60 + j0.26

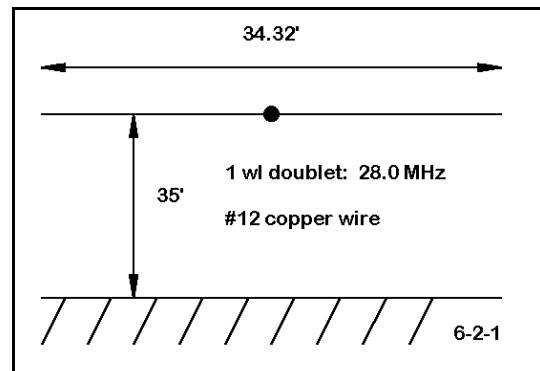
Comments: The simple half-wavelength dipole antenna is the chief cause of the temptation for antenna modelers to use no more than the minimum segmentation density. Even if the figures you derived for gain and source impedance are not identical to those listed in the reference columns, the spread is unlikely to make a significant operational difference to almost any imaginable task.

Nevertheless, notice that variations in the figures are largest between steps at the lowest levels of segmentation. Although the differences in gain and impedance are not operationally significant between segmentation densities of 5 and 17 segments per half-wavelength, they are more numerically significant than those between 23 and 41 segments per half-wavelength. Given the speed of modern computers, there is no reason to adhere to the lowest possible segmentation density except with the most complex antenna structures that press the limits of resources and run-time.

6-2.NEC: The full-wavelength doublet

Our second model is physically identical to the first: a #12 copper wire 34.32' long at a height of 35' above a Sommerfeld-Norton average ground.

The only difference, as noted in **Figure 6-2-1**, is that the antenna will be modeled at 28.0 MHz. To survey similar (but not identical) segmentation densities, we shall begin with 11 segments for the wire and increase by 10 segments to an upper exercise limit of 71, moving the source segment with each increase. Collect data on gain in dBi and on the source impedance ($R \pm jX$ in Ohms). Place your output data in the table below.



6-2 Test Data			Reference	
No. of Segments	Gain dBi	Source Z (R±jX) Ohms	Gain dBi	Source Z (R±jX) Ohms
11			9.30	3767 + j1435
21			9.33	4299 - j 141
31			9.34	4148 - j 801
41			9.35	3991 - j1120
51			9.35	3868 - j1302
61			9.36	3773 - j1419
71			9.36	3699 - j1500

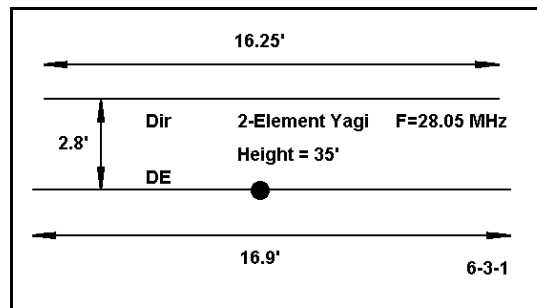
Comments: The results of this exercise yield a tighter group of gain numbers, but a rapidly varying set of impedance figures. Whether or not the model is well-converged may depend to a degree on one's understanding of antennas themselves. We expect a high source impedance. However, looking at the chart, we see that the reactance reverses its type, while the resistive part of the impedance reaches a peak and declines at the very same point. These data indicate that the wire is cut very close to full-wavelength resonance. In this region, only exceptionally small physical changes are needed to generate very large excursions in the antenna impedance.

In addition, the length of the source segment can make a difference in the reported source impedance, especially in regions of the antenna where the current is changing rapidly. Once you have worked through Chapter 8's material on source placement, you may wish to return to this exercise and the preceding one, using multiple sources or a constant-length source segment to re-evaluate source impedance changes with levels of segmentation density.

In general, it is unreasonable to expect the impedance figures to converge closely without a very high segmentation density. However, for most general modeling purposes, a density of about 15 segments per half-wavelength will reduce the impedance excursions to a manageable level.

6-3.NEC: A simple 2-element Yagi

Model 6-3.NEC shows a simple 2-element Yagi of "driver-director" design for 28.05 MHz. Its 0.5" diameter 6061-T6 aluminum elements have a constant diameter along their length (also known as being "monotapered"). Once more the height is 35' above average earth. The top view in **Figure 6-3-1** captures the essential dimensions.



```
CM Convergence test 3: 2-element DE/Dir Yagi
CE
GW 1 41 -8.125 2.8 35 8.125 2.8 35 .02085
GW 2 41 -8.45 0 35 8.45 0 35 .02085
GS 0 0 .3048
GE 1
GN 2 0 0 0 13 .005 0 0 0 0
EX 0 2 21 0 1 0
LD 5 1 1 11 2.4938E7
LD 5 2 1 11 2.4938E7
FR 0 1 0 0 28.05 1
RP 0 1 360 1000 76 0 1 1
FR 0 1 0 0 28.05 1
RP 0 181 1 1000 -90 90 1 1
EN
```

6-3-2

For reference, the standard model screen is shown in **Figure 6-3-2**. Make special note of the source location, since it must remain centered on this wire for the resegmentation exercise.

For this model, we shall gather information from the tables on the gain in both the forward and rearward direction

(90 and 270 degrees azimuth), as well a source information. Enter your data on the table at the top of the next page.

6-3 Test Data			
No. of Segs/El.	Forward Gain dBi	Rear Gain dBi	Source Z (R±jX) Ohms
11			
15			
21			
25			
31			
35			
41			
45			

Comments: Compare your data to the reference data below. Between the lowest and highest segmentation densities, forward gain varies by about 0.16 dB. The resistive component of the source impedance varies by about 1.6 Ohms, while the reactive component varies by under 2.7 Ohms. All of these differentials are for most purposes

operationally insignificant, and we may judge this simple 2-element Yagi model to be well-converged even at the lowest segmentation density.

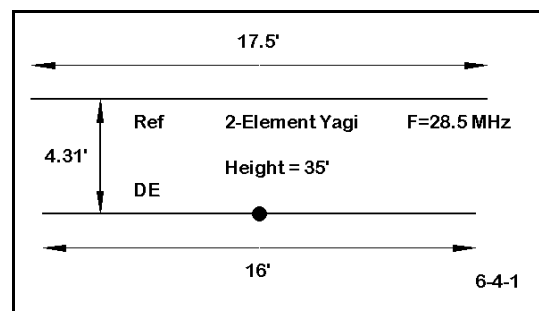
6-3 Reference Data			
No. of Segs/El.	Forward Gain dBi	Rear Gain dBi	Source Z (R±jX) Ohms
11	11.56	-4.25	23.20 - j27.25
15	11.60	-4.48	22.68 - j26.35
21	11.65	-4.68	22.24 - j25.67
25	11.67	-4.77	22.05 - j25.39
31	11.69	-4.86	21.85 - j25.06
35	11.71	-4.91	21.74 - j24.89
41	11.72	-4.97	21.62 - j24.68
45	11.72	-5.00	21.56 - j24.56

While the forward gain varies only minutely, the rear gain varies seemingly by a greater amount (0.75 dB). The rear gain figure is an indicator of one type of front-to-back measure where the 180-degree front-to-back ratio is simply the difference between the forward and the rear gain figures. In terms of front-to-back ratio, there is nearly a 1 dB difference between the lowest and highest segmentation densities.

In most Yagi service, differentials of up to a full dB are not especially significant or detectable in operation. Hence, the slightly larger spread of numerical values does not alter the judgment of convergence. Nonetheless, a segmentation density of at least 20 per half-wavelength will shrink the differentials considerably.

6-4.NEC: A different 2-element Yagi

The next exercise, 6-4.NEC, also involves a 2-element Yagi, this time of driver-reflector design at 35' above average earth at 28.5 MHz. **Figure 6-4-1** shows the overall dimensions of this 6061-T6 aluminum antenna. What the figure does not show is a slight change in the construction of the antenna.



```

CN Convergence test 4: 2-element 10-meter Yagi
CE
GW 1 10 -8 0 35 -6 0 35 .03645
GW 2 41 -6 0 35 6 0 35 .04165
GW 3 10 6 0 35 8 0 35 .03645
GW 4 10 -8.75 -4.31 35 -6 -4.31 35 .03645
GW 5 41 -6 -4.31 35 6 -4.31 35 .04165
GW 6 10 6 -4.31 35 8.75 -4.31 35 .03645
GS 0 0 .3048
GE 1
GN 2 0 0 0 13 .005 0 0 0 0
EX 0 2 21 0 1 0
LD 5 1 1 2 2.4938E7
LD 5 2 1 9 2.4938E7
LD 5 3 1 2 2.4938E7
LD 5 4 1 2 2.4938E7
LD 5 5 1 9 2.4938E7
LD 5 6 1 2 2.4938E7
FR 0 1 0 0 28.5 0
RP 0 181 1 1000 -90 90 1 1
FR 0 1 0 0 28.5 0
RP 0 1 360 1000 76 0 1 1
EN

```

6-4-2

As **Figure 6-4-2** shows in the wire lines, each element of the antenna is composed of three wires: a 1" diameter center section, 12' long, with end sections of 2' for the driven element and 2.75' for the reflector.

Enter your data in the following table. The segment column shows the pattern of segmentation for each element, with the source segment number on the driver center wire shown in parentheses. (For example, "2-9-2 (5)" indicates that the end sections of each element have 2 segments, both center sections have 9 segments, and the driver center wire source location is segment 5.) Although

we shall use fewer steps in this exercise, We shall change the segmentation density of each element from 11 up to 61 segments per half-wavelength.

6-4 Test Data			
No. of Segs/El.	Forward Gain dBi	Rear Gain dBi	Source Z (R±jX) Ohms
2-9-2 (5)			
4-17-4 (9)			
6-25-6 (13)			
8-33-8 (17)			
10-41-10 (21)			

Comments: Refer to the reference data for 6-4.NEC below. Although this antenna appears reasonably well-converged, it bears some suspicious signs. First, in all the examples examined so far, gain (forward and, where relevant, rear) has increased with increasing segmentation. In this example, both forward and rear gain decrease. In addition, the general trend of the resistive component of the source impedance has also been to decrease. In this case, that component increases. Something seems amiss.

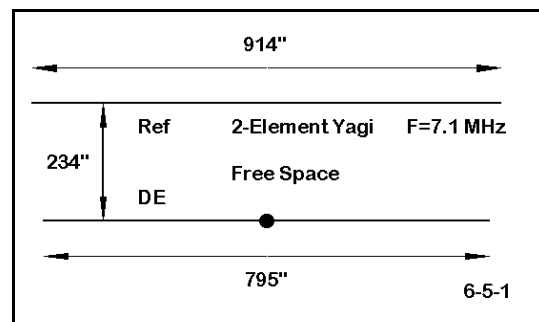
6-4 Reference Data			
No. of Segs/El.	Forward Gain dBi	Rear Gain dBi	Source Z (R±jX) Ohms
2-9-2 (5)	11.65 (11.66)	-0.69 (-0.76)	35.53 + j3.61 (35.38 + j2.95)
4-17-4 (9)	11.60 (11.64)	-0.63 (-0.74)	36.90 + j6.35 (36.11 + j4.46)
6-25-6 (13)	11.57 (11.62)	-0.58 (-0.73)	37.61 + j7.69 (36.45 + j5.06)
8-33-8 (17)	11.55 (11.61)	-0.53 (-0.72)	38.08 + j8.53 (36.64 + j5.32)
10-41-10 (21)	11.53 (11.61)	-0.50 (-0.71)	38.41 + j9.11 (36.73 + j5.38)

The reference table for 6-4.NEC shows data in parentheses taken from running the same model on NEC-4. Although the same numerical trends occur, the figures are much more tightly converged, especially for segmentation densities above 20 per half-wavelength. Moreover, the gain (both front and rear) values of the NEC-2 data are closest to those of the more accurate NEC-4 values when NEC-2 segmentation density is the lowest.

The source of these trends is the stepped diameter (also called stepped radius) elements. Changes in wire diameter along a single linear element produce increasing errors with increasing segmentation. This particular example shows only a small error with increasing segmentation because the step occurs so far out along each element. The portions of the elements with the highest current levels are essentially monotapered. With a more radical set of element-diameter tapers, less tame results will occur, as in the next model.

6-5.NEC: A tapered-diameter element Yagi

Example 6-5.NEC is also a 2-element Yagi of driver-reflector design. The dimensions are in inches for 7.1 MHz. The deceptively simple overall dimensions appear in **Figure 6-5-1**. The actual model consists of 22 wires, 11 per element. The elements taper radically from 0.5" in diameter at the tips to 2.25" in diameter near the center. The model creator added a short wide section of wire at each element center to



account for the effects of the boom-to-element mounting hardware.

In the progression of models, changing the segmentation will require care. The data entry table shows the progression of segment numbers for wires 1 through 6, where wire 6 is the reflector center wire. Reverse the pattern at this point so that the segmentation for the entire element follows the pattern 2-1-1-2-2-1-2-2-1-1-2 for the first reflector example.

For the driver, reduce the end wire segments by 1 to account for its significantly shorter length. Wire 17 is the driver counterpart to the reflector wire 6. Be certain to correctly place the source at the center of this wire.

6-5 Test Data			
No. of Segs/El.	Forward Gain dBi	Rear Gain dBi	Source Z (R±jX) Ohms
2-1-1-2-2-1			
4-2-2-4-4-1			
6-3-3-6-6-3			
7-4-4-8-8-3			
8-5-5-10-10-3			

Comments: This exercise has covered a segmentation density range from 15 to 150 segments per half-wavelength. See the reference data below. Although it may be tempting to adopt one or another line of the chart as a reasonable facsimile of a converged model, in fact, none of the lines will do. The forward gain is in all cases too high, while the rear gain is too low. The impedance is far off the mark on every line.

6-5 Reference Data			
No. of Segs/El.	Forward Gain dBi	Rear Gain dBi	Source Z (R±jX) Ohms
2-1-1-2-2-1	6.87	-3.40	33.97 - j20.48
4-2-2-4-4-1	6.34	-3.21	39.84 - j13.53
6-3-3-6-6-3	6.21	-2.86	41.71 - j 8.56
7-4-4-8-8-3	6.21	-2.58	42.31 - j 4.51
8-5-5-10-10-3	6.22	-2.36	42.58 - j 2.12

Models using other software (NEC-4) suggest a forward gain of 6 to 6.05 dBi and a rear gain of about -4 to -4.5 dBi as more nearly correct. The feedpoint impedance is close to $41 - j25$ Ohms. However, even NEC-4 requires a quite high number of segments per wire to converge, given the very large step in diameter between the center sections of each element and the adjacent sections.

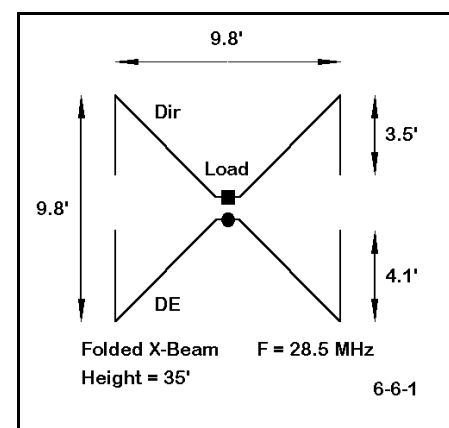
Multi-tapered linear antenna elements are an especial weakness of NEC-2. Corrective equations have been developed, the most prominent being the work of Dr. David Leeson. Essentially, these equations calculate a substitute mono-tapered element to replace the multi-tapered original. Substitute elements have produced excellent results. As we have seen (in 6-3.NEC), Yagis with monotapered elements converge quickly, that is, with a low segmentation density. See Chapter 9 for further information.

This particular model demonstrates that convergence is a necessary condition of model reliability. However, it does not alone suffice to guarantee that reliability.

There is another modeling flaw in the versions of 6-5.NEC that use low segment densities: the single segment center section is less likely to yield accurate results than a longer multi-segment (at least 3) section. However, such a move would constitute a different antenna model. Moreover, the effect of the stepped-diameter elements overrides the inaccuracies occasioned by using only one segment for the fat middle section of each element.

6-6.NEC: A folded X-beam

The model in 6-6.NEC is a folded X-beam, the overall outline of which is shown in **Figure 6-6-1**. This directional array consists ordinarily of a director and driven element. Each form a "V" at the center, which most constructors make from aluminum tubing. The model requires a short jumper from one arm to the other, which is useful in the model for placing the source and any loads. At the end of each (equal length) arm is a tail, normally of copper wire (#18). The approximate lengths of the director and the driven element tails are shown in the figure. Since these are rounded numbers, those in the model will involve more decimal places. This model is set for 28.5 MHz at a height of 35' above average earth.



Be sure to examine the model description closely. Note that the elements have separate material losses for copper and for aluminum for the appropriate wires. In addition, the director contains a load of -70 Ohms reactance placed at the center of the director to tune

the antenna for an approximation of maximum front-to-back ratio.

You may wish out of curiosity to examine the pattern for this compact array. Despite decent forward gain and a reasonable 180-degree front-to-back ratio, the quartering rear lobes make it susceptible to interfering signals from the rear.

The test data table lines indicate the segmentation in the order of director tail-(driver tail)-arm-center. The other side of the array is a mirror of these numbers. As in the preceding model, the center section is problematic when its length in relationship to adjacent wires (the arms) force the use of a single segment. Also suspicious is the close spacing of the two parallel center sections. However, these may be the least problematical aspects of trying to obtain convergence.

6-6 Test Data			
No. of Segs/El.	Forward Gain dBi	Rear Gain dBi	Source Z (R±jX) Ohms
5-(6) 8-1			
10-(12)-16-1			
15-(18)-25-3			
20-(24)-33-3			

Comments: The folded X-beam, when constructed of aluminum tubing arms and copper wire tails, simply will not converge.

6-6 Reference Data			
No. of Segs/El.	Forward Gain dBi	Rear Gain dBi	Source Z (R±jX) Ohms
5-(6) 8-1	10.51	1.69	89.48 + j 9.66
10-(12)-16-1	11.03	0.06	65.98 + j26.78
15-(18)-25-3	11.53	0.87	47.12 + j43.67
20-(24)-33-3	11.93	0.13	34.28 + j59.88

Here in a most dramatic case is an antenna model that will not converge, despite segmentation that exceeds 100 per half-wavelength. The reason for the convergence failure is the acute angular junction of wires of different diameters at each of the four corners of the array. One of the weaknesses of NEC-2 is the fact that models involving

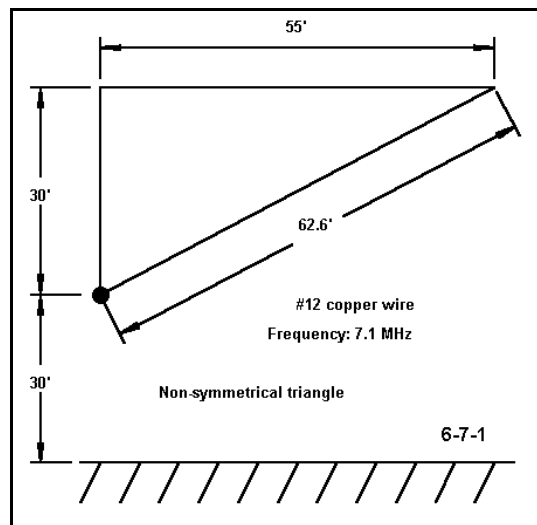
corner junctions of dissimilar diameter wires, such as the 4 corners of the X-beam in **Figure 6-6-1**, depart from reasonable values in virtually every output category.

It is possible to model the folded X-beam using single-diameter wires throughout. In some cases, the tightly acute angles may require length tapering for greatest accuracy, although with AWG wire sizes, this is rarely necessary. Fully tapered models of the folded X-beam tuned for maximum (180-degree) front-to-back ratio show forward gains of about 11.5 dBi and front-to-back ratios above 25 dB (although this does not include the large quartering rear lobes). Source impedances for models yielding these performance figures are consistently near 25 Ohms resistive.

6-7.NEC: A right triangle loop

6-7.NEC is the final example to examine for convergence. As **Figure 6-7-1** shows, the antenna is a right triangle, with the diagonal running from one upper corner to the opposing lower corner. Cut to be approximately resonate at 7.1 MHz, the antenna is #12 copper wire, with its lowest point 30' above average earth.

Since the antenna is designed to be fed at the corner forming its lowest point, the model uses a split feed. Instead of placing a single feedpoint on either one or the other side of the corner, there are two feedpoints: one on each of those immediately adjacent segments.



```

CM Convergence test 7: Non-symmetrical triangle
CE
GW 1 4 -27.5 0 30 -27.5 0 60 3.36778215223097E-03
GW 2 8 -27.5 0 60 27.5 0 60 3.36778215223097E-03
GW 3 9 27.5 0 60 -27.5 0 30 3.36778215223097E-03
SS 0 0 .3048
GE 1
GW 2 0 0 0 13 .005 0 0 0 0
EX 0 3 9 0 1 0
EX 0 1 1 0 1 0
LD 5 1 1 4 5.8001E7
LD 5 2 1 8 5.8001E7
LD 5 3 1 9 5.8001E7
FR 0 1 0 0 7.1 1
RP 0 1 360 1000 69 0 1 1
FR 0 1 0 0 7.1 1
RP 0 181 1 1000 -90 90 1 1
EN
    
```

Examine **Figure 6-7-2** and find the two sources. As you increase the segmentation density of this model, be certain the source positions remain at the corner on adjacent segments.

The source impedance of the antenna will be simply the sum of the two individual impedances, which are in series with each other. We shall have occasion with this model to look closely at those individual impedances.

The triangle model is composed of 3 wires in the order of vertical, horizontal, and diagonal, where end 2 of each connects or has the same coordinates as end 1 of the

succeeding wire (or end 1 of wire 1 in the case of end 2 of wire 3). The segmentation column lists the segmentation in the order of the wires, striving for roughly equal length segments. The gain figures may be derived from the table of elevation values, even though absolute maximum gain does not quite occur on the 90-270-degree axis.

6-7 Test Data			
No. of Segs/El.	Gain dBi	Source Z #1 (R±jX) Ohms	Source Z #2 (R±jX) Ohms
4-8-9			
8-16-18			
12-24-27			
16-32-36			
20-40-45			

Comments: The gain figure for the lowest level of segmentation (approximately 10 segments per half-wavelength) is significantly lower (numerically, although perhaps not operationally) than the remaining values. For some purposes, the next level of segmentation (approximately 20 segments per half-wavelength) may serve as the minimal convergence level.

6-7 Reference Data			
No. of Segs/El.	Gain dBi	Source Z #1 (R±jX) Ohms	Source Z #2 (R±jX) Ohms
4-8-9	2.23	21.83 + j7.57	19.26 + j6.79
8-16-18	2.41	20.03 + j5.23	18.82 + j4.96
12-24-27	2.43	19.68 + j4.66	18.88 + j4.50
16-32-36	2.44	19.51 + j4.35	18.91 + j4.24
20-40-45	2.44	19.41 + j4.16	18.92 + j4.07

However, examine the columns of source impedances. Only at the third level does the differential drop below 1 Ohm resistive. For virtually any purpose for which one might model this antenna, the model may be considered converged, despite the continuing small difference between the source impedances.

Since the antenna uses voltage sources, the currents in the fed segments (and therefore the source impedances reported) are a function of the interaction of all the segments in the antenna model. The antenna is not symmetrical on an axis bisecting the angle formed by the sides that are fed. Hence, the final currents in the fed segments are unequal. Part of that inequality arises from the fact that they are of very slightly unequal length. However, you may redesign this model so that the vertical and the diagonal sides are composed of two wires each, end to end. The wire from each pair approaching the fed corner may be made equal to its counterpart. For any reasonable level of segmentation density (for example, the highest level used in this model), the differential will persist.

As a supplemental exercise, you may reconstruct this model using current sources in place of the voltage sources. You will discover that the source impedances will differ even more radically and that convergence is more difficult to obtain. This result stems from the method of obtaining a current source within the program (a voltage source at a remote point via a transformation network). Although this system works reliably for symmetrical antenna structures relative to the source point, it yields somewhat anomalous results for non-symmetrical antennas, such as this triangle.

An alternative model for the split-feed triangle is to create a short fourth wire across the feedpoint region and to provide it with a single feed. Such a model would use the highest segmentation level in this exercise so that the new wire could be very short (about 1.4' long if placed between the 1' vertical mark and the 1' horizontal mark on the currently joining wires). Such models show reasonably good convergence with those using three

times the segmentation density. The gain is about 2.5 dBi with a source impedance of about $39 + j6.5$ Ohms. Although the model seems to solve any lingering questions concerning convergence, the antenna retains its lack of symmetry of currents in the feedpoint region.

Summing Up

The temptation to use the minimum number of segments possible in a model in order to speed the process of obtaining results can yield poor models of dubious reliability. Only the simplest linear antennas produce successful models with minimal segmentation density. For each antenna geometry, there is a minimal segmentation density for accurate results. For a few, as we have seen, no segmentation density will result in a converged model.

The actual minimum segmentation density to be used, however, is not determined by NEC-2 alone. Rather, the degree of convergence needed is also a function of the overall objectives of the modeling task, which may in turn be a function of a larger set of project objectives. Understanding your goals in modeling--whether they are set for you or you develop them yourself--is a key to effective antenna modeling.

Fortunately, antennas come in groups or types. Therefore, once you gain some familiarity with the modeling behaviors of representatives of an antenna type, you may transfer what you learn to other antennas of the same or similar types. However, whenever some new wrinkle occurs in the design, some further convergence testing is always appropriate in order to achieve the most reliable models possible.

User Notes

7. Frequency Specification

***Objectives:** The exercises in this chapter will develop an understanding of the importance of careful frequency specification for models. The chapter will guide you from one-frequency ("spot") modeling to various types of multi-frequency ("sweep") modeling. The chapter will also introduce you to potentials and pitfalls in frequency-scaling your models.*

The frequency specification for an antenna model is often overlooked, perhaps because some think it trivial or obvious. However, it is an important aspect of antenna modeling, worth spending some time pondering both its possibilities and its limitation for helping us gain a better understanding of the antennas we model.

For single frequency antennas, the specification is easy. However, these are not the only types of antenna models we shall encounter. Multi-frequency antennas, whether they have continuous coverage over a span of frequencies or operate at several discrete frequency bands, are commonplace projects for design and analysis. In each test, we must review the source position of relevance and the adequacy of segmentation for each frequency checked.

Moreover, we shall often be interested in the characteristics of antennas at other than their primary operating frequencies. The responses to other frequencies--normally above the primary operating frequency, but only sometimes harmonically related to a given antenna--may represent either bonuses or problems. For example, a 40-meter amateur-band antenna with a 50-Ohm source impedance at 7 MHz may show a low impedance also around 18 MHz. Such behavior may be viewed as a "bonus" insofar as it is close to the 17-meter amateur band. In contrast, An 80-meter antenna that is responsive to high power shortwave broadcasting station below 7.5 MHz and has a source impedance that allows efficient transfer of this energy to the receiving system may constitute a design problem for the antenna maker. The technique of modeling an antenna over an extended range of frequencies is called a **frequency sweep**.

We often perform frequency sweeps over more restricted frequency ranges. We may be interested in observing an antenna's characteristics across a band of frequencies that set limits to the antenna's operating bandwidth. Such factors as gain, front-to-back ratio, and source impedance (with attention to the VSWR relative to an intended transmission line) are all important design considerations. However, we may also extend the sweep outside the band of intended use to observe the antenna's characteristics for diagnostic

purposes. By observing both the peaks and the slopes of curves for gain, front-to-back ratio, and source impedance, we can make adjustments in the antenna's geometry to capture the best compromise among them, relative to the specific design goals governing our project.

A third dimension to frequency specification is called **frequency-scaling**. For most antenna types, it is possible to scale an antenna by reference to a ratio of design frequency to desired frequency. The scaling must include all antenna dimensions. Element length and spacing are automatically covered by scaling the geometric coordinates of a model in free space symmetrically positioned about the 0, 0, 0 point of the cartesian system. However, scaling only works if we also scale the element diameters. Converting a 14.4 MHz 2-element Yagi to 144 MHz requires that we shrink the element lengths and spacings by a factor of 10, and that we also shrink the element diameter by an equal factor. The result may yield an element size that is impractical or which varies from standard materials by enough to change the antenna's performance. In short, scaling is the beginning--not the end--of a new antenna modeling project.

There are enough interactive considerations connected with frequency specification to last us through several interesting exercises.

Exercise Preparation

We shall divide the exercises into three sections: spot frequency specification, frequency sweeping, and frequency-scaling. Our interest in each type of case will differ, so expect to develop different information for each of the exercises. In some cases, we shall only be interested in the paper planning form that defines the model to ensure that we have constructed as adequate a model as NEC-2 can handle. In other cases, we shall look at different types of output data, ranging over gain, front-to-back ratio (where that data is relevant to an antenna design), and source impedance in terms of both resistive and reactive components. We shall in some cases also request you to adjust one or more aspects of the model's geometry.

As always, if you save variants of the basic model, alter the filename before saving to preserve the original model. In addition, at least one exercise will develop a very sizable NEC output file (>1MB). This may be a good time to ensure that you have adequate storage memory available for these and future exercises. A large output file also indicates that considerable run time may be required. As models grow larger in terms of the number of wires and the number of segments, run times for the NEC-2 core will increase. Likewise, as we request multiple runs, as we do when performing a frequency sweep, run times will increase. The combination of the two may produce runs (within these exercise sets) of up to several minutes. The exact duration will depend upon the basic speed and the available working memory of your computer. Operations are slowed

further when NEC-2 must transfer some items to storage to make room to work on others. Do not prematurely decide that something has gone wrong. In virtually all cases, NEC-2 will work to successful completion of the model calculations.

7-1.NEC: A two-frequency coupled dipole set

Open file 7-1.NEC, the description for which appears at the right. The dipole pair is set up for operation at 10.125 MHz and at 18.118 MHz. both use 12.5 mm 6061-T6 aluminum elements, with all dimensions given in meters. The model, as presently given, shows a frequency specification for 10.125 MHz.

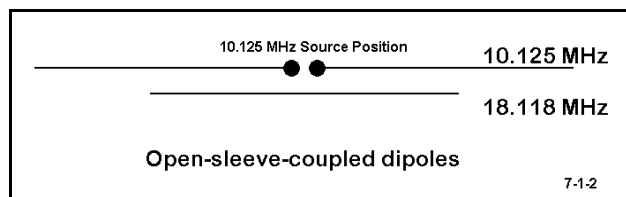
Your task for this antenna is to set up and run the model at the second frequency of operation, 18.118 MHz.

```

CM dipoles:  open sleeve coupling
CM 10.125MHz, 18.118 MHz
CE
GW 1 31 -7.2 0 15 7.2 0 15 .00625
GW 2 17 -4 .1 15 4 .1 15 .00625
GS 0 0 1
GE 1
GN 2 0 0 0 13 .005 0 0 0 0
EX 0 1 16 0 1 0
LD 5 1 1 31 2.4938E7
LD 5 2 1 17 2.4938E7
FR 0 1 0 0 10.125 0
RP 0 181 1 1000 -90 90 1 1
EN

```

7-1-1



Comments: You should have obtained source impedances in the low 60- Ω range for both runs. If you did not, the most likely source of error was attempting to change the source position from wire 1 to wire 2, since it was labeled as the 18.118 MHz element. However, notice that the

description of this antenna included the notation that it employs open-sleeve coupling. See **Figure 7-1-2**. This feed system uses the longer antenna as the single feedpoint for both frequencies. Hence, no action other than changing the initial frequency was needed to run the antenna model. Lesson: always determine (and never presume) the correct source position in an array for the frequency of interest.

Although only a change in frequency was called for as an action, several considerations should have been part of your pre-run effort. Is the element pair adequately segmented for the higher frequency? Using an arbitrary standard of about 10 segments per $1/2\lambda$, and given the shorter element length as about $1/2\lambda$, the segmentation more than meets this guideline. Given the close element spacing, are the segments well aligned between the two elements. Rather than calculate the length of each segment (0.46 m/seg for the 30-m element; 0.47 m/seg for the 17-meter element), you may gain more information from viewing the antenna structure graphic (NECVu). By displaying the segmentation, you can visually examine the relative lengths and their alignment. Note that because each element uses an odd number of segments, the center segments (with the highest current levels) are in fact aligned. You may wish to reduce the number of segments on the shorter wire by 1 and again view the alignment.

The model was placed 15 m above average earth. The difference in the elevation patterns for the two frequencies should arouse no surprise, given our past exercises dealing with take-off angles. However, notice that there is a very slight "front-to-back ratio" at each of the two frequencies. Although the elements are too close together and too diverse in length for significant directivity, they are not totally immune to parasitic interaction in the direction of the shorter element.

7-2.NEC: Nested 2-element quad beams for 14.175 and 28.5 MHz

Open file 7-2.NEC. The description to the right makes it seem relatively formidable compared to the antennas we have so far used in our exercises. Part of this is true and part illusion bred of many decimal places. Examine the last value in each wire line--the wire radius. The value is for #14 AWG wire. No harm would accrue to the model if you were to shorten the value in each line to 2.67-E3.

A second file stretcher is the 16 LD lines, each specifying the conductivity of copper for a

```

CM 10/20m Quad .16 wl spacing
CE
GW 1 15 -8.78 5.55 -8.78 8.78 5.55 -8.78 2.67060367454068E-03
GW 2 15 8.78 5.55 -8.78 8.78 5.55 8.78 2.67060367454068E-03
GW 3 15 8.78 5.55 8.78 -8.78 5.55 8.78 2.67060367454068E-03
GW 4 15 -8.78 5.55 8.78 -8.78 5.55 -8.78 2.67060367454068E-03
GW 5 15 -9.21 -5.55 -9.21 9.21 -5.55 -9.21 2.67060367454068E-03
GW 6 15 9.21 -5.55 -9.21 9.21 -5.55 9.21 2.67060367454068E-03
GW 7 15 9.21 -5.55 9.21 -9.21 -5.55 9.21 2.67060367454068E-03
GW 8 15 -9.21 -5.55 9.21 -9.21 -5.55 -9.21 2.67060367454068E-03
GW 9 7 -4.33 2.75 -4.33 4.33 2.75 -4.33 2.67060367454068E-03
GW 10 7 4.33 2.75 -4.33 4.33 2.75 4.33 2.67060367454068E-03
GW 11 7 4.33 2.75 4.33 -4.33 2.75 4.33 2.67060367454068E-03
GW 12 7 -4.33 2.75 4.33 -4.33 2.75 -4.33 2.67060367454068E-03
GW 13 7 -4.62 -2.75 -4.62 4.62 -2.75 -4.62 2.67060367454068E-03
GW 14 7 4.62 -2.75 -4.62 4.62 -2.75 4.62 2.67060367454068E-03
GW 15 7 4.62 -2.75 4.62 -4.62 -2.75 4.62 2.67060367454068E-03
GW 16 7 -4.62 -2.75 4.62 -4.62 -2.75 -4.62 2.67060367454068E-03
GS 0 0 .3048
GE 0
EX 0 1 8 0 1 0
LD 5 1 1 15 5.8001E7
LD 5 2 1 15 5.8001E7
LD 5 3 1 15 5.8001E7
LD 5 4 1 15 5.8001E7
LD 5 5 1 15 5.8001E7
LD 5 6 1 15 5.8001E7
LD 5 7 1 15 5.8001E7
LD 5 8 1 15 5.8001E7
LD 5 9 1 7 5.8001E7
LD 5 10 1 7 5.8001E7
LD 5 11 1 7 5.8001E7
LD 5 12 1 7 5.8001E7
LD 5 13 1 7 5.8001E7
LD 5 14 1 7 5.8001E7
LD 5 15 1 7 5.8001E7
LD 5 16 1 7 5.8001E7
FR 0 1 0 0 14.175 0
RP 0 1 360 1000 90 0 1 1
EN

```

separate wire. Although there are means of shortening this to a single line, wire geometry

input systems like the one in NECWin Plus tend to treat each wire separately. Although the number of lines multiplies, the simple ASCII file is not burdensome. Moreover, the NEC output file is not lengthened significantly by using the long form for registering wire conductivity.

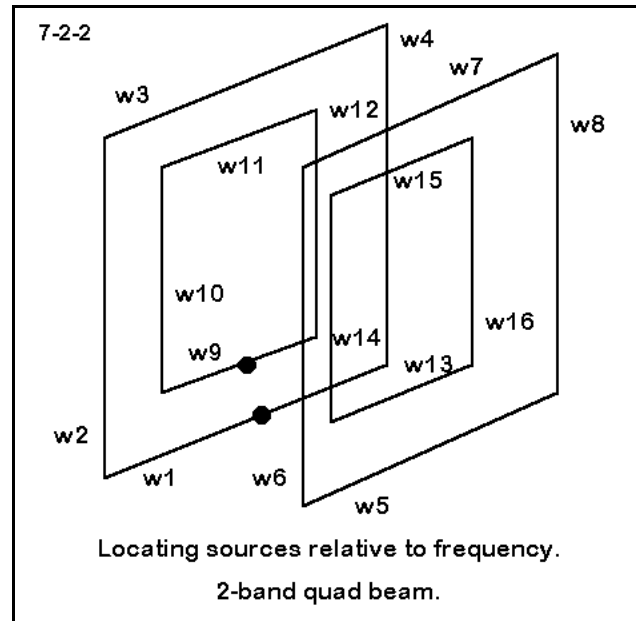
The antenna is actually 2 2-element beams in one overall space, each centered about the 0, 0, 0 axis coordinate. One pair of loop elements is for 14.185 MHz; the other is for 28.5 MHz. Since some of the Z-axis values are negative, the model must be set in free space or else there is an error in the geometry values. Verify the ground (or lack of ground) for the model. Also, verify the adequacy of segmentation for the highest frequency to be used with the model, using our 11-segments-per- $1/2\lambda$ working criterion.

As set up, the model uses the center of the lowest horizontal wire of the 14.175 MHz driven element (wire 1) for the source. Locating the source position for use of the array at 28.5 MHz can be puzzling unless you draw a sketch similar to **Figure 7-2-2**. Since the 14.175 MHz driven element is on the smaller of the 20-meter loops, the antenna configuration is a driver and a parasitic reflector. Without outside information, it is most probable that the 10-meter pair of loops follows the same configuration, placing the source on wire 9 at the center.

Run the model at 14.175 MHz. Then revise it to run at 28.5 MHz. Record the following data for each frequency: forward gain, worst-case front-to-back ratio, 180-degree front-to-back ratio, input impedance. Some of this data may be obtained from the requested azimuth pattern; other data must come from the tabular data either directly or by simple calculations shown in earlier exercises.

Comments: If the 28.5 MHz model refused to run fully without error, recheck your placement of the source. In moving it to wire 9, note that the wire has only 7 segments. The center segment is 4. Leaving the value at the 20-meter wire value of segment 8 (for 15 segments per wire) will cause NEC-2 to close prematurely and advise you of the existence of an error.

The figures for the 28.5 MHz run should come out close to those for the 14.175 MHz run: gain 7.0 dBi or slightly higher, worst case front-to-back ratio a little above or below 17 dB,



180-degree front-to-back ratio above 33 dB, and a source impedance near resonance in the 133-135- Ω range.

Although we have used the model for its frequency-specification purposes, like most models, it holds added interest. For example, use the 20-meter version of the model, with the source on wire 1, but run it at 28.5 MHz. Examine both the source impedance and the azimuth pattern. With the source close to resonance, the antenna is essentially a wide-spaced 2-element beam composed of 2λ loops (rather than the standard quad loop length of 1λ). Examine the Currents table for current maxima around the wire and compare those points to the directions of maximum gain. Now compare those values to the current maxima placement for either of the models run at its primary frequency.

This is only a sample of what we might learn about nested quad beams. We can also reconstruct the model so that the unused driven element is no longer a closed loop, but has a gap that models leaving the unused feedpoint an open circuit. With adjustments to the loops for resonance, we can also stretch wires 1 and 9 (by making more wires) to bring the feedpoints together into a common feed for the two antennas. Both projects will help refine our knowledge of quad beam performance.

7-3.NEC: A 51 MHz $1/4\lambda$ vertical with a sloping ground plane

File 7-3.NEC describes a $1/4\lambda$ vertical with a sloping ground plane for 51 MHz. The dimensions are in meters using 5 mm diameter aluminum for both the vertical element (1.425 m long) and the sloping ground plane wires. The coordinates for the ends of the ground plane wires indicate that they are at 45° angles relative to the horizontal. A little geometry reveals that they are about 1.243 m long. The feedpoint is at the lowest segment of the vertical element.

Run this model, recording the source impedance. Then revise the model, changing the diameter of all wires to 1 mm. Record the source impedance. Note the reactance. Reset the frequency until you find the resonant frequency (where the source impedance is a value of resistance ± 1 to 2 Ω reactance or less). Finally, return to the original frequency setting of 51 MHz and change the wire diameters to 25 mm. Record the source impedance and then find the resonant frequency of the antenna. Place your data on the following table. You may choose other wire diameters to extend the exercise.

CM Vertical, sloping gp, 51 MHz
CE
GW 1 30 0 0 1.425 0 0 0 .0025
GW 2 20 0 0 0 .8789 0 -.8789 .0025
GW 3 20 0 0 0 0 .8789 -.8789 .0025
GW 4 20 0 0 0 -.8789 0 -.8789 .0025
GW 5 20 0 0 0 0 -.8789 -.8789 .0025
GS 0 0 1
GE 0
EX 0 1 30 0 1 0
LD 5 1 1 30 2.4938E7
LD 5 2 1 20 2.4938E7
LD 5 3 1 20 2.4938E7
LD 5 4 1 20 2.4938E7
LD 5 5 1 20 2.4938E7
FR 0 1 0 0 51 0
RP 0 181 1 1000 -90 0 1 1
EN

7-3-1

7-3 Test Data			Reference Data	
Wire Diameter	Source Z (R ± j X Ω)	Resonant Frequency	Source Z (R ± j X Ω)	Resonant Frequency
5 mm		-----	47.0 - j 0.2	-----
1 mm			46.4 - j 11.1	51.65 MHz
25 mm			50.3 + j 12.0	49.75 MHz

Comments: The exercise illustrates the dependence of the resonant frequency of an antenna with linear elements upon the wire diameter. From the original diameter, we decreased and increased the diameter of all wires by a factor of 5. Thinning the wire had the effect of raising the resonant frequency--or of yielding a capacitively reactive source impedance at the original frequency. Fattening the wire has the opposite result: lowering the resonant frequency or yielding an inductively reactive source impedance at the original frequency. Similar results would accrue to almost any antenna whose elements are open-ended, including dipoles and longer wire antennas. Where an antenna design already shows a reactive feedpoint impedance, the increases and decreases will follow the same pattern.

In this exercise, we shall not exhaust our interest in the sloping ground-plane vertical. Placing it in free space was convenient to the main goal of the exercise. Placing it at various heights above real ground of various sorts and tacking the resonant frequency movement, if any, would be interesting. Equally useful would be to observe the azimuth pattern for maximum gain--and then comparing that figure with similar figures for a cluster of ground plane slopes ranging from horizontal down to near vertical below the main element.

7-4.NEC: A 51 MHz quad loop

Our next file, 7-5.NEC, is a free space vertically oriented quad loop using 6061-T6 5 mm wire and resonant at 51 MHz. With the source at the center of the lower horizontal wire, the antenna is horizontally polarized.

Run this antenna just as you did the sloping ground-plane vertical: first with the preset 5 mm wire, then with 1 mm and with 25 mm wire. In the table below, record the source impedance for each size wire at

```

CM Quad, 1-e1, 51 MHz, 5mm wire
CE
GW 1 7 -.791 0 -.791 .791 0 -.791 .0025
GW 2 7 .791 0 -.791 .791 0 .791 .0025
GW 3 7 .791 0 .791 -.791 0 .791 .0025
GW 4 7 -.791 0 .791 -.791 0 -.791 .0025
GS 0 0 1
GE 0
EX 0 1 4 0 1 0
LD 5 1 1 7 2.4938E7
LD 5 2 1 7 2.4938E7
LD 5 3 1 7 2.4938E7
LD 5 4 1 7 2.4938E7
FR 0 1 0 0 51 0
RP 0 1 360 1000 90 0 1 1
EN
    
```

51 MHz and then for the non-resonant cases, find the new resonant frequency.

7-4			Test Data			Reference Data		
Wire Diameter	Source Z ($R \pm j X \Omega$)	Resonant Frequency		Source Z ($R \pm j X \Omega$)	Resonant Frequency			
5 mm		-----		128.3 - j 0.9	-----			
1 mm				133.8 + j 47.4	50.10 MHz			
25 mm				121.5 - j 46.5	52.85 MHz			

Comments: If you compare this table to the one for the last exercise, you will immediately see that the impedance and resonant frequency patterns are opposite each other. Whereas open-ended antenna elements drop in resonant frequency as the element diameter increases, closed-geometry elements, such as the quad loop, increase in resonant frequency with increases in wire diameter. There are a number of antenna configurations, such as the folded X-beam (see Chapter 6), that are seemingly open-ended insofar as their elements terminate. However, in some cases, the close coupling of wire ends between elements gives them closed-geometry characteristics relative to wire size and resonant frequency.

7-5.NEC: A 2-element Yagi for 14.175 MHz

With 7-5.NEC, we turn from spot frequency discoveries to frequency sweeping. The 2-element Yagi described to the right uses 1" 6061-T6 elements in a driven element-reflector design, with dimensions measured in feet. For the exercise, free space will do fine as an environment.

```

CM Yagi, 2-el, 1" el
CE
GW 1 21 -17.5 0 0 17.5 0 0 .04165
GW 2 21 -16.05 9.63 0 16.05 9.63 0 .04165
GS 0 0 .3048
GE 0
EX 0 2 11 0 1 0
LD 5 1 1 21 2.4938E7
LD 5 2 1 21 2.4938E7
FR 0 1 0 0 14.175 0
RP 0 1 360 1000 90 0 1 1
EN

```

7-5-1

Although the frequency is specified as a single or spot frequency, we shall create a frequency sweep. The antenna is designed for the 20-meter amateur band, which extends from 14.0 to 14.35 MHz. We shall wish to check certain characteristics of the antenna across the band.

There are several input methods made available by different commercial implementations of NEC-2 for creating a frequency sweep.

1. Specify the starting frequency, the ending frequency, and the size of the interval between frequencies (or "step") for which NEC-2 will make a run. If the ending frequency is important, you must choose an interval or step which will finally coincide with the ending

frequency. Otherwise, NEC-2 will make its last run at the highest frequency not exceeding the ending frequency. For the present case, specifying 14.0, 14.35, .05 will create 8 runs (including the start and end frequencies).

2. Specify the starting frequency, the step, and the number of steps. In this input method, the ending frequency is determined by the size of the step and the number of them, relative to the starting frequency. If you require a specific end frequency, you must calculate the interval and number of steps needed to include that frequency. The difference in frequencies divided by the interval plus 1 is the number of steps needed. For this example, specifying 14.0, .05, 8 would produced the desired result.

In either input system, the resultant frequency card will read

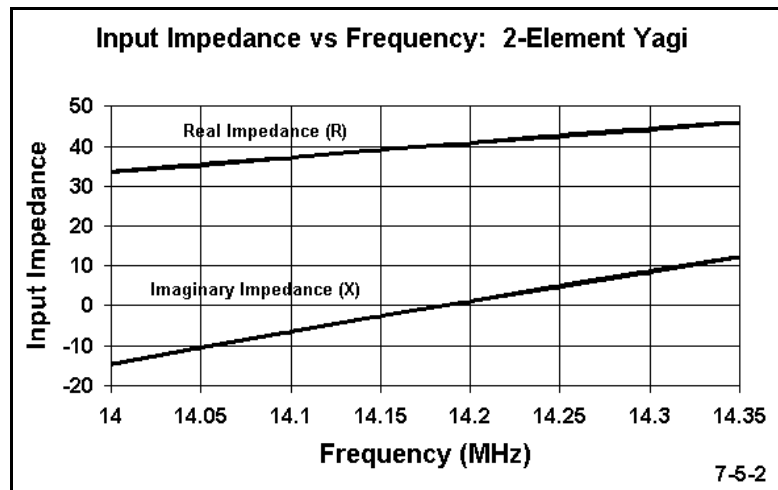
FR 0 8 0 0 14 .05

Transform the frequency card to this sweep and run the model. Record the figures for forward gain and for 180° front-to-back ratio in the table below.

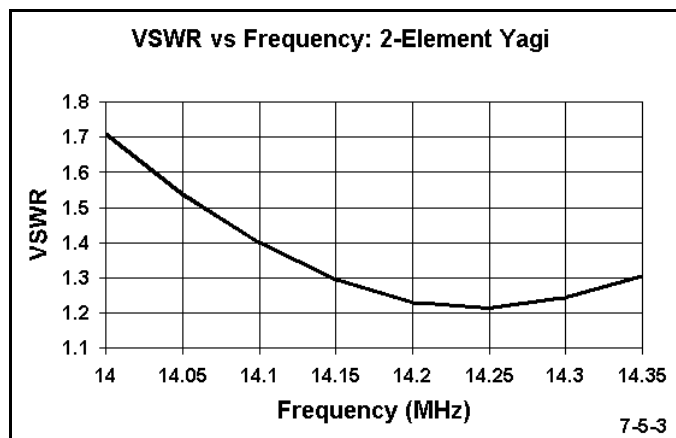
7-5 Test Data			Reference Data	
Frequency	Gain dBi	F-B dB	Gain dBi	F-B dB
14.00			6.45	10.83
14.05			6.36	11.01
14.10			6.27	11.10
14.15			6.18	11.09
14.20			6.10	11.03
14.25			6.02	10.91
14.30			5.94	10.75
14.35			5.87	10.57

Comments: The table makes clear that the 180° front-to-back ratio peaks between 14.1 and 14.15 MHz. The gain increases continuously as the frequency decreases, so that the peak gain of the antenna occurs at a frequency below those scanned.

In addition, we may obtain source impedance data. An alternative to tabulation is graphing, as shown in **Figure 7-5-2**. The antenna appears resonant at the design frequency of 14.175 MHz. The resistive portion of the impedance runs between 35 and 45 Ohms, which suggests that it might be directly matched to a 50- Ω coaxial cable within 2:1 VSWR limits. To check the correctness of this impression,



we may also create either a table or a graph of 50- Ω VSWR values across the frequency span. **Figure 7-5-3** shows the results at the top of the next page.



The question of the gain peak--and its associated value of 180° front-to-back ratio--might nag the antenna designer. Knowing the values outside the band limits might give some important clues concerning redesign of the antenna in order to achieve the best possible performance within the band limits. To do this check, we need not rerun the frequency span above 14.0 MHz. Instead, we may rewrite the frequency line to cover 13.7 to 14.0 MHz on 7 steps of 0.05 MHz each. If we think

there is other significant data within the first sweep, we may wish to give the second sweep file a new name.

If you make this run, you will discover that the maximum gain peak occurs at a frequency below 13.7 MHz. At that frequency, the front-to-back ratio is only about 7.5 dB. However, the front-to-back ratio passes 10 dB at about 13.9 MHz, where the gain is over 6.6 dBi. If the characteristics of the antenna can be shifted upward in frequency by about 0.1 MHz, the front-to-back ratio peak might be closer to the design frequency at mid-band, with an overall increase in antenna gain across the band. However, the source impedance would decrease, perhaps requiring a matching network for use with 50- Ω coaxial cable. The utility of frequency sweeps for both design and analysis of antennas is obvious.

7-6.NEC: A 3-element Yagi for 14.175 MHz

File 7-6.NEC contains a 3-element Yagi of the same materials (1" diameter 6061-T6 aluminum) in the same dimensional units (feet) at the same frequency (14.175 MHz) as the 2-element Yagi of 7-5.NEC. Of course, the 3-element Yagi adds a director to the 2-element Yagi's reflector and driven element.

Even though we fully expect the 3-element Yagi to have better performance figures than the 2-element Yagi in terms of forward gain and 180°

front-to-back ratio, it will be interesting to compare some of the trends in these numbers and the source impedance numbers for the two types of parasitic beams. We shall discover that the addition of a director to the driven element and reflector creates a different pattern of basic characteristics, one which characterizes even larger Yagis with numerous directors.

Therefore, let's run the same fundamental set of exercises for this antenna, using the span from 14.0 to 14.35 MHz in 8 0.05 MHz steps. Record your data on the table at the top of the next page.

```

CM Yagi, 3-el, 1" el
CE
GW 1 21 -17.7 0 0 17.7 0 0 .04165
GW 2 21 -16.7 6.67 0 16.7 6.67 0 .04165
GW 3 21 -15.57 15.5 0 15.57 15.5 0 .04165
GS 0 0 .3048
GE 0
EX 0 2 11 0 1 0
LD 5 1 1 21 2.4938E7
LD 5 2 1 21 2.4938E7
LD 5 3 1 21 2.4938E7
FR 0 1 0 0 14.175 0
RP 0 1 360 1000 90 0 1 1
EN

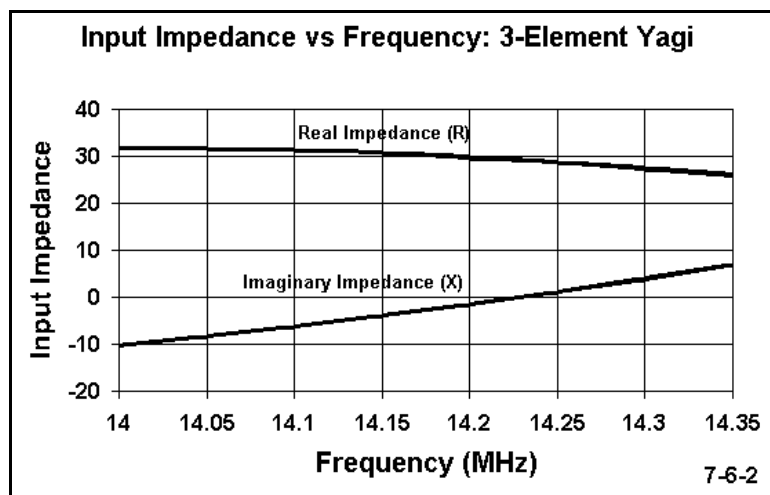
```

7-6-1

7-6 Test Data			Reference Data	
Frequency	Gain dBi	F-B dB	Gain dBi	F-B dB
14.00			7.15	21.52
14.05			7.16	21.87
14.10			7.17	22.11
14.15			7.20	30.69
14.20			7.23	37.18
14.25			7.27	35.58
14.30			7.32	29.12
14.35			7.38	24.94

Comments: As expected, the 3-element Yagi surpasses the 2-element Yagi in both gain and 180° front-to-back ratio. If we compare the Yagi in 7-6.NEC with some other 3-element designs, we may realize that it does not reach the gain levels of some designs (peak free space gains > 8 dBi). However, it shows excellent front-to-back characteristics across the band. (Nevertheless, check the worst-case values for the front-to-back ratio before reaching final conclusions.)

In contrast to the 2-element Yagi, the 3-element beam shows a steady increase in gain as the frequency increases. Indeed, the peak gain appears to occur well above the upper frequency limit of our sweep. The front-to-back ratio peaks within the band and close to the center frequency of the original design.



A graph of the source impedance in **Figure 7-6-2** shows another trend in Yagis with directors. Unlike the source impedance of the 2-element Yagi, the resistive component of the 3-element Yagi decreases as the frequency increases.

It should be clear that the ability to perform frequency sweeps across limited spans of interest provides at least two types of

important information. First, frequency sweeps give us important information relevant to the evaluation of given antenna designs. Second, they permit us to compare and contrast performance trends among different types of antennas.

7-7.NEC: A dipole resonant at 1 MHz

The antenna in 7-7.NEC is very simple: a 1 MHz copper dipole 145.59 m long and 25 mm in diameter. What is complex about this model is not the wire itself, but what we are going to do it. The frequency (FR) card is the clue. It calls for a frequency sweep starting at 1 MHz and proceeds for 91 0.1 MHz steps, to finish at 10 MHz. As with all frequency sweep models, before running it, verify

```

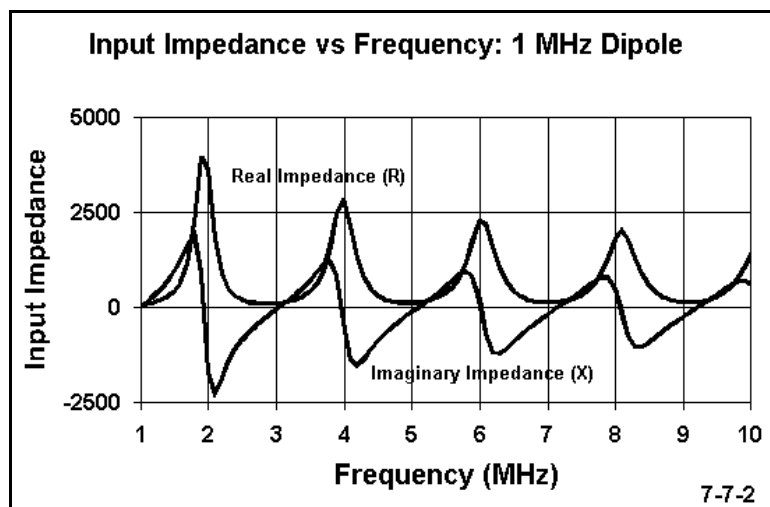
CM 1 MHz dipole: free space
CE
GW 1 111 145.59 0 0 0 0 0 .0125
GS 0 0 1
GE 0
EX 0 1 56 0 1 0
LD 5 1 1 111 5.8001E7
FR 0 91 0 0 1 .1
RP 0 1 2 1000 90 0 1 10
EN

```

7-7-1

that the segmentation is adequate at the highest frequency to be used. Unless you have access to all NEC-2 control cards or plenty of time, do NOT run this file.

91 patterns from 1 to 10 MHz would slow the calculations of NEC-2 to a crawl. Since we are interested in the progression of the source impedance through the frequency sweep, the patterns would be superfluous. We should execute the model with an XQ card to exclude pattern data. A simplified RP0 entry will do almost as well. Adding a PT-1 control card to exclude printing the unneeded current values would shorten the file. NECWin Plus does not access either the XQ or PT-1 cards, but always uses an RP card. (Refer to the NEC-2 Manual for details of NEC-2 input and control cards that are outside the scope of this guide.)



7-7-2

Comments: The graph of impedance values for the 1 MHz dipole has several interesting features. First, you may count the resonant points (including the initial 1 MHz point). Count one resonance for each place the reactance line crosses the zero line of the graph. Note the very broad resonances at low resistance values and the very sharp or narrow resonances at high resistance values.

The high resistance points, of course, mark antenna lengths of 1λ and multiples thereof as the frequency increases. Notice also that the first peak occurs prior to the 2 MHz

point, but the peaks grow further apart, since there are more wavelengths of wire, but only 2 ends to provide shortening effects.

There are innumerable uses for such broad frequency sweeps to check both the impedance and the pattern characteristics of antennas. Because NEC-2 slows down in handling very large matrices, you may not wish to make frequency sweep runs larger than this one. Instead, make multiple runs, for example from 1 to 10 MHz, then from 10 to 20 MHz, etc., where 91 to 101 steps per run is a practical maximum. You will save considerable time, since the file revision step between runs is quick.

NEC7-8.NEC: A scalable 3-element Yagi for 144.5 MHz

Once more, our subject file, 7-8.NEC, is a simple one--a 3-element 144.5 MHz Yagi composed of 3/16" (0.1875") 6061-T6 elements. The antenna is highly segmented (31 per element), and the source is at the center of the second element. Spacing is counted from the reflector forward to the director, and the elements are set symmetrically about the X-axis. The antenna is in free space and only a standard free space azimuth plot is requested.

```
CM Yagi, 3-el, 3/16" el
CE
GW 1 31 -20.181 0 0 20.181 0 0 .09375
GW 2 31 -19.228 13.341 0 19.228 13.341 0 .09375
GW 3 31 -18.078 27.508 0 18.078 27.508 0 .09375
GS 0 0 .02540
GE 0
EX 0 2 16 0 1 0
LD 5 1 1 31 2.4938E7
LD 5 2 1 31 2.4938E7
LD 5 3 1 31 2.4938E7
FR 0 1 0 0 144.5 0
RP 0 1 360 1000 90 0 1 1
EN
```

7-8-1

Initially, run the file and record the gain, 180-degree front-to-back ratio, and source impedance in the table below.

7-8 Test Data				
Frequency MHz	Element diameter (in.)	Gain dBi	F-B dB	Source Z (R ± jX Ω)
144.5	0.1875 (3/16")			
222.5	0.122			
222.5	0.125 (1/8")			
435	0.623			
435	0.10			
435	0.0641 (#14)			

As you can see, there will be further entries in this table once we decide what to do with the antenna. The frequencies listed suggest that we shall be **frequency-scaling** this

antenna for use at those other spots in the spectrum.

Frequency-scaling is a process of adjusting all antenna specifications to achieve the same performance at the new frequency as at the old. There are two processes by which we can scale and two ways of handling the antenna model. You may select any combination that suits you. As well, truncate the number of decimal places in each entry to a level suited to some presumed task.

A. **Element handling:** Two methods of treating antenna element dimensions correspond to traditional physical measures and to cartesian modeling coordinates.

1. **Physical measures:** Convert the antenna into a series of dimensions:

Reflector Length	40.362"
Driver length	38.456"
Director length	36.156"
Ref-to-Dr space	13.341"
Ref-to-Dir space	27.508"
Element diameter	0.1875"

2. **Model Coordinates:** Use the antenna model coordinates as a reference:

Reflector Length	X1	±20.181
Driver length	X2	±19.228
Director length	X3	±18.078
Ref-to-Dr space	Y2	13.341"
Ref-to-Dir space	Y3	27.508"
Element diameter	--	0.1875"

B. **Conversion to a new frequency:** Both direct and symbolic methods may be used for conversion, depending upon the anticipated number of frequency-scalings.

1. **Direct conversion:** Determine the frequency ratio between the present and the new frequency and multiply each dimension by the ratio. (In this example, we shall use the physical lengths of the elements, as specified in A.1. above.)

Old frequency	144.5
New frequency	222.5
Ratio of old to new	0.649438
New Reflector Length	26.213"
New Driver length	24.975"
New Director length	23.481"
New Ref-to-Dr space	8.664"

New Ref-to-Dir space 17.865"
 New Element diameter 0.1218"

2. **Conversion by fractions of a wavelength:** Determine the length of a wavelength at the original frequency in the units of measure of the original antenna. Create a set of dimensions as functions of a wavelength. Then apply to any new frequency by substituting its wavelength for the variable λ . (In this example, we shall use the coordinates described in 1.B. above.)

Wave length at 144.5 MHz 81.68066"
 Reflector Length X1 $\pm 0.24707 \lambda$
 Driver length X2 $\pm 0.23540 \lambda$
 Director length X3 $\pm 0.22132 \lambda$
 Ref-to-Dr space Y2 0.16333λ
 Ref-to-Dir space Y3 0.33677λ
 Element diameter -- 0.00230λ
 Wave length at 222.5 MHz 53.04654"
 Wave length at 435.0 MHz 27.13300"

Note that the equations for the antenna coordinates may be entered into the symbolic data entry system of NECWin Plus. As frequency is altered, the antenna will auto scale to the new frequency. Since element diameter is not part of the X, Y, Z coordinate system, be certain that there is an appropriate entry for the element diameter.

Create and run scaled models of the original antenna for 222.5 MHz and for 435 MHz, entering their data in the row that accurately lists the element diameter.

Comments: Compare your data to the reference table.

7-8				
Reference Data				
Frequency MHz	Element diameter (in.)	Gain dBi	F-B dB	Source Z (R \pm jX Ω)
144.5	0.1875 (3/16")	8.27	24.66	24.2 - j 0.6
222.5	0.122	8.26	24.59	24.2 - j 0.6
222.5	0.125 (1/8")	8.28	24.28	24.0 - j 0.2
435	0.0623	8.24	24.25	24.3 - j 0.5
435	0.10	8.56	18.60	19.4 + j 8.1
435	0.0641 (#14)	8.28	24.29	24.0 - j 0.1

Notice in the 222.5 MHz entry that the element diameter does not exactly correspond to a readily available wire, rod, or tubing size. Reset the diameter of each element to the nearest size of readily available material, for example, 1/8" (0.125"). Rerun the model at 222.5 MHz and record the results. In this case, the differences are likely to be judged to be too small to make a difference.

For the 435 MHz scaling of the original antenna, the element diameter specified by the scaling process is 0.0623. The nearest rod size may be 0.10" in diameter. Try this value as the element diameter and run the model at 435 MHz. Notice the differences in overall performance (which means not focusing on the higher gain figure alone). Now try #14 wire (diameter 0.0641"). The performance is now much closer to that of the perfect scaling and of the original antenna.

Frequency-scaling an antenna carries with it a set of cautions. In these monotapered element models, finding a suitable material close enough in diameter to the scaled requirement is a measure of the feasibility of the design. In the HF region, where elements may be tapered in diameter over many steps, frequency-scaling creates a consideration over and above finding relevantly similar materials. The scaled tapering schedule may not be structurally as sound as the original element--or it may be unnecessarily complex and heavy relative to the wind loading and other specifications for the design. As convenient and useful as frequency-scaling may be, it must always be used with due attention to the physical properties of the resulting design.

Summing Up

The frequency dimensions of antenna modeling offer many opportunities for generating good antennas from proven designs and for fully exploring the spot and extended frequency characteristics of any antenna under study. Spot checks and frequency sweeps are more than matters of casual interest: they are one of the fundamental tools for developing a fuller understanding of antennas in general and of specific designs.

The use of frequency checks, sweeps, and scalings is quite straightforward. More significant than merely knowing how to use these techniques is knowing when to use them. In these exercises, we have sampled only some of the many occasions calling for their use and only part of the information we can glean from their use. As you continue through future exercises, you will uncover many instances where running a frequency sweep is useful, just to expand your own comprehension of the antenna's properties. You will also see opportunities to try out a frequency-scaling of a design to determine its potential and feasibility at a frequency in which you have some interest. Whether or not the instructions set for an exercise requests added frequency work, feel free to go exploring with these tools.

8. Source Types and Placement

***Objectives:** The exercises in this chapter will focus upon types and placement of sources in antenna models. We shall encounter both voltage and current sources--as well as when each is best applied--along with single, split, and multiple sources. The exercises will also show you how to ensure that a source is exactly where you want it.*

The most fundamental energy source for an antenna modeled in NEC-2 is the **voltage source**. By selecting an arbitrary voltage and placing it at the antenna source point, NEC-2 can calculate all of the most significant electrical parameters of an antenna, using the calculation of mutual impedances as a basis. Since current at any point on the antenna will be proportional to the impedance for any given voltage, using a value of 1 volt suffices for most simple models. In most antennas, this will result in very low values of current, so some modelers choose higher voltages, such as 100, to elevate the current values. Such moves are strictly for convenience in reading current magnitude and make no difference to current distribution or current phase at any point on the antenna.

In NEC-2, it is necessary to place the antenna source on a specific segment, where it is in series with any loads, including distributed material loss loads, and in parallel with any transmission lines that might be added (in Chapter 15). For antennas which come to a point at the source--that is, which are composed of wires that join at an angle at the source--the modeler has both a dilemma and options. One may place the source on the nearest segment to the point, which provides inexact but, at low impedances, sufficiently accurate results for some purposes. One may also use **split sources**, that is, two sources on adjacent segments, so that the sum of their impedances is the antenna source impedance. One may also create an intervening wire with one or more segments to come between the joining wires and use on it a single source. Each technique has its proper application and limitations, which some of the exercises in this chapter will explore.

In addition to the use of single and substitute split sources, some types of antennas require **multiple sources** for analysis. Phased arrays, both vertically and horizontally polarized, are prime within this group, which also includes arrays of independently fed dipoles and the like. In a phased array, the feed system is often a calculated length of transmission line between one element that is also connected to the source of energy and one or more other elements. We often mistakenly think of them as having one driven element and one or more secondary elements. In fact, all of the elements are driven, and

the transmission line functions as a means of transforming the magnitude and phase of the current to the other element.

Such antennas can be studied by using multiple sources, one for each element. Each source provides its element with the proper current magnitude and phase for correct array operation. Such analyses make use of **current sources**, which are not native to NEC-2.

Rather, current sources are made available by the interface program, such as NECWin Plus. We shall see how they are created by looking at the .NEC file for identical antennas with voltage and with current sources, and we shall see what special steps need to be taken to derive certain data which they may obscure.

In addition, we shall look at the application of current sources to a simple phased array to see how we can use them to design an antenna with some prescribed properties. Along the way, we shall also learn why simple multiple voltage sources will not do the job so well, not to mention observing some odd but real phenomena, such as negative source impedances.

NEC-2 offers other types of sources for more advanced modeling purposes beyond the scope of NECWin Plus. Among these are incident plane waves, with options for linear and elliptic polarization, and the bicone voltage source.

Exercise Preparation

The exercises in this chapter will request that you make some considerable alterations in the modeling geometry of even simple antennas. (Modeling geometry, of course, is the system of wires with cartesian end coordinates. This is a reminder not to confuse the modeling geometry with the geometry of the physical antenna itself. We may construct a model having one wire from a physical antenna made from two wires. Likewise, we may model a real one-wire monopole with two or more wires.) The most common alteration will ordinarily involve cutting an initial model wire in two (usually at the center) and making of it two wires that join. Some examples will go so far as to convert one wire into three.

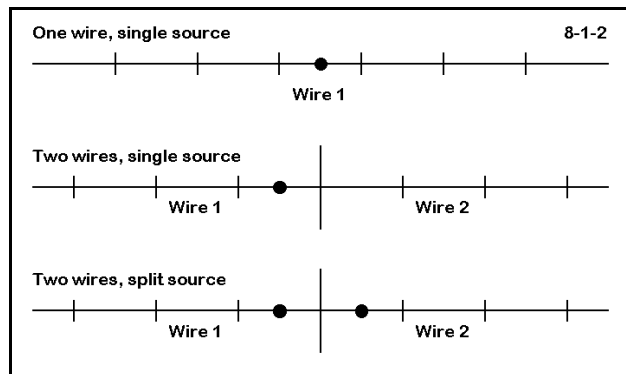
Therefore, you will end up with one or more variations on the beginning model file. In most cases, the disk accompanying this guide will contain a file showing you one of the ways (but not necessarily the only way) of accomplishing the assigned task as a check on your work. These files will normally be keyed to the initial file in this way: if the starting file is 8-1.NEC, a check file will be 8-1-1.NEC. If you save the modified files that you create, a sequence such as 8-1A.NEC, 8-1B.NEC, etc., will not overwrite either the original or the check files.

8-1.NEC: A simple dipole for 299.7925 MHz

Our first file, 8-1.NEC, contains a simple dipole in free space on which we shall conduct some preliminary exercises to see the effects of various ways of handling the source placement relative to the wire geometry. As given, the $1/2\lambda$ dipole consists of a single piece of (model) wire, fed at the center segment of an initial 11 segments. We shall not leave the antenna in this configuration.

```
CM Dipole in free space
CE
GW 1 11 -.2393 0 0 .2392 0 0 .0005
GS 0 0 1
GE 0
EX 0 1 6 0 1 0
FR 0 1 0 0 299.7925 0
RP 0 1 360 1000 90 0 1 1
EN
```

8-1-1



The first modification will be to increase the segmentation of the wire to 21, moving the source to segment 11. This move will make the segment lengths comparable to those in succeeding modifications, according to the sketch in **Figure 8-1-2**. The second modification will consist of "breaking" the wire in two at the center, that is, terminating wire 1 at 0,0,0 and starting wire 2 there to terminate at the former end of wire 1, with 10

segments for each of the 2 wires. Then place the source at either segment 10 of wire 1 or at segment 1 of wire 2: each is the segment adjacent to the geometric center of the antenna.

The third modification consists of adding a second source to the model just created. Whichever source you used in the second modification, add to it the other one listed. The sources are called a split source when placed on adjacent segments, even though they are on separate model wires. A "check" model description of this modification appears in **Figure 8-1-3**.

```
CM Dipole in free space
CM 2 wires, split source
CE
GW 1 10 -.2393 0 0 0 0 0 .0005
GW 2 10 0 0 0 .2392 0 0 .0005
GS 0 0 1
GE 0
EX 0 1 10 0 1 0
EX 0 2 1 0 1 0
FR 0 1 0 0 299.7925 0
RP 0 1 360 1000 90 0 1 1
EN
```

8-1-3

Save each of the modifications as a separate file. Should an error occur, you may quickly find it by comparing model descriptions. For each antenna, record the free space gain and the source impedance on the table at the top of the next page. Data entry is straightforward for the first two models. For the third, the split source arrangement requires a modicum of arithmetic to arrive at the effective source impedance. Since the two sources are in series, simply add the two resistive components

and add the reactive components. The result is the modeled source impedance for the antenna.

8-1 Test Data			Reference Data		
Model	Gain dBi	Source Z (R±jX Ω)		Gain dBi	Source Z (R±jX Ω)
1 wire, 1 source				2.13	72.0 + j 0.6
2 wires, 1 source				2.13	72.4 + j 0.5
2 wires, split source				2.13	72.3 + j 1.2

Comments: The data should be neither radical or surprising. For the model with the source on the segment adjacent to the element center, standard low impedance resonance rules apply. Placing the source slightly off-center at a low impedance point on a dipole does not change the source impedance much relative to exact center placement. The rate of change of impedance as a source is placed further off-center is very low at first and then increases ever more rapidly as one moves toward the element end.

The split source result shows a higher reactance because the current on either side of the dipole center does not change phase. Hence, each adjacent segment shows a slight inductive reactance. Do not presume that these cancel. In some instances of nonsymmetrical antennas, the reactances may appear as capacitive on one side and inductive on the other. Addition will yield the net, which is closest to reality.

8-2.NEC A 1λ center-fed wire

At the center of the $1/2\lambda$ dipole, the impedance changed slowly, and all three source methods yielded closely coincident impedance values. When a source is placed in a region of the antenna where the impedance is high and changing rapidly, the methods of placing a source may not show equal coincidence. File 8-2.NEC is a 1λ version of the previous $1/2\lambda$ model. It is center-fed, with about 20 segments per half wavelength.

```

CM 1 wl center-fed
CM in free space
CE
GW 1 41 -.4786 0 0 .4786 0 0 .0005
GS 0 0 1
GE 0
EX 0 1 21 0 1 0
FR 0 1 0 0 299.7925 0
RP 0 1 360 1000 90 0 1 1
EN

```

8-2-1

Use the given model for the first test run, then modify it in the same way as before. For

each of the two-wire versions, use 20 segments per wire. Record the data in the table at the top of the next page.

8-2			Test Data		Reference Data	
Model	Gain dBi	Source Z (R±jX Ω)		Gain dBi	Source Z (R±jX Ω)	
1 wire, 1 source				3.70	2328 - j 896	
2 wires, 1 source				3.87	2038 - j 791	
2 wires, split source				3.70	2672 - j 138	

Comments: A check model description for the split-source 2-wire version of the antenna appears in **Figure 8-2-2**. The single-source, adjacent-segment version of the model would be identical with the removal of one of the EX cards. Of special note is the rapid change of source impedance, even slightly off center in this antenna. This is exactly what one should expect in a high voltage, low current region of the antenna, where the source is located.

```

CM 1 wl center-fed
CM in free space
CE
GW 1 20 -.4786 0 0 0 0 0 .0005
GW 2 20 0 0 0 .4786 0 0 .0005
GS 0 0 1
GE 0
EX 0 1 20 0 1 0
EX 0 2 1 0 1 0
FR 0 1 0 0 299.7925 0
RP 0 1 360 1000 90 0 1 1
EN

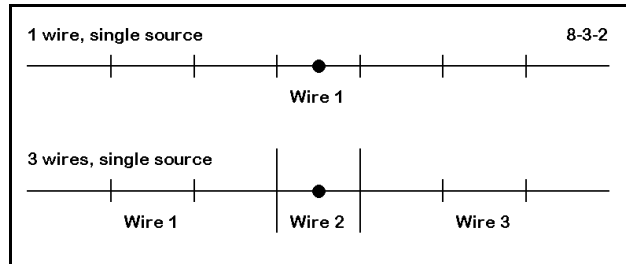
```

8-2-2

Examine carefully the single-source, adjacent-segment model azimuth pattern. Changing the source location not only changes the maximum gain, but also the shape of the pattern. Even though split-source model source impedance is as far off the center-fed value as is the single-source, adjacent-segment model, restoring balance to the source restores the antenna pattern as well as its gain value.

8-3.NEC A 3-wire dipole model

File 8-2.NEC presents another way to divide the antenna element geometry while placing a source in a prescribed position, in this case, the element center. Instead of using 1 or 2 wires, we use 3: 2 end wires and a short center segment on which we place the source.



```

CM Dipole in free space
CM 3 wire, single source
CE
GW 1 23 -.2393 0 0 -.005 0 0 .0005
GW 2 1 -.005 0 0 .005 0 0 .0005
GW 3 23 .005 0 0 .2393 0 0 .0005
GS 0 0 1
GE 0
EX 0 2 1 0 1 0
FR 0 1 0 0 299.7925 0
RP 0 1 360 1000 90 0 1 1
EN

```

8-3-1

Figure 8-3-2 on the next page shows the basic structure of the method of placing a source on a wire element, relative to the basic single-wire, single-source model.

We shall run this model as given, with 23 segments in each end wire, making them approximately the same length as the single segment in the center wire. Then, we shall modify this model in several ways. First, we shall decrease the segmentation of the end wires, first to 15 each and then to 10 each. Each decrease creates an increase in the disparity of length of the segment at the center and the immediately adjoining segments.

Next, we shall modify the model to place 3 segments in the center wire (wire 2). First we shall run the model with 23 segments per end wire, as in **Figure 8-3-3**. Then, we shall increase the number of segments per end wire to 70, which yields a segment length approximately equal to the segment length used in the center wire.

Record your results in terms of gain and source impedance in the table below.

```

CM Dipole in free space
CM 3 wires, single source
CE
GW 1 23 -.2393 0 0 -.005 0 0 .0005
GW 2 3 -.005 0 0 .005 0 0 .0005
GW 3 23 .005 0 0 .2392 0 0 .0005
GS 0 0 1
GE 0
EX 0 2 2 0 1 0
FR 0 1 0 0 299.7925 0
RP 0 1 360 1000 90 0 1 1
EN

```

8-3-3

8-3 Test Data			Reference Data		
Model (by segments)	Gain dBi	Source Z (R±jX Ω)		Gain dBi	Source Z (R±jX Ω)
23-1-23				2.15	72.1 + j 1.4
15-1-15				2.37	68.4 + j 0.9
10-1-15				2.61	64.5 + j 0.4
23-3-23				2.16	71.8 + j 0.9
70-3-70				2.14	72.4 + j 1.8

Comments: The source is sensitive to disparities of segment length in the segments immediately adjoining the one on which the source is placed. Since this antenna is the same as the one in exercise 8-1, you can check its source impedance and gain values for a single-wire, single source configuration. When the source wire has a single segment, it is crucial to ensure that the adjoining wires are segmented to yield segment lengths quite close to the length of the center wire. As you depart from this condition, as in the second and third lines of the table, the gain increases and the source impedance decreases, both unrealistically.

A recommended alternative procedure is to use 3 segments for the center wire on which the source is placed. This arrangement assures equal length segments on each side of the source segment. The last line of the table provides end-wire segment lengths that are close to the lengths of the center-wire segments, and its values closely coincide with those of the table's first line and the single-wire, single-source model. The fourth line on the table establishes end-wire segment lengths that are considerably different from those of the center wire. Although some variation from the last line is apparent, it is considerably less than when the length disparity occurs on segments immediately adjacent to the source segment. In effect, the added segments on the source wire desensitizes the source to moderate segment length changes as one moves to the wires connected to the source wire.

These first three exercises have no direct application, since a center-fed dipole is best modeled as a single wire with an odd number of segments, so that the source is placed on the center segment. However, they are important preliminary exercises in making you aware of the various alternatives to the single-wire, single-source model and to the elements of care that are required when using them. The remaining question is whether the alternatives have some real uses.

8-4.NEC: A 14 MHz inverted-Vee

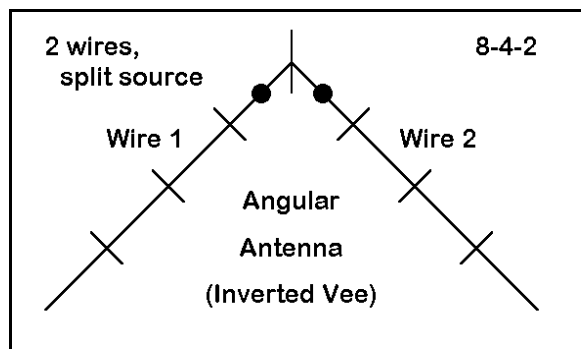
The inverted-Vee antenna in 8-4.NEC is representative of a number of antennas whose source point is also the apex of a wire angle. This free space #12 AWG copper wire Vee for 14 MHz uses $Z=0$ as its base; placing the antenna over a real ground would require modification of the Z-axis values.

```

CM Inverted vee: 14 MHz FS
CE
GW 1 20 -12.35 0 0 0 0 12.35 3.36778E-03
GW 2 20 0 0 12.35 12.35 0 0 3.36778E-03
GS 0 0 .3048
GE 0
EX 0 1 20 0 1 0
EX 0 2 1 0 1 0
FR 0 1 0 0 14 0
RP 0 1 360 1000 90 0 1 1
EN

```

8-4-1



The model comes with a split source, as shown in **Figure 8-4-2**. For assured accuracy, the split source is the simplest system. However, one might also reason that the source impedance will be low in this modified $1/2\lambda$ antenna. Hence, using a single source on either segment immediately adjoining the element apex may yield quite acceptable results.

To test this hypothesis, run the model, and add the two source values to obtain the model source impedance. Then remove either EX card and obtain the single source impedance value. Also obtain the maximum gain values as a check on the reasonableness of the results. Record your data in the following table.

8-4 Test Data			Reference Data	
Model	Gain dBi	Source Z (R±jX Ω)	Gain dBi	Source Z (R±jX Ω)
Split			1.65	42.7 + j 4.0
Single			1.65	42.7 + j 3.9

Comments: For this particular antenna, there is no significant difference in using either a split feed or a single source on one of the wire segments immediately adjoining the antenna center. However, the reliability of the adjacent-segment source placement would not have been known without the split-source model for comparison, plus some knowledge of the what value of source impedance to expect from a wire antenna bent to form a 90° angle. (In this regard, you may wish to further modify the inverted-Vee, using larger apex angles until it approaches a straight dipole. You may find the changes in

pattern shape, the vertically and horizontally polarized components of the far field pattern, and the impedance values to be interesting as they form a continuum.)

Other antennas, such as deltas and other triangles, fed at corners, may not show a low impedance. In such cases, a split-source placement may be necessary to arrive at a reasonable source impedance value. Where the current is not the same on either side of the actual feed point, as in the triangle we examined in Chapter 6, using a single-source on an adjacent segment to the actual source point can yield highly misleading results. You may wish to review that exercise for further insight into the source placement question.

As an additional exercise to do on your own, you may wish to create a 3-wire version of the inverted-Vee. Create a short horizontal wire at least 1.5' long with 3 segments at the top height of the present Vee and place it symmetrically about the X=0 axis. Then separate the upper ends of the present Vee by connecting each to an end of this new wire. Resegment the end wires so their segment lengths are equal to those in the new wire. When you run this version of the model, expect to see significant inductive reactance in the source impedance, since this model has lengthened the antenna element. You may also wish to change segmentation density of the end wires to check the sensitivity of the gain and source impedance values to this factor for an antenna that is not a straight line.

You can perform a similar operation on the right triangle antenna in Chapter 6, effectively blunting one corner to create a short 3-segment source wire. Compare the source impedance of the new version with the values obtained with the original antenna.

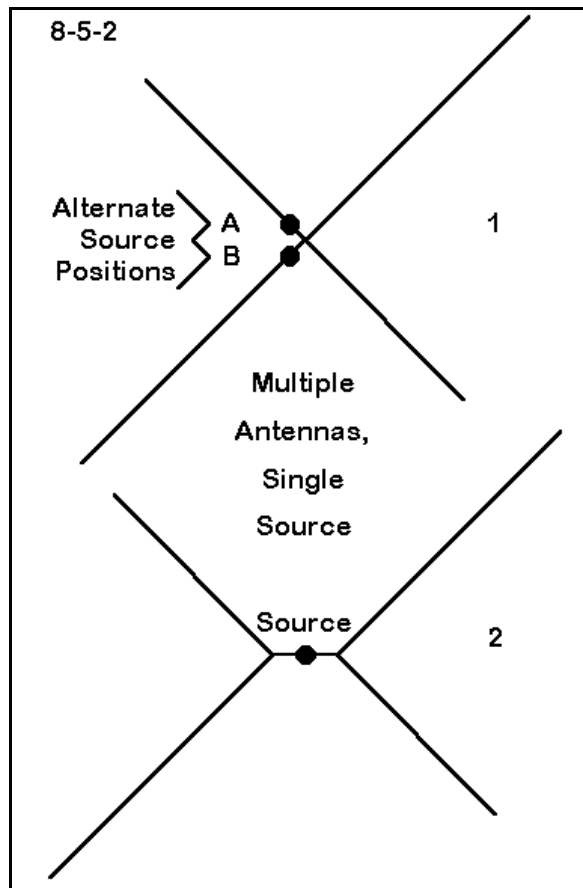
8-5.NEC Crossed dipoles for 14 and 21 MHz with a single source

Crossed dipoles with a single feedpoint present a modeling problem, as we shall discover when we run 8-5.NEC. This free space pair of #12 AWG copper dipoles for 14 and 21 MHz are at 90° angles to each other. In reality, we would feed them at a common point, where "point" means a very small space relative to the lengths of the antenna wires.

```

CM Crossed dipoles
CM 14 & 21 MHz
CE
GW 1 25 -12 -12 0 0 0 0 3.36778E-03
GW 2 25 0 0 0 12 12 0 3.36778E-03
GW 3 17 -7.92 7.92 0 0 0 0 3.36778E-03
GW 4 17 0 0 0 7.92 -7.92 0 3.36778E-03
GS 0 0 .3048
GE 0
EX 0 1 25 0 1 0
LD 5 1 1 25 5.8001E7
LD 5 2 1 25 5.8001E7
LD 5 3 1 17 5.8001E7
LD 5 4 1 17 5.8001E7
FR 0 1 0 0 14 0
RP 0 1 360 1000 90 0 1 1
EN

```



Note: We have used free space throughout these exercises so that we would not confuse source impedance value changes occasioned by changes in the model with those created by ground influences. We shall continue this practice throughout the chapter.

The key question for the model, whose structure is reflected in part 1 of **Figure 8-5-2**, is where to place the source. As given, the only option open to the modeler is to use a segment adjacent to the junction of the wires. However, we are still unguided as to whether to place the source on a 14 MHz wire (wire 1 or wire 2) or to set it on a 21 MHz wire (wire 3 or wire 4). The only solution is to do both and to check the gain and source impedance values for both frequencies from each position.

Run this model and its revision, recording your gain and source impedance data in the table at the top of the next page. The entries

list the source wire number (W_{xx}) and segment number (S_{xx}), as well as the frequency for the run.

8-5 Test Data			Reference Data	
Model (by source)	Gain dBi	Source Z ($R \pm jX \Omega$)	Gain dBi	Source Z ($R \pm jX \Omega$)
W1S25: 14			2.10	70.1 - j 12.7
W1S25: 21			1.65	90.9 + j385.5
W3S17: 14			1.13	9.2 - j302.9
W3S17: 21			2.18	72.0 - j 9.5

Comments: Which set of values is correct? Scanning the table may lead us to simply discard the wholly unreasonable values and use the remainder. The 14 MHz values seems on the surface to be reasonable when the source is on the 14 MHz wire, and

likewise for the 21 MHz values when the source is on its wire. In fact, the two antennas seem not to interact at all, but to operate independently. Note the temptation to introduce into this problem a number of presumptions and lore regarding combined dipole antennas.

The only temptation that should overtake us here is the one directed toward further and better modeling. The model requires revision into a 5-wire model, with a central wire serving as a 3-segment common source wire.

One leg of each dipole is attached to each end of the central wire, corresponding to the sketch in part 2 of **Figure 8-5-2**. One version of such a model appears in **Figure 8-5-3**, which is a check model (8-5-1.NEC).

Run this model and record the values for gain and source impedance in the short table below.

```

CM Crossed dipoles
CM 14 & 21 MHz
CE
GW 1 25 -12 -12 0 -.75 0 0 .00336778
GW 2 25 .75 0 0 12 12 0 .00336778
GW 3 17 -7.92 7.92 0 -.75 0 0 .00336778
GW 4 17 .75 0 0 7.92 -7.92 0 .00336778
GW 5 3 -.75 0 0 .75 0 0 .00336778
GS 0 0 .3048
GE 0
EX 0 5 2 0 1 0
LD 5 1 1 25 5.8001E7
LD 5 2 1 25 5.8001E7
LD 5 3 1 17 5.8001E7
LD 5 4 1 17 5.8001E7
LD 5 5 1 3 5.8001E7
FR 0 1 0 0 14 0
RP 0 1 360 1000 90 0 1 1
EN
    
```

8-5-3

8-5 Test Data			Reference Data		
Model (by source)	Gain dBi	Source Z (R±jX Ω)		Gain dBi	Source Z (R±jX Ω)
14 MHz				2.09	60.1 + j 6.3
21 MHz				1.80	88.5 + j 3.0

The results of the composite model using a single source are quite unlike those obtained from moving the source to different positions. Due to the complex geometry of the model, even though the structure seems intuitively simple enough, the results will not be so stable as they are with purely linear elements. Hence, the degree of precision obtainable may be operationally satisfactory, but may not meet more stringent study and analysis requirements. You may verify this fact by altering both the segmentation of the end wires and the size of the common portion of the antenna.

8-6.NEC: A $1/2\lambda$ off-center-fed antenna

Model 8-6.NEC is a simple 7.15 MHz off-center-fed $1/2\lambda$ #14 AWG copper wire antenna 50' above an S-N average (cond. = .005, d.c. = 13) ground. The antenna uses standard modeling procedures common to many of the exercises. The wire is placed symmetrically around the X=0 axis.

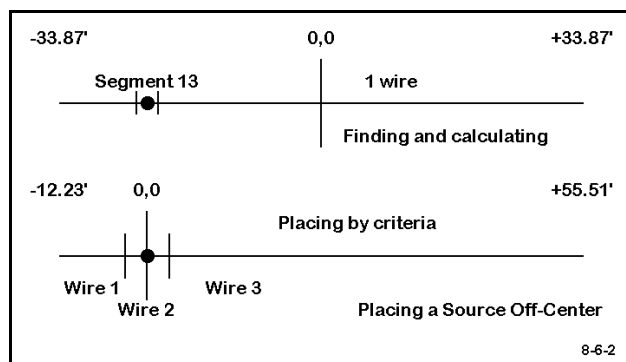
```

CM 7.15 MHz off-center-fed 1/2 wl
CE
GW 1 69 -33.87 0 50 33.87 0 50 .00267
GS 0 0 .3048
GE 1
GN 2 0 0 0 13 .005 0 0 0 0
EX 0 1 13 0 1 0
LD 5 1 1 69 5.8001E7
FR 0 1 0 0 7.15 0
RP 0 181 1 1000 -90 90 1 1
EN

```

8-6-1

Suppose your task were to locate the precise 300- Ω source point within $\pm 1\Omega$ and with no more than $\pm 1\Omega$ reactance. One technique, applicable to the model above is to establish a resonant center-fed $1/2\lambda$ antenna. Placing the source at the exact center of the wire would suffice for this task.



Then move the source outward toward one end of the antenna until you hit the correct segment. You would discover that as the source point moves outward, the resonant length of the antenna changes slightly. Hence, you would change the length and thereby move the source slightly, since its segment would also move. You might luckily hit a resonant length and be relatively close to the 300- Ω point. Run this antenna and verify that

with the source placed on segment 13 of the 69 total segments, the source impedance is between 297 and 298 Ω . Now calculate the exact lengths of wire on either side of this point. This exercise corresponds to the upper part of **Figure 8-6-2**.

There is an easier way, using the 3-wire technique. Establish a short wire with 3 segments. The recommended minimum length of this wire is about 0.02λ , or a little under 3' for the 7.15 MHz frequency. A 3' ($\pm 1.5'$) wire will do fine. Place the wire symmetrically about the X=0 axis, and set the source on segment 2, which places it at the X=0 point. The lower portion of **Figure 8-6-2** begins to emerge.

Now run a short wire (wire 1) from one end of the center wire and a long wire (wire 3) from the other. Adjust the extremities in the +X and -X directions until the wire is both resonant and shows a 300- Ω source impedance within the limits prescribed. Adjust the segmentation so that the length of each segment approximately matches that within the center wire, about 1' per segment.

```

CM 7.15 MHz off-center-fed 1/2 w1
CE
GW 1 11 -12.23 0 50 -1.5 0 50 2.67E-03
GW 2 3 -1.5 0 50 1.5 0 50 2.67E-03
GW 3 54 1.5 0 50 55.51 0 50 2.67E-03
GS 0 0 .3048
GE 1
GN 2 0 0 0 13 .005 0 0 0 0
EX 0 2 2 0 1 0
LD 5 1 1 11 5.8001E7
LD 5 2 1 3 5.8001E7
LD 5 3 1 55 5.8001E7
FR 0 1 0 0 7.15 0
RP 0 181 1 1000 -90 90 1 1
EN

```

8-6-3

The result is the model 8-6-1.NEC, shown in **Figure 8-6-3**. Run this model and verify the source impedance within the prescribed tolerances. The model provides instant information, with no calculation harder than addition on the total length of the wire and the lengths of each side of the feedpoint. Moreover, the precise 300- Ω point can be found, since adjustments to length on each side of center do not affect the position of the source. At most, the segment lengths within each of the wires are altered slightly. During the hunt for the 300- Ω source point, the segmentation can be brought back into tight accord with the center wire any time it drifts too far afield.

For many purposes, the demand for a ± 1 - Ω resistance and reactance margin is far too stringent to be operationally meaningful. However, for many numerical analysis and other purposes, such limits ensure smooth data curves showing operational trends. For example, repeat the exercise revising the model in 8-6-1.NEC to find the 100, 200, 400, 500, and 600 Ω source points. Construct a curve relative to overall resonant antenna length and another relative to the percentage of distance from the antenna center to tip for the source points uncovered. The precision of which NEC-2 is capable can yield very useful information about many antenna performance and physical specifications. To develop such data requires techniques of precision modeling, and the 3-wire source placement procedure is only one of them.

8.7.NEC: A 2-element horizontal phased array

To this point, we have used only voltage sources for our models. For most purposes, voltage sources are convenient to develop the desired data concerning antenna performance. They are somewhat less convenient if we wish to do a detailed analysis of the current magnitude along an antenna element, since the currents do not have a handy reference value when the source voltage is specified. However, this small handicap represents no real hindrance to the investigation.

There are applications for which the use of current sources is essential. Among them is

the development of data for phased arrays, whether they are composed of vertical or horizontal elements. One of the classic horizontal phased arrays is the two element beam that physically resembles a 2-element parasitic Yagi. Ordinarily, it uses a section of transmission line to establish a current magnitude and phase on the rear element--relative to that on the forward element--in order to achieve one or more desired performance characteristics. Common names for such arrays are the ZL Special and the HB9CV.

Let's begin the development of a phased array with a common 2-element Yagi, which is model 8-7.NEC. The model description shows two elements for 28.5 MHz, a 15.9' driver and a 17.3' reflector 5' apart and made from 1" diameter 6061-T6 aluminum in free space. Run this model. You should obtain a free space gain of about 6.28 dBi, with a 180° front-to-back ratio of around 10.95 dB, with a source impedance close to 41 Ω .

```

CM 2-element Yagi, 28.5 MHz
CE
GW 1 13 -7.95 0 0 7.95 0 0 .041665
GW 2 12 -8.65 -5 0 8.65 -5 0 .041665
GS 0 0 .3048
GE 0
EX 0 1 7 0 1 0
LD 5 1 1 13 2.4938E7
LD 5 2 1 12 2.4938E7
FR 0 1 0 0 28.5 0
RP 0 1 360 1000 90 0 1 1
EN

```

8-7-1

As the first step in our work, change the voltage source to a current source, with a current magnitude of 1 and a phase angle of zero. Verify that the data output of the model does not significantly vary from the data yielded with a voltage feed. For single source antennas with symmetrical currents (that is, equal in magnitude and phase on each side of the source point), the output data should be identical (within the limits of program rounding of values).

Let us suppose that using the antenna as a single-source parasitic Yagi provides too little front-to-back ratio for our needs. We can effect an increase by placing a source on both elements and establishing an optimizing ratio of current magnitudes and phases on the two elements. To see what values of current magnitude and phase we need, we shall have to revise the model to not only place the second source on the rear element, but as well to set the current conditions on each element.

```

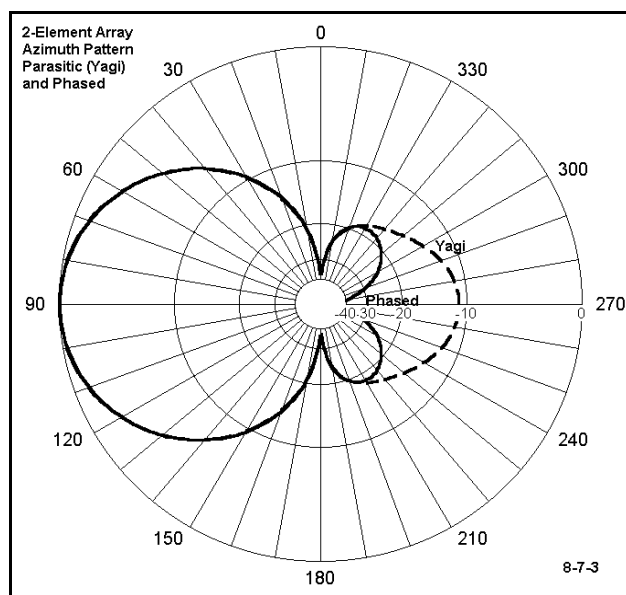
CM 2-element phased array
CM 28.5 MHz
CE
GW 1 13 -7.95 0 0 7.95 0 0 .041665
GW 2 13 -8.65 -5 0 8.65 -5 0 .041665
GW 901 1 9901.0000 9901.0000 9901.0000 9901.0001 9901.0001 9901.0001 .00001
GW 902 1 9902.0000 9902.0000 9902.0000 9902.0001 9902.0001 9902.0001 .00001
GS 0 0 .3048
GE 0
EX 0 901 1 0 1 0
EX 0 902 1 0 -.5787 .7407
LD 5 1 1 13 2.4938E7
LD 5 2 1 13 2.4938E7
NT 901 1 1 7 0 0 0 1 0 0
NT 902 1 2 7 0 0 0 1 0 0
FR 0 1 0 0 28.5 0
RP 0 1 360 1000 90 0 1 1
EN

```

8-7-2

Model 8-7-1.NEC, is the result. The model description holds a number of features that we must note in getting used to how NEC-2 handles current sources. Inspect the new lines on the model, especially the added GW lines, and the EX and NT lines.

NEC-2 programs create current sources at the antenna terminals by applying the native voltage source to a short wire at such a long distance from the antenna structure that it cannot affect the far field pattern. The new source wire is short and thin, as the new GW lines indicate. The source voltage goes to a network (NT) card, the output terminals of which are at the actual antenna source point, effecting a "forced" current magnitude and phase of specified dimensions.



Run either your own modification of 8-7.NEC or 8-7-1.NEC. The maximum 180° front-to-back ratio should occur with the source on wire 1 set at a magnitude of 1 with a phase angle of 0° and with the source on wire 2 set at a magnitude of 0.94 and a phase of 128°. In this configuration, the antenna should yield a forward free space gain of about 6.2 dBi, with a 180° front-to-back ratio exceeding 48 dB. See **Figure 8-7-3** for a comparison of the parasitic Yagi and the revised phased array. (You can create this graphic by importing the Yagi file into the polar plot facility of NECWin Plus, and then requesting both plots. This particular plot requests a normalized pattern on a

log scale. You may wish to re-examine the dual plot on a linear scale, both normalized

and non-normalized.)

There are two supplementary tasks to perform. First, vary the current magnitudes at the two sources, but keep their ratio constant and do not change the phase angle of either. For example, use a source 1 current magnitude of 0.5 and a source 2 current magnitude of 0.47. You should see no change in the antenna pattern. Second, return to the original magnitude values and now vary the current phases, keeping the rear current phase 128° greater than the forward current phase. For example, set the source 1 current phase at -28° and the rear current phase at $+100^\circ$. Again, you should see no pattern change.

As a third task, vary the rear current magnitude and phase in very small steps (magnitude = 0.01 per step; phase 1° per step) to see the rate at which the rear pattern degrades relative to its maximum 180° front-to-back ratio. As you move these values in certain directions, you should discover that the forward gain increases, while the rear gain does not exceed the level needed to maintain the worst-case front-to-back ratio of about 18 dB (as determined from **Figure 8-7-3**, by examining the remnant rear lobes). You may well ask yourself whether the added gain with a more uniform pattern of rear lobes might not make a superior antenna for some purposes than the lower gain version with the deep rear null. Note the current magnitude and phase values for what you consider the optimum phased array design.

Before moving to a fourth task, let's pause and inquire about the source impedance at our two antenna feedpoints. The program returns values for the remote sources, which do not reflect the values at the antenna terminals. To find these, open the NEC output file and find the "Network Connection Points" table. It will list excitation at both the antenna wire source points and the remote wire source points. **Figure 8-7-4** shows the portion of the table listing the impedances, with those applying to wires 1 and 2 indicated. You should translate the results into values of $39.4 + j27.9 \Omega$ for the wire 1 source and $33.0 + j3.5 \Omega$ for the wire 2 source. Likewise, find and record the antenna wire source impedances for what you recorded as your optimized version of this phased array.

NETWORK CONNECTION POINTS			
IMPEDANCE (OHMS)			
REAL		IMAG.	
3.94105E+01	2.78605E+01	W1	
3.29555E+01	3.53121E+00	W2	
1.91037E-03	-2.61610E+07		
3.66060E+00	-2.61610E+07		

8-7-4

The fourth task is to purposely create a poor antenna. Set the rear element current magnitude and phase to 1 and 135° , respectively. Set the forward element current magnitude and phase to 2 and 0° respectively. Run the model and examine the source impedances at the antenna wires. You will discover that the rear element exhibits a negative resistive component. This phenomenon is real and results from the rear element receiving more energy than it radiates. There are large arrays (20 or more) of independently-fed dipoles in which, depending upon the geometric configuration, some of

the antennas exhibit a negative resistance. Since we may use independent energy sources or networks to establish the current magnitudes and phases on each element of an array, it is possible (and common) to establish conditions under which one or more of those elements exhibits a negative resistive component to its impedance. If we use, as our means of setting the relative phasing of the array elements, transmission line sections to each element from a common source point, as is the case for many phased horizontal and vertical arrays, these conditions will normally not arise.

As a fifth task, attempt to redo any of the preceding tasks using only voltage sources to determine the conditions of both elements that will yield the goals of each of these tasks. Be especially determined in trying to create a negative resistive component to the impedance on the rear element.

Your last task is to vary the geometry of the array in 8-7-1.NEC by alternately changing the length of the elements and changing their spacing. For example, make the element of equal length, alternately choosing the length of the forward element, the length of the rear element, and some intermediate length as your basis for equal length elements. Likewise, vary the spacing between the elements from about 0.1λ to about 0.2λ in small increments, using the original element lengths and your equalized versions. In each case, leaving the forward element with a source current magnitude and phase of 1 and 0° , find the rear element source current magnitude and phase that yields a maximum 180° front-to-back ratio, recording the gain and source impedances for each case. For each set of element lengths, you should discover an interesting pattern to the relationship between the element spacing and the required current magnitude and phase ratio for maximum 180° front-to-back ratio.

You may, as a supplemental task, create $1/4\lambda$ vertical monopoles over perfect ground for any frequency and use the same current source techniques to create phased arrays with the deepest nulls.

Summing Up

NEC-2 has additional advanced capabilities with respect to the types of sources that may be employed for various kinds of antenna performance analysis. However, single and multiple voltage and current sources are the most common ones used in antenna investigations. As we have seen, these basic sources require careful attention if they are not to yield misleading or downright erroneous results.

Source segments are sensitive to their surroundings in terms of the immediately adjoining segment lengths, not to mention the symmetry of current magnitude and phase in those neighboring segments. Nevertheless, there are a variety of methods we may use to assure accuracy of both position and resulting source impedance data. We have

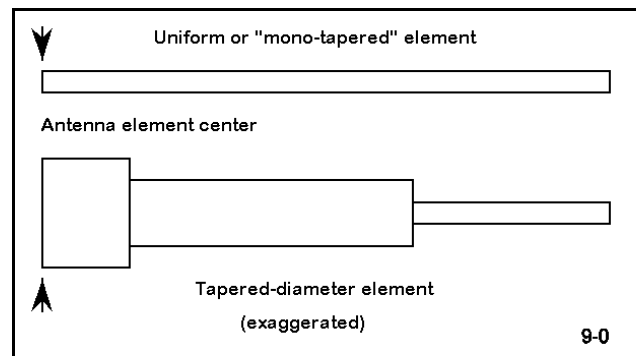
surveyed a number of the most fundamental techniques in these exercises. We shall have occasion to return to these techniques when we consider the placement of loads on Chapter 14.

Equally important to the condition within which we place sources is the type of source we use for various kinds of antenna analysis. Although voltage sources suffice for most single-source applications, current sources are necessary to both create and evaluate phased antenna arrays of many types. In this exercise set, we have tried to reveal how current sources are constructed in NEC-2 and to demonstrate their versatility and parameters. As with most of our work, we shall have to classify these efforts as scratching the surface, but hopefully in a direction that yields for you a patterned etching of useful modeling techniques.

9. Tapered-Diameter Elements

Objectives: *NEC-2's inability to model accurately physical elements with a tapering diameter has resulted in a standard work-around modeling method. These exercises will familiarize you with the detailed terms of the limitation, the requirements for correctly applying the substitute model, and limitations associated with the use of the corrective.*

Since the program's introduction, NEC-2 users have been aware that the program does not accurately model linear antenna elements which employ subsections of differing diameters. See **Figure 9-0** for an illustration of a "tapered-diameter element" (or TDE). The inaccuracies in NEC models of TDEs severely limited the program's ability to serve innumerable designers and analysts of antennas used from 3 to 50 MHz, where combinations of aluminum tubing often form the physical structure of antenna elements.



The solution to this problem emerged in the form of a series of equations, sometimes called the Leeson equations, although there are variations upon them. By calculating a series of parameters related to the self-impedance of a linear TDE in a near-resonant condition, one might substitute in its place an equivalent "mono-tapered" or uniform-diameter (cylindrical) antenna element with the same relevant characteristics with respect to modeling data outputs. Interestingly, the equations have been closely calibrated to results for highly segmented TDEs and equivalent mono-tapered elements produced by MININEC (version 3), which does not demonstrate the limitation with TDEs that is inherent in NEC-2.

For a detailed account of the techniques involved in the calculations, and in their origins, see Dr. David B. Leeson, *Physical Design of Yagi Antennas* (Newington: ARRL, 1992), especially Chapter 8. The notes at the end of the chapter contain valuable references to earlier work on which Leeson's equations are based.

NEC-2 very accurately models cylindrical elements. Although hand calculation of the

substitute monotapered element length and diameter can be tedious, especially for a multi-element array, implementations of NEC-2 can perform the calculation routinely and swiftly--so swiftly that a casual user of the program might be unaware of the substitution. The feature is almost always a user option, allowing one to model the antenna without the correction feature in operation.

The substitute mono-taper element can be implemented in one of two ways. It might be precalculated so that a new model replaces the input data that would have been received by the NEC-2 core from the modeler's specifications. The calculation can also be implemented within the NEC-2 core. In either case, the substitute dimensions will always be available for inspection within the NEC Output file.

The standard method of handling TDEs has proven very accurate, with reports of less than 1% error being common. An error of 1% is normally within the construction variables encountered in the structure of physical antennas, which include the connectors between sections of tubing and the element mounting assembly to either a mast or a boom, depending upon the complexity of the array.

However, it is possible to mismanage models involving TDEs in both subtle and more obvious ways. The ability of the technique to produce reliable equivalent uniform-diameter elements depends upon meeting the conditions of near-resonance, element linearity, and adequate segmentation. Therefore, it is important to acquire enough experience with handling TDE models to get a good feel for their operation and their limitations. The exercises in this chapters are designed to do just that.

Exercise Preparation

In these exercises, we shall explore a series of linear elements--some of uniform diameter, others of tapered diameter--in order to obtain a good "feel" for the use of substitute elements in modeling TDEs via NEC-2. Therefore, some of the exercises will involve models that yield unreliable results. Use care to recognize and note these models as simple comparators and not confuse them with models that are intended to produce reliable output data. View any unfamiliar configuration with the program's structure viewing facility (NECVu). As always, use care in renaming model files when you create variants.

Although the models will be scattered across the HF range, you can replicate many of the exercises using scaled or modified versions for the lower VHF range. You may wish to devise empirical experiments using such antenna elements to verify the principles of substitution involved in NEC-2 modeling of TDEs. Models in the 30 to 60 MHz range can be more easily constructed and tested at several wavelengths above ground than counterparts in the 7 to 21 MHz range. Moreover, the light physical structure should also

allow easier control of the construction variables that might otherwise obscure test results.

9-1.NEC: Monotapered dipoles for 14.0 MHz

The first step in the process of grasping NEC-2's method of handling TDEs is to have a set of reference dipoles with relevantly similar diameters to the TDEs we shall use in exploring program limits and their corrective. Open model 9-1-2.NEC. Note that the model uses a 7/8" (0.875" or 0.0279') diameter 6061-T6 element that is highly segmented. We may work in free space for this and succeeding exercises in this chapter.

```

CM Dipole: 14.0 MHz
CE
GW 1 81 -16.75 0 0 16.75 0 0 .04165
GS 0 0 .3048
GE 0
EX 0 1 41 0 1 0
LD 5 1 1 81 2.4938E7
FR 0 1 0 0 14 0
RP 0 1 360 1000 90 0 1 1
EN
    
```

9-1-1

Run the model, modifying its length until resonance is achieved ($\pm 1 \Omega$ source reactance). Then change the diameter, first to 1" and then to 3/4" (in feet, 0.0833 and 0.625), each time bringing the antenna element to resonance. (You may also use models 9-1-1.NEC and 9-1-3.NEC for these runs.) Record the length and source impedance in the table provided. Note that the model is constructed with dimensions symmetrically about a zero-center point. Be sure to translate the dimensions into the antenna's full length.

9-1 Test Data			Reference Data	
Diameter inches	Length feet	Source Z $R \pm jX \Omega$	Length feet	Source Z $R \pm jX \Omega$
0.75"			33.60	72.1 - j 0.0
0.875"			33.56	72.1 + j 0.3
1.0"			33.50	72.0 - j 0.1

Comments: The point of running these three dipoles is to establish a set of reasonable expectations of models that follow. All three of these models report a free space gain of 2.13 dBi, to go with very consistent source impedance reports. As expected, the required length for resonance decreases slightly with increasing element diameter.

These data become the baseline against which we shall either accept or hold suspect other data received from variations on these models.

9-2.NEC: Tapered-diameter dipoles for 14.0 MHz (uncorrected)

In this exercise, we shall look at the data returned by uncorrected NEC-2 for a dipole with a simple 2-step taper, using 1" and 3/4" tubing. Again, the dipole is 6061-T6 aluminum in

free space. We shall look at data results with the inner larger tube extending about 1/4, 1/2, and 3/4 of the way to the outer end. The models of relevance are 9-2-1.NEC, which uses an 8' section of 1" tubing, 9-2-2.NEC, which increases the length of 1" tubing to 16', and 9-2-3.NEC, which employs 24' of the 1" tubing. Beginning with the shortest length of 1" tubing, we shall adjust the outer end to resonance for each.

Each model is to have a total of 81 segments. To maintain a relatively close match in segment lengths in the different size tubing, use 21 segments on the 8' center section, with 30 segments each on the outer ends. For the 16' center section, use 41 segments, with 20 each on the outer ends. Use 61 segments on the 24' section of 1" tubing, with 10 each on the outer 3/4" sections. Model 9-2-1.NEC, shown at the right, illustrates the process.

```

CM Dipole: 14.0 MHz
CM 1"/.75" dia: 8' center
CE
GW 1 30 -16.85 0 0 -4 0 0 .03125
GW 2 21 -4 0 0 4 0 0 .04165
GW 3 30 4 0 0 16.85 0 0 .03125
GS 0 0 .3048
GE 0
EX 0 2 11 0 1 0
LD 5 1 1 30 2.4938E7
LD 5 2 1 21 2.4938E7
LD 5 3 1 30 2.4938E7
FR 0 1 0 0 14 0
RP 0 1 360 1000 90 0 1 1
EN
    
```

9-2-1

Use the table below to record resonant data for total length, free space gain, and source impedance for each of the three models.

9-2 (not cor.)		Test Data	
Center Length feet	Total Length feet	Gain dBi	Source Z R ± jX Ω
8			
16			
24			

Comments: Some of the data ought to make us quite suspicious of the accuracy of the reports. Although the source impedance figures appear plausible at first sight, notice the behavior of the antenna length. The resonant length with uncorrected NEC-2 is longest when the inner 1" diameter section is about 1/2 the total antenna length. You may check your work against the reference data at the top of the next page.

Of even greater significance is the reported excessive gain of the uncorrected model. Any value higher than 2.13 dBi would be suspicious. As the transition of diameters occurs closer to the antenna center (the high current node), the gain becomes higher. (As a supplementary exercise, you may wish to repeat this modeling run using off-center

feed and various modes of physical construction, for example either centered around the new feed point or centered around the antenna mid-point.) Excessive gain on each of several elements tends to accumulate, as we shall see in a later exercise that uses a multi-element array.

9-2 (not cor.)			
		Reference	Data
Center Length feet	Total Length feet	Gain dBi	Source Z $R \pm jX \Omega$
8	33.70	2.24	70.6 - j 0.7
16	33.78	2.19	71.6 - j 0.1
24	33.72	2.15	71.8 - j 0.9

9-2.NEC: Tapered-diameter dipoles for 14.0 MHz (corrected)

Enable the correction feature for NEC-2. Rerun the models labeled 9-2-1.NEC through 9-2-3.NEC, recording the gain and source impedance. Then adjust the length for resonance by adjusting only the outer ends of the smaller diameter tubing. Record the new data. Use the following table.

9-2 (cor.)					
		Test Data			
Center L feet	Gain dBi	Source Z $R \pm jX \Omega$	New Total L feet	Gain dBi	Source Z $R \pm jX \Omega$
8					
16					
24					

Comments: Compare your work with the reference data below. Note the consistency of the gain in all cases, which lends immediate plausibility to the corrected figures. However, note also the fact that the required antenna length for resonance is longest when the larger diameter section occupies 1/2 the total antenna length. Also note that all resonant lengths are significantly longer than resonant lengths when NEC-2 is uncorrected.

9-2 (cor.)		Reference Data			
Center L feet	Gain dBi	Source Z $R \pm jX \Omega$	New Total L feet	Gain dBi	Source Z $R \pm jX \Omega$
8	2.12	70.1 - j 8.7	33.94	2.13	71.9 - j 0.7
16	2.12	69.3 - j11.8	34.10	2.13	71.9 - j 0.6
24	2.12	70.0 - j 8.6	33.96	2.13	71.9 - j 0.6

9-3.NEC: Substitute mono-tapered dipoles for 14.0 MHz

The corrected model runs were not accomplished using the same models that were run when the correction factor was disabled. Instead, the program created substitute models having a uniform diameter. Each section of the original antenna was replaced by a section of the new diameter, with the length adjusted as the conversion equations required. However, the segmentation of each section remained as given in the original model.

From the model files for the 9-2-x.NEC series, extract the substitute dimensions and create three new models: 9-3-1.NEC through 9-3-3.NEC. Retain the 3-wire construction and the segmentation. However, substitute the new diameter for all 3 wires and replace the old coordinates with the new ones. A sample (9-3-1.NEC) is shown at right.

Enter the dimensions of the substitute antennas in the table below. You will have to translate the diameter, given in feet as a radius in the NEC records, into inches for the table. Also confirm the gain and source impedance of the models.

```

CM Dipole equivalent: 14.0 MHz
CE
GW 1 30 -16.781 0 0 -3.956 0 0 .0329
GW 2 21 -3.956 0 0 3.956 0 0 .0329
GW 3 30 3.956 0 0 16.781 0 0 .0329
GS 0 0 .3048
GE 0
EX 0 2 11 0 1 0
LD 5 1 1 30 2.4938E7
LD 5 2 1 21 2.4938E7
LD 5 3 1 30 2.4938E7
FR 0 1 0 0 14 0
RP 0 1 360 1000 90 0 1 1
EN

```

9-3-1

9-3 Test Data					
Old Center L feet	Outer L feet	Inner L feet	Diameter inches	Gain dBi	Source Z $R \pm jX \Omega$
8					
16					
24					

Comments: Notice that the overall dimensions of the substitute elements conform to the general rules for uniform-diameter elements: smaller the diameter, the longer the length of a given resonant frequency. However, this item may be the least significant piece of information the table reveals. Examine the progression of diameters. The original model with the shortest center section (8') converts to a true cylindrical model just over 3/4" in diameter, with a consequent length that is the greatest of the three. This fact corresponds to the uncorrected model returning the highest (erroneous) gain value. In contrast, the original model with the longest center section (24') converts to a substitute model with the shortest length and a diameter just under 1". The original model reported the least error in gain.

9-3 Reference Data					
Old Center L feet	Outer L feet	Inner L feet	Diameter inches	Gain dBi	Source Z $R \pm jX \Omega$
8	33.562	7.912	0.789	2.13	71.9 - j 0.7
16	33.532	15.734	0.879	2.13	71.9 - j 0.6
24	33.502	23.676	0.959	2.13	71.9 - j 0.6

Notice also that uniform-diameter substitute models are significantly shorter than their tapered counterparts. Moreover, the original baseline models on the 9-1-x.NEC series are all shorter than the resonated lengths of the tapered elements, regardless of the length of the center section. In general, tapered-diameter elements will always require--for resonance on any given frequency--a length greater than a uniform-taper element of the smallest diameter used in the tapered element.

9-4.NEC: A highly tapered dipole for 7.1 MHz

Open 9-4.NEC and examine element taper. The sample model at right carries the description only through the EX line and omits the rest, which will be found when you open the file within NECWin Plus. This 6061-T6 aluminum dipole for 7.1 MHz has all dimensions in inches, for convenience in exploring the element diameter taper. Six different size tubes are used each side of the center point.

The model is interesting not only for its extensive tapering, but as well for the large-diameter, short-length center section. Such sections are common in HF beam designs that attempt to account for the plates and hardware used to connect the element to the boom. Conversion equations are available in Chapter 9 of the Leeson reference noted earlier.

```

CM Dipole, tapered element
CM 7.1 MHz
CE
GW 1 2 -426.5 0 0 -372 0 0 .25
GW 2 2 -372 0 0 -306 0 0 .375
GW 3 2 -306 0 0 -240 0 0 .5
GW 4 3 -240 0 0 -120 0 0 1
GW 5 3 -120 0 0 -12 0 0 1.125
GW 6 1 -12 0 0 12 0 0 2.342
GW 7 3 12 0 0 120 0 0 1.125
GW 8 3 120 0 0 240 0 0 1
GW 9 2 240 0 0 306 0 0 .5
GW 10 2 306 0 0 372 0 0 .375
GW 11 2 372 0 0 426.5 0 0 .25
GS 0 0 .02540
GE 0
EX 0 6 1 0 1 0

```

9-4

Note that the total number of segments for this element is 25, a number usually accounted as sufficient for monotapered elements. Since this element will be converted to a monotapered element, one might reason that this level of segmentation is sufficient.

Run this model both as an uncorrected model and as a corrected model, recording its gain and source impedance in the next table.

Now open model 9-4-1.NEC, a more highly segmented version of the same 6061-T6 aluminum antenna element for 7.1 MHz. Once more, only the lines through EX appear in the description at right. In this model, the short, fat center section has been divided into 3 segments, for a net length of 8" per segment. The remaining sections of the antenna use the closest approximation to 8" per segment possible with the given lengths. The total number of segments in this scheme is 107.

Run this model both as an uncorrected model and as a corrected model, recording the same data as for 9-4.NEC in the table below.

```

CM Dipole, tapered element
CM 7.1 MHz
CE
GW 1 7 -426.5 0 0 -372 0 0 .25
GW 2 8 -372 0 0 -306 0 0 .375
GW 3 8 -306 0 0 -240 0 0 .5
GW 4 15 -240 0 0 -120 0 0 1
GW 5 14 -120 0 0 -12 0 0 1.125
GW 6 3 -12 0 0 12 0 0 2.342
GW 7 14 12 0 0 120 0 0 1.125
GW 8 15 120 0 0 240 0 0 1
GW 9 8 240 0 0 306 0 0 .5
GW 10 8 306 0 0 372 0 0 .375
GW 11 7 372 0 0 426.5 0 0 .25
GS 0 0 .02540
GE 0
EX 0 6 1 0 1 0

```

9-4-1

9-4 Test Data			Reference Data		
Model	Gain dBi	Source Z $R \pm jX \Omega$		Gain dBi	Source Z $R \pm jX \Omega$
9-4-uncor				3.09	64.5 + j 14.7
9-4-cor				2.31	68.9 - j 0.7
9-4-1-uncor				3.69	60.7 + j 30.9
9-4-1-cor				2.13	72.0 + j 0.1

Comments: The corrected models for both versions of the dipole produce far more plausible gain and source impedance figures than either of the uncorrected models. However, note that the corrected version of the model with a low segment count yields a high gain figure and a low source impedance figure. As we learned when working with segment lengths adjacent to a source (when not mixed with tapered diameter problems), inequalities of segment length in the immediate source area can generate erroneous output data from NEC-2. Just because the program produces a monotapered substitute element, we cannot assume that the segmentation in it will be satisfactory. The model must be constructed to ensure that--to the degree possible--all segments are approximately equal in length.

To a degree, the model in 9-4-1.NEC may be extreme in its dense segmentation. As a supplementary exercise, resegment the model, using a single segment for the center (fat) section of the antenna. Since that segment is now 24" long, use this length as the approximate segment length for all other sections of the antenna. Run this new model, making any necessary length adjustment for resonance to the outer "tip" sections only. Record your results for a corrected version of the antenna. You may also wish to check the results for an uncorrected version of this new model.

A second trend should emerge from this modeling sequence. Dense segmentation of an uncorrected element does not yield results that are closer to those derived from the substitute models. Quite the opposite is true. The highly segmented version of the antenna, when run uncorrected, produced the highest (most unrealistic) gain and the lowest source impedance of the group. Uncorrected, tapered-diameter elements are not suitable models for convergence testing.

9-5.NEC: A 3-element Yagi for 21.22 MHz

A number of consequences of failing to use corrected substitute elements for TDEs tend to accumulate with larger arrays, such as Yagi beams. For this reason, we shall use model 9-5.NEC, shown at right through the EX line. Note that the model description of the 6061-T6 aluminum antenna shows a short, large diameter (2.945") center section. The remainder of the elements consist of 0.75, 0.625, and 0.5 inch tubes. The elements are moderately segmented (47, 43, and 41 for the reflector, driver, and director, respectively), using the 6" long center section as a guide.

First, we shall frequency sweep this beam in both the uncorrected and corrected modes. The sweep will begin at 21.0 MHz and use 4 0.15 MHz steps to sample performance across the 15-meter amateur band. We shall record the maximum free space forward gain, the 180° front-to-back ratio, and the source impedance.

```

CM 3-e1 Yagi: 21.22 MHz
CE
GW 1 14 -143.75 0 0 -60 0 0 .25
GW 2 6 -60 0 0 -24 0 0 .3125
GW 3 3 -24 0 0 -3 0 0 .375
GW 4 1 -3 0 0 3 0 0 1.4725
GW 5 3 3 0 0 24 0 0 .375
GW 6 6 24 0 0 60 0 0 .3125
GW 7 14 60 0 0 143.75 0 0 .25
GW 8 12 -132.62 48 0 -60 48 0 .25
GW 9 6 -60 48 0 -24 48 0 .3125
GW 10 3 -24 48 0 -3 48 0 .375
GW 11 1 -3 48 0 3 48 0 1.4725
GW 12 3 3 48 0 24 48 0 .375
GW 13 6 24 48 0 60 48 0 .3125
GW 14 12 60 48 0 132.62 48 0 .25
GW 15 11 -126.75 140 0 -60 140 0 .25
GW 16 6 -60 140 0 -24 140 0 .3125
GW 17 3 -24 140 0 -3 140 0 .375
GW 18 1 -3 140 0 3 140 0 1.4725
GW 19 3 3 140 0 24 140 0 .375
GW 20 6 24 140 0 60 140 0 .3125
GW 21 11 60 140 0 126.75 140 0 .25
GS 0 0 .02540
GE 0
EX 0 11 1 0 1 0

```

9-5

Second, we shall remove the fat center section from only the driver. The simplest way to do this is to convert the diameter of the middle element center section to 0.75" to coincide with the diameter of adjacent wires. This change corresponds to using a well-insulated plate for the driven element such that it and its associated hardware do not contribute significantly to the apparent length of the element. We shall make the same uncorrected and corrected frequency sweeps as we did for the basic version of the model.

Third, we shall remove the excess diameter from the remaining elements, so that all elements show a continuous 0.75" diameter from -24 to + 24 inches relative to the center-line of the model. Once more, after modifying the model, we shall make our two frequency sweeps. We shall record all data in the following table.

9-5 Test Data						
Frequency MHz	Gain dBi	F-B dB	Source Z $R \pm j X \Omega$	Gain dBi	F-B dB	Source Z $R \pm j X \Omega$
Basic		Uncor.			Cor.	
21.0						
21.15						
21.3						
21.45						
D.E. mod.		Uncor.			Cor.	
21.0						
21.15						
21.3						
21.45						
All el. mod.		Uncor.			Cor.	
21.0						
21.15						
21.3						
21.45						

Comments: The data indicate several trends that are significant to modelers. First, the uncorrected gain of the 3--element Yagi in its native form with a large-diameter center section is unnaturally high--equal in fact to what one might expect from a very long-boom 5-element Yagi. The source of these high gain figures emerges from examining the subsequent uncorrected gain figures for the modified models. Simply removing the large center section from the driven element, where the current is higher than any other place on the antenna elements, lowers the gain to more reasonable, if still inaccurate, levels.

Second, the artificiality of the gain figures for the uncorrected unmodified model becomes completely apparent when all the data is compared to the uncorrected model with a driver lacking the large-diameter center section. For example, the front-to-back ratio does not vary to the hundredth's place, despite a drop of well over 2 dB in the gain figures. However, in conjunction with the reduced gain, the source impedance rises dramatically in the uncorrected model.

Third, removing all of the large-diameter center sections from the array further reduces gain and front-to-back ratio, but does not change the pattern of the figures. The gain rises continuously across the operating band, while the front-to-back ratio peaks at the lower end of the band or just outside that band. The driven element resonant frequency is not materially changed by the alterations in the reflector or director.

9-5						
			Reference	Data		
Frequency MHz	Gain dBi	F-B dB	Source Z $R \pm j X \Omega$	Gain dBi	F-B dB	Source Z $R \pm j X \Omega$
Basic		Uncor.			Cor.	
21.0	10.40	23.55	10.2 - j11.8	7.55	26.64	19.2 - j35.9
21.15	10.48	18.45	9.7 - j 8.4	7.56	38.53	19.9 - j29.8
21.3	10.58	15.07	9.1 - j 4.6	7.61	24.51	19.9 - j23.6
21.45	10.69	12.40	8.3 - j 0.5	7.68	19.20	19.4 - j17.2
D.E. mod.		Uncor.			Cor.	
21.0	7.85	23.55	18.3 - j20.6	7.55	26.13	19.5 - j30.3
21.15	7.93	18.45	17.6 - j14.2	7.56	39.10	20.2 - j24.2
21.3	8.03	15.07	16.4 - j 7.3	7.61	24.84	20.3 - j18.0
21.45	8.14	12.40	14.9 + j 0.2	7.69	19.38	19.7 - j11.5
All el. mod.		Uncor.			Cor.	
21.0	7.81	22.81	18.7 - j20.6	7.56	42.28	19.7 - j31.0
21.15	7.90	18.02	17.8 - j14.2	7.60	26.45	19.9 - j24.9
21.3	8.01	14.74	16.5 - j 7.3	7.67	20.15	19.4 - j18.5
21.45	8.12	12.11	15.0 + j 0.3	7.76	16.38	18.3 - j11.7

Turning to the corrected model, the gain does not change at all across the operating band when the center section is removed from the corrected model. This lack of change is a correct result, since changing the length of the driven element changes the source impedance but not the overall performance of a well-designed parasitic beam. The actual change in impedance of the corrected but modified model appears mostly as a reduction in the capacitive reactance designed into the original model.

Removing the large-diameter center sections from the parasitic elements does have an effect upon the antenna performance. Essentially, the smaller, more constant diameter elements result in performance curves that are lowered in frequency, in this case by

about 0.15 MHz. This shift may initially seem counter-intuitive, since with simple dipoles, a reduction in diameter would push any given gain curve upward in frequency and require a slight lengthening of the antenna element to bring it back down to its original frequency. However, a parasitic array involves a complex set of element interactions, and the downward shift in frequency when removing a large-diameter center section from all elements is typical.

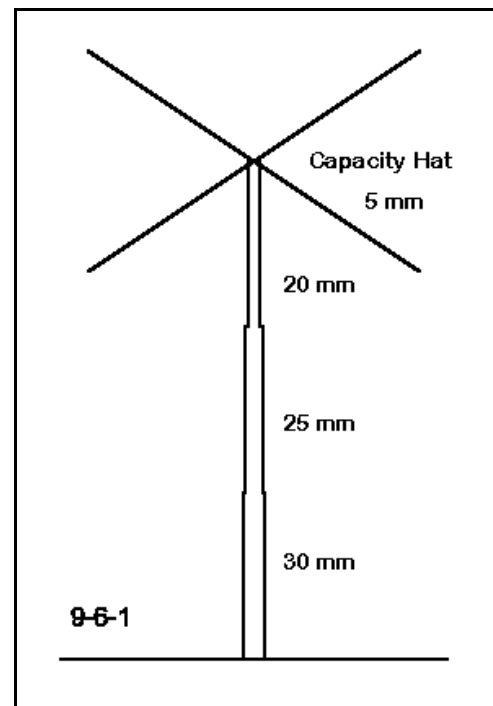
As a supplemental exercise, obtain the substitute element lengths and diameters for all three models. From them, construct 3-element Yagis composed of a single wire per element and segmented at the original density of 47, 43, and 41 for the reflector, drive, and director, respectively. Compare the data either for the design frequency of 21.22 MHz or for a full frequency sweep between the new models (for which 9-5-1.NEC through 9-5-3.NEC are check models) and the original models in the corrected mode. What differences in performance data emerge and to what degree are they functions of the differences between the wholly equal segment lengths of the new models and the remaining irregularities of length on the originals?

9-6.NEC: A capacity-hat short vertical for 10.0 MHz

In some instances, the geometry of an antenna will prevent you from using the TDE correction system. Consider a capacity-hat short vertical for 10 MHz, where the vertical section is composed of three sections, each with a different diameter, as illustrated in **Figure 9-6-1**. Since the activation of the TDE correction requires a linear structure without angular junctions, you cannot obtain a correct model for this antenna.

The model (9-6.NEC) for this basic antenna shows the 6 m long vertical section to consist of equal lengths of 20 mm, 25 mm, and 30 mm diameter 6061-T6 aluminum. The same material is used for the 5 mm top-hat wires. (We shall look into the ability of NEC-2 to model top hats in the next chapter.) The goal is to make this antenna resonant at 10 MHz. The antenna is over perfect ground for this exercise. The resulting gain figures may not reflect real performance, but they will be entirely satisfactory for comparing values to determine whether the reported results are plausible.

Since the antenna is symmetrically vertical, a single elevation plot will suffice--or you may consult the Radiation Pattern table to obtain the gain value.



Run this model and record both the gain in dBi and the source impedance in terms of resistance and reactance.

```

CM 1/4 wave short vertical
CM Capacity-hat load
CE
GW 1 8 0 0 0 0 0 2 .015
GW 2 8 0 0 2 0 0 4 .0125
GW 3 8 0 0 4 0 0 6 .01
GW 4 3 0 0 6 .65 0 6 .0025
GW 5 3 0 0 6 0 .65 6 .0025
GW 6 3 0 0 6 -.65 0 6 .0025
GW 7 3 0 0 6 0 -.65 6 .0025
GS 0 0 1
GE 1
GN 1
EX 0 1 1 0 1 0
LD 5 1 1 8 2.4938E7
LD 5 2 1 8 2.4938E7
LD 5 3 1 8 2.4938E7
LD 5 4 1 3 2.4938E7
LD 5 5 1 3 2.4938E7
LD 5 6 1 3 2.4938E7
LD 5 7 1 3 2.4938E7
FR 0 1 0 0 10 0
RP 0 181 1 1000 -90 0 1 1
EN

```

9-6

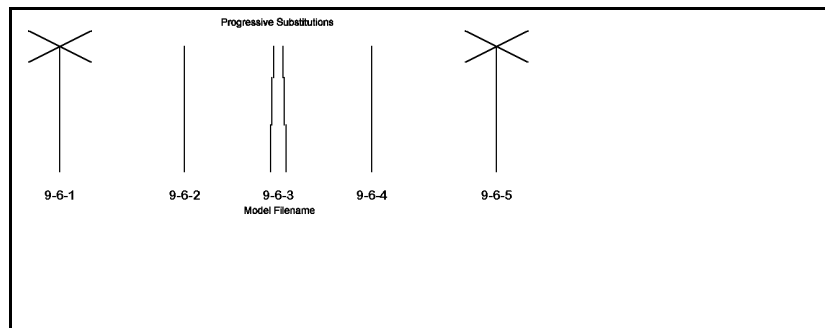
The reported values (which should read about 5.18 dBi and $34.3 + j 4.3 \Omega$ for gain and source impedance, respectively) may seem initially plausible. However, the gain is in excess of what is possible. Over perfect ground, the maximum gain of a lossless full-length $1/4\lambda$ radiator is 2.15 dBi plus 3 dB for ground reflection, minus losses in this case for the use of 6061-T6 aluminum and for shortening the radiator. Any value over about 5.1 dBi is suspect. Hence, both the gain and the source impedance values must be held dubious.

Although the values might be close enough to begin casual construction, allowing for extensive field adjustment, they are wholly inadequate for tasks requiring more rigorous engineering. For example, planning an array of such antennas, perhaps with switchable phasing to obtain directional patterns with specified properties, is not possible from these questionable results. An alternate strategy is required.

In a 5-step process, it is possible to develop a very reliable stand-in model for the original in 9-6.NEC.

Figure 9-6-2 provides a simple way to track the process. The sample we shall present presumes that the lengths of both the vertical and the top-hat rods

are adjustable. If either dimension turns out to be fixed by the terms of a project, then the process will be a bit slower to execute, but not appreciably different.



Step 1, shown in model 9-6-1.NEC on the next page, simply replaces the vertical sections of the antenna with a uniform diameter element with an estimated average diameter. In this case, a diameter of 25 mm serves adequately. Without changing the dimensions of the hat assembly, adjust the height of the vertical portion of the antenna until arriving at resonance at 10 MHz.

In every step, we shall record the height of the antenna, the gain and the source impedance. Run this step and verify that resonance at 10 MHz occurs at a height of about 5.90 m. The gain should be close to 5.09 dBi, with a source impedance of about $33.6 - j 0.3 \Omega$. Note that the gain figure is very reasonable for an aluminum antenna over perfect ground.

Unfortunately, we are still shy of reliable data, unless the actual antenna uses a constant diameter vertical section. Since the equivalent diameter and length of a tapered-diameter element is quite specific, we do not yet know if our averaging step yields wholly accurate results.

```

CM 1/4 wave short vertical: 10 MHz
CM Substitute 25 mm version
CE
GW 1 8 0 0 0 0 0 1.9 .0125
GW 2 8 0 0 1.9 0 0 3.9 .0125
GW 3 8 0 0 3.9 0 0 5.92 .0125
GW 4 3 0 0 5.92 .65 0 5.92 .0025
GW 5 3 0 0 5.92 0 .65 5.92 .0025
GW 6 3 0 0 5.92 -.65 0 5.92 .0025
GW 7 3 0 0 5.92 0 -.65 5.92 .0025
GS 0 0 1
GE 1
GN 1
EX 0 1 1 0 1.414214 0
LD 5 1 1 8 2.4938E7
LD 5 2 1 8 2.4938E7
LD 5 3 1 8 2.4938E7
LD 5 4 1 3 2.4938E7
LD 5 5 1 3 2.4938E7
LD 5 6 1 3 2.4938E7
LD 5 7 1 3 2.4938E7
FR 0 1 0 0 10 0
RP 0 181 1 1000 -90 0 1 1
EN

```

9-6-1

```

CM 1/4 wave short vertical
CM Resonant at Fa
CE
GW 1 8 0 0 0 0 0 1.9 .0125
GW 2 8 0 0 1.9 0 0 3.9 .0125
GW 3 8 0 0 3.9 0 0 5.92 .0125
GS 0 0 1
GE 1
GN 1
EX 0 1 1 0 1 0
LD 5 1 1 8 2.4938E7
LD 5 2 1 8 2.4938E7
LD 5 3 1 8 2.4938E7
FR 0 1 0 0 12.1 0
RP 0 181 1 1000 -90 0 1 1
EN

```

9-6-2

Step 2 in the process involves removing the hat from the initial monotapered vertical antenna section and determining the resonant frequency of the vertical portion alone. Model 9-6-2.NEC shows this step. You should not use this model until you have modified model 9-6-1.NEC and arrived at its resonant frequency, recording as well

the gain and source impedance.

You should arrive at resonance at about 12.10 MHz, with a gain of about 5.14 dBi and a source impedance of about $26.0 + j 0.2 \Omega$. Note that the antenna is a full $1/4\lambda$ at 12.1 MHz with no hat—hence, the higher gain report.

For Step 3, construct a tapered-diameter vertical (with no hat) using the original diameters specified (30 mm, 25 mm, and 20 mm), as illustrated in model 9-6-3.NEC. Make the section approximately equal in length. Using the correction system, resonate this vertical at 12.10 MHz. Because the antenna is truly linear, the correction system will function well. Since tapered elements are normally longer than uniform elements of the same average diameter, expect this construction to be slightly longer than the element in model 9-6-2.NEC. In fact, you should obtain a model about 5.99 m long, with a source impedance of about $36.0 + 0.4 \Omega$.

```

CM 1/4 wave short vertical
CM TDE w/o cap hat
CE
GW 1 8 0 0 0 0 0 2 .015
GW 2 8 0 0 2 0 0 4 .0125
GW 3 8 0 0 4 0 0 6.03 .01
GS 0 0 1
GE 1
GN 1
EX 0 1 1 0 1 0
LD 5 1 1 8 2.4938E7
LD 5 2 1 8 2.4938E7
LD 5 3 1 8 2.4938E7
FR 0 1 0 0 12.1 0
RP 0 181 1 1000 -90 0 1 1
EN

```

9-6-3

Record the height of this structure. It is the height of the actual antenna that hypothetically will be constructed from the tapered-diameter tubing sections.

To begin Step 4, obtain the section dimensions of the substitute element used by the correction system to model the TDE. Construct a uniform-diameter vertical antenna using these dimensions, as shown in model 9-6-4.NEC. The substitute section will have a total height of 5.907 m and a diameter of 25.4 mm. Running this model, you should find it resonant at 12.10 MHz with a source impedance of about $35.8 - j 0.8 \Omega$, very close to the TDE model values.

```

CM 1/4 wave short vertical
CM Substitute vertical
CE
GW 1 8 0 0 0 0 0 1.959 .0127
GW 2 8 0 0 1.959 0 0 3.919 .0127
GW 3 8 0 0 3.919 0 0 5.907 .0127
GS 0 0 1
GE 1
GN 1
EX 0 1 1 0 1.414214 0
LD 5 1 1 8 2.4938E7
LD 5 2 1 8 2.4938E7
LD 5 3 1 8 2.4938E7
FR 0 1 0 0 12.1 0
RP 0 181 1 1000 -90 0 1 1
EN

```

9-6-4

```

CM 1/4 wave short vertical: 10 MHz
CM substitute with cap hat
CE
GW 1 8 0 0 0 0 0 1.959 .0127
GW 2 8 0 0 1.959 0 0 3.919 .0127
GW 3 8 0 0 3.919 0 0 5.907 .0127
GW 4 3 0 0 5.907 .655 0 5.907 .0025
GW 5 3 0 0 5.907 0 .655 5.907 .0025
GW 6 3 0 0 5.907 -.655 0 5.907 .0025
GW 7 3 0 0 5.907 0 -.655 5.907 .0025
GS 0 0 1
GE 1
GN 1
EX 0 1 1 0 1.414214 0
LD 5 1 1 8 2.4938E7
LD 5 2 1 8 2.4938E7
LD 5 3 1 8 2.4938E7
LD 5 4 1 3 2.4938E7
LD 5 5 1 3 2.4938E7
LD 5 6 1 3 2.4938E7
LD 5 7 1 3 2.4938E7
FR 0 1 0 0 10 0
RP 0 181 1 1000 -90 0 1 1
EN

```

9-6-5

Step 5 consists of reconstructing the hat on top of the latest model and adjusting the length of the spokes for 10.0 MHz. Model 9-6-5.NEC illustrates this construction. The spokes were lengthened from the original model to 0.655 m each for a resonant source impedance of $33.5 -j 0.9 \Omega$. The gain value returned is 5.09 dBi, just what we would expect.

Model 9-6-5.NEC is now a very accurate and usable stand-in model for the original model, 9-6.NEC. For more complex arrays or for other modeling studies that might change materials, ground situations, and other factors, the stand-in will yield very good results. However, you must

remember that the height of 5.907 m is not the height of the physical antenna that you would construct. That height remains 5.99 m, as determined through model 9-5-3.

This example used a very smooth and small set of transitions among sections of the vertical TDE. Hence, the numbers of the final model and those of the initial estimated average diameter model are very close. In fact, they are of numeric but not constructional significance. However, you may verify the aptness of the technique by constructing other models with more radical changes in diameter. For example, try a 3 MHz, 40' vertical antenna with top-hat, where the vertical portion is composed of sections beginning with a short 6" diameter portion, followed by sections of 5, 4.5, 4, and 2 inches in diameter to make up the total length. Vary the percentage of the total length occupied by each diameter of tubing.

This exercise is only one of many ways in which limitations in the applicability of the TDE correction system can be effectively overcome through the use of carefully constructed stand-in models.

Summing Up

The inability of NEC-2 to handle directly tapered-diameter elements with accuracy has yielded an ingenious correction system that employs substitute models having identical relevant characteristics as the original TDE. Part of the goal has been to acquaint you sufficiently with the terms of the correction factor to give you confidence in the accuracy of

its results.

The correction factor is subject to a number of limitations. First, it applies only to linear elements with no intervening or terminal junctions with other wires that are at an angle other than 180° with the subject element. For accurate results, the TDE must be within a small amount (about 15%) of resonance. Only a single source at the element center is permitted, although with open-end elements, such as dipoles, a split source is permissible if the element center is the junction of two segments or wires. For grounded elements, such as monopoles, the source must be on the lowest segment. Identical rules apply to loads, and mid-element loads are not permitted. Only one transmission line may be used in the element--at the center of open-ended elements or the bottom of a grounded element. If a transmission line is used for an open-ended element, the element center must also be a segment center. Within these limits, which enclose a wide spectrum of simple and complex antennas, the correction system yields very reliable antenna performance data.

Where some limitation is overrun by an antenna design, the TDE system can often be used to develop a stand-in model for the original tapered-diameter version using the substitute created by the correction system as a replacement for the TDE section of the antenna. Although the technique is not suitable to every TDE circumstance, it expands the utility of NEC-2 to encompass modeling situations that might otherwise not be covered. It also serves as a primary example of an assortment of work-arounds available when models seem to press the limits of the core program.

10.

Geometry Limitations

Objectives: *In this set of exercises, you will learn of some NEC-2 limitations for which there are no direct work-arounds. Of equal importance, you will learn something of the process by which such limitations are analyzed and evaluated in a small series of detailed modeling tests.*

Every method-of-moments modeling system has limitation in terms of geometries that are difficult if not impossible to model. The tapered-diameter element is one limitation of NEC-2 for which there is a work-around in terms of substituting a reliable non-tapered element. However, the substitute only works if the element is linear and meets other criteria for invoking the corrective.

Some other geometric configurations do not model well within NEC-2, and for many of them, there are no correctives. In this set of exercises, we shall explore some of these problematical geometries. One of our goals is to acquaint ourselves with them to the extent that we automatically raise a caution flag when we encounter modeling tasks involving them.

However, there is a second, equally important goal, which is to introduce some of the methods we employ to determine that we in fact have a geometric limitation. Therefore, our work with the individual models will be more extensive than in some preceding exercises, as we work through a process of validating models or limitations that suggest a model may be less than fully reliable.

In general, there are four questions we may pose in the process of limitation detection:

1. Is there a reliable theoretical method of establishing a standard against which to measure a model? A known, credible mathematical formulation often serves this purpose.
2. Is there a different modeling program which is known to be reliable in the given case against which to measure the NEC-2 model? The most commonly available programs are MININEC (3.13) and NEC-4. Each has its own advantages and constraints, which means that the use of them must be judicious.

3. Are there any tests internal to NEC-2 which one may use to check a model's plausibility? Convergence, encountered in Chapter 6, is one of the primary tests used to validate NEC results, but in this application, it may best be used in conjunction with other methods.
4. Can one build and test the antenna modeled to determine the accuracy of the model? In some case, building and testing may require more resources than are available. However, one may devise more easily constructed alternative antennas to test the same potential limitation.

The last entry on our list of questions is a strong reminder that modeling antennas does not occur in a vacuum. Rather it is a tool whose use begins with and ends with actual antennas used in telecommunications. For this reason, all but a few antennas modeled throughout this guide are derived from functional antennas that have been used or are in use. The few exceptions--for example, those arbitrarily set to a 1-meter wavelength and using lossless wire in free space--are designed to let you connect practical antennas to the fundamentals of antenna theory. Between these poles of theory and construction, antenna modeling has its natural home.

Exercise Preparation

In this set of exercises, we shall encounter fewer distinctly different antennas and more variations on the selected use of the models. To investigate model reliability requires that we have "check" models of known accuracy against which to assess--either initially or finally--whether our modeling attempt is plausible. Moreover, we shall need to create numerous routine and systematic variations on our models. In this chapter, most check models are supplied on the accompanying disk, but systematic variants you will generate yourself as you move through an exercise.

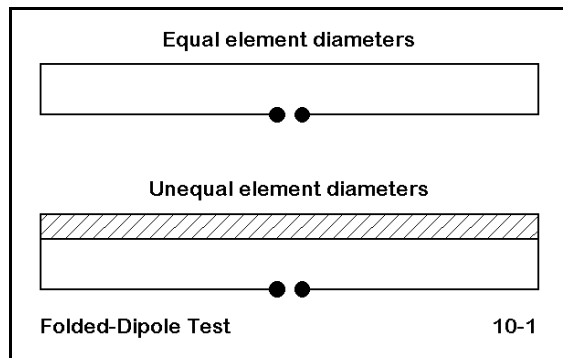
The model filenames will take a slightly different look in this chapter. For example, the models for the first exercise will be 10-1-1.NEC through 10-1-4.NEC. Therefore, if you save variants, be sure to use filenames that allow separable saving and as well give clues to the source model. When asked to do a convergence test, for instance, you may wish to use a filename such as 10-2-3A.NEC to preserve 10-2-3.NEC and to mark it as the source model for the revision you generate.

Although some of the exercises are routine and repetitive, going all the way through them yourself is crucial to mastering the skill of evaluating model reliability and getting a good sense of where certain limitations in NEC-2 begin. Therefore, be prepared to spend some time with each modeling exercise--both in conducting the hands-on operations and in developing your understanding of the results and their consequences for further modeling effort.

10-1.NEC: A folded dipole for 28.5 MHz

NEC-2 models standard folded dipoles, wherein both closely spaced elements have the same diameter, with good accuracy. Of course, such models should adhere to the practice of setting wire segment junctions precisely parallel to each other for maximum accuracy. Another easily obtained modeling program, MININEC, also models standard folded dipoles with roughly equivalent accuracy.

As a check on this, we shall start with two standard folded dipoles, both resonated close to 28.5 MHz. Each uses a spacing of 0.25' (3"). However, one uses 0.5" diameter wire, while the other uses #12 AWG (0.0808") wire. For this exercise, we shall model the folded dipoles in free space and use lossless wire, since neither ground affects nor wire loss play a role in our investigation.



Our task, as indicated by the sketch in **Figure 10-1**, will be to use the baseline accuracy of these antenna models and then to explore the accuracy of models using unequal wire diameters in the folded-dipole configuration.

Open file 10-1-1 (0.5" diameter wire) and then 10-1-2.NEC (#12 AWG). Compare the descriptions shown on this page to verify that the only differences are in the wire lengths--needed to resonate the antennas--and the wire diameters.

```

CM Folded dipole 0.5" dia. el.
CE
GW 1 67 -8.05 0 0 8.05 0 0 .02085
GW 2 1 8.05 0 0 8.05 .25 0 .02085
GW 3 67 8.05 .25 0 -8.05 .25 0 .02085
GW 4 1 -8.05 .25 0 -8.05 0 0 .02085
GS 0 0 .3048
GE 0
EX 0 1 34 0 1 0
FR 0 1 0 0 28.5 0
RP 0 1 360 1000 90 0 1 1
EN
10-1-1

```

```

CM Folded dipole #12 wires
CE
GW 1 67 -8.14 0 0 8.14 0 0 3.36778E-03
GW 2 1 8.14 0 0 8.14 .25 0 3.36778E-03
GW 3 67 8.14 .25 0 -8.14 .25 0 3.36778E-03
GW 4 1 -8.14 .25 0 -8.14 0 0 3.36778E-03
GS 0 0 .3048
GE 0
EX 0 1 34 0 1 0
FR 0 1 0 0 28.5 0
RP 0 1 360 1000 90 0 1 1
EN
10-1-2

```

Run the models to determine their maximum gain and their source impedances in terms of resistance and reactance. Record your results on the table on the next page. For comparison, reference data is provided in parentheses from the output of a MININEC program. Note that there are spaces left for further entries that will be related to the folded dipole with unequal

element diameters. Our initial goal is to establish that both programs yield reasonably good results for these basic models. The segmentation density is established by the need in MININEC to use many segments to avoid "clipping" corners.

10-1 Test Data			Reference Data	
Model	Gain dBi	Source Z (R±jX Ω)	Gain dBi	Source Z (R±jX Ω)
10-1-1			2.23 (2.23)	285.8 + j 4.2 (285.5 + j 1.5)
10-1-2			2.19 (2.19)	286.4 + j 1.1 (286.2 - j 0.0)
10-1-3			0.98 (2.22)	398.8 + j23.7 (530.0 + j 4.5)
10-1-4			0.96	394.0 - j 3.0

Comments: Your modeling should have yielded figures very close to those for the same model run on MININEC. (There is a 1 segment difference between the two models per long element, since center feeding in MININEC requires placement of the source on a segment junction, whereas in NEC-2, one places the source on a segment itself. Therefore, for linear elements, NEC-2 prefers an odd number of segments, while MININEC prefers an even number of segments.)

The general accuracy of the source impedances is assured by the general knowledge that a folded dipole with equal wire diameters provides a 4:1 impedance transformation over a resonant dipole of similar diameter to the two-wire combination. Given that such a dipole would have a source impedance between 70 and 72 Ω, the range of expected folded dipole source impedances would be between 280 and 288 Ω. Both NEC-2 and MININEC meet this expectation.

Open file 10-3-3.NEC. This file contains a folded dipole using a fed element of #12 AWG wire (0.0808" diameter) and a secondary element of 0.5" diameter wire. The 3" spacing and other modeling parameters are identical to that in the check models. Run this model and enter its maximum gain and source impedance into the table above. Once you have entered the data, compare it with the corresponding data from the MININEC model of the same antenna.

```

CM Folded dipole 0.5"/#12 wires
CE
GW 1 67 -8.1 0 0 8.1 0 0 3.36778E-03
GW 2 1 8.1 0 0 8.1 .25 0 3.36778E-03
GW 3 67 8.1 .25 0 -8.1 .25 0 .02085
GW 4 1 -8.1 .25 0 -8.1 0 0 3.36778E-03
GS 0 0 .3048
GE 0
EX 0 1 34 0 1 0
FR 0 1 0 0 28.5 0
RP 0 1 360 1000 90 0 1 1
EN

```

10-1-3

Not only does the NEC-2 model show an unexpectedly low maximum gain, its source impedance diverges widely from the MININEC report of source impedance. On the possibility that the disparity might be a result of the non-resonance of the folded dipole in the NEC-2 model, revise the length of 10-1-3.NEC to resonance.

```

CM Folded dipole 0.5"/#12 wires
CE
GW 1 67 -8.05 0 0 8.05 0 0 3.36778E-03
GW 2 1 8.05 0 0 8.05 .25 0 3.36778E-03
GW 3 67 8.05 .25 0 -8.05 .25 0 .02085
GW 4 1 -8.05 .25 0 -8.05 0 0 3.36778E-03
GS 0 0 .3048
GE 0
EX 0 1 34 0 1 0
FR 0 1 0 0 28.5 0
RP 0 1 360 1000 90 0 1 1
EN

```

10-1-4

File 10-1-4.NEC contains the reresonated folded dipole with unequal element diameters. Unfortunately, the gain figure remains low, although the source impedance rises somewhat. The remaining question is whether there is a decisive means of evaluating the differences between the MININEC and the NEC-2 models.

Standard antenna theory for folded dipoles evaluates the ratio of the folded dipole's source impedance against a single dipole's source impedance in terms of the spacing and relative diameters of the folded dipole elements.

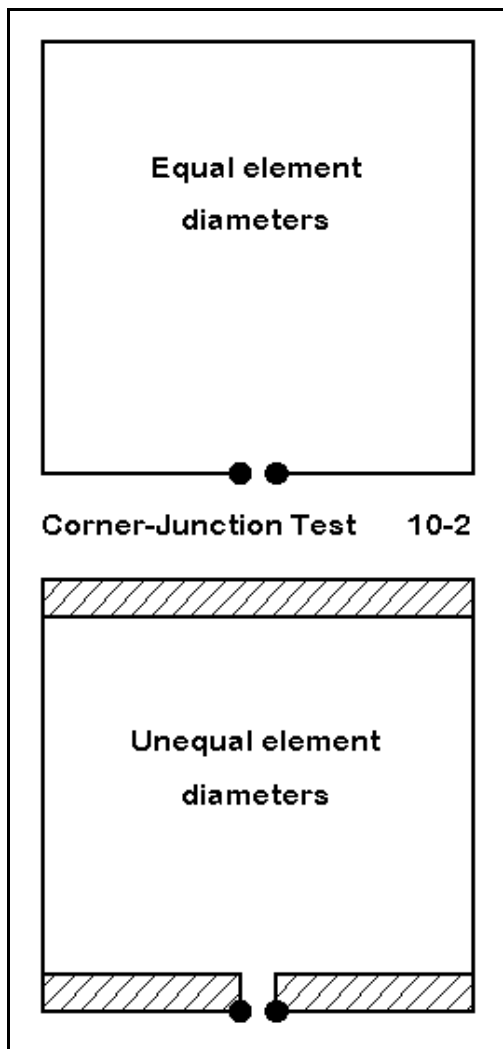
$$R = \left(I + \frac{\log \frac{2s}{d_1}}{\log \frac{2s}{d_2}} \right)^2 \quad 1$$

where R is the impedance transformation ratio, s is the center-to-center wire spacing, d_1 is the diameter of the fed wire, and d_2 is the diameter of the second wire, and where s , d_1 , and d_2 are given in the same units. It should be clear that for equal diameter wires of any reasonable spacing, the transformation ratio will be 4. For a spacing of 3", a fed wire diameter of 0.0808", and a second wire diameter of 0.5", the resultant transformation ratio is about 7.47. For a linear dipole impedance between 70 and 72 Ω , the anticipated folded dipole impedance would be between 523 and 538 Ω . We might expect some variation, since the equation does not account for the length or diameter of the connecting wires, which are #12 AWG in this model. However, that variation should be slight.

The MININEC source impedance value falls squarely within the range of anticipated source impedances for the model folded dipole. In contrast, the NEC-2 model provides not only an unreasonably low maximum gain, but as well a source impedance well outside the range of those anticipated. Therefore, the modeler would be justified in treating the NEC-2 model as unreliable. Moreover, one may also note that here is a category of wire geometries for which NEC-2 does not generally produce reliable results. All folded dipoles with unequal-diameter elements must henceforth be approached with caution.

Not all cases in which we meet a doubtful model will we have ready equations by which to judge decisively the model's reliability. In many cases, we shall have to use a combination of tests, and even then, the results--short of building and testing a particular antenna--may be suggestive rather than decisive. However, even suggestive results should mean that we approach future models of that type with caution.

10-2: A quad loop for 28.5 MHz



We may begin our investigation into quad loops in the same manner as we approached the study of folded dipoles: with some models that are accurate in both MININEC and in NEC-2. Our eventual task will be to evaluate the adequacy of NEC-2 models of quad loops using different diameter wires for the horizontal and vertical members, as suggested in **Figure 10-2**. Once more, we begin with the partial goal of establishing the general accuracy of models using a uniform wire diameter throughout, and for this, we may once more use 0.5" diameter wire in one model and #12 AWG (0.0808") wire in the other.

```

CM Quad loop 0.5" wire
CE
GW 1 61 -4.682 0 -4.682 4.682 0 -4.682 .02085
GW 2 61 4.682 0 -4.682 4.682 0 4.682 .02085
GW 3 61 4.682 0 4.682 -4.682 0 4.682 .02085
GW 4 61 -4.682 0 4.682 -4.682 0 -4.682 .02085
GS 0 0 .3048
GE 0
EX 0 1 31 0 1 0
FR 0 1 0 0 28.5 0
RP 0 1 360 1000 90 0 1 1
EN

```

10-2-1

File 10-2-1.NEC contains the file for the half-inch wire loop, while 10-2-2.NEC contains the #12 model. Carefully compare the two models to ensure they are the same except for the wire size and the loop length necessary for (approximate) resonance.

As with the folded dipoles, run these models and record their maximum gain and source impedances in the appropriate lines of the table on the next page. The reference table once more provides MININEC data in parentheses to establish the rough coincidence of the models in each system. The high segmentation per side is again a necessity in MININEC in order to minimize corner cutting by that program's method of handling current pulses and wire junctions at an angle. That segmentation density will become an issue for NEC-2.

```

CM Quad loop #12 wire
CE
GW 1 61 -4.573 0 -4.573 4.573 0 -4.573 3.36778E-03
GW 2 61 4.573 0 -4.573 4.573 0 4.573 3.36778E-03
GW 3 61 4.573 0 4.573 -4.573 0 4.573 3.36778E-03
GW 4 61 -4.573 0 4.573 -4.573 0 -4.573 3.36778E-03
GS 0 0 .3048
GE 0
EX 0 1 31 0 1 0
FR 0 1 0 0 28.5 0
RP 0 1 360 1000 90 0 1 1
EN
    
```

10-2-2

10-2 Test Data			Reference Data	
Model	Gain dBi	Source Z (R±jX Ω)	Gain dBi	Source Z (R±jX Ω)
10-2-1			3.37 (3.37)	129.7 - j 0.2 (129.4 - j 3.6)
10-2-2			3.30 (3.30)	125.7 - j 1.9 (125.2 - j 7.3)
10-2-3			3.59 (3.63)	170.4 + j122 (136.9 - j 5.2)
10-2-3A			3.39	133.4 - j 0.4
10-2-4			3.58	135.2 - j 2.7

Comments: Once more, the MININEC and the NEC-2 models of the quad loops with a uniform wire diameter are in close agreement. Now we may approach the question concerning quad loops where the horizontal members are significantly different in diameter from the vertical members.

Open file 10-2-3.NEC. Except for the variable wire diameter, the model uses the same parameters as the first two models in this sequence. Run the model and record the values received for maximum gain and source impedance. Note the heavy segmentation density, since this model was also run in MININEC to produce the parenthetical values on line 3 of table 10-2.

```

CM Quad loop .5"/#12 wires
CE
GW 1 61 -5.075 0 -5.075 5.075 0 -5.075 .02085
GW 2 61 5.075 0 -5.075 5.075 0 5.075 3.36778E-03
GW 3 61 5.075 0 5.075 -5.075 0 5.075 .02085
GW 4 61 -5.075 0 5.075 -5.075 0 -5.075 3.36778E-03
GS 0 0 .3048
GE 0
EX 0 1 31 0 1 0
FR 0 1 0 0 28.5 0
RP 0 1 360 1000 90 0 1 1
EN
    
```

10-2-3

The source impedance for this model shows the model to be seriously off resonance. Revise this model by uniformly reducing the dimensions until the model is resonant. A value of $\pm 4.78'$ per side should bring the model close to resonance. Save this model as 10-2-3A.NEC.

It is tempting to call the job done at this point. The gain value is more modest than the MININEC value, but the source impedance is apparently nearly correct relative to the preceding models. Hence, we have a possibly undecidable difference in the requisite loop lengths called out by NEC-2 and MININEC: 9.56' per side vs. 10.15' per side. This amounts to a 2.36' overall difference in loop length. Perhaps only an empirical test may decide the issue.

Although empirical tests are always in order, we may waste a good bit of time if we do not first exhaust the modeling tests available to us. We earlier noted the heavy segmentation density used in the MININEC model and transported uncritically to the NEC-2 model. Let us perform an extended convergence test on 10-2-3A, noting not only the gain and source impedance, but as well, the step-by-step differences in the resistive and reactive components of the source impedance. As you modify 10-2-3A for segments per side, be sure to relocate the source segment correctly to ensure that the bottom horizontal wire is always fed in the center. Record your results in the following table.

10-2-3A		Test Data			
Segments Side	Gain dBi	Source Resistance	ΔR	Source Reactance	ΔX
5					
11					
21					
31					
41					
51					
61					
71					
81					
91					

You may check your work against the reference table on the next page. What should be clear is that the model never reaches convergence. While the gain figures are well converged, the source impedance resistive and reactive components never reach even a 1 Ω change from step to step. Nor is it clear what level of segmentation density one should select for the most accurate model. Because the gain continues to drop slowly with further segmentation, the exercise seems to lead in the wrong direction.

With cases like the one at hand, where there is a large change of wire diameter at a sharp angle, convergence testing fails as an independent test of model adequacy. However, together with the MININEC results, it provides a clue to our next step.

10-2-3A		Reference Data			
Segments Side	Gain dBi	Source Resistance	Δ R	Source Reactance	Δ X
5	3.41	118.9	-----	-89.2	-----
11	3.41	121.5	2.6	-62.7	48.7
21	3.40	125.3	2.8	-40.5	22.2
31	3.40	128.0	2.7	-26.6	13.9
41	3.39	130.1	2.1	-16.2	10.4
51	3.39	131.9	1.8	- 7.7	8.5
61	3.39	133.4	1.5	- 0.4	7.3
71	3.38	134.8	1.4	6.0	6.4
81	3.38	136.1	1.3	11.8	5.8
91	3.38	137.3	1.2	17.2	5.6

Although the lowest level of convergence shows the lowest source resistance and reactance, it also shows the highest gain. The result suggests of one more task to perform. Reresonate the loop at a segmentation level of 5 per side. Record your results in the original table.

The dimensions you arrive at should be close to those shown in the check file 10-2-4.NEC. At 5.0' per side, the quad loop with unequal

```

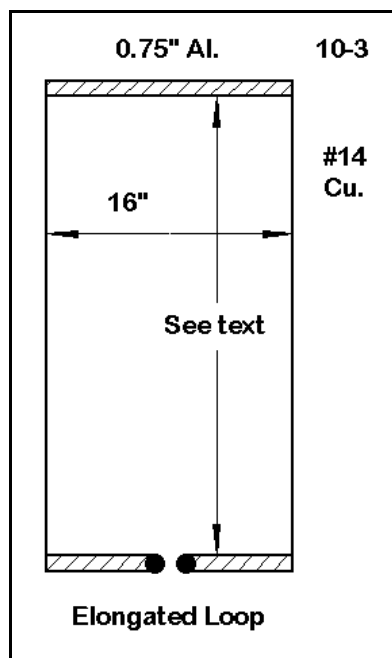
CM quad loop .5/#12
CE
GW 1 5 -5 0 -5 5 0 -5 .02085
GW 2 5 5 0 -5 5 0 5 3.36778E-03
GW 3 5 5 0 5 -5 0 5 .02085
GW 4 5 -5 0 5 -5 0 -5 3.36778E-03
GS 0 0 .3048
GE 0
EX 0 1 3 0 1 0
FR 0 1 0 0 28.5 1
RP 0 1 360 1000 90 0 1 1
EN
    
```

wire diameters yields a NEC-2 gain of 3.58 dBi with a source impedance of $135.2 - j2.7\Omega$. These numbers are not far off the MININEC figures of 3.63 dBi gain and $136.9 - j5.2\Omega$.

From results such as these emerges the guideline to model angular corners with wires of dissimilar diameters with the lowest number of segments possible. Notice, however, that this guideline can exist only because MININEC is thought to be relatively reliable of this class of model. Nothing within NEC-2 and the standard internal tests for model adequacy would justify the guideline or certify the result as even probably accurate.

In the end, the only remaining desideratum is to build a test antenna and measure at least the source impedance. However, with only 0.15' (less than 2") per side difference between the MININEC and NEC models, exceptionally careful construction would be required to differentiate them.

10.3: An elongated quad loop for 146 MHz



A more decisive and buildable test antenna may be devised to test the adequacy of closed geometry loops using different wire diameters. The elongated loop shown in **Figure 10-3** can be made from hardware store aluminum tubing and house wiring, along with a PVC or wood support system (to minimize the chances for metallic influences to alter the antenna performance). The elongated form of the quad loop provides for a convenient match to 50- Ω coaxial cable for connection to either rudimentary or sophisticated antenna analyzers (or even SWR meters with a signal source). Although the modeling is done in free space, any height above $3-4\lambda$ will negate any significant influence from ground reflections on the source impedance. Since the antenna is modeled for 146 MHz, the required height is about 20' for the tests.

The 0.75" diameter horizontal members are aluminum, while the #14 (0.0641") wires are copper. If you construct this antenna for a test, minimize the size of connection "lumps" where the copper wire meets the aluminum tubing. Also, minimize lead length to the transmission line connector so that it does not inadvertently lengthen the lower horizontal wire.

Lest we leap over careful modeling procedures and begin with a minimally segmented version of the antenna, we should replicate relevant portions of the preceding test, especially some part of the convergence test. Open file 10-3-1.NEC. Create your own table for convergence testing, beginning at the given segmentation of 14 horizontal and 42 vertical (since the ratio of height to base is about 2:1). Reduce this in steps through 14/28 and 7/14 to a final density of 3/5. At each step, reresonate the antenna simply by reducing the values on the Z-axis. For ease in this task, the model has been set up with a baseline Z-value of zero, minimizing the number of entries needed to change the height.

```

CM Elongated quad loop: 146 MHz
CM 0.75" Al., #14 Cu.
CE
GW 1 21 -8 0 0 8 0 0 .375
GW 2 42 8 0 0 8 0 29.4 .032047244
GW 3 21 8 0 29.4 -8 0 29.4 .375
GW 4 42 -8 0 29.4 -8 0 0 .032047244
GS 0 0 .02540
GE 0
EX 0 1 11 0 1 0
LD 5 1 1 21 2.4938E7
LD 5 2 1 42 5.8001E7
LD 5 3 1 21 2.4938E7
LD 5 4 1 42 5.8001E7
FR 0 1 0 0 146 0
RP 0 1 360 1000 90 0 1 1
EN

```

10-3-1

Record the maximum gain and source impedance for each of these steps. You should see a steady rise in maximum gain as the segmentation density decreases. As well, the resonant (or approximately resonant) source resistance should decrease from a value in the mid-60s to a value close to 52Ω .

```

CM Elongated quad loop: 146 MHz
CM 0.75" Al., #14 Cu.
CE
GW 1 3 -8 0 0 8 0 0 .375
GW 2 5 8 0 0 8 0 33.1 .032047244
GW 3 3 8 0 33.1 -8 0 33.1 .375
GW 4 5 -8 0 33.1 -8 0 0 .032047244
GS 0 0 .02540
GE 0
EX 0 1 2 0 1 0
LD 5 1 1 3 2.4938E7
LD 5 2 1 5 5.8001E7
LD 5 3 1 3 2.4938E7
LD 5 4 1 5 5.8001E7
FR 0 1 0 0 146 0
RP 0 1 360 1000 90 0 1 1
EN

```

10-3-2

The final height for the 3/5 segmentation level should be about 33.1", as shown in file 10-3-2.NEC. The source impedance should be $52.0 - j0.8\Omega$, with a maximum modeled gain of 5.08 dBi. You should note that the segmentation used to achieve these numbers is below the conservative minimum level of 10 segments per $1/2\lambda$ that we have been using.

Both a fully tapered segment-length model and a highly segmented model within MININEC, using the same materials and the same horizontal dimension, show a source impedance of $51.8 + j0.6\Omega$ and a maximum gain of 5.09 dBi. These values are essentially the same as for the NEC-2

minimal segment model. However, the MININEC model calls for a vertical length of 33.7".

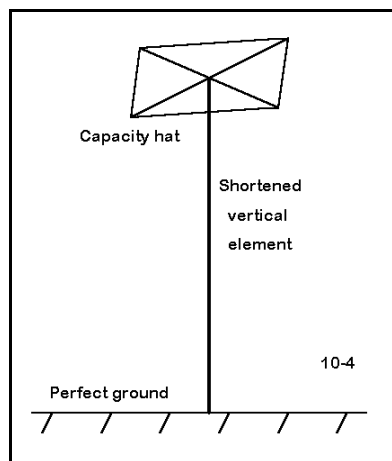
With normal construction, you should be able to build a test antenna capable of validating this region (33.1" to 33.7") as correct. With great construction care, you should also be able to differentiate the two models to determine which is the more accurate. For a test of this order, it is always wise to replicate it on other frequencies, for example, 52 MHz, and to build multiple test antennas in order to eliminate construction variables from the test

data.

Beyond validating the technique of modeling closed geometries in NEC-2 with minimal segmentation, both the use of MININEC for comparative purposes and test antenna building may be required on a number of alternative closed shapes and on nearly-closed shapes. An example of the latter is the folded X-beam. One version of this antenna examined in Chapter 6 used differential wire diameters on various parts of the structure. The antenna features sharp (45°) angles at corners and very close coupling between element ends. Validating an appropriate NEC-2 model will be a challenging exercise.

10-4: A capacity-hat short vertical for 3.75 MHz

The difficulty NEC-2 has with differential diameters at angular junctions varies among antenna types. The further away from the high current node of the antenna, the less the problem shows itself. For example, you may model an inverted-L antenna over perfect ground using a 1" diameter vertical section of 42.1' and a 30' long horizontal section of #12 AWG wire. Since the material transition occurs well away from the antenna source at the base, there is only about a $10\text{-}\Omega$ reactance difference between a MININEC and a NEC-2 model, when both are fairly heavily segmented (86 segments total).



There are also models with significant diameter transitions which are immune to the effect. The shortened vertical with a "capacity" hat is one such example. **Figure 10-4** shows the general outline of such an antenna over perfect ground.

The vertical is short for the frequency. The horizontal assembly at the top completes the length necessary for resonance or some other specified condition. Because the assembly is spread, it requires less space than an equivalent horizontal section for an inverted-L antenna. For the same 42.1' vertical 1" diameter aluminum section, the inverted-L required a 30' horizontal wire. The spoke in the hat in the sketch are only 6.258' long.

Hats may take many shapes: squares, hexagons, octagons, etc. They may or may not include a perimeter wire, and may be of any density, including a solid circular plate. What they all have in common is the best feasible symmetry so that the radiation from any horizontal member is canceled by the radiation from another member or combination of members.

Open file 10-4-1.NEC. This is a model of the capacity-hat vertical just described, using a 4-spoke hat with a perimeter wire.

Since our interest in this antenna is limited to validating the model geometry, the perimeter wires are modeled as single wires, rather than setting wire junctions midway between spokes. For a correct report of current magnitude and phase along the perimeter wires, see model 5-5-2.NEC and its associated guidelines in Chapter 5.

Note the segmentation level in the model. For the length given, segmentation is greater than 40 per $1/2\lambda$. Run this model and record its maximum gain and source impedance in the table at the top of the next page. Compare your results with those derived from a MININEC run of the same model.

```

CM Short vertical: 3.75 MHz
CM Capacity-hat
CE
GW 1 25 0 0 0 0 0 42.1 .041665
GW 2 3 0 0 42.1 6.258 0 42.1 .00336778
GW 3 3 0 0 42.1 0 6.258 42.1 .00336778
GW 4 3 0 0 42.1 -6.258 0 42.1 .00336778
GW 5 3 0 0 42.1 0 -6.258 42.1 .00336778
GW 6 5 6.258 0 42.1 0 6.258 42.1 .00336778
GW 7 5 0 6.258 42.1 -6.258 0 42.1 .00336778
GW 8 5 -6.259 0 42.1 0 -6.258 42.1 .00336778
GW 9 5 0 -6.258 42.1 6.258 0 42.1 .00336778
GS 0 0 .3048
GE 1
GN 1
EX 0 1 1 0 1 0
LD 5 1 1 25 2.4938E7
LD 5 2 1 3 5.8001E7
LD 5 3 1 3 5.8001E7
LD 5 4 1 3 5.8001E7
LD 5 5 1 3 5.8001E7
LD 5 6 1 5 5.8001E7
LD 5 7 1 5 5.8001E7
LD 5 8 1 5 5.8001E7
LD 5 9 1 5 5.8001E7
FR 0 1 0 0 3.75 0
RP 0 181 1 1000 -90 90 1 1
EN
    
```

10-4-1

10-4 NEC-2 Test Data			MININEC Data		
Model	Gain dBi	Source Z (R±jX Ω)		Gain dBi	Source Z (R±jX Ω)
10-4-1				5.00	27.7 - j 3.1

Comments: Your data should be insignificantly different from the MININEC model data. The same techniques may be applied to linear dipole elements (or similar parasitic elements without an independent source). Indeed, you may view dipole elements in free space as two vertical elements over perfect ground placed feedpoint to feedpoint, for that is, in fact, how NEC-2 generates antenna data over perfect ground.

From the series of exercises so far, you should see an emergent pattern. As an angular junction of wires with dissimilar diameters grows closer to the high current node, the greater the difficulty NEC-2 has in developing accurate modeling data. The further away the junction, or the less involved in the far field radiation the junction may be, the greater the accuracy of the model and the more normal the convergence progression.

10-5: A 14 MHz dipole and a close-spaced wire

A number of physical configurations of antenna elements place second wires very close to the main antenna element. The Tee-match uses a bar placed from 3" to 1' from the main element. Open-sleeve coupled elements may be only a few inches apart in some designs. These near-by wires may be of the same or of different diameters relative to the primary element. To evaluate the ability of NEC-2 to handle such cases, we shall sample a few of the exercises we might run.

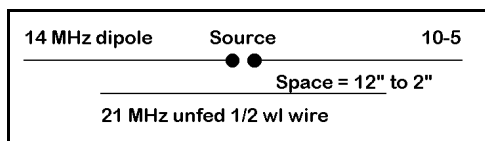


Figure 10-5 gives us an idea of a type of test we might run. Consider a dipole at some arbitrary frequency such as 14 MHz. Then consider a second wire, ordinarily shorter and placed close to the driven wire. In this simple situation, we have

many variables we might explore. We can vary the relative diameters of the two wires. Even within the constraint of making the secondary wire shorter, we can investigate various wire length ratios. We can also vary the spacing in regular increments.

Beyond these modeling experiments, we may put our assembly at different frequencies, using the same or different wire diameters. We may also reverse the situation, feeding the short wire and checking the influence of the longer wire at different spacings, different diameter ratios, and different length ratios. A final set of tests might include discovering whether the test results truly scale—that is, turn out to be the same if we change the wavelength, the wire lengths, the wires diameters, and the wire spacing: all by an equal factor.

To sample these tests, open file 10-5-1.NEC. It consists of a 1" diameter 6061-T6 aluminum dipole for 14 MHz in free space. In the model, all dimensions are in inches. The secondary wire, also 1" diameter 6061-T6 aluminum, was originally independently resonated as a dipole for 21 MHz, providing a length ratio of approximately 3:2 between the driven and undriven wires. This initial model sets a spacing of 12" between the wires.

```

CM 14 MHz Dipole with 21 MHz wire
CM Spacing = 12"
CE
GW 1 35 -203 0 0 203 0 0 .5
GW 2 23 -133.5 12 0 133.5 12 0 .5
GS 0 0 .02540
GE 0
EX 0 1 18 0 1 0
LD 5 1 1 35 2.4938E7
LD 5 2 1 23 2.4938E7
FR 0 1 0 0 14 0
RP 0 1 360 1000 90 0 1 1
EN

```

10-5-1

The test we shall run consists of decreasing the spacing of the wires in 2" increments down to a minimum distance of 2" center-to-center between the wires. This final spacing presses the limits of recommended wire separation for NEC-2. We shall record the maximum gain, the slight front-to-back ratio, and the source impedance at each increment of spacing.

```

CM 14 MHz Dipole with 21 MHz wire
CM Spacing = 2"
CE
GW 1 35 -204.7 0 0 204.7 0 0 .5
GW 2 23 -133.5 2 0 133.5 2 0 .5
GS 0 0 .02540
GE 0
EX 0 1 18 0 1 0
LD 5 1 1 35 2.4938E7
LD 5 2 1 23 2.4938E7
FR 0 1 0 0 14 0
RP 0 1 360 1000 90 0 1 1
EN
    
```

10-5-2

At each new spacing, we shall reresonate the dipole by changing its length until the source reactance is less than $\pm 1\Omega$. In this way, we may better review the resonant source impedance changes as wholly resistive values. In addition, we shall also record the resonant lengths of the 14 MHz dipole at each spacing. The model for a 2" spacing appears at left to provide an idea of the magnitude of the anticipated changes. The final chart will be a reasonably complete account of the antenna's behavior in the presence of at least one kind of closely spaced wire.

10-5		Test Data			NEC-2
Spacing Inches	Length Inches	Gain dBi	F-B Ratio dB	Source Z $R\pm jX \Omega$	
12					
10					
8					
6					
4					
2					

Comments: The data you collect will provide an interesting pattern, although its meaningfulness may be limited. The decrease in source resistance and the increase in gain as the spacing between wires narrows will be interesting, but there is so far no way to determine if the curves result from actual antenna phenomena or from the nature of the modeling program.

Once more, we may begin the evaluative process by comparing data from a comparable program, MININEC. A similar chart was developed from essentially the same models. The only differences were the reduction of segments in each wire by one in order to keep the source centered on the 14 MHz wire. (The reduction in the undriven wire kept the segment junctions as well aligned as they are in the NEC-2 model.)

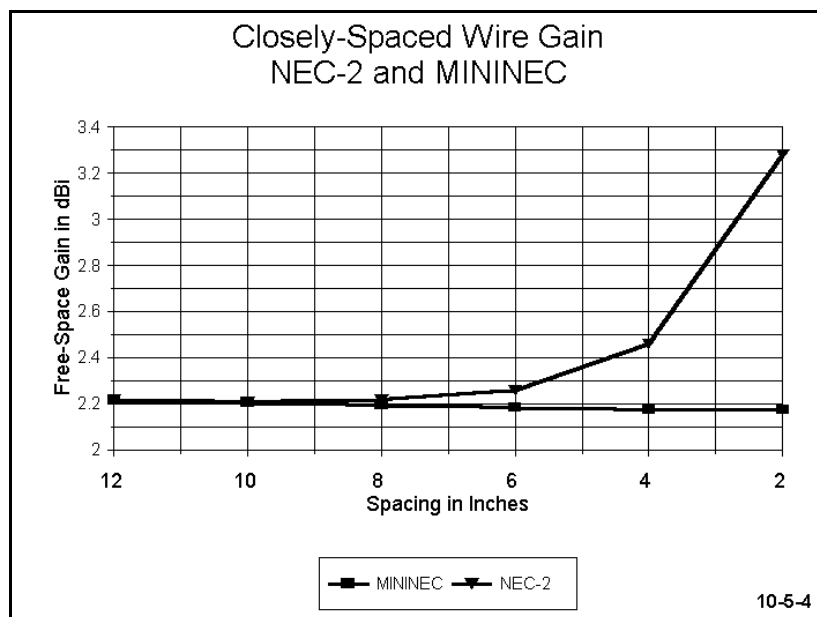
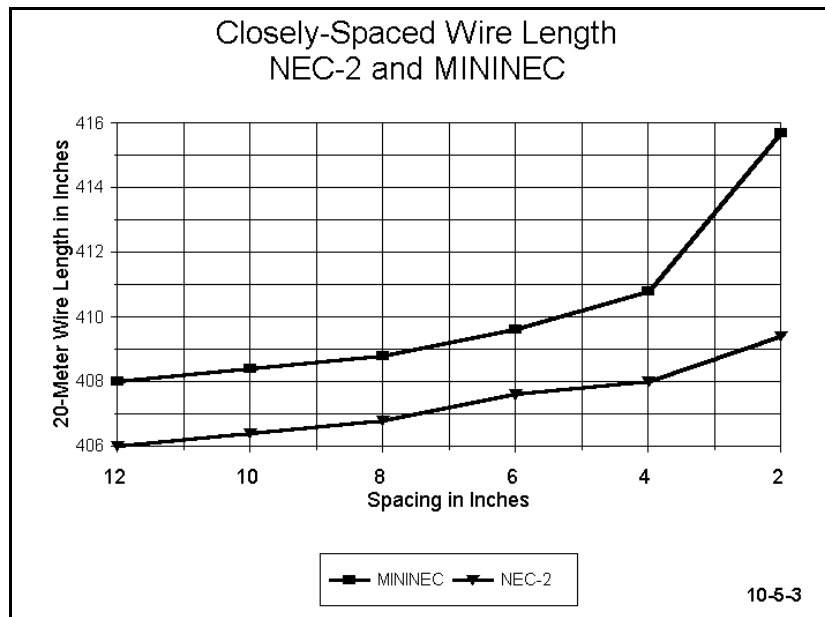
10-5		Reference Data		MININEC
Spacing Inches	Length Inches	Gain dBi	F-B Ratio dB	Source Z $R \pm jX \Omega$
12	204.0	2.22	0.16	74.6 - j 0.3
10	204.2	2.21	0.14	74.9 + j 0.0
8	204.4	2.20	0.12	75.3 + j 0.1
6	204.8	2.19	0.10	76.2 + j 0.5
4	205.4	2.18	0.07	77.8 + j 0.3
2	207.7	2.17	0.05	84.4 + j 0.1

The data reveal some immediate differences. First, the resonant lengths in the two programs differ. The version of MININEC used was not frequency corrected, and therefore shows a slight offset from the NEC-2 numbers. This offset, which is corrected in some implementations of MININEC, does not affect the validity of any trends that may emerge from the number.

Second, the front-to-back ratios for the two programs are virtually identical. Although this fact may seem to trivialize the data gathering, in fact it reveals something important. Whatever else may differ in the trends as spacing decreases, the shapes of the far field patterns generated by the two programs are very close to being the same. Any differences between results, therefore, will have to be attributed to factors other than the field shape calculated by the programs.

The chief areas of variance among the two charts concern resonant wire length, gain, and source resistance at resonance. Reviewing the data trends is often best done by charting the data in a spread sheet and then graphing the results. Virtually any such program will be more than adequate for the simple graphs we need.

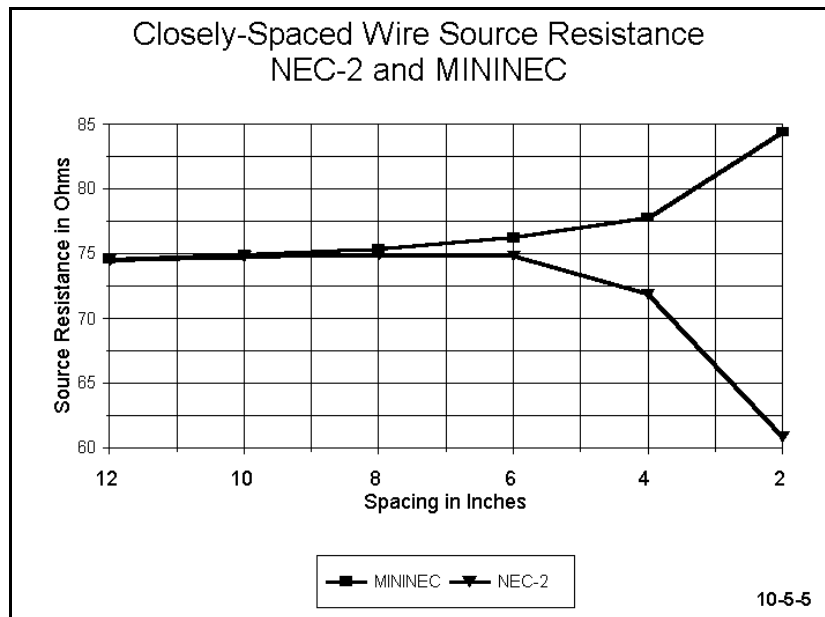
Figure 10-5-3 plots the resonant wire lengths for both the NEC-2 and the MININEC data. Besides the offset already noted, the steepness of the curve for MININEC calls itself to our attention. However, do not overlook the slight irregularity in the NEC-2 curve in the 6" spacing region: it is not an error. Keep the change in curve shape between the 8" and 4" space points in mind as we review other data from the charts. Indeed, you may wish to go back and redo the NEC-2 chart at 1" increments to watch the development of the curve shape change more closely.



The gain curves in **Figure 10-5-4** provide some of the most interesting data. The MININEC curve is very flat, with a total decrease in gain across the spacing changes of merely 0.05 dB. In contrast, the NEC-2 curve is more complex. It tracks the MININEC curve for the first two entries. However, at the 8" spacing mark, it reverses direction and begins to rise in almost exponential fashion. At a spacing of 4", which is well within published tolerances for NEC-2 wires, the gain has

increased over 0.25 dB to a figure that is unreasonable to expect of this configuration of wires. The smooth curve up to the highest value tends to confirm the initial suspicion that the NEC-2 data for close spaced wires is becoming unreliable. Note that the region of gain curve reversal--in the 8" region--corresponds to the beginning of the curve change for resonant wire length.

The curves for the resonant source resistance, shown in **Figure 10-5-5**, reveal an opposite trend from the gain. The MININEC curve shows a continuing trend upward. Moreover, the curve is smooth and modest. In contrast, the NEC-2 curve begins a gradual rise in source resistance up to the 8" spacing point. Then, the source resistance reported by NEC-2 begins to decrease at an ever-faster rate, reaching a level that is below what we may expect for such wires.



There is a correspondence between the gain and source resistance curves that bears further investigation. Since far field strength and hence the maximum gain value are a function of the current magnitudes along the antenna wires, and since a low source impedance at a current node may be associated with generally higher current levels along the wire, you may wish to explore the Currents and Location table and extract a pattern among their levels for various spacings of the two wires.

In short, the data you have so far collected and graphed represent only the beginning of an investigation into the unreliability of models with very closely spaced wires. You may alter the models at will to explore differences that may be a product of the relative diameters of the two wires or the relative lengths of the two wires. These curves, while showing the same overall trend, will help refine the conditions of its occurrence, allowing you to develop a more complete profile. Such a profile provides more detailed warning of when a projected antenna geometry may be approaching the limits of accurate output data. In all cases, you may refine the data collection by more closely spacing the points of each variable you explore.

The Gain Averaging Test

The error patterns in gain and source impedance exposed in comparative modeling between NEC-2 and MININEC, as demonstrated by Exercise 10-5, are also revealed within NEC-2 in a special test of model adequacy called the Gain Averaging Test. The

Gain Averaging Test is a necessary but not a sufficient condition of model adequacy. Models failing the test are considered inadequate, while models meeting the test might fail to be adequate for other reasons.

The conduct of the Gain Averaging Test requires either that the antenna be modeled in free space or with a perfect ground. For all but monopoles connected to ground at one end, free space is the more common environment for the test. Additionally, the test uses perfect (lossless) wire for the elements, and sets all real parts (resistive components) of transmission lines and networks to zero. Under these conditions, one can take a sufficient sample of readings over the free space sphere or the perfect ground hemisphere to derive an average power gain for the model. The radiated power equals the input power for an adequate model, which yields an average power gain of 1 for free space and of 2 for perfect ground. Inadequate models that press various limitations of NEC-2 tend to yield average power gains that depart from these ideal figures.

For many purposes, a model that yields a free space average gain figure ranging from 0.95 to 1.05 may be considered to have passed the test and, unless defective in ways that the Gain Averaging Test cannot detect, is likely to be highly accurate. Values between 0.9 and 0.95 and between 1.05 and 1.1 result in models that are usable for most purposes, with errors only up to 1 dB. Models that depart further from the ideal are considered progressively worse, and those yielding free space power gain values less than 0.8 or greater than 1.2 are subject to question and require refinement. For application of the test over perfect ground, the figures cited in this evaluation note should be doubled.

For models that do not yield average gain values very close to 1 in free space (or 2 over perfect ground), the results of the test may be used to provide approximate corrections to both gain and the resistive component of the source impedance. The corrected power gain will be the computed gain divided by the average gain. (Multiply the computed gain by 2 if the average gain is taken over perfect ground.) Since the correction applies to power ratios, the user will have to convert the correction factor to dB or back out a value for the power ratio from gain values specified in dBi for radiation directions of interest.

The resistive component of the source impedance can be corrected by multiplying the computed value by the average gain (divided by 2 if over perfect ground). The reactive component of the source impedance is not affected by the procedure. Hence, other derived figures--for example, VSWR relative to a standard impedance--will also change if the corrective is introduced.

The application of the Gain Averaging Test is, strictly speaking, limited to lossless wire models in free space or over perfect ground. In many applications, one may use the corrective derived from the test to yield reasonably accurate results with models that employ highly conductive wire and that have no other loads, networks, or transmission

lines. You may wish to run the test for the close-spaced element models just explored and examine the consequences of applying the correctives, using the MININEC figures as a comparator. However, the main function of the Gain Averaging Test is to determine so far as possible the adequacy of the model and not to correct NEC-2 calculations under all conditions. Since the test is made available in NEC-Win Plus, it is advisable to run it for any model whose geometry may be considered the least bit complex.

The chief ramification of the investigation in this chapter is that a number of common antenna structures may not be reliably modeled in NEC-2. For each frequency region and each combination of element length and diameter, there is a "breaking point" such that spacing antenna elements and other linear structures any closer will likely inflate gain and deflate the source impedance inaccurately. Matching sections that make use of long bars that parallel a driven element may, if physically modeled with the antenna itself, alter the antennas gain values without yielding a reliable source impedance value.

You will, undoubtedly encounter similar structural antenna features in your future work. In each case, you may have to perform tests similar to the ones in this exercise to determine the relative probability of being able directly to model an antenna geometry with confidence in the data you then generate.

Summing Up

We have lingered over each of our models in this set of exercises, not only to acquaint you with some of the geometric limitations of NEC-2, but as well, to familiarize you with some of the procedures by which you may assess whether your model is near or within these caution zones. Since no single set of exercises can exhaust the list of limitations of any modeling program, you must be prepared to be skeptical about your own results--especially when they defy intuition and theory, and to perform appropriate reliability tests yourself.

Only a limited number of cases, such as the folded dipole, have convenient formulations which permit an easy decision about modeling results. The use of an alternative program, such as MININEC, does not itself validate a test result, since that program may also be operating within a zone of unreliability. Only where the comparative program has an established record of being in concert with both theory and empirical tests can its results be used as a comparative standard for NEC-2.

The purpose of these exercises has not been to cause a loss of faith in NEC-2 as a highly competent antenna modeling program. Quite the opposite is true. By learning some of the geometric limitations of NEC-2 and tests to detect them, you may more readily and confidently develop antenna models which are clearly within these boundary conditions. And you will know when you are approaching the boundaries and work with appropriate caution.

User Notes

11

Grounds and Applications

Objectives: *This exercise set will acquaint you with the many ground options (including the no-ground or "free space" choice) available within NEC-2. In addition, you will work with some of the primary applications of the grounds, in some cases finding ways to speed your analysis or development work by making the most optimal selection.*

NEC-2 offers the modeler several different choices of grounds beneath the antenna, including no-ground (free space). Each has its own set of best applications for both speeding preliminary work and for final analysis of greatest accuracy. In this chapter, we shall sample some of these applications.

First, let's familiarize ourselves with the types of ground, their typical entry in a .NEC file, and what they mean.

1. **Free Space:** the term "free space" indicates the absence of any surface beneath the antenna. Therefore, the antenna radiates in all directions without reflections (other than those that are a function of the modeled antenna structure itself). Choice of free space or "no-ground" is often the best for comparison of antennas of similar types. Moreover, it usually provides the most rapid calculation speeds and yields the highest accuracy output data.

The absence of ground may appear in a .NEC file as simply no ground entry, that is, no GN card. It may also appear as the following:

GN -1

2. **Perfectly Conducting Ground:** This option places beneath the antenna a perfectly conducting surface with perfect reflection properties--at a distance specified by the entries in the Z-axis column of the wire geometry cards. A vertical wire may contact a perfect ground, but a horizontal wire should have a height several times greater than the wire radius ($h > 3a$) for valid results.

Since a perfect ground creates an image antenna identical to the original, it requires twice as long to fill the interaction matrix as a free space model. However, it is still faster than

the use of either of the ground condition approximation systems. Thus, it has some interesting developmental applications. Selection of a perfect ground results in the following GN card entry:

GN 1

3. Finite Ground: Reflection Coefficient Approximation: Sometimes called the "fast" or "real" ground, this system employs an image model modified by Fresnel plane-wave reflection coefficient approximations for near fields. This system loses accuracy as an antenna is brought within several tenths of a wavelength toward the ground or lower and is most suitable for relatively compact antenna structures. Nonetheless, it yields quite reasonable results, especially for preliminary developmental work, and is faster than the more accurate Sommerfeld-Norton method.

Every finite ground requires at least the specification of values for the conductivity (in S/m) and the dielectric constant (permittivity) of the ground. A table of typical values for various types of soil appears in the Appendix of this guide. In general, vertical antennas close to the ground are more sensitive to changes in soil type than are horizontal antennas at their typical heights well above the ground surface. A typical GN card for a "fast" ground using "average" soil would appear as follows:

GN 0 0 0 0 13 .005

The reflection coefficient ground method also has provision for a second medium that extends a specified radius within ground specified in the card just shown. The interior medium is generated by entering a ground radial screen. Through a GD card, NEC-2 also has provision for adding a second medium beyond the one selected in the GN card, and this medium may be at some height lower than the GN specification. Both of these inputs are most applicable to vertical or vertically polarized antennas, where the modeler wishes to differentiate local conditions affecting the antenna source impedance from those affecting the far field pattern.

4. Finite Ground: Sommerfeld-Norton Method: The more accurate Sommerfeld-Norton (S-N) ground method uses exact solutions for fields in the presence of the specified ground and is accurate very close to ground. Horizontal wires should be above ground by a factor of at least the following: $(h^2 + a^2)^{1/2} > 10^{-6}\lambda$, where h is the wire height and a is the wire radius. The wire should also have a height several times greater than the wire radius ($h > 3a$). Except for the entry immediately following the card identification, a simple S-N ground entry looks identical to a reflection coefficient approximation ground entry card. For example,

GN 2 0 0 0 13 .005

The S-N ground extends indefinitely to the horizon. For our initial sampling of ground applications, we shall confine ourselves to simple grounds, that is to grounds whose properties extend from the antenna to infinity.

Exercise Preparation

In the following exercises, you will be asked to change the ground system of many of the models supplied on the accompanying disk. In some cases, you will modify the antenna geometry, for example, by changing an element length until a specified condition is reached or by changing the height of the antenna. Each of these changes will alter the model. Hence, you may wish to save any variants of interest under alternative file names. Or, at the conclusion of the exercise, you may return the model to its original condition.

11-1.NEC: A 16-element Yagi for 432 MHz

File 11-1.NEC is a 16-element Yagi of 6061-T6 aluminum for 432 MHz. The dimensions are in millimeters, including the 5 mm element diameters. As the "zero" entries in the Z-axis column indicate, along with the absence of a ground (GN) card, the antenna is initially in free space. The elements are each 21 segments long, resulting in a total of 336 segments for the antenna.

We shall use this antenna to make some comparative runs using the ground options at our disposal. We shall record the gain, the 180-degree front-to-back ratio, and the source impedance for the antenna, along with the run time in seconds. You may use any convenient start and stop points, so long as you use them consistently for all runs. The "start" and "stop" announcements for the NEC-2 run screen are handy. Ultra-precision is unnecessary for this exercise, since you will only need to become familiar with the relative lengths of run times for the computer you are using.

When you move from free space to the first of the grounds, you will have to increase the value of Z in all wire entries to 9000 mm. This height places the antenna many wavelengths above ground. If you make an error in adjusting the

```

CM 16-el Yagi: 432 MHz
CE
GW 1 21 -173.1 0 0 173.1 0 0 2.5
GW 2 21 -169.5 124 0 169.5 124 0 2.5
GW 3 21 -157.2 178 0 157.2 178 0 2.5
GW 4 21 -154.305 0 154.305 0 2.5
GW 5 21 -150.8 454 0 150.8 454 0 2.5
GW 6 21 -149.2 629 0 149.2 629 0 2.5
GW 7 21 -147.7 822 0 147.7 822 0 2.5
GW 8 21 -145.3 1032 0 145.3 1032 0 2.5
GW 9 21 -143.3 1251 0 143.3 1251 0 2.5
GW 10 21 -143.3 1480 0 143.3 1480 0 2.5
GW 11 21 -141.7 1721 0 141.7 1721 0 2.5
GW 12 21 -140.1 1972 0 140.1 1972 0 2.5
GW 13 21 -139.3 2232 0 139.3 2232 0 2.5
GW 14 21 -138.9 2496 0 138.9 2496 0 2.5
GW 15 21 -138.1 2766 0 138.1 2766 0 2.5
GW 16 21 -137.3 3042 0 137.3 3042 0 2.5
GS 0 0 .001
GE 0
EX 0 2 11 0 1 0
LD 5 1 1 21 2.4938E7
LD 5 2 1 21 2.4938E7
LD 5 3 1 21 2.4938E7
LD 5 4 1 21 2.4938E7
LD 5 5 1 21 2.4938E7
LD 5 6 1 21 2.4938E7
LD 5 7 1 21 2.4938E7
LD 5 8 1 21 2.4938E7
LD 5 9 1 21 2.4938E7
LD 5 10 1 21 2.4938E7
LD 5 11 1 21 2.4938E7
LD 5 12 1 21 2.4938E7
LD 5 13 1 21 2.4938E7
LD 5 14 1 21 2.4938E7
LD 5 15 1 21 2.4938E7
LD 5 16 1 21 2.4938E7
FR 0 1 0 0 432 0
RP 0 1 360 1000 90 0 1 1
EN

```

11-1

values for Z, refer to check file 11-1-1.NEC on the disk. Be certain to enter average ground values (cond. = 0.005 S/m, die. const. = 13) in the correct places for the real/reflection coefficient and for the S-N ground methods. Also, change the theta (zenith) angle to 89.9° (elevation angle = 0.1°). Use the table below to record your values.

11-1 Test Data				
Ground Type	Run Time Sec	Gain dBi	F-B dB	Source Z $R \pm jX \Omega$
Free Space				
Perfect				
Real/Fast				
S-N				

Comments: With respect to the performance values recorded, you will notice that, between the two "real" ground systems, there is no difference in any category. When antennas are many wavelengths above the ground surface, the difference in the calculated results for the two systems disappear. The loss due to "average" ground conditions are also minimal when compared to the results over perfect ground. Relative to free space, however, the antenna shows a 6.0 dB increase in forward gain, which is the theoretical maximum gain increase due to ground reflections. Losses due to real grounds are less than 0.1 dB.

11-1 Reference Data				
Ground Type	Run Time Sec	Gain dBi	F-B dB	Source Z $R \pm jX \Omega$
Free Space	30	16.31	24.34	51.6 - j 1.9
Perfect	36	22.32	24.37	51.6 - j 1.9
Real/Fast	42	22.27	24.38	51.6 - j 1.9
S-N	80	22.27	24.38	51.6 - j 1.9

The timing runs in the reference table were made on a relatively slow computer with limited memory resources. Consequently, they emphasize any timing differences. Since the run times account for all calculations made by the NEC-2 core, the longer run of the S-N ground is partially, but not completely obscured. Overall, there is little to choose

among free-space, perfect, and fast grounds with respect to time. However, as we shall see, there are other good reasons for selecting free-space for some runs and perfect ground for others. In addition, we shall see applications for the fast and S-N ground methods as well.

11-2.NEC: A 2-element wire Yagi for 7.15 MHz

11-3.NEC: A 2-element wire Moxon for 7.15 MHz

```

CM 2-el wire Yagi: 7.15 MHz
CE
GW 1 21 -32.8 0 0 32.8 0 0 3.36778E-03
GW 2 21 -34.5 -21 0 34.5 -21 0 3.36778E-03
GS 0 0 .3048
GE 0
EX 0 1 11 0 1 0
LD 5 1 1 21 5.8001E7
LD 5 2 1 21 5.8001E7
FR 0 1 0 0 7.15 0
RP 0 1 360 1000 90 0 1 1
EN

```

11-2

```

CM Moxon rectangle: 7.15 MHz
CE
GW 1 7 -24.78 2.75 0 -24.78 10.76 0 3.36778E-03
GW 2 45 -24.78 10.76 0 24.78 10.76 0 3.36778E-03
GW 3 7 24.78 10.76 0 24.78 2.75 0 3.36778E-03
GW 4 9 -24.78 1.42 0 -24.78 -8.21 0 3.36778E-03
GW 5 45 -24.78 -8.21 0 24.78 -8.21 0 3.36778E-03
GW 6 9 24.78 -8.21 0 24.78 1.42 0 3.36778E-03
GS 0 0 .3048
GE 0
EX 0 2 23 0 1 0
LD 5 1 1 7 5.8001E7
LD 5 2 1 45 5.8001E7
LD 5 3 1 7 5.8001E7
LD 5 4 1 9 5.8001E7
LD 5 5 1 45 5.8001E7
LD 5 6 1 9 5.8001E7
FR 0 1 0 0 7.15 0
RP 0 1 360 1000 90 0 1 1
EN

```

11-3

We shall look at files 11-2.NEC and 11-3.NEC together. Our purpose will be to make some comparisons between these two directional wire antennas, both of #12 AWG copper and both designed for 7.15 MHz. We shall want to know which is

better--not to mention what might be the proper standards by which to make the comparison. For our initial side-by-side work, placing the antennas in free space is the fastest way to proceed.

Notice that the Moxon rectangle is more highly segmented than the Yagi, owing to its rectangular and nearly closed geometry. However, neither antenna model would suffer from moderate reductions in segmentation density. The dimensions of each antenna are in feet, with the height set to zero for our free-space exercise.

Run both antennas and record gain, 180-degree front-to-back ratio, and the source impedance in the table provided. Using either model as a starter, import the file of the other and overlay the two azimuth patterns for comparison.

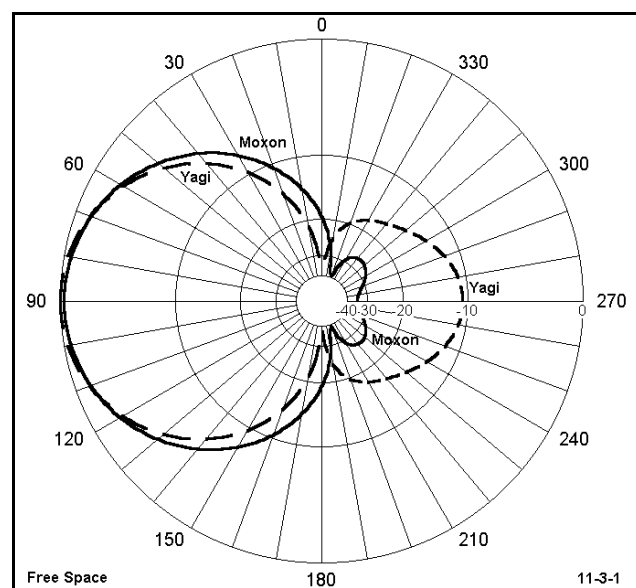
11-2 & 11-3 Test Data			
Antenna	Gain dBi	F-B dB	Source Z $R \pm j X \Omega$
Yagi			
Moxon			

Comments: The table shows that the Moxon rectangle has a much greater front-to-back ratio than the Yagi, while the Yagi is a bit superior in gain. (You did, of course, refer to the Power gain table to calculate the 180° front-to-back ratio of the Moxon, due to the cardioidal shape of its pattern.) The source impedances are quite comparable, both providing an acceptable match to widely-used 50- Ω coaxial cables. Verify this fact by consulting the VSWR data output. However, the numbers in these tables do not show everything we should know about the antennas.

11-2 & 11-3 Reference Data			
Antenna	Gain dBi	F-B dB	Source Z $R \pm j X \Omega$
Yagi	6.07	10.64	45.3 - j 0.3
Moxon	5.79	34.06	58.2 + j 0.6

The pattern comparison in **Figure 11-3-1** supplies additional information that is not apparent in the table. First, it tells us whether the high front-to-back figure for the Moxon is justified. Second, it reveals that the -3 dB beamwidth of the Moxon is greater than that of the Yagi (78° vs. 69°). These factors may play a role in determining which is the better array for an application. Note that since both antennas are wire arrays, they are likely to be in fixed positions.

As convenient and quick as free space patterns may be, they do not provide complete information. Until many

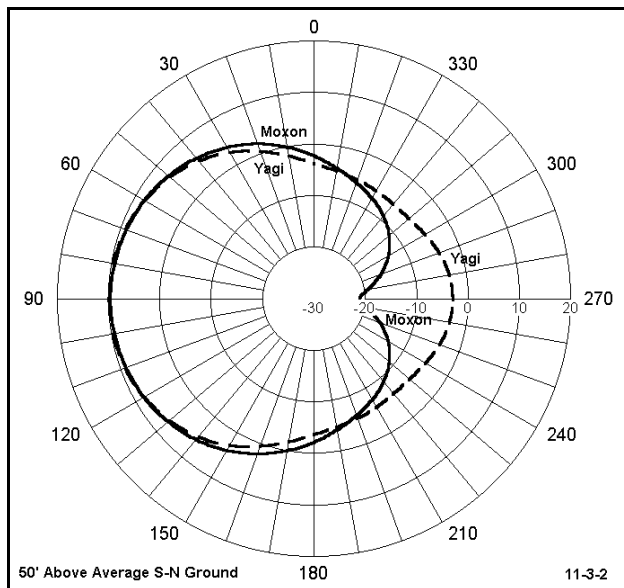


directive antennas approach 1λ in height above ground, their patterns may deviate significantly from their free space patterns. Since a wavelength at the indicated frequency is about 140' long, these antennas are unlikely to be installed at more than about $5/8\lambda$ high.

Revise both the Yagi and the Moxon models to place them successively at 50', 70', and 90' above average soil (cond. = 0.005 S/m; die. const. = 13). For each antenna height, run an initial theta (elevation) pattern to determine the TO angle. Then revise the file once more to run a phi (azimuth) pattern at the indicated angle. Once more, gather the tabular data and then overlay the patterns for the two antennas at each height.

Fill in the data you gather for each height on the table below.

11-2 & 11-3			
Test Data			
Antenna	Gain dBi	F-B dB	Source Z R ± j X Ω
Yagi: 90'			
Moxon: 90'			
Yagi: 70'			
Moxon: 70'			
Yagi: 50'			
Moxon: 50'			



Files 11-2-1.NEC and 11-3-1.NEC provide check models for your work over ground. **Figure 11-3-2** samples the comparative patterns you will produce, in this case, for 50' over average S-N ground (chosen because the antenna is not much above $1/4\lambda$ above ground).

Which antenna is better? None of the data sets answers that question directly. Develop several sets of operating specifications and develop answers relative to those objectives. If you had an answer in mind before creating the clusters of operating goals, analyze what presumed goals lay behind your choice.

Besides the data gathered here, you may

well wish to continue this exercise by performing frequency sweeps across the band of frequencies to be used (here, the radio amateur 40-meter band from 7.0 to 7.3 MHz). Look not only at the source impedance and the 2:1 SWR bandwidth for each antenna, but also look at how well the antenna characteristics hold up over the 300 kHz span of intended operation.

11-4.NEC: A capacity-hat vertical over perfect ground for 14.175 MHz

11-5.NEC: A capacity-hat dipole in free space for 14.175 MHz

Once more, we shall examine two different models in one exercise, but for a completely different purpose. We have examined separately in earlier exercises both the capacity-hat vertical and the capacity-hat dipole, but we have not explored how they might be related to each other. Moreover, if we experimented with changing the design frequency of any of these earlier models, we discovered that developing the correct dimensions for the capacity hat could be a slow process, even if we use symbolic dimensions or other programmatic short-cuts.

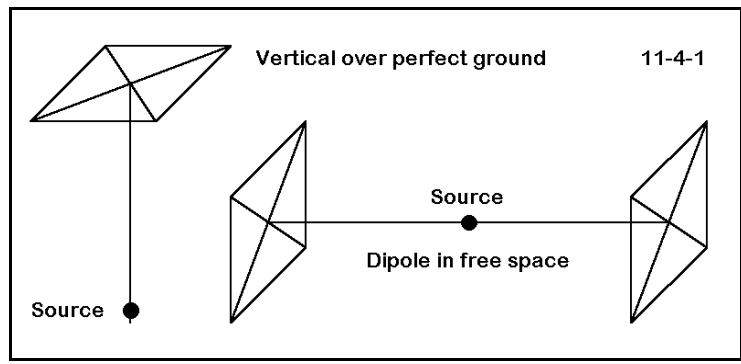
Consider the capacity-hat dipole of file 11-5.NEC, which is actually the second of our two models. As long as this file may be, it is actually a short-cut version which does not acknowledge the true element ends, which are at the mid-points of the perimeter wires on the hats. However, since our hypothetical task is simply developing dimensions for a free-space resonant capacity-hat dipole at 14.175 MHz, we may use the smaller model and restore the element ends later.

The model consists of a linear element of 6061-T6 aluminum 166.4" long. At each end is a 4-spoke hat assembly with a perimeter wire. The hat assembly uses #12 AWG copper wire. One might have specified an octagon for each hat with both a perimeter wire and an intermediate wire touching each spoke at its midpoint. In fact, you should construct a few models of this order of complexity for the practice. This is not an idle suggestion, but instead a recommendation that you develop orderly model construction procedures to ensure that everything ends up in the right place with the right connections in the right order.

```

CM Capacity-hat dipole: 14.175 MHz
CE
GW 1 5 -133.2 0 23.02 -133.2 23.02 0 4.04E-02
GW 2 5 -133.2 23.02 0 -133.2 0 -23.02 4.04E-02
GW 3 5 -133.2 0 -23.02 -133.2 -23.02 0 4.04E-02
GW 4 5 -133.2 -23.02 0 -133.2 0 23.02 4.04E-02
GW 5 3 -133.2 0 0 -133.2 0 23.02 4.04E-02
GW 6 3 -133.2 0 0 -133.2 23.02 0 4.04E-02
GW 7 3 -133.2 0 0 -133.2 0 -23.02 4.04E-02
GW 8 3 -133.2 0 0 -133.2 -23.02 0 4.04E-02
GW 9 51 -133.2 0 0 133.2 0 0 .5
GW 10 3 133.2 0 0 133.2 0 23.02 4.04E-02
GW 11 3 133.2 0 0 133.2 23.02 0 4.04E-02
GW 12 3 133.2 0 0 133.2 0 -23.02 4.04E-02
GW 13 3 133.2 0 0 133.2 -23.02 0 4.04E-02
GW 14 5 133.2 0 23.02 133.2 23.02 0 4.04E-02
GW 15 5 133.2 23.02 0 133.2 0 -23.02 4.04E-02
GW 16 5 133.2 0 -23.02 133.2 -23.02 0 4.04E-02
GW 17 5 133.2 -23.02 0 133.2 0 23.02 4.041E-02
GS 0 0 .02540
GE 0
EX 0 9 26 0 1 0
LD 5 1 1 5 5.8001E7
LD 5 2 1 5 5.8001E7
LD 5 3 1 5 5.8001E7
LD 5 4 1 5 5.8001E7
LD 5 5 1 3 5.8001E7
LD 5 6 1 3 5.8001E7
LD 5 7 1 3 5.8001E7
LD 5 8 1 3 5.8001E7
LD 5 9 1 51 2.4938E7
LD 5 10 1 3 5.8001E7
LD 5 11 1 3 5.8001E7
LD 5 12 1 3 5.8001E7
LD 5 13 1 3 5.8001E7
LD 5 14 1 5 5.8001E7
LD 5 15 1 5 5.8001E7
LD 5 16 1 5 5.8001E7
LD 5 17 1 5 5.8001E7
FR 0 1 0 0 14.175 0
RP 0 1 360 1000 90 0 1 1
EN
    
```

11-5



The task of systematically varying the size of the capacity hat assemblies on each end of the dipole is fraught with opportunities for entry errors. However, we may cut the job in half--literally--by considering **Figure 11-4-1**. With only minor adjustments, you may think of the dipole in free space as simply two identical vertical antennas of the same design end

to end. By placing only one of these antennas over perfect ground, we let NEC-2 create the other half of the antenna.

Open file 11-4.NEC. Making adjustments for the reorientation of the antenna element, compare it with one half of the dipole in 11-5.NEC. There is only one small adjustment. The source of the vertical is on the first segment above ground, since NEC-2 does not allow a source in contact with the ground. However, since the offset is very small and the anticipated impedance is low at this high current node, the source impedance error relative to the centered source of the dipole is likely to be insignificant. Otherwise, the models are identical.

Run both models and gather data on the maximum gain and the source impedance, placing them in the table below.

```

CM Capacity-hat vertical: 14.175 MHz
CE
GW 1 25 0 0 0 0 0 133.2 .5
GW 2 3 0 0 133.2 23.02 0 133.2 .0404
GW 3 3 0 0 133.2 0 23.02 133.2 .0404
GW 4 3 0 0 133.2 -23.02 0 133.2 .0404
GW 5 3 0 0 133.2 0 -23.02 133.2 .0404
GW 6 5 23.02 0 133.2 0 23.02 133.2 .0404
GW 7 5 0 23.02 133.2 -23.02 0 133.2 .0404
GW 8 5 -23.02 0 133.2 0 -23.02 133.2 .0404
GW 9 5 0 -23.02 133.2 23.02 0 133.2 .0404
GS 0 0 .02540
GE 1
GN 1
EX 0 1 1 0 1 0
LD 5 1 1 25 2.4938E7
LD 5 2 1 3 5.8001E7
LD 5 3 1 3 5.8001E7
LD 5 4 1 3 5.8001E7
LD 5 5 1 3 5.8001E7
LD 5 6 1 5 5.8001E7
LD 5 7 1 5 5.8001E7
LD 5 8 1 5 5.8001E7
LD 5 9 1 5 5.8001E7
FR 0 1 0 0 14.175 0
RP 0 181 1 1000 -90 0 1 1
EN
    
```

11-4

11-4 & -5 Test Data			Reference Data	
Antenna	Gain dBi	Source Z $R \pm jX \Omega$	Gain dBi	Source Z $R \pm jX \Omega$
Vertical			5.01	55.5 - j 3.8
Dipole			2.00	27.8 - j 1.7

Comments: By simple arithmetic, you can see that the source impedance of the vertical is 1/2 that of the dipole. The gain of the vertical is precisely 3 dB higher than the gain of the dipole, owing to the ground reflection calculations for the image antenna. These figures give you a foundation for further developments in complex but symmetrical free space models, since you may use half the antenna placed vertically over a perfect ground to shorten your work. Of course, use symbolic notation and other shortcuts provided by your program to further ease the development burden.

For further experience in this technique, adjust the hat dimensions alone to resonate the antenna first at 14.0 MHz, then at 14.35 MHz. When the vertical is complete in each case, transfer the dimensions to the dipole and run it for confirmation. Finally, for all three models, transfer the final dipole to 1λ above ground, making any final hat adjustments necessary.

11-6.NEC: A dipole for 1.9 MHz

Our exercise for the 1.9 MHz #14 copper wire dipole is simply to compare results between the fast and the S-N ground methods. The antenna is center fed using the simplest modeling technique of placing all of the wire length in the End-1 X column, with all dimensions in feet. However, you will be required to vary the height or Z values in 20' increments downward from the present 140' value. Since few installations can elevate a full length dipole for the 160-meter amateur band higher than 140', we can expect results to coincide with those for any such antenna at $1/4\lambda$ up and lower. Record your maximum gain and source impedance results for both the fast and the S-N ground methods in the following table.

```

CM 160m dipole
CE
GW 1 21 250.8 0 140 0 0 140 2.67E-03
GS 0 0 .3048
GE 1
GN 0 0 0 0 13 .005
EX 0 1 11 0 1 0
LD 5 1 1 21 5.8001E7
FR 0 1 0 0 1.9 1
RP 0 181 1 1000 -90 90 1 1
EN
    
```

11-6

11-6 Test Results				
Height feet	Fast Gain dBi	Fast Source Z $R \pm jX \Omega$	S-N Gain dBi	S-N Source Z $R \pm jX \Omega$
140'				
120'				
100'				
80'				
60'				
40'				

Comments: As in an earlier experiment, you should notice increasingly divergent results as the antenna more closely approaches the ground. Results converge very closely above about $1/3\lambda$, with results above that point being virtually interchangeable. This refresher exercise is simply a reminder of where the borders of accuracy lie for the fast of reflection coefficient approximation method of handling ground reflections.

If you made your runs sequentially within each of the ground systems, you also noticed in both increased speed of execution after the first run. This quite real impression stems from the manner in which NEC-2 and NECWin Plus handle ground calculations. The calculations are stored in a file so that subsequent runs using the same ground specifications simply call upon the first run's results. It is possible to store S-N results in separate files for reuse, a feature of NEC-2 that is very useful for design work that focuses upon a limited number of discrete frequencies.

11-6				
		Reference Results		
Height feet	Fast Gain dBi	Fast Source Z $R \pm jX \Omega$	S-N Gain dBi	S-N Source Z $R \pm jX \Omega$
140'	6.26	91.2 + j 1.6	6.28	91.0 + j 1.0
120'	6.54	84.1 + j 10.3	6.53	84.3 + j 9.4
100'	6.84	73.1 + j 16.1	6.79	73.8 + j 14.9
80'	6.88	59.4 + j 17.3	6.75	61.2 + j 16.0
60'	6.54	45.0 + j 13.3	6.17	48.9 + j 12.0
40'	5.48	32.3 + j 5.8	4.49	40.4 + j 4.5

```

CM 6-el Yagi: 21.2 MHz
CE
GW 1 41 -3.562 0 30 3.562 0 30 .0125
GW 2 41 -3.328 1.4266 30 3.328 1.4266 30 .0125
GW 3 41 -3.214 2.9714 30 3.214 2.9714 30 .0125
GW 4 41 -3.153 5.1806 30 3.153 5.1806 30 .0125
GW 5 41 -3.24 8.747 30 3.24 8.747 30 .0125
GW 6 41 -3.118 12.125 30 3.118 12.125 30 .0125
GS 0 0 1
GE 1
GN 0 0 0 0 13 .005
EX 0 2 21 0 1 0
LD 5 1 1 41 2.4938E7
LD 5 2 1 41 2.4938E7
LD 5 3 1 41 2.4938E7
LD 5 4 1 41 2.4938E7
LD 5 5 1 41 2.4938E7
LD 5 6 1 41 2.4938E7
FR 0 1 0 0 21.2 0
RP 0 1 360 1000 83 0 1 1
EN

```

11-7

11-7.NEC: A 6-element Yagi for 21.2 MHz

Above a certain antenna height, use of the fast ground method can speed antenna development work. Let us take as an example 11-7.NEC, a 6-element Yagi of 6061-T6 aluminum for 21.2 MHz. All dimensions for this antenna are in meters, along with the 30 m height. The model is heavily segmented in order to expand time-dependent functions to a noticeable level.

Run this antenna and record the source impedance for both the fast and the S-N grounds. You will notice that the source impedance has a high value of capacitive reactance. Beginning with the fast system, begin to adjust the length of the driven element (wire 2) only until the antenna registers a reactance of less than 1Ω . To make the task a bit more interesting, for each adjustment toward resonance, check the source impedance value obtained against the S-N ground method. Then return to the fast method to make the next adjustment. Record your results for the initial and final source impedance on the table below.

When the run is complete, you may also wish to compare the performance data for this antenna. The fundamental question is this: does the alteration of the length of the driven element make a significant difference upon the operating properties of the antenna? As

always, there is a second question behind the first: what would count as a significant difference under varying operating specifications?

11-7		
Test Data		
Antenna Model	Fast Source Z $R \pm jX \Omega$	S-N Source Z $R \pm jX \Omega$
Initial		
Final		

Comments: Your results should be close to those in the reference table. You may check your final dimensions against the check file 11-7-1.NEC on the disk accompanying this guide.

11-7		
Reference Data		
Antenna Model	Fast Source Z $R \pm jX \Omega$	S-N Source Z $R \pm jX \Omega$
Initial	18.82 - j 15.29	18.83 - j 15.28
Final	20.26 + j 0.37	20.26 + j 0.38

Obviously, there is no problem associated with using the fast ground system for extensive antenna development and analysis work, when the antenna height is well above $1/2\lambda$. This antenna at roughly 2λ up shows no difference either in the source impedance or the other key performance data outputs. However, since use of the S-N ground method is somewhat of a *de facto* standard, you should likely reference final results to that system.

11-8.NEC: A center-loaded vertical dipole for 7.15 MHz

Open file 11-8.NEC. The antenna element is 6061-T6 aluminum for this 50 mm diameter antenna to be used at 7.15 MHz. Notice in the antenna description that a resistance-reactance load is positioned at the antenna midpoint: a roughly 300 Ω inductance with a reactance of 500 Ω and a series resistance of 1.7 Ω . We shall look at loads in detail in the next two chapters, but the function of the load is to block any intuitions about what the gain of this antenna should be under various conditions. The load also shortens the antenna, lowering its source position. Notice that the antenna extends from 2 to 13 meters above ground.

```

CM vertical dipole
CE
GW 1 21 0 0 2 0 0 13 .025
GS 0 0 1
GE 1
GN 0 0 0 0 13 .005
EX 0 1 11 0 1 0
LD 4 1 11 11 1.7 500 0
LD 5 1 1 21 2.4938E7
FR 0 1 0 0 7.15 0
RP 0 181 1 1000 -90 0 1 1
EN

```

Initially check the source impedance of this antenna using both the fast and the S-N ground methods. You will notice considerable inductive reactance. Shorten the antenna by adjusting only the top height until it is resonant by both systems (reactance is less than $\pm 1 \Omega$). Record the source data for both ground methods.

11-8 Test Data		
Antenna Model	Fast Source Z $R \pm jX \Omega$	S-N Source Z $R \pm jX \Omega$
Initial		
Final		

Comments: You should notice an approximate 2.5 Ω difference in the source impedances provided by the two ground methods. However, both systems place resonance at the same antenna length, a top height of about 12.62 m. This occurs with the source about 7.5 m above ground.

11-8 Reference Data		
Antenna Model	Fast Source Z $R \pm jX \Omega$	S-N Source Z $R \pm jX \Omega$
Initial	23.70 + j 25.24	26.19 + j 25.58
Final	22.23 - j 0.20	24.68 + j 0.24

We have another mission for your resonated vertical dipole, which you can check against

The reference table below will serve as a check upon your work.

11-8-1	Ref. Data	2-12.62 m	Ref. Data	12-12.7 m
Soil Type Cond./D.C.	Source Z $R \pm jX \Omega$	Gain dBi TO angle	Source Z $R \pm jX \Omega$	Gain dBi TO angle
.001/80	24.3 + j 2.0	1.95 / 72	15.3 + j 0.6	2.72 / 78
.0303/20	25.2 + j 2.0	1.41 / 72	15.1 + j 0.6	1.30 / 79
.01/14	25.2 + j 0.9	-0.10 / 69	15.1 + j 0.8	-0.31 / 77
.0075/12	25.1 + j 0.5	-0.50 / 69	15.1 + j 0.9	-0.57 / 76
.006/13	24.8 + j 0.4	-0.55 / 68	15.2 + j 0.9	-0.36 / 76
.005/13	24.7 + j 0.2	-0.60 / 68	15.2 + j 0.9	-0.25 / 76
.002/13	23.9 + j 0.1	-0.47 / 67	15.3 + j 0.9	0.47 / 75
.002/10	23.9 - j 0.4	-0.89 / 66	15.3 + j 1.0	0.19 / 74
.001/5	22.9 - j 1.7	-1.66 / 65	15.4 + j 1.2	0.32 / 72
.001/3	22.7 - j 3.1	-2.43 / 64	15.4 + j 1.4	0.25 / 71

Comments: Although these soil types are often considered to be in decreasing order of quality, the results of modeling antennas--especially vertical antennas--over the various soils casts doubt upon whether the idea of decreasing quality has a direct relationship to the effect of these soils on far fields. With the vertical closest to the ground, there is only one small anomaly in our expectation of a steady curve--which occurs with the 0.002/13 value set. When the antenna is elevated considerably, that anomaly becomes a large jump in far field strength, one that carries through to the end of the chart. Even with the poorest soil, far field strength does not drop to the level it has with the 0.01/14 value set.

Although the values in this chart have been taken from accepted tables of soil types, there is nothing in the assignment of values for conductivity and permittivity that excludes any reasonable combination. (In fact, you have by now likely plugged in the two values in reverse order, and still arrived at results, even if hardly credible results.) Therefore, you may wish to design and execute a special project of testing a matrix of value combinations (conductivity from 0.001 to 0.01; dielectric constant from 1 to 80) with a standard (vertical) antenna. You may wish to run the chart with the antenna at three selected heights, one close to the earth, one at a modest height, and one an equal increment higher. When you have examined your resulting tables for patterns in the values, you may next wish to investigate the Sommerfeld-Norton equations in the basic NEC-2 literature to find the causes of the patterns you find.

Summing Up

The various types of grounds available within NEC-2, including no-ground or free space, offer the modeler numerous opportunities to model both efficiently and accurately by judiciously selecting the best ground system for the right task. Perfect ground, reflection coefficient approximations and the Sommerfeld-Norton method each offer something profitable to both the casual and the serious modeler. Growing familiar and natural with the behavior of the various ground systems has been the goal of this set of exercises.

In addition, modelers should have a working familiarity of the types of soil conditions which are available by the selection of values for ground conductivity and relative permittivity (dielectric constant). Different far field pattern strengths result from different ground choices, especially where a vertically polarized antenna is at stake, with different patterns of values resulting from the choice of antenna height. Understanding these variations is crucial to good modeling practice.

Further ground structuring potentials are available within NEC-2. Chapter 17 will take up some of the more productive possibilities. In the end, an effective antenna modeler is a well-grounded modeler.

User Notes

12

Resistive Loads

***Objectives:** This chapter will explore resistive loads. Resistive loads may be distributed or "spot" loads. Distributed loads, or the conductivity of the wire material, are integral to all but theoretic antennas. Spot loads, with specific resistance values and segment placement, will be useful in a variety of applications.*

In this chapter, we shall begin our exploration of antenna loading. The concept of loading has two related but fairly distinct meanings. In one sense, all antennas made from real materials are loaded, that is, suffer losses from the finite conductivity of the materials used. This form of loading tends to be distributed throughout the antenna structure or specific portions of it.

Antenna loading also refers to the introduction at specific locations on the antenna structure of non-radiating components that alter the performance characteristics of the antenna relative to its operation without those components. Load components may have resistance or reactance, or both. Here, we shall confine ourselves to resistive loads, and devote the next chapter to reactive (and combination resistive-reactive) loads.

In actuality, being physical structures, "spot" loading components exhibit some radiation, but it is ordinarily so small relative to that of the remainder of the antenna structure that it may be ignored. In fact, NEC-2 treats spot loads as mathematical entities, not as physical entities. We shall specify only the component value. If the component has a physical make-up that may affect the radiation pattern of the antenna, we must separately model that structure.

Both distributed and spot resistive loads involve ohmic losses. However, NEC-2 provides each with its own distinctive input card. Let's look at a sample of each.

1. **Distributed Loads:** All forms of antenna loading that are not modeled solely as physical elements require the use of a load or LD card. Antenna material load cards are "type 5."

LD 5 3 1 15 5.8001E7

The load card type is the first entry. Next comes the "tag" or wire number in the order of the GW wire geometry cards, in this case wire 3. The following two numbers indicate the range of segments to which the material load is assigned, in this instance, segments 1 to 15. Ordinarily, the higher number will be the same as the total number of segments on the wire. The final value is the conductivity of the material used: copper for this wire.

The Appendix lists the conductivities (and resistivities) of common antenna materials. Both conductivity and resistivity are unit-length concepts so that their units of measure are Siemens (or mhos) per meter and Ohms per meter, respectively.

We have employed materials loads in most of the exercise models encountered so far. For real antennas, they are inevitable, since every round wire has an internal impedance, taking into account the skin depth for a given conductivity.

2. Spot Resistive Loads: We have several options for specifying a purely resistive load in a NEC model, since all spot loads are available for combinations of either resistance and reactance or resistance, inductance, and capacitance. Perhaps the simplest means of entering a purely resistive load (assuming we do not later plan to make it more complex) is to use the series resistance-reactance option, which calls for a load card of "type 4." Here is an example.

```
LD 4 6 11 11 50 0 0
```

The first entry specifies the load type (4), while the second designates the wire number (6). For loads occupying one segment (the most common type), the third and fourth entries will be identical and name the segment (11) on which the load is placed. Spot loads may be viewed as being placed at the center of the segment, but are distributed throughout the segment. The next value (50) gives the value of the resistive load in Ohms. The final zeroes are reserved for functions we shall encounter in Chapter 13.

It is possible to specify more than one load for the same wire segment, in which case the loads will be in series. So too will be any source (or transmission line--see Chapter 14) placed on the same segment as the load. Although the complex elements of a single load may be set in parallel (as we shall see in the next chapter), organizing loads, sources, and transmission lines in parallel calls for special techniques and work-arounds.

Both distributed material loads and spot ohmic loads are significant in various antenna design and analysis ventures. Distributed loads often play a role in the specification of antenna materials and in comparative analyses of performance with various materials. Spot resistive loads are integral parts of some types of antenna arrays, such as the Beverage, the Vee-beam, and the Rhombic. We may also use resistive loads to generate data on certain kinds of modeling constructs, such as parallel transmission lines. The more aware we are of the importance of resistive loads and the more facile our

handling of them, the more opportunities we give ourselves for effective antenna modeling. So let's tackle a series of exercises making use of each kind of resistive load.

Exercise Preparation

We shall organize the work of this chapter into its natural divisions, working first with distributed material loads (type 5) and then with spot resistive loads (type 4). The first portion of the work will require that you make extended series of changes to antenna material entries and, in some cases, to antenna dimensions. Therefore, be careful to save variants of the initial model under separate filenames. The second portion of the work will call for changes in frequency and other entries, again creating numerous variants upon the original file.

12-1.NEC: A dipole for 7.0 MHz

The first step in mastering distributed material loads is not specifying them. In most cases, programs such as NECWin Plus make the entry of the material simple and often non-numerical. You need only enter the name of the material, and the corresponding load card is generated for the wire or wires involved.

```

CM Dipole in Free Space: 7.0 MHz
CE
GW 1 11 20.86 0 0 0 0 0 .000814
GS 0 0 1
GE 0
EX 0 1 6 0 1 0
FR 0 1 0 0 7 1
RP 0 1 360 1000 90 0 1 1
EN

```

12-1

The true first step is becoming aware of what happens when you change materials for an antenna. Open file 12-1.NEC, a simple #14 wire dipole for 7.0 MHz in free space. All dimensions are in meters. Note the absence of an LD 5 card, indicating that the model uses a perfect conductor. We shall not let this perfect conductor stay in place past the first run.

Makes a series of runs for this file. After each run, change the conductivity of the material to the value specified in the next line of the table on which you will record your results. For each material selection, verify the conductivity value in the resulting .NEC file. The table lists only the conductivity values. Consult the Appendix to correlate these values to the materials to which they apply. This extra "inconvenience" will familiarize you with these correlations so that you can begin to recognize a material just from the conductivity value in the .NEC file.

For each material, record the maximum gain, source impedance, and efficiency of the antenna. Efficiency figures can be obtained from the NEC Output File table. In fact, you may wish to use the NEC Output File exclusively in your data gathering, since paging through this file may be faster than separately opening the source impedance file and the polar plot facility.

12-1 Test Data			
Conductivity S/m	Gain dBi	Source Z R ± jX Ω	Efficiency %
Perfect			
6.2893E7			
5.8001E7			
3.7665E7			
3.0769E7			
2.4938E7			
1.5625E7			
9.0909E6			
1.3889E6			

Comments: Even for so simple an antenna as the wire dipole, the selection of materials can make a difference in performance. (How significant the difference is depends upon operational goals that we have not here specified.) Note especially the major breaks in the table. The first occurs when we substitute any real material for a perfect conductor, resulting in a 2% efficiency drop for even so fine a conductor as silver.

The largest break occurs between Phosphor Bronze and Stainless Steel, in the grades given. Note that stainless steel is widely used in antenna work. Phosphor bronze, once heavily used in the early days of radio communication but later dropped in favor of copper as it became more economically feasible, is now making a come back for wire antennas.

A second notable point about the table is the absence of a 2.15 dBi entry for the perfect wire dipole. You may wish to review basic antenna theory to determine why the value for the test dipole--carefully resonated to less than $\pm 1 \Omega$ reactance--does not reach the standard value for a "dipole in free space."

Allied to this situation is the fact that our test antenna is longer than 20 meters, even though the amateur band to which it is set is called "40 meters." What is the actual wavelength of 7 MHz? Note also that both the source resistance and reactance rise as the conductivity of the material decreases, with no other changes in the antenna structure. Since the reactance makes the antenna inductively reactive--or long, relative to resonance--how much of the impedance rise is due to material conductivity change and how much due to the antenna being long?

12-1 Reference Data			
Conductivity S/m	Gain dBi	Source Z $R \pm jX \Omega$	Efficiency %
Perfect	2.13	72.2 + j 0.1	100.00
6.2893E7	2.04	73.7 + j 1.4	98.09
5.8001E7	2.04	73.7 + j 1.5	98.01
3.7665E7	2.02	74.1 + j 1.8	97.54
3.0769E7	2.01	74.3 + j 1.9	97.28
2.4938E7	2.00	74.6 + j 2.2	96.98
1.5625E7	1.96	75.2 + j 2.7	96.19
9.0909E6	1.91	76.2 + j 3.6	95.02
1.3889E6	1.55	83.0 + j 8.8	87.53

12-2.NEC: Dipole for 4 MHz

The trends we noted in 12-1.NEC have consequences for antenna construction. We can approach the ramifications of decreasing conductivity from many angles, but perhaps this simple and tedious exercise will do as a start.

Open file 12-2.NEC. This simple 4 MHz dipole will be our test vehicle for meeting a specification. In this case, it is an arbitrary one, but in real antenna design cases, something similar might emerge. Our task will be to determine the smallest AWG wire size (in even numbers) that will permit a resonated 4 MHz dipole to achieve a free space maximum gain of 1.75 dBi.

```

CM Dipole 4MHz
CE
GW 1 11 36.36 0 0 0 0 0 .001632
GS 0 0 1
GE 0
EX 0 1 6 0 1 0
LD 5 1 1 11 1.3889E6
FR 0 1 0 0 4 0
RP 0 1 361 1000 90 0 1 1
EN

```

12-2

The model in 12-2.NEC is already set for stainless steel, which requires #8 AWG wire. This fact should give you a strategy. All other minimum wire sizes to achieve the same gain threshold will be smaller, since their conductivity will be higher. Use the standard list of wire materials from stainless steel up through silver. Where a wire size is not listed as an automated input selection, use the wire size table in the Appendix to determine the wire diameter. Since all dimensions are in meters, be sure to convert the Appendix entry, which is in millimeters. Moreover, be sure to change the antenna length to bring it to resonance for each material change and each wire size change. Resonance will be a

limit of $\pm 1 \Omega$ reactance.

For each run (including for the baseline model in stainless steel, record the following data in the table below: source impedance, efficiency, free space gain, length, and AWG wire size.

12-2 Test Data					
Material	Source Z $R \pm jX \Omega$	Efficiency %	Gain dBi	Length Meters	AWG Wire Size
Stls. Steel					
Ph. Bronze					
Brass					
6061-T6					
6063-T832					
Pure Alum.					
Copper					
Silver					

Comments: You may compare your results with the reference table at the top of the next page. The model description in **Figure 12-2-1** is a check model, 12-2A.NEC, which gives usable final dimensions for the case of silver as the antenna material. Be certain to read the antenna wire size as the radius and double it to determine the corresponding AWG wire size.

```

CM Dipole 4 MHz
CE
GW 1 11 36.57 0 0 0 0 0 .0002555
GS 0 0 1
GE 0
EX 0 1 6 0 1 0
LD 5 1 1 11 6.2893E7
FR 0 1 0 0 4 0
RP 0 1 361 1000 90 0 1 1
EN

```

12-2-1

In the data, you may notice certain trends. The gain threshold would be ideally constant, but the numbers do waver a bit, due to the requirement to hit a minimum gain level rather than a precise gain number. Within the limits set by that fact, certain other numbers are equivalently stable and nearly constant. One such figure is the source impedance, which varies only by the degree of fluctuation of the actual gain and by the $\pm 1 \Omega$ reactance limits for defined resonance. Equally stable are the efficiency percentages, which hold within similar limits. The test of this stability is the slight variation in the numbers for 6063-T832 aluminum, which shows a slightly higher gain and efficiency, but a slightly lower source impedance, because the next smaller wire size allowed (#22) would not achieve the threshold gain value.

The resonant antenna length itself rose continuously as the wire size decreased. This, of course, was a wholly expected result.

12-2 Reference Data					
Material	Source Z $R \pm jX \Omega$	Efficiency %	Gain dBi	Length Meters	AWG Wire Size
Stls. Steel	78.3 + j 0.1	91.64	1.75	36.36	# 8
Ph. Bronze	78.3 - j 0.4	91.75	1.75	36.46	#16
Brass	78.1 + j 0.1	92.06	1.77	36.50	#18
6061-T6	78.1 - j 0.0	92.08	1.77	36.52	#20
6063-T832	77.5 - j 0.6	92.85	1.81	36.52	#20
Pure Alum.	78.3 - j 0.5	91.88	1.76	36.53	#22
Copper	78.4 - j 0.5	91.76	1.75	36.55	#24
Silver	78.2 + j 0.4	92.08	1.77	36.57	#24

12-3.NEC: 3-element Yagi for 225 MHz

The issues surrounding the selection of materials often involve comparing antenna performance against a series of non-performance standards, such as structural integrity. Wind survival, chemical resistance, long-term stability, and a host of other factors may enter into the structural integrity question.

Open 12-3.NEC, a 3-element Yagi for 225 MHz, with dimensions given in millimeters. Since the antenna position will be several

wavelengths above ground, free space modeling is adequate for the present test. The antenna is of standard design with 3 mm diameter elements.

```

CM 3-element Yagi, 225 MHz
CE
GW 1 31 -329.2 0 0 329.2 0 0 1.5
GW 2 31 -313.7 217.6 0 313.7 217.6 0 1.5
GW 3 31 -294.9 448.7 0 294.9 448.7 0 1.5
GS 0 0 .001
GE 0
EX 0 2 16 0 1 0
LD 5 1 1 31 2.4938E7
LD 5 2 1 31 2.4938E7
LD 5 3 1 31 2.4938E7
FR 0 1 0 0 225 0
RP 0 1 360 1000 90 0 1 1
EN

```

12-3

The question to resolve is this: which of two versions will be chosen for a selected site, where the antenna will be in a fixed position for point-to-point communications. The aluminum version, shown in the initial model, has proven--in this hypothetical case--to

require replacement in less than 2 years due to mechanical and chemical stresses on the elements. A stainless steel (type 302) version of the antenna will be several times heavier, but is anticipated to last at least 5 years in the same environment. Performance requirements are at least 7.9 dBi free space gain and at least 20 dB 180° front-to-back ratio. The present antenna meets those criteria. Will a stainless steel version of the same antenna be up to the task?

Run the aluminum Yagi and record data on the gain, 180° front-to-back ratio, and the source impedance. Then change the material to stainless steel, using the standard conductivity figure for type 302 given in the Appendix. Record the data for the antenna, after making any and all element length adjustments required by radical change in material conductivity.

12-3 Test Data			
Material	Gain dBi	F-B dB	Source Z $R \pm jX \Omega$
6061-T6 Aluminum			
Stainless Steel Type 302			

Comments: The result of the exercise should initially be surprising, if you have used the preceding models as a gauge. No modifications in the antenna are required for a stainless steel version, as your data should show. In fact, with a gain deficit under 0.2 dB and a front-to-back ratio deficit of just over 1 dB, the stainless steel Yagi is quite fit for duty from the perspective of performance figures.

12-3 Reference Data			
Material	Gain dBi	F-B dB	Source Z $R \pm jX \Omega$
6061-T6 Aluminum	8.25	24.80	24.4 - j 0.8
Stainless Steel Type 302	8.08	23.65	25.0 + j 0.1

Complex antenna arrays using elements of significant diameter relative to the wavelength in question--as in the case of our VHF Yagi--show far less loss of performance when using lower conductivity materials than thin wire antennas such as the dipoles previously

modeled. In fact, stainless steel is routinely used in a variety of antenna applications requiring strength, durability, and immunity from chemical atmospheres. More recent materials, such as titanium-aluminum alloys, promise lighter weights with equal or better physical and chemical properties than stainless steel.

Developing the right expectation curves of various materials requires experience with them in a variety of diameters and antenna configurations. This model is one step in that direction. As further steps, you may take any number of previously used models in this guide and convert them from copper or aluminum to materials with lower conductivity in order to develop a large assortment of comparisons. The correct intuitions about material performance can save much time in future modeling efforts.

12-4.NEC: A 50- Ω quad loop for 50 MHz

Open file 12-4.NEC. You will recognize that the horizontal members of this quad loop are 0.375" in diameter, while the vertical members are #14 wire. The loop is designed to present a source impedance of about 50 Ω at 50 MHz when several wavelengths above ground. Hence, the antenna is modeled in free space for convenience.

Since NEC-2 does not provide exceptionally accurate results when angular junctions bring together wires of dissimilar diameters, the antenna is sparsely segmented (in accord with the practical work-around we examined in Chapter 10). Nonetheless, the results will be sufficiently accurate to reveal any trends relative to our current investigation.

The horizontal members are 6061-T6 aluminum, while the vertical wires are copper. Some implementations of NEC-2 require a single material for all wires in a single model. However, NECWin Plus permits a wire-by-wire specification of material. Run the model. Then create two variations, one of all copper, the other of all 6061-T6. Record the maximum gain and source impedance on the following table.

```

CM Elongated loop: 50 MHz
CE
GW 1 5 -21.5 0 -45.2 21.5 0 -45.2 .1875
GW 2 10 21.5 0 -45.2 21.5 0 45.2 .03204
GW 3 5 21.5 0 45.2 -21.5 0 45.2 .1875
GW 4 10 -21.5 0 45.2 -21.5 0 -45.2 .03204
GS 0 0 .02540
GE 0
EX 0 1 3 0 1 0
LD 5 1 1 5 2.4938E7
LD 5 2 1 10 5.8001E7
LD 5 3 1 5 2.4938E7
LD 5 4 1 10 5.8001E7
FR 0 1 0 0 50 0
RP 0 1 360 1000 90 0 1 1
EN

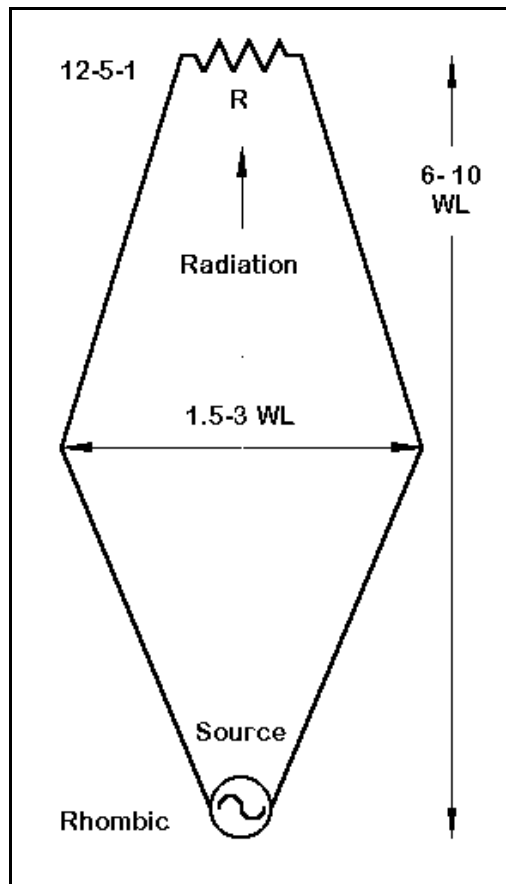
```

12-4			Test Data		Reference Data	
Material	Gain dBi	Source Z $R \pm jX \Omega$		Gain dBi	Source Z $R \pm jX \Omega$	
Mixed				4.61	49.57 + j 3.97	
Copper				4.62	49.52 + j 3.92	
6061-T6 Al.				4.59	49.84 + j 4.21	

Comments: Although brief, the example shows the limits of an excessive concern with slight differences in material performance. The differences in the performance data for the three variants of the 50 MHz elongated loop are too small to have more than numerical interest. In practical antenna performance terms, they are not detectable differences. In fact, the probable error within the model--given NEC-2 limitations with this type of configuration--is larger than the differences among the variations of it. A good part of developing an experienced hand at modeling is understanding when differences make a difference and when they do not. When results diverge less than the likely modeling error itself, then the disparity can have no reliable significance.

12-5.NEC: A Rhombic for 14 to 28 MHz

To this point, we have dealt exclusively with distributed material or type 5 loads. We shall now turn to spot resistive loads handled as type 4 loads. Unlike material specification, these loads will have to be placed on a designated segment in much the same manner as a source. Moreover, we shall have to enter a precise resistance value (in contrast to the conductivity values we used with material loads). In short, we shall be modeling resistors, but only as mathematical values and not as physical objects.



Numerous antennas require a resistive termination and are sometimes called traveling wave antennas. Among them is the Rhombic antenna, a very large wire diamond with highly directional properties--when terminated with a resistor of about $800\ \Omega$. Moreover, the terminating resistor provides a relatively stable source impedance. For the general outline of a typical rhombic antenna, see **Figure 12-5-1**.

```

CM Rhombic: 14-28 MHz
CE
GW 1 1 -57.53 -.5 21 -57.53 .5 21 .0010265
GW 2 50 -57.53 .5 21 0 28 21 .0010265
GW 3 50 0 28 21 57.53 .5 21 .0010265
GW 4 1 57.53 .5 21 57.53 -.5 21 .0010265
GW 5 50 57.53 -.5 21 0 -28 21 .0010265
GW 6 50 0 -28 21 -57.53 -.5 21 .0010265
GS 0 0 1
GE 1
GN 2 0 0 0 13 .005 0 0 0 0
EX 0 1 1 0 1 0
LD 4 4 1 1 800 0 0
LD 5 1 1 1 5.8001E7
LD 5 2 1 50 5.8001E7
LD 5 3 1 50 5.8001E7
LD 5 4 1 1 5.8001E7
LD 5 5 1 50 5.8001E7
LD 5 6 1 50 5.8001E7
FR 0 1 0 0 21 1
RP 0 181 1 1000 -90 0 1 1
FR 0 1 0 0 21 1
RP 0 1 360 1000 81 0 1 1
EN

```

12-5

Open file 12-5.NEC. The #12 AWG copper wire rhombic is over 100 m long by nearly 60 m wide. The antenna is set 21 m above average S-N ground. The initial frequency is 21 MHz, although the antenna is designed for use from 14 through 28 MHz.

The model uses two short wires at each end of the diamond. The first 1-segment wire positions the source, while the second places the load. The overall antenna is under-segmented for run-time speed in this exercise. For more exacting results, double the number of segments for each leg of the diamond, using 3 segments for each of the short wires. If you make this change, be certain to center both the source and the load on their short wires. Nevertheless, with the segmentation given, the figures will be approximately correct and the trends will be accurate.

The type 4 load calls for $800\ \Omega$ resistance with no reactance. If you simply ignore the reactance input box, a zero will be entered. Since the resistance-reactance load type

places the two elements in series, a purely resistive load will result.

Notice that the model calls for 2 patterns, an elevation and an azimuth pattern. The elevation pattern is needed to obtain the take-off angle for each frequency checked, after which you will adjust the elevation angle for the requested azimuth pattern. For each of the frequencies on the following table, record the forward gain, the take-off angle, the beamwidth, the 180-degree front-to-back ratio, and the source impedance. You may obtain all of the data (or calculate it) from the NEC Output file or you may use various smaller tabular and graphical outputs to obtain the data.

12-5 Test Data					
Frequency MHz	Gain dBi	T-O angle degrees	Beamwidth degrees	F-B dB	Source Z $R \pm jX \Omega$
14					
18.12					
21					
24.9					
28					

Comments: The rhombic with its terminating resistor shows remarkably consistent performance across the frequency range, with very high gain and an excellent front-to-back ratio. Moreover, the source impedance does not depart radically from the value of the terminating resistor, the model load. As with any horizontally oriented antenna, the take-off angle is a function of the height above ground in terms of fractions of a wavelength. Notice also that the beamwidth to -3 dB points exhibits a parallel narrowing with frequency increases.

The significance of the terminating resistor can easily be shown in models. As an additional exercise, reduce the value of the terminating resistor to zero. (You may leave the load specification in place and change only the resistance value. NEC-2 will correctly calculate all values as if the LD input card was not present.) Redo all runs and compare the patterns and other information with the data obtained for the original configuration.

12-5 Reference Data					
Frequency MHz	Gain dBi	T-O angle degrees	Beamwidth degrees	F-B dB	Source Z $R \pm jX \Omega$
14	16.00	14	18	34.31	812 - j 74
18.12	17.81	10	14	21.67	906 - j 54
21	18.36	09	12	30.39	799 - j 30
24.9	18.17	07	10	27.87	869 + j 2
28	17.19	06	8	24.70	793 + j 11

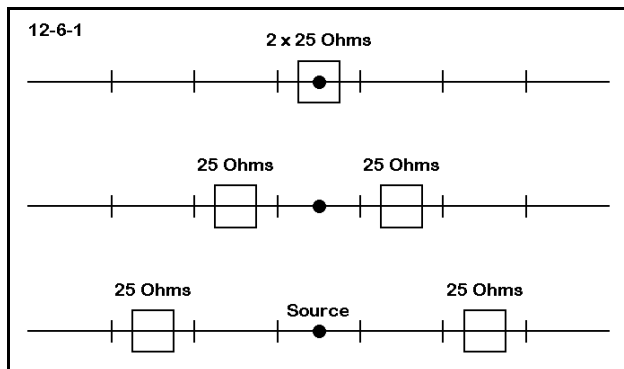
There are two further exercises you may wish to run. First, alter the value of the terminating resistor in regular steps from 400 to 1200 Ω in 200- Ω steps. Record the same data set as obtained with the initial 800- Ω resistor. Rhombic antennas were originally designed to be an approximate match to wide-spaced site-constructed parallel transmission lines. This practice limited reactance excursions along the line, allowing easier impedance transformation to the transmitter output impedance with balance link-coupled antenna tuning units. What ramifications emerge from altering the value of the terminating resistor?

Second, alter the shape of the diamond by widening and narrowing its width. Using the 800- Ω terminating resistor--or other values you discover to your liking--check the revised antenna throughout its operating range. The original very large array has a considerable number of minor lobes. Is there a shape that maximizes gain with at least 20 dB front-to-back ratio while minimizing the minor lobes? If you find such a shape for any frequency, does the benefit extend across the total operating frequency range of the antenna? Are the diamond shape and the terminating resistor value interrelated?

Remember that "no" answers to some of these questions are as important as "yes" answers and their accompanying quantifiable differences from the basic model.

12-6.NEC: A loaded dipole for 7.0 MHz

The position of any load along a radiating antenna element has a large bearing upon its effect. Resistive loads can dramatize the effect, since they convert into heat some energy that otherwise would contribute to the antenna's far field radiation pattern.



In this exercise, we shall familiarize ourselves with the consequences of changing the position of a load along a radiator, as illustrated in **Figure 12-6-1**. We shall begin with an unloaded antenna, the 7 MHz dipole of model 12-1.NEC. Note that the antenna has 11 segments. We shall obtain the maximum gain, efficiency, and source impedance for the antenna.

Next, we shall load the antenna with a total of 50Ω . Initially, we shall place the load at the antenna center, where it appears in series with the source. Since it is in series, we can place a single load of 50Ω . Then, we shall split the load into two $25\text{-}\Omega$ loads and place them on the segments adjacent to the center source segment (#5 and #7). In successive steps, we shall move the loads outward by one segment per step until they are on the outermost segments (#1 and #11).

After collecting initial data from model 12-1.NEC, open model 12-6.NEC. Verify that except for the added load entry, it is the same antenna as in 12-1.NEC. Note the LD entry, along with the position and value of the load. Obtain the data for this model. Then, replace the single load with two $25\text{-}\Omega$ loads placed on segments 5 and 7. Repeat the process until data has been obtained for all the entries on the table below.

```

CM Dipole in Free Space: 7.0 MHz
CE
GW 1 11 20.86 0 0 0 0 0 .000814
GS 0 0 1
GE 0
EX 0 1 6 0 1 0
LD 4 1 6 6 50 0 0
FR 0 1 0 0 7 1
RP 0 1 360 1000 90 0 1 1
EN

```

12-6

12-6 Test Data			
Load Position Segment(s)	Maximum Gain dBi	Efficiency (%)	Source Z $R \pm jX \Omega$
No load			
6 (center)			
5-7			
5-8			
3-9			
2-10			
1-11			
12-6 Reference Data			
Load Position Segment(s)	Maximum Gain dBi	Efficiency (%)	Source Z $R \pm jX \Omega$
No load	2.13	100	72.2 + j 0.1
6 (center)	-0.16	59.09	122.2 + j 0.1
5-7	-0.02	60.96	118.4 - j 1.6
5-8	0.37	66.68	108.2 - j 2.6
3-9	0.95	76.23	94.6 - j 2.2
2-10	1.59	88.31	81.7 - j 1.0
1-11	2.05	98.29	73.5 - j 0.1

Comments: Since the modeled antenna used perfectly conducting wire, all reductions in efficiency are a function of the load and its position. As the load moves further outward, the efficiency increases towards 100%. If you were to more highly segment this dipole, you would discover that the efficiency approaches 100% as the load occupies a smaller space at the ends of the element. An examination of the current levels on each side of the loaded segments will prove instructive.

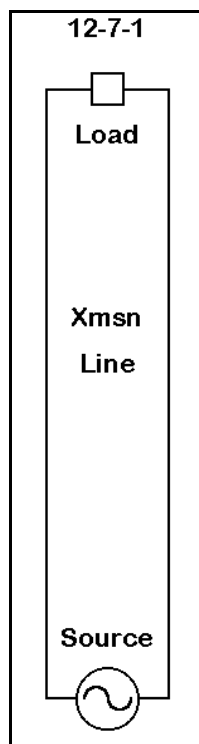
It was not necessary to list the efficiency figures, since the data at hand for these resonant dipoles permits efficiency calculations. Simply divide the source resistance of the unloaded dipole by the source resistance of any of the loaded dipoles. As the center-loaded case illustrates, the total source resistance is the sum of the antenna source

resistance plus the effects of the load. With a center load, the source resistance is the native 72.2Ω plus the $50\text{-}\Omega$ load resistance. You may also calculate the antenna gain knowing efficiency, since that number represents power not lost. The power level for the center-loaded model is about 2.29 dB lower than the unloaded gain of 2.13 dBi, or -0.16 dBi.

As the load moves outward, the efficiency, gain, and source impedance values all form curves. Because using only a few steps does not yield a smooth curve when graphed, you should double or triple the number of segments in the model. Move the load progressively outward and graph the results. In addition, you may also change the load value and rerun the entire exercise (using either the original short version or the longer version just suggested).

Finally, for each step outward from the center, increase the value of the loads equally until you reduce the performance figures to those for the center-loaded model. What conclusions do you reach from this exercise?

12-7.NEC: A parallel transmission line



Spot resistive loads are useful for a number of subsidiary modeling tasks. We shall sample just one: the calibration of a physically modeled parallel transmission line. Since this type of transmission line consists of two wires that parallel each other, NEC-2 is capable of modeling it well, so long as the wires are not too close together.

There are a number of qualifications to modeling parallel transmission lines. First, they will not directly replicate actual lines in which the insulation used to bind the wires in parallel creates a velocity factor of less than 1.0. Modeled transmission lines in NEC-2 have no medium other than a vacuum (or, as a good approximation thereof, air). If you use a physically modeled transmission line to analyze what is occurring on an actual antenna system, you will have to take the velocity factor of the actual line into account in dimensioning your model.

Second, because NEC-2 is most accurate when angular junctions have wires of the same diameter, you may have to calculate a substitute transmission line of the same characteristic impedance as the one in use.

If your actual transmission line uses #18 AWG wire to an antenna using #12 AWG wire, you should model an equivalent transmission line using #12 AWG wire for the system.

Third, NEC-2 models of transmission lines are not in full agreement with the results of standard equations for calculating such lines. For parallel transmission lines in open air, the most frequently cited equations are these:

$$Z_o = 276 \log_{10} \frac{2S}{d} \quad \text{or} \quad Z_o = 120 \cosh^{-1} \frac{S}{d} \quad 1$$

where Z_o is the characteristic impedance in Ohms, S is the center-to-center spacing between wires, and d is the diameter of each wire, with S and d given in the same units (inches, millimeters, etc.). As our sample, let's assume a parallel transmission line using #12 AWG wire, with a diameter of 0.0808" and a spacing between wires of 3". The standard (left) equation gives us a characteristic impedance of 516.3 Ω . With this number in hand, we may now try to model the line.

The initial method for determining the characteristic impedance of a modeled line involves setting up a model like the sketch of **Figure 12-7-1**. The model should be in free space. The #12 AWG copper wires are set 3" apart and made $1/4\lambda$ long. If we arbitrarily choose 14 MHz for our model, 1λ is 843.06" long, with the required section being 210.77" long. (You may carry this out to further decimal places, if you wish, in order to avoid an accumulation of rounding errors.)

The model (illustrated by file 12-7.NEC) should have short (3") wires connecting both the top and bottom ends of the parallel lines. For easiest examination of the currents along these lines, construct the model from one corner progressively around the "loop."

Segmenting the model requires that the short wires have 1 segment. To keep the segment lengths approximately equal, the long wires require about 70 segments each. On the top short wire, place a type 4 resistive load of 50-

Ω (or some other favored low value). Since the $1/4\lambda$ section will form a transformer, we may expect a high impedance at the source with a rapidly changing reactance, a situation that will allow a more precise determination of resonance.

Run either your model or 12-7.NEC.

Comments: The use of the calculated 210.77" line results in a reactive line. Model 12-7 achieves resonance (less than $\pm 1 \Omega$) with a length of 208.46". Notice that the original calculation of the characteristic impedance did not include the connecting wires we used

```

CM Parallel transmission line
CM Calculated: 516.3 Ohms
CE
GW 1 1 0 0 0 3 0 0 4.04133858267717E-02
GW 2 70 3 0 0 3 0 208.46 4.04133858267717E-02
GW 3 1 3 0 208.46 0 0 208.46 4.04133858267717E-02
GW 4 70 0 0 208.46 0 0 0 4.04133858267717E-02
GS 0 0 .02540
GE 0
EX 0 1 1 0 1.414214 0
LD 4 3 1 1 50 0 0
LD 5 1 1 1 5.8001E7
LD 5 2 1 70 5.8001E7
LD 5 3 1 1 5.8001E7
LD 5 4 1 70 5.8001E7
FR 0 1 0 0 14 0
RP 0 1 360 1000 90 0 1 1
EN

```

in the model.

The source resistance should be about 5971.4 Ω . The characteristic impedance of the line will be

$$Z_0 = \sqrt{Z_L Z_S} \quad 2$$

where Z_0 is the characteristic impedance, Z_L is the load impedance, and Z_S is the source impedance, when all are resistive. With our 50- Ω load, $Z_0 = 546.4 \Omega$.

```

CM Parallel transmission line
CM Calculated: 516.3 Ohms
CE
GW 1 1 0 0 0 3 0 0 4.04133858267717E-02
GW 2 140 3 0 0 3 0 419 4.04133858267717E-02
GW 3 1 3 0 419 0 0 419 4.04133858267717E-02
GW 4 140 0 0 419 0 0 0 4.04133858267717E-02
GS 0 0 .02540
GE 0
EX 0 1 1 0 1.414214 0
LD 4 3 1 1 50 0 0
LD 5 1 1 1 5.8001E7
LD 5 2 1 140 5.8001E7
LD 5 3 1 1 5.8001E7
LD 5 4 1 140 5.8001E7
FR 0 1 0 0 14 0
RP 0 1 360 1000 90 0 1 1
EN

```

12-7A

The requirement to shorten the line by over 1% from a true $1/4\lambda$ and the divergence of the characteristic impedance from its expected value suggests that the model may be only in the ballpark and not fully accurate.

To test this suspicion, double the line length and the number of segments on each long wire, as shown in file 12-7A.NEC. This process should give us a $1/2\lambda$ wire, and the load resistance should appear as the source impedance.

Run your version of this $1/2\lambda$ transmission line (or model 12-7A.NEC). Resonate the

line by adjusting the length. You will note that the required length, 419", is over 2" longer than a simple doubling of the $1/4\lambda$ test line. The resistive impedance of about 51.7 Ω accounts not only for the original load, but as well for the finite conductivity of the copper wire.

Since the $1/2\lambda$ line did not turn out to be a true doubling of the $1/4\lambda$ line, we still have reason to distrust the characteristic impedance reported by the short line. However, we cannot determine the characteristic impedance of the line from a $1/2\lambda$ section. Instead, our third step involves increasing the line length to $3/4\lambda$. Using the $1/2\lambda$ line as a basis, we may simply try $3/2$ its length, or 628.5". One reason underlying this move is that the longer we make the line, the smaller the error introduced by the short wires at each end of the transmission line.

As in model 12-7B.NEC, you should be certain to increase the number of segments along the line to about 210. This will extend the run time of the model. (For this reason alone, many modelers do not go beyond the first step of the method.) If you carefully make the runs, you will discover that the line resonates at a length of about 629.582", very close to the $3/2$ calculation. The resonant source impedance will be about 5774.2, which will yield, by equation (2), a characteristic impedance of about 537.3.

```

CM Parallel transmission line
CM Calculated: 516.3 Ohms
CE
GW 1 1 0 0 0 3 0 0 4.04133858267717E-02
GW 2 210 3 0 0 3 0 629.582 4.04133858267717E-02
GW 3 1 3 0 629.582 0 0 629.582 4.04133858267717E-02
GW 4 210 0 0 629.582 0 0 4.04133858267717E-02
GS 0 0 .02540
GE 0
EX 0 1 1 0 1 0
LD 4 3 1 1 50 0 0
LD 5 1 1 1 5.8001E7
LD 5 2 1 210 5.8001E7
LD 5 3 1 1 5.8001E7
LD 5 4 1 210 5.8001E7
FR 0 1 0 0 14 0
RP 0 1 360 1000 90 0 1 1
EN

```

12-7B

Notice the difference in this impedance from both the value yielded by the $1/4\lambda$ line and by the original calculation. The utility of the value just derived, however, is established by the very low difference in the predicted and the actual length of the $3/4\lambda$ line. Moreover, the $3/4\lambda$ line is 99.6% of a true value (632.30") for 14 MHz.

This exercise should suffice to give you expectations that NEC-2 physically modeled transmission lines will exhibit slightly higher (about 4% in this case) values than lines calculated from the standard equation (1). Whether that differential is significant depends upon the required precision of the model as determined by the project goals.

Before leaving this subject, you should perform two supplementary exercises. First, suppose that you need a value of 500Ω as the characteristic impedance of a line. Back calculate through equation (1) to determine what values it calls for either in terms of an adjusted spacing or of wire size. (In the practical world, the diameter adjustment may be too small to be feasible.) Then adjust the spacing of model wires to achieve a value of 500Ω within 1%. Second, create modeled lines with characteristic impedances of 400, 500, and 600Ω , using #18, #14, and #12 AWG copper wire. Compare them with calculated results from equation (1) and graph the trends.

Summing Up

Both distributed (material) resistive loads and spot resistive loads present a diverse collection of modeling considerations. Because of that diversity, many modelers overlook resistive loading as relatively simple or unimportant. The exercises in this chapter should have dispelled both misconceptions.

As we discovered when exploring material conductivity questions, selection of materials can be very significant to the success of an antenna project. There are direct relationships among antenna efficiency, gain, and source impedance when moving from one material to another. At the other end of the scale, as the wire size increases relative

to the wavelength of operation, increases in efficiency slow to the point that selection of materials may be for reasons other than electrical performance of the antenna.

The utilization of spot (type 4) resistive loads may be intrinsic to an antenna design or it may simply open opportunities for calibrating partial models to be used in larger modeled assemblies. Perhaps of greatest importance is understanding how the placement of resistive loads along an antenna element affects the performance of that element. This aspect of resistive loading will remain with us in the next chapter, which will explore reactive loading. For many cases of reactive loading, we shall have to consider the Q of the loading component--and that requirement will return us once more to resistive loading.

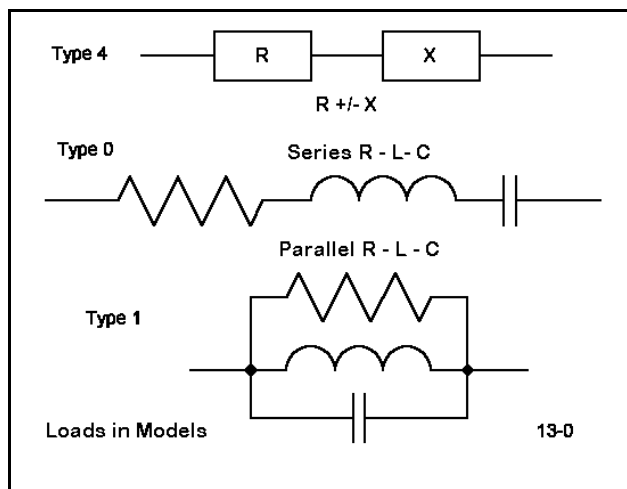
13

Reactive Loads

Objectives: Reactive loads (which also include resistive components) are so commonplace in antenna design that NEC-2 offers three distinct ways of incorporating them in models. These exercises will familiarize you with some applications of reactive loads and also the best techniques for modeling them in each application.

We insert inductive and capacitive reactance into an antenna structure for many different reasons: to change the resonant frequency, to alter the phase relationships among parts of the assembly, to effect impedance transformations, to create high impedance traps, among others. NEC-2 offers the modeler the ability to introduce reactance loads to any segment of any wire of the model. These loads appear in series with sources and transmission lines appearing on the same segment.

NEC-2 permits the modeler to construct reactive loads in a number of ways, of which we shall work with three in this chapter: the series resistance-reactance load (type 4), the series resistance, inductance, capacitance load (type 0), and the parallel resistance, inductance, capacitance load (type 1). These types, shown in **Figure 13-0**, cover the most common applications of loads. Let's look at the entry methods of these load types one at a time.



Type 4--Complex Resistance-Reactance

Type 4 loads consist of entries for resistance and reactance, where these numbers are known or obtainable. Reactance is entered according to common conventions: "+" = inductive; "-" = reactive. Either value may be zero. The typical entry line for a type 4 load (with a resistance of 5Ω and a capacitive reactance of 750Ω placed on wire 5, segment 3) would appear as follows:

LD 4 5 3 3 5 -750

The first numerical entry registers the load type, followed by the wire (tag) number. The next two entries record the starting and ending segments for the load. (The loads in these exercises will be confined to a single segment per load). The following entries record the resistance and reactance, respectively.

Since virtually all methods of introducing reactance are frequency dependent, this type is not the most apt for antennas to be modeled over a range of frequencies. However, it has certain advantages for developing antenna models which we shall examine in the exercises. As may be evident, the purely resistive spot loads we examined in the last chapter are actually a special case of the complex series resistance-reactance load where the reactance value was zero.

Type 0--Series Resistance-Inductance-Capacitance

Series loads using inductance and capacitance values are very useful in the HF range for introducing inductors (and accounting for their series resistance) or capacitors (for which Q is not usually an issue at HF). Such loads automatically convert to the correct impedance loading at each frequency at which the antenna is modeled. Values are introduced in the sequence given using Ohm, Henrys, and Farads (that is, basic units). Engineering notation may be used for entries.

A series load consisting of an inductance of 7 μH , 45 pF, and 2 Ω on wire 6, segment 18 would yield the following load card:

LD 0 6 18 18 2 7E-6 4.5E-11

The first numeric entries indicates the load type, and the next three are the same as for type 4 loads. The values that follow are for resistance, inductance, and capacitance, all in basic units. If a load has only some of the components, enter zeroes for the missing ones. Hence, a capacitive load consisting only of a 45 pF capacitance would read 0 0 4.5E-11.

Type 1--Parallel Resistance-Inductance-Capacitance

Parallel loads are especially apt for modeling traps, that is, parallel circuits containing inductance and reactance where the coil Q creates also a resistance for which the entry must account after conversion to a parallel equivalent resistance. A parallel load consisting of 25 k Ω , 1.5 μH , and 37 pF on wire 9, segment 11 would yield the following load entry:

LD 1 9 11 11 2.5E4 1.5E-6 3.7E-11

If the parallel circuit lacks any of the three components, enter a zero in its place. NEC-2 does NOT interpret zeroes in parallel circuits as a short circuit. Instead, it treats zero as indicating a missing component. For example, if the resistance is missing, you need not create an artificial very high value for the entry. A zero will suffice to give correct results from the load specification. However, if the inductance of the parallel circuit has a finite Q, resulting in a resistance in series with the inductance, both the resistance and the inductance values must be converted into parallel equivalents prior to entry into the type 1 load line.

In the following exercises, we shall look at both load phenomena in antenna models and applications of the various kinds of loads just enumerated. Although the treatment cannot be exhaustive, we can at least obtain a sure feel for working with reactive loads.

Exercise Preparation

The following exercises will be a mixture of simple antennas on which we shall perform many modifications and some complex antennas calling for a careful sorting of modeled wires. Use extreme care when saving variations of the models on the disk accompanying this guide so as not to overwrite another model in the sequence. Variant filenames for this chapter might well use multi-letter codes to indicate the kind of alteration made. For example, when moving an inductive load outward along an antenna element, you might append "LD[segment #]" to the basic model designation.

As with every exercise, it is important that you model each variation on the basic model and chart the results, even though reference data is available. Not only will this procedure allow you to detect modeling errors and to calibrate your version of NEC-2 against the one used in creating these exercises, the procedures will naturalize the process of modeling more fully, enabling future work to proceed smoothly and efficiently.

13-1.NEC & 13-2.NEC: A shortened and loaded dipole for 14.175 MHz

We shall begin with a simple shortened dipole, 6 m long and 25 mm in diameter and test it at 14.175 MHz. Although the comment card calls this antenna a loaded dipole, there is yet no load.

After recording the source impedance of this antenna, create a type 4 load with zero resistance and place it at the center segment (where it will be in series with the source). This will constitute "center-loading" for the dipole. For the reactance, explore values of capacitive and/or inductive reactance until the antenna is once more

```

CM Loaded dipole: 14.175
CE
GW 1 11 -3 0 0 3 0 0 .0125
GS 0 0 1
GE 0
EX 0 1 6 0 1.414214 0
LD 5 1 1 11 2.4938E7
FR 0 1 0 0 14.175 0
RP 0 1 360 1000 90 0 1 1
EN

```

resonant, as indicated by a source reactance of less than $\pm 1 \Omega$.

Once you have this data in hand, along with the maximum gain for both the unloaded and loaded versions of the antenna, consider that you have just inserted a load with an infinite Q. Since component Q is simply the ratio of reactance to resistance in a series circuit, a resistance value of zero provides a likely unrealistic set of expectations. As a supplement to this simple exercise, systematically alter the Q of the series resistance-reactance circuit for Q values of 500 down to 50, which represents a reasonable (although optimistic) span of real values encountered in antenna work. Model 13-2.NEC provides a sample for a Q of 300. In each case, re-resonate the antenna. Record the values of resistance and reactance used for each level of Q, the maximum gain of the antenna, and the source impedance.

```

CM Loaded dipole:  14.175
CE
GW 1 11 -3 0 0 3 0 0 .0125
GS 0 0 1
GE 0
EX 0 1 6 0 1.414214 0
LD 4 1 6 6 1.45 434 0
LD 5 1 1 11 2.4938E7
FR 0 1 0 0 14.175 0
RP 0 1 360 1000 90 0 1 1
EN

```

13-2

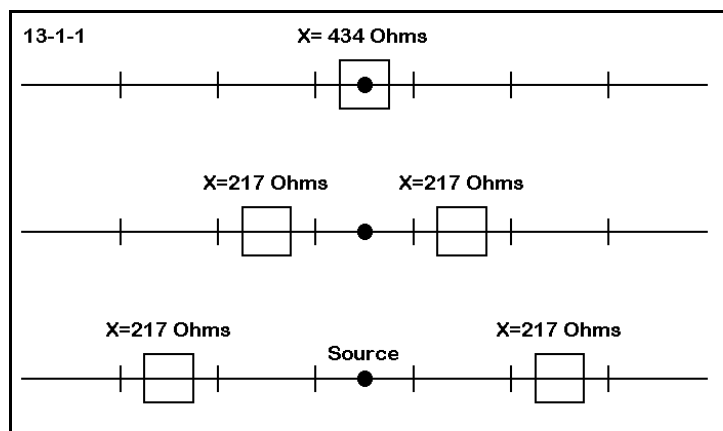
13-1/13-2		Test Data		
Q	Reactance Ω	Resistance Ω	Gain dBi	Source Z $R \pm jX \Omega$
Unloaded	0	0		
"Infinite"		0		
500				
400				
300				
200				
100				
50				

Comments : The antenna required no adjustments in the reactance as the Q decreased in order to maintain resonance. In fact, for single linear elements, the resistive and reactive components of the complex impedance load operated independently. The inductive reactance established resonance. In fact, the capacitive reactance at the source provided the clue to what kind and exactly what amount of reactance to set into the load.

The load resistance alone affected both the gain and the source resistance of the

antenna. For this center-loading situation, the source impedance increased exactly as the load resistance increased, which was in turn a function of decreasing Q.

13-1/13-2		Test Data		
Q	Reactance Ω	Resistance Ω	Gain dBi	Source Z $R \pm jX \Omega$
Unloaded	0	0	1.86	19.2 - j434.3
"Infinite"	434	0	1.86	19.2 - j 0.3
500	434	0.87	1.67	20.1 - j 0.3
400	434	1.09	1.62	20.3 - j 0.3
300	434	1.45	1.55	20.7 - j 0.3
200	434	2.17	1.40	21.4 - j 0.3
100	434	4.34	0.98	23.6 - j 0.3
50	434	8.68	0.24	27.9 - j 0.3



We are not finished with our simple loaded dipole. We wish to examine (as we did for purely resistive loads) what happens as we move the purely reactive load outward from the center position. Using 13-2.NEC, set the resistance to zero, but retain the 434- Ω reactive load at the center (segment 6). Then, in a series of modifications sketched in **Figure 13-1-1**, split and move the resulting pair of 217- Ω reactive loads

outward along the antenna, one segment pair at a time (5 and 7, 4 and 8, etc.), until finally the loads are on segments 1 and 11. Check both the maximum gain and the source impedance.

Once you have recorded the data for the consequences of moving the purely reactive load outward, change the value of the load reactance until the antenna is once more resonant. Record both the gain and the source resistance with this new load. As a final step. change the Q of the load for each segment-pair position to 300 for both the moving

pair of 217- Ω loads and the loads that yield resonance. Recheck both the gain and the source impedance. Record your data in the tables (13-2) on the next page. The bracketed values already in place are sample check values.

13-2 Test Data				
Position	Reactance Ω	Resistance Ω	Gain dBi	Source Z $R \pm jX \Omega$
"Infinite" Q	Constant	Load		
6 (center)	434	0	[1.86]	[19.3 - j0.3]
5-7	217-217	0		
4-8	217-217	0	[1.87]	[25.2 - j173]
3-9	217-217	0		
2-10	217-217	0		
1-11	217-217	0	[1.86]	[19.6 - j427]
Q = 300	Constant	Load		
6 (center)	434	1.45	[1.55]	[20.7 - j0.3]
5-7	217-217	0.72-0.72		
4-8	217-217	0.72-0.72	[1.69]	[26.3 - j173]
3-9	217-217	0.72-0.72		
2-10	217-217	0.72-0.72		
1-11	217-217	0.72-0.72	[1.86]	[19.6 - j427]

Comments: Because repetition of the entire table for reference purposes would require so much room, a few sample values have already been inserted in the "Test Data" table as checkpoints for your own modeling.

For an indefinitely high Q (zero resistance in the load), the gain of the shortened dipole remains constant, although the inductively reactive load has less and less affect upon the source reactance. Notice that the resistive component of the source impedance peaks when the load is placed about 1/3 of the way (segments 4 and 8) between the centered source and the element end.

When a finite Q is selected--in this case, 300--the source reactance is almost wholly

unaffected, and the source resistance is changed by a decreasing amount as the load moves toward the element ends. The source resistance peaks with the load at the same position as for the case of an indefinitely high Q.

13-2 Test Data				
Position	Reactance Ω	Resistance Ω	Gain dBi	Source Z $R \pm jX \Omega$
"Infinite" Q	Resonating	Load		
6 (center)	434	0	[1.86]	[19.3 - j0.3]
5-7		0		
4-8	322-322	0	[1.87]	[29.7 - j0.6]
3-9	453-453	0		
2-10		0		
1-11	2637-2637	0	[1.89]	[46.2 + j0.4]
Q = 300	Resonating	Load		
6 (center)	434	1.45	[1.55]	[20.7 - j0.3]
5-7				
4-8	322-322	1.07-1.07	[1.59]	[31.6 - j0.7]
3-9	453-453			
2-10				
1-11	2637-2637	8.79-8.79	[1.27]	[53.3 - j0.2]

Once more, some check values have been inserted into the Test Data table.

As the load is moved outward, the value of reactance needed to arrive at resonance increases to a very high value: over 2500 Ω each side of center. (In general, it is unwise other than in an exercise of this kind to place loads on the end of a wire. Because current is changing rapidly in this region, power dissipation in the load and other factors may be inaccurate.) The resonating value for a load positioned midway between the element center and its ends approaches the value of the single center load. Despite the very high values of reactance required near the element ends to achieve resonance, the source impedance rises slowly, slowly approaching the value for a full-size self-resonant dipole.

With a Q of 300, the increasingly high level of reactance yields sufficient resistance in the load to reduce gain beyond the segment 3-9 position. The source impedance, however, is only higher than the high-Q case by the amount of the load resistance. Once more, only the reactance affects resonance.

The loaded dipole with which we have been working has one more lesson to teach us, this time about placing loads precisely. As a start, let the loads on each side of center be exactly 500Ω each. Position them so that the antenna achieves resonance. Use any number of segments necessary to reach the desired result. Then determine the distance from center for each of the loads.

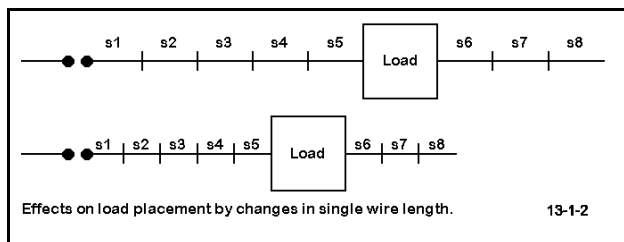
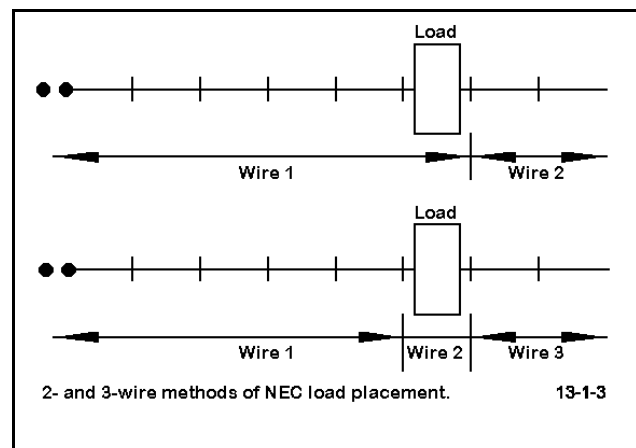


Figure 13-1-2 illustrates something of the difficulty of the process. If we vary the wire length, the segment lengths also change. If we leave the length constant, then the load arrives at a correct point either by lucky accident or by the use of a very large number of segments.

As we discovered when placing sources off center, we have alternative means of placing loads to position them more precisely. By breaking the dipole wire into separate wires, with the load either on a segment of its own (the "3-wire" method) or at the end of a wire (the "2-wire" method), we can achieve some precision of load placement. For most cases, the 2-wire method is sufficient. However, if the length of the loading component is significant to the model, the 3-wire method should be used. The length of the loading segment, which should reflect the length of the physical loading component, determines the segment lengths in the adjacent wires. Of course, the labels "2-wire" and "3-wire" refer to each side of a center-fed antenna element.



```

CM Loaded dipole: 14.175
CE
GW 1 6 -3 0 0 -1.912 0 0 .0125
GW 2 21 -1.912 0 0 1.912 0 0 .0125
GW 3 6 1.912 0 0 3 0 0 .0125
GS 0 0 1
GE 0
EX 0 2 11 0 1 0
LD 4 2 21 21 0 500 0
LD 4 2 1 1 0 500 0
LD 5 1 1 6 2.4938E7
LD 5 2 1 21 2.4938E7
LD 5 3 1 6 2.4938E7
FR 0 1 0 0 14.175 0
RP 0 1 360 1000 90 0 1 1
EN

```

13-2-1

Construct a "2-wire" method model to position the 500- Ω loads more precisely to achieve resonance with the 6-meter aluminum dipole at 14.175 MHz. Although no specific segmentation is requested, a minimum of about 30 segments overall is a good number (about 0.2 m per segment) to represent a likely length for the loading inductance.

Check model 13-2-1.NEC provides one of many possible solutions to this task. On your own, you may wish to try a "3-wire" solution to the assignment.

13-3.NEC: A center-loaded 2-element Yagi for 28.5 MHz

13-4.NEC: A mid-element-loaded 2-element Yagi for 28.5 MHz

13-5.NEC: A full-size 2-element Yagi for 28.5 MHz

In this set of exercises, we shall make use of 3 simple 2-element Yagis. The first is a center-loaded short-element beam, found in 13-3.NEC. The 1" diameter 6061-T6 aluminum elements are 11.6' and 12.16' long at a 4.25' spacing. The center of each element is loaded with 223 Ω of inductive reactance and 0.73 Ω resistance, simulating a Q=300 inductor. All of the models will be run in free space and have a design center frequency of 28.5 MHz. All are resonant at this frequency.

```

CM Center-loaded Yagi: 28.5 MHz
CE
GW 1 31 -5.8 0 0 5.8 0 0 .04165
GW 2 31 -6.08 -4.25 0 6.08 -4.25 0 .04165
GS 0 0 .3048
GE 0
EX 0 1 16 0 1 0
LD 4 1 16 16 .74 223 0
LD 4 2 16 16 .74 223 0
LD 5 1 1 31 2.4938E7
LD 5 2 1 31 2.4938E7
FR 0 1 0 0 28.5 0
RP 0 1 360 1000 90 0 1 1
EN

```

13-3

The second short-element Yagi makes use of the same dimensions as the center-loaded model. 13-4.NEC presents a mid-element-loaded version of the Yagi. In place of center inductive reactance, each element has inductive reactance approximately 1/2 the way outward to the element end. The driven element has type 4 loads of 216 Ω reactance and 0.72 Ω resistance, while the reflector loads are 218 Ω reactance and 0.72 Ω resistance. Both value sets simulate Q=300 inductors at the indicated points.

```

CM Mid-element loaded yagi: 28.5 MHz
CE
GW 1 31 -5.8 0 0 5.8 0 0 .04165
GW 2 31 -6.08 -4.25 0 6.08 -4.25 0 .04165
GS 0 0 .3048
GE 0
EX 0 1 16 0 1 0
LD 4 2 8 8 .73 218 0
LD 4 2 24 24 .73 218 0
LD 4 1 8 8 .72 216 0
LD 4 1 24 24 .72 216 0
LD 5 1 1 31 2.4938E7
LD 5 2 1 31 2.4938E7
FR 0 1 0 0 28.5 0
RP 0 1 360 1000 90 0 1 1
EN

```

13-4

The final beam, 13-5.NEC, is full size, but uses 1" diameter 6061-T6 aluminum like the shorter version of the antenna. The driven element is 15.8' long, while the reflector is 17.34' long. The elements are 4.25' apart. This unloaded Yagi, also for 28.5 MHz, provides us with a standard of comparison for the two shortened and loaded Yagis. With it, we shall derive some general characteristics of beams whose elements are loaded with inductive reactance.

```

CM 2el Yagi: 28.5 MHz
CE
GW 1 31 -7.9 0 0 7.9 0 0 .04165
GW 2 31 -8.67 -4.25 0 8.67 -4.25 0 .04165
GS 0 0 .3048
GE 0
EX 0 1 16 0 1 0
LD 5 1 1 31 2.4938E7
LD 5 2 1 31 2.4938E7
FR 0 1 0 0 28.5 0
RP 0 1 360 1000 90 0 1 1
EN
    
```

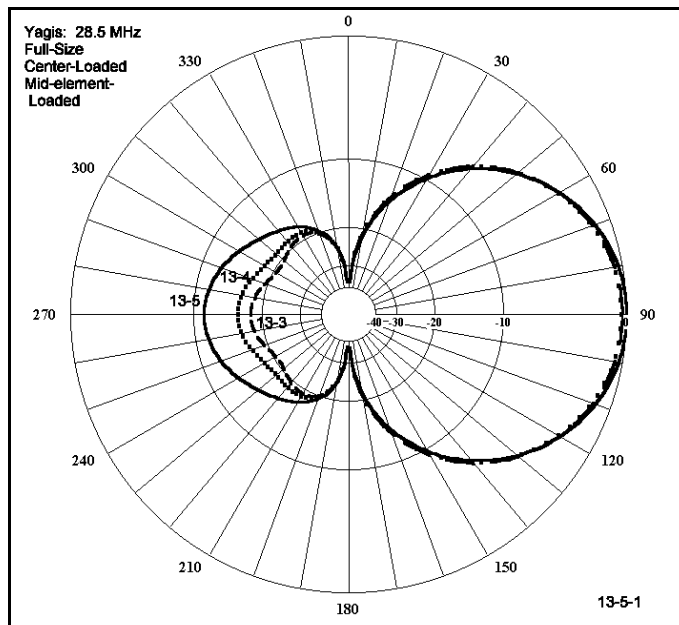
13-5

We shall perform several tasks with these antennas, but the initial job is to take some reference readings from them. Initially, gather data at the design frequency for the maximum forward gain, the 180-degree front-to-back ratio, and the source impedance. Besides entering the data into the table, make comparative azimuth patterns.

13-3/4/5 Test Data			
Antenna	Gain dBi	F-B dB	Source Z R ± jX Ω
13-3			
13-4			
13-5			

Comments: Of immediate notice is that both loaded Yagis have less gain but higher front-to-back ratios than the full-size Yagi. The polar plot in **Figure 13-5-1** makes the differences visually evident, while the table makes them numerically clear.

Both loaded Yagis have source impedances lower than the full-size Yagi, but the center-loaded version has the lowest source impedance--about 1/2 that of the full-size model. Note that this relationship holds only for Yagis shortened to about 3/4 the size of their full-size counterparts. Shorter Yagis with higher center



loading have correspondingly lower source impedances.

13-3/4/5			
		Reference Data	
Antenna	Gain dBi	F-B dB	Source Z R ± jX Ω
13-3	5.99	17.62	17.0 + j 0.3
13-4	5.96	15.58	26.5 + j 0.5
13-5	6.25	11.23	33.0 + j 0.4

Our task will be only to note their characteristics of these beams. Of special importance is that the full-size beam characteristics are dependent upon its geometry alone. In part, the characteristics of each of the loaded and shortened models are dependent also upon the Q of the loading inductances. A Q of 300 for the loads is not beyond reach, but is often optimistic from a practical perspective. Component weathering often reduces the Q as a result of chemical reactions on both the inductors and their junctions with the main elements. Hence, it is always in order to explore the effects of lowered Q, that is, of increases in the resistive components of the complex loading impedances.

The next task is therefore to revise each loaded Yagi by lowering the load Qs to values of 200, 100, and 50. You can simply divide the reactance values by these numbers to obtain the appropriate replacement values for resistance. Enter the gain, front-to-back ratio and source impedance values for each loaded beam in the table below.

13-3/4 Test Data			
Antenna Q-Resistance	Gain dBi	F-B dB	Source Z $R \pm jX \Omega$
Center-loaded	13-3.NEC		
300-0.74/0.74	5.99	17.62	17.0 + j 0.3
200-1.12/1.12			
100-2.23/2.23			
50-4.46/4.46	4.50	13.45	21.3 - j 1.9
Mid-loaded	13.4.NEC		
300-0.72/0.73	5.96	15.58	26.5 + j 0.5
200-1.08/1.09			
100-2.16/2.18	5.36	14.09	29.0 - j 0.9
50-4.32/4.36			

Comments: Partial check data is included in the table. The effect of reactance Q on gain and the 180° front-to-back ratio is evident, as both deteriorate with decreasing Q. The source impedances respond to the rising resistance that decreasing Q represents, but that change is not drastic. Except for the difference in source impedance, the performance of the Yagis under the two methods of loading does not differ significantly.

As we view the Table 13-3/4, a question should occur to us. Can any of these decreases be attributed more to decreasing Q in one element than to decreasing Q in the other? We have a way to determine an answer: rerun the exercise with decreasing Q, but hold first one element and then the other at the Q=300 level. Use tables 13-3 and 13-4 for your results.

13-3			
		Test Data	Center-load
Antenna Q-Resistance	Gain dBi	F-B dB	Source Z $R \pm jX \Omega$
Reflector	Q=300	Drive	Q=X
300-0.74/0.74	5.99	17.62	17.0 + j 0.3
200-1.12/0.74			
100-2.23/0.74			
50-4.46/0.74	5.13	17.61	20.8 + j 0.3
Driver	Q=300	Reflector	Q=X
300-0.74/0.74	5.99	17.62	17.0 + j 0.3
200-0.74/1.12			
100-0.74/2.23	5.71	15.65	17.2 - j 0.6
50-0.74/4.46			

13-4			
		Test Data	Mid-load
Antenna Q-Resistance	Gain dBi	F-B dB	Source Z $R \pm jX \Omega$
Reflector	Q=300	Drive	Q=X
300-0.72/0.73	5.96	15.58	26.5 + j 0.5
200-1.08/0.73			
100-2.16/0.73			
50-4.32/0.73	5.12	15.60	32.2 + j 0.2
Driver	Q=300	Reflector	Q=X
300-0.72/0.73	5.96	15.58	26.5 + j 0.5
200-0.72/1.09			
100-0.72/2.18	5.71	14.08	26.8 - j 0.8
50-0.72/4.36			

As in the previous table, a few check values have been inserted in these tables.

Among the trends you will discover is that--for both types of loaded beams--when only the driver losses increase, the gain diminishes and the resistive component of the source impedance increases roughly in line with similar changes when both elements exhibit higher losses or lower Q loads. The front-to-back ratio and the reactance tend to remain close to constant. When only the reflector load shows higher losses, the front-to-back ratio decreases and changes in reactance parallel those of the case where both element loads show lower Q values. The gain also decreases, but at a slower rate than when the driver load Q is directly altered. Understanding detailed trends in the behavior of antenna structures in the face of increased losses of sundry sorts can aid in the diagnosis of both gradual and sudden changes in antenna performance.

Thus far, we have employed complex impedance loads consisting of resistance and reactance values. So long as we stay on a single frequency, it makes no difference whether we use a type 4 load or a type 0 load. However, type 4 loads do not alter their reactive values as we change frequencies. Whenever a frequency sweep is required, type 4 loads should be converted into their series R-L-C equivalents. To illustrate the importance of this change, let us first make the intentional error of performing a frequency sweep of 13-3.NEC--using the Q=300 values of resistance--from 28.0 to 29.0 MHz in 0.25 MHz steps. List the impedance and VSWR values relative to 17.0Ω in the following table.

13-3			Test Data			Reference Data		
Frequency MHz	Source Z $R \pm jX \Omega$	VSWR 17Ω		Source Z $R \pm jX \Omega$	VSWR 17Ω			
28.0				9.3 - j 16.4	3.83			
28.25				12.9 - j 7.3	1.74			
28.5				17.0 + j 0.3	1.02			
28.75				20.9 + j 6.6	1.50			
29.0				24.2 + j 12.0	1.97			

From data such as this, one might reach the conclusion that the center-loaded Yagi has a 2:1 VSWR operating bandwidth of better than 800 kHz when the design center frequency is 28.5 MHz.

Convert the type 4 load to a type 0 load using series values of resistance, inductance, and capacitance. The equations for conversion are the standard ones for deriving inductance and inductive reactance from each other. For reference, we shall include at

this point the conversion equations for both inductance and capacitance and their respective values of reactance.

$$X_L = 2 \pi f L \qquad L = \frac{X_L}{2 \pi f} \qquad 1$$

where L is the inductance in Henrys, X_L is the reactance in Ω , and f is the frequency in Hertz.

$$X_C = \frac{1}{2 \pi f C} \qquad C = \frac{1}{2 \pi f X_C} \qquad 2$$

where C is the capacitance in Farads, X_C is the reactance in Ω , and f is the frequency in Hertz.

For model 13-3.NEC, replace the type 4 load with the calculated values for a type 0 series load. You may use engineering notation for the value of inductance (for example, 1.245E-6). Be sure to place a zero for the missing value of capacitance. Now perform the same frequency sweep using your revised model or check model 13-3-1.NEC. Record your data for source impedance and VSWR relative to 17 Ω in the following table.

```

CM Center-loaded Yagi: 28.5 MHz
CE
GW 1 31 -5.8 0 0 5.8 0 0 .04165
GW 2 31 -6.08 -4.25 0 6.08 -4.25 0 .04165
GS 0 0 .3048
GE 0
EX 0 1 16 0 1 0
LD 0 1 16 16 .74 .000001245 0
LD 0 2 16 16 .74 .000001245 0
LD 5 1 1 31 2.4938E7
LD 5 2 1 31 2.4938E7
FR 0 1 0 0 28.5 0
RP 0 1 360 1000 90 0 1 1
EN
    
```

13-3-1

13-3-1 Test Data			Reference Data	
Frequency MHz	Source Z $R \pm jX \Omega$	VSWR 17 Ω	Source Z $R \pm jX \Omega$	VSWR 17 Ω
28.0			7.8 - j 23.0	6.49
28.25			11.6 - j 10.1	2.22
28.5			17.0 + j 0.3	1.02
28.75			22.0 + j 8.3	1.64
29.0			25.9 + j 15.1	2.25

The data for the frequency sweep using a type 0 series R-L-C load reflect the change of load impedance at each frequency. As a consequence, the 2:1 VSWR operating bandwidth shows itself to be narrower than the erroneous frequency sweep we ran using a type 4 load. Since almost every loaded antenna is designed for a band of frequencies--

or the analysis of the antenna makes off-frequency performance important data--convert type 4 loads to type 0 loads early in the developmental or analytical process.

As a confirming exercise, perform the same set of "erroneous" and correct frequency sweeps on 13-4.NEC and 13-4-1.NEC, the mid-element-loaded Yagi alternately set up with type 4 and type 0 series loads. Be sure to use 26.4 Ω or 26.5 Ω as the VSWR reference impedance. You should see a very similar set of curves to those just developed. Since model 13-5.NEC, the full size Yagi, is available for comparison, perform a frequency sweep on it as well, using 33.0 Ω as the VSWR reference value. Note the comparatively wider operating bandwidth for the full size Yagi compared to either of the loaded versions. For more exacting curves, you may wish to decrease the frequency sweep step to 0.2 MHz or even to 0.1 MHz for all of the models. Overlaid graphs of the results are especially useful visual cues to the different performance results for the three antennas.

```

CM Mid-element loaded yagi: 28.5 MHz
CE
GW 1 31 -5.8 0 0 5.8 0 0 .04165
GW 2 31 -6.08 -4.25 0 6.08 -4.25 0 .04165
GS 0 0 .3048
GE 0
EX 0 1 16 0 1 0
LD 0 1 8 8 .72 .000001206 0
LD 0 1 24 24 .72 .000001206 0
LD 0 2 8 8 .73 .000001217 0
LD 0 2 24 24 .73 .000001217 0
LD 5 1 1 31 2.4938E7
LD 5 2 1 31 2.4938E7
FR 0 1 0 0 28.5 0
RP 0 1 360 1000 90 0 1 1
EN

```

13-4-1

As a supplementary exercise, you may convert the type 4 load used with 13-2.NEC, the dipole for 14.175 MHz, to a type 0 load and run an appropriate frequency sweep from 14.0 to 14.35 MHz in either 0.07 or 0.05 MHz steps.

To these notes on type 0 series R-L-C loads, we must add a word of caution. Do NOT convert the reactance values for open or shorted transmission line stubs used as reactive loads into type 0 loads. The rate of change of reactance with frequency differs between transmission line stubs and standard inductive and capacitive components. We shall note a method for directly handling transmission line stubs used as loads in the next chapter.

13-6.NEC: An extended double Zepp for 7.15 MHz

13-7.NEC: A Severns modified extended double Zepp for 7.15 MHz

The use of series inductive loads in antenna structures is perhaps the most common form of loading, since--at least in the LF to HF range--major design efforts have gone into creating smaller antenna structures with performance that most closely approximated the performance of a full size antenna. However, series capacitive loading also has a variety of functions. (Note: a "capacity-hat" is not a capacitive load in the sense that a capacitor or an open-ended transmission line stub may be a substitute for it. Capacity hats should always be modeled as physical structures.)

Not all uses of loading are designed to either electrically lengthen or shorten a physical

structure. In some cases, inductive or capacitive reactance may be used to alter current magnitude and phase along an antenna element in order to achieve some specified goal. To sample this particular use of reactive loading, we shall consider two versions of the extended double Zepp antenna.

Consider model 13-6.NEC, a standard #12 AWG copper wire extended double Zepp for 7.15 MHz. The antenna is 51.8 m long, about 1.25λ . The length is not critical, since the antenna is nonresonant by design. Instead, it is designed to achieve the highest gain possible in a single-wire bidirectional antenna. As the antenna is further lengthened to 1.5λ and beyond, the 2 major lobes break up into several lobes, both major and minor.

```

CM Extended double Zepp: 7.15 MHz
CE
GW 1 31 -25.9 0 25 25.9 0 25 .000814
GS 0 0 1
GE 1
GN 0 0 0 0 13 .005
EX 0 1 16 0 1 0
LD 5 1 1 31 5.8001E7
FR 0 1 0 0 7.15 0
RP 0 181 1 1000 -90 90 1 1
FR 0 1 0 0 7.15 0
RP 0 1 360 1000 67 0 1 1
EN
    
```

This particular model is set at a height of 25 m. Run the model and verify from the elevation pattern that the corresponding azimuth pattern uses the correct take-off angle. Then examine the azimuth pattern, noting especially the maximum bi-directional gain, the -3 dB beamwidth, and the gain of the secondary lobes. Also check the source impedance of the antenna. Record your data in the table below.

13-6 & 13-7		Test Data		
Antenna	Gain dBi	-3 dB Beamwidth	2ndary lobe Gain dBi	Source Z $R \pm jX \Omega$
Standard EDZ				
Severns EDZ				

```

CM Extended double Zepp: 7.15 MHz
CM Capacitive loading
CE
GW 1 12 -25.9 0 25 -7.62 0 25 .000814
GW 2 7 -7.62 0 25 7.62 0 25 .000814
GW 3 12 7.62 0 25 25.9 0 25 .000814
GS 0 0 1
GE 1
GN 0 0 0 0 13 .005
EX 0 2 4 0 1 0
LD 0 1 12 12 0 0 .0000000000091
LD 0 3 1 1 0 0 .0000000000091
LD 5 1 1 12 5.8001E7
LD 5 2 1 7 5.8001E7
LD 5 3 1 12 5.8001E7
FR 0 1 0 0 7.15 0
RP 0 181 1 1000 -90 90 1 1
FR 0 1 0 0 7.15 0
RP 0 1 360 1000 67 0 1 1
EN

```

13-7

Dr. Rudy Severns developed a modification for the standard EDZ to change two elements of the antenna's performance while retaining both its gain and physical length. He introduced a capacitor on each side of the center source point using an experimentally determined value (9.1 pF) and position. The results appear in model 13-7.NEC. Note the division of the physical wire into 3 model wires so that the capacitors may be placed more precisely. Also note that the type 0 load cards set the inductance as zero, since it is "missing," and the resistance at zero, since capacitor Q is not an issue at the antenna operating frequency of 7.15 MHz. Otherwise, the antenna is the same as 13-6.NEC.

Run the model and record the values for maximum gain, beamwidth, minor lobe gain, and source impedance in the table above.

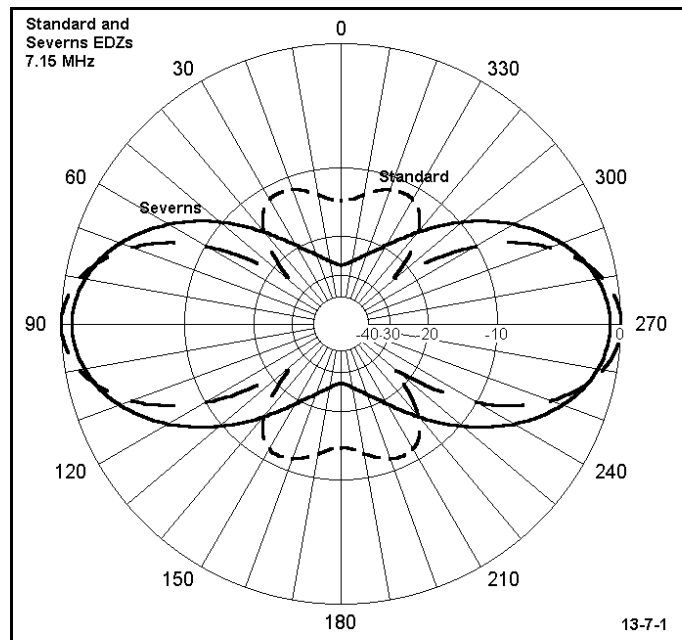
13-6 & 13-7		Reference Data		
Antenna	Gain dBi	-3 dB Beamwidth	2ndary lobe Gain dBi	Source Z $R \pm jX \Omega$
Standard EDZ	10.92	36°	-0.31	176.5 - j 1071
Severns EDZ	10.24	46°	-----	216.6 + j 11

Comments: The tabular data makes clear that the 9.1 pF "loading" capacitors have changed the antenna performance specification. The antenna has suffered a very small loss of gain but has increased its beam width. There are no minor lobes in the Severns antenna, and the source impedance is nearly resistive with a value that permits a match to coaxial cable via a 4:1 impedance matching device (a balun transformer).

The pattern differential between the standard and loaded EDZ shows up most clearly in a comparative azimuth pattern graphic such as **Figure 13-7-1**.

The graphic emphasizes the advantages of eliminating the minor lobes in terms of highly increased front-to-side rejection.

You should examine closely the currents at corresponding positions along the two versions of the EDZ antenna in order to better grasp the alterations created by the addition of the capacitors. In addition, do a frequency sweep of the modified EDZ from 7.0 to 7.3 MHz at 0.05 MHz intervals to determine if both the pattern and the source impedance remain adequate across the 40-meter amateur band.



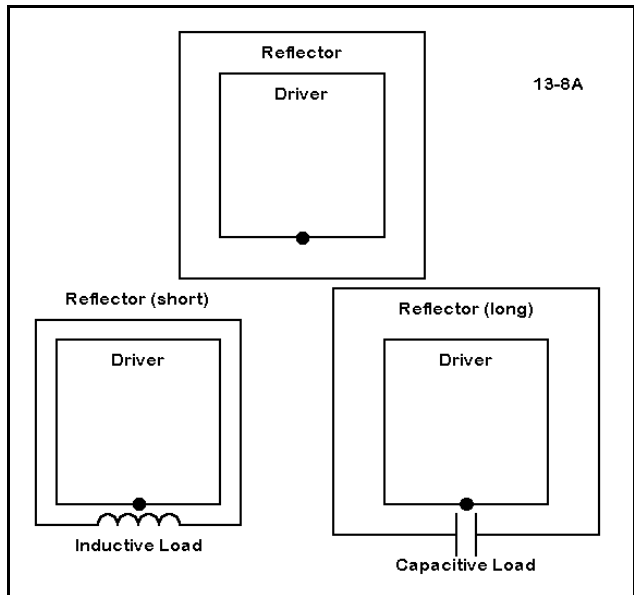
13-8.NEC: Three versions of a 2-element quad beam for 21.22 MHz

In this exercise, we shall use type 0 loads to adjust the performance of 2 variations of a standard 2-element quad beam for 21.22 MHz. Each quad consists of #14 AWG copper wire, with all dimensions in meters. The basic model, 13-8.NEC, has each element optimized for a combination of free space gain (>7.0 dBi) and 180° front-to-back ratio (>20 dB), with a resonant source impedance close to 100 Ω (which provides an easy match to a 50-Ω coaxial cable feedline through a 1/4λ matching section of 75-Ω cable). You may verify the antenna properties by running the model. Indeed a frequency sweep from 21.0 to 21.45 MHz in 0.09 MHz steps will be instructive.

You should note both the change of azimuth pattern across the swept frequencies, as well as the VSWR with a 100-Ω reference value. Every HF antenna design is essentially a compromise that will involve these parameters.

```

CM 2e1 Quad: 21.22 MHz
CM Standard version
CE
SW 1 11 -1.7739 0 -1.7739 1.77394 0 -1.7739 .000814
SW 2 11 1.77394 0 -1.7739 1.77394 0 1.77394 .000814
SW 3 11 1.77394 0 1.77394 -1.7739 0 1.77394 .000814
SW 4 11 -1.7739 0 1.77394 -1.7739 0 -1.7739 .000814
SW 5 11 -1.8684 -1.766 -1.8684 1.86842 -1.766 -1.8684 .000814
SW 6 11 1.86842 -1.766 -1.8684 1.86842 -1.766 1.86842 .000814
SW 7 11 1.86842 -1.766 1.86842 -1.8684 -1.766 1.86842 .000814
SW 8 11 -1.8684 -1.766 1.86842 -1.8684 -1.766 -1.8684 .000814
SS 0 0 1
GE 0
EX 0 1 6 0 1 0
LD 5 1 1 11 5.8001E7
LD 5 2 1 11 5.8001E7
LD 5 3 1 11 5.8001E7
LD 5 4 1 11 5.8001E7
LD 5 5 1 11 5.8001E7
LD 5 6 1 11 5.8001E7
LD 5 7 1 11 5.8001E7
LD 5 8 1 11 5.8001E7
FR 0 6 0 0 21 .09
RP 0 1 360 1000 90 0 1 1
EN
    
```



Our task, however, only uses the basic quad as a reference. In **Figure 13-8A**, we see two variants of the design, one with the reflector shortened, the other with the reflector lengthened. Use models 13-8-1.NEC and 13-8-2.NEC to determine the new reflector lengths. Then set up a design procedure to determine the type and degree of loading to return these variants to as close to the design specifications as possible.

Finally, perform a frequency sweep of the finished quad and compare it with the results you obtained for the unloaded reference quad. Record the three sets of swept VSWR values in the table at the bottom of this page.

13-8	Test Data					VSWR
Antenna	21.0	21.09	21.18	21.27	21.35	21.45
13-8						
13-8-1						
13-8-2						

Comments: As you develop the project, you may begin the loading by using type 0 loads, with pure guesses about the amount of inductance and capacitance the loading may require. However, beginning with a type 4 load and using reactance values may be quicker. The short reflector will require lengthening or inductive reactance. Since the shortening is small, you can use a few tens of Ohms and then zero in on the best value to

replicate the unloaded quad. The unloaded quad has a gain of 7.18 dBi with a 180° front-to-back ratio of 23.18 dB and a source impedance of 98.9 Ω resistive.

With an inductive load reactance of 56 Ω , the quad returns a gain of 7.19 dBi, a front-to-back ratio of 22.60 dB, and a source impedance of 96.3 Ω resistive. In contrast, the long reflector required less reactive loading, since it was lengthened less from the unloaded value. A capacitive reactance load of -31 Ω returns values of 7.19 dBi for the gain, 23.20 dB for the front-to-back ratio, and 99.7 Ω resistive for the source impedance. Note that amount of required reactive loading is crudely proportional to the amount of shortening and lengthening involved.

Before you can run accurate frequency sweeps for these two "optimized" quads, you must convert the reactive loads into appropriate values of inductance and capacitance at the design frequency of 21.22 MHz. The results are 0.42 μ H and 242 pF, respectively. You may reasonably ask yourself how fast you might have arrived at these values had you begun with type 0 loads, which you will now use to replace the type 4 complex impedance loads. For the moment, let the value of resistance in both cases remain at zero.

```

CM 2el Quad: 21.22 MHz
CM Inductively loaded
CE
GW 1 11 -1.7739 0 -1.7739 1.77394 0 -1.7739 .000814
GW 2 11 1.77394 0 -1.7739 1.77394 0 1.77394 .000814
GW 3 11 1.77394 0 1.77394 -1.7739 0 1.77394 .000814
GW 4 11 -1.7739 0 1.77394 -1.7739 0 -1.7739 .000814
GW 5 11 -1.8288 -1.766 -1.8288 1.8288 -1.766 -1.8288 .000814
GW 6 11 1.8288 -1.766 -1.8288 1.8288 -1.766 1.8288 .000814
GW 7 11 1.8288 -1.766 1.8288 -1.8288 -1.766 1.8288 .000814
GW 8 11 -1.8288 -1.766 1.8288 -1.8288 -1.766 -1.8288 .000814
GS 0 0 1
SE 0
EX 0 1 6 0 1 0
LD 0 5 6 6 0 .00000042 0
LD 5 1 1 11 5.8001E7
LD 5 2 1 11 5.8001E7
LD 5 3 1 11 5.8001E7
LD 5 4 1 11 5.8001E7
LD 5 5 1 11 5.8001E7
LD 5 6 1 11 5.8001E7
LD 5 7 1 11 5.8001E7
LD 5 8 1 11 5.8001E7
FR 0 6 0 0 21 .09
RP 0 1 360 1000 90 0 1 1
EN

```

13-8-1

```

CM 2el Quad: 21.22 MHz
CM Capacitively loaded
CE
GW 1 11 -1.7739 0 -1.7739 1.77394 0 -1.7739 .000814
GW 2 11 1.77394 0 -1.7739 1.77394 0 1.77394 .000814
GW 3 11 1.77394 0 1.77394 -1.7739 0 1.77394 .000814
GW 4 11 -1.7739 0 1.77394 -1.7739 0 -1.7739 .000814
GW 5 11 -1.8897 -1.766 -1.8897 1.88976 -1.766 -1.8897 .000814
GW 6 11 1.88976 -1.766 -1.8897 1.88976 -1.766 1.88976 .000814
GW 7 11 1.88976 -1.766 1.88976 -1.8897 -1.766 1.88976 .000814
GW 8 11 -1.8897 -1.766 1.88976 -1.8897 -1.766 -1.8897 .000814
GS 0 0 1
SE 0
EX 0 1 6 0 1 0
LD 0 5 6 6 0 0 .000000000242
LD 5 1 1 11 5.8001E7
LD 5 2 1 11 5.8001E7
LD 5 3 1 11 5.8001E7
LD 5 4 1 11 5.8001E7
LD 5 5 1 11 5.8001E7
LD 5 6 1 11 5.8001E7
LD 5 7 1 11 5.8001E7
LD 5 8 1 11 5.8001E7
FR 0 6 0 0 21 .09
RP 0 1 360 1000 90 0 1 1
EN

```

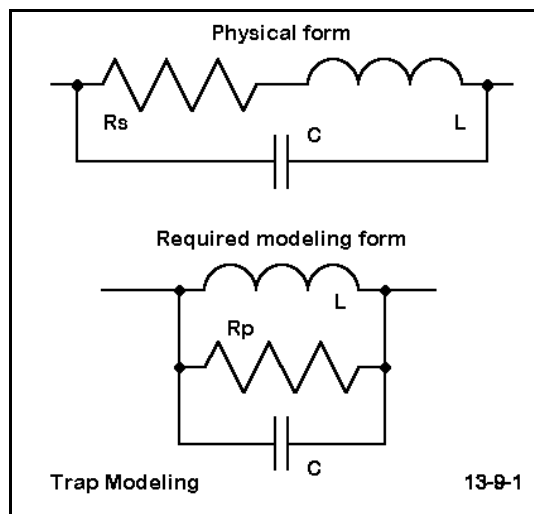
13-8-2

13-8	Ref. Data					VSWR
Antenna	21.0	21.09	21.18	21.27	21.35	21.45
13-8	1.79	1.36	1.09	1.10	1.27	1.42
13-8-1	1.90	1.42	1.12	1.10	1.27	1.42
13-8-2	1.77	1.35	1.08	1.10	1.27	1.42

The models in 13-8-1.NEC and 13-8-2.NEC, despite differences in source impedance that have a minor effect on the SWR values, show some real trends as well. The more rapid change of resistance and reactance, especially visible below the design frequency, is real, typical, and would be further evident had we included a finite Q for the inductive loading component. The slightly broadening of response in the case of capacitive loading is also real and typical, even though the amount in this case is too small to be of practical relevance. As important as these effects is the flattening of the quad SWR curve above the design frequency. To arrive at a smooth SWR curve with roughly equal values at both ends of the swept frequency range, one might move the driver resonance point lower without adversely affecting either the gain or the front-to-back ratio.

13-9.NEC: A trap dipole for 14.175 and 28.5 MHz

A trap antenna element is one designed to operate on two frequencies. At the upper frequency, a parallel tuned circuit--ordinarily tuned to somewhat below the operating frequency--electrically terminates the element so that between traps on a dipole element the length is resonant at the desired frequency. On the lower frequency, the trap has an inductive reactance equal to that of the inductive and capacitive components in parallel (which is not the reactance of the coil alone). The inductance physically shortens the length of antenna needed for resonance at the lower frequency.



Modeling traps is a primary use of parallel R-L-C loads (type 1) in HF antennas. We shall only sample the procedure here, since traps involve some special treatment that would distract us from mastering the art of creating and inserting loads into antenna structures.

The chief caution to observe in modeling traps is to account properly for the trap Q, which is almost exclusively a function of the trap coil. As shown in **Figure 13-9-1**, the coil Q is a function of a series resistance and reactance. We must convert the series resistance and reactance in the inductor into their parallel equivalents. We

perform such conversions using the standard equations for series and parallel values of resistance and reactance:

$$R_P = \frac{R_S^2 + X_S^2}{R_S} \quad X_P = \frac{R_S^2 + X_S^2}{X_S} \quad 3$$

and

$$R_S = \frac{R_P X_P^2}{R_P^2 + X_P^2} \quad X_S = \frac{R_P^2 X_P}{R_P^2 + X_P^2} \quad 4$$

where R_S and X_S as series values of resistance and reactance, and R_P and X_P are parallel values of resistance and reactance.

Let us create a trap that is self-resonant at 27.76 MHz, consisting of a 1.2 μH coil and a 27.4 pF capacitor. The coil has a Q of about 200. At the trap frequency, the coil reactance is about 209.3 Ω , for a series resistance of about 1.02 Ω . The parallel equivalents are 42960 Ω resistance and 209.3 Ω reactance. These will count as the components of the parallel tuned load for each side of the dipole at points 8.18' from the feedpoint. These are the values used in model 13-9-10.NEC, the 28.5 version of the model.

```
CM 20-10 m trap dipole
CM 28.5 MHz
CE
GW 1 12 -14.59 0 0 -8.18 0 0 .02085
GW 2 31 -8.18 0 0 8.18 0 0 .02085
GW 3 12 8.18 0 0 14.59 0 0 .02085
GS 0 0 .3048
GE 0
EX 0 2 16 0 1.414214 0
LD 1 2 1 1 42960 .0000012 .0000000000274
LD 1 2 31 31 42960 .0000012 .0000000000274
LD 5 1 1 12 2.4938E7
LD 5 2 1 31 2.4938E7
LD 5 3 1 12 2.4938E7
FR 0 1 0 0 28.5 0
RP 0 1 360 1000 90 0 1 1
EN
```

13-9-10

```
CM 10-20 m trap dipole
CM 14.175 MHz
CE
GW 1 12 -14.59 0 0 -8.18 0 0 .02085
GW 2 31 -8.18 0 0 8.18 0 0 .02085
GW 3 12 8.18 0 0 14.59 0 0 .02085
GS 0 0 .3048
GE 0
EX 0 2 16 0 1.414214 0
LD 1 2 1 1 21360 .0000012 .0000000000274
LD 1 2 31 31 21360 .0000012 .0000000000274
LD 5 1 1 12 2.4938E7
LD 5 2 1 31 2.4938E7
LD 5 3 1 12 2.4938E7
FR 0 1 0 0 14.175 0
RP 0 1 360 1000 90 0 1 1
EN
```

13-9-20

At 14.175 MHz, the net reactance of the two components is 147.5 Ω inductive reactance. Converted with the given series resistance, the parallel resistance becomes about 21360 Ω to go with the 1.2 μH inductance and the 27.4 pF capacitance. Model 13-9-20.NEC presents the 14.175 MHz version of the model. Careful examination shows that the only difference between it and the 10-meter version is the value of the parallel-equivalent resistor. All other dimensions and parameters remain the same in both models.

Run both models and obtain values for maximum gain and source impedance.

Comments: The gain values for the two models are only about 0.1 dB apart (1.97 dBi vs. 2.08 dBi), a desired condition for trap-loaded elements. The resonant source impedance

at 14.175 MHz is about 63Ω , partly a function of element shortening and inductive loading. At 28.5 MHz, the resonant source impedance is about 86Ω , partly the result of tuning the trap below the operating frequency. The element is slightly long and capacitively loaded to resonance.

A full treatment of practices and procedures for designing trap-loaded elements requires considerable external study. This example has used a 2:1 frequency ratio. Frequency ratios above 3:1 present problems of pattern shape distortion, since the outer portions are long enough at the higher frequency to count as collinear elements approaching, reaching, or passing self-resonance. We have simply positioned the traps at the end of the inner, higher frequency element to include them in that element length, and the segmentation has been arbitrarily set. As well, we have overlooked questions of trap Q at both frequencies of operation. In this example, the trap exhibits a Q of about 150 at both 28.5 and 14.175 MHz. Other design questions can be generated, for example, the use of multiple traps in a single element (say, for 20, 15, and 10 meters).

Historically, trap design has been based largely on experimentation and simplified calculations. Modeling traps as parallel R-L-C loads offers a fertile field of investigation to refine our understanding of their operation.

Summing Up

Reactive loads comprise an array of important tools in antenna design. We have not done justice to the topic of reactive loading as it applies to antenna theory and development, but we have surveyed reasonably well how to model reactive loads. As we have noted along the way, when to use a particular method is as significant a decision as which method to use in the first place.

Complex impedance loads consisting of series resistances and reactances provide a means for faster development at specific frequencies. Often, one can easily estimate a needed reactance value and calculate an accompanying resistance value from considerations of component Q. Beginning with inductance or capacitance (or both) is normally a slower more tedious process, one that requires conversion into reactance to determine associated resistance values from Q. Unless dictated by other factors, such as a set of known load component values, design and analysis often begins with type 4 loads.

All such loads must be converted to type 0 or type 1 loads if modeling is to be accurate over a range of frequencies. Since data for frequencies even at small distances from the design frequency is crucial to a full understanding of an antenna's performance characteristics, series and parallel R-L-C loads will play an inevitable role in careful modeling.

As we saw at the beginning of this extensive series of exercises, modeling also has much to teach us about the behavior of loaded elements. Although we left nearly as many questions unanswered as answered, the methods and maneuvers encountered along the way should provide a foundation for developing a more complete data set.

14. Transmission Lines

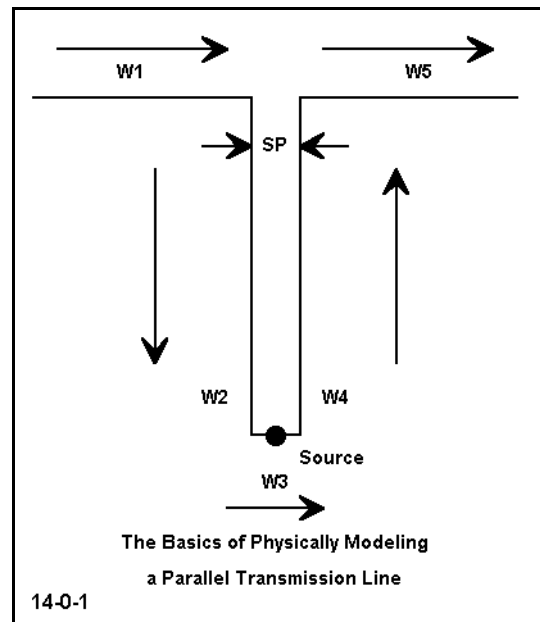
Objectives: *The final major ingredient that we shall explore is NEC-2's transmission line function. In addition to developing an understanding of how to implement transmission lines within the program, we shall also look at ways of modeling some of the major applications of transmission lines in various antenna configurations.*

Although coaxial cables are impractical to model physically within NEC-2, we may in fact physically model parallel transmission lines in a straightforward manner. **Figure 14-0-1** shows the basic layout for such a model. For greatest accuracy with respect to selecting a characteristic impedance, the test procedure used in Chapter 12 should precede the use of the line in a model. Moreover, the wire diameter of the antenna and of the transmission line should be the same size to avoid NEC-2 inaccuracies resulting from the angular junction of wires having dissimilar diameters.

NEC-2 offers an alternative means of modeling transmission lines of any type, the TL input card.

In selecting this option, you should be aware of its limitations as well as opportunities. First, the transmission lines created via the TL input are mathematical only. Therefore, they do not interact with near or far field patterns. Hence, a TL-type transmission line will not show any radiation. A separate wire must be physically modeled (that is, be a part of the GW inputs) to show such radiation. Second, NEC-2 transmission lines are lossless. If you need to know the affects on the source impedance of losses in a real line, you will have to calculate them separately, perhaps via one of a number of available utility programs. Third, TL entries are accurate only if conditions are balanced.

In exchange for these limitations, the TL input permits you to place one or more transmission lines anywhere within the model. The line may have any characteristic



impedance (Z_0) and any velocity factor (VF). In fact, NEC-2 itself does not recognize the VF. The input portion of your program may accept these figures and precalculate the electrical length of the line, or you may have to precalculate the electrical length of the line by dividing the physical length by the VF.) The modeled transmission lines do not add to the total wire and segment count, which will permit faster core runs and larger (or more finely detailed) antenna structures within the programmed limit of segments.

Every transmission line appears in series with the wire segment on which it appears, and also with any loads on that segment. However, it appears in parallel with any sources on the segment. Multiple transmission lines on the same segment appear in parallel with each other. Every transmission line must run between two wires. For transmission lines run to sources only, rather than to other antenna elements, we may create a very short, thin wire anywhere—even a 100λ away from the antenna structure. This move places the source segment well away from any possible significant interaction with the primary elements of the antenna structure. The transmission line will have a length that is specified in the TL input.

The complete TL entry looks like this:

TL	1	8	2	1	50	10.6	0	0	0	0
	(1)	(2)	(3)	(4)	(5)	(6)	(7)	(8)	(9)	(10)

Entries (1) and (2) specify the wire number and segment of one end of the transmission line, while (3) and (4) specify the corresponding data for end 2. Entry (5) provides the Z_0 of the line, while (6) gives the length of the line in meters. (Automated entry conversion for wire lengths may not also automatically convert transmission lines lengths in units other than meters, so you should precalculate the line length in meters as part of your conversion to electrical length of the physical line and its associated velocity factor.) If the length entry (6) is zero, then NEC-2 uses the actual distance between the two wire/segment combinations as the length of the line. Entry pairs (7) and (8), and (9) and (10), permit the specification of values for shunt admittance (in terms of real and imaginary values, that is, as conductance and susceptance) at ends 1 and 2 of the line respectively. For ordinary transmission lines, these values are zero. However, we shall use this facility for end 2 in creating open and shorted transmission line stubs.

Figure 14-0-2 provides a view of the transmission-line entry screen you may call up to create the TL entry. Although the label shows no transmission lines defined, you can see the line above in the process of creation. All of the entries show a straightforward correlation to the sample TL line with the possible exception of the "phase reversal" options. For straight lines, no phase reversal is selected. Some lines may call for a half twist to effect a phase reversal, and this, in turn, requires selection of the phase reversal option. The only difference you will see in the TL line under phase reversal is that the Z_0 of the line will be entered as a negative number.

The screenshot shows a dialog box titled "Transmission Lines" with a sub-tab "Options" and a label "14-0-2". The main title is "Transmission Line #1 of 1".

Under "Place Transmission Line", there are two columns: "From" and "To:".

- From:** Wire #: 1, Segment #: 8
- To:** Wire #: 2, Segment #: 1

Under "Shunt Admittance", there are two rows: "End One" and "End Two". Each row has two input fields: "Real" and "Imaginary", both with units "mhos".

- End One: Real: 0, Imaginary: 0
- End Two: Real: 0, Imaginary: 0

Under "Transmission Line Type", there are two radio button options:

- No Phase Reversal
- 180° Phase Reversal

At the bottom, there are four buttons: "Previous", "OK", "Cancel", and "Next".

Additional fields at the bottom left:

- Characteristic Impedance (ohms): 50
- Electrical Length (m): 10.6

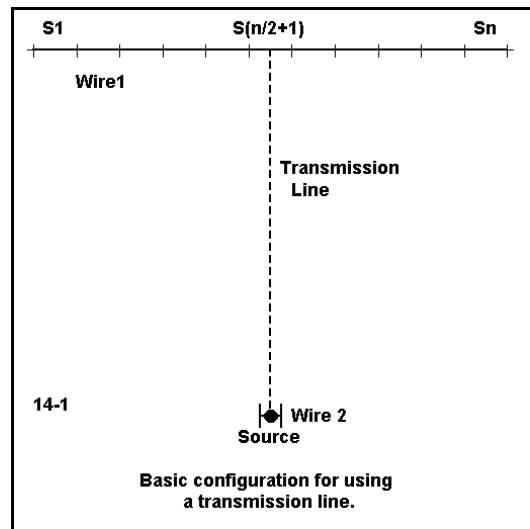
Exercise Preparation

The exercises which follow attempt to expose you to enough antenna modeling transmission line applications to make the process thoroughly natural. Most of them involve either progressions of model variation or of additions to the base model, with only a few check models along the way with which to compare your work. Nonetheless, you should use standard care in saving variants so as not to overwrite the basic and check models unless that is your intention.

Because our focus is on transmission lines, the actual antenna structures will be rather simple. However, the transmission lines can take on a certain complexity of their own as we embellish the base models.

14-1.NEC: A dipole for 21 MHz fed with a transmission line to the source

Figure 14-1 shows perhaps the most fundamental use of a transmission line: to connect a remote source to the antenna. In many cases, adding wire 2 to the model, along with the transmission line that connects the two wires together, is unnecessary. However, the step can be useful in investigating the behavior of resistance and reactance at the antenna wire source at various distances from the antenna wire. Moreover, it is a simple matter to change the characteristics of the transmission line by altering the TL entry.



```

CM Dipole: 21 MHz
CE
GW 1 21 -3.418 0 15 3.418 0 15 .000814
GS 0 0 1
GE 1
GN 2 0 0 0 13 .005 0 0 0 0
EX 0 1 11 0 1 0
LD 5 1 1 21 5.8001E7
FR 0 4 0 0 21 .15
RP 0 181 1 1000 -90 90 1 1
EN

```

14-1

So let's begin by exploring the changes in resistance and reactance at the antenna source of a simple #14 AWG copper wire dipole for 21.0 to 21.45 MHz at a height of 15 meters over average (S-N) ground. Note that the frequency

entry calls for a 4-point sweep of the frequencies between the limits at 0.15 MHz intervals. Record both the source impedance and the VSWR relative to 50- Ω and 75- Ω transmission lines in the table below. Note that the table has places for the next step in the process--the addition of a wire and a transmission line between the dipole and the new short segment.

The check model 14-1-1.NEC contains one version of the 6 we shall create. The listed Z_0 of the line is 75 Ω , but we shall also run the model with a 50- Ω line. The listed line length is 15 meters. However, we shall make subsequent runs (with both lines) using lengths of 20 meters and 25 meters. In this exercise, we shall simply assume that the velocity factor (VF) of the lines is 1.0, making their physical and electrical lengths identical. However, you may wish to multiply these lengths by VFs of 0.66 and 0.78 to see what physical lengths correspond to the listed electrical lengths, using values common for solid and foam dielectric coaxial cables.

```

CM Dipole--xmsn line: 21 MHz
CE
GW 1 21 -3.418 0 15 3.418 0 15 .000814
GW 2 1 -.1 0 5 .1 0 5 .000814
GS 0 0 1
GE 1
GN 2 0 0 0 13 .005 0 0 0 0
EX 0 2 1 0 1 0
LD 5 1 1 21 5.8001E7
LD 5 2 1 1 5.8001E7
TL 1 11 2 1 75 15 0 0 0 0
FR 0 4 0 0 21 .15
RP 0 181 1 1000 89 90 -1 1
EN

```

14-1-1

14-1		Test Data			
Line Length	Z_0	21.0 MHz $R \pm jX \ \Omega$ VSWR	21.15 MHz $R \pm jX \ \Omega$ VSWR	21.3 MHz $R \pm jX \ \Omega$ VSWR	21.45 MHz $R \pm jX \ \Omega$ VSWR
No line	50 Ω				
	75 Ω				
15 m line	50 Ω				
	75 Ω				
20 m line	50 Ω				
	75 Ω				
25 m line	50 Ω				
	75 Ω				

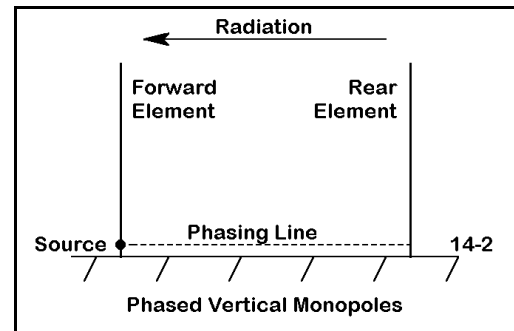
Comments: The pattern of VSWR for each cable should not be surprising. Despite changes in the resistance and reactance values along the transmission line, the 50- Ω and the 75- Ω VSWR values remain the same. (Numerical values may show a 1-digit change in the last recorded decimal place due to rounding conditions within any program.) Since the reflection coefficient does not change and since the transmission line is lossless, the SWR will be the same everywhere along any length of line you use.

14-1		Reference Data			
Line Length	Z_o	21.0 MHz $R \pm jX \ \Omega$ VSWR	21.15 MHz $R \pm jX \ \Omega$ VSWR	21.3 MHz $R \pm jX \ \Omega$ VSWR	21.45 MHz $R \pm jX \ \Omega$ VSWR
No line	50 Ω	66.3 - j 20.2 1.56	62.4 - j 9.7 1.41	68.7 + j 0.9 1.37	70.0 + j 11.5 1.47
	75 Ω	66.3 - j 20.2 1.36	62.4 - j 9.7 1.19	68.7 + j 0.9 1.09	70.0 + j 11.5 1.19
15 m line	50 Ω	49.7 - j 22.6 1.57	54.4 - j 17.5 1.41	60.7 - j 14.0 1.38	68.8 - j 13.1 1.47
	75 Ω	57.8 - j 11.4 1.37	63.4 - j 2.8 1.19	71.2 + j 5.0 1.09	81.7 + j 11.6 1.19
20 m line	50 Ω	71.4 + j 16.3 1.56	63.2 + j 15.9 1.41	56.5 + j 15.6 1.37	51.8 + j 19.6 1.19
	75 Ω	95.2 - j 17.2 1.37	80.7 - j 12.4 1.19	70.5 - j 4.9 1.10	63.7 + j 3.8 1.19
25 m line	50 Ω	36.7 + j 10.7 1.56	37.1 + j 7.2 1.41	36.8 + j 3.3 1.37	34.0 + j 0.7 1.47
	75 Ω	78.2 + j 23.5 1.36	83.9 + j 10.1 1.19	81.1 - j 3.6 1.09	71.9 - j 12.6 1.19

Examine also the pattern of impedance values either in your chart or the reference table. Note the regularity of the changes as the line length increases. You may wish to relate these values to standard equations for calculating the impedance on a transmission line at any distance from a specified load on the line. Numerous utility programs exist for making such calculations. One such program for lossless lines exists in the collection of utilities written in GW BASIC and available under the name HAMCALC from George Murphy, 77 McKenzie Street, Orillia, ON L3V 6A6, Canada for a small donation to cover the costs of disk and mailing (\$5 US). You may chart at 5° (electrical) the changes in resistance and reactance (along with voltage and current magnitude and phase) along any length of line. Another program that will take into account line losses is TL, available with some American Radio Relay League publications.

14-2.NEC: Phased $1/4\lambda$ vertical monopoles for 7.1 MHz

Transmission lines are often used to create differentials of current magnitude and phase between two or more antenna elements. The purpose is to control one or more aspects of an antenna array's operating specifications, for example, gain, front-to-back ratio, or source impedance. **Figure 14-2** shows the general situation with a pair of vertical monopoles and a connecting transmission line, with the forward element serving as the array source. (The source need not be at the forward element, but may be at the rear element or between elements, depending upon design.) The connecting transmission line is often called a phasing line, although what is at stake is both the relative magnitude and phase of the current.



The connecting transmission line is often called a phasing line, although what is at stake is both the relative magnitude and phase of the current.

```

CM Phased 7.1 MHz verticals
CE
GW 1 25 0 0 0 0 0 33 .0625
GW 2 25 34.63 0 0 34.63 0 33 .0625
GS 0 0 .3048
GE 1
GN 1
EX 0 1 1 00 1 0
LD 5 1 1 25 2.4938E7
LD 5 2 1 25 2.4938E7
FR 0 1 0 0 7.1 0
RP 0 1 361 1000 89 0 1 1
EN
14-2

```

Let's begin our development of phased 1.25" diameter 6061-T6 aluminum vertical monopoles for 7.1 MHz with model 14-2.NEC. This model contains just the two monopoles (no phasing line), each 33' tall over perfect ground and spaced 34.63' apart. Feed only one of the verticals at its lowest segment above ground and check the forward gain, the 180° front-to-back ratio, and the source impedance of the array. In this condition, you will recognize that the rear element is parasitic relative to the forward element. Record

your check values in the table atop the next page.

Now create a transmission line to run between wire 1, segment 1 and wire 2, segment 1. Specify the line at -50Ω (indicating a phase reversal) and use a line length of 16.459 meters. (Note that the transmission line length is in meters, even though the antenna geometry dimensions were originally specified in feet. We shall momentarily work with this length value more extensively.) With this line in place, per check model 14-2-1.NEC, run the model and determine the forward gain, the 180° front-to-back ratio, and the source impedance. Record these values on the same table as you used for the values without the phasing line in place.

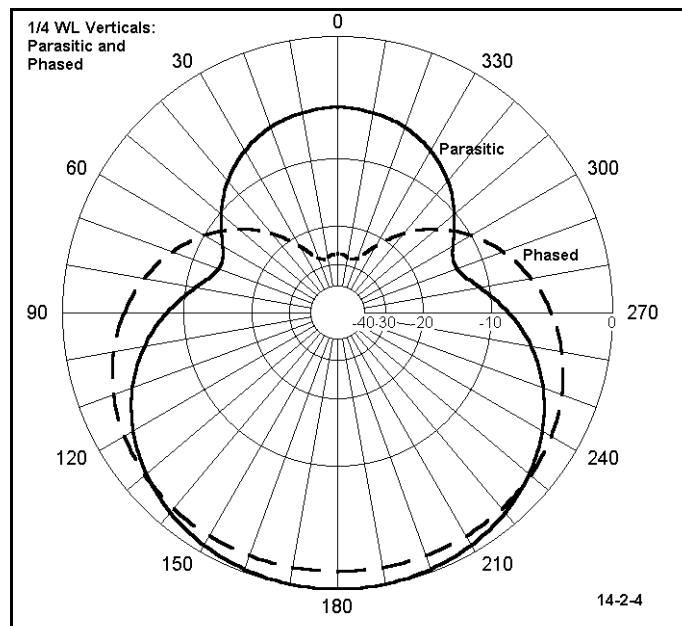
```

CM Phased 7.1 MHz verticals
CE
GW 1 25 0 0 0 0 0 33 .0625
GW 2 25 34.63 0 0 34.63 0 33 .0625
GS 0 0 .3048
GE 1
GN 1
EX 0 1 1 00 1 0
LD 5 1 1 25 2.4938E7
LD 5 2 1 25 2.4938E7
TL 1 1 2 1 -50 16.459 0 0 0 0
FR 0 1 0 0 7.1 0
RP 0 1 361 1000 89 0 1 1
EN
14-2-1

```

14.2 Test Data				
Antenna	Gain dBi	F-B dB	Source Z $R \pm j X \Omega$	50- Ω VSWR
No phase line				
Phase line				

Comments: Notice, first of all, the differences in both gain and front-to-back ratio between the parasitic and phased versions of this array. Gain has decreased by over 1 dB, while the front-to-back ratio has increased by over 25 dB. These figures reveal what tends to be one chief purpose in using phased rather than parasitic arrays: to maximize rejection from the rear. However, in more complex arrays, phasing lines may be used to control directivity in both the forward and rearward directions.



Examine also the azimuth patterns for the two versions of the array. Note the apparent broadening of the -3 dB beamwidth of the array. With a triangle of elements, one might provide directional reception or transmission over the 360° horizon in three zones.

14.2 Reference Data				
Antenna	Gain dBi	F-B dB	Source Z $R \pm j X \Omega$	50- Ω VSWR
No phase line	9.39	5.08	$31.1 + j 14.3$	1.81
Phase line	8.26	25.26	$38.6 - j 3.7$	1.31

However, we may wish to pose another question: Will a standard 50-Ohm coaxial cable with a common velocity factor of 0.66 serve as the phasing line for this array? (For this exercise, we shall ignore any problems of physical layout occasioned by the phase reversal in the line.) The required line is 14.46 m long, which translates into 0.39λ at 7.1

MHz, where a full wavelength is about 42.22 m. This is also 140.3 electrical degrees in length. Each of these figures may be useful in different types of calculations we may need from time to time. Hence, moving swiftly and easily from one way of measuring to another is a desirable skill.

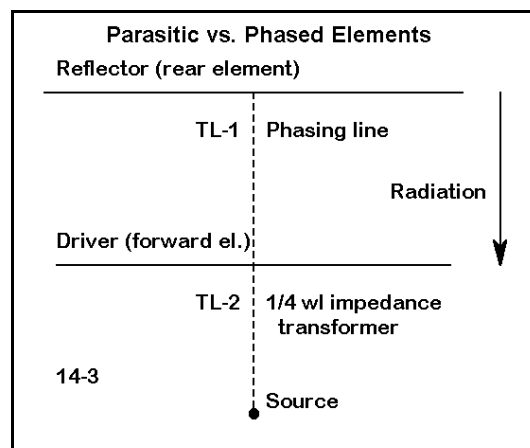
The antenna elements are given as 34.63' apart. The required line length translates to 54.0' at a velocity factor of 1.0. If we try a 0.66 VF line, the length is 35.64' or just about enough to reach between the two elements. (Examine the minimal slack value in this calculation and consider whether the line length would be adequate for elevated antennas at the same distance apart. Be sure to allow for line sag between the elements.) Had the line length been inadequate, one might have considered coaxial cable with a VF of 0.75 to 0.8, typical of lines using a foam dielectric.

As a supplementary exercise, develop the length of phasing line necessary to achieve the same results without a phase reversal. Once you have achieved this result, calculate the change in current magnitude and phase along this length of line. Also calculate the impedance at the connection point to the rear element. You may also use a technique we earlier explored (in Exercise 8-7) of using current sources for both elements without the transmission line between them. Adjust the current magnitude and phase on the rear element until you arrive at exactly the same gain and front-to-back ratio. Compare the relative magnitudes and phases of the two sets of source values .

Once you have collected all of the figures, compare the electrical length of the line with the phase of the rear element current relative to the phase of the forward element. Do the same for the element impedance when converted into a second source (reading the source impedance as a magnitude and phase rather than as a resistance and a reactance). You may also wish to compare the current magnitude and phase on the rear element of the model we called "parasitic."

14-3.NEC: Phased 2-element horizontal beam for 28.5 MHz

The horizontal beam in **Figure 14-4** represents a 3-stage exercise for us. The initial version of this 12 mm diameter 6061-T6 aluminum 2-element array in free space will begin as a Yagi, with only the forward element fed as a driver. Next, we shall add a phasing line between elements, followed in the final stage by the addition of an impedance matching section to permit connection of a 50- Ω transmission line to the transmitting and receiving equipment. At each stage of the development, we shall track the gain, 180° front-to-back ratio, source impedance and 50- Ω VSWR



to provide a record of the course of improvements in performance.

```

CM 2-element Yagi: 28.5 MHz
CE
GW 1 21 -2.44 0 0 2.44 0 0 .006
GW 2 21 -2.65 -1.46 0 2.65 -1.46 0 .006
GS 0 0 1
GE 0
EX 0 1 11 0 1.414214 0
LD 5 1 1 21 2.4938E7
LD 5 2 1 21 2.4938E7
FR 0 5 0 0 28 .25
RP 0 1 360 1000 90 0 1 1
EN

```

14-3

Model 14.3.NEC provides the information for the parasitic version of the beam. The 4.88 and 5.30 m elements, spaced 1.46 m apart provide typical 2-element driver-reflector Yagi performance. The elements are spaced to provide the user with the option of directly feeding the antenna with a 50- Ω coaxial cable or through a network for a more precise match to the transmission line. Note the frequency sweep from 28.0 to 29.0 MHz in 5 steps 0.25 MHz apart. All three

versions of the antenna will request an identical sweep.

The second version of the antenna (check model 14-3-1.NEC) requires that you add a 35- Ω 0.66 VF phasing line between the center of wire 1 and the center of wire 2 (segment 22 in each case). Specify a physical length of 1.47 m, which is an electrical length of 2.2273 m. Be sure to specify a phase reversal for the line. Rerun the frequency sweep for the antenna.

For stage 3 (14-3-2.NEC), add a short, thin wire, one-segment (3) at some distance from the antenna. From the present source position to the new wire, create a transmission line of 35 Ω (0.66 VF). Then move the source to wire 3. This transmission line will function as a $1/4\lambda$ impedance transformer to match the new lower impedance at the center of the forward element to a 50- Ω main feed line. Although a 1.736 m physical line is required for the design center frequency of 28.5 MHz, the electrical length will be 2.630 m. Run the frequency sweep from 28.0 through 29.0 MHz, recording the results in the table.

```

CM 2-element Yagi w/ phase &
CM matching lines: 28.5 MHz
CE
GW 1 21 -2.44 0 0 2.44 0 0 .006
GW 2 21 -2.65 -1.46 0 2.65 -1.46 0 .006
GW 3 1 -.05 0 -10 .05 0 -10 .0015
GS 0 0 1
GE 0
EX 0 3 1 0 1.414214 0
LD 5 1 1 21 2.4938E7
LD 5 2 1 21 2.4938E7
LD 5 3 1 1 2.4938E7
TL 1 11 2 11 -35.00 2.2273 0 0 0 0
TL 1 11 3 1 35 2.630303 0 0 0 0
FR 0 5 0 0 28 .25
RP 0 1 360 1000 90 0 1 1
EN

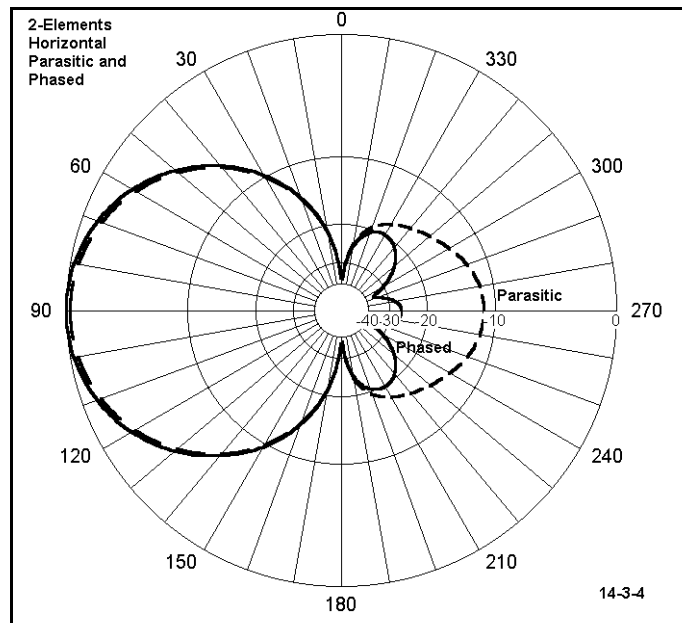
```

14-3-2

14-3		Test Data		
Model Frequency	Gain dBi	F-B dB	Source Z $R \pm j X \Omega$	50- Ω VSWR
14-3	28.00			
	28.25			
	28.50			
	28.75			
	29.00			

14-3 Continued		Test Data		
Model Frequency	Gain dBi	F-B dB	Source Z $R \pm j X \Omega$	50- Ω VSWR
14-3-1	28.00			
	28.25			
	28.50			
	28.75			
	29.00			
14-3-2	28.00			
	28.25			
	28.50			
	28.75			
	29.00			

Comments: Although the Yagi version of the beam is adequate for many purposes and is simpler in construction than the subsequent version, it lacks good front-to-back performance, and its direct match to a 50- Ω feed system is marginal at best. Adding the feedline between elements creates a version of a phased 2-element array variously called the ZL-Special or HB9CV. The phasing line provides a compromise setting of current magnitude and phase to the rear element--relative to the forward element--to achieve a balance between gain and rejection from the rear. As with the vertical array, pressing for a perfect rear null would have reduced the gain below the level obtained in the parasitic version. Achieving a deep rear null would also have required a phasing line not readily available.



The $1/4\lambda$ section of 35- Ω line from the forward element to the new source point raises the source impedance to a very reasonable match for the 50- Ω system feed line. Notice that the range of reactance change from one end of the frequency sweep to the other is much less for the phased and matched array than for the parasitic beam by a factor of about 3:1. Although less stable across the swept band of frequencies than the performance numbers for the Yagi model, the phased array averages about 0.25 greater gain and over 10 dB greater front-to-back ratio than the parasitic version. For this reason, some designers select the phased system on the grounds that the performance advantages outweigh the potential problems of greater system complexity.

Similar performance can also be obtained by using a 50- Ω phasing line. However, with this line, the position for the matching section is not at the forward element. Rather, it is at a point about 0.15 m (6") from the forward element toward the rear. As a supplemental exercise, create a pair of 50- Ω transmission lines to meet between elements. With a short forward section and a long rear section, achieve the best balance of performance. Then add the matching section of 35- Ω transmission line. Add short, thin 1-segment wires where necessary as terminations for the transmission lines.

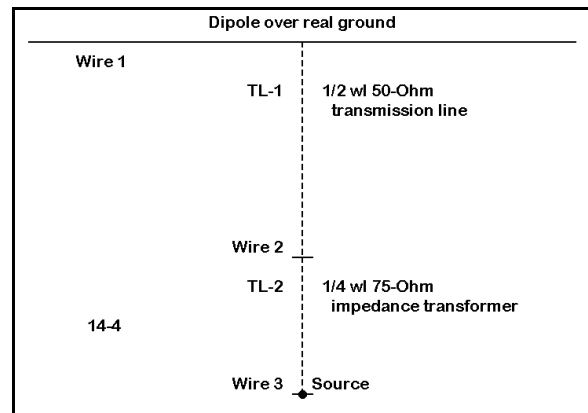
In addition, you may wish to try to create a maximum front-to-back ratio version of this antenna system, using a transmission line with whatever value of characteristic impedance the task calls for and not being concerned if such a line exists in reality. Such an exercise is often useful, since lines may be created from combination of existing lines

or specially fabricated for specified tasks. When you get as close to a perfect rear null as possible, frequency sweep the result to determine the range over which the null persists at a larger value than the front-to-back ratio of model 14-3-2.NEC.

14-3		Reference Data			
Model Frequency		Gain dBi	F-B dB	Source Z R ± j X Ω	50-Ω VSWR
14-3	28.00	6.61	10.18	30.3 - j 19.3	2.00
	28.25	6.38	10.93	35.1 - j 8.8	1.51
	28.50	6.16	11.06	39.8 + j 1.1	1.26
	28.75	5.96	10.78	44.2 + j 10.6	1.29
	29.00	5.78	10.31	48.4 + j 19.6	1.49
14-3-1	28.00	5.94	19.59	15.6 + j 2.8	3.21
	28.25	6.17	25.94	18.2 + j 3.4	2.77
	28.50	6.42	26.16	21.9 + j 3.5	2.30
	28.75	6.67	18.71	27.3 + j .1	1.83
	29.00	6.91	14.07	33.9 - j 3.6	1.49
14-3 Continued		Reference Data			
Model Frequency		Gain dBi	F-B dB	Source Z R ± j X Ω	50-Ω VSWR
14-3-2	28.00	5.93	19.57	77.3 - j 10.3	1.59
	28.25	6.17	25.94	65.7 - j 11.2	1.40
	28.50	6.42	26.15	54.5 - j 8.9	1.21
	28.75	6.67	18.71	44.4 - j 3.8	1.15
	29.00	6.91	14.07	36.0 + j 3.7	1.41

14-4.NEC: A broadband wire dipole for 7.0 to 7.3 MHz

Multiple series matching "sections" using commonly available transmission lines can effect a match from almost any antenna source impedance to almost any line. Dr. Frank A. Regier worked out the calculations necessary for precision systems. However, modeling experimentally can often turn up some useful results on its own. For example, consider **Figure 14-4**, a sketch of a #14 AWG copper wire dipole for 7.0 through 7.3 MHz set 15 m above average (S-N) ground. At this height, the source impedance would be above 72Ω by a significant amount, complicating a match to a $50\text{-}\Omega$ system feedline.



We shall develop a simple broadband matching system for this antenna in three steps, beginning with a 4-step frequency sweep of the antenna alone, looking at the source impedance and the $50\text{-}\Omega$ VSWR. Then we shall add a $1/2\lambda$ section of $50\text{-}\Omega$ transmission line. At center frequency (7.15 MHz), the impedance at both ends of the cable is the same. However, this is not true even small distances away from the center frequency. Finally, we shall add a $1/4\lambda$ section of $75\text{-}\Omega$ cable to see the results of the final step in the matching system.

```

CM 40 dipole 7.15MHz
CM w/ 1/2 wl 50-Ohm &
CM 1/4 wl 75-Ohm lines
CE
GW 1 25 -10.22 0 15 10.22 0 15 .000814
GW 2 1 -.1 0 5 .1 0 5 .000814
GW 3 1 -.1 0 2 .1 0 2 .000814
GS 0 0 1
GE 1
GN 2 0 0 0 13 .005 0 0 0 0
EX 0 3 1 0 1 0
LD 5 1 1 25 5.8001E7
LD 5 2 1 1 5.8001E7
LD 5 3 1 1 5.8001E7
TL 1 13 2 1 -50 20.96364 0 0 0 0
TL 2 1 3 1 75 10.48182 0 0 0 0
FR 0 4 0 0 7 .1
RP 0 181 1 1000 -90 90 1 1
EN

```

14-4-2

The model 14-4-2.NEC is shown to the right. From it, you can derive the description of the earlier stages, simply by deleting the appropriate transmission line and wire entries dependent upon them. Be certain that the source is correctly located for each stage of development. Record your results in the following table.

14-4					Test Data				
Model	7.0 MHz		7.1 MHz		7.2 MHz		7.3 MHz		
	$R \pm jX \ \Omega$	VSWR							
14-4.NEC									
14-4-1.NEC									
14-4-2.NEC									

Comments: There is, of course, no difference in the 50- Ω VSWR between the first two steps of the development. However, the resistive components of the impedance have risen, making the values better candidates for transformation to values closer to 50 Ω with a 75- Ω $1/4\lambda$ matching section. With the rise on the resistive component of the complex impedance, there was also a drop in the reactive component, a condition that creates a smaller remnant reactance after transformation by the matching section. The result is a relatively flat VSWR across the entire frequency sweep for the final stage of development.

14-4					Reference Data				
Model	7.0 MHz		7.1 MHz		7.2 MHz		7.3 MHz		
	$R \pm jX \ \Omega$	VSWR							
14-4.NEC	83.4 - j 34.8	2.08	86.5 - j 12.7	1.78	89.6 + j 9.4	1.82	92.9 + j 31.4	2.14	
14-4-1.NEC	90.7 - j 29.6	2.08	87.3 - j 10.6	1.78	90.3 + j 6.9	1.82	99.9 + j 23.3	2.14	
14-4-2.NEC	55.2 + j 17.0	1.40	63.3 + j 7.4	1.31	61.8 - j 4.5	1.26	52.8 - j 11.2	1.25	

Over the narrow bandwidth covered by the 40-meter amateur band, the matched VSWR shows a single curve. However, in the 3.5 MHz to 4.0 MHz amateur band, the curve begins to show a double "dip" where the design center frequency is the geometric mean between the two minima. As a supplemental exercise, repeat the modeling experiment with a dipole resonant for the center of that band of frequencies. Set the antenna at various heights between $1/4\lambda$ and $3/4\lambda$ above ground and check the results. Also, increase the length of the 50- Ω section in increments of $1/2\lambda$ and compare curves. For detailed examination of such curves, you may wish to take readings every 0.05 MHz and transfer your readings to a spread sheet--or use the VSWR graphing facilities of NECWin

Plus.

14-5.NEC: A stub-loaded dipole for 14.175 MHz

Transmission line stubs are used extensively in various facets of antenna design. NEC-2 permits you to model them using the TL facility. Like all transmission lines, each end must terminate on a wire segment. To create a stub requires you to create this wire and give it special properties, revealed by the following TL entry line:

TL	1	8	2	1	50	10.6	0	0	1E10	1E10
	(1)	(2)	(3)	(4)	(5)	(6)	(7)	(8)	(9)	(10)

The entries in positions (9) and (10) specify a set of values for shunt (parallel) conductivity and susceptance (or "real" and "imaginary" components of shunt admittance). The high positive values shown in the example create a short circuit across the "far" end of the transmission line. To create an open circuit, specify 1E-10 for both values. (You may be better able to picture the open and closed circuit by taking the inverse of the values given, which sets values for a complex shunt impedance across the far terminals of the transmission line.)

The reactance of the stub is determined by standard equations involving both the characteristic impedance and the electrical length of the line. For shorted transmission lines,

$$X = Z_o \tan \beta l \quad 1$$

where X is reactance, Z_o is the characteristic impedance of the line, and βl is the line length in electrical degrees or radians. Using the equation in either direction (toward reactance or toward line length) requires conversions to and from the length as a physical measure and the length in electrical degrees.

For open stubs, the useful equations are

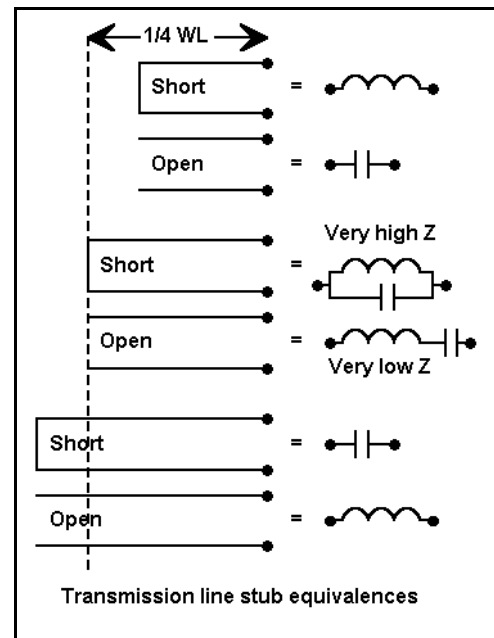
$$X = Z_o \cot \beta l \quad \text{or} \quad X = \frac{Z_o}{\tan \beta l} \quad 2$$

where all terms have the same meaning as they did with the shorted stub equation.

Whether the reactances are inductive (positive) or capacitive (negative) depends upon the line length. You may wish to calculate a number of values using different transmission lines, lengths, and reactance values. In general, the lower the characteristic impedance of the line, the longer a shorted stub will be for the same reactance value. For open stubs, the opposite rule applies.

Be certain to take the velocity factor of the transmission line into account when calculating the electrical line length. NEC-2 itself requires all transmission line dimensions to be their electrical, not their physical, length.

The second wire used to terminate a stub can be any distance away from the antenna structure. Very short wires, even of ordinary wire diameters, have virtually negligible affect on the performance outputs of NEC-2. Hence, they may be placed at a far but reasonable distance from the antenna with no problems. For antenna structures that you suspect might be sensitive to wires in the radiation field, place the terminating wire very far (100λ) from the antenna.



```

CM Dipole: 14.175 MHz
CM Reactance loaded
CE
GW 1 101 -2.564 0 0 2.564 0 0 .000814
GS 0 0 1
GE 0
EX 0 1 51 0 1 0
LD 4 1 25 25 0 870.4 0
LD 4 1 77 77 0 870.4 0
LD 5 1 1 101 5.8001E7
FR 0 1 0 0 14.175 0
RP 0 1 360 1000 90 0 1 1
EN
14-5

```

To test the use of transmission line stubs, we can use a simple short dipole that requires the insertion of reactance. Model 14-5.NEC begins a conversion process by showing the antenna with type 4 reactive loads in place on segments 25 and 77 of the wire. The design frequency of this #14 AWG copper wire antenna is 14.175 MHz. For resonance, the required reactive loads (ignoring Q for the present) are each 870.4Ω .

We may convert the reactance to a corresponding inductance ($9.77E-6 \mu\text{H}$). Check model 14-5-1.NEC uses this type 0 load for the same antenna. However, we may equally replace the inductor with shorted transmission line stubs that provide the same reactance. If you calculate the required electrical line lengths for both $50\text{-}\Omega$ and $450\text{-}\Omega$ transmission lines, you will get values of 5.0942 m and 3.681 m, respectively. These values appear in check models 14-5-2.NEC and 14-5-3.NEC. If you run all these models for the single frequency, 14.175 MHz, you will discover that they are all resonant within $\pm 1 \Omega$ reactance at a source resistance of about 26.0Ω .

However, our interest in stub-loading is not just to establish the equivalency of the models at resonance. All of the models except the one using a type 4 load are set up for a 4-step frequency sweep between 14.0 and 14.3 MHz in 0.1 MHz steps. Run models 14-5-1.NEC through 14-5-3.NEC, checking especially on the source impedance at each of the swept frequencies. Record the values in the table below.

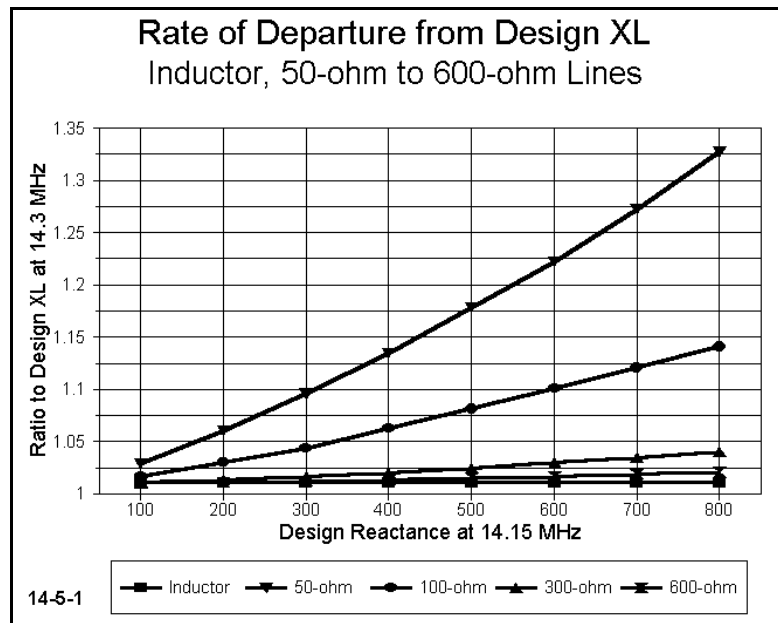
14-5 Test Data				
Load Type	14.0 MHz	14.1 MHz	14.2 MHz	14.3 MHz
Inductive				
50- Ω Stub				
450- Ω Stub				

Comments: The rate of change of both source resistance and source reactance resulting from the changes in the load reactance as the frequency moves away from design resonance is least for the inductive load. Often, the rate of change for inductive loads is inappropriately presumed to be the case for loading stubs as well. A more detailed look at stub loading quickly dispels the misimpression.

14-5 Reference Data				
Load Type	14.0 MHz	14.1 MHz	14.2 MHz	14.3 MHz
Inductive	24.6 - j 50.5	25.4 - j 21.5	26.2 + j 8.1	27.1 + j 38.3
50- Ω Stub	19.6 - j355.1	22.4 - j193.1	27.7 + j 88.0	41.4 + j718.1
450- Ω Stub	24.1 - j 81.3	25.1 - j 35.7	26.3 + j 12.6	27.6 + j 64.1

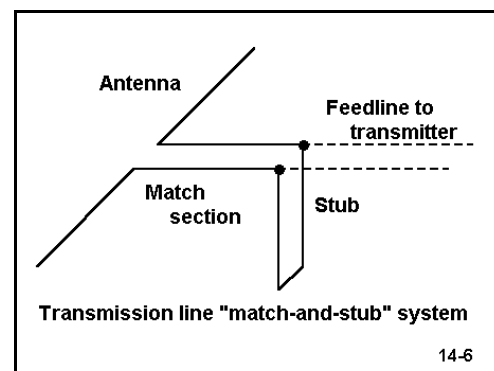
Changes in load reactance in stubs as the frequency departs from the design center are not simply direct functions of changes in frequency. Changes vary with the tangent (or cotangent, for open stubs) of the electrical length of the line, which itself varies with frequency. In general, as your data testifies, the lower the Z_0 of the transmission line, the more rapid the change of reactance for the same variation in frequency.

For reference, we may let the rate of change of reactance in an inductor be set flat at some frequency offset from the design center. In **Figure 14-5-1**, the design center is 14.15 MHz and the offset frequency is 14.3 MHz. The rate of departure from this flat value for lines of different characteristic impedances provides a portrait of stub performance for load reactances from 100 to 600 Ω . The 600- Ω line most closely approaches the rate of change of the inductor, but does not reach it. You may verify these curves by creating stubs of many line Z_0 s and reactance values as an extra exercise. You may expand the exercise to include both center loading and loading at a variety of points along the antenna element.



14-6.NEC: A "stub-matched" extended double Zepp for 28.5 MHz

When the source impedance of an antenna represents a serious mismatch to a system feedline, one system to effect a match consists of two lengths of transmission line, as shown in **Figure 14-6**. The series or "match" section is calculated to effect a change in the resistive component of the complex impedance to the Z_0 of the system feedline, while the stub provides the parallel equivalent of the compensating reactance necessary to equal the series reactance present at the junction with the system feedline. (Since the provision of equal but opposite reactance at the junction point could, less conveniently, be accomplished with a series reactive component, this matching system is a variant on the Regier series matching calculations.)



"Match-and-stub" systems can be calculated using a Smith chart, by hand, or by the use of readily available utility programs (such as the one included in the HAMCALC collection). All make use of the reflection coefficient to determine the correct junction point and thereafter, standard transmission line equations for calculating the series reactance, its parallel equivalent, and the stub length necessary to effect the compensation. (Of course, stubs may be replaced with equivalent reactive lumped components.) Essentially, there are four solutions to every match-and-stub problem, since there are two points within each $1/2\lambda$ where the resistive component of the impedance has the correct value, and for each of these points, there is an open and a shorted stub that may be used. The designer ordinarily picks the solution resulting in either the shortest total length of match-and-stub line or the most convenient lengths for the particular installation. Although most match-and-stub systems use the same transmission line for both components, this is not necessary. Finally, not all transmission line Z_0 values will provide a match in all situations.

```
CM Extended duble Zepp: 28.5 MHz
CE
GW 1 31 -6.74 0 0 6.74 0 0 .000814
GS 0 0 1
GE 0
EX 0 1 16 0 1 0
LD 5 1 1 31 5.8001E7
FR 0 1 0 0 28.5 0
RP 0 1 360 1000 90 0 1 1
EN
```

14-6

As an exercise in modeling match-and-stub, let's begin with a familiar extended double Zepp antenna: #14 AWG copper wire in free space for 28.5 MHz. Model 14-6.NEC provides this basic model without a matching system added to it. Run this model at 28.5 MHz to determine the source impedance. Your value should be close to $137.2 - j663.6 \Omega$. This is the values which a match-and-stub system must convert to 50Ω , which

represents the system coaxial cable feedline.

Using any means at your disposal, calculate the required lengths of the match line and the stub line. (Model 14-6-1.NEC already contains a 1.5875-m match line and a 0.430-m shorted stub, both of $450\text{-}\Omega$ transmission line.) Note that to reconstruct the original model to contain these lines, you will have to add two wires: one for the junction of the match line, the system feedline, and the stub (which will also become the new source segment); and the other for the termination of the shorted stub. As always with transmission lines, you may place these wires anywhere at a considerable distance from the antenna element itself.

```
CM Extended duble Zepp: 28.5 MHz
CE
GW 1 31 -6.74 0 0 6.74 0 0 .000814
GW 2 1 -.01 -10 0 .01 -10 0 .000814
GW 3 1 -.01 -10 -10 .01 -10 -10 .000814
GS 0 0 1
GE 0
EX 0 2 1 0 1 0
LD 5 1 1 31 5.8001E7
LD 5 2 1 1 5.8001E7
LD 5 3 1 1 5.8001E7
TL 1 16 2 1 450 1.5875 0 0 0 0
TL 2 1 3 1 450 .43 0 0 10000000000 10000000000
FR 0 6 0 0 28 .2
RP 0 1 360 1000 90 0 1 1
EN
```

14-6-1

Run model 14-6-1.NEC in a frequency sweep from 28.0 through 29.0 MHz on 0.2 MHz

steps. Record both the source impedance and the 50- Ω VSWR in the table below. Although our interests are in the source impedance and its match to the 50- Ω feedline system, you should always check the azimuth (or elevation) plots to ensure that our expectations are being met--in short, that the match-and-stub system make no significant difference to the antenna's radiation fields.

14-6						
	Test Data					
	28.0 MHz	28.2 MHz	28.4 MHz	28.6 MHz	28.8 MHz	29.0 MHz
$R \pm j X \Omega$						
SWR						

Comments: The table serves a double function. First, it provides a guide to field adjustments we might have to make in a real antenna. By reference to the numbers in the chart, we may be able to make educated judgments concerning how much to trim from or add to each piece to center the impedance match at the desired frequency. Performing a frequency sweep often proves useful even if a given antenna is to be used at only one frequency. Understanding how an antenna performs over a frequency range, whether narrow or broad, gives many clues to aid in making a particular antenna achieve its performance potential.

Second, the table also shows the 2:1 50-Ohm VSWR operating bandwidth of the antenna: just under 0.8 MHz. You may compare this figure with the operating bandwidth of a simple dipole of the same material or with other antennas. Moreover, you may construct similar match-and-stub systems with lines having other Z_0 values. Then, compare the operating bandwidth of each additional match-and-stub system with this model which uses 450- Ω transmission line.

14-6						
	Reference Data					
	28.0 MHz	28.2 MHz	28.4 MHz	28.6 MHz	28.8 MHz	29.0 MHz
$R \pm j X \Omega$	98.5-j34.9	73.4-j20.5	56.4-j 6.5	44.6+j 8.1	36.2+j17.4	30.0+j27.2
SWR	2.29	1.66	1.19	1.19	1.68	2.33

In the application of stubs both as reactive loads and as reactances for matching networks, length adjustment can be expected. Accounting for the velocity factor of a transmission line is one (by now) obvious area of modification of the electrical lengths used in models. Velocity factor may be specified by a transmission line manufacturer, but often it varies a bit from product lot to product lot. In addition, NEC-2 transmission lines are lossless. For lines under $1/2\lambda$ long, the resulting modeled lengths are generally close

enough for ready field adjustment. However, for lines of longer length, losses may alter performance in a significant way.

Summing Up

We have sampled uses of transmission lines across a wide area of modeling. Still, we have only begun to look into their use in both models and in real antennas. We shall investigate some more complex uses of transmission lines in Part C, when we look at both horizontal and vertical phased arrays in more detail. For now, simple antennas will suffice to acquaint us with modeling procedures and applications.

The TL or transmission line entry is among the control cards within a NEC-2 model. Correct entry requires terminating wires for both ends of the mathematical model used to capture the characteristic impedance and the electrical length of transmission lines. The core will return an error message if both wires are not present. Moreover, use of the TL facility within NEC-2 should ensure that 1. lossless transmission lines are satisfactory for the application at hand and 2. the conditions of application are balanced. A TL entry should not be used to simulate a linear load placed midway between the source and the wire end. The TL entry will not correctly capture the imbalance of currents on the two wires of such a load. The result will be an inaccurate model of the element and its linear load. Some uses of parallel transmission lines must be physically modeled.

Advanced applications of transmission lines permit the modeler to tailor the shunt admittance at either or both ends of the line to simulate any number of conditions. Although we have simulated short and open circuits as the two most common uses of this feature, others are certainly possible.

We may model with transmission lines using only trial and error techniques. However, expert use of transmission lines in models calls for calculating adjuncts to the NEC-2 program. Smith charts, utility programs, or even hand calculation from basic equations tends to be more efficient than simply trying a set of values to see where they lead. As with all facets of modeling with NEC-2, the better the quality of our inputs, the better the quality of the program output.

15.

Monopoles and Ground Planes

***Objectives:** In these exercises, you will become familiar with modeling techniques useful for $1/4\lambda$ and similar monopoles and their associated ground planes over perfect ground and above real ground. In addition, you will learn some substitute techniques for modeling ground planes that are below ground.*

The $1/4\lambda$ monopole presents some unique challenges to antenna modelers. Some of the difficulties stem from NEC-2's inability to handle wires below the ground surface, one of the usual places to find a ground plane structure for a monopole. Other challenges arise from the fact that method-of-moments modeling and calculating place monopoles in a different perspective than traditional ways of looking at these simple antennas. Adjusting our presumptions about monopoles is one of the first steps toward effectively and accurately modeling them.

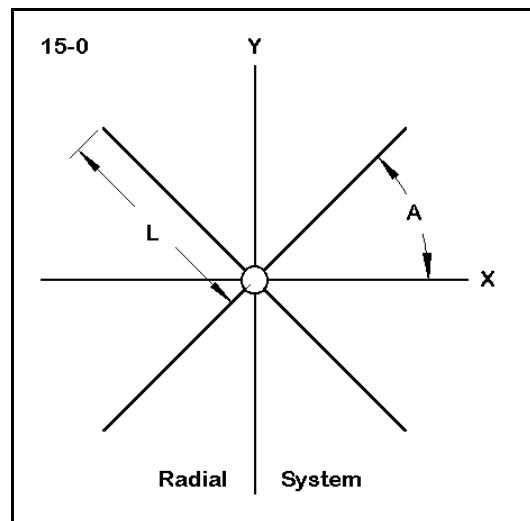
One of the facilities offered by NEC-2 is the ability to model monopoles over perfect ground. In these models, the program creates the image antenna, with gain and source impedance adjusted for the perfect reflection. The process speeds modeling compared to the time required for creating radials systems (and for creating complex symmetrical free space models, as well). Perfect ground simplifies the process of comparing models in a preliminary manner.

However, the modeler cannot avoid modeling radial systems for use with $1/4\lambda$ monopoles, if the work is eventually to be used for the design or analysis of antennas to be used in the real world. We shall begin our exercises in this arena with some free space and highly elevated models over some divergent soil types. We shall next compare flat and sloping ground planes. Eventually, we shall place the radial system close to the ground. NEC-2 is limited by the fact that it cannot directly model buried radials, although we can simulate buried radials by placing them very close to the ground.

In addition to the challenge of modeling radials, $1/4\lambda$ monopoles offer a number of interesting configurations worth modeling. For example, a height of approximately $5/8\lambda$ yields the maximum gain for monopoles, and we shall want to look at such antennas. Comparing "standard" and long monopoles over both perfect ground and over lossier ground conditions, even with an extensive ground plane, will give us an opportunity to

compare textbook ideal figures with more realistic expectations of performance.

Perhaps the greatest temptation in modeling vertical monopoles is always to use perfect ground in order to avoid having to create large models involving many radials. However, modeling a radial system is a straightforward task with simple rules which are amenable to symbolic model entry or to advanced calculation to determine the radial end-points. **Figure 15-0** shows a typical radial system with 8 radials surrounding a center antenna that passes through the page. To construct or symbolize a set of radials, you may use any system similar to the following:



Set the X-axis as the reference line. Let L be the length of each radial (so that a sample radial might have the values at end 1 of $X=0$ and $Y=0$ and at end 2 of $X=L$ and $Y=0$). If N is the number of radials, then the angle (A) between each radial is $A=360/N$. The radials will then have end-2 coordinates as follows:

Radial Number	End-2 X	End-2 Y
1	$X1 = \cos A * L$	$Y1 = \sin A * L$
2	$X2 = \cos (2 * A) * L$	$Y2 = \sin (2 * A) * L$
N	$Xn = \cos (N * A) * L$	$Yn = \sin (N * A) * L$

In this example, radial N is the one which will extend from the center point to the values $X=L$ and $Y=0$. You may set this table into a modeling program offering symbolic dimensional notation, or you may prepare the table and its results as a preliminary exercise on a prepared form to keep your work systematic and traceable.

Symbolic entry does allow revision of the length of the entire radial system with a single change for the value of L . You must, however, have an entry for each radial in the system. Hence, changing the number of radials in a system requires the introduction of the correct number of wires to complete the array.

Once you have modeled radial systems with various numbers of wires, you should save your collection under some system of filenames. You may pull them from the files, scale them to the frequency of a present project as well as to the desired wire size and type, adjust X , Y , and Z values to position them for the new project, and then construct the new

radiating wires atop them.

Exercise Preparation

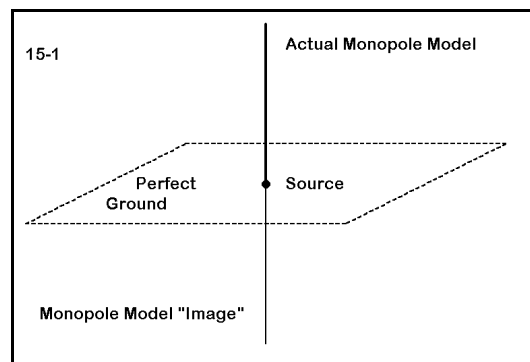
In the following exercises, we shall use a mixed bag of media, involving free space, perfect ground, and Sommerfeld-Norton grounds of varying qualities. It will be important that you track the medium within which each model is run in order to prevent inappropriate comparisons among antennas until you develop a thorough familiarity with what to expect from an antenna type in each medium.

Additionally, we shall in some cases require the revision of models without much fanfare. Therefore, be certain that you track the filenames used for variations on models, especially if you wish to save the original and some of the more significant variants.

Because the modeling perspective on vertical monopoles does not always clearly reflect fundamental theoretical considerations found in standard texts on the subject, you may wish to review monopole theory either before or during these exercises.

15-1.NEC: A $1/4\lambda$ vertical monopole over perfect ground at 3 MHz

When you choose perfect ground, NEC-2 creates an image antenna of the actually modeled wire(s), as illustrated in **Figure 15-1**. Using perfect ground can provide a relatively swift way of comparing various antenna models of relevantly similar sorts, as well as giving you a means of rapidly checking the benefits of modifications to a model. Perfect ground models are related in very regular ways to free space models containing both the actual and image elements within the wire structures.



```

CM 1/4 wave vertical: 3 MHz
CE
GW 1 35 0 0 0 0 0 24.13 .0127
GS 0 0 1
GE 1
GN 1
EX 0 1 1 0 1 0
LD 5 1 1 35 2.4938E7
FR 0 1 0 0 3 0
RP 0 181 1 1000 -90 0 1 1
EN
15-1

```

Open model 15-1.NEC. The antenna consists of a single 6061-T6 aluminum monopole 24.13 m long with a 25.4 mm diameter. The antenna is over perfect ground with one end in contact with the ground (coordinates 0, 0, 0). The antenna has 35 segments, with the lowest segment used for the source. The antenna is constructed to be resonant at 3 MHz over the perfect ground.

We shall perform some modifications upon this antenna, but first we should compare it with a dipole in free space to refresh our memories about the relationship between free-

space dipoles and perfect-ground monopoles.

Open model 15-1-1.NEC. You should recognize the model as the free-space dipole equivalent of the perfect-ground monopole. The antenna is 48.26 m long and 25.4 mm in diameter, using 6061-T6 aluminum. There are 71 segments so that the source can be exactly centered on segment 36.

```

CM 1/2 wave free space dipole: 3 MHz
CE
GW 1 71 -24.13 0 0 24.13 0 0 .0127
GS 0 0 1
GE 0
EX 0 1 36 0 1 0
LD 5 1 1 71 2.4938E7
FR 0 1 0 0 3 0
RP 0 1 360 1000 90 0 1 1
EN

```

15-1-1

Run both models and record the results in the following table.

15-1 Test Data		
Antenna	Gain dBi	Source Z $R \pm jX \Omega$
Monopole-perfect gnd		
Dipole-free space		

Comments: As we have seen in an earlier exercise, the gain of the perfect-ground monopole is almost exactly 3 dB higher than the gain of the free-space dipole. The source impedance of the monopole is half that of the dipole, allowing for the minuscule displacement of the source between the two models.

15-1 Reference Data		
Antenna	Gain dBi	Source Z $R \pm jX \Omega$
Monopole-perfect gnd	5.14	36.15 + j 0.32
Dipole-free space	2.13	72.27 + j 0.48

You may use these relationships as a guide for other modeling ventures. As a supplementary exercise, select a 3-element Yagi in free space from an earlier chapter and reconstruct half the antenna as a 3-element vertical over perfect ground. Compare the resulting values and elevation pattern with the original values and azimuth pattern. Replicate this experiment with other antennas used in preceding chapters.

A common question raised about vertical monopoles (and other linear antennas) concerns the degree to which we may shorten them and still retain usable gain. Our monopole over perfect ground provides a ready vehicle for developing a preliminary

answer. In successive steps, shorten the antenna to 80, 60, 40, and finally to 20 percent of its original height. Determine the gain and source impedance of the shortened antenna and record your data in the following table.

15-1 Test Data			
% of Full Length	Length Meters	Gain dBi	Source Z $R \pm jX \Omega$
100			
80			
60			
40			
20			

Comments: Although the source impedance shows a rapidly decreasing resistance and a rapidly increasing capacitive reactance, the gain of the element holds up surprisingly well. A 20% of its full length, the monopole has lost less than 0.5 dB gain. At 2/3 of the full length, the antenna has lost less than only about 0.2 dB gain. A rule of thumb used in some applications is to attempt to keep an antenna at least 2/3 full size to achieve close to maximum performance with top loading.

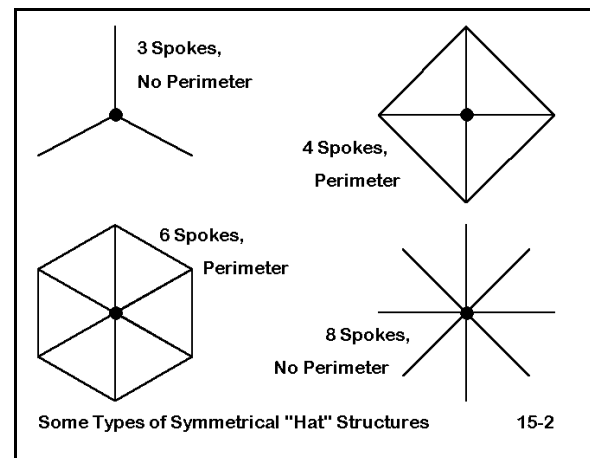
15-1 Test Data			
% of Full Length	Length Meters	Gain dBi	Source Z $R \pm jX \Omega$
100	24.130	5.14	36.2 + j 0.32
80	19.304	4.99	19.4 - j 129
60	14.478	4.88	9.8 - j 279
40	9.652	4.79	4.1 - j 505
20	4.826	4.71	1.1 - j1055

You may expand this chart to any desired degree--for example, using 5% increments. The resulting table will serve as a long-term reference table, as well as provide a basis for developing some useful graphics. Since the antenna element is quite thin for the frequency used, you may also wish to repeat the exercise for antenna elements with larger diameters--perhaps up to 150 mm (about 6").

In addition, replicate this experiment with the free-space dipole. Compare the dipole data in detail with the results for the monopole.

15-2.NEC: A "hat-loaded" monopole over perfect ground for 3 MHz

Shortened vertical monopoles are common practice from the VLF range upward. One technique of "loading" the monopole to resonance is called the "capacity hat," a symmetrical array of wires (or even a disc or cylinder) at the end of the monopole furthest from the ground and source. Since the hat structure is symmetrical and at right angles to the monopole portion of the antenna, its radiation is self-cancelling. One rule of thumb used in some areas of antenna engineering suggests that the monopole be no less than 2/3 full (self-resonant) length for maximum gain.



Hat structures, as illustrated in **Figure 15-2** can take many forms, but often consist of spokes radiating from the tip of the monopole. This configuration is physically identical to the structure of most ground-plane radial systems, and the construction for a model is identical, except for the Z-axis value. So long as the radials are arranged symmetrically, any number from 2 to n may be used, with about 32 being the limit for a NEC-2 model, given recommendations for the maximum number of wires having a common junction.

The length of the spokes can be shortened by connecting their tips with a perimeter wire, as indicated in some of the hats in **Figure 15-2**. The effective size of the "spoke + perimeter" hat, compared to a "spoke only" hat, is very roughly equal to the length of the spoke plus 1/2 the length of the wire connecting any two spoke tips. Obviously, the greater the number of spokes, the smaller the decrease in hat size effected by using a "spoke + perimeter" style hat. However, in the construction of real antennas using capacity hats, interconnecting wires at both the tips and intermediate points may have structural as well as electrical functions.

For VLF through MF, a series of equations based upon the analogy of antennas with transmission lines permits the rough calculation of hat sizes for disc construction. These equations, available in most standard antenna engineering texts, require that the monopole wire diameter be very small relative to a wave length, since the transmission line analogy presumes an increasing antenna wire diameter which the actual parallel sides of a wire only approximate. The equations lose accuracy in the HF range. For

modeling purposes, the hat may be viewed as simply a physical extension of the antenna that has no net radiation due to its symmetry. Often, it is easier to determine experimentally the required length for spokes in a model than it is to calculate and then make adjustments for the lack of coincidence between equations and modeling results.

We shall examine some hats of various sizes for a 3 MHz vertical monopole composed of 25.4 mm 6061-T6 aluminum over perfect ground. The monopole is just over 16 m long, just about 2/3 full size.

```

CM 1/4 wave short vert--cap load
CM 6 spokes
CE
GW 1 25 0 0 0 0 0 16.0324 .0127
GW 2 3 0 0 16.0324 3.8481 0 16.0324 .000161
GW 3 3 0 0 16.0324 1.92405 3.33255 16.0324 .000161
GW 4 3 0 0 16.0324 -1.924 3.33255 16.0324 .000161
GW 5 3 0 0 16.0324 -3.8481 0 16.0324 .000161
GW 6 3 0 0 16.0324 -1.924 -3.3325 16.0324 .000161
GW 7 3 0 0 16.0324 1.92405 -3.3325 16.0324 .000161
GS 0 0 1
GE 1
GN 1
EX 0 1 1 0 1 0
LD 5 1 1 25 2.4938E7
LD 5 2 1 3 2.4938E7
LD 5 3 1 3 2.4938E7
LD 5 4 1 3 2.4938E7
LD 5 5 1 3 2.4938E7
LD 5 6 1 3 2.4938E7
LD 5 7 1 3 2.4938E7
FR 0 1 0 0 3 0
RP 0 181 1 1000 -90 0 1 1
EN
    
```

15-2-6S

Initially, we shall look at models using only spokes in numbers ranging from 3 to 32, according to the table below. Begin with model 15-2-3S.NEC, which indicates the 3-spoke version. (Shown to the right is the model for a 6 spoke hat.) Record the maximum gain from the elevation pattern once you assure

yourself that the spokes are of a length that yields resonance within $\pm 1 \Omega$ reactance. In the table below, record the source impedance at resonance and the length of the equal spokes. Then rebuild the spoke system for the next level of complexity, using the models on the disk only to check your work. (Models 15-2-nS.NEC indicate spoke-only hat models for this exercise.

15-2: Sp-Only		Test Data	
Number of Spokes	Spoke-Length Meters	Gain dBi	Source Z $R \pm jX \Omega$
3			
4			
6			
8			
12			
16			
24			
32			

Comments: As the number of spokes increased, the length decreased from a maximum with 3 spokes of nearly 6 m to less than 2 m with 32 spokes. The antenna gain is nearly constant throughout the exercise, with a variation of only 0.04 dB. The source impedance can be considered constant.

15-2: Sp-Only		Reference	Data
Number of Spokes	Spoke-Length Meters	Gain dBi	Source Z $R \pm jX \Omega$
3	5.994	4.96	27.9 -j 0.7
4	4.966	4.98	27.8 -j 0.7
6	3.848	4.99	27.9 +j 0.4
8	3.239	4.99	27.9 +j 0.4
12	2.611	5.00	27.9 -j 0.2
16	2.297	5.00	27.9 -j 0.9
24	2.007	5.00	27.9 -j 0.3
32	1.861	5.00	28.0 -j 0.2

Repeat the experiment using model 15-2-3P.NEC, the smallest spoke + perimeter wire design. The model-type is illustrated to the right, using the 3-spoke version. Note that the number of hat wires per model is automatically doubled, resulting in quite lengthy models by the time you reach 32 spokes.

In these examples, we have taken the shortcut of using a

single wire between the tips of the spokes. The detailed current magnitude and phase information provided by starting each perimeter wire at its center was not useful to our task. Should that data be important to a given model tasks, more complex models would have been necessary. Moreover, segmentation has been standardized so that the length of segments is not constant from one model to the next or from one portion of the hat to

```

CM 1/4 wave short vert--cap load
CM 3 spokes: perimeter wire
CE
GW 1 25 0 0 0 0 0 16.0324 .0127
GW 2 3 0 0 16.0324 2.9845 0 16.0324 .000161
GW 3 3 0 0 16.0324 -1.4922 2.58465 16.0324 .000161
GW 4 3 0 0 16.0324 -1.4922 -2.5846 16.0324 .000161
GW 5 5 2.9845 0 16.0324 -1.4922 2.58465 16.0324 .000161
GW 6 5 -1.4922 2.58465 16.0324 -1.4922 -2.5846 16.0324 .000161
GW 7 5 -1.4922 -2.5846 16.0324 2.9845 0 16.0324 .000161
GS 0 0 1
GE 1
GN 1
EX 0 1 1 0 1 0
LD 5 1 1 25 2.4938E7
LD 5 2 1 3 2.4938E7
LD 5 3 1 3 2.4938E7
LD 5 4 1 3 2.4938E7
LD 5 5 1 5 2.4938E7
LD 5 6 1 5 2.4938E7
LD 5 7 1 5 2.4938E7
FR 0 1 0 0 3 0
RP 0 181 1 1000 -90 0 1 1
EN

```

15-2-3P

the next, since the aim of the exercise is to show some trends. Should you be required to produce more accurate work for a design or analysis project, you would, of course, make every attempt to equalize the segment lengths throughout the model.

Record the same data (spoke length, gain, and source impedance at resonance) in the table below, and then increase the number of spokes. Use the models in the 15-2-nP.NEC series on the accompanying disk as checks upon your work.

15-2: Sp+Per		Test Data	
Number of Spokes	Spoke-Length Meters	Gain dBi	Source Z $R \pm jX \Omega$
3			
4			
6			
8			
12			
16			
24			
32			

Comments: Although the use of a perimeter wire reduces spoke length by about half for the 3-spoke design, the perimeter wire version of the hat is only marginally smaller than the spoke-only version when the number of spokes is 32. Since the rate of hat-size shrinkage is much lower with a perimeter wire, the antenna designer may choose a hat with fewer spokes for structural simplicity in some cases without sacrificing much by way of small size. Once more, the gain and source impedance vary only insignificantly from one model to the next.

15-2: Sp+Per			
		Reference Data	
Number of Spokes	Spoke-Length Meters	Gain dBi	Source Z $R \pm jX \Omega$
3	2.985	4.97	28.1 + j 0.1
4	2.591	4.98	28.1 + j 0.6
6	2.280	4.99	28.0 + j 0.8
8	2.096	4.99	27.9 - j 0.5
12	1.918	5.00	28.0 + j 0.1
16	1.808	5.00	27.9 - j 0.8
24	1.701	5.00	27.9 - j 0.3
32	1.640	5.00	28.0 - j 0.2

The monopoles and the hat wires in this exercise are both thin: about 1" and #28 AWG wire, respectively. You may wish to increase alternately the diameters of the monopole and the hat wires for some of the simpler models to see the effects of each increase upon the required hat size to achieve resonance. Once you have arrived at a set of interesting results, transpose those selected diameters to one or more of the more complex models with many spokes to see if the effects diminish with the increasing number of spokes, and to what degree. You may also create a graph of the results from 3 through 32 spokes for each type of hat. Allow for the fact that the spoke numbers do not increase directly in either an arithmetic or geometric progression. Can you nonetheless extrapolate a point in terms of the number of spokes where the addition of further spokes will no longer decrease the hat radius by any significant amount?

Besides introducing you to an important facet of shortened monopole design, this exercise has, of course, also introduced you to the construction of radial systems of wires with a common connection at a vertical antenna element. You may have used symbolic model data entry or independent calculation to derive the coordinates for the outer points of the radials. In effect, you have performed precisely the tasks necessary for constructing ground planes.

15-3.NEC: An elevated monopole with ground plane for 7.05 MHz

Although many treatments of vertical monopoles with ground-plane structures begin at ground level, method-of-moments modeling may equally begin in free space. Moreover, ground-plane monopoles find uses at heights well above ground, so exploring the characteristics of these antennas at these heights is relevant to developing an overall understanding of their operation.

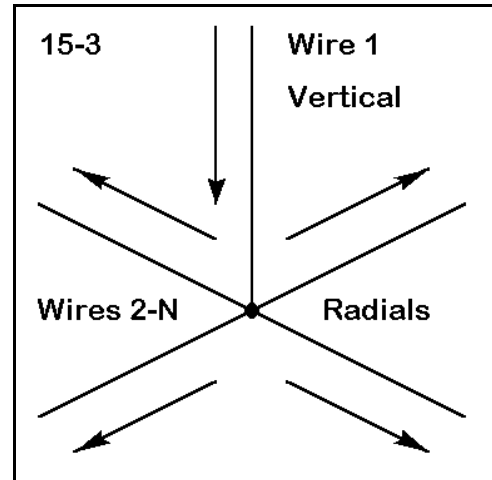


Figure 15-3 introduces us to the need for developing some convention in our modeling to make it systematic. The sketch shows through arrows the directions of modeling wires from end 1 to end 2 of each wire. One might as easily work in precisely the opposite direction. However, the models used in this exercise follow the sketch. The monopole will always be wire 1, with the radial wires following.

Open model 15-3-1.NEC, a free-space vertical monopole with 4 ground-plane radials designed for 7.05 MHz. The vertical element is 50 mm in diameter (nearly 2"), while the radials are 6.35 mm in diameter (about 0.25"). The vertical element is a resonant monopole, that is, $1/4\lambda$ long electrically over a perfect ground, and the radials have been cut to establish resonance in free space. The antenna is fed at the lowest segment of the vertical element. Segmentation is limited to 10 segments per element. For increased accuracy, one might use more segments per wire. However, we shall explore models using 4, 8, 16, and 32 radials. The largest of these has 330 segments. Hence, for this exercise, 10 segments per $1/4\lambda$ will suffice to accurately establish trends. For a specific design or analysis project, you may either use more segments or taper the length of the segments toward the source and the junction of the radials for greater accuracy. (If you choose the latter course of model design, ensure that the segment above the source segment is equal in length to the source segment and to the first segment of each radial wire.)

```

CM 1/4 w1 w/GP: 7.05 MHz
CM 4 radials
CE
GW 1 10 0 0 10.1346 0 0 0 .025
GW 2 10 0 0 0 11.7957 0 0 .00317
GW 3 10 0 0 0 11.7957 0 0 .00317
GW 4 10 0 0 0 -11.795 0 0 .00317
GW 5 10 0 0 0 0 -11.795 0 .00317
GS 0 0 1
GE 0
EX 0 1 10 0 1 0
LD 5 1 1 10 2.4938E7
LD 5 2 1 10 2.4938E7
LD 5 3 1 10 2.4938E7
LD 5 4 1 10 2.4938E7
LD 5 5 1 10 2.4938E7
FR 0 1 0 0 7.05 0
RP 0 181 1 1000 -90 0 1 1
EN
    
```

In this exercise, you will change the number of radials from 4 to 8 to 16 and finally to 32,

using one of the standard techniques. For each radial system, you will first record the gain and source impedance of the model in free space and then over various S-N ground qualities with the antenna base and radial system at a height of 40 m (about 1λ). Use the table below to record the results of your work.

15-3		Test Data			
# Radials	4	8	16	32	
Free Space					
Gain					
Source Z					
VG Ground					
Gain/TO ang					
Source Z					
Ave Ground					
Gain/TO ang					
Source Z					
VP Ground					
Gain/TO ang					
Source Z					

The ground qualities used in this test are "Very Good" (cond. = 0.0303 s/m; perm. = 20), "Average" (cond. = 0.005 s/m; perm. = 13), and "Very Poor" (cond. = 0.001 s/m; perm. = 5). Should you encounter difficulties in constructing these variants, you may consult check models 15-3-1.NEC through 15-3-4C.NEC. A sample is shown at right for the 4-radial model over very good soil, with the base at 40 m and the tip of the vertical at 50.1346 m.

You should notice that, holding the length of the vertical element constant, the required radial length to achieve resonance increases as the number of radials increases. From 4 to 32 radials, the radials increase in length about 1 m from a low of 11.796 m to a high of 12.863 m.

```

CM 1/4 wl w/GP: 7.05 MHz
CM 4 radials
CE
GW 1 10 0 0 50.1346 0 0 40 .025
GW 2 10 0 0 40 11.7957 0 40 .00317
GW 3 10 0 0 40 0 11.7957 40 .00317
GW 4 10 0 0 40 -11.795 0 40 .00317
GW 5 10 0 0 40 0 -11.795 40 .00317
GS 0 0 1
GE 1
GN 2 0 0 0 20 .0303 0 0 0 0
EX 0 1 10 0 1 0
LD 5 1 1 10 2.4938E7
LD 5 2 1 10 2.4938E7
LD 5 3 1 10 2.4938E7
LD 5 4 1 10 2.4938E7
LD 5 5 1 10 2.4938E7
FR 0 1 0 0 7.05 0
RP 0 181 1 1000 -90 0 1 1
EN
    
```

15-3-1A

15-3 Reference Data				
# Radials	4	8	16	32
Free Space				
Gain	1.29	1.24	1.21	1.15
Source Z	21.5 - j 0.5	21.9 + j 0.2	22.1 - j 0.7	22.5 - j 0.4
VG Ground				
Gain/TO ang.	5.15 / 26	5.17 / 26	5.18 / 26	5.19 / 26
Source Z	21.4 - j 0.1	21.8 + j 0.6	22.1 - j 0.2	22.5 + j 0.7
Ave Ground				
Gain/To ang	3.35 / 26	3.36 / 25	3.38 / 25	3.39 / 25
Source Z	21.4 - j 0.2	21.8 + j 0.5	22.1 - j 0.3	22.5 - j 0.2
VP Ground				
Gain/TO ang	3.32 / 11	3.31 / 11	3.31 / 11	3.29 / 11
Source Z	21.4 - j 0.3	21.9 + j 0.4	22.1 - j 0.4	22.5 - 0.1

Comments: The table is interesting in several respects. First, the source impedance does not change by moving the model from free space to a height of 1λ above ground,

regardless of the soil type. Second, as the number of radials is increased for each of the soil types, the gain figures wander a bit, but do not indicate any significant change of antenna performance. At high antenna placements for monopoles with ground planes, the use of extensive radial systems is unnecessary, so long as the smaller ground plane systems maintain symmetry. As a supplementary exercise, you may wish to experiment by shortening a single radial wire by about 5%. Check the effects of the change upon the overall azimuth pattern at the indicated take-off angle for small and large radial systems.

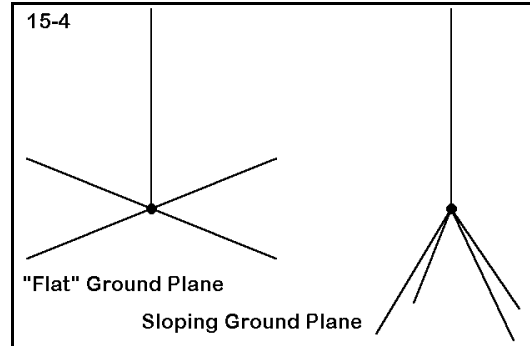
Finally, notice the effects of the soil type on both the gain and the take-off angle. Between the very good and the average soil types, the take-off angle does not change by much, although the gain difference is nearly 2 dB. Between the average soil and the very poor soil, the gain does not change much, but the take-off angle is nearly 15 degrees lower over the worse soil. To see this graphically, overlay the elevation patterns for any of the average soil models on any of the very poor soil models. You should see a change in strength in both of the lowest two lobes of the pattern between the two models.

Do not discard any of the variants of our original model. We shall further modify them for another exercise a bit farther on in the chapter.

15-4.NEC: A sloping ground-plane monopole for 7.05 MHz

Because the source impedance of a typical monopole with a ground plane is low, many ground planes are designed to have radials that slope downward, as illustrates in **Figure 15-4**. The downward slope increases the source impedance to a value intermediate between that of the standard ground plane monopole and that of a dipole. In addition, the radiation from the ground plane wires now has both a vertically polarized and a horizontally polarized component.

Although the horizontal component cancels as with a standard ground plane monopole, the vertical component adds to the antenna's overall radiation.



Open model 15-4-0.NEC. This 4-radial model is identical to those used in the preceding exercises, with a 50 mm diameter 6061-T6 vertical elements and 6.35 mm diameter radials. It is placed at a base height of 40 m above average soil and will be the standard against which we shall measure the other models in this group.

From the original model, you may construct monopoles with ground planes that slope 30°, 45°, and 60° downward relative to the horizon. Model 15-4-30 demonstrates the 30° downward slope model. Notice that as you increase the angle of the radials downward, the length for resonance of the system decreases: 10.4 m for the 30° model, 9.8 m for the 45° model, and 9.3 m for the 60° model. If you have difficulties constructing the required models from the original, consult models 15-4-30.NEC through 15-4-60.NEC for guidance.

```

CM 1/4 wl vert: 7.05 MHz
CM 30-degree g-p.
CE
GW 1 10 0 0 50.1346 0 0 40 .025
GW 2 10 0 0 40 9.00666 0 34.8 .00317
GW 3 10 0 0 40 0 9.00666 34.8 .00317
GW 4 10 0 0 40 -9.0066 0 34.8 .00317
GW 5 10 0 0 40 0 -9.0066 34.8 .00317
GS 0 0 1
GE 1
GN 2 0 0 0 13 .005 0 0 0 0
EX 0 1 10 0 1 0
LD 5 1 1 10 2.4938E7
LD 5 2 1 10 2.4938E7
LD 5 3 1 10 2.4938E7
LD 5 4 1 10 2.4938E7
LD 5 5 1 10 2.4938E7
FR 0 1 0 0 7.05 0
RP 0 181 1 1000 -90 0 1 1
EN
    
```

15-4-30

Our project for this exercise will consist not only of constructing the sloping-radial monopoles, but as well of checking their performance at various heights above ground. For each of the models, including the standard ground-plane monopole, check the gain and take-off angle, as well as the source impedance, at heights of 40 m, 30 m, and 20 m above ground as measured by the height of the junction of the radials with the vertical element. These heights correspond roughly to heights of 1λ , $3/4\lambda$, and $1/2\lambda$ above ground. Record your findings in the following table below.

15-4 Test Data				
Radial Slope	0°	30°	45°	60°
40 m (1λ)				
Gain/TO ang				
Source Z				
30 m ($3/4\lambda$)				
Gain/TO ang				
Source Z				
20 m ($1/2\lambda$)				
Gain/TO ang				
Source Z				

Comments: At a height of 1λ above ground, the gain increases as the radials are sloped further toward the vertical, with only a very small increase in the take-off angle. The increasing slope to the ground-plane radials also increases the source impedance to

virtually a perfect match for a 50- Ω feedline system.

At a height of about $3/4\lambda$ above average soil, the gain remains fairly constant as the radials increase in downward slope. The take-off angle increases a bit more than at 1λ in height, and the source impedance also shows this more rapid increase.

At a junction height of $1/2\lambda$, increases in the slope of the radials show a decrease in gain. At the greatest radial slope downward, the tips of the radials are just above $1/4\lambda$ from the ground. The take-off angle shows a transition between the dominance of the lower two lobes, with the lowest lobe becoming dominant with the greatest downward slope of the radials.

15-4				
Reference Data				
Radial Slope	0°	30°	45°	60°
40 m (1λ)				
Gain/TO ang	3.35 / 26	3.77 / 27	3.95 / 28	4.15 / 28
Source Z	21.4 - j 0.2	40.3 + j 0.5	46.9 + j 0.6	50.7 + j 0.9
30 m ($3/4\lambda$)				
Gain/TO ang	3.39 / 33	3.31 / 36	3.28 / 37	3.32 / 37
Source Z	21.5 - j 1.0	41.7 - j 0.2	48.7 + j 0.4	52.6 + j 1.1
20 m ($1/2\lambda$)				
Gain/TO ang	2.37 / 45	1.35 / 49	0.78 / 49	0.77 / 13
Source Z	21.8 + j 0.5	38.7 + j 1.7	44.4 + j 1.6	47.6 + j 1.5

The $3/4\lambda$ junction height represents a transition point below which the ground begins to exert effects upon the antenna that are not evident above that point. As portions of the antenna structure approach a height of $1/4\lambda$ above ground, the effects become quite strong. As a supplementary exercise, you may lower the standard ground-plane monopole to 10 m above ground (about $1/4\lambda$) and check its performance at that height in terms of gain, take-off angle, source impedance, and elevation pattern.

15-5.NEC: A ground-plane monopole for 7.05 MHz at ground level

At heights well above ground (above $1/2\lambda$), the number of radials in a vertical monopole system made little difference to performance. However, in bringing the sloping-radial antennas lower than $1/2\lambda$ above ground, we began to notice a much stronger influence of the ground upon the antenna's performance characteristics. Close to earth, the ground effects become very strong--strong enough to influence the way in which we design ground-plane vertical monopoles. In this exercise, we shall look at those effects a little more closely.

One common form of the ground plane places the radials at or just below the surface of the ground. NEC-2 cannot directly model this situation, because wires touching the ground or below the ground are disallowed. However, the program can simulate the situation closely enough to provide valuable information.

Open model 15-5-4.NEC, a vertical monopole with its ground plane just above the surface of the ground. Except for its height above ground, this 4-radial monopole for 7.05 MHz is identical to one we examined in free space and high above the ground.

NEC-2 permits wires to be very close to the ground, and heights as low as 0.001λ can simulate a ground plane in contact with the ground. Precision may be less than with antennas at great heights, but the trends revealed by changes in antenna performance with changes

in design will hold good. Since a wavelength at 7.05 MHz is about 42.5 m, 0.0425λ would be a minimum ground plane height, which we may round to 0.05 m for this exercise.

In successive steps, run the model at heights of 0.05 m, 0.1 m, 0.25 m, and 1.0 m above ground (remembering to increase the Z coordinate of the top of the vertical as the base height is raised). Then open model 15-5-32, a 32-radial version of the same monopole. Make the same runs and record the gain, take-off angle, and source impedance in the following table.

```

CM 1/4 wl vert: 7.05 MHz
CM 4 radials, 0.05 m
CE
GW 1 10 0 0 10.1846 0 0 .05 .025
GW 2 10 0 0 .05 11.796 0 .05 .00317
GW 3 10 0 0 .05 0 11.796 .05 .00317
GW 4 10 0 0 .05 -11.796 0 .05 .00317
GW 5 10 0 0 .05 0 -11.796 .05 .00317
GS 0 0 1
GE 1
GN 2 0 0 0 13 .005 0 0 0 0
EX 0 1 10 0 1 0
LD 5 1 1 10 2.4938E7
LD 5 2 1 10 2.4938E7
LD 5 3 1 10 2.4938E7
LD 5 4 1 10 2.4938E7
LD 5 5 1 10 2.4938E7
FR 0 1 0 0 7.05 0
RP 0 181 1 1000 -90 0 1 1
EN

```

15-5-4

15-5 Test Data				
Height Meters	15-5-4 Gain / TO	15-5-4 Source Z	15-5-32 Gain / TO	15-5-32 Source Z
0.05				
0.1				
0.25				
1.0				

Comments: Immediately apparent should be the high variability of performance figures for the 4-radial monopole in contrast to the relative stability of the figures for the 32-radial model. In the smaller model, small changes of height created large differences of gain and source impedance. In the 32-radial antenna, little changed.

15-5 Reference Data				
Height Meters	15-5-4 Gain / TO	15-5-4 Source Z	15-5-32 Gain / TO	15-5-32 Source Z
0.05	-1.57 / 26	49.4 + j 52.4	0.12 / 26	33.4 - j 0.4
0.1	-0.83 / 26	40.9 + j 32.6	0.17 / 25	32.0 - j 2.1
0.25	-0.40 / 25	36.3 + j 14.9	0.17 / 25	31.1 - j 4.3
1.0	-0.08 / 24	32.0 - j 0.0	0.16 / 24	29.5 - j 5.9

At a height of 1 m above ground, the performance of the two antennas begins to approach coincidence, both in terms of gain and source impedance. At the lowest height, the gain of the 4-radial version is less by about 1.5 dB. More significant to some designers is the increase in source impedance by over 15Ω , which many interpret to represent losses due to the ground by virtue of an insufficient ground plane assembly. As a result, ground plane assemblies consisting of 60 to 120 radials are common practice in the MF through lower HF range.

You may perform further checks upon this progression by using the 8- and 16-radial 7.05 MHz monopoles used in an earlier exercise (15-3). Lower each of these systems to the heights designated in this sampling and record the additional values. You may also wish to create some graphic curves and attempt to extrapolate a size for a radial system that will represent a point of diminishing returns, where further increases in the number of

radials will produce no further improvements worthy of the investment.

Although NEC-2 cannot certify the precision of the results of modeling ground-contact radials with radials that are immediately adjacent to the ground, the overall trends coincide reasonably with empirical measurements of those same trends. Nonetheless, modeling results in other aspects of ground radial systems have resulted in considerable re-evaluation of traditional methods of calculating such systems, especially where elevated but low radial systems are involved.

15-6.NEC: $1/4\lambda$ vs. $5/8\lambda$ monopole ground-plane systems for 7.05 MHz

Just as the 1.25λ center-fed horizontal wire antenna exhibits gain over a 0.5λ dipole, a $5/8\lambda$ vertical monopole can be expected to show gain over a correspondingly positioned $1/4\lambda$ monopole. Beyond the $5/8\lambda$ height, the monopole begins to break up with higher angle lobes dominating the pattern. Hence, the $5/8\lambda$ monopole represents one type of limit in monopole design, already about 2.5 times longer than the standard $1/4\lambda$ monopole. If the longest monopole proves too long for the construction project, which it may easily do at LF through MF, and if the source impedance presents no insurmountable problems, then a height between the extremes may be selected.

Open model 15-6-1.NEC, a $1/4\lambda$ vertical monopole over perfect ground. Essentially, this is the same monopole we have been using, but without a ground plane. We shall increase the height of this monopole by factors of 1.5, 2.0, and 2.5 as we move to a $3/8\lambda$, $1/2\lambda$, and finally a $5/8\lambda$ monopole. Record the maximum gain and source impedance in the chart below for each of these vertical lengths. The $5/8\lambda$ version of the monopole is shown to the right as a sample.

```

CM 5/8 w1 vert: 7.05 MHz
CM Perfect ground
CE
GW 1 10 0 0 25.4615 0 0 0 .025
GS 0 0 1
GE 1
GN 1
EX 0 1 10 0 1 0
LD 5 1 1 10 2.4938E7
FR 0 1 0 0 7.05 0
RP 0 181 1 1000 -90 0 1 1
EN
15-6-1C

```

When you have finished these runs, open model 15-6-2.NEC. This model uses the vertical element of the model just run plus a 32-radial ground plane 0.05m above the ground over average soil. As with the model over perfect ground, increase the height to $3/8\lambda$, $1/2\lambda$, and $5/8\lambda$, recording the gain and take-off angle as well as the source impedance.

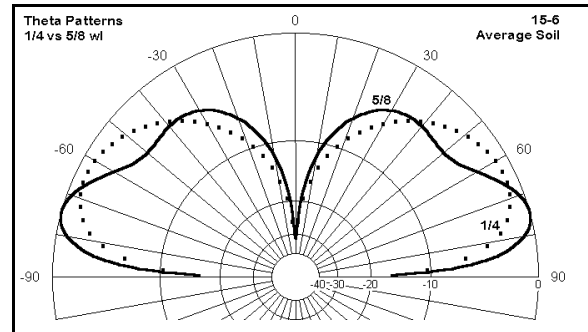
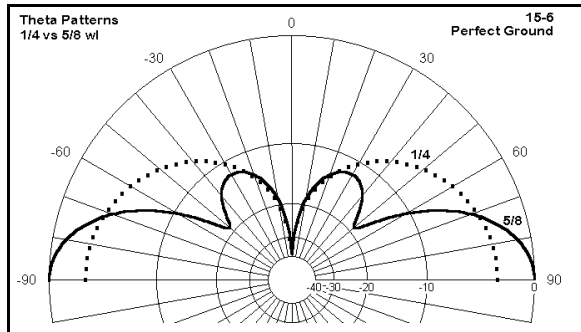
15-6 Test Data				
Height (λ)	15-6-1 Gain	15-6-1 Source Z	15-6-2 Gain / TO	15-6-2 Source Z
0.25				
0.375				
0.50				
0.625				

Comments: If we focus only upon the results over perfect ground, the $5/8\lambda$ monopole shows a 2.8 dB gain over the $1/4\lambda$ monopole. Intermediate lengths also show advantageous gain and may be worth considering in a design project.

15-6 Test Data				
Height (λ)	15-6-1 Gain	15-6-1 Source Z	15-6-2 Gain / TO	15-6-2 Source Z
0.25	5.14	$36.5 + j 2$	0.12 / 26	$33.4 - j 0$
0.375	5.72	$153.5 + j 288$	0.24 / 23	$131.9 + j286$
0.50	6.70	$1131.5 + j 415$	0.48 / 19	$1105.5 + j574$
0.625	7.96	$184.4 - j 456$	0.90 / 16	$184.4 - j456$

Over average soil, with a ground plane at the surface, the gain advantage of the longer monopole shrinks. However, the lower take-off angle for the $5/8\lambda$ antenna may be useful enough on its own to justify the investment in the longer monopole.

A comparison of perfect ground numbers and real ground numbers often turns up a disparity of performance promise. We can see the same disparity by comparing elevation patterns for the $1/4\lambda$ and the $5/8\lambda$ antennas over the two ground media, as in **Figure 15-6** below.



Although the patterns on the left show the classic textbook comparison between the standard and long monopoles, the patterns on the right show what the designer might expect to achieve with the ground plane and soil conditions specified. The $5/8\lambda$ monopole shows its distinct advantage in both gain and take-off angle. However, whether these benefits form enough of an advantage to justify the added complexity of construction and maintenance will remain an open question until clear design objectives can provide the foundation for an answer.

As a supplementary exercise, you may wish to develop--for any of the antennas we have examined in this chapter--radial systems with longer radials. Radials over 0.4λ and longer have been used for MF broadcast stations. You may also wish to exercise your ingenuity in creating ground planes with up to 120 radials using junctions close to but not at the main element so that no junction exceeds about 30 wires.

Summing Up

We have explored some of the dimensions of vertical monopole modeling, but certainly not all of them. Central to the exercises was a growing naturalness in modeling radial systems, whether for ground planes or for capacity hat and other structures. In fact, the array of structures provided in the models can form the basis for a collection that you may recall and scale to other frequencies (considering both wire length and diameter). Reinventing the wheel of a radial system for each model can become a bit tedious; and a few models on file can ease the process considerably.

Once constructed, ground planes do not lose their fascination. The requirements for highly elevated and for surface ground planes appear to differ considerably, with minimal radials needed higher up and very many needed close to or upon the earth. One of the more interesting territories still in need of extensive work is the region between about $1/2\lambda$ up and the surface. The performance of ground plane monopoles at various heights in this region over the wide variety of soil conditions is open to systematic study both with models and with real antennas.

Indeed, there remain a number of open questions about the adequacy of antenna models using NEC in all its forms to represent actual ground plane antennas close to the earth. For example, the use of slightly elevated radials, perhaps 0.05λ to 0.1λ above ground, has emerged from modeling studies which also suggest that as few as 6 to 8 such radials might substitute for the formerly used systems of over 120 buried radials. However, empirical measurements by different experimenters appear to yield conflicting results, some tending to confirm the findings, others tending to contradict them. It would appear that one of radio communications' most fundamental antennas is not so simple an affair as it might seem at first sight.

16. Vertically Polarized Antennas and Arrays

***Objectives:** In these exercises, you will meet a wide variety of vertically polarized antennas and arrays, ranging from the vertical dipole to 1λ loops of phased verticals to directional vertical antenna systems. Some arrays will employ parasitic techniques, while others will use phased elements.*

The ground-plane vertical monopole does not exhaust the collection of vertically polarized antennas that find extensive use in communications systems. Indeed, the special place of the ground-plane vertical emerged from the earliest days of radio communications and broadcasting as nearly the only practical antenna for the low and very low frequencies used. The opening of the short wave (HF) region of the spectrum saw the development of both horizontal and vertical antennas which used the $1/2\lambda$ dipole as the fundamental element.

The fundamental difference between the collection of antennas (with an exception or 2) in this chapter and those in the last chapter is that our new additions will model perfectly well in free space. That is, they do not require either a ground plane or an image antenna (through the use of perfect ground) to be complete. This fact does not mean that these antennas will not be affected by the ground: the effects will be profound. However, without the addition of a ground plane, these antennas can function at any height above the ground. We may call them "self-contained."

As we shall discover in a later chapter, many of these self-contained verticals offer potential for VHF and UHF applications in addition to their "normal" HF uses. With respect to HF applications, we shall find that we may use NEC-2 to uncover some properties of vertically polarized self-contained antennas, including their response over soils of various qualities in both the immediate antenna vicinity and in the antenna's far field. In almost all cases, we shall be interested in both the elevation and azimuth patterns for the antennas, since one of the reasons for using these lower gain antennas is the signal-to-noise ratio improvement occasioned by the absence of high-angle radiation pattern lobes.

Although the basic antennas--the dipoles--are omni-directional, some of the self-contained verticals have bi-directional patterns ranging from barely detectable ovals to distinct "figure 8s." Not only can we use parasitic and phasing techniques to create

directional antennas from the omni-directional basic types, but as well we can enhance the initial bi-directivity of other versions to create quite effective uni-directional arrays. Along the way, we shall not neglect to explore some of the directional potential for $1/4\lambda$ monopoles. In the end, we shall find that vertically polarized antennas and arrays comprise a fertile field for design and analysis through modeling.

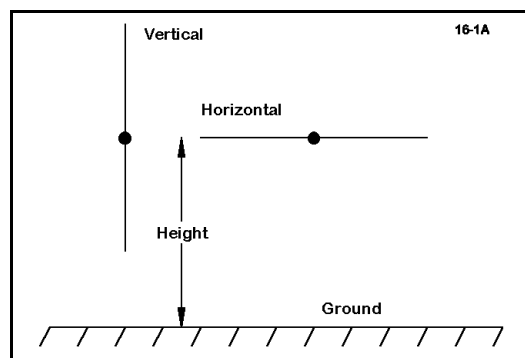
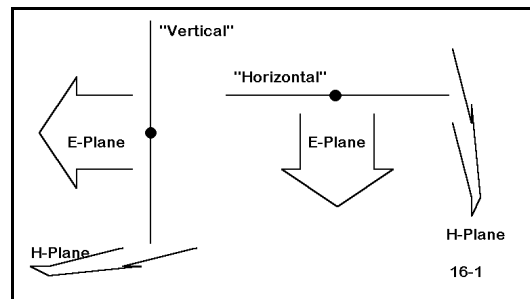
Exercise Preparation

The exercises in this collection will be quite diverse. Some will involve comparisons of vertical and horizontal antennas. Others will require that you create ground planes and change soil types in order to explore various antenna properties. Still others will be shortened and require either end-loading or inductive loading. Some will demand close attention to wire placement to ensure correct modeling. Finally, we shall employ transmission lines to create a rudimentary phased array. Virtually everything you practiced in Part B of this guide may come into play somewhere in the collection of models we shall create.

As always, use care in saving variants of the supplied models to ensure that you preserve (and can later find) any interesting model you encounter.

16-1.NEC: Vertical and horizontal dipoles for 10 MHz

Models 16-1-1.NEC and 16-1-2.NEC are identical except for one fact: one is extended along the Z-axis, while the other is extended along the Y-axis. In free space, this difference makes no difference to performance, but it does make a difference to terminology. "Vertical" and "horizontal" are terms which only make sense when there is a ground or other plane of reference.



As shown in **Figure 16-1**, in free space we refer to the E and H planes of the antenna's radiation, depending upon whether we are referring to radiation in the plane of the wire or at right angles to the wire. For the two antennas, the E-planes are at right angles to each other.

Over ground or some other reference plane, as illustrated in **Figure 16-1A**, the terms "vertical" and "horizontal" acquire meaning and have become the modeling terms of choice for most

purposes. A convention with less universality is placing the height of a vertical antenna at the source, ordinarily the center of the length of the wire, as indicated in the illustration. In many instances, the term "vertical" is retro-fitted to free space if the main length of wire lies along the Z-axis. If the main length of wire lies along either the X- or the Y-axis, then by convention, we call the antenna horizontal, even in free space.

With these reminders, we can begin work on models 16-1-1.NEC, a vertical dipole in free space, and 16-1-2.NEC, a horizontal dipole in free space. The only difference between the models is the axis along which the main element wire lies: Z in the case of the vertical and X in the case of the horizontal. Both are 1" diameter 6061-T6 aluminum center-fed wires 47.1' long, resonant at 10 MHz.

```

CM Vertical Dipole: 10.0 MHz
CM Free Space
CE
GW 1 21 0 0 0 0 47.1 .041665
GS 0 0 .3048
GE 0
EX 0 1 11 0 1 0
LD 5 1 1 21 2.4938E7
FR 0 1 0 0 10 1
RP 0 181 1 1000 -90 0 1 1
FR 0 1 0 0 10 1
RP 0 1 360 1000 90 0 1 1
EN
16-1-1
    
```

```

CM Horizontal Dipole: 10.0 MHz
CM Free Space
CE
GW 1 21 0 0 0 47.1 0 0 .041665
GS 0 0 .3048
GE 0
EX 0 1 11 0 1 0
LD 5 1 1 21 2.4938E7
FR 0 1 0 0 10 1
RP 0 181 1 1000 -90 0 1 1
FR 0 1 0 0 10 1
RP 0 1 360 1000 90 0 1 1
EN
16-1-2
    
```

Run both of these antenna, recording the maximum gain and the source impedance in the table below. Then for each antenna create a S-N average ground (cond.=0.005; perm.=13), and place the antenna centers at three successively lower heights: 2λ , 1λ , and 0.5λ . Since a wavelength at 10 MHz is about 98.357' you may round the height numbers to 200, 100, and 50 feet. From the initial run of each model, determine from the elevation pattern the take-off angle and place this figure into the azimuth pattern request for the specific model variant.

16-1 Test Data				
Antenna Height (λ)	Vertical: Gain dBi/TO	Vertical: Source Z	Horizontal: Gain dBi/TO	Horizontal: Source Z
Free Space				
2λ				
1λ				
0.5λ				

Comments: Of immediate note is the lower gain of the vertical dipole at each level, despite the equality of the antennas in free space. However, if you compare azimuth patterns, you will see why: the figure-8 pattern of the horizontal dipole over ground has both nulls and lobes, compared to the circular azimuth pattern of the vertical dipole. However, do not stop the comparison at this point. Examine the elevation patterns as well, noting the multiple and high lobes of the horizontal dipole. Since radiation off the ends of a dipole is minimal, the vertical dipole has no "straight-up" lobe.

There are less obvious differences between the antennas. For example, note the significant change of source reactance with the change of horizontal antenna height, along with a change of resistance that is larger than for the vertical antenna. Moreover, note the variability of the vertical antenna take-off angle while the take-off angle for the horizontal dipole moves in a regular progression upward as the antenna height is reduced.

16-1 Reference Data				
Antenna Height (λ)	Vertical: Gain dBi/TO	Vertical: Source Z	Horizontal: Gain dBi/TO	Horizontal: Source Z
Free Space	2.13 / ---	71.9 - j 0.1	2.13 / ---	71.9 - j 0.1
2 λ	4.62 / 6°	71.8 + j 0.0	8.00 / 6°	70.0 - j 2.2
1 λ	3.23 / 27°	71.3 + j 0.2	7.82 / 14°	68.7 - j 4.7
0.5 λ	0.61 / 77°	69.0 + j 0.9	7.57 / 63°	65.4 - j 8.8

Short of dragging the bottom of the vertical dipole on the ground, you may supplement this exercise with additional runs using smaller distances between antenna heights. The lower limit for comparability on the terms established (setting the antenna centers at the same height) is roughly $1/4\lambda$ above the ground. However, even with this limitation, you will find some interesting patterns to both the lobes of the antenna patterns and the source impedance.

16-2.NEC: A 7.05 MHz vertical dipole over various soils

In this exercise, we may consider two questions at once: What are the performance characteristics of a vertical dipole over various soils types. Does the presence of a ground plane beneath the antenna improve the performance of the vertical dipole. Of course, we must assess these questions at various antenna heights. Our aim is to develop the beginnings of a systematic study, so the selection of the test antenna, the heights to be used, and the size of the ground plane will be of considerable import.

Figure 16-2, on the next page, shows the basic structure of the models. Eliminating the ground plane structure, the evaluation of the dipole will be a simple task. For a model with a ground plane beneath, we may adapt the 32-radial system used with a $1/4\lambda$ monopole close to the earth--within about 2" at 7.05 MHz.

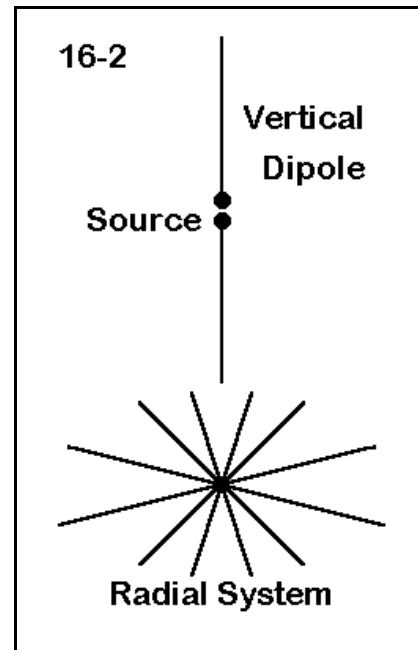
To assess the properties of the antenna under varying conditions, let's use the following antenna heights as defined by the center or source point for the dipole: 2λ (280'), 1λ (140'), 0.5λ (70'), and 0.25λ (35'). Since the dipole is 66.6' long, the lowest height for the center will bring the lower end within 1.7' of the ground.

```

CM vert dipole w/gp: 7.05 MHz          16-2-2
CM 32-radial ground plane
CE
GW 1 21 0 0 313.3 0 0 246.7 .08335
GW 2 10 0 0 .164 42.2 0 .164 .0104
GW 3 10 0 0 .164 41.389 8.233 .164 .0104
GW 4 10 0 0 .164 38.988 16.149 .164 .0104
GW 5 10 0 0 .164 35.088 23.445 .164 .0104
GW 6 10 0 0 .164 29.84 29.84 .164 .0104
GW 7 10 0 0 .164 23.445 35.088 .164 .0104
GW 8 10 0 0 .164 16.149 38.988 .164 .0104
GW 9 10 0 0 .164 8.233 41.389 .164 .0104
GW 10 10 0 0 .164 0 42.2 .164 .0104
GW 11 10 0 0 .164 -8.233 41.389 .164 .0104
GW 12 10 0 0 .164 -16.149 38.988 .164 .0104
GW 13 10 0 0 .164 -23.445 35.088 .164 .0104
GW 14 10 0 0 .164 -29.84 29.84 .164 .0104
GW 15 10 0 0 .164 -35.088 23.445 .164 .0104
GW 16 10 0 0 .164 -38.988 16.149 .164 .0104
GW 17 10 0 0 .164 -41.389 8.233 .164 .0104
GW 18 10 0 0 .164 -42.2 0 .164 .0104
GW 19 10 0 0 .164 -41.389 -8.233 .164 .0104
GW 20 10 0 0 .164 -38.988 -16.149 .164 .0104
GW 21 10 0 0 .164 -35.088 -23.445 .164 .0104
GW 22 10 0 0 .164 -29.84 -29.84 .164 .0104
GW 23 10 0 0 .164 -23.445 -35.088 .164 .0104
GW 24 10 0 0 .164 -16.149 -38.988 .164 .0104
GW 25 10 0 0 .164 -8.233 -41.389 .164 .0104
GW 26 10 0 0 .164 0 -42.2 .164 .0104
GW 27 10 0 0 .164 8.233 -41.389 .164 .0104
GW 28 10 0 0 .164 16.149 -38.988 .164 .0104

```

The antenna will be a 2" diameter 6061-T6 aluminum dipole, as partially shown on the left, with a 32-radial ground plane. Simply omit the wires beyond the first one to picture the dipole without a ground plane. These are models 16-2-1.NEC (no ground plane) and 16-2-2.NEC (with ground plane). Note that the vertical dipole uses 21 segments for its $1/2\lambda$, while the $1/4\lambda$ radials use 10 segments each.



For the exercise, you will have to adjust the dipole height $\pm 33.3'$ in the Z-axis column relative to the specified center heights. For the 2λ height, this gives an end 1 Z of 313.3' and an end 2 Z of 246.7' for wire 1. Only wire 1 need be changed for the tests.

The soils we shall use conform to standard definitions, as listed in the Appendix to this guide: "very good" (conductivity = 0.0303 s/m; permittivity = 20), "average" (conductivity = 0.005 s/m; permittivity = 13), "poor" (conductivity = 0.002 s/m; permittivity = 13), and "very poor" (conductivity = 0.001 s/m; permittivity = 5). In other exercises, we have noted that performance figures over different soils do not create smooth curves, so we should not anticipate values before they emerge from the calculations.

For the dipole alone and the dipole with a ground plane beneath it, and for each soil type,

record the maximum gain in dBi, the take-off angle in degrees, and the source impedance in terms of resistance and reactance in the appropriate boxes within the table on the next page. Since the table is large, a few reference values are scattered throughout it in lieu of providing a separate reference table. The 32-radial model is large (about 340 segments), so expect longer run times on slower computers.

16-2		Test Data			
Antenna & Height	Very Good	Average	Poor	Very Poor	
Alone 2 λ		4.45 / 7° 71.7 + j 0.1			
W/GP 2 λ			4.78 / 06° 71.7 + j 0.1		
Alone 1 λ	5.21 / 27° 71.0 + j 0.2				
W/GP 1 λ				3.77 / 12° 71.4 + j 0.3	
Alone 0.5 λ				1.39 / 16° 69.6 + j 1.0	
W/GP 0.5 λ		0.30 / 13° 69.0 + j 1.0			
Alone 0.25 λ			0.22 / 19° 95.8 + j 4.3		
W/GP 0.25 λ	2.01 / 15° 96.6 + j 7.5				

Comments: Although the take-off angle shows a consistent rise as the soil quality grows worse, the antenna gain is subject to more erratic variations. Although the gain over poor soil with an antenna height of 1 λ is less than the gain for either average or very poor soil, by the time the antenna reaches a height of 1/4 λ at its center, the gain over poor soil is higher than for either average or very poor soil.

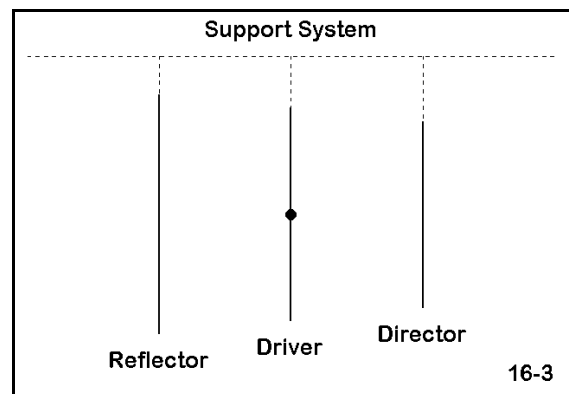
Noticeable differentials of gain, although not at a level making any operational difference to an antenna installation, begin to occur when the antenna is centered at the 1/2 λ mark. The differentials are more noticeable with the antenna at its lowest height, but the amounts never rise above 0.8 dB. The table suggests that the rise in differential gain between having no ground plane and having a ground plane might be a relatively smooth

curve as the antenna is brought from the $1/2\lambda$ mark down to the $1/4\lambda$ point. Do not make this assumption. As a supplemental exercise, test the antenna at each 5' increment between the half and quarter wavelength points and record the data. The gain peaks that you will encounter over some soils may surprise you. Moreover, where no peak is detectable within the specified range of heights, make further tests at 5' intervals above the $1/2\lambda$ mark. These test will be especially apt for the dipole over poor and very poor soils.

Since the improvement in gain effected by the 32-radial ground plane appears somewhat marginal on a cost-benefit basis, it is legitimate to wonder if the same benefits might be garnered from a simpler radial pattern, perhaps one with only 4 radials. As another supplement to this study, create a 4-radial ground plane and test the dipole at 5' intervals from the $1/2\lambda$ center point down to the $1/4\lambda$ center position. You may also wish to complete the data study by doing the same for 8-radial and 16-radial systems, graphing either the gain results or the source impedance figures for all of the radial system and for the dipole alone.

16-3.NEC: A 3-element vertical Yagi for 7.05 MHz

Converting the omni-directional pattern of a vertical antenna into a directional pattern is straightforward. You may use either parasitic or phasing techniques to achieve the goal. In this exercise, you will work with a 3-element vertically oriented parasitic beam, as sketched in **Figure 16-3**. The support system shown is apt to wire construction, wherein a heavy overhead line may support the elements easily. Other construction methods are equally common. Note that the element designations correspond to those you will encounter in the chapter devoted entirely to Yagi antennas.



```

CM 3-el vert Yagi: 7.05 MHz
CM 1/2 wl above ground
CE
GW 1 21 0 0 103.3 0 0 36.7 .08335
GW 2 21 20 0 100 20 0 40 .08335
GW 3 21 -20 0 106 -20 0 34 .08335
GS 0 0 .3048
GE 1
GN 2 0 0 0 13 .005 0 0 0 0
EX 0 1 11 0 1 0
LD 5 1 1 21 2.4938E7
LD 5 2 1 21 2.4938E7
LD 5 3 1 21 2.4938E7
FR 0 1 0 0 7.05 0
RP 0 181 1 1000 -90 0 1 1
FR 0 1 0 0 7.05 0
RP 0 1 360 1000 77 0 1 1
EN

```

16-3-1

Open models 16-3.NEC and 16-3-1.NEC. The first model is simply the same vertical dipole with a center height of $1/2\lambda$ that we have used in the preceding exercise. The heavier 2" diameter 6061-T6 aluminum element may be much more difficult to suspend from an overhead rope, but the model will serve as a comparator for its companion, a 3-element beam made from the same material. This model, shown at the left, uses 20' spacing between elements, with a shorter director and longer reflector, relative to the driven element, as one might expect in such designs. The model was designed so that the

driven element would be the same length as the dipole alone. Only the driver is fed at its center.

For the dipole and the parasitic array, record (as applicable) the gain, the 180° front-to-back ratio, and the source impedance in the table on the next page. As well pay close attention to the elevation and azimuth patterns for the antenna.

16-3 Test Data			
Antenna	Gain dBi	F-B dB	Source Z $R \pm jX \Omega$
Vertical Dipole			
3-El. Array			

Comments: The array shows very considerable gain over the dipole alone, and at the same take-off angle. The front-to-back ratio is considerable. The source impedance for this design permits direct use of a $50\text{-}\Omega$ system feedline. Of equal importance with these performance specifications is the operating beamwidth of the array. The -3 dB points are 128° apart, providing a wide span of coverage.

16-3 Reference Data			
Antenna	Gain dBi	F-B dB	Source Z $R \pm jX \Omega$
Vertical Dipole	0.22	----	$68.6 + j 0.8$
3-El. Array	4.71	18.05	$47.0 + j 0.5$

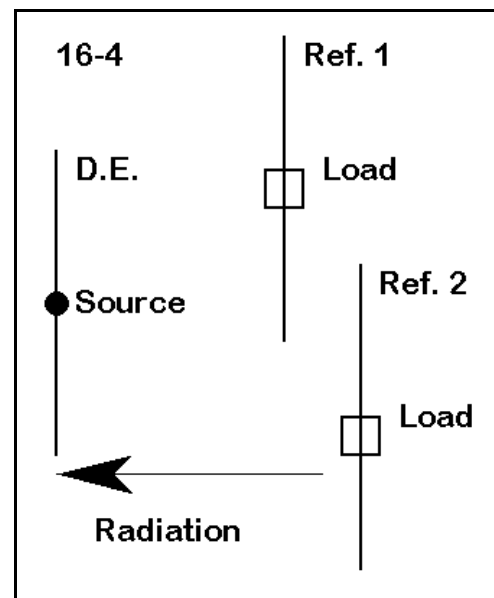
This array was not designed to provide either the maximum gain possible or the highest front-to-back ratio that might be obtained. Rather, it was designed for the convenience of the source impedance, while still providing useful gain and rear nulling. As a supplemental exercise, you may wish to work with the dimensions to achieve improvements in performance, accepting whatever source impedance emerges. Second, you should also reduce the wire size to a lighter copper AWG size which might permit overhead support for the elements. Adjust the element lengths and spacings to restore or improve upon the performance achieved with the aluminum model.

Third, the array is initially set very high. Test the performance of the antenna--or any of the improved or wire versions you create--at lower heights. It will be useful to also model the driven element alone as a simple dipole in order to sort out changes in the performance figures. You will wish to know not only what affects the lower heights produce, but as well what improvements the 3-element array can offer over the dipole at each height. Finally, decrease the length of the reflector to the length of the director. Then place an inductive load at the element center to increase its electrical length and restore the array's performance. Now consider ways to use the results of this modeling task to create a reversible array with a simple remote switching system. You may also design the director at reflector length and place a capacitive load at its center.

16-4.NEC: A triangular parasitic array for 7.05 MHz

The array we have just considered is in principle reversible, providing bi-directional coverage. Full coverage of the entire horizon would require the addition of at least two more elements. However, vertical arrays have a certain versatility of geometry that makes them attractive choices for some applications. For instance, we may set 3 elements in a triangle about $1/4\lambda$ on a side, as shown in **Figure 16-4**. One element functions as a driver, while the other two act as reflectors. Although the highest achievable gain is less than for a true 3-element Yagi, this array provides the ability to cover virtually the entire horizon in three steps with only three vertical elements.

Note that the reflectors have loads at their centers. This fact indicates that the elements are not inherently sized to act as reflectors. If each reflector is the correct size to be a driven element, then an inductively reactive load can electrically lengthen the element to serve when needed as a reflector.



```

CM triangle array: 7.05 MHz
CE
GW 1 21 0 0 101.9 0 0 38.1 .08335
GW 2 21 -30 17.5 101.9 -30 17.5 38.1 .08335
GW 3 21 -30 -17.5 101.9 -30 -17.5 38.1 .08335
GS 0 0 .3048
GE 1
GN 2 0 0 0 13 .005 0 0 0 0
EX 0 1 11 0 1 0
LD 4 2 11 11 0 90 0
LD 4 3 11 11 0 90 0
LD 5 1 1 21 2.4938E7
LD 5 2 1 21 2.4938E7
LD 5 3 1 21 2.4938E7
FR 0 1 0 0 7.05 0
RP 0 181 1 1000 -90 0 1 1
FR 0 1 0 0 7.05 0
RP 0 1 360 1000 77 0 1 1
EN

```

16-4

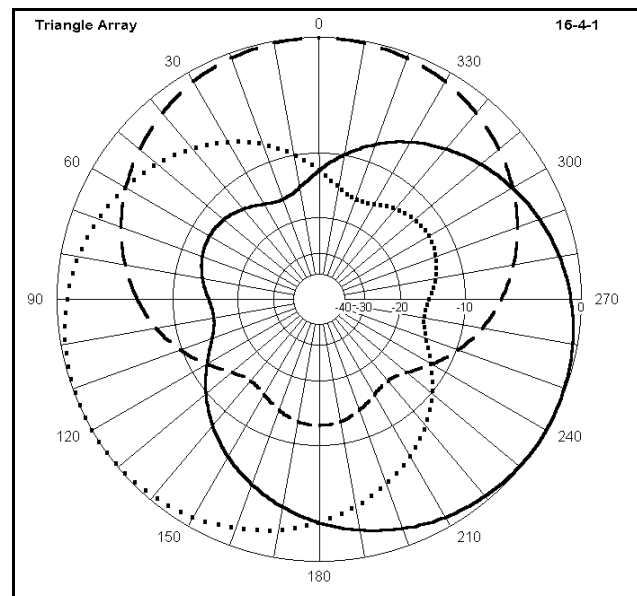
Open model 16-4.NEC. This model follows our progression of 2" diameter aluminum element vertical arrays elevated $1/2\lambda$ at their center. This triangle of elements has wire 1 as the driven element and wires 2 and 3 as the loaded reflectors. The elements are shorter than those used for the dipoles because this array consists only of a driver and reflectors, without a director. Simple type 4 loads are used to place a reactance of $90\ \Omega$ in the center of each reflector. At a more advanced stage of

design, you may replace the type 4 loads with R-L-C loads and factor in the Q of the required inductor as well. Only with R-L-C loads can a frequency sweep be effectively run.

Run the model. You should obtain a gain of about 4.62 dBi, with a 180° front-to-back ratio of about 12.5 dB. The source impedance will be about $62 - j6\ \Omega$. The beamwidth of the antenna will be approximately 126° between -3 dB points. Although not as effective in nulling signals to the rear of the array as the 3-element vertical Yagi, the antenna provides significant improvements over a single vertical dipole centered in the same position.

Now systematically replace the load on one reflector with the source and the source on its element with one load. Rerun the model. Repeat the procedure once more to obtain the third azimuth pattern possible with this array. combine the azimuth patterns into a single plot, similar to the one shown in **Figure 16-4-1**.

The purpose of the exercise is to demonstrate the relative simplicity of obtaining virtually full horizon coverage with three directional beams composed of a total of only 3 elements with a remote switching system. There are numerous possible switching systems involving relays and other devices. Switching can occur at the elements themselves or at a central point. For example, transmission lines can transform reactances along their length. You may wish to calculate various loads and transmission line lengths to achieve a remote value of $90\ \Omega$ inductive reactance at the reflector elements, while the



transmission line used becomes just one more section of the main feedline for the driven element.

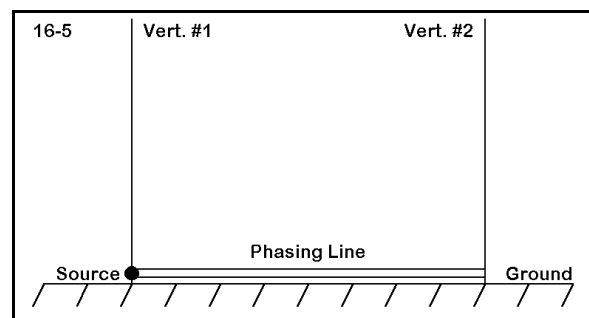
Like the model used in the preceding exercise, this triangle uses large diameter aluminum elements set very high. As a supplemental set of exercises, rerun the model at various lower heights and with both aluminum and copper materials of various diameters. For any design of interest, replace the R-X loads with suitable series R-L-C loads and include a value of resistance that reflects a reasonable assumption about the Q of the loading inductors. Scale the array to other frequencies of interest. Take frequency sweeps to determine the operating bandwidth for both the source impedance and the desired performance figures.

It is also possible to ensure that almost no dips in gain occur anywhere along the horizon with a vertical array of 4 elements.

16-5.NEC: A phased array of $1/4\lambda$ monopoles for 10 MHz

Directional gain with arrays of vertical antennas may employ phasing techniques as well as parasitic methods. In this exercise, we shall look at a pair of $1/4\lambda$ vertical monopoles spaced about $1/4\lambda$ apart. Each element will be 7.25 mm in diameter copper "wire." We shall initially model the antennas over perfect ground with separate current feeds in order to establish relatively ideal phase conditions for a maximum rearward null. Then we shall replace the separate feeds with a simple phasing transmission line. Finally, we shall place the assembly on ground planes over real soil conditions.

Figure 16-5 shows the general scheme of our system, including the phasing line, but omitting the details of the eventual ground plane. Open model 16-5.NEC. In this version of the model, you will note the addition of a third wire at a remote position. This wire contains the source and network termination necessary to effect a current source for the antenna. Should you be interested in the source impedance, you would look in the network termination portion of the tabular NEC output file.



```

CM Phased 1/4 wl monopoles
CM Separate current sources
CE
GW 1 21 0 0 7.255 0 0 0 .003625
GW 2 21 7.495 0 7.255 7.495 0 0 .003625
GW 3 2 2997.925 2997.925 2997.925 2997.985 2997.985 2997.985 .000814
GS 0 0 1
GE 1
GN 1
EX 0 3 1 0 0 1.414214
EX 0 3 2 0 1.414214 -.0000002199
LD 5 1 1 21 5.8001E7
LD 5 2 1 21 5.8001E7
LD 5 3 1 2 5.8001E7
NT 3 1 1 21 0 0 0 1 0 0
NT 3 2 2 21 0 0 0 1 0 0
FR 0 1 0 0 10 0
RP 0 1 360 1000 89 0 1 1
EN
    
```

16-5

The two sources have identical current magnitude specifications, but the second element source has a phase that is -90° relative to the first element source. Since each element is approximately resonant, the sourcing system should produce close to the maximum null

possible for these two elements in the given arrangement. Run this model and record the maximum gain and the 180° front-to-back ratio (as derived from the radiated power table figures) on the table on the next page. The source impedance figures will not be important for our purposes, but you may check them out of interest. Since the ground is perfect, we need not concern ourselves with the take-off angle.

Open model 16-5-1.NEC. The elements of this model are the same as those used in the first model, but the dual current source has been replaced by a single voltage source and a phasing (transmission) line from the source on one element to the former position of the source on the second element. Note that the $50\text{-}\Omega$ line reverses connections between the two ends. The line length of 11.356 m is equivalent to a direct connection with a line velocity factor of 0.66. The particular transmission line used in the model represents a readily available commercial transmission line (coaxial cable). Run this model and record the gain, 180° front-to-back ratio, and the source impedance in the table on the next page.

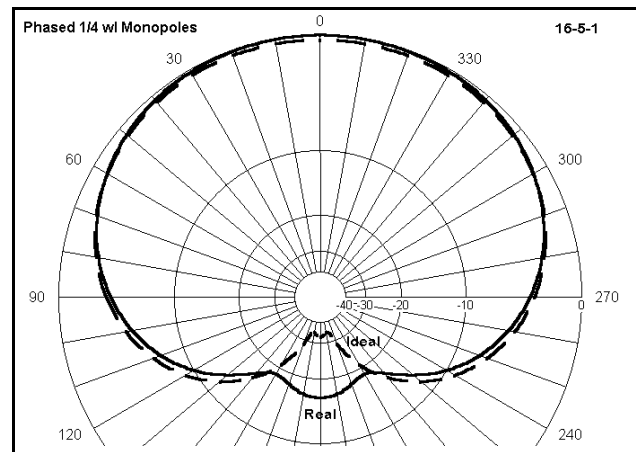
```

CM Phased 1/4 wl monopoles
CM Transmission line phasing: simple
CE
GW 1 21 0 0 7.255 0 0 0 .003625
GW 2 21 7.495 0 7.255 7.495 0 0 .003625
GS 0 0 1
GE 1
GN 1
EX 0 2 21 0 1 0
LD 5 1 1 21 5.8001E7
LD 5 2 1 21 5.8001E7
TL 1 21 2 21 -50 11.35578 0 0 0 0
FR 0 1 0 0 10 0
RP 0 1 360 1000 89 0 1 1
EN
    
```

16-5-1

16-5 Test Data				
Model	Gain dBi	T-O Angle	F-B dB	Source Z $R \pm jX \Omega$
16-5		-----		-----
16-5-1		-----		
16-5-2				

Comments: Although the gain of the line-phased system is slightly higher than that of the ideal system, the front-to-back ratio is considerably lower. **Figure 16-5-1** makes the difference visually evident in the overlay of the "ideal" pattern atop the pattern for the "real" or line-phased system. The limitation in the obtainable null is a function of two factors: the transmission line chosen for the task of phasing and the simple direct line phasing method.



You may wish to supplement the exercise so far by trying values of impedance and velocity factor for the simple transmission line phasing arrangement until you obtain the best null possible. As an alternative, you may wish to create a third wire (position anywhere) that is both short (1-segment) and thin. Place the source on the wire. Remove the transmission line between the two elements and create transmission lines between each element and the new wire. Be certain to place the junctions on the lowest segment of each wire. Ensure that the transmission line to the second element has reversed connections. Now try various lengths of transmission line for each of the two new lines. Using standard commercial lines, work toward the shortest combination of lines that together would still be long enough to reach from one element to the other, allowing for velocity factor--and of course, which together yield the deepest rear null.

Note that in a phased pair of vertical radiators, the deepest null does not coincide with the point of maximum gain. In fact, the maximum gain point may be well above 1 dB higher than the gain with the deepest rear null. Consider various applications and try to imagine circumstances which might call for the maximum gain at the expense of front-to-back ratio, on the one hand, and on the other, call for the greatest rejection to the rear, regardless of the forward gain. Also imagine situations which might call for a compromise gain vs. rear null combination. In these hypothetical situations, the source impedance has not been considered a significant issue. You may wish to add it into the mix of significant parameters to make the problem more complex.

One line remains on the table: open model 16-5-2.NEC. This model places the antenna over average real ground (S-N: cond. = 0.005 s/m; perm. = 13). To effect this move, we had to elevate the model slightly, since NEC-2 ground must be above the surface by at least 0.001λ . The 4-radial ground plane for each element was created by modeling the element in isolation in free space and attaching a radial system which would bring the system to resonance. Since the resultant radials, even rotated to form a pairs of Xs, would overlap at two points, one radial system was elevated further so that the wires would not make contact and create an error condition for the model.

Run the model, and enter in the table the gain, front-to-back ratio, take-off angle, and source impedance.

```

CM Phased 1/4 wl monopoles: 10 MHz
CM Transmission line phasing: simple
CM Average ground
CE
GW 1 21 0 0 7.285 0 0 .03 .003625
GW 2 21 0 0 .03 5.86899 5.86899 .03 .003625
GW 3 21 0 0 .03 -5.86899 5.86899 .03 .003625
GW 4 21 0 0 .03 -5.86899 -5.86899 .03 .003625
GW 5 21 0 0 .03 5.86899 -5.86899 .03 .003625
GW 6 21 7.495 0 7.295 7.495 0 .04 .003625
GW 7 21 7.495 0 .04 13.3639 5.86899 .04 .003625
GW 8 21 7.495 0 .04 1.62601 5.86899 .04 .003625
GW 9 21 7.495 0 .04 1.62601 -5.86899 .04 .003625
GW 10 21 7.495 0 .04 13.3639 -5.86899 .04 .003625
GS 0 0 1
GE 1
GN 2 0 0 0 13 .005 0 0 0 0
EX 0 2 21 0 1 0
LD 5 1 1 21 5.8001E7
LD 5 2 1 21 5.8001E7
LD 5 3 1 21 5.8001E7
LD 5 4 1 21 5.8001E7
LD 5 5 1 21 5.8001E7
LD 5 6 1 21 5.8001E7
LD 5 7 1 21 5.8001E7
LD 5 8 1 21 5.8001E7
LD 5 9 1 21 5.8001E7
LD 5 10 1 21 5.8001E7
TL 1 21 2 21 -50 12.27912 0 0 0 0
FR 0 1 0 0 10 0
RP 0 181 1 1000 -90 0 1 1
FR 0 1 0 0 10 0
RP 0 1 360 1000 67 0 1 1
EN

```

16-5-2

16-5 Reference Data				
Model	Gain dBi	T-O Angle	F-B dB	Source Z $R \pm jX \Omega$
16-5	8.21	-----	32.13	-----
16-5-1	8.52	-----	16.44	39.7 - j 1.9
16-5-2	-0.58	23°	12.41	69.2 + j 56.2

Comments: The projected performance of the phased array over real ground may seem initially disappointing. However, this model uses only 4 radials per antenna element. In addition, the soil chosen typically calculates poorer performance figures than either very good or poor soil. Supplementary to this exercise, create increasingly larger radial systems for the array until the performance ceases to improve by any significant amount. Doubling the number of radials with each model is advisable. (Determining what constitutes a significant amount of improvement is a part of the work.) Additionally, try

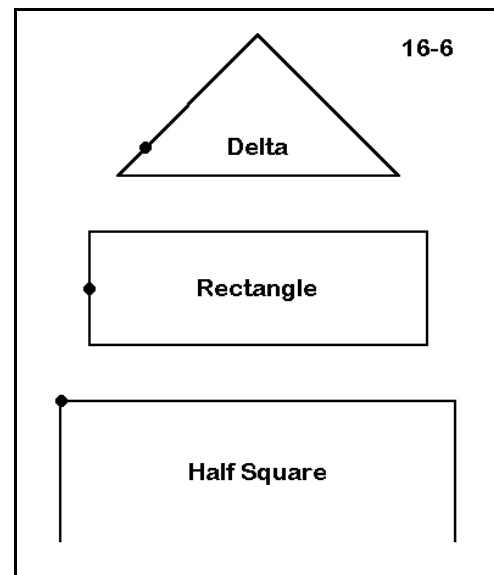
each new system over various soils: minimally, very good, average, poor, and very poor.

In the process of developing larger radial systems, you may wish to place the radials at the same height above ground. This will require you to terminate radials where they intersect radials from the other element, a system often shown for commercial installation designs. Alternatively, you may also wish to create a single screen of wires to cover the area that a radial system would occupy.

16-6.NEC: 1λ vertically polarized antennas for 7.15 MHz

Vertically polarized antennas need not have a vertical appearance. In this exercise, we shall look at some "SCVs," self-contained vertically polarized 1λ wire antennas as possible alternatives to the standard vertical monopole and dipole. Since the antennas are self-contained, that is, they do not require a ground plane to complete the antenna electrically, we may model them directly over real soil with no ground plane beneath them.

Figure 16-7 shows three potential configurations for the SCVs, along with their common names. For each antenna, examine the source point, indicated by the dot. For the delta--here a right triangle--the source is a $1/4\lambda$ from the apex of the triangle. The source for the rectangle is mid-side, a position $1/4\lambda$ from the center of the horizontal wires. In the half square, the source is at the junction of one of the vertical wires and the horizontal wire, $1/4\lambda$ from the vertical's tip. In each case, the antenna shows maximum (but not exclusively) vertically polarized radiation with the source at the indicated positions. The horizontal wire connecting the source point with a corresponding position on the opposite side of the array constitutes a current phase-reversing line, which permits the radiation of the two vertical sections to add in a direction broadside to the array.



```

CM Right-Angle Delta: 7.15 MHz
CE
GW 1 15 -30.4 0 19.6 0 0 50 3.36778215223097E-03
GW 2 15 0 0 50 30.4 0 19.6 3.36778215223097E-03
GW 3 19 30.4 0 19.6 -30.4 0 19.6 3.36778215223097E-03
GS 0 0 .3048
GE 1
GN 2 0 0 0 13 .005 0 0 0 0
EX 0 1 3 0 1 0
LD 5 1 1 15 5.8001E7
LD 5 2 1 15 5.8001E7
LD 5 3 1 19 5.8001E7
FR 0 1 0 0 7.15 0
RP 0 181 1 1000 -90 90 1 1
FR 0 1 0 0 7.15 0
RP 0 1 360 1000 70 0 1 1
EN

```

16-6-1

Open model 16-6-1.NEC, a right-angle delta for 7.15 MHz using #12 AWG copper wire. The apex of the triangle is limited to 50' above average soil, a trait that all of the models in this exercise will share. The source is located on wire 1, segment 3, about 15% of the way up the leg. Run this model, recording in the table on the next page the maximum gain, the take-off angle, and the source impedance.

Open model 16-6-2.NEC, a rectangle for 7.15 MHz, also constructed of #12 AWG copper wire. Like the delta, the maximum height allowed for the antenna is 50' above ground. If you examine the model, you will instantly discover that it has too many wires for a single rectangle. Side-fed single rectangles have very low source impedances. To raise the source impedance, you may create an impedance transformer from the antenna itself by using a double loop. Only one end vertical wire is fed. At the opposite ends, the wires cross (with a small space between them) creating a continuous wire run for the two loops. The effect is an approximate 4:1 impedance step-up ratio relative to a single loop. Spacing is not critical, and the overall effect is similar to that created with a folded dipole relative to a single dipole

```

CM Rectangle (double): 7.15 MHz
CE
GW 1 31 -29 0 50 29.1 0 50 3.36778215223097E-03
GW 2 7 29.1 0 50 29.1 3 37 3.36778215223097E-03
GW 3 31 29 0 37 -29 0 37 3.36778215223097E-03
GW 4 7 -29 0 37 -29 0 50 3.36778215223097E-03
GW 5 31 -29 3 50 29 3 50 3.36778215223097E-03
GW 6 7 29 3 50 29 0 37 3.36778215223097E-03
GW 7 31 29.1 3 37 -29 3 37 3.36778215223097E-03
GW 8 7 -29 3 37 -29 3 50 3.36778215223097E-03
GS 0 0 .3048
GE 1
GN 2 0 0 0 13 .005 0 0 0 0
EX 0 4 4 0 1 0
LD 5 1 1 31 5.8001E7
LD 5 2 1 7 5.8001E7
LD 5 3 1 31 5.8001E7
LD 5 4 1 7 5.8001E7
LD 5 5 1 31 5.8001E7
LD 5 6 1 7 5.8001E7
LD 5 7 1 31 5.8001E7
LD 5 8 1 7 5.8001E7
FR 0 1 0 0 7.15 0
RP 0 181 1 1000 -90 90 1 1
FR 0 1 0 0 7.15 0
RP 0 1 360 1000 73 0 1 1
EN
    
```

16-6-2

Run the model and record in the table below the maximum gain, take-off angle, and source impedance for the rectangle.

```

CM Half Square 7.15 MHz
CE
GW 1 11 70.5 0 15.5 70.5 0 50 3.36778215223097E-03
GW 2 21 70.5 0 50 0 0 50 3.36778215223097E-03
GW 3 11 0 0 50 0 0 15.5 3.36778215223097E-03
GS 0 0 .3048
GE 1
GN 2 0 0 0 13 .005 0 0 0 0
EX 0 1 11 0 1 0
LD 5 1 1 11 5.8001E7
LD 5 2 1 21 5.8001E7
LD 5 3 1 11 5.8001E7
FR 0 1 0 0 7.15 0
RP 0 181 1 1000 -90 90 1 1
FR 0 1 0 0 7.15 0
RP 0 1 360 1000 72 0 1 1
EN
    
```

16-6-3

Much simpler is the half square model, 16-6-3.NEC. With only 3 #12 AWG copper wires, the antenna also adheres to the 50' height limitation. The source point is on the last segment of the first wire. Should you require a more precise corner source placement, you may use a split feed for it. Record the gain, take-off angle, and source impedance of the half square in the table with the figures for the other SCVs.

16-6 Test Data			
Antenna	Gain dBi	Take-Off Angle	Source Z R ± jX Ω
Delta			
Rectangle			
Half Square			

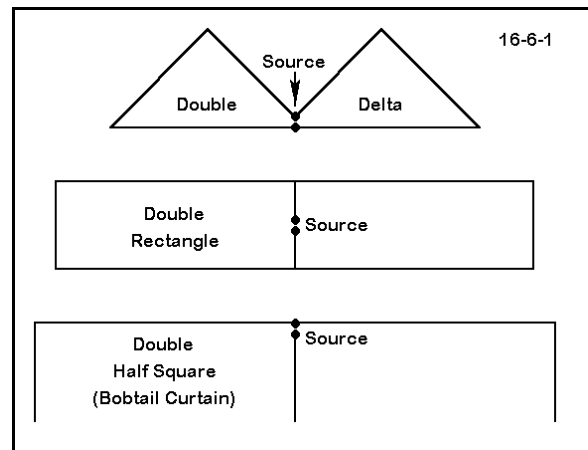
Comments: In this initial experiment with SCVs, the doubled rectangle has the highest gain and the lowest take-off angle. All three provide a good match for a 50- Ω feedline system. Examine both the elevation and azimuth plots for each antenna. You should discover that the greatest side rejection accompanies the highest gain. Although these antennas will never compete in gain with horizontal directional beams placed at great heights, they do constitute low-cost fixed arrays with some desirable characteristics. They exhibit very low gain at high radiation angles, thus providing a high signal-to-noise ratio for radiation coming in at the very low angles typical of long distance skip signals. However, this condition only exists at a low installation height.

16-6 Reference Data			
Antenna	Gain dBi	Take-Off Angle	Source Z R \pm jX Ω
Delta	1.89	20°	61.6 - j 0.2
Rectangle	3.46	17°	54.6 - j 7.3
Half Square	2.99	18°	50.1 - j 4.7

To supplement this initial modeling, raise the height of each antenna in small increments (about 5' per rerun) and recheck the gain, take-off angle, and the elevation pattern. Continue to raise the antenna until each shows about the same amount of higher angle secondary lobe in its pattern. This height represents the practical height limit for effective use of the SCVs.

Each version of the antenna has advantages as well as disadvantages. Although the delta shows the lowest gain, it requires only a single high mounting point, thus permitting construction where the other SCVs might not be practical. The rectangle is the most compact of the shapes, but in the doubled version requires twice the wire. The half square is mounted with the horizontal wire upward so that the high current region of the verticals is as high as possible. However, that advantage is offset by difficulties associated with running the feedline to the source point.

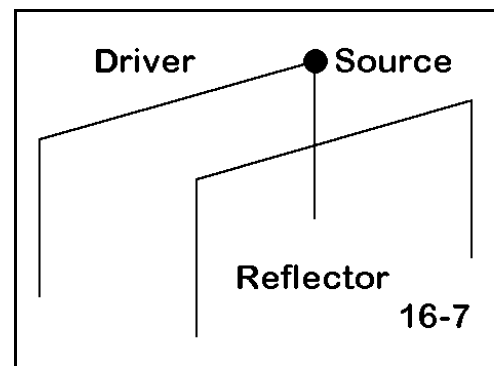
Basic SCVs are shape sensitive with respect to gain. You may experiment with the shapes by placing them in free space to determine a variant that yields the highest gain. For example, the delta may have its base extended with a consequent reduction in height. Some of the shapes are frequency sensitive, while others are not. Frequency scale the antennas by a factor of 3 (to about 22 MHz) and reshape each for maximum gain. In the process of reshaping the antennas, note the consequences for the source impedance.



Additional gain can emerge from open-face double versions of each of the basic SCV configuration. Interestingly, the antennas shown in **Figure 16-6-1** all require longer and lower dimensions than would be obtained simply by placing the simple antennas side-by-side. As a historical note, the double half square actually made its appearance first under the name "bobtail curtain," with the simplified version a later development. Develop maximum gain versions of each "double" and compare their characteristics.

16-7.NEC: Parasitic half square arrays for 7.15 MHz

Just as vertical monopoles and dipoles may be placed in parasitic arrays for additional directional gain, so too may any of the SCVs. In this exercise, we shall explore the parasitic half square, as shown in outline in **Figure 16-7**. However, any of the SCVs are apt to similar treatment. The most common form of parasitic array uses the second element as a reflector. This version normally provides a wider operating bandwidth and a more manageable source impedance than a driver-director array.



```

CM Half Square 7.15 MHz
CM Full-size reflector
CE
GW 1 11 19.0347 0 3.81 19.0347 0 15.24 .00103
GW 2 21 19.0347 0 15.24 0 0 15.24 .00103
GW 3 11 0 0 15.24 0 0 3.81 .00103
GW 4 11 19.0347 -6.096 3.3528 19.0347 -6.096 15.24 .00103
GW 5 21 19.0347 -6.096 15.24 0 -6.096 15.24 .00103
GW 6 11 0 -6.096 15.24 0 -6.096 3.3528 .00103
GS 0 0 1
GE 1
GN 2 0 0 0 13 .005 0 0 0 0
EX 0 1 11 0 1.414214 0
LD 5 1 1 11 5.8001E7
LD 5 2 1 21 5.8001E7
LD 5 3 1 11 5.8001E7
LD 5 4 1 11 5.8001E7
LD 5 5 1 21 5.8001E7
LD 5 6 1 11 5.8001E7
FR 0 1 0 0 7.15 0
RP 0 1 361 1000 71 0 1 1
EN
    
```

16-7-1

Open model 16-7-1.NEC. This pair of half squares actually matches the half square we previously examined, but the dimensions for this model are given in meters rather than in feet. Both horizontal wires are the same length. The reflector vertical wires are longer than the driver vertical wires by the amount necessary to maximize gain and front-to-back ratio at the 7.15 MHz operating frequency. With a preset maximum height of 50' (15.24 m), the

reflector verticals extend within about 11' (3.35 m) of the ground.

Open model 16-7-2.NEC. This version of the parasitic half square array uses a different method of reflector formation. The reflector is the same physical size as the driver, so that the verticals extend down only to the 12.5' (3.81 m) point. At the position on the reflector corresponding to the source on the driver, an inductive reactance of 67 Ω is installed (as a type 4 load). The load electrically lengthens the reflector to achieve the same results as longer wires.

```

CM Half Square 7.15 MHz
CM Loaded reflector
CE
GW 1 11 19.0347 0 3.81 19.0347 0 15.24 .0010265
GW 2 21 19.0347 0 15.24 0 0 15.24 .0010265
GW 3 11 0 0 15.24 0 0 3.81 .0010265
GW 4 11 19.0347 -6.096 3.81 19.0347 -6.096 15.24 .0010265
GW 5 21 19.0347 -6.096 15.24 0 -6.096 15.24 .0010265
GW 6 11 0 -6.096 15.24 0 -6.096 3.81 .0010265
GS 0 0 1
GE 1
GN 2 0 0 0 13 .005 0 0 0 0
EX 0 1 11 0 1 0
LD 4 4 11 11 0 67 0
LD 5 1 1 11 5.8001E7
LD 5 2 1 21 5.8001E7
LD 5 3 1 11 5.8001E7
LD 5 4 1 11 5.8001E7
LD 5 5 1 21 5.8001E7
LD 5 6 1 11 5.8001E7
FR 0 1 0 0 7.15 0
RP 0 1 360 1000 71 0 1 1
EN
    
```

16-7-2

Since the load is placed non-symmetrically on the antenna element, you may question whether it can be as effective as lengthening both vertical wires by equal amounts. Run the antennas and record the requisite data in the table on the next page.

16-7 Test Data			
Antenna	Gain dBi Take-Off Angle	Front-to-Back Ratio dB	Source Z R ± jX Ω
Full Reflector			
Loaded Reflector			

Comments: There is no significant difference in the performance of these two arrays, given the figures for gain, front-to-back ratio, and source impedance. However, the load provided was a pure reactance, which did not account for the Q of the inductance

providing the reactance. You may replace the type 4 load with a series R-L-C load, including a reasonable value of R to reflect a sensible Q for the inductor. With this load in place, you may then perform a frequency sweep from 7.0 through 7.3 MHz to test the operating bandwidth of both the source impedance and the performance characteristics.

16-7 Reference Data			
Antenna	Gain dBi Take-Off Angle	Front-to-Back Ratio dB	Source Z $R \pm jX \Omega$
Full Reflector	6.64 / 19°	20.46	78.9 + j 3.5
Loaded Reflector	6.55 / 19°	19.41	78.9 + j 4.9

For an additional challenge, consider the length of a shorted stub of 50- Ω or 75- Ω coaxial cable necessary to effect the required reflector load. Can you design this load so that at a mid-point between the elements, you may install a simple remote switching system? In each position, the transmission line would function as an added length of line to the driver and as a stub to the reflector, thus creating a reversible directional array.

Finally, create directional arrays using pairs of each of the other types of SCVs explored in the preceding exercise.

Summing Up

In this short set of exercises, we have sought to sample a wide variety of vertically polarized antennas and arrays, ranging from the simple vertical dipole to parasitic and phased arrays. (Indeed, the last exercise can be viewed as a parasitic array of phased verticals.) Numerous other arrangements of vertical and vertically polarized antenna elements await modeling analysis. Some involve hosts of individually driven elements, others employ phasing systems for up to four elements, while still others form long vertical Yagis and log periodic arrays.

The goal of this chapter has been to acquaint you with the fundamental concerns and considerations that go into developing adequate models for vertical antenna systems. Unlike horizontal antennas, for which the ground is only a reflecting medium, vertical antenna design and analysis requires close attention to the ground as a loss medium as well as a reflecting medium. In addition, we must be aware of and honor limitations of the modeling program to ensure that the models make sense. Finally, we must be aware of what transmission lines offer by way of opportunities and what they impose as limitations.

Nonetheless, once we take the ground into proper account, vertical antennas offer a fertile field for design ingenuity, both electrically and mechanically. In many instances, the

electrical design may be the easier part of the equation. The mechanical portion of the work requires a balance of physical and fiscal factors that combine to yield unendingly variable task goals for the antenna designer.

For further examples to model, open almost any antenna handbook to the section on vertically polarized arrays.

User Notes

17.

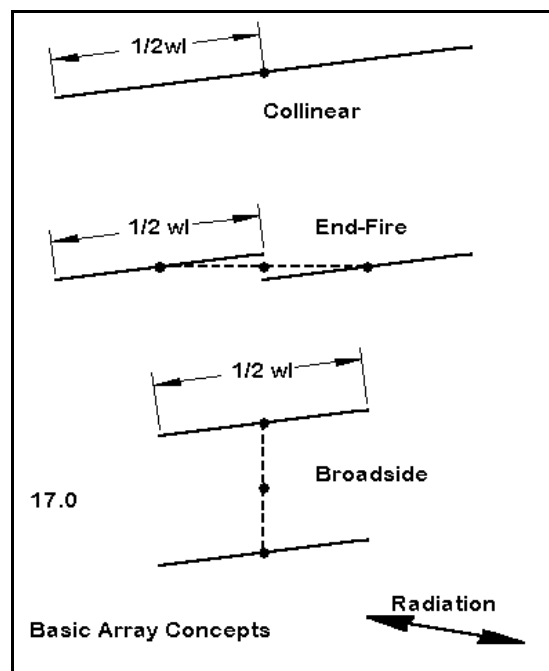
Bi-Directional Wire Arrays

Objectives: Although less prominent than other types of antennas today, bi-directional wire arrays occupy an important niche in MF and HF radio communications. In these exercises, you will become acquainted with the modeling techniques necessary to develop and analyze this diverse group of antennas, including the routine use of transmission lines as part of the design.

Bi-directional wire arrays comprise a class of antennas composed of multiple $1/2\lambda$ antenna elements arranged to produce antenna patterns that serve specific purposes. Familiarity with the antenna types and their principles of operation is necessary to understand the modeling challenges they present.

If we adopt the $1/2\lambda$ resonant length of wire as our basic unit, then we can make sense out of the operative vocabulary of bi-directional wire array. The two key questions are these: a. How are the elements arranged relative to each other? b. With a given arrangement, what is the main axis of radiation?

Figure 17.0 shows three basic arrangements that yield the fundamental categories within which these arrays are specified. Elements are **collinear** when they are arranged end-to-end so that the main radiation lobes are tangential to the wire. The ends may touch, as in the illustration, or they may be separated by a phasing section, a length of wire or transmission line that alters the current phase and magnitude at the point of junction. Ordinarily, these lines are used to increase the strength of the main radiation lobes.



When elements are parallel to each other, in a plane that is parallel to the ground surface,

and the strongest radiation lobes are tangential to the wires, we have an **End-Fire** array. Most commonly for bi-directional arrays, the two elements are fed 180° out of phase with each other. The simplest means of achieving this goal is to create two transmission lines of equal length to a central source wire (junction). One line is reverse connected to its element. Since the current magnitude and phase shift along each line is identical, the reverse connection on one of the lines ensures the out-of-phase condition.

A **Broadside** array places elements (normally) in a vertical plane, with the main radiation lobe again tangential to the wires. In this configuration, we feed the wire elements in phase with each other. Once more, the simplest feed system is to use equal lengths of transmission line to a common junction, but normal connections are used for both lines. Ordinarily, the slight differences in the source impedance of the two wires, given their different distances from the earth's surface, is not sufficient to disturb the relative phasing. However, in very sensitive systems, networks may be used to achieve critical phasing adjustments.

Most bi-directional wire arrays use combinations of these techniques. For most applications, a 1λ wire is the shortest collinear element having sufficient gain to use in either a broadside or end-fire array. Longer elements, such as the 1.25λ extended double Zepp (EDZ), are commonplace. Moreover, we may combine both end-fire and broadside techniques into single arrays.

For many of the bi-directional array designs, absolute precision is less important than with other types of antennas. A 5% variation in the length of a $1/2\lambda$ element may make little difference to the performance of the array. Indeed, as arrays grow larger, modeling does not so much determine an exact construction version as it looks at trends in both performance and source impedance to guide field adjustment of the physical antenna. In addition, we should not expect source impedances that are ready matches to a $50\text{-}\Omega$ system feedline. Instead, we shall find a wide variety of source impedances that challenge us to develop feed networks that fall outside the scope of our efforts in this guide.

Although bi-directional arrays date from the earliest days of radio communications, they reached a zenith of design effort in the 1930s as short wave broadcasting became commonplace. Great "antenna farms" involving acres of land emerged as stations built multiple fixed-position antennas beaming power with narrow beamwidths at selected reception areas. Although new ideas in bi-directional arrays surface more slowly today, engineering an antenna of this type to serve a specific communications need is still a significant engineering enterprise.

In some applications, especially in the upper HF range, the Yagi and other rotatable parasitic antennas have supplanted the bi-directional array. However, up to about 10 MHz, the bi-directional array is still the antenna of choice for most fixed stations.

Moreover, even above 10 MHz, these antennas offer a cost-benefit ratio that make them attractive alternatives to other techniques.

Exercise Preparation

The exercises in this chapter all involve wire antennas. For simplicity, every model will use #12 AWG copper wire. However, actual commercial antenna installations may use much fatter wire, while many casual installations might use thinner wire. Therefore, a standard supplemental exercise for each antenna will be to test the design with other wire diameters to discover whether wire diameter makes a difference to the required dimensions, the bandwidth over which a certain radiation pattern holds good, and the source impedance of the array.

Many of the antennas will use phase-line sections--shorted parallel lengths of wire. The models will physically model these lines. Wherever they occur, you may wish to experiment with shorted transmission line sections to see if you can replicate the model with these replacements.

Transmission lines will also be a part of sourcing both end-fire and broadside arrays. These lines will run to a short wire junction on which you will place the source. For convenience, the models will place this source wire exactly between the array wires and use the actual distance to it as the transmission line length. You may wish to experiment with other line lengths to see their effect upon the composite source impedance for the array. For both end-fire and broadside arrays, keep the transmission line lengths equal to each other to preserve phasing. With some line lengths, you may arrive at a source impedance that is more desirable from one or another perspective. All transmission lines will presume a velocity factor of 1.0. You may wish to recalculate the line-lengths for other velocity factors that correspond to those used in commercially available transmission lines.

For all of the arrays, take careful note of the segmentation density, which has been set at about 15 segments per half-wavelength wherever feasible within the segmentation allowance of NECWin Plus. On paper, a sketch of a large array may look smaller than it really is, tempting you to inadequate segmentation. On the other hand, it is fairly easy to imagine an array of multiple elements, each 5λ or more long. Hence, for some models that you develop, less than optimal segmentation densities may be necessary until you can access professional level programs with relatively unlimited wire segment capacities.

Because wire arrays involve long elements--and often several of them--expect run times to be longer than with the simple antennas encountered in the earlier parts of this guide. As always, you will be asked to perform tests with frequencies other than the one specified in the original model. Use care to provide new filenames for the revised models if you wish to preserve the original.

17-1.NEC: A 1λ center-fed collinear array for 14.175 MHz

The 1λ center-fed wire is, for our purposes, a collinear array of 2 1/2λ elements with no phasing adjustment between the elements. Model 17-1.NEC shows how simple a bi-directional wire array can be.

This antenna is perhaps the most commonly used bi-directional array, since every doublet operated on its second harmonic creates this array. The dimensions need only approximate a full wavelength to obtain good performance, as the rounded dimension numbers in the model suggest.

```
CM 1 wl center-fed: 14.175 MHz
CE
GW 1 31 -32 0 35 32 0 35 3.367E-03
GS 0 0 .3048
GE 1
GN 2 0 0 0 13 .005 0 0 0 0
EX 0 1 16 0 1 0
LD 5 1 1 31 5.8001E7
FR 0 1 0 0 14.175 0
RP 0 1 361 1000 63 0 1 1
FR 0 1 0 0 14.175 0
RP 0 181 1 1000 -90 90 1 1
EN
```

17-1

```
CM 1/2 wl center-fed: 14.175 MHz
CE
GW 1 15 -16.94 0 35 16.94 0 35 3.367E-03
GS 0 0 .3048
GE 1
GN 2 0 0 0 13 .005 0 0 0 0
EX 0 1 8 0 1 0
LD 5 1 1 15 5.8001E7
FR 0 1 0 0 14.175 0
RP 0 1 360 1000 63 0 1 1
FR 0 1 0 0 14.175 0
RP 0 181 1 1000 -90 90 1 1
EN
```

17-1-1

To form a basis for understanding the operation of the collinear 1λ wire, open model 17-1-1.NEC, a resonant 1/2λ center-fed dipole at the same height and wire type (35' above average S-N ground, #12 copper wire). Run both models, recording in the table below the maximum gain, the take-off angle, the -3 dB beamwidth of the main lobes, and the source impedance.

For these models and the ones to come, both azimuth and elevation plots are specified. Use the elevation plot to determine the take-off angle of maximum radiation and do not rely upon the initial angle specified in the azimuth plot. Likewise, determine the maximum gain from the azimuth plot set at the take-off angle, since for some models that are not absolutely symmetrical, the elevation plot and the azimuth plot may show different maximum gain figures.

17-1		Test Data		
Antenna	Gain dBi	T-O angle	Beamwidth	Source Z R ± jX Ω
1 λ				
1/2 λ				

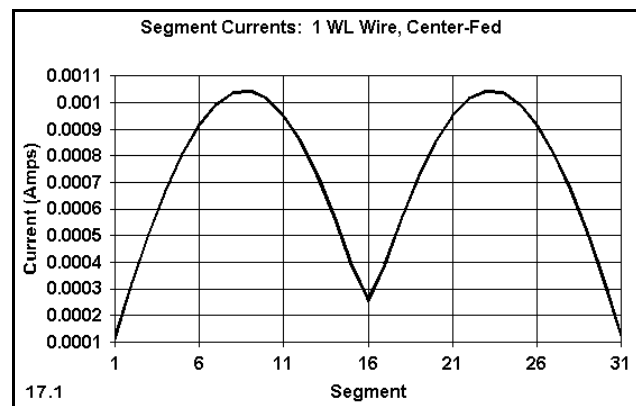
Comments: Both antennas are bi-directional and exhibit identical take-off angles. Therefore, the 1.5 dB gain of the full-wave antenna over its half-wavelength counterpart must come largely from the power in the main lobe. The added main lobe strength results in a narrowing of the beamwidth that is significant to potential communications

purposes. For some types of communications, the 28° narrower beamwidth of the 1λ antenna may be too narrow; for other purposes, it may be precisely what is needed.

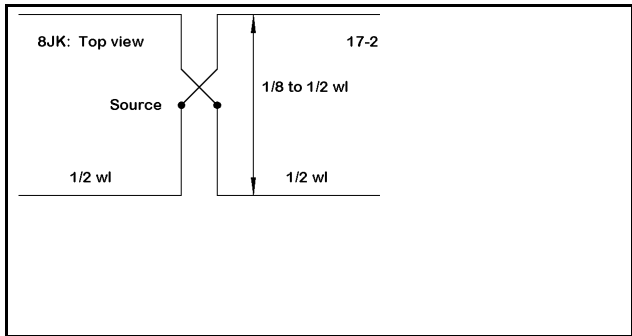
17-1		Reference Data		
Antenna	Gain dBi	T-O angle	Beamwidth	Source Z $R \pm jX \Omega$
1λ	8.92	27°	58°	$3073 + j 2374$
$1/2\lambda$	7.40	27°	86°	$68.6 + j 0.4$

The very high source impedance of the 1λ antenna should recall a much earlier exercise in which we explored the rapid rate of change of both resistance and reactance in the vicinity of $n\lambda$ points. You may wish to experiment in very small increments of length with this antenna to find the point where the reactance shifts from inductive on the short side to capacitive on the long side of 1λ .

Let's carry this simple exercise one step beyond a review of the fundamentals of antenna length. Create a graph of the current levels along the antenna, similar to the one shown in **Figure 17.1**. The exact magnitudes (a function of the chosen voltage source value) are less important than the repeated curves on each side of the center source point. If you also look at the current tables (or create a second graph), you will see that the current magnitudes and phases are additive, creating the greater gain of the 1λ antenna over the $1/2\lambda$ dipole. Graphs of this order can be useful aids in the design or analysis of other bi-directional arrays.



17-2.NEC: the 8JK end-fire array for 14.175 MHz.



The antenna shown in **Figure 17.2** goes under many names, including the "flat-top array" and the "8JK array." The latter name arises from the amateur radio call sign of its inventor, Dr. John Kraus, a pioneer in antennas whose text is still widely used for teaching and for reference.

The basic antenna consists of two 1λ collinear elements spaced from $1/8\lambda$ to $1/2\lambda$ apart. Because the antenna is an end-fire array, both elements are fed, but 180° out of phase, as indicated by the "half-twist" in one of the connecting transmission lines from the source.

Model 17-2.NEC begins with the 8JK elements spaced about $1/2\lambda$ (35') apart (farther apart than some individuals might allow for a true 8JK array).

The wire dimensions, the height above average ground, and the test frequency are the same as for model 17-1.NEC so that we can make a fair comparison of the results.

```

CM 8JK: End-Fire Array: 14.175 MHz
CE
GW 1 31 -32 17.5 35 32 17.5 35 3.367E-03
GW 2 31 -32 -17.5 35 32 -17.5 35 3.367E-03
GW 3 1 -.2 0 35 .2 0 35 3.367E-03
GS 0 0 .3048
GE 1
GN 2 0 0 0 13 .005 0 0 0 0
EX 0 3 1 0 1 0
LD 5 1 1 31 5.8001E7
LD 5 2 1 31 5.8001E7
LD 5 3 1 1 5.8001E7
TL 1 16 3 1 -600 0 0 0 0 0
TL 2 16 3 1 600 0 0 0 0 0
FR 0 1 0 0 14.175 0
RP 0 1 360 1000 63 0 1 1
FR 0 1 0 0 14.175 0
RP 0 181 1 1000 -90 90 1 1
EN
    
```

Run this model, recording the gain, take-off angle, beamwidth, and source impedance in the table below. Then modify the model to reduce the element spacing to $3/8\lambda$ (26.25'), $1/4\lambda$ (17.5'), and $1/8\lambda$ (8.75'). The transmission line connections to the center source point will automatically shorten with each change if you take equal amounts away from the Y values for each element.

17-2 Test Data				
Spacing	Gain dBi	T-O angle	Beamwidth	Source Z $R \pm jX \Omega$
$1/2 \lambda$				
$3/8 \lambda$				
$1/4 \lambda$				
$1/8 \lambda$				

Comments: Note that the gain of the array increases as the spacing decreases down to about $1/4\lambda$, at which point the gain begins to decrease. In contrast, the composite source

impedance shows an inverse curve to the gain. As a separate exercise, you may independently analyze the transmission line lengths to determine the reasons for the impedance curve.

Compare the gain and beamwidth figures to those for the $1/2\lambda$ and 1λ antenna we just examined. Note that the 8JK provides about 1.8 dB gain at its peak over the single 1λ antenna and over 3 dB gain more than the dipole. In the process, the beamwidth shrinks to 50° or so. Of note is the further lowering of the take-off angle to 25° . (You may wish to undertake an analysis of why the composite patterns of end-fire arrays tend to show a lower angle of maximum radiation than the patterns of single or collinear elements.) Although the 8JK is structurally more complex than the collinear 1λ antenna, its greater gain and narrower beamwidth may justify the added work under some circumstances.

17-2		Reference Data		
Spacing	Gain dBi	T-O angle	Beamwidth	Source Z $R \pm jX \Omega$
$1/2 \lambda$	10.25	26°	54°	$44.2 - j 4.7$
$3/8 \lambda$	10.56	25°	52°	$36.9 - j127.4$
$1/4 \lambda$	10.73	25°	50°	$38.0 - j320.2$
$1/8 \lambda$	10.64	25°	50°	$71.4 - j968.9$

To establish that it is possible to obtain additional gain by stacking end-fire arrays composed of 1λ elements, examine model 17-2-1.NEC, to the right. Two 8JKs are spaced vertically by $1/2\lambda$ ($35'$). All transmission line leads come to a central junction wire (Wire 3) on which the source is placed. Note that the transmission lines to the forward elements are reversed to preserve the 180° out-of-phase condition of the forward elements relative to the rear elements. You may examine the construction of the antenna by using the NEC-Vu feature of your program.

Run this antenna, recording the gain, take-off angle, beamwidth, and source impedance.

```

CM 2-8JKs stacked: 14.175 MHz
CM Combined End-Fire & Broadside Array
CE
GW 1 31 -32 17.5 35 32 17.5 35 3.367E-03
GW 2 31 -32 -17.5 35 32 -17.5 35 3.367E-03
GW 3 1 -.2 0 52.5 .2 0 52.5 3.367E-03
GW 4 31 -32 17.5 70 32 17.5 70 3.367E-03
GW 5 31 -32 -17.5 70 32 -17.5 70 3.367E-03
GS 0 0 .3048
GE 1
GN 2 0 0 0 13 .005 0 0 0 0
EX 0 3 1 0 1 0
LD 5 1 1 31 5.8001E7
LD 5 2 1 31 5.8001E7
LD 5 3 1 1 5.8001E7
LD 5 4 1 31 5.8001E7
LD 5 5 1 31 5.8001E7
TL 1 16 3 1 -600 0 0 0 0 0
TL 2 16 3 1 600 0 0 0 0 0
TL 4 16 3 1 -600 0 0 0 0 0
TL 5 16 3 1 600 0 0 0 0 0
FR 0 1 0 0 14.175 0
RP 0 1 360 1000 74 0 1 1
FR 0 1 0 0 14.175 0
RP 0 181 1 1000 -90 90 1 1
EN

```

17-2-1

Comments: The antenna shows over 2 dB more gain (12.44 dBi) than the $1/2\lambda$ spaced version of a single 8JK. Because the second flat-top is at a 70' height, the overall take-off

angle is much lower than the single 8JK at a 35' height: 16° elevation. The beamwidth is about the same (54°), but the source impedance seems to have a manageable value of $38.0 + j 98.7 \Omega$.

The overall impression given by the models we have so far examined is that the more elements we add in various $1/2\lambda$ configurations, the higher the gain of the array. To a large degree, this is a true impression. However, the increasing complexity of the antenna structures needed to achieve this gain is also evident. Hence, designers have sought to achieve the desired gain more compactly.

17-3.NEC: A Lazy-H broadside array for 14.175 MHz

An alternative to the 8JK flat-top array is a similar structure set up vertically: single 1λ elements fed in phase (with transmission-line connection non-reversed to the center source wire) and spaced by perhaps $1/2\lambda$. Model 17-3.NEC shows a version of such an antenna, dubbed the "Lazy-H" by virtue of its appearance of being the letter H on its side. The only other difference between this antenna and the others we have examined is that the elements are somewhat longer (68' vs. 64'). The bottom wire for this 14.175 MHz example is 35' above average S-N ground. All of our antennas so far have used #12 AWG copper wire and 600- Ω transmission line. Before running this and other models, be certain that, for all models involving transmission line feed-systems, you do not inadvertently reverse or unreverse transmission line connections.

```

CM Lazy-H: 1 wl: 14.175 MHz
CM Vertical Space = 1/2 wl
CE
GW 1 31 -34 0 35 34 0 35 3.367E-03
GW 2 31 -34 0 70 34 0 70 3.367E-03
GW 3 1 -.2 0 52.5 .2 0 52.5 3.367E-03
GS 0 0 .3048
GE 1
GN 2 0 0 0 13 .005 0 0 0 0
EX 0 3 1 0 1 0
LD 5 1 1 31 5.8001E7
LD 5 2 1 31 5.8001E7
LD 5 3 1 1 5.8001E7
TL 1 16 3 1 600 0 0 0 0 0
TL 2 16 3 1 600 0 0 0 0 0
FR 0 1 0 0 14.175 0
RP 0 1 360 1000 73 0 1 1
FR 0 1 0 0 14.175 0
RP 0 181 1 1000 -90 90 1 1
EN

```

17-3

```

CM Lazy-H: 1 wl: 14.175 MHz
CM Vertical Space: 5/8 wl
CE
GW 1 31 -34 0 35 34 0 35 3.367E-03
GW 2 31 -34 0 79 34 0 79 3.367E-03
GW 3 1 -.2 0 57 .2 0 57 3.367E-03
GS 0 0 .3048
GE 1
GN 2 0 0 0 13 .005 0 0 0 0
EX 0 3 1 0 1 0
LD 5 1 1 31 5.8001E7
LD 5 2 1 31 5.8001E7
LD 5 3 1 1 5.8001E7
TL 1 16 3 1 600 0 0 0 0 0
TL 2 16 3 1 600 0 0 0 0 0
FR 0 1 0 0 14.175 0
RP 0 1 360 1000 75 0 1 1
FR 0 1 0 0 14.175 0
RP 0 181 1 1000 -90 90 1 1
EN

```

17-3-1

Model 17-3.NEC shows a 35' vertical spacing between wires, about $1/2\lambda$. Other spacings between vertical elements are possible, with $5/8\lambda$ tending to show gain advantages that outweigh the small increase in overall antenna height. Open model 17-3-1.NEC, which is the same Lazy-H, but with the upper element raised to 79' and the center source junction wire moved accordingly to preserve in-phase feeding.

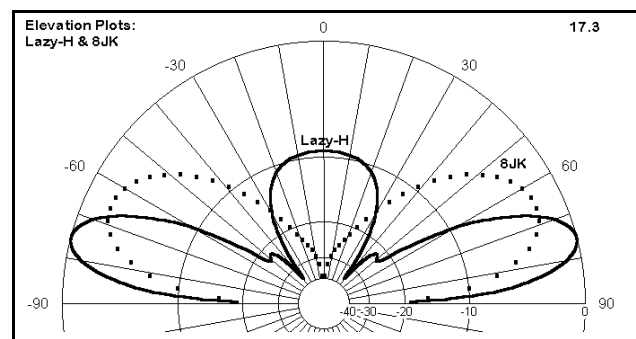
Run both models, recording the gain, take-off angle, beamwidth, and source impedance in the table below.

17-3 Test Data				
Spacing	Gain dBi	T-O angle	Beamwidth	Source Z $R \pm jX \Omega$
$1/2 \lambda$				
$5/8 \lambda$				

Comments: The Lazy-H, even with the smaller spacing, shows performance figures that rival the full 4-element double 8JK (technically 8 elements, since each element is a collinear array of 2 $1/2\lambda$ wires). With an extra $1/8\lambda$ spacing, the gain exceeds that of the complex array with very comparable beamwidth and take-off angle values. Structurally, the antenna saves about 35' of linear space and possibly a pair of vertical supports for the wires.

17-3 Reference Data				
Spacing	Gain dBi	T-O angle	Beamwidth	Source Z $R \pm jX \Omega$
$1/2 \lambda$	12.29	17°	52°	$30.9 - j 3.1$
$5/8 \lambda$	12.66	15°	50°	$29.4 + j136.3$

However, the charted numbers do not tell us everything. **Figure 17.3** shows comparative elevation plots for the 8JK and the Lazy-H spaced $5/8\lambda$. For some applications, the very high angle lobe of the Lazy-H (which is not present on the model spaced $1/2\lambda$) may be sensitive to near-vertical incidence signals that might interfere with the desired signals from lower angle paths. Such a requirement would then favor arrays without high angle lobes. Re-examine the elevation plots for all of the arrays to determine which ones might meet the new specification.



17-4.NEC: An extended double Zepp for 28.5 MHz

```

CM Extended Double Zepp: 28.5 MHz
CE
GW 1 51 -22.2 0 35 22.2 0 35 3.367E-03
GS 0 0 .3048
GE 1
GN 2 0 0 0 13 .005 0 0 0 0
EX 0 1 26 0 1.414214 0
LD 5 1 1 51 5.8001E7
FR 0 1 0 0 28.5 0
RP 0 1 360 1000 76 0 1 1
FR 0 1 0 0 28.5 0
RP 0 181 1 1000 -90 90 1 1
EN
    
```

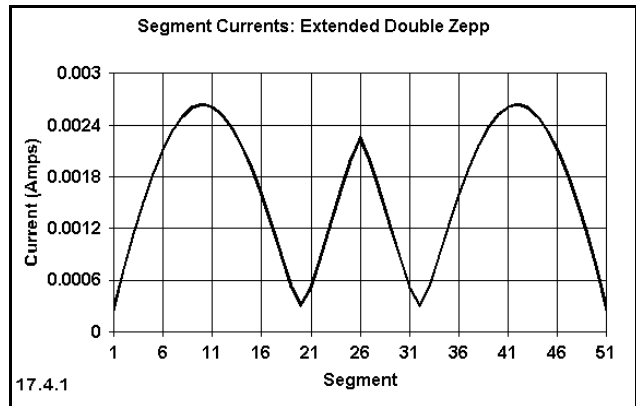
17-4

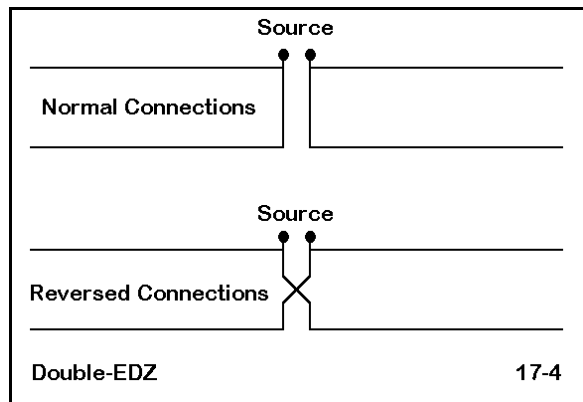
The extended double Zepp (EDZ) is a 1.25λ non-resonant antenna that is actually $2 \frac{1}{2}\lambda$ elements phased by a $\frac{1}{4}\lambda$ wire to produce maximum gain. The length need only be approximated, since the gain curve is shallow as one makes the wire longer or shorter. Model 17-3.NEC supplies a #12 AWG copper version for 28.5 MHz at 35' above average S-N ground. Remember that 35' at this frequency is a 1λ height. Run the model, recording the gain, take-off angle, beamwidth, and source impedance in the table.

take-off angle, beamwidth, and source impedance in the table.

17-4 Test Data					
Antenna	Gain dBi	F-B dB	T-O Angle	Beam-width	Source Z $R \pm jX \Omega$
EDZ		-----			
DEDZ: Norm					
DEDZ: Rev					

Comments: We shall fill in the blanks in the table shortly. First, let's create a current graph for the EDZ to help us understand how it works. As shown in **Figure 17.4.1**, the large smooth current curves appear at the outer parts of the antenna, each covering a $\frac{1}{2}\lambda$ space. The center portion of the array adds little to the antennas gain, but does space the half wavelength sections far enough apart to increase their gain. In fact, the center section of the antenna is a convenience, not a necessity. Create a model of $2 \frac{1}{2}\lambda$ center-fed dipoles, with their ends separated by $\frac{1}{4}\lambda$. For all other aspects of the antenna, match the EDZ model. Compare the azimuth and elevation patterns with those of the EDZ.





Before looking at some true arrays with the EDZ as their bases, let's look at a pair of models that are easy to misread. The figure at the left shows their configurations. They resemble models we have already run, except that they are fed on one wire, with the transmission line run normally or in reversed connections to the second element of the same length. We may call the antennas the Double EDZ or DEDZ for short. Models 17-4-1.NEC and 17-4-2.NEC contain the versions with normal and with reversed connections, respectively.

The only difference between the two models occurs in the TL entry, where the 600-Ω transmission line shows a negative sign on one model.

```
CM Dual EDZ w/600 ohm line
CM Normal Connections: 28.5 MHz
CE
GW 1 51 -22.2 0 35 22.2 0 35 3.367E-03
GW 2 51 -22.2 -4.31 35 22.1 -4.31 35 3.367E-03
GS 0 0 .3048
GE 1
GN 2 0 0 0 13 .005 0 0 0 0
EX 0 1 26 0 1.414214 0
LD 5 1 1 51 5.8001E7
LD 5 2 1 51 5.8001E7
TL 1 26 2 26 600 0 0 0 0 0
FR 0 1 0 0 28.5 0
RP 0 1 360 1000 76 0 1 1
FR 0 1 0 0 28.5 0
RP 0 181 1 1000 -90 90 1 1
EN
```

17-4-1

```
CM Dual EDZ w/600 ohm line
CM Reverse Connections: 28.5 MHz
CE
GW 1 51 -22.2 0 35 22.2 0 35 3.367E-03
GW 2 51 -22.2 -4.31 35 22.2 -4.31 35 3.367E-03
GS 0 0 .3048
GE 1
GN 2 0 0 0 13 .005 0 0 0 0
EX 0 1 26 0 1.414214 0
LD 5 1 1 51 5.8001E7
LD 5 2 1 51 5.8001E7
TL 1 26 2 26 -600 0 0 0 0 0
FR 0 1 0 0 28.5 0
RP 0 1 360 1000 76 0 1 1
FR 0 1 0 0 28.5 0
RP 0 181 1 1000 -90 90 1 1
EN
```

17-4-2

Run these models, recording in the blank lines the gain, take-off angle, beamwidth, and source impedance. Add the small front-to-back value from the azimuth pattern analysis.

17-4 Reference Data					
Antenna	Gain dBi	F-B dB	T-O Angle	Beam-width	Source Z R ± jX Ω
EDZ	10.77	-----	14°	32°	121.5 - j615.1
DEDZ: Norm	11.69	2.36	14°	32°	56.9 - j 10.0
DEDZ: Rev	11.08	0.66	14°	30°	41.1 - j 20.3

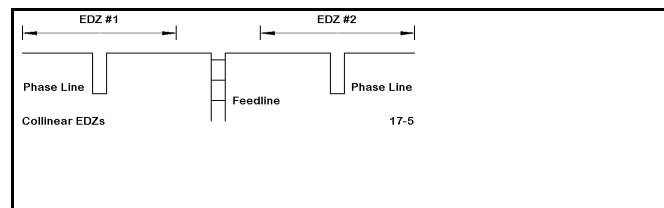
Comments: The gain of an EDZ surpasses that of a 1λ center-fed wire by a worthy amount. The beamwidth narrows considerably as well, making a highly directive array. However, the source impedance is considered by many to be inconvenient. Models 17-4-1.NEC and 17-4-2.NEC appear to be phased arrays of some sort, but they yield only a

tiny front-to-back ratio, and no more gain in one direction than about half of the front-to-back ratio, despite having 2 elements spaced about $1/8\lambda$ apart. Examine the current tables for these antennas. You will discover that one of the elements carries little or no current, while the other carries virtually the same current as the single-wire EDZ. The function of the forward wire is to effect an impedance transformation to a source impedance value that is suitable for use with a 50- Ω system feedline. Assuming that such a double-wire EDZ is suitable to some application or another, run a frequency sweep from 28.0 through 29.0 MHz to determine the 2:1 VSWR operating bandwidth of each version of the DEDZ.

The purpose of introducing the DEDZ at this point is to caution you not to read prematurely the function of a phasing line from its appearance. In this case, appearances can deceive until the model is run through its paces and all of the relevant data examined.

17-5.NEC: A collinear EDZ for 21.225 MHz

An EDZ consists of two $1/2\lambda$ (180°) wires connected by a 90° wire. A collinear EDZ consists of 2 EDZs (each 450°) connected by a 90° wire, as shown in **Figure 7-5**. The result is an antenna about 2.75λ long. Although a center-fed wire of this length would radiate at angles near the wire ends, the collinear EDZ radiates broadside to the wire.



The EDZ yields about 3 dB more gain than a dipole, while the collinear EDZ provides a little under 3 dB further gain over a single EDZ. Since gain in a bi-directional array comes largely at the expense of beamwidth, we can expect a further reduction in that parameter.

Model 17-5.NEC, shown at right, provides a sample of a collinear EDZ for 21.225 MHz, using our standard #12 AWG wire. The wire height is 46' above average S-N ground, or 1λ high. In this model, the phasing lines are physically modeled with a 0.5' spacing between wires. This spacing is not critical. You may wish to try alternatives to this model using more closely spaced phasing line wires or shorted section of transmission line.

First, make a basic run of the model, recording for 21.225 MHz the gain, take-off angle, beamwidth, and source impedance. As we have indicated, the VSWR operating bandwidth is not usually an issue for bi-directional wire arrays. However, designers are very much interested in

the frequency span over which an array holds its pattern and produces useful gain and approximately the same beamwidth. Therefore, modify the model to make a frequency sweep from 20.5 through 22.0 MHz in 4 0.5 MHz steps. Record your results in the following table.

```

CM Collinear EDZs: 21.225 MHz
CE
GW 1 33 -64.5 0 46 -36.25 0 46 3.367E-03
GW 2 5 -36.25 0 46 -36.25 0 39 3.367E-03
GW 3 1 -36.25 0 39 -35.75 0 39 3.367E-03
GW 4 5 -35.75 0 39 -35.75 0 46 3.367E-03
GW 5 61 -35.75 0 46 35.75 0 46 3.367E-03
GW 6 5 35.75 0 46 35.75 0 39 3.367E-03
GW 7 1 35.75 0 39 36.25 0 39 3.367E-03
GW 8 5 36.25 0 39 36.25 0 46 3.367E-03
GW 9 33 36.25 0 46 64.5 0 46 3.367E-03
GS 0 0 .3048
GE 1
GN 2 0 0 0 13 .005 0 0 0 0
EX 0 5 31 0 1 0
LD 5 1 1 33 5.8001E7
LD 5 2 1 5 5.8001E7
LD 5 3 1 1 5.8001E7
LD 5 4 1 5 5.8001E7
LD 5 5 1 61 5.8001E7
LD 5 6 1 5 5.8001E7
LD 5 7 1 1 5.8001E7
LD 5 8 1 5 5.8001E7
LD 5 9 1 33 5.8001E7
FR 0 1 0 0 21.225 0
RP 0 1 360 1000 76 0 1 1
FR 0 1 0 0 21.225 0
RP 0 181 1 1000 -90 90 1 1
EN
    
```

17-5

17-5 Test Data				
Frequency MHz	Gain dBi	T-O angle	Beamwidth	Source Z $R \pm jX \Omega$
21.225				
20.5				
21.0				
21.5				
22.0				

Comments: The collinear EDZ produces nearly 13 dBi gain at a take-off angle of 76° (14° elevation) for the entire span of the frequency sweep. The lowest value is only about 0.5 dB less than the peak value. The beamwidth is close to constant. The source impedance varies considerably across the frequency span. However, if the exact source impedance is not an issue, the antenna promises to be fairly non-critical in construction, providing close to the highest level of performance obtainable if fairly close to the design ideal. Expressed in other terms, one can design the antenna slightly high in frequency

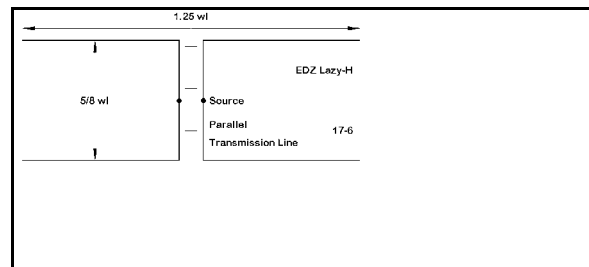
and the natural stretch of the 129' wire over time will not significantly affect performance. However, the changing length of the wire will be detectable in terms of periodic source impedance measurements.

17-5 Reference Data				
Frequency MHz	Gain dBi	T-O angle	Beamwidth	Source Z $R \pm jX \Omega$
21.225	13.52	14°	18°	249 - j 734
20.5	13.01	14°	18°	612 - j 1327
21.0	13.43	14°	18°	314 - j 891
21.5	13.50	14°	16°	199 - j 564
22.0	12.96	14°	16°	159 - j 298

The exceptionally narrow beamwidth of this antenna requires careful attention to its orientation at installation. It is better suited, perhaps, to point-to-point communications rather than to general area communications.

17-6.NEC: An EDZ Lazy-H for 28.5 MHz

The EDZ also lends itself to other array configurations, one of the most useful of which is the Lazy-H. **Figure 17-6** shows the general layout for model 7-6.NEC.



```

CM EDZ Lazy-H: 28.5 MHz
CE
GW 1 51 -22 0 35 22 0 35 3.367E-03
GW 2 51 -22 0 57 22 0 57 3.367E-03
GW 3 1 -.2 0 46 .2 0 46 3.367E-03
GS 0 0 .3048
GE 1
GN 2 0 0 0 13 .005 0 0 0 0
EX 0 3 1 0 1.414214 0
LD 5 1 1 51 5.8001E7
LD 5 2 1 51 5.8001E7
LD 5 3 1 1 5.8001E7
TL 1 26 3 1 450 0 0 0 0 0
TL 2 26 3 1 450 0 0 0 0 0
FR 0 1 0 0 28.5 0
RP 0 1 360 1000 80 0 1 1
FR 0 1 0 0 28.5 0
RP 0 181 1 1000 -90 0 1 1
EN
    
```

The design frequency is 28.5 MHz for this array of 2 EDZs vertically spaced by about $5/8\lambda$, with the lower element 35' (1λ at the design frequency) above average S-N ground. The two EDZs are fed in phase at the center of the connecting run of 450-

Ω parallel transmission line.

Since the lower wire is about $1/2\lambda$ above ground at 14 MHz and nearly $1/2\lambda$ long at 10 MHz, the antenna may be useful at a number of frequencies below the design frequency. Modify the FR entry for the antenna and check its performance (including the acceptability of the azimuth pattern) at the frequencies indicated in the table on the next page. You will have to find the correct take-off angle from the elevation patterns to set up the azimuth pattern to reflect maximum gain.

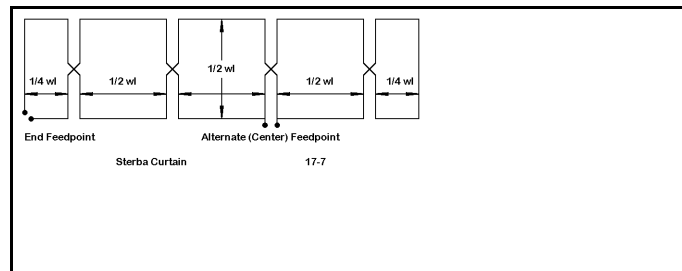
17-6 Test Data				
Frequency MHz	Gain dBi	T-O angle	Beamwidth	Source Z $R \pm jX \Omega$
28.50				
24.94				
21.22				
18.12				
14.15				
10.12				

Comments: The EDZ Lazy-H provides useful performance over a very wide range of frequencies: almost a range of 3:1. The gain decreases as the antenna wire grows shorter as a fraction of a wavelength. The take-off angle increases as the height of the lower wire becomes a decreasing fraction of a wavelength above ground. However, even at the lowest frequency checked, the antenna performs at least as well as a dipole at $1/2\lambda$ above ground. Above about 23 MHz, the array provides very high gain as compared to other arrays we have examined. The source impedance excursions, however, can be a challenge. As noted in the preparation for these exercises, you are encouraged to experiment with different line lengths connecting the source junction wire, so long as you use equal lines lengths from the source to each wire.

17-6 Reference Data				
Frequency MHz	Gain dBi	T-O angle	Beamwidth	Source Z $R \pm jX \Omega$
28.50	14.65	10°	32°	53.9 + j 356
24.94	14.33	11°	42°	17.2 + j 96
21.22	12.28	12°	52°	23.0 - j 29
18.12	10.56	16°	62°	49.0 - j 141
14.15	9.09	20°	74°	494.6 - j 416
10.12	7.40	28°	88°	50.9 + j 93

17-7.NEC: A Sterba Curtain for 3.6 MHz and for 7.2 MHz

The arrays we have examined, and other combinations of and variations upon them, do not exhaust the available designs in use at various types of installations. One of the early designs (now supplanted by more advanced curtains) is the Sterba curtain, a sample of which appears in **Figure 17-7**. A horizontal $1/4\lambda$ section



is installed at each end, but the center area may have any number of $1/2\lambda$ sections. Each added $1/2\lambda$ section increases the gain and narrows the beamwidth of the array.

Standard installation of a Sterba curtain calls for placing the bottom wire at $1/2\lambda$ above ground, with the top wire another $1/2\lambda$ above that. At each transition point, the top and bottom wires are cross-connected with vertical "half-twist" parallel wires. Although these wires in practice may consist of parallel transmission line, the models we shall explore physically model the wires.

```

CM Sterba curtain: 3.6 MHz
CM Bottom-Corner Source
CE
GW 1 15 0 1 134 0 0 268 3.36778215223097E-03
GW 2 8 0 0 268 67 0 268 3.36778215223097E-03
GW 3 15 67 0 268 67 0 134 3.36778215223097E-03
GW 4 15 67 0 134 201 0 134 3.36778215223097E-03
GW 5 15 201 0 134 201 0 268 3.36778215223097E-03
GW 6 15 201 0 268 335 0 268 3.36778215223097E-03
GW 7 15 335 0 268 335 0 134 3.36778215223097E-03
GW 8 15 335 0 134 469 0 134 3.36778215223097E-03
GW 9 15 469 0 134 469 0 268 3.36778215223097E-03
GW 10 8 469 0 268 536 0 268 3.36778215223097E-03
GW 11 15 536 0 268 536 0 134 3.36778215223097E-03
GW 12 8 536 0 134 469 1 134 3.36778215223097E-03
GW 13 15 469 1 134 469 1 268 3.36778215223097E-03
GW 14 15 469 1 268 335 1 268 3.36778215223097E-03
GW 15 15 335 1 268 335 1 134 3.36778215223097E-03
GW 16 15 335 1 134 201 1 134 3.36778215223097E-03
GW 17 15 201 1 134 201 1 268 3.36778215223097E-03
GW 18 15 201 1 268 67 1 268 3.36778215223097E-03
GW 19 15 67 1 268 67 1 134 3.36778215223097E-03
GW 20 8 67 1 134 0 1 134 3.36778215223097E-03
GS 0 0 .3048
GE 1
GN 2 0 0 0 13 .005 0 0 0 0
EX 0 20 8 0 .707107 0
EX 0 1 1 0 .707107 0

```

17-7

Model 17-7.NEC (shown only through the source or EX lines) demonstrates one technique useful in modeling large structures with numerous parallel wires. One set of wires (Wires 1-10) is offset from the other set (wires 11-20) by a constant amount (along the Y-axis in this model). The spacing is 1' in the model for 3.6 MHz. This maneuver ensures that the vertical wires are modeled in opposite directions with a constant spacing and yet connect to the correct wires at each end. Since the 1' offset is only a tiny fraction of a wavelength, the modeling gambit makes no significant difference to the performance figures calculated for the

antenna. You may more closely space the vertical wires if you wish to reflect the actual distance between wires of a particular transmission line you wish to use for them.

In our initial model, the source is the lower corner of one end of the array. The model uses a split source, that is two sources on the adjacent corner segments. In this type of model, using segment lengths that are approximately equal in length through out the model, and especially in the vicinity of the source, is crucial to developing accurate results.

Model 7-7-1.NEC is essentially the same antenna as model 17-7.NEC, with one exception. An additional wire has been added across one of the interior ends of the vertical wires between $1/2\lambda$ sections.

A single source is used on this 1-segment wire, shown schematically as the alternative source point in the initial sketch of the Sterba curtain. Although the source impedance value for the end connection has been viewed by some to be more convenient, the more centered location of the source has been judged to provide higher performance by developing more equal currents on the sections of the antenna.

```

CM Sterba curtain: 3.6 MHz
CM Bottom-Center Source
CE
GW 1 15 0 1 134 0 0 268 3.36778215223097E-03
GW 2 8 0 0 268 67 0 268 3.36778215223097E-03
GW 3 15 67 0 268 67 0 134 3.36778215223097E-03
GW 4 15 67 0 134 201 0 134 3.36778215223097E-03
GW 5 15 201 0 134 201 0 268 3.36778215223097E-03
GW 6 15 201 0 268 335 0 268 3.36778215223097E-03
GW 7 15 335 0 268 335 0 134 3.36778215223097E-03
GW 8 15 335 0 134 469 0 134 3.36778215223097E-03
GW 9 15 469 0 134 469 0 268 3.36778215223097E-03
GW 10 8 469 0 268 536 0 268 3.36778215223097E-03
GW 11 15 536 0 268 536 0 134 3.36778215223097E-03
GW 12 8 536 0 134 469 1 134 3.36778215223097E-03
GW 13 15 469 1 134 469 1 268 3.36778215223097E-03
GW 14 15 469 1 268 335 1 268 3.36778215223097E-03
GW 15 15 335 1 268 335 1 134 3.36778215223097E-03
GW 16 15 335 1 134 201 1 134 3.36778215223097E-03
GW 17 15 201 1 134 201 1 268 3.36778215223097E-03
GW 18 15 201 1 268 67 1 268 3.36778215223097E-03
GW 19 15 67 1 268 67 1 134 3.36778215223097E-03
GW 20 8 67 1 134 0 1 134 3.36778215223097E-03
GW 21 1 201 0 134 201 1 134 3.36778215223097E-03
GS 0 0 .3048
GE 1
GN 2 0 0 0 13 .005 0 0 0 0
EX 0 21 1 0 1 0

```

17-7-1

In addition to these models, open 17-7-2.NEC and 17-7-3.NEC, end-fed and center-fed

versions of the antenna for 7.2 MHz. run all four models at their design frequencies, and record the gain, take-off angle, beamwidth, and source impedance in the following table.

17-7 Test Data				
Antenna	Gain dBi	T-O angle	Beamwidth h	Source Z $R \pm jX \Omega$
3.6 MHz End-Fed				
3.6 MHz Center-Fed				
7.2 MHz End-Fed				
7.2 MHz Center-Fed				

Comments: The models of the center-fed versions of the Sterba curtain consistently show slightly higher gains than the end-fed versions. To discover why, study the current tables or graphics for the models. Note not only the current level, but as well, where along the horizontal $1/2\lambda$ sections that the peaks occur. You should notice a difference between the end-fed and center-fed models. As a supplemental exercise, you may adjust the distance between the lower and upper wires in an attempt to center the current magnitude peaks on each segment--and then determine whether that makes a significant difference to the overall antenna gain.

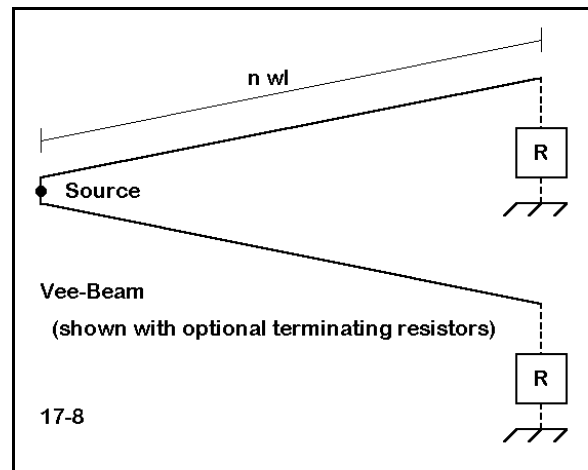
In viewing the elevation and azimuth patterns for these models, note the degree to which each type of model departs from a true broadside pattern. The end-fed version shows a peak gain up to 3° off center. The center-fed model, because of the number of $1/2\lambda$ sections used, is not quite center-fed and exhibits a main lobe about 1 degree off center. The side lobes are not quite symmetrical.

Finally, perform a frequency sweep for each antenna to determine the effective operating bandwidth for the high-gain, narrow-beamwidth pattern. The Sterba curtain turns out to be a high-performance but frequency-specific antenna. Of course, you should also create larger Sterba curtains to test the amount of gain added with each new $1/2\lambda$ section. The samples we have examined are somewhat small at 2λ long.

17-7		Reference Data		
Antenna	Gain dBi	T-O angle	Beam -width	Source Z $R \pm jX \Omega$
3.6 MHz End-Fed	14.81	17°	27°	733.0 - j 11.8
3.6 MHz Center-Fed	15.15	17°	27°	1503 + j 450
7.2 MHz End-Fed	14.74	17°	26°	677.5 + j 43.8
7.2 MHz Center-Fed	15.08	17°	26°	1352 + j 313

17-8.NEC: A Vee-beam for 14.175 MHz

Another departure from the basic arrays we studied early in this chapter is the Vee-beam, a many-wavelength long wire antenna. With the terminating resistors shown in **Figure 17-8**, the antenna becomes a directional "traveling-wave" array, similar in principle to the terminated rhombic we encountered in Chapter 12. Without the terminating resistors, the Vee-beam (as well as the rhombic) is bi-directional, with a tiny front-to-back ratio. In general, for equal lengths, the rhombic tends to have slightly more gain than the Vee-beam.



Since Vee-beams are ordinarily 5λ or longer, they require many segments, which can challenge a computer with limited resources. The segmentation density must be large enough so that the feed segment is about the same length as the segments in the long arms. Alternatively, you can use a split feed and bring the arms to a point. Nonetheless, the resultant models tend to be large (400-500 segments) with longer run times.

```

CM Vee beam: 14.175 MHz
CE
GW 1 220 107 -35 15.24 0 -.15 15.24 .0010265
GW 2 1 0 -.15 15.24 0 .15 15.24 .0010265
GW 3 220 0 .15 15.24 107 35 15.24 .0010265
GS 0 0 1
GE 1
GN 2 0 0 0 13 .005 0 0 0 0
EX 0 2 1 0 1.414214 0
LD 5 1 1 220 5.8001E7
LD 5 2 1 1 5.8001E7
LD 5 3 1 220 5.8001E7
FR 0 1 0 0 14.175 0
RP 0 1 361 1000 76 0 1 1
FR 0 1 0 0 14.175 0
RP 0 181 1 1000 -90 0 1 1
EN
    
```

Open model 17-8.NEC. This 5λ Vee-beam has two main legs plus a short feedpoint segment. Since we are working with bi-directional arrays, the model has no terminating resistors. The dimensions are in meters. The two legs depart from the center line between them by a certain angle, about 18° on each side. The first question to answer is how to determine this angle.

Begin with a single wire antenna whose length is equal to one of the Vee-beam legs. Model 17-8-1.NEC is such an antenna. Like the model in 17-8.NEC, the antenna is 15.24 m (50') above average S-N ground. The single leg is 112.58 m long. Run this model, paying special attention to the azimuth pattern. Determine the azimuth angle of maximum radiation relative to the axis along which the antenna wire runs.

```

CM 5 wl long wire, end fed: 14.175 MHz
CE
GW 1 220 0 0 15.24 112.58 0 15.24 .0010265
GS 0 0 1
GE 1
GN 2 0 0 0 13 .005 0 0 0 0
EX 0 1 1 0 1.414214 0
LD 5 1 1 220 5.8001E7
FR 0 1 0 0 14.175 0
RP 0 181 1 1000 -90 17 1 1
FR 0 1 0 0 14.175 0
RP 0 1 360 1000 75 0 1 1
EN

```

17-8-1

For the 1-wire model, the angle is 17-18° and this determines the angle for each of the Vee-beam wires as they depart from the center line. Of the remaining data, perhaps the most important item is the maximum gain of 11.67 dBi. While we are viewing the azimuth pattern, we may also note the great number of minor lobes.

Having set the angle for our Vee-beam, we may now run the model. Gather data on the gain, front-to-back ratio (if any), take-off angle, beamwidth, and source impedance for each of the frequencies on the table.

17-8 Test Data					
Frequency MHz	Gain dBi	F-B dB	T-O Angle	Beamwidth	Source Z R ± jX Ω
14.175					
18.118					
21.225					
24.94					
28.5					

Comments: Like rhombics, Vee-beams are designed to be useful on frequencies above the design frequency. The usual frequency limits are a ratio of 2:1 with the design frequency, depending upon the angle chosen for the beam. As the tabular data shows, the Vee-beam exhibits excellent gain with a narrow beamwidth through 28.5 MHz. The front-to-back ratio is small compared to directional antennas, but large enough to make the orientation of the Vee an important consideration. The source impedance values show large variations.

Whether the Vee-beam is useful in a particular application may depend upon the

tolerance for the many side lobes that remain in the azimuth pattern. Some of the minor lobes are less than 10 dB below the main lobe on some frequencies. Consequently, despite the simplicity of the Vee-beam in its bi-directional form, some of the other array designs may turn out to be more practical.

17-8 Reference Data					
Frequency MHz	Gain dBi	F-B dB	T-O Angle	Beam-width	Source Z $R \pm jX \Omega$
14.175	14.47	2.54	14°	14°	275 + j 486
18.118	15.77	2.82	11°	12°	249 + j 345
21.225	16.45	2.73	10°	10°	3073 - j 542
24.94	16.63	3.00	8°	10°	535 + j 799
28.5	16.35	3.33	7°	8°	203 - j 128

Open to question is whether the model we have explored has chosen the optimal angle between wires for a. the design frequency or b. the range of frequencies in the test. As a supplemental exercise, test the Vee-beam on all of the assigned frequencies using both larger and smaller angles between the wires.

Summing Up

Our foray into bi-directional wire arrays has attempted to sample the modeling challenges offered by the diverse assortment of antennas in this realm. We began with the basic element of the array, the $1/2\lambda$ wire, and then combined these into collinear, end-fire, and broadside arrays. From there, it was only a small step into using phased collinear elements, such as the EDZ, in similar but larger arrays with enhanced performance. Finally, we examined the modeling challenges of array types that do not easily fit the main categories, such as the Sterba curtain and the Vee-beam. And this is only the beginning.

The proper modeling evaluation of a wire array requires access to almost all of the collections of data produced by NEC-2: elevation and azimuth patterns, source impedance information, current magnitude and phase tables and graphics, frequency sweeps, and much more. Unlike some types of antennas for which limited information is sufficient to guide further development, wire arrays demand attention to virtually everything we can calculate if we are to perfect a design or to understand its potentials and limitations.

In large bi-directional wire arrays, field strength is often purchased at the expense of -3 dB beamwidth. For some applications, the very high-gain narrow-beamwidth pattern is

precisely required. For others, it inhibits communications. Consequently, the selection of an array to use for a particular purpose requires multi-faceted thinking if that selection is to be judicious.

Of course, most bi-directional arrays are large, when measured in terms of wavelengths. Hence, we must pay equal attention to our model construction to ensure adequate levels of segmentation without exceeding program or run-time limitations. The use of transmission lines to feed elements either in phase or out of phase is another facet of model construction requiring care. Because a complex wire array may involve many wires and many transmission lines, it serves as a paradigm case for the warning to check carefully all models before running them.

As a class of antennas, the bi-directional wire arrays hold a fascination for many antenna designers and experimenters. By careful modeling, one might convert many of the designs into directional antennas via parasitic or phasing techniques.

18.

Yagis

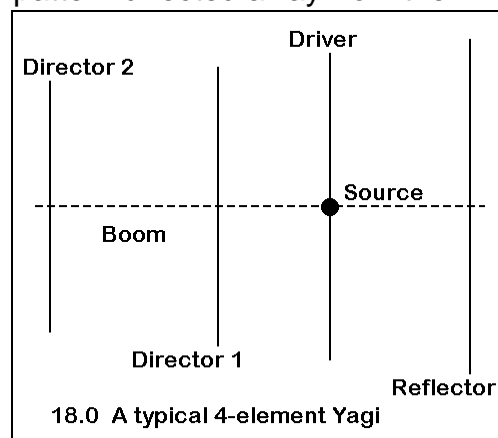
Objectives: The Yagi antenna is among the most common and varied horizontally polarized antenna design used from HF through UHF. In these exercises, you will become acquainted with some of the characteristics of parasitic antenna element modeling and operation. You will also work with multi-band Yagis and with stacks.

The Yagi, named for the Yagi-Uda discoveries and developments of the 1920s, has become a *de facto* standard for multi-element antenna arrays in the HF through UHF range. Used as horizontally polarized beams at HF, Yagis also perform as vertically polarized antennas at VHF and UHF. Versions of the antenna range from 2-element copper wire antennas for lower HF operation to long-boom giants, including up to 40+ elements for UHF use.

In these exercises, we shall confine ourselves to HF Yagis, since a future chapter will pay special attention to VHF and UHF antenna designs. Even within these limits, there are too many design variations to sample adequately. Therefore, we shall focus instead on some of the primary characteristics of Yagis as revealed by some common members of this family of antennas.

The Yagi is based on principles of parasitic elements, that is, elements not directly fed by an energy source. These elements achieve their ability to alter and focus the radiation pattern by the currents induced in them by radiation from the driven element. According to their length and spacing from the driven element, the parasitic elements become either directors or reflectors. Directors are shorter than the driven element (by 1 to 5%, depending upon spacing) and result in the radiation pattern being sharply distorted in the direction of the director. Reflectors are longer than the driven element (again, by 1 to 5%, depending upon spacing) and result in a radiation pattern directed away from them.

It is possible to create Yagi arrays with just two elements--either a director-driver combination or a reflector-drive combination. However, Yagis acquire significantly more gain and a better controlled front-to-back ratio when they employ at least three elements. Normally, for Yagis of 3 or more elements, there is one reflector and one driver, with additional elements being directors. **Figure 18-0** illustrates a 4-element Yagi to give a general impression of the taper of the elements. Traditional Yagi design tends toward reducing the



length of each director forward of the driver. However, some designs optimized for various purposes may have equal length directors or even one that is shorter than its adjacent directors.

Recommended reading on Yagi design includes Dr. James L. Lawson's *Yagi Antenna Design* (Newington: ARRL, 1986), which developed a large body of systematic data about many aspects of Yagi design via computer models. Although a number of ingredients in Lawson's analysis have undergone refinement, basic principles remain intact. The dependency of Yagis for gain upon boom length rather than the number of elements and the recognition of the role of tapered-diameter elements are but two of many Lawson precepts.

Despite intensive work by many over the decades since the 1920s, Yagi design is far from exhausted. Moreover, design debate continues to this day. For example, some designers prefer high gain and accept a narrower operating bandwidth and lower source impedance as the cost of that gain. Others opt for a higher source impedance and wider operating bandwidth at a cost of either less gain or an additional element for a given boom length.

In this set of exercises, we shall first look at models exhibiting basic Yagi properties and limitations. We shall then move to models that exemplify some of the design trade-offs inherent in Yagis. Finally, we shall explore a few multi-band Yagi models to discover additional trade-offs involved in multi-frequency design.

Yagi antennas generally refer to a subclass of parasitic antenna arrays, normally those involving a $1/2\lambda$ driven element and parasitic elements close to $1/2\lambda$ long. However, parasitic arrays can also include other antenna types, including vertical monopoles and non-resonant driver arrays. For example, we have known since the mid-1930s how to create a parasitic array from two extended double Zepp (1.25λ) elements.

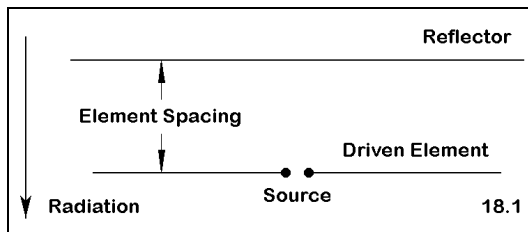
ExercisePreparation

The characteristics of most Yagi beams or arrays are best gathered by running a frequency sweep across a band of frequencies of interest. The antennas in this set of exercises are designed for the amateur radio high frequency spectrum, where bandwidths may range from 13% of the band center frequency down to 0.4%. These bandwidths present Yagi designers with very different challenges, which may call for different types of configurations of reflectors and/or directors.

All of the Yagi designs in this exercise set have placed the point of maximum front-to-back ratio at the design center frequency, midway between the frequency sweep limits built into the initial models. Since the frequency of maximum gain ordinarily does not coincide with the frequency of maximum front-to-back ratio in Yagi design, the peak gain obtainable from a design may be near the frequency sweep limit at one or the other end of a band--or it may lie outside the band. In actual designs, the front-to-back ratio peak may be moved closer to one or the other end of a range of frequencies to achieve the best pattern balance across a band. In addition, the driven elements have been resonated at the design center frequency. In reality, the driver may change its length by a considerable amount without affecting either the gain or the front-to-back ratio. This feature permits the designer to make the driver either capacitively or inductively reactive to suit a particular matching system of choice, if the source impedance does not match the system feedline characteristic impedance.

Some exercises may call for supplemental frequency sweeps in addition to the one programmed into the model. Be sure to save these additional sweeps as separate models, using whatever filename scheme you have developed to this point. More importantly, please do make the recommended additional sweeps.

18-1.NEC: A 2-element driver-reflector Yagi for 28.5 MHz



One of the most fundamental Yagi designs is the 2-element configuration, consisting of a driven element (or driver) and a reflector, as sketched in **Figure 18.1**. The reflector is longer than the driver, but the exact amount depends upon element spacing. We shall sample two different spacings to catalog their effect on performance

and source impedance.

Model 18-1.NEC uses element spacing close to $1/8\lambda$, a typical value in 2-element design. This and the next model use 0.75" diameter 6061-T6 aluminum elements, with dimensions in feet. For convenience, these models are in free space. However, upon completing the work of this exercise, you should systematically examine the performance and source impedance characteristics of both models at heights ranging from $1/2\lambda$ to 2λ above various qualities of ground in order to develop a fuller understanding of their operation.

```

CM 2-element Yagi:  DE/Ref-.123w1 sp
CE
GW 1 13 -7.96 0 0 7.96 0 0 .03125
GW 2 13 -8.67 -4.25 0 8.67 -4.25 0 .03125
GS 0 0 .3048
GE 0
EX 0 1 7 0 1 0
LD 5 1 1 13 2.4938E7
LD 5 2 1 13 2.4938E7
FR 0 6 0 0 28 .2
RP 0 1 360 1000 90 0 1 1
EN

```

18-1

Yagis

```

CM 2-el Yagi: de-ref--.174 wl spacing
CE
GW 1 13 -7.92 0 0 7.92 0 0 .03125
GW 2 13 -8.67 -6 0 8.67 -6 0 .03125
GS 0 0 .3048
GE 0
EX 0 1 7 0 1 0
LD 5 1 1 13 2.4938E7
LD 5 2 1 13 2.4938E7
FR 0 6 0 0 28 .2
RP 0 1 360 1000 90 0 1 1
EN

```

18-1-1

Model 18-1-1.NEC, shown on the next page, increases the spacing closer to $3/16\lambda$, a small fractional increase, but a real distance of 1.75' at 28.5 MHz, the design center frequency of both models. Note that the reflectors of both models have the same length. However, the driven elements differ in resonant length, with the one in the wider-spaced model being marginally (1") shorter.

For this exercise, run both models across the span from 28 to 29 MHz in 0.2 MHz steps. Record the forward gain (90°), the rearward gain (270°), the resulting 180° front-to-back ratio, the source impedance, and the 50- Ω VSWR for each step.

18-1 Test Data					
Frequency MHz	Forward Gain dBi	Rear Gain dBi	F-B dB	Source Z R \pm jX Ω	50- Ω VSWR
28.0 18-1 18-1-1					
28.2 18-1 18-1-1					
28.4 18-1 18-1-1					
28.6 18-1 18-1-1					
28.8 18-1 18-1-1					
29.0 18-1 18-1-1					

Comments: There are two different aspects to the data you have collected. One facet is the comparison of 2-element Yagis of different spacings. The other is the general pattern of reflector-driver design performance.

Although the differences are small in practical operational terms, the closer-spaced Yagi shows consistently higher gain and front-to-back ratio than the wide-spaced model. However, the wider-spaced version has a source impedance that is closely matched to the typical 50- Ω coaxial cable system feedline. The wider spacing between reflector and

driven element yields a higher source impedance, but a longer boom. Operationally, then, the final decision between these designs would involve mechanical as well as electrical factors.

The two designs nevertheless have a number of significant features in common, features that are earmarks of the basic arrangement of elements. First, the gain increases as the frequency decreases. The gain diminishes slowly with frequency increases. However, as the frequency goes down, there will be a point at which the gain no longer increases. In a small span, the antenna will reverse direction, with maximum gain on the reflector side of the array. You should revise the frequency sweep to run from 26 to 30 MHz in 0.5 MHz steps in order to track the gain curve more closely.

At a frequency below the bandwidth scanned in this exercise but above the reversal frequency region, the antenna will exhibit a free space gain above 7 dBi. However, at that point, the front-to-back ratio will be negligible (4 to 7 dB), and the source impedance will be very low (10 to 15 Ω).

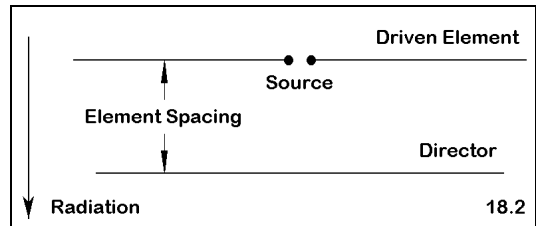
Second, the source impedance increases as the frequency increases. Despite the design differences and the average value of the resistive component of the source impedance, the resistance increases by about the same amount for both designs across the 1 MHz scanned range.

18-1 Reference Data						
Frequency MHz		Forward Gain dBi	Rear Gain dBi	F-B dB	Source Z R ± jX Ω	50-Ω VSWR
28.0	18-1	6.72	-3.26	9.98	24.1 - j20.0	2.49
	18-1-1	6.45	-3.46	9.91	41.9 - j16.8	1.50
28.2	18-1	6.55	-4.23	10.78	27.4 - j11.7	1.96
	18-1-1	6.30	-4.12	10.42	45.7 - j 9.8	1.25
28.4	18-1	6.38	-4.77	11.15	30.7 - j 3.9	1.64
	18-1-1	6.15	-4.52	10.67	49.3 - j 3.1	1.07
28.6	18-1	6.21	-4.97	11.18	34.0 + j 3.7	1.48
	18-1-1	6.01	-4.69	10.70	52.8 + j 3.3	1.09
28.8	18-1	6.05	-4.91	10.96	37.2 + j10.9	1.47
	18-1-1	5.87	-4.70	10.57	56.1 + j 9.5	1.24
29.0	18-1	5.91	-4.71	10.62	40.4 + j17.9	1.57
	18-1-1	5.75	-4.60	10.35	59.3 + j15.6	1.39

Despite the limitations of this design, it is able to operate across an entire MHz in the vicinity of 30 MHz. Of course, these figures would be proportionately lower as one decreases the frequency, amounting to about 0.5 MHz in the 15 MHz region. In terms of Yagi design, the reflector-drive configuration is considered a broad-band antenna.

18-2.NEC: A 2-element driver-director Yagi for 28.5 MHz

A 2-element Yagi composed of a driven element and a director can achieve higher gain and front-to-back ratios than a 2-element driver-reflector design. However, as we shall see, the antenna exhibits a fairly narrow operating bandwidth, especially when compared to the reflector-drive configuration.



```
CM 2-e1 Yagi: de/dir-.072 spacing
CE
GW 1 13 -8.02 0 0 8.02 0 0 .03125
GW 2 13 -8.59 -2.5 0 8.59 -2.5 0 .03125
GS 0 0 .3048
GE 0
EX 0 2 7 0 1 0
LD 5 1 1 13 2.4938E7
LD 5 2 1 13 2.4938E7
FR 0 6 0 0 28 .2
RP 0 1 360 1000 90 0 1 1
EN
```

18-2

Model 18-2.NEC is a typical driver-director design set at a design center frequency of 28.5 MHz. Like the reflector designs, the material is 0.75" diameter 6061-T6 aluminum, and the antenna is modeled in free space. The spacing of this model is about 0.07λ , typical of the close spacing needed for maximum performance while maintaining a source impedance high enough to avoid the loss of a serious percentage of power to the resistance of connections and other mechanical junctions.

The companion model, 18-2-1.NEC, spaces the elements further apart by a bit under 0.9λ . Even though this increase amounts to only 0.5', the effects on the element lengths are very noticeable. The wider-spaced version has a slightly shorter driven element and a more significantly shorter director.

```
CM 2-e1 Yagi: de/dir-0.87 w1 spacing
CE
GW 1 13 -7.95 0 0 7.95 0 0 .03125
GW 2 13 -8.54 -3 0 8.54 -3 0 .03125
GS 0 0 .3048
GE 0
EX 0 2 7 0 1 0
LD 5 1 1 13 2.4938E7
LD 5 2 1 13 2.4938E7
FR 0 6 0 0 28 .2
RP 0 1 360 1000 90 0 1 1
EN
```

18-2-1

For both of these antennas, we shall perform the same frequency sweep as before: from 28 to 29 MHz in 0.2 MHz steps. As well, we shall record the same data: forward gain, reverse gain, front-to-back ratio, source impedance, and 50-Ω VSWR. Use the table on the next page to record the results of the sweep.

Comments: As with the first design that we explored, the data for the driver-director design has two aspects: a comparison between the two models and a set of

characteristics common to all Yagis of this configuration. Comparatively, both models have similar gain curves, but the closer-spaced model achieves much better front-to-back ratios. Both antennas are designed to show a peak in the 180° front-to-back ratio near the design center frequency. However, the cost for the better rearward rejection is a lower source impedance. The rate of change of both the resistive and reactive components of the source impedance are similar for the two antennas.

18-2 Test Data					
Frequency MHz	Forward Gain dBi	Rear Gain dBi	F-B dB	Source Z $R \pm jX \Omega$	50-Ω VSWR
28.0 18-2 18-2-1					
28.2 18-2 18-2-1					
28.4 18-2 18-2-1					
28.6 18-2 18-2-1					
28.8 18-2 18-2-1					
29.0 18-2 18-2-1					

Consistent with each other, both driver-director designs show a high rate of change of both resistance and reactance at the source. This factor alone tends to limit the operating bandwidth to under 0.5 MHz in the 30 MHz region, with correspondingly smaller operating bandwidths at lower frequencies. Consequently, the design is rarely used on the wider amateur radio allocations at 20, 15, and 10 meters. However, the design can prove entirely adequate for the 30, 17, and 12 meter bands, each of which is at most 0.1 MHz wide.

Unlike the reflector designs, director designs increase in gain with increases in frequency, and they show a decreasing source impedance with frequency increases. The gain continues to increase beyond the range scanned in this exercise, although the front-to-back ratio almost disappears and the source impedance soon descends to about 10 Ω . At some higher frequency, the pattern will reverse, with the most gain in the opposite direction from the director. You should expand the frequency sweep to go from 28 to 30 MHz on 0.25 MHz steps to find the reversal region in the vicinity of 29.75 MHz for model

18-2.NEC.

The trends for virtually all operating parameters are opposite for the two types of configurations possible in 2-element Yagis. You should feel free to develop further models with different spacings to test these conclusions and to develop expectations for the rates of change for each of the major specifications. Element spacings for reflector designs have ranged from 0.1 to 0.25λ , while director designs have used spacings from 0.05 to 0.125λ .

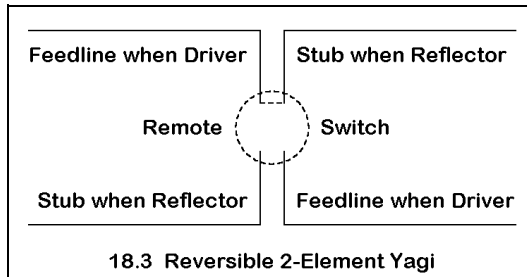
18-2 Reference Data						
Frequency MHz		Forward Gain dBi	Rear Gain dBi	F-B dB	Source Z $R \pm jX \Omega$	50- Ω VSWR
28.0	18-2	5.60	- 6.84	12.44	31.9 - j20.0	
	18-2-1	5.71	- 6.97	12.68	35.1 - j18.9	
28.2	18-2	5.93	- 9.74	15.67	27.5 - j12.7	
	18-2-1	6.03	- 9.21	15.24	31.3 - j11.9	
28.4	18-2	6.30	-15.12	21.42	22.9 - j 4.2	
	18-2-1	6.36	-11.58	17.94	27.0 - j 3.9	
28.6	18-2	6.67	-17.05	23.72	18.6 + j 5.0	
	18-2-1	6.71	-10.72	17.43	22.9 + j 5.1	
28.8	18-2	7.03	- 8.40	15.43	14.8 + j15.4	
	18-2-1	7.02	- 6.49	13.51	19.1 + j15.0	
29.0	18-2	7.29	- 2.84	10.13	11.7 + j26.6	
	18-2-1	7.26	- 2.40	9.66	15.8 + j25.9	

18-3.NEC: A reversible wire Yagi for 10.1-10.15 MHz

Although aluminum Yagis are available for use on frequencies below 12 MHz, fixed-position copper wire Yagis often serve important communications functions. The principles of operation are identical to those employed with Yagis using larger diameter elements, although the operating bandwidth of a wire Yagi may be relatively smaller. Wire Yagi installations often prompt the use of elements of identical lengths, with a reflector electrically lengthened by the insertion of an inductive reactance. Although inductively reactive loads can significantly reduce gain when applied to the driven element, their use in parasitic elements with lower current levels produces few noticeable ill-effects.

Run model 18-3.NEC, a 2 element #12 AWG copper wire beam with a design center frequency of 10.125 MHz. This free space model has identical 46.24' elements spaced 14.2' (slightly less than 0.15λ) apart. The reflector is center loaded with a type 4 reactive

load of 75Ω . You should obtain a free space gain of about 6.07 dBi and a front-to-back ratio of about 10.90 dB, with a source impedance of $43.5 - j 0.1 \Omega$.



The question is how best to implement the required load. We might add an inductance to the reflector. However, let's consider another option. If we use a transmission line stub, either shorted or open, we can make the Yagi reversible. By adding stubs to each element and bringing them to a central point--either elevated or near the ground--we can use one line as a stub and the other as a section of the system feedline.

A simple remote switching system would permit role reversal for the two sections of line. The system is sketched in **Figure 18.3**.

Since we may use either a shorted stub or an open-ended stub to accomplish the same loading task, we may choose the stub type that results in the best length for the installation. Refer to the chapter on reactive loads for information on calculating suitable stubs.

Models 18-3-1.NEC through 18-3-3.NEC provide examples of stubs suitable for use in such an installation. 18-3-1.NEC, shown at right, uses a 15.21' (4.636 m) shorted stub of $50\text{-}\Omega$ transmission line ($VF = 1.0$). (Note that you may have to enter transmission line data in meters even if the antenna dimensions are in feet or inches. As well, you may have to separately calculate the effects of the line's velocity factor on the physical length of the stub.)

```
CM 2-el bi-directional Yagi: 10.1-10.15 MHz
CM Shorted stub load on reflector
CE
GW 1 13 -23.12 0 0 23.12 0 0 3.36778215223097E-03
GW 2 13 -23.12 -14.2 0 23.12 -14.2 0 3.36778215223097E-03
GW 3 1 -.2 -14.2 -20 .2 -14.2 -20 1.05643044619423E-03
GS 0 0 .3048
GE 0
EX 0 1 7 0 1 0
LD 5 1 1 13 5.8001E7
LD 5 2 1 13 5.8001E7
TL 2 7 3 1 50 4.636008 0 0 10000000000 10000000000
FR 0 6 0 0 10.1 .01
RP 0 1 360 1000 90 0 1 1
EN
```

18-3: 1-3

Model 18-3-2.NEC is identical except for the use of a shorted stub that is 63.78' (19.44 m) long. At the design center frequency, this line is exactly $1/2\lambda$ longer than the preceding model's stub. Note once more that since NEC-2 transmission lines are mathematical rather than physical, they do not account for losses in the line. Model 18-3-3.NEC uses the same antenna dimensions with a transmission line stub that is open and 39.48' (12.034 m) long.

Apart from slight differences in losses within each length of stub, the choice of stub type and length should have no affect on antenna performance. Rather than presume that this claim is a fact, let's model each of these systems and run a frequency sweep from 10.1 MHz through 10.15 MHz in 0.01 MHz steps.

Yagis

For each model, record for each frequency step the free space forward gain, the rear gain, the 180° front-to-back ratio, the source impedance, and the 50-Ω VSWR. Use the table at the top of the next page for your data.

Note that the models do not use a length of transmission line on the driven element of these driver-reflector designs. However, as a supplementary exercise, you may add such a line and run it to an added short wire, placing the source on the new wire. These additions will not add materially to the run-time for the modified models. Note especially if the length of line makes a significant difference in the source impedance.

18-3 Test Data					
Frequency MHz	Forward Gain dBi	Rear Gain dBi	F-B dB	Source Z $R \pm jX \Omega$	50-Ω VSWR
10.10 18-3-1 18-3-2 18-3-3					
10.11 18-3-1 18-3-2 18-3-3					
10.12 18-3-1 18-3-2 18-3-3					
10.13 18-3-1 18-3-2 18-3-3					
10.14 18-3-1 18-3-2 18-3-3					
10.15 18-3-1 18-3-2 18-3-3					

Comments: As we expected, there is no significant difference in the performance of the simple Yagi with any of the stub-loading systems used. Consequently, you can choose whichever of the three (or other) stub type and lengths that will provide the correct length to reach the design position of the remote switching box. Of course, you should independently take into account losses in the stubs, especially as their length increases to over $1/2\lambda$.

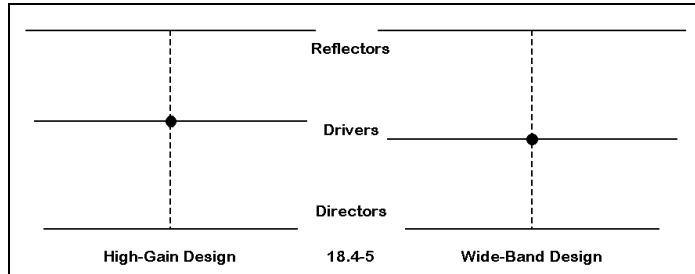
The narrow band of frequencies over which the beam is expected to operate simplifies the design considerations for this array. However, you may well revise the frequency span to test the antenna over a wider range of frequencies.

As wire beams, the designs in 18-3-1.NEC through 18-3-3.NEC will not have as broad a set of responses as antennas using larger diameter elements. Indeed, you may wish to redesign the antenna using either larger monotapered elements or tapered-diameter elements to simulate an aluminum Yagi for this band. You may use either an unloaded or a loaded reflector for your aluminum version of the beam. Once you have effected the design changes, compare the results with those you obtained for the wire models.

18-3		Reference Data			
Frequency MHz	Forward Gain dBi	Rear Gain dBi	F-B dB	Source Z $R \pm jX \Omega$	50-Ω VSWR
10.10	18-3-1 6.18	-4.60	10.78	41.3 - j 4.3	1.24
	18-3-2 6.22	-4.48	10.70	40.6 - j 4.4	1.26
	18-3-3 6.20	-4.53	10.73	40.9 - j 4.4	1.25
10.11	18-3-1 6.14	-4.72	10.86	42.2 - j 2.6	1.20
	18-3-2 6.16	-4.65	10.81	41.8 - j 2.7	1.21
	18-3-3 6.15	-4.68	10.83	42.0 - j 2.6	1.20
10.12	18-3-1 6.09	-4.80	10.89	43.1 - j 0.9	1.16
	18-3-2 6.10	-4.79	10.89	43.0 - j 0.9	1.17
	18-3-3 6.10	-4.79	10.89	43.0 - j 0.9	1.16
10.13	18-3-1 6.05	-4.87	10.92	44.0 + j 0.7	1.14
	18-3-2 6.04	-4.88	10.92	44.1 + j 0.7	1.13
	18-3-3 6.05	-4.87	10.92	44.0 + j 0.7	1.14
10.14	18-3-1 6.00	-4.91	10.91	44.9 + j 2.4	1.13
	18-3-2 5.98	-4.92	10.90	45.3 + j 2.4	1.12
	18-3-3 5.99	-4.91	10.90	45.1 + j 2.4	1.12
10.15	18-3-1 5.96	-4.93	10.89	45.8 + j 4.0	1.13
	18-3-2 5.92	-4.94	10.86	46.4 + j 4.0	1.12
	18-3-3 5.94	-4.93	10.87	46.1 + j 4.0	1.12

18-4.NEC and 18-5.NEC: High-gain and wide-band 3-element Yagis for 14.175 MHz

In this exercise, we shall examine two contrasting designs for 3-element Yagis, both consisting of one reflector and one director. They reflect two different design philosophies, sketched in **Figure 8.4-5**. One design tries to achieve the maximum gain possible (with a reasonable front-to-back ratio) for the given boom length (23').



The compromise for this "high gain" version of the Yagi is that it must hold the gain as well as possible over a frequency spread from 14.0 MHz through 14.35 MHz.

The second design strives to achieve wide-band operation, with stable (although lower) values for gain, good front-to-back ratio, and a direct match across the operating bandwidth with a 50-Ω system feedline. The sketch of the two antenna layouts reveals the different element positioning required to achieve this goal.

Open model 18.4.NEC, the high-gain Yagi. Like its counterpart, it has 1" diameter 6061-T6 aluminum elements and is modeled in free space. You will wish to compare antenna dimensions with the next model. Note especially the spacing of the driven element from the reflector (125.5").

```
CM 3-el. Yagi: wide-band: 14.0-14.35 MHz
CE
GW 1 21 -215 0 0 215 0 0 .5
GW 2 21 -199 141 0 199 141 0 .5
GW 3 21 -181 271 0 181 271 0 .5
GS 0 0 .02540
GE 0
EX 0 2 11 0 1 0
LD 5 1 1 21 2.4938E7
LD 5 2 1 21 2.4938E7
LD 5 3 1 21 2.4938E7
FR 0 6 0 0 14 .07
RP 0 1 360 1000 90 0 1 1
EN
```

```
CM 3-el. Yagi: high gain: 14-14.35 MHz
CE
GW 1 21 -207.4 0 0 207.4 0 0 .5
GW 2 21 -198 125.5 0 198 125.5 0 .5
GW 3 21 -186.3 270.5 0 186.3 270.5 0 .5
GS 0 0 .02540
GE 0
EX 0 2 11 0 1 0
LD 5 1 1 21 2.4938E7
LD 5 2 1 21 2.4938E7
LD 5 3 1 21 2.4938E7
FR 0 6 0 0 14 .07
RP 0 1 361 1000 90 0 1 1
EN
```

Next, open model 18-5.NEC, the wide-band version of the 3-element Yagi. Compare the reflector-driver spacing to that of the high-gain version.

Run the indicated frequency sweep of the two beams from 14.0 through 14.35 MHz in 0.07 MHz steps. Record the same data we have used throughout this exercise.

18-4/5		Test Data			
Frequency MHz	Forward Gain dBi	Rear Gain dBi	F-B dB	Source Z $R \pm jX \Omega$	50- Ω VSWR
14.0 18-4 18-5					
14.07 18-4 18-5					
14.14 18-4 18-5					
14.21 18-4 18-5					
14.28 18-4 18-5					
14.35 18-4 18-5					

Comments: As we did with the 2-element Yagis, we shall divide our observations of these beams into two categories: how they contrast and what they have in common. The contrast between the beams is especially apparent in the gain column, where the high-gain version averages about 1 dB additional gain across the band of frequencies we swept. The front-to-back ratios are comparable, although the wide-band version shows a smoother curve. (For most Yagi applications, a 20 dB front-to-back ratio is considered adequate in designs with more than 2 elements. However, you may wish to explore the azimuth patterns to ascertain both the front-to-rear ratio and the worst-case front-to-back ratio before making final judgments.)

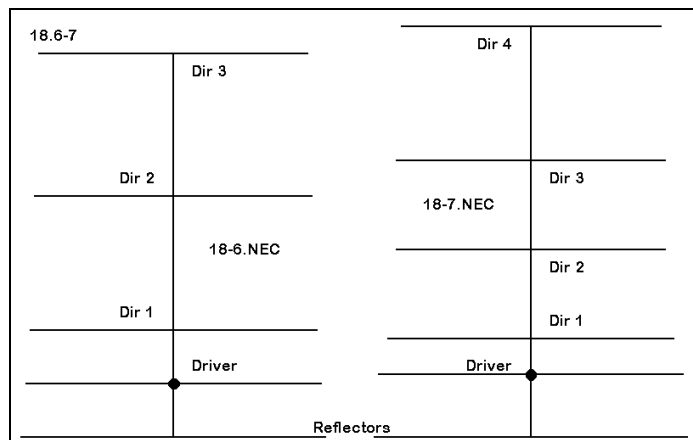
The wide-band Yagi exhibits a very low VSWR relative to a 50- Ω system feedline, thus simplifying matching the antenna to the line. In contrast, the high-gain version requires the use of a matching network. Any common matching system (gamma, beta, Tee, $1/4\lambda$ transmission line) will provide full bandwidth coverage in view of the small changes in both the resistive and reactive components of the source impedance. Whether the advantage of higher gain outweighs the wide-band version's smoother performance curves and direct system feedline match is a decision beyond the scope of this exercise.

18-4/5		Reference Data				
Frequency MHz		Forward Gain dBi	Rear Gain dBi	F-B dB	Source Z $R \pm jX \Omega$	50- Ω VSWR
14.0	18-4	7.94	-12.98	21.92	27.1 - j13.2	2.02
	18-5	7.06	-13.47	20.53	47.1 - j 9.3	1.22
14.07	18-4	8.00	-17.39	25.39	26.8 - j 8.5	1.94
	18-5	7.08	-13.77	20.85	46.9 - j 5.6	1.14
14.14	18-4	8.07	-20.55	28.62	26.2 - j 3.5	1.92
	18-5	7.11	-13.82	20.93	46.5 - j 1.7	1.08
14.21	18-4	8.15	-16.77	24.92	25.3 + j 1.7	1.98
	18-5	7.15	-13.59	20.74	45.8 + j 2.2	1.10
14.28	18-4	8.24	-12.51	20.75	24.7 + j 7.2	2.12
	18-5	7.20	-13.09	20.29	45.0 + j 6.4	1.19
14.35	18-4	8.34	- 9.31	17.65	22.9 + j13.0	2.36
	18-5	7.27	-12.35	19.62	43.9 + j10.7	1.30

What these two beams have in common is that the gain increases and the source impedance decreases across the band of frequencies we swept. Yagis with three elements share this property with the 2-element driver-director design. The phenomena are indicators that, to a very large degree, the directors control the operating characteristics of the Yagi array. The reflector cannot easily be eliminated from Yagi design. To a significant degree, it provides the Yagi with a wide operating bandwidth. Of greater importance is that fact that the reflector length and spacing from the driver controls the source impedance of the Yagi. Although this factor may be modified via the addition of an extra director more closely spaced to the driver, the reflector is an essential ingredient in the determination of the source impedance characteristics of the beam.

18-6.NEC and 18-7.NEC: Long-boom Yagis for 14.175 MHz

It is often useful to frequency sweep a Yagi design across the band of frequencies for which it is intended in order to make comparative evaluations of performance potentials. Models 18-6.NEC and 18-7.NEC are both long boom Yagis intended to provide about 10 dBi free space gain



with a front-to-back ratio in excess of 20 dB and to be matched to a 50- Ω system feedline. As **Figure 18.6-7** illustrates, they take quite different design approaches to this goal.

```

CM 5-el. Yagi: 14.175 MHz 18-6
CE
GW 1 5 -215.6 0 0 -156 0 0 .3125
GW 2 3 -156 0 0 -120 0 0 .375
GW 3 4 -120 0 0 -72 0 0 .4375
GW 4 13 -72 0 0 72 0 0 .5
GW 5 4 72 0 0 120 0 0 .4375
GW 6 3 120 0 0 156 0 0 .375
GW 7 5 156 0 0 215.6 0 0 .3125
GW 8 4 -205.95 79.8 0 -156 79.8 0 .3125
GW 9 3 -156 79.8 0 -120 79.8 0 .375
GW 10 4 -120 79.8 0 -72 79.8 0 .4375
GW 11 13 -72 79.8 0 72 79.8 0 .5
GW 12 4 72 79.8 0 120 79.8 0 .4375
GW 13 3 120 79.8 0 156 79.8 0 .375
GW 14 4 156 79.8 0 205.95 79.8 0 .3125

```

Model 18-6.NEC is a tapered-diameter 6061-T6 aluminum Yagi with 5 elements, only two of which are shown at left. The design uses the spacing (with attention to element length) between the driver and the reflector as well as the first director to establish a source impedance compatible with a 50- Ω feed system. As we shall see, although the source impedance is adequate, it leaves room for perfection. However, further enhancement of the source impedance would have required additional spacing between the reflector and the driver, requiring a boom longer than the design limit of 45'

and would also have required additional spacing between directors. (Impedances closer to 50 Ω have been achieved at the design frequency of 14.175 MHz with booms of 53 to 55 feet.)

Model 18-7.NEC is also comprised of 6061-T6 tapered-diameter elements, this time 6 of them on a 48' boom. Again, only the reflector and driver appear in the description box, since the full model description would be longer than this page. However, you can view the full description via NECWin Plus. The principle behind the design is to use a wider spacing between the reflector and driver to increase the source impedance and to control those characteristics through a close-spaced first director. Attaining the desired gain and front-to-back ratio characteristics requires 3 directors in the remaining boom space, giving the beam a total of six elements. Designs willing to settle for a lower source impedance (in the 25- Ω range) can achieve similar gain and front-to-back ratio results using only 5 elements.

```

CM 6-el Yagi: 14.175 MHz 18-7
CE
GW 1 7 -217.73 0 0 -152 0 0 .25
GW 2 4 -152 0 0 -116 0 0 .3125
GW 3 4 -116 0 0 -72 0 0 .375
GW 4 2 -72 0 0 -48 0 0 .4375
GW 5 9 -48 0 0 48 0 0 .5
GW 6 2 48 0 0 72 0 0 .4375
GW 7 4 72 0 0 116 0 0 .375
GW 8 4 116 0 0 152 0 0 .3125
GW 9 7 152 0 0 217.73 0 0 .25
GW 10 6 -210.7 90 0 -152 90 0 .25
GW 11 4 -152 90 0 -116 90 0 .3125
GW 12 4 -116 90 0 -72 90 0 .375
GW 13 2 -72 90 0 -48 90 0 .4375
GW 14 9 -48 90 0 48 90 0 .5
GW 15 2 48 90 0 72 90 0 .4375
GW 16 4 72 90 0 116 90 0 .375
GW 17 4 116 90 0 152 90 0 .3125
GW 18 6 152 90 0 210.7 90 0 .25

```

Run a frequency scan for both 18-6.NEC and 18-7.NEC from 14.0 through 14.35 MHz in 0.07 MHz steps. Record the forward gain, front-to-back ratio, source impedance, and 50- Ω VSWR for each beam in order to compare the results.

18-6 & 18-7		Test Data			
Frequency MHz		Forward Gain dBi	F-B dB	Source Z $R \pm jX \Omega$	50- Ω VSWR
14.00	18-6 18-7				
14.07	18-6 18-7				
14.14	18-6 18-7				
14.21	18-6 18-7				
14.28	18-6 18-7				
14.35	18-6 18-7				

Comments: By now, you have run enough examples to determine the 180° front-to-back ratio without need for recording the rear gain. You have also experienced the value of using this parameter to determine the frequency of maximum rearward null as a design factor. However, remember that the front-to-rear ratio and the worst-case front-to-back ratio remain equally valuable measures of antenna performance. Clearly, both antennas perform comparably with respect to gain and front-to-back ratio across the band of frequencies swept in the test. However, the source impedance of the longer boom model, with its extra controlling director, is clearly superior with respect to forming a direct match with 50- Ω feedline systems. Losses in the transmission line may be less, especially where long cable runs are required. Moreover, some equipment exhibits great sensitivity in its sensors to even low values of VSWR, reducing the available power output for values as low as 1.5:1. In these and similar situations, the 48' boom design might be advisable. Nevertheless, the 45' boom design would be entirely satisfactory in many other situations.

As the boom length and number of elements in a Yagi increase, it becomes possible to control various of the performance curves and to make them converge within the limits of the frequency coverage of the antenna. The 45' boom Yagi brings the gain and front-to-back curves to near coincidence, although the source impedance continues to rise across the span from 14.0 through 14.35 MHz. In contrast, the 48' boom model achieves a close coincidence of the source impedance and front-to-back ratio curves, while the gain continues to rise beyond the limits of the frequency sweep. Although some design tasks

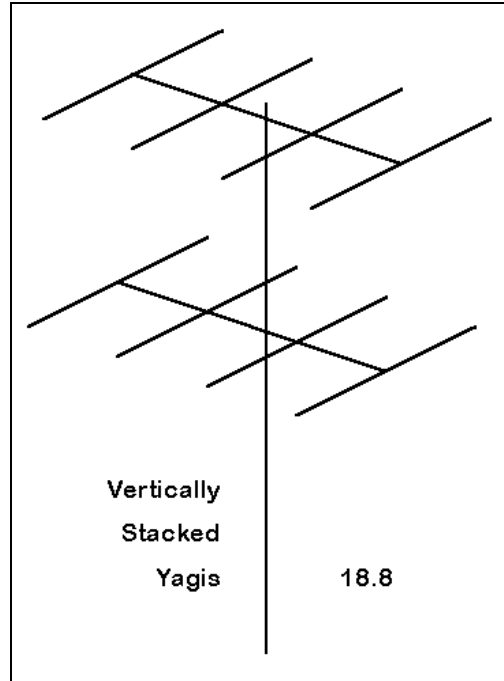
may single out only one of the many performance specifications to optimize--gain, for instance--an ideal Yagi design strives to control as many of the performance characteristics as possible. Although achieving a coincident peak of gain, front-to-back ratio, and source impedance at a desired value is theoretically possible, it is likely to result in a mechanically unfeasible design.

18-6 & 18-7		Reference Data			
Frequency MHz		Forward Gain dBi	F-B dB	Source Z $R \pm jX \Omega$	50- Ω VSWR
14.00	18-6	10.05	21.09	31.6 - j 11.2	1.71
	18-7	10.09	24.64	41.6 - j 0.8	1.20
14.07	18-6	10.13	25.86	31.6 - j 7.7	1.65
	18-7	10.15	28.83	43.1 + j 0.9	1.16
14.14	18-6	10.21	36.69	31.9 - j 3.9	1.58
	18-7	10.20	30.88	44.3 + j 1.9	1.14
14.21	18-6	10.26	31.91	33.3 - j 0.5	1.50
	18-7	10.25	27.90	44.8 + j 2.0	1.13
14.28	18-6	10.27	24.59	33.6 + j 0.5	1.41
	18-7	10.28	24.76	43.8 + j 0.9	1.14
14.35	18-6	10.21	21.45	35.4 - j 3.7	1.43
	18-7	10.30	22.68	39.8 - j 0.9	1.26

18-8.NEC: Stacked 4-element Yagis for 14.175 MHz

A common technique for increasing the gain of a Yagi antenna system without added boom length is to stack 2 or more Yagis of the same design, as illustrated in **Figure 18.8**. Since very long booms result in many mechanical challenges, stacking Yagi beams becomes an attractive design alternative for achieving up to 3 dB gain for each additional antenna.

However, finding the correct stacking separation for maximizing gain becomes a challenge in itself. The optimal stacking distance varies significantly with the gain of the individual antennas and to a lesser extent with the height of the lower antenna above ground. As an exercise in basic theory, you may wish to examine the elevation patterns of many Yagis of varying gain to extrapolate the pattern data necessary to calculate (with due regard for ground reflections) optimal separation for stacks of 2 or more beams.



```

CM 4-el. Yagi 70' up: 14.175
CM Stack of 2, both fed in phase
CE
GW 1 21 -17.38 0 70 17.38 0 70 .04165
GW 2 21 -16.41 6 70 16.41 6 70 .04165
GW 3 21 -16.29 11 70 16.29 11 70 .04165
GW 4 21 -15.26 25.5 70 15.26 25.5 70 .04165
GW 5 21 -17.38 0 123 17.38 0 123 .04165
GW 6 21 -16.41 6 123 16.41 6 123 .04165
GW 7 21 -16.29 11 123 16.29 11 123 .04165
GW 8 21 -15.26 25.5 123 15.26 25.5 123 .04165
GS 0 0 .3048
GE 1
GN 2 0 0 0 13 .005 0 0 0 0
EX 0 2 11 0 1 0
EX 0 6 11 0 1 0
LD 5 1 1 21 2.4938E7
LD 5 2 1 21 2.4938E7
LD 5 3 1 21 2.4938E7
LD 5 4 1 21 2.4938E7
LD 5 5 1 21 2.4938E7
LD 5 6 1 21 2.4938E7
LD 5 7 1 21 2.4938E7
LD 5 8 1 21 2.4938E7
FR 0 1 0 0 14.175 0
RP 0 1 360 1000 81 0 1 1
EN
    
```

Model 18-8.NEC is a single 4-element Yagi that forms the basis for this small stacking exercise. The version at the left is model 18-8-1.NEC, a stack of two of the beams separated by about 0.75λ , which is optimal for this particular Yagi in view of both its gain and the 1λ height of the lower antenna. The beams are standard 6061-T6 aluminum monotapered 1" diameter element designs, with the lower antenna 70' above average soil using the S-N ground system. Note that the source positions are both on segment 11 of wires 2 and 6, the lower and upper driver, respectively.

Our interest in this stack will be confined to the ways in which the antennas can be operated. We may feed both together in phase, both together out of phase, the lower beam only, or

the upper beam only. Run all 4 configurations at the design center frequency of 14.175 MHz. Either modify model 18-8-1.NEC or use check models 18-8-2.NEC through 18-8-4.NEC to achieve the desired set-up. Note that setting one source at 180° relative to the

other source results in a negative value for the source voltage in the EX line of the model description.

18-8				
		Test Data		
Feed System	TO Angle degrees	Gain dBi	F-B dB	Source Z $R \pm jX \Omega$
Both in phase				
Both out of phase				
Bottom only				
Top only				

Comments: Note that only the scheme of feeding both antennas in phase results in additional gain for the assembly. The other schemes show gain ranging from 2.4 to 2.9 dB less than the in-phase combination. However, raw stack gain is not the only parameter worth noting.

Under various ionospheric conditions, the required take-off angle for transmission and reception may vary considerably. The use of the remaining stack options, especially the "bottom-only" and the "out-of-phase" options, results in a variety of angles for the strongest lobe of the array. It is possible to design not only a manual switching system, but as well, an automated system to switch to the option resulting in the strongest received signal.

18-8				
		Reference Data		
Feed System	TO Angle degrees	Gain dBi	F-B dB	Source Z $R \pm jX \Omega$
Both in phase	9	16.58	23.14	25.9 - j30.4 L 25.2 - j30.4 U
Both out of phase	22	13.73	21.39	27.5 - j27.3 L 26.9 - j27.5 U
Bottom only	14	13.77	21.35	26.8 - j28.8
Top only	8	14.17	24.66	26.1 - j29.0

Note: L = lower antenna; U = upper antenna

Note that feeding both antennas in phase results in a slightly lower elevation angle of maximum radiation than feeding the top beam only. This result will hold true of any stacking arrangement, since the composite pattern results from combining the top beam output with that of a beam with a much higher take-off angle relative to the horizon. The difference is real, although it has little operational significance.

Numerous follow-up exercises are possible and advisable. You may wish to perform frequency sweeps across the 20-meter amateur radio band to determine whether the anticipated results from the stack are frequency specific or more general. Additionally, you may wish to experiment with the spacing of the two beams in the stacked array to determine whether the present separation is indeed optimal from both the gain and front-to-back ratio perspectives. Few beams exhibit maximum front-to-back ratio and gain at the same separation. The disparity between optimum, heights for both varies widely from one design to another, and you may wish to model numerous Yagi designs to determine what patterns, if any, can be extracted from the exercise.

18-9.NEC: A non-interlaced multi-band Yagi for 18.2 and 24.95 MHz

The next stage in Yagi design involves achieving desired levels of performance on multiple separated frequencies with one set of elements, some of which may have principle duties on only one of the bands. The simplest type of set-up is to have two (or more) Yagis on the same boom, such that each set of elements is relatively independent of the other set.

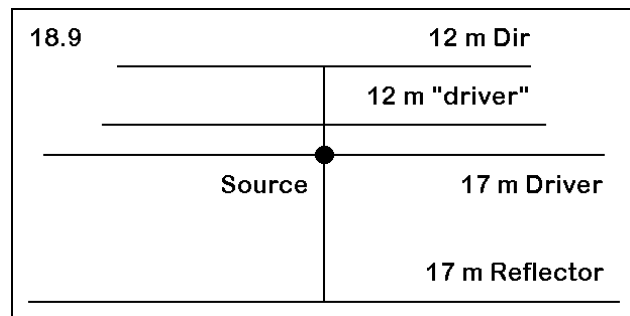


Figure 18.9 shows one such system for the amateur radio 17 and 12 meter bands. The forward (shorter) elements form a 2-element driver-director array for 24.95 MHz. Since this allocation is only 100 kHz wide, the driver-director arrangement has sufficient bandwidth to cover the entire band. The rear (longer elements) form a driver-reflector array for 18.112 MHz, with more than enough bandwidth to serve another 100 kHz allocation. The spacing was selected for a source impedance compatible with a 50-Ω system feedline.

The only "oddity" in this simple design is the use of open sleeve coupling between the lower frequency driven element, marked with a source position, and the higher frequency driver. By close coupling and careful adjustment of the 12-meter driver length and spacing from the 17-meter driver, a single feedpoint may be used on the 17 meter driver for both bands. On the higher frequency band, the single driver exhibits close to a 50-Ω source impedance and the forward elements operate as a normal driver-director array. The model, 18-9.NEC, has tapered-diameter 6061-T6 elements, with all dimensions shown in meters.

Because of the length of the model description, only the rear elements are shown to the right. The model is initially set up for a 3-step frequency sweep from 18.068 to 18.168 in 0.05 MHz steps. After making this modeling run, change the frequency (but not the source location) to create a 3-step frequency sweep from 24.89 through 24.99 MHz in 0.05 MHz steps. Record the forward free space gain, the 180° front-to-back ratio, the source impedance in terms of resistance and reactance, and the 50-Ω VSWR for the two sweeps.

```

CM 4-el Yagi: 12 m & 17 m                               18-9
CE
GW 1 5 -2.8956 .94488 0 -1.9812 .94488 0 .00476
GW 2 5 -1.9812 .94488 0 -.762 .94488 0 .00635
GW 3 2 -.762 .94488 0 -.3048 .94488 0 .00794
GW 4 3 -.3048 .94488 0 .3048 .94488 0 .00953
GW 5 2 .3048 .94488 0 .762 .94488 0 .00794
GW 6 5 .762 .94488 0 1.9812 .94488 0 .00635
GW 7 5 1.9812 .94488 0 2.8956 .94488 0 .00476
GW 8 5 -3.0419 .10668 0 -1.9812 .10668 0 .00476
GW 9 5 -1.9812 .10668 0 -.762 .10668 0 .00635
GW 10 2 -.762 .10668 0 -.3048 .10668 0 .00794
GW 11 3 -.3048 .10668 0 .3048 .10668 0 .00953
GW 12 2 .3048 .10668 0 .762 .10668 0 .00794
GW 13 5 .762 .10668 0 1.9812 .10668 0 .00635
GW 14 5 1.9812 .10668 0 3.0419 .10668 0 .00476
    
```

18-9 Test Data			
Parameter	18.068	18.118	18.168
Gain dBi			
F-B dB			
Source Z (R±jXΩ)			
50-Ω VSWR			
	24.89	24.94	24.99
Gain dBi			
F-B dB			
Source Z (R±jXΩ)			
50-Ω VSWR			

Comments: In principle, this antenna is very easy to create, both as a model and as a physical reality. Its performance shows higher than normal gain on the lower frequency span. On the upper band, gain is also higher than one might normally expect. Part of these figures owe to the fact that the 12-meter elements act partially as directors on 17 meters. As well, on the 12 meter band, the 17 meter elements act somewhat as reflectors. You may examine the current table for the antenna to verify that the current on the seemingly inactive elements is not quite low enough to count as wholly negligible.

However, part of the unexpectedly high performance owes to the close spacing of the two driver elements, which are also unequal in length. As we noted in a past set of exercises, NEC-2 tends to produce higher than normal gain figures for such situations, along with

Yagis

source impedance figures that may be inaccurate. In this case, the 17-meter gain may be up to 0.15 dB higher than reality, which the 12-meter gain may be as much as 0.5 dB higher than one can attain with a physical implementation of this antenna. Nonetheless, even when figures are reduced by these amounts, the antenna produces very respectable 2-element-per-band performance on a 10' boom.

18-9 Reference Data			
Parameter	18.068	18.118	18.168
Gain dBi	6.56	6.49	6.42
F-B dB	11.40	11.50	11.53
Source Z ($R \pm jX\Omega$)	41.1 - j 1.5	43.7 + j 1.2	46.3 + j 3.7
50- Ω VSWR	1.22	1.15	1.12
	24.89	24.94	24.99
Gain dBi	6.92	7.00	7.09
F-B dB	24.32	27.84	33.08
Source Z ($R \pm jX\Omega$)	63.6 - j 1.9	55.9 - j 1.9	47.7 - j 0.3
50- Ω VSWR	1.27	1.12	1.05

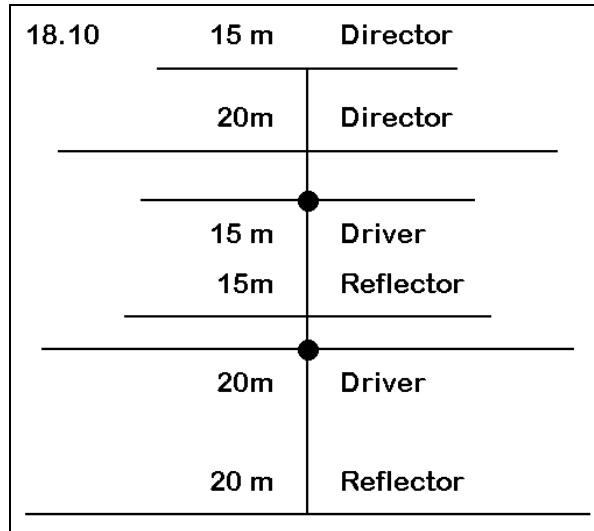
Because the model may yield incorrect source impedance figures, the lengths of the direct and the coupled drivers may not be exact, nor might the spacing be correct. However, both specifications will be close enough to allow experimental determination during construction of the correct values. Remember that when using open sleeve coupling, the coupled driver length will affect both the resistive and reactive components of the source impedance at the higher frequency. In cases like this one, the model provides a guide to the start of experimentation, but not a wholly reliable model of all construction and performance details.

18-10.NEC: Interlaced Yagis for 14.175 and 21.2 MHz

High gain multi-band Yagis cannot easily use the principle of separation (sometimes called "forward stagger" employed in the previous exercise without ending up with long booms that present numerous mechanical challenges. Consequently, some degree of element interlacing is required. Interlacing results in longer director elements for lower bands falling forward of shorter director elements for higher bands. When the elements are for adjacent bands up to a frequency ratio of 1:1.5, the longer elements tend to act as reflectors at the higher frequency, disrupting the function of the higher frequency element.

When bands are harmonically related, the longer element may be excited to a significant current level. The result can be an enhancement of the higher frequency forward gain. However, this function may also limit the higher frequency operating bandwidth, since the lower frequency element tends to be long relative to an antenna element wavelength at the higher frequency. The standard counteragent to such problems is the use at upper frequencies of a higher than normal number of elements for a given level of gain and operating bandwidth.

For our exercise, we shall examine a relatively modest interlacing situation for 3-element Yagis, shown in **Figure 18.10**. The goal of the design project was to achieve as short a boom length as possible while preserving as closely as possible the full performance of the independent antennas. If you re-examine the 3-element high-gain Yagi in model 18-4.NEC, you can get some idea of the performance expectations.



```

CM Interlaced Yagis: 20 m & 15 m
CE
GW 1 21 -5.2832 0 0 5.2832 0 0 .008
GW 2 21 -5.0038 3.2258 0 5.0038 3.2258 0 .008
GW 3 21 -4.7752 6.985 0 4.7752 6.985 0 .008
GW 4 15 -3.5052 3.4798 0 3.5052 3.4798 0 .00625
GW 5 15 -3.3147 5.969 0 3.3147 5.969 0 .00625
GW 6 15 -3.1877 8.4836 0 3.1877 8.4836 0 .00625
GS 0 0 1
GE 0
EX 0 2 11 0 1 0
LD 5 1 1 21 2.4938E7
LD 5 2 1 21 2.4938E7
LD 5 3 1 21 2.4938E7
LD 5 4 1 15 2.4938E7
LD 5 5 1 15 2.4938E7
LD 5 6 1 15 2.4938E7
FR 0 3 0 0 14 .175
RP 0 1 360 1000 90 0 1 1
EN
    
```

Model 18-10.NEC is one solution to the problem of interlacing. Two of the 15-meter elements (reflector and driver) lie between the 20-meter driver and director. Commercial designs tend to group all reflectors behind all drivers, with all directors placed forward of these two element sets. Such design may also cover up to three separate frequency bands.

This 6061-T6 aluminum model uses uniform-diameter elements: 16 mm diameter elements for the 14 MHz and 12.5 mm diameter elements for 21 MHz. An operational version of this array would undoubtedly require tapered-diameter elements. Note that there are separate sources for each band. Be sure to correctly place the source on wire 2, segment 11 for 20 meters and wire 5, segment 8 for 15 meters.

For this exercise, we may simply sample the performance at mid-band and at the band edges. Therefore, set a 20 meter frequency sweep from 14.0 through 14.35 MHz in 3 steps with a 0.175 MHz interval. Then set a 15 meter frequency sweep from 21.0 through 21.45 MHz with a 0.225 MHz interval. Record the gain, front-to-back ratio, and source impedance. We may by-pass the VSWR reading, since each set of elements will require

a suitable matching network for a 50- Ω feedline system.

18-10			
Test Data			
Parameter	14.00	14.175	14.35
Gain dBi			
F-B dB			
Source Z ($R \pm jX\Omega$)			
	21.00	21.225	21.45
Gain dBi			
F-B dB			
Source Z ($R \pm jX\Omega$)			

Comments: Both beams exhibit slightly higher gains than we might expect from monoband models, owing to the "forward stagger effect," which you can confirm from examining the current tables for this model. At the higher frequency range, however, the front-to-back ratio drops, as does the source impedance. Although the figures still represent highly usable performance, they do mark the consequences of interlacing elements. As a supplemental exercise, you may wish to move the 15 meter elements totally forward of the 20-meter elements--making suitable adjustments in element spacing and length--to restore full monoband performance.

18-10			
Reference Data			
Parameter	14.00	14.175	14.35
Gain dBi	8.12	8.29	8.50
F-B dB	23.05	22.04	15.03
Source Z ($R \pm jX\Omega$)	23.8 - j 24.9	23.3 - j 10.8	21.7 + j 5.1
	21.00	21.225	21.45
Gain dBi	8.11	8.16	8.30
F-B dB	16.70	18.45	14.36
Source Z ($R \pm jX\Omega$)	16.0 - j 23.4	17.8 - j 11.3	17.5 + j 0.5

Often in multi-band Yagi design, some elements require placement at virtually identical positions on the boom. For directors and reflectors, some designers employ traps, although the use of traps in driven elements has diminished, due to their losses in these high-current elements. In addition, driven element designs may use separately fed drivers (often with a remote switch), or they may employ open-sleeve coupling, "log" cells, or directly coupled drivers to achieve single-feedline operation. The variant designs of multi-band Yagis present you with innumerable supplemental exercises.

Summing Up

These exercises have progressed from the simplest Yagi designs to moderate levels of complexity in long-boom designs, stacking, and multi-band considerations. Despite the length and number of the exercises, we have only made an entry into an antenna design realm with almost unlimited diversity. For example, we have not looked in this chapter at methods of antenna element loading, commonly used at 7 MHz and below to make Yagi antennas more manageable mechanically. Nor have we tried to model "linear loads" (folded wire configurations), which NEC-2 does not handle well if the linear load wires are different in diameter relative to the main element diameter. We have limited our investigation to 5 element Yagis, although 7- and 8-element Yagis are used near 30 MHz. We have avoided models using traps and have not directly modeled matching systems. Of course, VHF and UHF Yagis have been reserved for another chapter.

Despite these restrictions, the exercises have introduced you to fundamental properties and behavior of Yagi antennas, including their potentials and their limitations. Understanding the applications of Yagi theory is enhanced by the ability to try out and optimize various designs as models, a much more rapid procedure than building physical models of every design modification. Developing appropriate anticipations about Yagi designs is crucial to choosing quickly the right design directions in development tasks. At the same time, it is important also not to convert anticipations into preconceptions about the limitations of Yagi design. Some of the best recent advances in Yagi antenna performance have emerged from a process of setting aside preconceptions.

The role of amateur radio, with its complex assortment of frequency allocations and operational demands, has made it inseparable from engineering efforts in the search for improved Yagi antennas. Besides some original work developed for these exercises, the designs used as models have been adapted from published designs and models by Brian Beezley, K6STI; William Orr, W6SAI; Jack Reeder, W6NGZ; Jim Breakall, WA3FET; Nathan Miller, NW3Z; and R. Dean Straw, N6BV. The work of other excellent Yagi designers has been omitted, but deserves detailed study by any student both of modeling and of parasitic antenna design.

19. Horizontal Parasitic and Phased Arrays

***Objectives:** Horizontal directional arrays are not limited to Yagis. In this set of exercises, you will encounter a variety of simple and complex horizontally polarized antennas using either parasitic or phase-line arrangements. In fact, in at least one case, the antenna will use both types of arrangements.*

The name "Yagi" is usually only applied to parasitic beam antennas whose elements are approximately $1/2\lambda$ long. However, parasitic arrays can be composed of elements of almost any length whatsoever. In our foray into vertical arrays, we met some interesting and useful configurations. Horizontally polarized antennas can yield an even wider assortment of parasitic beam antennas.

In this chapter, we shall begin by looking at the cubical quad antenna, which is composed of 1λ loops of wire. (The 1λ loop is already an "array" of sorts.) The name "cubical quad" stems from the fact that the square is the most common form of the loop, and the 2-element array is the most used parasitic form of this directional beam antenna: hence, the rough shape of a cube. However, a quad element can use loops of almost any uniform shape, ranging from a triangle (sometimes called the "delta") to a smooth circle (used only at VHF and above, where tubing can hold the continuous arc).

Collinear arrays, such as the extended double Zepp (EDZ), can also be placed in parasitic arrangements in order to achieve further gain and a uni-directional pattern. While looking at a parasitic EDZ, we may also learn some useful facts about parasitic antenna elements. In the end, virtually any broadside and/or collinear array can be set up in pairs to become an end-fire parasitic array. The chief design question then becomes a matter of selecting the most practical array to meet a set of project goals and specifications.

Parasitic arrays employ antenna wire geometry--and the resultant current distribution--to achieve gain in a single direction and pattern strength reduction in all other directions. However, as we saw when working with vertical antennas, arrays of horizontal elements can also be phase-fed to achieve much the same results. Horizontal phase-fed arrays, which include the ZL-Special and the HB9CV variant upon this basic design, can employ networks to adjust the magnitude and phase of the current at the source of each antenna

element. Such methods result in the most precise regulation of the antenna pattern.

More common in casual antenna design are phasing lines constructed from transmission lines. These lines will transform the current magnitude and phase to provide one or both elements with values that are necessary to achieve a given order of performance. We shall examine a number of designs that make use of phasing lines. Moreover, we shall look at some that make use of multiple transmission lines, each of which will have its own function.

Nothing in antenna theory and practice prevents us from combining both parasitic and phase-line techniques in a single overall antenna. Although we shall examine but a single model of such an antenna, it will allow us to open at least two significant areas of inquiry. One area involves the techniques of design that yield the best possible performance from such a composite design. The other area involves making a set of relevant comparisons to determine whether the resultant design is best for a task at hand.

The goal of this chapter is to acquaint you with the variety of antenna types that are amenable to either (or both) parasitic or phase-line treatment to achieve a set of design goals, where one of the goals is having a uni-directional array. The end result should be an increase in the number of possibilities at your disposal as you encounter later the question of how best to achieve certain orders of gain and directionality.

Exercise Preparation

The exercises in this chapter will present you with antenna elements that require more than linear thinking. Each element may demand attention to 2, if not 3, dimensions, and the resulting arrays may also show variability in all 3 dimensions. Therefore, you may wish to increase the amount of paper sketching you do in order to assure that the models you construct or modify work correctly the first time. The paper forms shown in an early chapter may be of use in this regard. You should alter them as needed to account for some of the models that have a large number of wires.

In addition, transmission lines will be used as a matter of course in constructing both phase lines and matching systems for some antennas. A review of the transmission line chapter may be in order so that you may effectively track not only the position and termination points of transmission lines, but as well the function of each. In fact, you may wish to thumb through the preceding chapters of this guide to note models that have some relevance to the central thrust of this chapter.

As always, the exercises will request that you modify many of the models in order to perform additional tasks beyond those for which check models are provided. If you wish

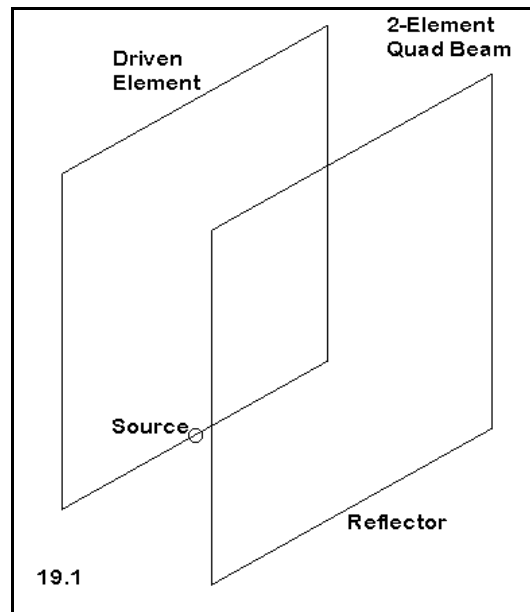
to preserve the original models supplied with the guide, you should use care in giving your variants filenames.

19-1.NEC: A 2-element cubical quad beam for 21.22 MHz

The cubical quad directional array is composed of 2 or more continuous loops of wire, each about 1λ long. Each of the loops can be viewed initially as $2 \frac{1}{2}\lambda$ linear wires with the ends bent to meet.

In the square version, the source for horizontal polarization is midway on one of the horizontal wires. Side-fed, the square would show vertical polarization relative to some presumed ground surface. Loops may range from triangular to circular, although the straight-wire requirement of NEC-2 restricts us to only approximations of true circles. Even the square may be set up as a diamond and fed either at its bottom peak for horizontal polarization or at its side peak for vertical polarization.

With only a single source, the quad loop shows at the position opposing the source point a roughly equal current and voltage magnitude, but both are 180° out of phase with the source. As a result, the quad loop is roughly equivalent to $2 \frac{1}{2}\lambda$ dipoles fed in phase with each other and spaced about $\frac{1}{4}\lambda$ apart. The gain of the loop in free space over a single $\frac{1}{2}\lambda$ dipole is a little over 1 dB.



```

CM 2el Quad: 21.22 MHz
CE
GW 1 11 -5.82 0 -5.82 5.82 0 -5.82 2.67E-03
GW 2 11 5.82 0 -5.82 5.82 0 5.82 2.67E-03
GW 3 11 5.82 0 5.82 -5.82 0 5.82 2.67E-03
GW 4 11 -5.82 0 5.82 -5.82 0 -5.82 2.67E-03
GW 5 11 -6.15 -5.794 -6.15 6.15 -5.794 -6.15 2.67E-03
GW 6 11 6.15 -5.794 -6.15 6.15 -5.794 6.15 2.67E-03
GW 7 11 6.15 -5.794 6.15 -6.15 -5.794 6.15 2.67E-03
GW 8 11 -6.15 -5.794 6.15 -6.15 -5.794 -6.15 2.67E-03
GS 0 0 .3048
GE 0
EX 0 1 6 0 1 0
LD 5 1 1 11 5.8001E7
LD 5 2 1 11 5.8001E7
LD 5 3 1 11 5.8001E7
LD 5 4 1 11 5.8001E7
LD 5 5 1 11 5.8001E7
LD 5 6 1 11 5.8001E7
LD 5 7 1 11 5.8001E7
LD 5 8 1 11 5.8001E7
FR 0 1 0 0 21.22 0
RP 0 1 360 1000 90 0 1 1
EN

```

19-1

Figure 19.1 shows a 2-element cubical quad directional array, where the reflector element is a parasitic element and larger in overall circumference than the driven element. A version of this antenna appears in model 19-1.NEC. The antenna uses #14 AWG copper wire in two loops to form a beam (or directional array) whose design center frequency is 21.22 MHz. The free-space model is constructed with a common center at coordinates 0,0,0. Hence, the driver and reflector are equal distances from this point in the Y-axis. Note also the source position at the center

equal distances from this point in the Y-axis. Note also the source position at the center

of the bottom wire of the driver loop.

Modify this model for a frequency sweep from 21.0 through 21.45 MHz in 6 0.9 MHz steps. Record your results in the table on the next page.

19-1 Test Table				
Frequency MHz	Gain dBi	F-B dB	Source Z $R \pm jX \Omega$	108- Ω VSWR
21.00				
21.09				
21.18				
21.27				
21.56				
21.45				

Comments: The 2-element cubical quad parasitic array shows an average gain of about 1 dB over an equivalent 2-element driver-reflector Yagi. However, the front-to-back ratio is significantly better than one can obtain from the Yagi. The center-frequency impedance of the model is 108 Ω , and that figure was used to develop the VSWR curve for the antenna.

Note that, as in the case of the 2-element driver-reflector Yagi, the gain peaks outside the lower end of the band of frequencies swept. You may perform a supplemental frequency-sweep exercise using a lower starting frequency to locate the frequency of maximum gain. This model was designed to place the peak 180° front-to-back ratio on or close to the design center frequency.

Of special note are the source impedance and VSWR curves. Notice that the curve is much steeper below the design center frequency than above it.

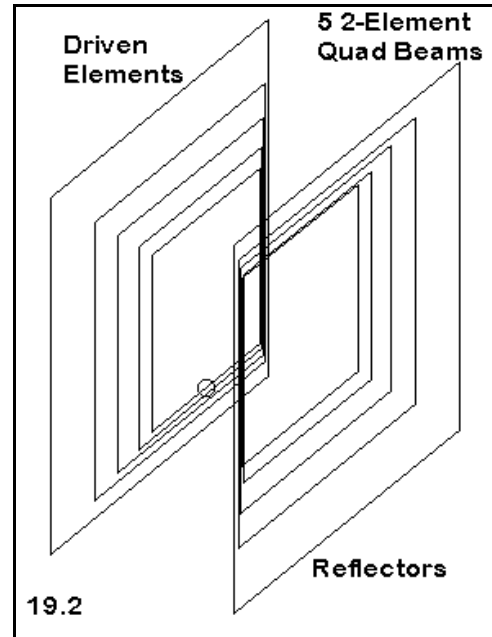
19-1 Reference Table				
Frequency MHz	Gain dBi	F-B dB	Source Z $R \pm jX \Omega$	108- Ω VSWR
21.00	7.45	16.10	76.0 - j 31.3	1.63
21.09	7.29	20.31	89.2 - j 16.4	1.29
21.18	7.12	23.77	102.7 - j 3.9	1.06
21.27	6.95	22.02	115.8 + j 6.3	1.09
21.56	6.78	18.71	128.0 + j 14.5	1.23
21.45	6.62	16.16	138.9 + j 21.2	1.36

Since the gain and front-to-back specifications of the antenna are relatively independent of the resonant frequency of the driven element, you may alter its length to set the resonant frequency lower in order to attain approximately equal values of VSWR at the band edges. In lengthening the element, be sure to increase the values in both the X and Z axes. Now add another 1-segment wire at a distance from the source position and create a $1/4\lambda$ section of 75- Ω transmission line between the source segment and the new wire. Transfer the source to the new wire. Setting up a frequency sweep identical to the original, develop a 50- Ω VSWR profile for the revised model. Try to establish the lowest VSWR levels of equal value at both ends of the swept band. To achieve this goal, you may alter the resonant frequency of the driver or the length of the matching section of transmission line--or both.

Return to the original model set at 21.22 MHz. If you run the model at this frequency, you will obtain a free space gain of about 7.04 dBi, a 180° front-to-back ratio of about 23.59 dB, and a source impedance of about 108.6 + j 0.9 Ω . Change the diameter of all wires to #18 AWG copper wire. Alter the dimensions of the driver and the reflector to restore the original operating specifications as closely as possible, including resonating the driver within a value of $\pm j 1.0 \Omega$. Then modify the wire diameter once more to #10 AWG copper wire and perform the same task. You should note that with closed loop geometries, the relationship of wire diameter to length for resonance and other specified antenna parameters is the reverse of that for linear elements. Increased wire diameter in the quad loops calls for an increase of circumference to restore the antenna properties, while decreased wire diameter calls for a decrease in circumference.

19-2.NEC: 5 nested 2-element cubical quad arrays for 14-28 MHz

If cubical quad arrays are nested, their interactions tend to be minimal, requiring only slight readjustments of dimensions due to the presence of nearby larger and smaller loops. (This design presumes that unused driver elements form closed loops; open loops change the interactions dramatically.) Hence, nested multi-band arrays of cubical quads are commonplace designs. Some mechanical designs use a common boom with 4 insulated arms. This design provides a constant physical spacing for the elements of each band but a different spacing in terms of fractions of a wavelength. The design scheme in **Figure 19.2** uses a central hub with angular support arms for the loops, thus maintaining a constant spacing in terms of fractions of a wavelength. Both mechanical systems may yield successful arrays of approximately equal performance on all frequencies.



Open model 19-2.NEC. The partial description to the right shows only the driver and reflector loops for 14.175 MHz and for 21.22 MHz, along with the driver for 28.5 MHz. The full model has 40 wires (5 bands, 2 loops per band, 4 wires per loop). Note the specification of the source position for each test frequency in **Figure 19-2**. In testing the model, change both the source wire and source segment numbers for each frequency.

```

CM 5 2-element quads optimized
CM Sources: 14.175 Mhz = W17S8
CM           18.112   = W33S7
CM           21.22    = W 9S6
CM           24.94    = W25S5
CM           28.5     = W 1S4
CE
GW 1 7 -4.32 2.155 -4.32 4.32 2.155 -4.32 2.67060367454068E-03
GW 2 7 4.32 2.155 -4.32 4.32 2.155 4.32 2.67060367454068E-03
GW 3 7 4.32 2.155 4.32 -4.32 2.155 4.32 2.67060367454068E-03
GW 4 7 -4.32 2.155 4.32 -4.32 2.155 -4.32 2.67060367454068E-03
GW 5 7 -4.6 -2.155 -4.6 4.6 -2.155 -4.6 2.67060367454068E-03
GW 6 7 4.6 -2.155 -4.6 4.6 -2.155 4.6 2.67060367454068E-03
GW 7 7 4.6 -2.155 4.6 -4.6 -2.155 4.6 2.67060367454068E-03
GW 8 7 -4.6 -2.155 4.6 -4.6 -2.155 -4.6 2.67060367454068E-03
GW 9 11 -5.815 2.897 -5.815 5.815 2.897 -5.815 2.67060367454068E-03
GW 10 11 5.815 2.897 -5.815 5.815 2.897 5.815 2.67060367454068E-03
GW 11 11 5.815 2.897 5.815 -5.815 2.897 5.815 2.67060367454068E-03
GW 12 11 -5.815 2.897 5.815 -5.815 2.897 -5.815 2.67060367454068E-03
GW 13 11 6.03 -2.897 -6.03 6.03 -2.897 -6.03 2.67060367454068E-03
GW 14 11 6.03 -2.897 -6.03 6.03 -2.897 6.03 2.67060367454068E-03
GW 15 11 6.03 -2.897 6.03 -6.03 -2.897 6.03 2.67060367454068E-03
GW 16 11 -6.03 -2.897 6.03 -6.03 -2.897 -6.03 2.67060367454068E-03
GW 17 15 -8.75 4.334 -8.75 8.75 4.334 -8.75 2.67060367454068E-03
GW 18 15 8.75 4.334 -8.75 8.75 4.334 8.75 2.67060367454068E-03
GW 19 15 8.75 4.334 8.75 -8.75 4.334 8.75 2.67060367454068E-03
GW 20 15 -8.75 4.334 8.75 -8.75 4.334 -8.75 2.67060367454068E-03
    
```

Notice that the loops for each have a different segmentation density. However, the length of each segment in the model is as nearly constant as the total number of segments in the model will permit. Thus, the segment junctions are fairly well aligned throughout the model. Since the frequency steps forming the design frequencies for each pair of loops do not form a linear sequence, uniformity can only be approximate.

Run this model at each of the specified frequencies and record the free-space gain, the 180° front-to-back ratio, and the source impedance.

19-2 Test Table				
Frequency MHz	Source Location	Gain dBi	F-B dB	Source Z $R \pm jX \Omega$
14.175				
18.112				
21.22				
24.94				
28.50				

Comments: Note that the gain and front-to-back figures are generally a bit higher for the nested quad arrays than for the 21.22 model we took as typical of the genre. However, before deciding that these higher gain figures are themselves a trend, run a frequency sweep for each band of frequencies: 14.0 - 14.35 in 6 steps, 21.0 - 21.45 in 6 steps, 28.0 - 29.0 in 6 steps, 18.068 - 18.168 in 3 steps, and 24.89 - 24.99 in 3 steps. For each band, note the approximate frequency of maximum front-to-back ratio as well as the VSWR relative to the source impedance at the design center frequency.

19-2 Reference Table				
Frequency MHz	Source Location	Gain dBi	F-B dB	Source Z $R \pm jX \Omega$
14.175	Wi 17, Seg 8	7.23	28.98	84.3 - j 0.1
18.112	Wi 33, Seg 7	7.26	30.30	59.7 - j 1.3
21.22	Wi 9, Seg 6	7.18	25.24	52.3 - j 0.5
24.94	Wi 25, Seg 5	7.32	25.84	41.4 + j 0.2
28.50	Wi 1, Seg 4	7.48	20.27	40.9 - j 0.3

From your frequency sweep of each band, you may be able to place the resonant point for each driver loop at a position resulting in equal VSWR values at each end of each band. Be sure to recheck performance on all bands to see if changing the driver length on any one band has an affect on the others.

The nesting of the quad arrays has its most dramatic effect upon the source impedance for each test frequency. The source impedance of those arrays having both higher and lower frequency arrays surrounding them is about half the source impedance of an

independent array of 2 elements. The impedance at 14.175 MHz is highest, since this array lacks another that is larger. The source impedance for 28.5 MHz is lowest, since it lacks a smaller array inside it. The source impedance for 24.94 MHz is also low due to interactions with the 28.5 MHz elements, which are within the size limits for an active director. You may wish to check the current table for each test frequency to determine the most or the significantly active elements.

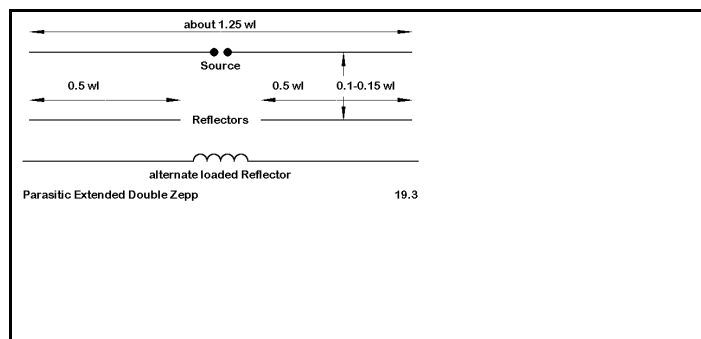
Cubical quads for either a single frequency band or for multiple bands have been built using as many as 6 or more elements. In multi-band arrays, element spacing rapidly becomes far off the optimal range for at least some of the frequency bands, resulting in less gain (or less front-to-back ratio—or a compromise between the two specifications) than in an optimized mono-band version. However, the ability to nest antennas for multiple frequency bands in a single assembly often becomes the driving factor in setting a final design.

Some quad designs bring all of the driven elements to a single point. Modeled, this source point would be a single wire of three segments, each about the same length as the average segment length along the remainder of the wires. Because the circumference of the drivers will change in this arrangement, adjustments to the dimensions of all drivers will be necessary, and there may be consequential required changes to the reflectors.

As a supplemental exercise, you may wish to modify the 5-band model quad array for a single source point for all bands. After modification, check each test frequency for gain, front-to-back ratio, and source impedance. Check the patterns also for any modifications due to driver interactions, especially interactions between 14.175 MHz and 28.5 MHz and between 24.94 MHz and 28.5 MHz. Consult the current tables and compare the current levels for every element on each band with those you obtained for the quad arrays when independently fed in the original model.

19-3.NEC: A parasitic extended double Zepp array for 28.5 MHz

Other types of arrays may also become directional when set up in parasitic fashion. The extended double Zepp (EDZ) is a bi-directional collinear pair of $1/2\lambda$ elements connected at the center by a phasing and spacing line. Usually center fed, the antenna exhibits a very high capacitive reactance. However, the bi-directional gain over a single $1/2\lambda$ dipole is significant, while the beamwidth is much narrower. **Figure 19.3** shows two



schemes for converting the EDZ into a directional array.

The alternate scheme with the loaded reflector preserves the look of the EDZ pair, but at the cost of a large loading inductor (up to 1000 Ω reactance). The coil losses, due to its finite Q, lead to the system of using separate, unconnected $1/2\lambda$ reflectors, since the center section of the antenna contributes little to the overall pattern and performance of the antenna.

```

CM Parasitic  EDZ:  28.5 MHz
CE
GW 1 31 -6.35 0 0 6.35 0 0 .00103
GW 2 13 -6.35 -1.34 0 -1.1 -1.34 0 .00103
GW 3 13 1.1 -1.34 0 6.35 -1.34 0 .00103
GS 0 0 1
GE 0
EX 0 1 16 0 1.414214 0
LD 0 1 16 16 4.6 5.17e-6 0
LD 5 1 1 31 5.8001E7
LD 5 2 1 13 5.8001E7
LD 5 3 1 13 5.8001E7
FR 0 1 0 0 28.5 0
RP 0 1 360 1000 90 0 1 1
EN

```

19-3

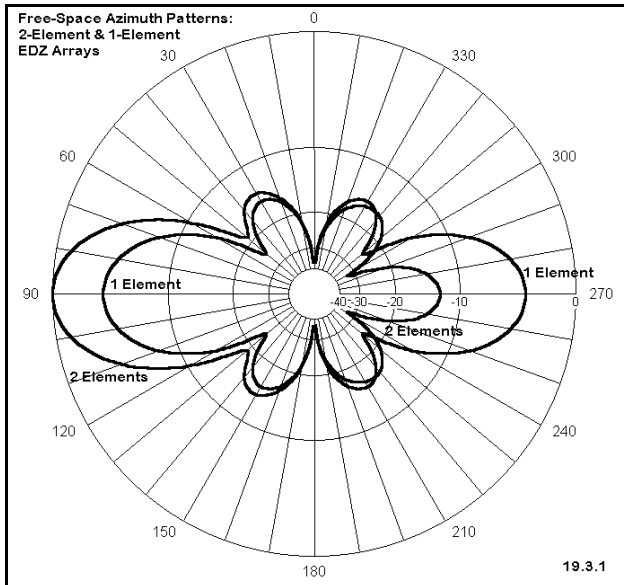
Open model 19-3.NEC. This free-space model of a parasitic EDZ beam uses the split-reflector configuration on a design center frequency of 28.5 MHz. Dimensions are in meters, and the wire is #12 AWG copper. As a model, the EDZ beam is very simple.

To determine if the antenna provides significant advantages that will outweigh the added mechanical challenge of supporting two

wire elements on a relatively even plane 1.34 m apart, we should compare the beam configuration with the single-wire EDZ. Check model 19-3-1.NEC supplies the free-space driver-only model for this antenna. Run both antennas at the design center frequency and record the gain, front-to-back ratio (where relevant) and source impedance in the table at the top of the next page.

19-3 Test Data			
Antenna	Gain dBi	F-B dB	Source Z $R \pm jX \Omega$
2-El. EDZ Beam			
1-El. EDZ			

Comments: The EDZ parasitic beam provides nearly 4 dB forward gain more than the bi-directional single EDZ antenna. The front-to-back ratio is not outstanding compared to that of some other antennas, but its advantage over the standard EDZ becomes apparent when comparing azimuth patterns, as in **Figure 19.3.1**.



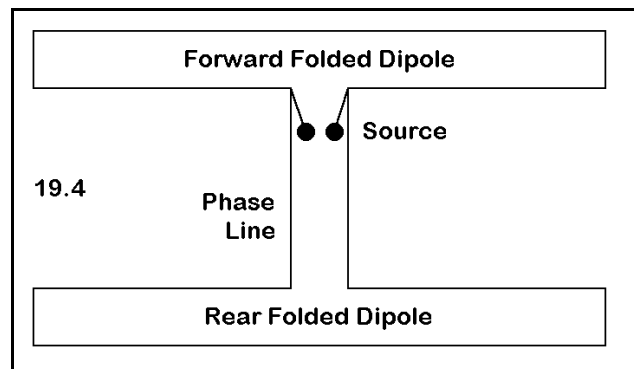
Both antennas have been provided with inductive loads to bring them to resonance. Thus, you may take VSWR curves around their source impedances of 121.0 Ω for the beam and 241.0 Ω for the single wire EDZ. However, of equal concern is whether the directional pattern holds up across any significant band width or whether it is a "single-frequency" array. Therefore, as a supplemental exercise, do a frequency sweep of the array from 28.0 to 29.0 MHz in no smaller than 0.2 MHz steps. Record the gain, front-to-back ratio, and source impedance, but also pay special attention to the azimuth patterns. Evaluate the performance bandwidth of the antenna. The pattern of the EDZ

beam has the side lobes characteristic of the basic EDZ antenna. Create variant designs, using a slightly longer driven element and then optimizing the reflector lengths for maximum gain or front-to-back ratio. Check the relationship of the main lobe gain to the gain of the side lobes and to the source impedance.

19-3		Reference Data	
Antenna	Gain dBi	F-B dB	Source Z $R \pm jX \Omega$
2-El. EDZ Beam	8.56	12.56	121.0 - j 0.7
1-El. EDZ	4.88	-----	241.0 - j 0.9

19-4.NEC: A folded-dipole phased horizontal array for 28.5 MHz

An alternative to parasitic end-fire arrays is the phase-fed end-fire array. Among the more typical of these arrays is the "ZL-Special," a 2-element horizontal beam brought to prominence in the late 1940s by a New Zealand antenna experimenter. Among the resultant designs is the one shown in **Figure 19.4**. The two antenna elements are fed by phasing lines. The forward element phase-line length is zero,



while the phasing line to the rear has a definite length.

Experimenters discovered that the required transformation of current magnitude and phase did not occur in standard commercially-made transmission lines in the length required by the separation of elements. By placing the folded dipoles in the horizontal plane, the feed-point positions were drawn closer together while the outer dimensions maintain close to the desired $1/8\lambda$ spacing. By juggling the lengths of the forward and rear elements, experimenters reached a combination that provided outstanding rear rejection. Only much later were the parameters of calculating phase lines for this type of antenna worked out in detail.

```

CM ZL Special: Trombone; 300 ohm
CM TL normal connection; rear el. reversed
CE
GW 1 41 -7.684 0 35 7.684 0 35 .01565
GW 2 2 7.684 0 35 7.684 -.368 35 .01565
GW 3 41 7.684 -.368 35 -7.684 -.368 35 .01565
GW 4 2 -7.684 -.368 35 -7.684 0 35 .01565
GW 5 41 7.842 -4.28 35 -7.842 -4.28 35 .01565
GW 6 2 -7.842 -4.28 35 -7.842 -3.912 35 .01565
GW 7 41 -7.842 -3.912 35 7.842 -3.912 35 .01565
GW 8 2 7.842 -3.912 35 7.842 -4.28 35 .01565
GS 0 0 .3048
GE 1
GN 2 0 0 0 13 .005 0 0 0 0
EX 0 3 21 00 1.00000 0.00000
LD 5 1 1 41 5.8001E7
LD 5 2 1 2 5.8001E7
LD 5 3 1 41 5.8001E7
LD 5 4 1 2 5.8001E7
LD 5 5 1 41 5.8001E7
LD 5 6 1 2 5.8001E7
LD 5 7 1 41 5.8001E7
LD 5 8 1 2 5.8001E7
TL 3 21 7 21 300.00 1.350264 0 0 0 0
FR 0 1 0 0 28.5 0
RP 0 1 360 1000 76 0 1 1
EN
    
```

19-4

Model 19-4.NEC is an example of the folded-dipole ZL-Special. Because the folded dipoles required considerable spacing between wires, they were originally made from thin copper tubing and rounded at the ends, lending the name "trombone" to this style of array. The 0.375" elements of this copper antenna are set 35' above average soil using the S-N ground system. The phasing line is shown as 1.35 m of 300-Ω parallel line with a normal connection. However, note that the rear element is constructed in the opposite direction from the forward element, placing the requisite "half-twist" at the element itself.

The design center frequency is 28.5 MHz for this array. Modify the model to perform a frequency sweep from 28.2 through 28.8 MHz in 4 0.2 MHz steps. Record the gain, front-to-back ratio, and source impedance for each step in the sweep. Also check the azimuth patterns for this antenna at the indicated TO angle.

19-4 Test Data				
Frequency	28.2	28.4	28.4	28.8
Gain dBi				
F-B dB				
Source Z				

Comments: The pattern for this trombone ZL-Special holds up very well indeed across the specified frequency sweep band width. The rear null peaks beyond 40 dB, with the

180° front-to-back ratio no worse than about 26 dB at the specified band edges. The worst-case front-to-back ratio is around 18 dB, resulting in an excellent overall front-to-rear ratio for a 2-element antenna.

The forward gain increases as the frequency increases, typical of phase-fed arrays of this type. The values are approximately those obtainable from a similarly spaced 2-element driver-reflector Yagi: the Yagi values will show a higher peak but a more rapid drop across the band. Moreover, the source impedance is relatively stable. Providing a capacitive shunt reactance to effect a beta match would provide a reasonable match to 50-Ω coaxial cable throughout the bandwidth swept in this exercise.

One remaining question connected with this model may revolve around the legitimacy of the modeling technique. Standard design of closely spaced horizontal phase-fed arrays calls for the use of a phase line length of around 0.125λ with a half twist to provide 135° (0.375λ) phasing. This model twisted the element and left the phase-line with normal terminations.

The rough-and-ready design rules for ZL-Specials are actually erroneously based on the double cycle of impedance in a single wavelength of transmission line. Correct transmission line use in phasing is concerned

with the voltage and current cycles, which require a full wavelength of transmission to repeat themselves. For a given length of transmission line and a set of load conditions, the transformation of current magnitude and phase along the line can be no more than the line length permits. Placing the twist in the line or in the element makes no difference.

Run check model 19.4-1.NEC, which models the antenna with the rear element oriented like the forward element, but with a reversal in the transmission line termination. You will obtain the same results.

```

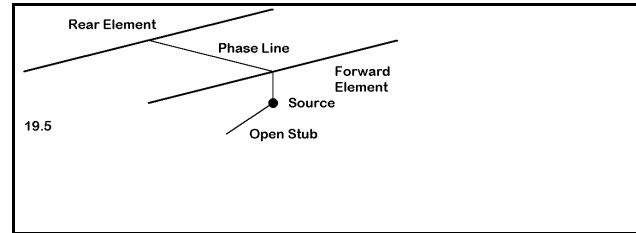
CM ZL Special: Trombone; 300 ohm
CM TL reverse connection; rear el. normal
CE
GW 1 41 -7.684 0 35 7.684 0 35 .01565
GW 2 2 7.684 0 35 7.684 -.368 35 .01565
GW 3 41 7.684 -.368 35 -7.684 -.368 35 .01565
GW 4 2 -7.684 -.368 35 -7.684 0 35 .01565
GW 5 41 -7.842 -4.28 35 7.842 -4.28 35 .01565
GW 6 2 7.842 -4.28 35 7.842 -3.912 35 .01565
GW 7 41 7.842 -3.912 35 -7.842 -3.912 35 .01565
GW 8 2 -7.842 -3.912 35 -7.842 -4.28 35 .01565
GS 0 0 .3048
GE 1
GN 2 0 0 0 13 .005 0 0 0 0
EX 0 3 21 0 1 0
LD 5 1 1 41 5.8001E7
LD 5 2 1 2 5.8001E7
LD 5 3 1 41 5.8001E7
LD 5 4 1 2 5.8001E7
LD 5 5 1 41 5.8001E7
LD 5 6 1 2 5.8001E7
LD 5 7 1 41 5.8001E7
LD 5 8 1 2 5.8001E7
TL 3 21 7 21 -300 1.350264 0 0 0 0
FR 0 1 0 0 28.5 0
RP 0 1 360 1000 76 0 1 1
EN
    
```

19-4-1

19-4	Reference Data			
Frequency	28.2	28.4	28.4	28.8
Gain dBi	11.77	11.84	11.91	11.97
F-B dB	26.60	32.42	34.13	27.64
Source Z	31.7 + j 17.5	32.8 + j 24.6	33.9 + j 31.9	34.9 + j 39.4

19.5.NEC: A linear-dipole phased horizontal array for 28.5 MHz

For mechanical rigidity, many designers favor horizontal phased arrays constructed from linear, tubular elements. However, such designs show low impedances at both element source points. The phase line must be a lower impedance type, and the resultant source impedance will often also be very low. The source impedance may thus require a matching network, perhaps a match-and-stub arrangement, shown in **Figure 19.5**.



```

CM ZL3MH: 28.5
CE
GW 1 51 -7.94 0 35 7.94 0 35 .04165
GW 2 51 7.62 -4.31 35 -7.62 -4.31 35 .04165
GW 3 1 -.1 0 34.716 .1 0 34.716 1.05643E-03
GW 4 1 1051 1051 1051 1051.1 1051.1 1051.1 1.05643E-03
GS 0 0 .3048
GE 1
GN 2 0 0 0 13 .005 0 0 0 0
EX 0 3 1 0 1 0
LD 5 1 1 51 2.4938E7
LD 5 2 1 51 2.4938E7
LD 5 3 1 1 5.8001E7
LD 5 4 1 1 5.8001E7
TL 1 26 2 26 71 1.959864 0 0 0 0
TL 1 26 3 1 71 .1292352 0 0 0 0
TL 3 1 4 1 71 2.1336 0 0 0 0
FR 0 1 0 0 28.5 0
RP 0 1 361 1000 76 0 1 1
EN
19-5

```

Model 19-5.NEC is an example of such a phased array using 1" diameter 6061-T6 aluminum elements. The phasing, matching, and stub line sections are all 71- Ω transmission line. If parallel transmission line of this characteristic impedance is not available, the use of coaxial line in the phasing section will require special care to prevent unwanted coupling to the element-support boom. In this model, the rear element is reversed, and the phase line

uses normal terminations. Be sure to sort out the functions of all wires and transmission lines in the model.

The model is set 35' above average soil in the S-N ground system, identical in position to the last model. Hence, you may think of these models as competing designs. Therefore, run the same frequency sweep--from 28.2 MHz through 28.8 MHz in 4 0.2 MHz steps. Record the gain, front-to-back ratio, and source impedance. Since this model is provided with a matching section, also record the 50- Ω VSWR for each frequency. In addition, check the azimuth patterns at the indicated elevation angle to see how well the pattern for this version of the ZL-Special holds up.

19-5				
Test Data				
Frequency	28.2	28.4	28.4	28.8
Gain dBi				
F-B dB				
Source Z				
50- Ω VSWR				

Comments: Before adding some notes on performance, we should reinspect the wire chart for this antenna. Note that the rear element is in fact shorter than the forward element. Because the antenna was designed to use available transmission lines as the phase line, the geometry was optimized to yield a maximum null at the design center frequency (over 37 dB) with a 71- Ω phasing line. This condition could only be fulfilled if the rear element was shortened below the length of the forward element. The fact that in other designs the rear element is longer than the forward element is not because such designs follow Yagi rules of element length. Rather, the rear elements are the length they are because each particular length yields the correct conditions for a given phasing line characteristic impedance and length in pursuit of a maximum rear null.

As the test results reveal, the reverse taper of element lengths does not adversely affect performance. Gain values between 19-4.NEC and 19-5.NEC are within 0.1 dB, while the 180° front-to-back figures are also too close to make an operational difference. The matching system provides a 2:1 VSWR operating bandwidth considerable in excess of the frequencies swept in this exercise and likely would permit operation from 28.0 through 29.0 MHz. You may expand the frequency sweep as a supplemental exercise to find the precise limits of the 2:1 VSWR operating bandwidth.

19-5				
Reference Data				
Frequency	28.2	28.4	28.4	28.8
Gain dBi	11.60	11.73	11.86	11.98
F-B dB	25.43	35.07	32.32	23.60
Source Z	37.2 + j 11.7	46.4 + j 5.3	53.0 - j 7.5	50.9 - j 23.9
50- Ω VSWR	1.49	1.14	1.17	1.60

These two examples of horizontally polarized phase-fed arrays do not exhaust the

possibilities for designing such system. Each of these cases has focused upon achieving a maximum rearward null. However, not all designs seek this goal.

A number of designs set front-to-back specifications lower than those shown in these examples. Notice that the maximum null (>30 dB) is a fairly narrow-band phenomenon. If we set a threshold level of perhaps 20 dB as a reasonable value for the front-to-back ratio, then we may optimize the array for other properties. The most common property for which designers strive is gain. Although a phased array may achieve a bit over 7 dBi free space forward gain, this figure cannot be realized without severe deterioration of the front-to-back ratio. More realistic is a gain of about 6.5 dBi. Antennas designed with these goals are often classified as HB9CV designs, after the work of a European experimenter.

We have already analyzed such a design. Exercise 14-3.NEC involved a 2-element Yagi converted to a phase-fed array with all of the characteristics just noted. To achieve the design objectives, the model used elements following the Yagi pattern of using a longer rear element. Moreover, the model employs a different matching system than the linear model in 19.4.NEC.

In order to fully appreciate the role of relative current magnitude and phase upon the performance of 2-element arrays, you may strip the models we have so far examined and place current sources on both the forward and rear elements. Leaving the forward element current source set at a magnitude of 1 and a phase angle of zero, alternately adjust the phase angle and the magnitude of current on the rear element until you arrive at a set of design goals. Then you may calculate or experimentally determine the phasing line needed to replicate these conditions. Your initial experiments with the models need not restrict themselves to commercially-made lines.

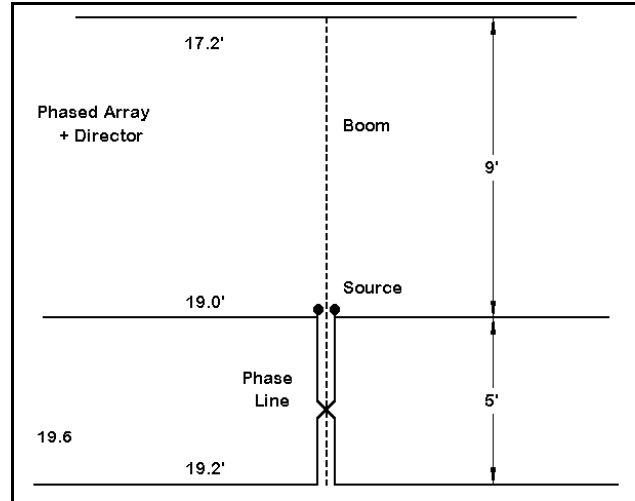
Among the advisable modeling exercises in this series should be the construction of a pair of resonant dipoles. Place the rear element at a regular series of increasing distances from the forward element and determine for each distance the correct value of rear element source current magnitude and phase to achieve a maximum rear null. You may then replicate the exercise with elements having different lengths. Gaining a systematic familiarity with the properties of these types of phased arrays will significantly shorten design time in the future. If you have any serious anticipations of designing horizontally polarized phased arrays in the future, you should thoroughly review the applicable theory and methods of calculation.

19-6: A 3-element combined parasitic-phased array for 24.94 MHz

Nothing in antenna theory or practice forbids combining parasitic and phased elements in the same design. In general, the addition of parasitic reflectors to a phased array adds little, if anything, to the design. Indeed, in parasitic designs, reflectors tend to control mostly the source impedance. However, directors control both the forward gain and the

front-to-back ratio of a Yagi. They exert similar control on a combined parasitic-phase-fed design as well. Therefore, we shall focus our attention upon a sample of this type of design, a 3-element array.

Figure 19.6 shows the general outline and dimensions of a design for 24.94 MHz. Model 19-6.NEC shows the details. The 0.75" diameter 6061-T6 elements, with 41 segments per element, form a 2-element phased array with a parasitic director on a 14' boom. The phasing line consists of 6.6' of 0.66 VF coaxial cable, which translates into 10' or 3.048 m of line with a velocity factor of 1.0. The source point does not contain a matching network.



```

CM 3 el ZL Sp 12m exp.
CE
GW 1 41 -8.6 9 0 8.6 9 0 .03125
GW 2 41 -9.5 0 0 9.5 0 0 .03125
GW 3 41 -9.6 -5 0 9.6 -5 0 .03125
GS 0 0 .3048
GE 0
EX 0 2 21 0 1 0
LD 5 1 1 41 2.4938E7
LD 5 2 1 41 2.4938E7
LD 5 3 1 41 2.4938E7
TL 2 21 3 21 -50 3.048 0 0 0 0
FR 0 1 0 0 24.94 0
RP 0 1 360 1000 90 0 1 1
EN
    
```

Perform a frequency sweep on this model from 24.89 through 24.99 MHz in 0.05 MHz steps. Record the free space gain, the 180° front-to-back ratio, and the source impedance across this 100 kHz-wide amateur radio band. Record your results in the table below. You may wish to examine the azimuth patterns for each of these frequencies as well as the numerical data.

19-6 Test Data			
Frequency	Gain dBi	F-B dB	Source Z R ± jX Ω
24.89			
24.94			
24.99			

Comments: This composite design achieves a very good level of forward gain with a very small rear lobe. The source impedance is low, but not out of the reach of a capacitive shunt reactance beta match. The characteristics are at least stable enough to cover a narrow frequency range such as the 12-meter amateur radio band.

We should pose at least two further questions of this design. First, since geometry alone does not tell the complete story with phased arrays, how was the design achieved? Second, how well do the performance specifications match up to competing 3- and 4-element Yagi designs?

19-6 Reference Data			
Frequency	Gain dBi	F-B dB	Source Z $R \pm jX \Omega$
24.89	8.54	27.69	15.1 + j 21.6
24.94	8.63	33.93	15.5 + j 23.0
24.99	8.71	40.08	16.0 + j 24.5

To answer the first question, open check model 19-6-1.NEC. As the description to the right reveals, this model contains only the phased elements and omits the director. Run this model, checking the gain and 180° front-to-back ratio. Looking at the azimuth pattern may also be instructive.

```
CM 2 e1 ZL Sp 12m exp.
CE
GW 1 41 -9.5 0 0 9.5 0 0 .03125
GW 2 41 -9.6 -5 0 9.6 -5 0 .03125
GS 0 0 .3048
GE 0
EX 0 1 21 0 1 0
LD 5 1 1 41 2.4938E7
LD 5 2 1 41 2.4938E7
TL 1 21 2 21 -50 3.048 0 0 0 0
FR 0 1 0 0 24.94 0
RP 0 1 360 1000 90 0 1 1
EN
```

19-6-1

You should obtain a free space gain of about 7.17 dBi, with a front-to-back ratio of about 10.09 dB.

These figures represent very close to the absolute maximum gain (between 7.2 and 7.3 dBi) that can be achieved by a pair of phased elements at the given spacing. The phased elements are set to maximum gain, with the director then responsible for additional gain and the reduction of the rear lobe. The spacing and length of that element produces the final results. (Setting the phased portion of the array for maximum rear null would not have produced the forward gain of the given design, since the director could not have added more gain than the present difference between the phased portion and the total array.)

```
CM 3 e1 Yagi: 24.95 MHz
CE
GW 1 41 -9.822 0 0 9.822 0 0 .02605
GW 2 41 -9.378 5.942 0 9.378 5.942 0 .02605
GW 3 41 -8.824 12.812 0 8.824 12.812 0 .02605
GS 0 0 .3048
GE 0
EX 0 2 21 0 1 0
LD 5 1 1 41 2.4938E7
LD 5 2 1 41 2.4938E7
LD 5 3 1 41 2.4938E7
FR 0 1 0 0 24.94 0
RP 0 1 360 1000 90 0 1 1
EN
```

19-6-2

```
CM 4 e1 Yagi: 24.94 MHz
CE
GW 1 41 -9.771 0 0 9.771 0 0 .03125
GW 2 41 -9.255 3.833 0 9.255 3.833 0 .03125
GW 3 41 -9.1 7.667 0 9.1 7.667 0 .03125
GW 4 41 -8.469 14.5 0 8.469 14.5 0 .03125
GS 0 0 .3048
GE 0
EX 0 2 21 0 1 0
LD 5 1 1 41 2.4938E7
LD 5 2 1 41 2.4938E7
LD 5 3 1 41 2.4938E7
LD 5 4 1 41 2.4938E7
FR 0 1 0 0 24.94 0
RP 0 1 360 1000 90 0 1 1
EN
```

19-6-3

To answer our second question, we should

compare the antenna design of model 19-6.NEC to one or more relevantly similar designs. In this case, models 19-6-2.NEC and 19-6-3.NEC provide examples of high gain Yagi designs, one a 3-element design on a 13' boom, the other a 4-element design on a 14.5' boom. Hence both are similar physically to the composite design.

The 3-element design uses 5/8" diameter 6061-T6 elements, while the 4-element version uses 3/4" elements of the same material. Run these designs at the design center frequency and record the data for gain, front-to-back ratio, and source impedance, adding in the data from the previous table for the performance of the composite design.

19-6A			
Test Data			
Antenna	Gain dBi	F-B dB	Source Z $R \pm jX \Omega$
Composite			
4-el. Yagi			
3-el. Yagi			

Comments: All three designs offer similar performance within broad limits. However, the gain of the composite design is superior to even that of the 4-element Yagi, despite the use of one-less element. The gain advantage of the 3-element composite design is about 0.5 dB over the 3-element Yagi.

The front-to-back ratios of the three antennas show differences, but they may largely disappear when the overall rear patterns are examined. All three can be considered superior designs with respect to this parameter. The source impedance of the 3-element Yagi is the highest, although the figures for the 4-element Yagi and the composite design are similar.

19-6A			
Test Data			
Antenna	Gain dBi	F-B dB	Source Z $R \pm jX \Omega$
Composite	8.63	33.93	15.5 + j 23.0
4-el. Yagi	8.49	25.38	17.9 - j 19.3
3-el. Yagi	8.17	25.49	24.8 + j 1.1

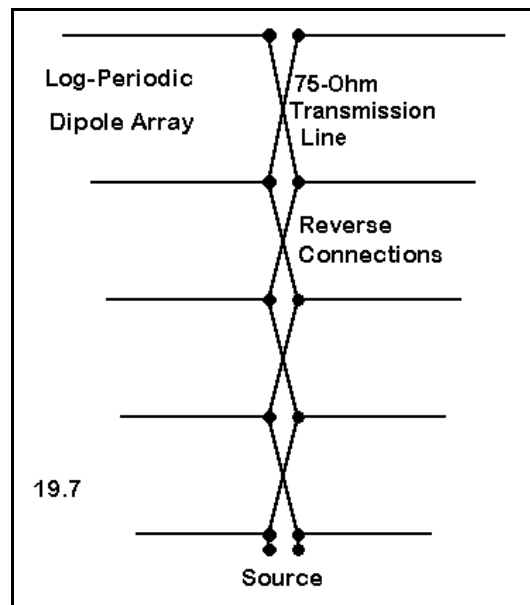
Whether the two comparative beams represent a fair test of the composite design is something that your growing experience with the possibilities of various types of antennas

will eventually decide. That evaluation can await the future, since--without further information concerning project goals and specifications--we could not make a decision concerning the selection of antenna designs anyway. However, the exercise does provide some insight into both the capabilities and the limitations of composite phase-fed and parasitic designs.

19-7.NEC: A log-periodic array for 19-29 MHz

One of the most interesting phased arrays is the log-periodic dipole array (LPDA) antenna. The antenna is capable in principle of performance rivaling at least a long boom 3-element Yagi, but over a frequency span that can be as high as 10:1 with a single feedline. Elements are arranged in ascending order of length from the source via a transmission line that makes reverse connections with each element along the way, as shown in **Figure 19.7**.

Ordinarily, for the upper HF region, the boom will consist of 2 tubular sections spaced to create a transmission line of the desired characteristic impedance. Elements are then mounted alternately to each boom section. However, wire versions of the LPDA are common, often being mounted within solid or flexible non-conducting frameworks.



The design of an LPDA results from the applications of a set of equations involving the angle created by the taper of the element ends, the ratio of element spacing from one to the next, and, where applicable, the angle between the two element-support booms. In our example, the last angle is zero, simplifying the calculations. In general, the shallower the element taper angle and the more elements used, the better the performance in terms of gain, front-to-back ratio, and consistency across the frequency range of the design. Utility programs for designing LPDAs are available as freeware.

```

CM Log Periodic: 19-29 MHz
CE
GW 1 21 0 -3.7225 0 0 3.72252 0 .01
GW 2 21 2.38241 -3.3502 0 2.38241 3.35027 0 .01
GW 3 19 4.52659 -3.0152 0 4.52659 3.01524 0 .01
GW 4 19 6.45634 -2.7137 0 6.45634 2.71372 0 .01
GW 5 19 8.19312 -2.4423 0 8.19312 2.44235 0 .01
GS 0 0 1
GE 0
EX 0 5 10 0 1 0
LD 5 1 1 21 2.4938E7
LD 5 2 1 21 2.4938E7
LD 5 3 1 19 2.4938E7
LD 5 4 1 19 2.4938E7
LD 5 5 1 19 2.4938E7
TL 1 11 2 11 -75 0 0 0 0 0
TL 2 11 3 10 -75 0 0 0 0 0
TL 3 10 4 10 -75 0 0 0 0 0
TL 4 10 5 10 -75 0 0 0 0 0
FR 0 1 0 0 21 0
RP 0 1 360 1000 90 0 1 1
EN

```

19-7

Our sample LPDA, model 19-7.NEC, uses only 5 elements on an 8.2 m boom to create an LPDA of modest performance for the 10-MHz span from 19 through 29 MHz. With 20 mm diameter 6061-T6 aluminum elements, the design uses 75- Ω transmission line in an effort to provide gain and rear nulling, along with an acceptable match to a 50- Ω system feedline, across the design spectrum. (An operational version of this array would undoubtedly use tapered-diameter elements. Moreover, this model omits details of obtaining the required boom

structure to present a 75- Ω characteristic impedance.)

Convert the frequency entry of this model to a frequency sweep from 19 through 29 MHz in 6 2-MHz steps. Record the gain, 180° front-to-back ratio, source impedance, and 50- Ω SWR for each step in the following table.

19-7 Test Data				
Frequency MHz	Gain dBi	F-B dB	Source Z $R \pm jX \Omega$	50- Ω VSWR
19				
21				
23				
25				
27				
29				

Comments: As with all antennas for which handy design equations exist, the real performance rarely coincides exactly with the seeming simplicity of the calculational process. This antenna shows considerable fluctuation in all performance categories. The gain and front-to-back ratio peak near 21 MHz, with severe gain and front-to-back ratio drops at the design spectrum extremes. The source impedance varies widely, although it almost manages to stay within the 2:1 VSWR limits usually set for HF antennas used with a 50- Ω system feedline.

19-7				
		Reference Data		
Frequency MhZ	Gain dBi	F-B dB	Source Z $R \pm jX \Omega$	50- Ω VSWR
19	6.76	8.68	44.9 - J 7.1	1.20
21	8.49	29.23	69.4 - J 13.1	1.48
23	8.39	12.78	52.6 - J 41.4	2.20
25	7.50	19.59	33.7 - J 41.4	1.65
27	6.83	14.74	30.7 + J 1.5	1.63
29	5.81	12.91	51.2 + J 18.7	1.44

Without doubt, additional elements (a tighter spacing ratio) and a longer boom (a narrower element-end angle) would yield better and more consistent performance across the design spectrum. However, at a certain point (dependent upon the design objectives), the added mechanical complexity and weight may offset the convenience of having a single source point and continuous frequency converge over a particular frequency spectrum. Nonetheless, the LPDA represents a direction in phased arrays well-worth supplemental study and redesign of our sample model.

Summing Up

In this set of exercises, we have looked at the application of parasitic techniques for the development of directional antennas applied to arrays of elements more complex than the $1/2\lambda$ dipole. In addition, we have explored the rudiments of phase-feeding horizontal arrays. Finally, we looked at composite parasitic-phased beams and LPDAs.

However, our small expedition is but the beginning of a long journey into complex horizontally polarized arrays. In principle, it is possible to combine every principle of horizontal antennas into a single array of great gain, high front-to-back ratio, and narrow beamwidth. As a single example, consider a model based on a collinear array of two extended double Zepps. Take a pair of these long wires and phase-feed them for a balance of gain and front-to-back ratio. Then stack two of these pairs and feed them in phase. This immodestly complex array might be capable of greater than 20 dB forward gain over ground with a beamwidth less than 18 degrees. Greater gains and narrower beamwidths yet are possible.

For some applications, such antennas might be all wrong. As the LPDA example illustrates, frequency coverage may be as important in some design projects as gain is in

others. In the world of known applications, modeling serves the needs of antenna projects--both developmental and analytical--where the goals and specifications precede the modeling task and help to define it.

Nevertheless, where no task, project, or application has been preset, there are no rules against experimental modeling. This chapter has only touched the surface of a field of endless antenna design possibilities. You never know what might emerge from exploring a pathway not hitherto taken.

20. VHF/UHF Antennas

***Objectives:** The VHF/UHF range (30-3,000 MHz) presents a diversity of modeling challenges, ranging from very large arrays of "HF-type" antennas to special purpose antennas. We shall survey a part of the assortment in order to become acquainted with concerns unique to modeling the smaller physical elements in varied applications.*

For equivalent gain, front-to-back ratio, and source impedance, VHF and UHF antennas are proportionately smaller than their HF counterparts. However, this one fact is enough to alert the skilled modeler to a number of differences in modeling practice.

VHF element diameters are likely to be larger fractions of a wavelength than the HF counterparts. This fact offers the opportunity of a wider operating bandwidth, but as well may require considerable antenna redesign to achieve the performance specifications of the comparable HF antenna.

VHF and UHF antennas may be placed at physical heights equivalent to those of HF antennas, but these heights represent multiple wavelengths. Above certain heights--with a rough dividing line of about 5λ --accurate assessment of elevation patterns may require much finer readouts, ordinarily using increments of every 0.1° instead of the standard 1.0° used at HF.

The smaller physical size of the elements offers the opportunity to design very large arrays electrically. Since each half wavelength requires a certain minimum segmentation, the overall model size can quickly grow to the limits of the modeling software or the practical run-time limits for the computer used.

These guidelines apply most readily to the wide variety of parasitic arrays used in both the VHF and UHF region. Not only do these regions show very long-boom Yagis and similar types, but as well, many operations call for cluster of Yagis spaced both vertically and horizontally to achieve maximum gain.

High-gain arrays do not dominate antenna design at VHF and UHF. Communications

requirements often call for omni-directional antennas to provide coverage over a specific geographic area. Many services specifically use vertical polarization, since the simplest omni-directional antenna is the vertical dipole or monopole with ground plane. "Improved types" of these antennas are commonplace.

Some issues surrounding polarization involve the heavy signal strength loss occasioned when antennas at each end of a link are cross polarized, one vertical, the other horizontal. Early practice was to press horizontal antennas with gain and directivity into service by reorienting them vertically. One consequence was a change in beamwidth (ordinarily much wider) and some loss of gain below a certain height (in wavelengths). Therein began a search of alternative designs.

The polarization question combined with the special communications needs for which the point-to-point nature of VHF and UHF propagation are most apt carry with them a change in design goals. Instead of looking solely at gain, front-to-back ratio, beamwidth, operating bandwidth, and source impedance--which are typically paramount in HF design--VHF and UHF designers may be more concerned to tailor an antenna's pattern and polarization to suit a specific communications requirement. Power and gain may take a back seat to pattern shape and response to signals of different polarization.

In short, antennas in the realm of VHF and UHF communications offer a number of challenges and design considerations quite different from those common to HF practice. These exercises at most will point in certain directions, but they cannot survey the entire territory. In part, this limitation emerges from simple space considerations. But as well, that territory is just now being developed.

Exercise Preparation

As you have progressed through the practical antenna design and modeling considerations of Part C, the number of supplemental exercises for you to conduct on your own in extension of the basic modeling tasks has increased. That trend will continue in the exercises to follow. Because of the diversity of antenna types used in the VHF and UHF region, the sampling must be smaller, and therefore, the remaining work for you to do on your own will expand. If time is no object, you may perform all of the supplemental exercises at leisure. However, if time is pressing, you may need to be selective, playing out certain design directions because they most focally interest you.

The exercises in this set, as always, tend to begin with a very basic antenna and proceed to more complex or intriguing designs. The number of possible variations on a basic model supplied with this guide will be nearly endless. Hence, you will need to use great care in keeping various models well sorted by filenames and even storage techniques (for example, on separate disks or in separate subdirectories). Eventually, you will discover that even the large numbers of files you collect here is only a beginning to your ultimate

collection of models.

20-1.NEC: 6-element Yagis for 51 MHz

Open model 20-1.NEC. As shown at the right, this is a model of a fairly standard 6-element Yagi using 6.25 mm 6061-T6 elements. The layout is an adaptation of a wide-band HF design by Dr. James Breakall. Initially, we shall model this antenna in free space, taking interest in the gain, 180° front-to-back ratio, and source impedance, all to be recorded on the table below.

```

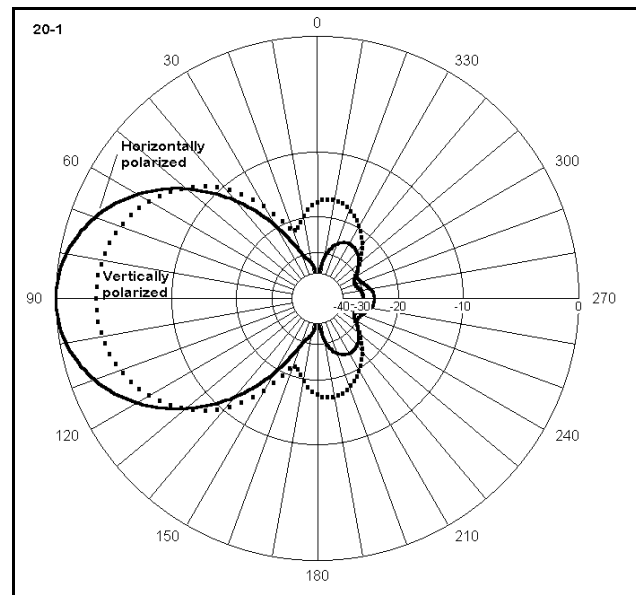
CM 6 el 51 MHz: Free space
CE
GW 1 15 -1.492 0 0 1.492 0 0 .00313
GW 2 15 -1.444 .639 0 1.444 .639 0 .00313
GW 3 15 -1.377 .99 0 1.377 .99 0 .00313
GW 4 15 -1.336 1.893 0 1.336 1.893 0 .00313
GW 5 15 -1.336 2.757 0 1.336 2.757 0 .00313
GW 6 15 -1.287 4.045 0 1.287 4.045 0 .00313
GS 0 0 1
GE 0
EX 0 2 8 0 1 0
LD 5 1 1 15 2.4938E7
LD 5 2 1 15 2.4938E7
LD 5 3 1 15 2.4938E7
LD 5 4 1 15 2.4938E7
LD 5 5 1 15 2.4938E7
LD 5 6 1 15 2.4938E7
FR 0 1 0 0 51 0
RP 0 1 360 1000 90 0 1 1
EN
    
```

However, we shall revise the model of this antenna to place it at a height of 12 m (about 2λ) above average soil. To the list of recorded data, we shall add the take-off angle. For reference, see model 20-1-1.NEC. Finally, we shall revise the model further to keep the center line at the 12-meter height, while turning the elements to a vertical position. One convenient way to do this from scratch is to set the model in free space and set the element ends as "plus" and "minus" values about Z=0. Then simply add 12 to each value of Z for both ends of each element, and add the required ground input. You may use model 20-1-2.NEC as a reference.

20-1 Test Data				
Orientation	Gain dBi	T-O angle	F-B dB	Source Z R ± jX Ω
Free Space		-----		
Horizontal				
Vertical				

Comments: Although the 180° front-to-back ratio and the source impedance for this beam show insignificant differences between the horizontal and vertical orientations, the forward gain at the angle of maximum radiation shows a considerable (nearly 2.9 dB) difference with the antenna at a height of 2λ above the ground. Moreover, the take-off angles differ by a degree. Although this latter difference may have little operational impact, it does suggest that the antenna does not perform in quite the same way when horizontal as when vertical.

The difference becomes apparent as soon as we overlay the azimuth patterns for the two variations in position. The antenna in the vertical orientation has an obviously wider beamwidth, not only in the forward direction, but rearward as well. The wider beamwidth accounts largely (but not necessarily totally) for the decrease in forward gain. Notice also the change in the position of the side-rejection nulls relative to each pattern. To obtain a fuller picture of what is going on, you should not only overlay azimuth patterns, as in **Figure 20-1**, but as well overlay elevation patterns (or investigate 3-dimensional portraits of the overall patterns). It is clear, at least in a preliminary way, that at the given height, the antenna's performance will be significantly different depending on orientation.



This exercise leaves a number of questions unanswered. For example, is there a height above ground at which the differential in gain will largely disappear. The way to answer this question is to change the height of the antenna in roughly $1/2\lambda$ increments until either the gain differential disappears or you decide that the curves you generate will never converge for practical purposes. (However, note that what may seem impractical heights in terms of wavelength for 50 MHz may well become practical heights above 300 MHz or some higher frequency. Therefore, you may wish to carry the experiment as high as 20λ up, about 240 m.) You will have to begin with an elevation pattern to determine the new take-off angle for each new height. Remember that if you exceed about 5λ in height, decrease the angular increment for the elevation pattern to about 0.1° .

20-1		Reference Data		
Orientation	Gain dBi	T-O angle	F-B dB	Source Z $R \pm jX \Omega$
Free Space	10.25	-----	26.70	$45.0 + j 1.0$
Horizontal	15.88	7°	26.13	$45.0 + j 0.7$
Vertical	13.00	6°	26.89	$45.0 + j 1.0$

The antenna modeled in this exercise is a wide-band array, designed to hold both its pattern and source impedance specifications across a fairly wide range of frequencies.

You should check this by performing a frequency sweep for both the horizontal and vertical versions from about 49.5 MHz through about 52 MHz. You may use a wider range if you desire to see the points where performance falls off significantly in one or another category on our table. Is there a difference in wide-band performance between the vertical and the horizontal orientations of the antenna?

20-2.NEC: A long-boom Yagi for 432 MHz

Yagi designs for high-gain, narrow-beamwidth communications work have applications well into the UHF region of the spectrum. Among the pioneers in the development of these designs is Guenter Hoch (DL6WU), who developed a large number of long-boom antennas. We shall sample his work with model 20-2.NEC, a 26-element Yagi for 432 MHz, using 4 mm diameter 6061-T6 elements. The wire portion of the model is shown at right, down through the EX input line. The model uses the maximum allowable segmentation per element (19) permitted by a program with a 500-segment limit.

```

CM DL6WU Original, 26 el 432 MHz
CE
GW 1 19 0 .1703 0 0 -.1703 0 .002
GW 2 19 .1388 .165 0 .1388 -.165 0 .002
GW 3 19 .1908 .1508 0 .1908 -.1508 0 .002
GW 4 19 .3158 .1496 0 .3158 -.1496 0 .002
GW 5 19 .465 .1478 0 .465 -.1478 0 .002
GW 6 19 .6384 .1461 0 .6384 -.1461 0 .002
GW 7 19 .8328 .1446 0 .8328 -.1446 0 .002
GW 8 19 1.0409 .1432 0 1.0409 -.1432 0 .002
GW 9 19 1.2595 .1421 0 1.2595 -.1421 0 .002
GW 10 19 1.4886 .1411 0 1.4886 -.1411 0 .002
GW 11 19 1.728 .1402 0 1.728 -.1402 0 .002
GW 12 19 1.9778 .1394 0 1.9778 -.1394 0 .002
GW 13 19 2.238 .1387 0 2.238 -.1387 0 .002
GW 14 19 2.5087 .138 0 2.5087 -.138 0 .002
GW 15 19 2.7863 .1374 0 2.7863 -.1374 0 .002
GW 16 19 3.0639 .1369 0 3.0639 -.1369 0 .002
GW 17 19 3.3414 .1364 0 3.3414 -.1364 0 .002
GW 18 19 3.619 .1359 0 3.619 -.1359 0 .002
GW 19 19 3.8966 .1354 0 3.8966 -.1354 0 .002
GW 20 19 4.1742 .135 0 4.1742 -.135 0 .002
GW 21 19 4.4518 .1346 0 4.4518 -.1346 0 .002
GW 22 19 4.7294 .1342 0 4.7294 -.1342 0 .002
GW 23 19 5.007 .1338 0 5.007 -.1338 0 .002
GW 24 19 5.2845 .1335 0 5.2845 -.1335 0 .002
GW 25 19 5.5621 .1331 0 5.5621 -.1331 0 .002
GW 26 19 5.8397 .1328 0 5.8397 -.1328 0 .002
GS 0 0 1
GE 0
EX 0 2 10 0 1 0

```

One feature of Hoch's designs is the ability to "clip" the beam at various points and still have a quite effective Yagi for the boom length that remains. In this exercise, we shall experiment with Yagis with 21, 16, 14, and 10 elements in models that you either create yourself or consult from models 20-2-1.NEC through 20-2-4.NEC. If you create your own models from the original, simply delete the elements beyond those you wish to retain, deleting also the associated material load cards. Record the gain, 180° front-to-back ratio, the source impedance, and the boom length for each version of the antenna.

20-2 Test Data				
No. elements	Gain dBi	F-B dB	Source Z $R \pm jX \Omega$	Boom Length m
26				
21				
16				
14				
10				

Comments: From the source impedance column of the table, it is clear that these Yagis were designed for direct feed from a 50- Ω feedline system. Alternative Hoch designs have used a folded dipole as a driver to obtain a higher source impedance. With a source impedance of 200 Ω , 4 of these antennas might be placed in an array that uses custom equal-length feedlines from each Yagi source to a parallel junction to form a common 50- Ω source. We shall sample such arrays in a later exercise in this chapter.

Also of note is the fact that the boom-length vs. forward gain curve shows a slowly decreasing rise in gain with each additional increment of boom length. Between 10 and 14 elements, we obtain a 1.8 dB gain increase with a 1.02-m increase in boom length. Between 21 and 26 elements, we achieve nearly 1 dB of further gain with a 1.39-m increase in boom length.

20-2 Reference Data				
No. elements	Gain dBi	F-B dB	Source Z $R \pm jX \Omega$	Boom Length m
26	18.60	22.19	50.2 + j 0.1	5.84
21	17.63	20.42	48.9 - j 1.1	4.45
16	16.28	18.04	47.4 - j 3.9	3.06
14	15.69	26.58	55.5 + j11.3	2.51
10	13.89	29.71	49.6 + j10.6	1.49

The slight variations in source reactance can be easily removed with a small adjustment of the driven element length. Likewise, if a more exacting match to a 50- Ω system is

desired, either the driven element or the reflector spacing may be adjusted slightly without significant effect upon the remaining performance specifications for the antenna. Of greater impact on the antenna will be the boom itself, if not a good insulator at 432 MHz, and such accessories as a feedline connector attached to the driven element.

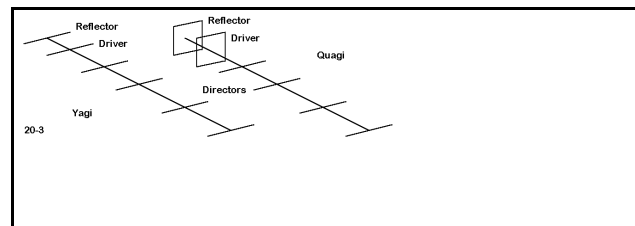
Innumerable supplemental modeling tasks suggest themselves for this sequence of long-boom Yagis. For instance, there are numerous other cutting points one might use in shortening the antenna design for various purposes. One might clip the antenna in 1-element increments, checking both the performance and the source impedance with each cut. If the source impedance is not a very good match for a 50- Ω feed system, one might then adjust the driver (and reflector, if necessary) to achieve a 50- Ω match to see if this can be done without significant jeopardy to the antenna performance. Even at the cuts made in this exercise, some slight juggling of the reflector length and/or spacing might be used to increase the front-to-back ratio as far above 20 dB as possible without reducing gain or throwing off the source impedance by any great amount.

You should also be curious about the operating bandwidth of these Yagis with respect to both the 2:1 SWR bandwidth and to the performance characteristics of the antenna. How far from design center frequency can you go with only an acceptable degradation in either the forward gain or the front-to-back ratio. If you inspect the azimuth patterns for these antennas, you will discover that they are a far cry from the smooth patterns typical of HF Yagis with low element numbers. Side and rear lobes abound, and part of the design goal is to keep them within acceptable limits (where acceptability may be a function of application). Therefore, when checking the antenna at distances from the design frequency, inspect the azimuth patterns to ensure that all unwanted side lobes are within reasonable limits.

20-3.NEC: 8-element Yagis and quagis for 432 MHz

Designs for Yagis rarely show maximum gain and front-to-back ratio when the source impedance is 50 Ω . Rather, maximum performance tends to occur with a source impedance between 20 and 25 Ω . One alternative is to use a folded dipole to raise the source impedance.

Since double and triple element reflectors are common in long-boom VHF/UHF Yagis, a second option has emerged: design a hybrid long boom parasitic array using a quad loop for the driven element and for the reflector. The result is called a "quagi," as illustrated in **Figure 20-3**. Let's compare an 8-element Yagi with an 8-element quagi.



```

CM 8-el Yagi: 432 MHz
CE
GW 1 15 -.172 0 0 .172 0 0 .000814
GW 2 15 -.1618 .0694 0 .1618 .0694 0 .000814
GW 3 15 -.1599 .1405 0 .1599 .1405 0 .000814
GW 4 15 -.1571 .283 0 .1571 .283 0 .000814
GW 5 15 -.1544 .491 0 .1544 .491 0 .000814
GW 6 15 -.1519 .738 0 .1519 .738 0 .000814
GW 7 15 -.1515 1.01 0 .1515 1.01 0 .000814
GW 8 15 -.1523 1.208 0 .1523 1.208 0 .000814
GS 0 0 1
GE 0
EX 0 2 8 0 1 0
LD 5 1 1 15 5.8001E7
LD 5 2 1 15 5.8001E7
LD 5 3 1 15 5.8001E7
LD 5 4 1 15 5.8001E7
LD 5 5 1 15 5.8001E7
LD 5 6 1 15 5.8001E7
LD 5 7 1 15 5.8001E7
LD 5 8 1 15 5.8001E7
FR 0 1 0 0 432 0
RP 0 1 360 1000 90 0 1 1
EN

```

20-3-1

Open model 20-3-1.NEC, the 8-element Yagi composed of #14 AWG copper wire elements, as shown at left. The free space model uses a 1.21-meter boom. Note also that as the models progress, we shall use a somewhat random selection of composition techniques. Whereas the long-boom Yagis placed the elements across the Y-axis, this model places them across the X-axis. (In other models, the reflector may not be at 0, but at some "minus" point relative to the driver or to the antenna center.) For this model, record the forward gain, 180° front-to-back ratio, and source impedance in the table on the next page. Use the gain tables

wherever necessary to calculate the front-to-back ratio.

Next, open model 20-3-2.NEC, the 8-element Quagi. This model is composed of #12 AWG copper wire. The model initially appears more complex, because the first 8 entries on the wire table make up the reflector and the driven element. The source point is the lower horizontal section of the driven element. Beyond quad loops, the antenna uses standard Yagi-type directors on a 1.37-m boom. Once more, record on the table on the next page the gain, front-to-back ratio, and source impedance.

While examining these models, compare the boom length with the boom length of the 10-element version of the Yagi in exercise 20-2. That 10-element model uses a boom length of about 1.49 m to achieve a gain of about 13.9 dBi in free space. Note that the Quagi boom is about 0.12 m shorter, while the Yagi boom is 0.29 m shorter (nearly 5" and over 11", respectively, at a frequency where a wavelength is under 28"). Therefore, it will be useful to compare the gain of the 2 antennas in this exercise with that of its closest counterpart in the long-boom exercise.

```

CM 8-el quagi: 432 MHz
CE
GW 1 7 -.0939 0 -.0939 .09398 0 -.0939 .00103
GW 2 7 .09398 0 -.0939 .09398 0 .09398 .00103
GW 3 7 .09398 0 .09398 -.0939 0 .09398 .00103
GW 4 7 -.0939 0 .09398 -.0939 0 -.0939 .00103
GW 5 7 -.0914 .1436 -.0914 .09144 .1436 -.0914 .00103
GW 6 7 .09144 .1436 -.0914 .09144 .1436 .09144 .00103
GW 7 7 .09144 .1436 .09144 -.0914 .1436 .09144 .00103
GW 8 7 -.0914 .1436 .09144 -.0914 .1436 -.0914 .00103
GW 9 15 -.1495 .2785 0 .1495 .2785 0 .00103
GW 10 15 -.1484 .5563 0 .14843 .5563 0 .00103
GW 11 15 -.1476 .7049 0 .14763 .7049 0 .00103
GW 12 15 -.1468 .9266 0 .14684 .9266 0 .00103
GW 13 15 -.146 1.143 0 .14605 1.143 0 .00103
GW 14 15 -.1452 1.37 0 .14525 1.37 0 .00103
GS 0 0 1
GE 0
EX 0 5 4 0 1 0
LD 5 1 1 7 5.8001E7
LD 5 2 1 7 5.8001E7
LD 5 3 1 7 5.8001E7
LD 5 4 1 7 5.8001E7
LD 5 5 1 7 5.8001E7
LD 5 6 1 7 5.8001E7
LD 5 7 1 7 5.8001E7
LD 5 8 1 7 5.8001E7
LD 5 9 1 15 5.8001E7
LD 5 10 1 15 5.8001E7
LD 5 11 1 15 5.8001E7
LD 5 12 1 15 5.8001E7
LD 5 13 1 15 5.8001E7
LD 5 14 1 15 5.8001E7
FR 0 1 0 0 432 0
RP 0 1 360 1000 90 0 1 1
EN

```

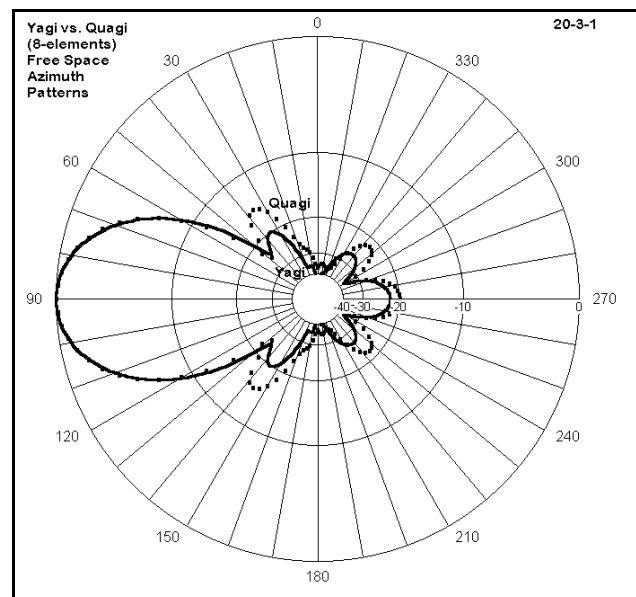
20-3-2

20-3 Test Data			
Model	Gain dBi	F-B dB	Source Z $R \pm jX \Omega$
8-el Yagi			
8-el Quagi			

Comments: The quagi indeed achieves a 50- Ω source impedance with performance that is only about 0.1 dB less in gain and about 0.5 dB less in front-to-back ratio relative to the Yagi used for comparison. If a 50- Ω source impedance is crucial to an application, then the quagi might be a strong candidate, despite its longer boom length. Note that both these designs are optimized for gain rather than front-to-back ratio, when compared to the 10-element version of the long-boom Yagi in exercise 20-2. With only 8 elements and shorter booms, their gain is lower by only about 0.5 dB, although the front-to-back ratios are significantly lower than the long-boom 50- Ω model.

20-3 Reference Data			
Model	Gain dBi	F-B dB	Source Z $R \pm jX \Omega$
8-el Yagi	13.48	21.98	21.4 - j 17.5
8-el Quagi	13.39	19.59	50.4 + j 5.1

These performance specifications do not exhaust the relevant comparisons among these antennas. For example, perform frequency sweeps of all three antennas to see how well the performance holds up across a range of frequencies. To check the SWR operating bandwidth, you may wish to bring the 8-element Yagi driver to resonance and check the SWR relative to the source impedance that emerges from lengthening that element. Although many applications will not press whatever limits arise from the frequency sweep, such information is always useful for any antenna you model. In addition, compare



the azimuth patterns of the antennas for undesirable side lobes. **Figure 20-3-1** compares the Yagi and quagi azimuth patterns, where the quagi side lobes (dotted line) become apparent in contrast to the Yagi side lobes (solid line).

20-4.NEC: Arrays of 8-element Yagis for 144.2 MHz

```

CM 8-el Yagi: 144.2 MHz
CE
GW 1 15 -.5153 0 0 .51531 0 0 .00238
GW 2 15 -.4848 .20779 0 .48483 .20779 0 .00238
GW 3 15 -.4789 .4208 0 .47894 .4208 0 .00238
GW 4 15 -.4706 .84709 0 .47061 .84709 0 .00238
GW 5 15 -.4625 1.47137 0 .46253 1.47137 0 .00238
GW 6 15 -.4551 2.21053 0 .45514 2.21053 0 .00238
GW 7 15 -.4538 3.026 0 .45387 3.026 0 .00238
GW 8 15 -.4562 3.6195 0 .4562 3.6195 0 .00238
GS 0 0 1
GE 0
EX 0 2 8 0 1 0
LD 5 1 1 15 2.4938E7
LD 5 2 1 15 2.4938E7
LD 5 3 1 15 2.4938E7
LD 5 4 1 15 2.4938E7
LD 5 5 1 15 2.4938E7
LD 5 6 1 15 2.4938E7
LD 5 7 1 15 2.4938E7
LD 5 8 1 15 2.4938E7
FR 0 1 0 0 144.2 0
RP 0 1 360 1000 90 0 1 1
EN

```

20-4

Because very long-boom Yagis can become mechanically unwieldy, the pursuit of gain from Yagi arrays takes a different turn at certain points. Instead of steadily increasing boom length, designers turn to arrays of Yagis. Although the number of Yagis in a given array is unlimited, we shall restrict ourselves to arrays involving 2 and 4 Yagis. Each array will use 8-element Yagis based on designs by Brian Beezley (K6STI) with 6061-T6 aluminum elements about 3/16" in diameter, as shown at left, with the dimensions in meters.

To determine how much various configurations may improve performance over a single antenna, we shall begin with the basic "1 Yagi" model (20-4.NEC), shown above. Models 20-4-1.NEC and 20-4-2.NEC will place two of these antennas side-by-side and one above the other with spacings that achieve maximum gain for each configuration. The next step (20-4-3.NEC) creates a 4-antenna square from the vertical and horizontal arrays. Finally, 20-4-4.NEC places four beams in a diamond configuration with a vertical dimension somewhat greater than the cross-point dimension of the square. Our question will be whether or not we derive sufficient benefit for the complexity involved.

Attend closely to the construction technique for the models in the arrays. Each antenna is a copy of the original, with the dimension values adjusted in the axes appropriate to the array type. The adjustment factors are taken as constant figures added or subtracted from the X, Y, or Z values of the original. You may achieve this end on paper in advance of modeling or you may enter the values symbolically for easy adjustment of the model later.

Record the gain, -3 dB beamwidth, front-to-back ratio, and source impedance(s) of the various arrays in the next table. If the source impedance values among the beams in the array do not vary among themselves by a significant amount, record only a single average value.

20-4		Test Data		
Array	Gain dBi	Beamwidth	F-B dB	Source X R ± jX Ω
1				
2-Horizontal				
2-Vertical				
4-Square				
4-Diamond				

Comments: The 2-beam arrays have the same free space gain. However, note that the vertical array has the same beamwidth as the single antenna, while the horizontal array narrows that beamwidth by half. The utility of each array might well be determined by the beamwidth rather than the gain figures. The gain is about 2.7 dB greater than the single Yagi.

By placing 4 of the Yagis in a square, we can achieve another 2.8 dB of gain, but only at the narrower beamwidth, controlled by having 2 pairs of horizontally arranged beams. The diamond configuration adds still another 0.8 dB to the total gain over a single antenna, again at the 20° beamwidth determined by having 2 Yagis side-by-side. Throughout the growth of the array, the source impedances of the individual antennas remained quite stable. So, too, did the front-to-back ratio.

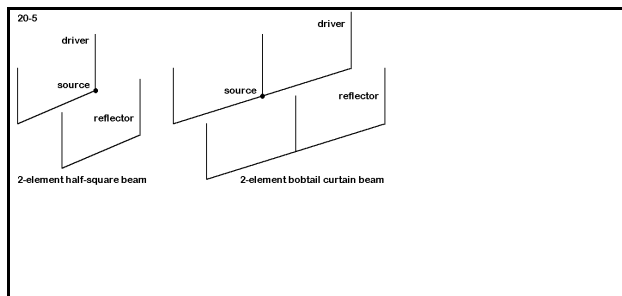
The 4-square and 4-diamond arrays provide gain over the longest of the long-boom Yagis, the 26-element version with a boom length of nearly 6 m at 432 MHz, the equivalent of about 18 m at the test frequency of these 144 MHz arrays. In contrast, the 8-element Yagis have individual booms just over 3.6 m. However, what the array saves in length, it takes up in height and width.

20-4				
		Reference Data		
Array	Gain dBi	Beamwidth	F-B dB	Source X R ± jX Ω
1	13.48	40°	22.09	21.4 - j 17.6
2-Horizontal	16.19	20°	23.21	22.7 - j 18.0
2-Vertical	16.19	40°	24.04	20.8 - j 18.5
4-Square	19.01	20°	24.51	20.0 - j 18.3
4-Diamond	19.78	20°	21.74	20.3 - j 16.5

To supplement this exercise, you may perform several interesting tasks. One is to perform a frequency sweep on each of the arrays to discover which, if any, has significantly wider-band or narrower-band characteristics than the others. You may also adjust the spacings of the 2- and 4-Yagi arrays to strive for improved performance without degrading any of the specifications along the way. Finally, on software with relatively unrestricted segment maxima, you may try to create even larger arrays.

20-5.NEC: Vertically polarized parasitic arrays for 146 MHz

In exercise 20-1, we learned that turning a Yagi vertical does not always yield a beamwidth as narrow as some application may require. In this exercise, we shall look at some parasitic beam designs with predominantly vertically polarized radiation, but with other characteristics remarkable like those of a Yagi in its primary orientation: that is, the beamwidth will be reasonably narrow and the rear lobes will not be excessive. **Figure 20-5** shows two versions of these arrays, based respectively on the half square and the bobtail curtain.



In the present VHF application for 146 MHz, the standard HF practice of placing the horizontal section of the antenna high relative to the $1/4\lambda$ vertical elements no longer makes a difference: performance is identical with the horizontal up or down. These models all place the horizontal low in order to bring the feedline beneath the antenna.

All of the models will use 0.5" diameter 6061-T6 elements for simplicity of model composition. However, each may be easily redesigned for a combination of element sizes, for example, a fat horizontal for structural strength with thinner vertical elements for

wind slippage. Test versions to empirically check the models can easily be constructed from house wiring with some form of support that is transparent to RF at VHF frequencies.

Open model 20-5-1.NEC. Examine also models 20-5-2.NEC and 20-5-3.NEC. The progression of models use the half square by itself, in a 2-element design, and finally in a 3-element design. All modes use a horizontal member 40" long, setting the widest point of the array. The strongest radiation is broadside to the horizontal section. Adjustments for resonance and for parasitic performance change only the lengths of the vertical elements, as well as the spacing between elements. We shall use the single half square as a reference in order to see what we might gain from the parasitic versions. All antennas are 360" (30') above average S-N ground. In the table on the next page, record the gain, take-off angle, beamwidth, front-to-back ratio, and source impedance.

```

CM half square, 3-el Yagi 2M
CE
GW 1 11 -20 0 380.2 -20 0 360 .25
GW 2 22 -20 0 360 20 0 360 .25
GW 3 11 20 0 360 20 0 380.2 .25
GW 4 11 -20 -17.5 382 -20 -17.5 360 .25
GW 5 22 -20 -17.5 360 20 -17.5 360 .25
GW 6 11 20 -17.5 360 20 -17.5 382 .25
GW 7 11 -20 20.5 379.3 -20 20.5 360 .25
GW 8 22 -20 20.5 360 20 20.5 360 .25
GW 9 11 20 20.5 360 20 20.5 379.3 .25
GS 0 0 .02540
GE 1
GN 2 0 0 0 13 .005 0 0 0 0
EX 0 1 11 0 1 0
LD 5 1 1 11 2.4938E7
LD 5 2 1 22 2.4938E7
LD 5 3 1 11 2.4938E7
LD 5 4 1 11 2.4938E7
LD 5 5 1 22 2.4938E7
LD 5 6 1 11 2.4938E7
LD 5 7 1 11 2.4938E7
LD 5 8 1 22 2.4938E7
LD 5 9 1 11 2.4938E7
FR 0 1 0 0 146 0
RP 0 181 1 1000 -90 90 1 1
FR 0 1 0 0 146 0
RP 0 1 360 1000 87 0 1 1
EN
20-5-3

```

```

CM 21 Bobtail 2m
CE
GW 1 22 0 0 380 0 0 360 .25
GW 2 42 0 0 360 -40.5 0 360 .25
GW 3 22 -40.5 0 360 -40.5 0 380 .25
GW 4 42 0 0 360 40.5 0 360 .25
GW 5 22 40.5 0 360 40.5 0 380 .25
GW 6 22 0 -12 381.6 0 -12 360 .25
GW 7 42 0 -12 360 -40.5 -12 360 .25
GW 8 22 -40.5 -12 360 -40.5 -12 381.6 .25
GW 9 42 0 -12 360 40.5 -12 360 .25
GW 10 22 40.5 -12 360 40.5 -12 381.6 .25
GS 0 0 .02540
GE 1
GN 2 0 0 0 13 .005 0 0 0 0
EX 0 1 22 0 1 0
LD 5 1 1 22 2.4938E7
LD 5 2 1 42 2.4938E7
LD 5 3 1 22 2.4938E7
LD 5 4 1 42 2.4938E7
LD 5 5 1 22 2.4938E7
LD 5 6 1 22 2.4938E7
LD 5 7 1 42 2.4938E7
LD 5 8 1 22 2.4938E7
LD 5 9 1 42 2.4938E7
LD 5 10 1 22 2.4938E7
FR 0 1 0 0 146 0
RP 0 181 1 1000 -90 90 1 1
FR 0 1 0 0 146 0
RP 0 1 360 1000 87 0 1 1
EN
20-5-5

```

Open models 20-5-4.NEC and 20-5-5.NEC. These files contain the VHF bobtail curtain and a 2-element parasitic version of the bobtail. Like the half-square designs, the elements are uniformly 0.5" diameter 6061-T6 aluminum. The horizontal members are 81" long overall for both models, with the verticals pointed upward. Adjustments are accomplished by varying the length of the verticals (and for the parasitic version, the spacing). The base height is 360" over average S-N soil. Record the same data as for the half squares.

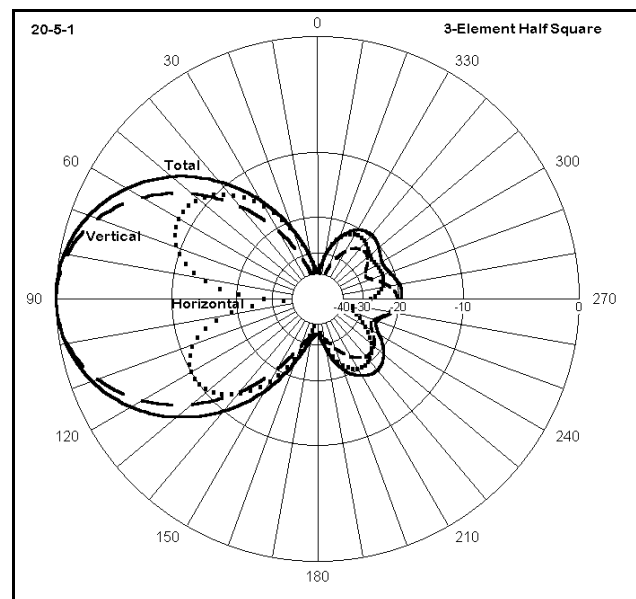
From exercises on vertical arrays, we may anticipate that the bobtail single and double versions will outperform the corresponding half-square versions. We should also anticipate that the pattern of the bobtail is more likely to be symmetrical about a center line through the

array, since the source is centered. In contrast the half squares are fed at one corner of each driver, offering the potential for some degree of asymmetry. How much may be

present we can determine from the azimuth patterns for the antennas.

20-5 Test Data				
Array	Gain dBi TO angle	Beamwidth	F-B dB	Source X R ± jX Ω
1 half square				
2 half squares				
3 half squares				
1 bobtail				
2 bobtails				

Comments: The half squares show a progression of gain from about 9.2 dBi up to about 14.6 dBi as we add parasitic elements to the basic antenna. The beamwidth figure is for a composite of vertically polarized radiation and remnant horizontally polarized radiation due to incomplete cancellation along the horizontal member of the antenna. **Figure 20-5-1** shows the components of the total field. Note that the horizontally polarized radiation has a null just in the direction where the vertically polarized radiation is strongest. Moreover, it is the horizontally polarized radiation that contributes to the asymmetry of the total pattern, especially in the rearward direction. You should examine closely all of the half-square azimuth patterns, noting the sharp side nulls of the single half square pattern as well as features of the two parasitic patterns.

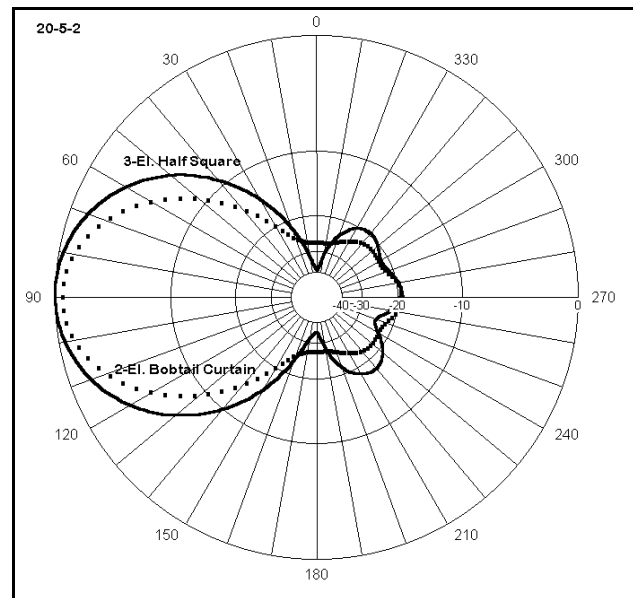


Similar horizontal and vertical radiation components, but symmetrically arranged, are also present in the bobtail patterns, which you should explore in detail. For example, the single bobtail exhibits a narrower beamwidth than the single half square, but without the sharp and deep side nulls. The single bobtail curtain has a 1.4 dB gain advantage over the single half square. Likewise, a 2-element bobtail array shows a 1.2 dB advantage over the 2-element half square. However, the 2-element bobtail has slightly less gain and a lower front-to-back ratio than the 3-element half square, despite the fact that each

antenna has exactly 6 vertical elements. For all cases, source impedances range from 36 to 59 Ω , values which appear to be quite manageable.

20-5		Reference Data		
Array	Gain dBi TO angle	Beamwidth	F-B dB	Source X R \pm jX Ω
1 half square	9.27 / 87°	77°	-----	55.8 - j 0.5
2 half squares	12.85 / 87°	71°	18.73	58.7 - j 1.9
3 half squares	14.55 / 87°	60°	20.02	36.7 + j 1.8
1 bobtail	10.66 / 87°	50°	-----	37.6 + j 1.7
2 bobtails	14.02 / 87°	48°	18.50	42.2 + j 0.4

For some applications, beamwidth may also be an issue in selecting a vertically polarized directional antenna. **Figure 20-5-2** overlays the total patterns for the 3-element half square and the 2-element bobtail curtain. Although the gain advantage of the half square is apparent, so too is the narrower beamwidth of the bobtail array--about 20% narrower. (Note that the half square beam width is already about 40% narrower than the beamwidth of 3- or 4-element Yagis tilted to a vertical orientation.)

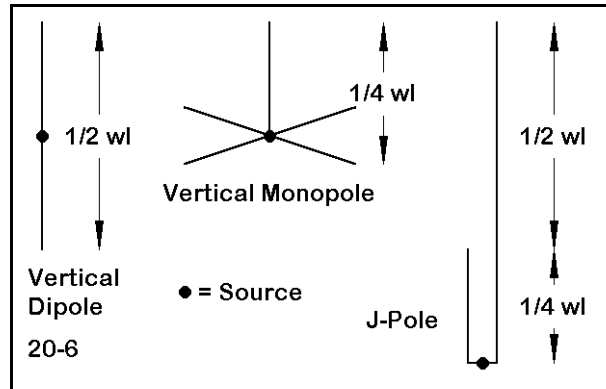


To supplement this exercise, you can of course create larger arrays. However, you may wish to consider another direction. The half square and bobtail arrays have vertical elements whose upper ends are unsupported. Moreover, of the SCVs, they have the largest broadside area. A closed loop is already commonly used for vertically polarized radiation: the side-fed quad loop in square or diamond form. As we discovered in examining SCVs for HF, the flattened rectangle offers significantly more gain than a square. Can you develop a maximum-gain side-fed rectangular loop and then further develop a parasitic version of the antenna for directional gain?

20-6.NEC: Vertically polarized omni-directional antennas for 146 MHz

In services requiring the use of vertically polarized antennas, directional gain may be less important to some applications than area coverage. Therefore, the requirement may be for an omni-directional antenna.

There are numerous omni-directional vertical antennas, of which we shall sample only a small number of basic types. **Figure 20-6** sketches the vertical dipole, the vertical monopole with a ground plane, and the J-pole. These single section antennas might be considered the basic VHF verticals.



```

CM Vertical dipole: 146 MHz
CM Free Space
CE
GW 1 21 0 0 37.55 0 0 0 .25
GS 0 0 .02540
GE 0
EX 0 1 11 0 1 0
LD 5 1 1 21 2.4938E7
FR 0 1 0 0 146 0
RP 0 1 360 1000 90 0 1 1
EN
20-6-1

```

Open model 20-6-1.NEC. The free space vertical dipole shown at left is perhaps the most fundamental antenna of the group, although it is

used less than some others. Providing a feedline at right angles to the antenna is the usual difficulty that prompts the use of other types in the group. The model, like the ones to come, uses 0.5" diameter 6061-T6 aluminum. Also open model 20-6-1A.NEC, the same antenna raised 360" (30') above average S-N ground, as measured from the lowest point of the antenna.

Model 20-6-2.NEC contains a free space vertical monopole with a ground plane. Although the base feedpoint of this antenna is more accessible, the antenna is more complex, with 5 wires required to complete it. Model 20-6-2A.NEC takes the same 6061-T6 aluminum antenna to the 360" point above average ground, as measured from the base of the ground plane.

```

CM 1/4 wl monopole-gp: 146 MHz
CM Free Space
CE
GW 1 21 0 0 18.75 0 0 0 .25
GW 2 21 0 0 0 24.4 0 0 .25
GW 3 21 0 0 0 0 24.4 0 .25
GW 4 21 0 0 0 -24.4 0 0 .25
GW 5 21 0 0 0 0 -24.4 0 .25
GS 0 0 .02540
GE 0
EX 0 1 21 0 1 0
LD 5 1 1 21 2.4938E7
LD 5 2 1 21 2.4938E7
LD 5 3 1 21 2.4938E7
LD 5 4 1 21 2.4938E7
LD 5 5 1 21 2.4938E7
FR 0 1 0 0 146 0
RP 0 1 360 1000 90 0 1 1
EN
20-6-2

```

```

CM J-pole: 146 MHz
CM Free Space
CE
GW 1 21 0 0 55.5 0 0 16.5 .25
GW 2 11 0 0 16.5 0 0 0 .25
GW 3 11 0 7 0 0 7 16.5 .25
GW 4 5 0 0 0 0 7 0 .25
GS 0 0 .02540
GE 0
EX 0 4 3 0 1 0
LD 5 1 1 21 2.4938E7
LD 5 2 1 11 2.4938E7
LD 5 3 1 11 2.4938E7
LD 5 4 1 5 2.4938E7
FR 0 1 0 0 146 0
RP 0 1 360 1000 90 0 1 1
EN
20-6-3

```

An interesting variation on the half wavelength vertical antenna requires end feeding with a parallel-wire matching section. The J-pole, so-called for its resultant appearance, has a number of forms that vary in minor detail. The model shown at left in 20-6-3.NEC is designed to be fed at the base connecting wire that shorts the parallel stub. The 6061-T6 0.5" aluminum elements call for a wider spacing of the matching section than is found in many versions. Variants of the antenna have been constructed from material as diverse as parallel transmission line and copper water pipe. Model 20-6-3A.NEC describes the same antenna 360" above average S-N ground, as measured from the bottom

of the "J" of the J-pole.

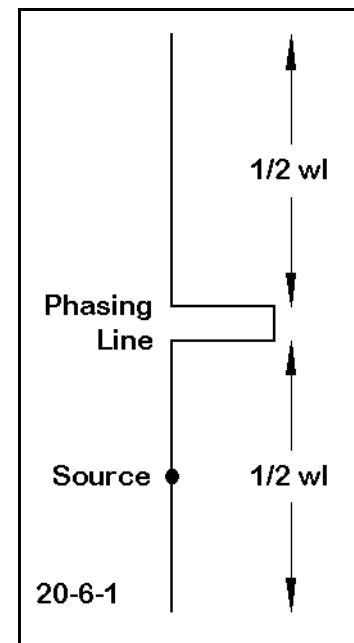
It is not necessary to restrict omni-directional vertical antenna design to single section antennas. **Figure 20-6-1** shows a collinear pair of vertical dipoles with a phasing line between them. The phasing line length depends upon its materials (wire diameter and spacing) and the requisite phase adjustment so that the fields from the two sections of the antenna add in the plane at right angles to the antenna elements. The 0.5" 6061-T6 version of the antenna shown in model 20-6-4.NEC uses a wide spaced line about $1/4\lambda$ long.

```

CM Collinear vertical dipoles: 146 MHz
CM Free space
CE
GW 1 21 0 0 0 0 0 41.5 .25
GW 2 11 0 0 41.5 19.5 0 41.5 .25
GW 3 1 19.5 0 41.5 19.5 0 44.5 .25
GW 4 11 19.5 0 44.5 0 0 44.5 .25
GW 5 21 0 0 44.5 0 0 81.5 .25
GS 0 0 .02540
GE 0
EX 0 1 11 0 1 0
LD 5 1 1 21 2.4938E7
LD 5 2 1 11 2.4938E7
LD 5 3 1 1 2.4938E7
LD 5 4 1 11 2.4938E7
LD 5 5 1 21 2.4938E7
FR 0 1 0 0 146 0
RP 0 1 360 1000 90 0 1 1
EN
20-6-4

```

In model 20-6-4A.NEC you will find the same antenna raised by 360" as measured from the lowest point on the antenna. For each of these 146 MHz antennas, record in the table below the gain and source impedance, as well as the take-off angle for the versions over ground.



20-6 Test Data			
Antenna	Gain dBi	T-O angle	Source Z $R \pm jX \Omega$
Dipole: F.S.		-----	
Dipole: 30'			
Monopole: F.S.		-----	
Monopole: 30'			
J-pole: F.S.		-----	
J-pole: 30'			
Collinear: F.S.		-----	
Collinear: 30'			

Comments: The relative gains of the various vertical omni-directional antennas should present no surprises. The monopole in free space and at highly elevated locations has about 1.35 dB less gain than the vertical dipole. The excess gain of the J-pole over the dipole is not to be explained by its greater height above ground, since the added gain also shows up in the free space model. Rather, the matching section of the J-pole provides some radiation, since the currents in the two wires are not exactly equal. Moreover, the asymmetrical structure distorts the pattern of the antenna from a true circle. Examine the azimuth pattern for the J-pole--or examine the gain table to discover the minor variations in the field (all too small to be operationally significant). The collinear array provides a more significant gain advantage over a single dipole: about 2 dB. Since the phasing line does not have exactly equal currents, there is a slight distortion of the pattern from being truly circular, but once more, not to a significant operational degree.

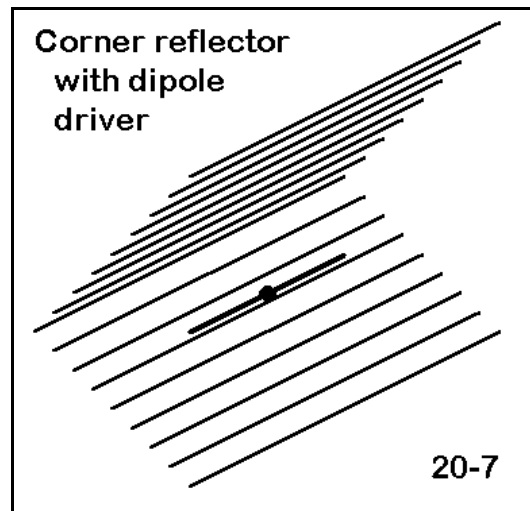
20-6 Reference Data			
Antenna	Gain dBi	T-O angle	Source Z R ± jX Ω
Dipole: F.S.	2.13	-----	71.9 - j 0.5
Dipole: 30'	6.57	3°	71.9 - j 0.5
Monopole: F.S.	0.78	-----	24.5 - j 0.6
Monopole: 30'	5.22	3°	24.5 + j 0.6
J-pole: F.S.	2.56	-----	47.6 - j 1.0
J-pole: 30'	6.92	3°	47.7 + j 0.9
Collinear: F.S.	4.16	-----	174.5 + j 4.2
Collinear: 30'	8.53	3°	174.7 + j 4.4

It is likely that for these runs you accepted the given model without alteration. However, since the version of the models over ground are about 5λ up, you should have altered the elevation plots of them all for an increment of 0.1° in the request for pattern entries. If you did not make this change, do so now and use the gain tables to find the more accurate angle of maximum radiation and its value. Be sure to explore various azimuth angles with the elevation pattern request in order to discover variations in the pattern strength at the new take-off angle. Alternatively, request an azimuth pattern at the take-off angle and examine the shape as revealed both in graphical form and as derived from tabular values.

You may wish to perform frequency sweeps for these antennas from 140 through 150 MHz. Use the resonant impedance of the antenna as the value for determining SWR. You may also create further collinear arrays of verticals for added gain. All of the antennas have been composed of a uniform material--0.5" diameter 6061-T6 aluminum--in order both to make the comparisons fair and to avoid modeling difficulties associated with angular junctions of materials with dissimilar diameters. You certainly should experiment with these antennas using materials of different diameters and composition.

20-7.NEC: A corner reflector array for 432 MHz

Techniques that are too ungainly for use at HF become very practical in the VHF and UHF ranges of the spectrum. The corner reflector, shown in outline in **Figure 20-7**, is one example of such techniques. Once used for UHF television reception, these antennas still find extensive use in communications links that must handle a wide frequency range. They tend to provide a relatively uniform pattern of gain and source impedance over a span of frequencies many times larger than a Yagi design would support. The reflector wires are each about 1.2λ long at the design frequency, with the aperture about 1.6λ long from top to bottom, and the same distance from the rear apex of the corner to the front edge. A $1/2\lambda$ dipole is positioned about 0.4λ from the deepest point of the corner. Refer to standard texts for more exacting determinations of corner reflector dimensions for various applications.



```

CM Corner refl + dipole: 432 MHz
CM Free space
CE
GW 1 11 -.1475 .2794 0 .14757 .2794 0 .005
GW 2 15 -.4064 0 0 .4064 0 0 .005
GW 3 15 -.4064 .0508 .0508 .4064 .0508 .0508 .005
GW 4 15 -.4064 .1016 .1016 .4064 .1016 .1016 .005
GW 5 15 -.4064 .1524 .1524 .4064 .1524 .1524 .005
GW 6 15 -.4064 .2032 .2032 .4064 .2032 .2032 .005
GW 7 15 -.4064 .254 .254 .4064 .254 .254 .005
GW 8 15 -.4064 .3048 .3048 .4064 .3048 .3048 .005
GW 9 15 -.4064 .3556 .3556 .4064 .3556 .3556 .005
GW 10 15 -.4064 .4064 .4064 .4064 .4064 .4064 .005
GW 11 15 -.4064 .4572 .4572 .4064 .4572 .4572 .005
GW 12 15 -.4064 .508 .508 .4064 .508 .508 .005
GW 13 15 -.4064 .5588 .5588 .4064 .5588 .5588 .005
GW 14 15 -.4064 .0508 -.0508 .4064 .0508 -.0508 .005
GW 15 15 -.4064 .1016 -.1016 .4064 .1016 -.1016 .005
GW 16 15 -.4064 .1524 -.1524 .4064 .1524 -.1524 .005
GW 17 15 -.4064 .2032 -.2032 .4064 .2032 -.2032 .005
GW 18 15 -.4064 .254 -.254 .4064 .254 -.254 .005
GW 19 15 -.4064 .3048 -.3048 .4064 .3048 -.3048 .005
GW 20 15 -.4064 .3556 -.3556 .4064 .3556 -.3556 .005
GW 21 15 -.4064 .4064 -.4064 .4064 .4064 -.4064 .005
GW 22 15 -.4064 .4572 -.4572 .4064 .4572 -.4572 .005
GW 23 15 -.4064 .508 -.508 .4064 .508 -.508 .005
GW 24 15 -.4064 .5588 -.5588 .4064 .5588 -.5588 .005
GS 0 0 1
GE 0
EX 0 1 6 0 1 0 20-7

```

Open model 20-7.NEC. 23 10-mm diameter rods compose the reflector structure, while a single 432 MHz dipole, also 10 mm in diameter, feeds the array. The material is 6061-T6 aluminum. The segmentation is limited in the reflector to hold the total number of segments within program limits. Ordinarily, the dipole is fed from the rear and is suspended by an RF-transparent rod or pair of rods.

Our goal with the corner reflector array is to test the wide-band potential of the antenna. For that purpose, we shall execute a frequency sweep from 400 through 500 MHz, despite the design frequency of 432

MHz. Record the gain, front-to-back ratio, beamwidth, and source impedance.

20-7 Test Data				
Frequency MHz	Gain dBi	F-B dB	Beamwidth degrees	Source Z $R \pm jX \Omega$
400				
410				
420				
430				
440				
450				
460				
470				
480				
490				
500				

Comments: The trends in the 100 MHz curves for this corner reflector show very good gain across the swept range, with only a 2.6 dB rising variation. The 180° front-to-back ratio reaches a minimum of about 25.4 dB at 470 MHz and is well above 30 dB at the range limits. You may wish to examine also the worst case front-to-back ratio, which holds rather uniformly across the swept range, despite variations in the 180° front-to-back values. The one very significant change with frequency is the narrowing of the -3 dB beamwidth by 20° (from 58° to 38°) as the frequency rises. The source impedance appears to change by a considerable amount. However, if the reference impedance is set to 105 Ω , the VSWR reaches 1.80:1 at the lower frequency limit and 1.74:1 at the upper frequency limit. You may create a graph of each of these sets of changes for reference, either within the program or with an external spread sheet.

From the trends in the gain and front-to-back numbers, it is clear that the corner reflector has not reached its limits in providing good performance numbers. However, the source impedance figures suggest that the antenna may be close to a 2:1 VSWR operating bandwidth limit. (There is nothing magic about the 2:1 VSWR ratio limit, and under certain operating conditions, the limit might well be extended.) As an additional task, then, expand the sweep range by 75 to 100 MHz on either end of the original sweep and determine an appropriate set of frequency limits for use of the antenna as modeled. Also,

you may wish to create a "bow tie" dipole and test it within the corner reflector to see if you can further expand the frequency range of the array.

20-7 Reference Data				
Frequency MHz	Gain dBi	F-B dB	Beamwidth degrees	Source Z R ± jX Ω
400	10.78	34.63	58	65.6 - j 30.2
410	10.92	33.18	58	74.6 - j 18.4
420	11.06	31.62	56	84.3 - j 7.5
430	11.22	30.08	56	94.6 + j 2.3
440	11.40	29.58	54	105.6 + j 10.9
450	11.61	27.19	52	116.9 + j 18.1
460	11.86	25.93	50	128.2 + j 23.7
470	12.17	25.39	48	139.1 + j 27.9
480	12.54	25.84	44	149.0 + j 31.1
490	12.90	28.47	42	158.3 + j 34.5
500	13.38	32.20	38	169.8 + j 38.0

20-8.NEC: Polarized omni-directional antennas for 300 MHz

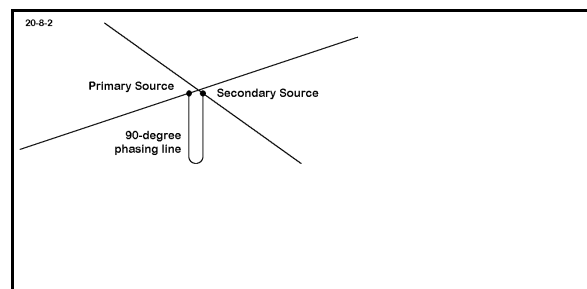
```

CM vertical dipole: 299.7925 MHz
CE
GW 1 21 0 0 -.239 0 0 .239 .0005
GS 0 0 1
GE 0
EX 0 1 11 0 1 0
LD 5 1 1 21 2.4938E7
FR 0 1 0 0 299.7925 0
RP 0 1 360 1000 90 0 1 1
EN
20-8-1

```

Special techniques need not be limited to obtaining gain or operating bandwidth. They may also extend to issues of polarization. In this exercise, we shall compare three antennas in terms of their polarization, with gain and source impedance figures being of secondary importance.

We may begin with model 20-8-1.NEC, a very simple 1 mm 6061-T6 aluminum vertical dipole for 299.7925 MHz (which is often rounded to 299.8 MHz), where a wavelength is exactly 1 m long. Run this model in free space and closely examine not only the total field, but as well the horizontally and vertically polarized components of the field. Record



the gain and source impedance figures.

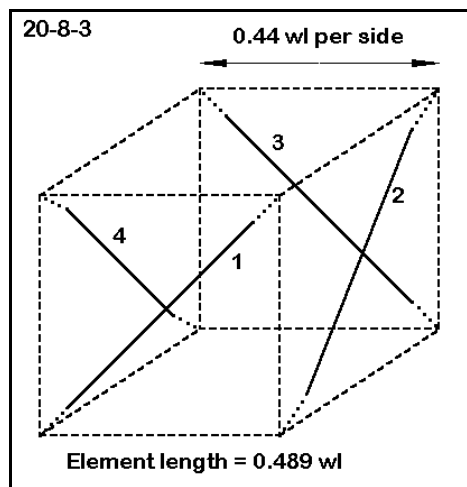
A second antenna of great interest is the turnstile, shown in **Figure 20-8-2**. This array uses two horizontal dipoles set at right angles to each other and crossing at their centers without touching. The antennas are phased by 90° via a transmission line of that length whose characteristic impedance matches the source impedance of the individual dipoles, that is, about 72Ω .

Model 20-8-2 provides a sample turnstile antenna for our same target frequency, composed of the same material as the vertical dipole. Run this model, recording the standard data, but paying close attention to the vertical and horizontal components of the antenna's total radiation field, as recorded in the free space azimuth plot.

```

CM Turnstile: 299.7925 MHz
CE
GW 1 21 -.239 0 .001 .239 0 .001 .0005
GW 2 21 0 -.239 -.001 0 .239 -.001 .0005
GS 0 0 1
GE 0
EX 0 1 11 0 1 0
LD 5 1 1 21 2.4938E7
LD 5 2 1 21 2.4938E7
TL 1 11 2 11 72 .25 0 0 0 0
FR 0 1 0 0 299.7925 0
RP 0 1 360 1000 90 0 1 1
EN
20-8-2

```



A third antenna for our group is a variation on the Lindenblad as originally modeled by Brian Beezley, and shown schematically in **Figure 20-8-3**. The antenna is composed of 4 independently fed dipoles set at 45° angles on the faces (ignoring the top and bottom) of an imaginary cube about 0.44λ on a side. Each dipole is about 0.49λ long.

```

CM Lindenblad--299.7925 MHz
CE
GW 1 21 .22 -.173 -.173 .22 .173 .173 .0005
GW 2 21 -.22 .173 -.173 -.22 -.173 .173 .0005
GW 3 21 .173 .22 -.173 -.173 .22 .173 .0005
GW 4 21 -.173 -.22 -.173 .173 -.22 .173 .0005
GS 0 0 1
GE 0
EX 0 1 11 0 1 0
EX 0 2 11 0 1 0
EX 0 3 11 0 1 0
EX 0 4 11 0 1 0
LD 5 1 1 21 2.4938E7
LD 5 2 1 21 2.4938E7
LD 5 3 1 21 2.4938E7
LD 5 4 1 21 2.4938E7
FR 0 1 0 0 299.7925 0
RP 0 1 360 1000 90 0 1 1
EN
20-8-3

```

Model 20-8-2.NEC is a model of the antenna using 1 mm aluminum and targeted at the 1-m wavelength. As with the other antennas, run the model, recording the standard data, but also attending to the horizontal and vertical components of the radiation fields. For all three antennas, you may obtain the horizontal and vertical field gain from the gain tables.

20-8 Test Data				
Antenna	Total Field Gain dBi	Horizontal Gain dBi	Vertical Gain dBi	Source Z $R \pm jX \Omega$
Vert. Dipole				
Turnstile				
Lind. variant				

Comments: The vertical dipole is the only antenna of the three to have a nearly perfect circular pattern. The gain figures for the other antennas are maximums drawn from the gain tables. The turnstile antenna gain (total field) varies by only about 1 dB (between -0.89 and -1.90) around the circumference of the pattern, while the Lindenblad variant total field varies even less (between 0.60 and 1.01).

What gives these three antennas interest as a group is the polarization. Obviously, the vertical dipole is almost perfectly vertically polarized, with only a remnant of horizontally polarized radiation. The turnstile, in contrast, is almost wholly horizontally polarized with only a trace of vertically polarized radiation. Between these extremes lie most antennas, with an irregular combination of both radiation components. The Lindenblad variant differs in that the horizontally polarized and vertically polarized fields are almost exactly equal, so closely equal that the differential is not operationally significant. The horizontally polarized component moves between -2.82 and -1.80 dBi, while the vertically polarized component moves between -2.04 and -2.21 dBi, both at 45° intervals. Since the maxima and minima for the two alternate, the total field is remarkably stable.

20-8 Reference Data				
Antenna	Total Field Gain dBi	Horizontal Gain dBi	Vertical Gain dBi	Source Z $R \pm jX \Omega$
Vert. Dipole	2.10	0.00	2.10	73.3 + j 0.0
Turnstile	-0.89	-0.89	0.00	36.0 + j 0.0
Lind. variant	1.01	-1.80	-2.04	113 + j4 (x4)

There are numerous applications which may call for an equality of vertically and horizontally polarized radiation from the same antenna, regardless of the antenna's power gain. In a region where television receivers may use either a vertical or a horizontal antenna, the television transmitting antenna might be required to provide equal signal strength to both. As a supplemental exercise, develop other applications where equality

of the polarized components of the total antenna field may be more significant than directional or omni-directional gain.

The antennas we have examined are also examples of a common modeling practice: they provide a basic model at a 1-m wavelength. Our task is then to frequency scale them to some working frequency, making adjustments in the model according to the difference between the material diameters that we contemplate using and the scaled diameters initially presented by the model. As a supplement to this exercise, scale the collection of three antennas for 54, 85, 213, and 480 MHz, using element diameters that are integers in millimeters and that are no larger than 4 mm and no smaller than 1 mm.

Summing Up

Our sampling of VHF and UHF concerns and techniques has only pointed the way to a domain of ever widening challenges, both in the field of antenna design and in the arena of antenna modeling. The goal of point-to-point long range communications still remains a significant aim, although there may be a more diverse range of targets that include terrestrial surface contact, moon-bounce signal detection, and satellite repeater retransmission. More local and area needs, especially with the growth of digital data transmission, have added specialized requirements to antennas so that gain may not be the main issue in many instances.

The structures we have examined in this chapter tell only part of the story. More advanced challenges lie ahead, for example, accurately modeling parabolic dishes, horns, and other special shapes, most of which require large numbers of segments and long run times. These projects have been omitted, since this guide is designed to use models that execute in a reasonably short time. NEC-Win Plus, however, can handle models of almost any practical size.

If these exercises have taught us anything, it is that we have only begun to model.

User Notes

21. Special Structures

Objectives: *In our final exercises, we shall encounter a medley of different physical and electrical structures. Most will have only occasional application; others introduce some advanced techniques; still others are simply odd but interesting. Their sum is the knowledge that many modeling projects require as much ingenuity as technical know-how.*

Not every modeling technique has a well-organized place in the scheme of modeling theory and practice. This fact is especially true, since we have restricted ourselves to the use of NEC-2 within the NEC-Win Plus package, with limitations on the available NEC input cards. Although this package is more than adequate for all of the types of antennas with which we have worked so far, some antennas may require professional-level packages, direct NEC card input, virtually unlimited segments per model, and multiple ground-type facilities.

Nevertheless, we can go a long way with the tools at hand toward modeling what seems at first sight beyond package capabilities. We have already sampled at least two examples of this practice. Theoretically, we should not have been able to model a vertical monopole composed of tapered-diameter sections and topped with a capacity hat. However, by the judicious creation of a substitute model for the tapered-diameter vertical element, we obtained quite accurate results. In modeling ground planes, which must be above ground with NEC-2, we found we could closely approximate buried radials by placing the system very close to the ground surface.

In this chapter, we shall look at a group of cases that are related only by the fact that we shall have to figure out ways to get the modeling task done. Some will involve interesting geometric shapes, such as helices. Although advanced NEC versions have helix-creating cards, we shall learn to create our own. Other examples will involve segment-eating structures, such as wire cages and tower sections. Although direct modeling is ideal, we shall generate satisfactory simpler substitutes so that the segment limitations do not inhibit modeling multi-element beams from caged wires or modeling complex antenna structures placed atop tower sections.

We shall also look at a sample of some electrical conundrums facing the modeler. For example, some antenna circuitry requires the placement of components across a source. However, all standard loads appear in series with the source. The creation of a parallel load that uses true inductive or capacitive values requires the creation of an additional

physical structure on the antenna element. We shall look at the construction steps necessary to ensure that modeling the added structure for a shunt load does not invalidate the model.

Not all structures that are relevant to the modeling of antennas are themselves antennas. In many instances, surrounding objects may play a role in the performance of an actual antenna. Modeling the objects would be useful in assessing potential antenna performance in a given environment. Cars, ships, planes, and helicopters have all been successfully modeled. We shall try our hand at a simple object to see what is involved in the modeling and what sorts of results we get from the effort.

Space limits how many nooks and crannies into which we may poke our modeling software in this guide. Nevertheless, these concluding exercises should convince you that it is possible to model far more antennas and auxiliary structures--both large and small--than an initial readout of NEC-2 specifications might seem to allow. Once you have realized this fact, you will be ready to go it alone, confident in your abilities to model within program restrictions almost any antenna system you might encounter.

Exercise Preparation

Besides the usual advice to save model variants under alternative names, there is only one caution to give for this final chapter. Be prepared to use any and all of the techniques encountered in the previous chapters in the exercises in this final chapter. Also be prepared to return to earlier models to use as comparators with models you develop in these exercises.

21-1: A helical dipole and a helical Yagi for 28.5 MHz

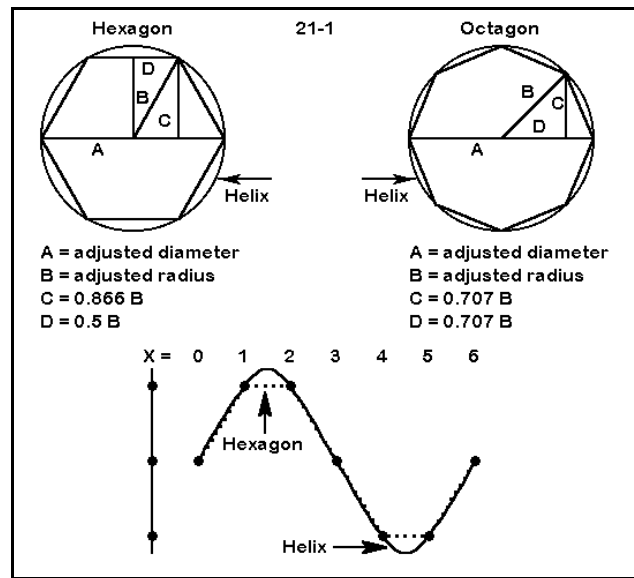
A helix is simply any wire wound in a spiral, ordinarily with a constant diameter and a constant pitch or distance between turns. Helices find use in antennas in at least two different applications. First, they can be used as spiral forms of linear elements in order to shorten the length of the element while sustaining gain so far as possible. The helix becomes especially useful at HF as the element become shorter than about 2/3 full length, since its losses are less than those of even high-Q loading inductors. However, there is a cost: ordinarily, the spiral wire requires a central support, adding to the weight of the structure.

A second common use is at UHF frequencies, where a helical element may be fed at its end with a reflector behind the feedpoint. If correctly calculated (see standard references), the helix will effectively radiate a signal with directional gain and circular polarization. Such antennas are useful in satellite communications and similar tasks where the signal source at the other end of a path may show a varying polarization due to positional changes. Circular polarization tends to reduce signal fading due to cross

polarization.

Advanced implementations of NEC have an input card which will create a helix to specifications. However, the modeler may create a helix manually without too much work. Since NEC uses straight wires, all helices are approximations of a true spiral. However, with enough segments, the approximations will be quite accurate. For antennas whose construction permits field adjustment, even a hexagon may be a satisfactory model.

Calculating a helix is a simple matter of creating one turn of the spiral and then repeating the shape. **Figure 21-1** outlines the procedure using simple geometric shapes as a starting point. Let X be the axis lengthwise along the spiral. The cross-sectional dimensions will use the Y- and Z-axes.



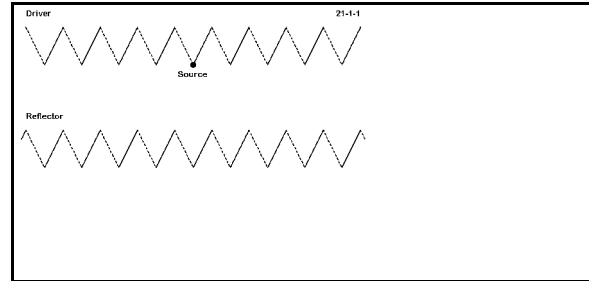
First, determine if the circumference needs to be truly accurate. A perfect circular circumference is 2π (6.283) times the radius. The outline of a hexagon is only 6 times a radial reaching a peak that lies on the circumference of a circle. An octagon outline is about 6.123 times a similar radial. If the area within the straight-line figure or the outline length of that figure is crucial, adjust the radial length to achieve the desired value.

21-1		First Helix		6-Sides			
W#-E#	X	Y	Z	W#-E#	X	Y	Z
1-1	0	-B	0	1-2	1	-D	0
2-1	1	-D	C	2-2	2	D	C
3-1	2	D	C	3-2	3	B	C
4-1	3	B	0	4-2	4	D	0
5-1	4	D	-C	5-2	5	-D	-C
6-1	5	-D	-C	6-2	6	-B	-C

The values to be used for the Y and Z values are shown in the drawing and on the table for the first full turn of the helix. The X values are determined by dividing the distance between equivalent positions on successive turns by the number of sides on the straight-line polygon. The figure and table show the situation for a hexagon. After completing the first turn, subsequent turns simply repeat the Y and Z value and add the actual value of $X=6$ to the second turn entries.

To test this work let's develop a 2-element helical Yagi for 28.5 MHz, as shown in **Figure 21-1-1**. We shall use #12 AWG copper wire.

Since we can always squeeze or spread turns in the final product, a hexagon will suffice. We have arbitrarily chosen a radial length of 0.1016 m (about 4") corresponding to a circular diameter of 0.2032 m. The pitch will be 0.3048 m/turn, so each step within a turn will be 0.0508 m along the X-axis. Of course, we shall begin with a dipole and then move on to the 2-element array.



GM Helical dipole: 28.5 MHz		21-1
CE		
GW	1 3 0 .1016 0 .0508 .0508 .08788 .0010265	
GW	2 3 .0508 .0508 .08788 .1016 -.0508 .08788 .0010265	
GW	3 3 .1016 -.0508 .08788 .1524 -.1016 0 .0010265	
GW	4 3 .1524 -.1016 0 .2032 -.0508 -.0878 .0010265	
GW	5 3 .2032 -.0508 -.0878 .254 .0508 -.0878 .0010265	
GW	6 3 .254 .0508 -.0878 .3048 .1016 0 .0010265	
GW	7 3 .3048 .1016 0 .3556 .0508 .08788 .0010265	
GW	8 3 .3556 .0508 .08788 .4064 -.0508 .08788 .0010265	
GW	9 3 .4064 -.0508 .08788 .4572 -.1016 0 .0010265	
GW	10 3 .4572 -.1016 0 .508 -.0508 -.0878 .0010265	
GW	11 3 .508 -.0508 -.0878 .5588 .0508 -.0878 .0010265	
GW	12 3 .5588 .0508 -.0878 .6096 .1016 0 .0010265	
GW	13 3 .6096 .1016 0 .6604 .0508 .08788 .0010265	
GW	14 3 .6604 .0508 .08788 .7112 -.0508 .08788 .0010265	
GW	15 3 .7112 -.0508 .08788 .762 -.1016 0 .0010265	
GW	16 3 .762 -.1016 0 .8128 -.0508 -.0878 .0010265	
GW	17 3 .8128 -.0508 -.0878 .8636 .0508 -.0878 .0010265	
GW	18 3 .8636 .0508 -.0878 .9144 .1016 0 .0010265	
GW	19 3 .9144 .1016 0 .9652 .0508 .08788 .0010265	
GW	20 3 .9652 .0508 .08788 1.016 -.0508 .08788 .0010265	
GW	21 3 1.016 -.0508 .08788 1.0668 -.1016 0 .0010265	
GW	22 3 1.0668 -.1016 0 1.1176 -.0508 -.0878 .0010265	
GW	23 3 1.1176 -.0508 -.0878 1.1684 .0508 -.0878 .0010265	
GW	24 3 1.1684 .0508 -.0878 1.2192 .1016 0 .0010265	
GW	25 3 1.2192 .1016 0 1.27 .0508 .08788 .0010265	
GW	26 3 1.27 .0508 .08788 1.3208 -.0508 .08788 .0010265	
GW	27 3 1.3208 -.0508 .08788 1.3716 -.1016 0 .0010265	
GW	28 3 1.3716 -.1016 0 1.4224 -.0508 -.0878 .0010265	
GW	29 3 1.4224 -.0508 -.0878 1.4732 .0508 -.0878 .0010265	
GW	30 3 1.4732 .0508 -.0878 1.524 .1016 0 .0010265	
GW	31 3 1.524 .1016 0 1.5748 .0508 .08788 .0010265	
GW	32 3 1.5748 .0508 .08788 1.6256 -.0508 .08788 .0010265	
GW	33 3 1.6256 -.0508 .08788 1.6764 -.1016 0 .0010265	
GW	34 3 1.6764 -.1016 0 1.7272 -.0508 -.0878 .0010265	
GW	35 3 1.7272 -.0508 -.0878 1.778 .0508 -.0878 .0010265	

Using the information just given, create the first and subsequent turns for a resonant dipole for 28.5 MHz. You may use model 21-1.NEC as a check. As you add turns and check resonance, be sure to move the source as close to the antenna center as possible. Because the hexagon facets have appreciable length, use about 3 segments per wire. When you achieve resonance, which may not be on a complete turn, record the gain and source impedance in the table on the next page.

At left is a partial model description, cut off so as not to reveal too easily the total number of turns necessary to achieve resonance.

Next, copy the dipole, but adjust all Y values by a factor of -1.524 m (about 5'), which will create a reflector. You will discover that the driver is too long. To maintain balance, remove a single section from each end of the driver element. Use NEC-Vu to check your work to ensure that all segments end up where you want them and that the reflector is longer than the driver by an equal amount on each end. You may check your work against model 21-1-1.NEC. Record the gain, 180° front-to-back ratio, and source impedance in the table on the next page.

21-1-1 Test Data			
Antenna	Gain dBi	F-B dB	Source Z $R \pm jX \Omega$
Dipole		-----	
Yagi			

Comments: The dipole and Yagi elements are only a bit longer than $1/4\lambda$, but both antennas perform closer to versions with element about 70% full size and loaded by conventional means. You may wish to check models of loaded elements and beams in early chapters for comparison--or you may create inductively loaded dipoles and Yagis as comparators. Indeed, the use of helical elements as a substitute for linear elements is most advantageous when the element lengths are about 45% to 55% of full size, leaving a reasonably wide pitch to the turns.

In addition, the Yagi version of the helical antenna is not resonant. Of course, the capacitive reactance may be left for use with a beta or similar matching network. However, try to resonate the driver by adding a short wire to each end that tracks where the next helix segment would go, but is short enough to achieve resonance with equal segments on each end. Alternatively, you may add a short segment to each end that brings you close to resonance. Then, move the free ends inward or outward to alter the resonant frequency. The result should be suggestive of actual construction and field alignment procedures.

21-1-1 Reference Data			
Antenna	Gain dBi	F-B dB	Source Z $R \pm jX \Omega$
Dipole	1.74	-----	25.3 + j 4.6
Yagi	6.05	18.08	17.2 - j 19.1

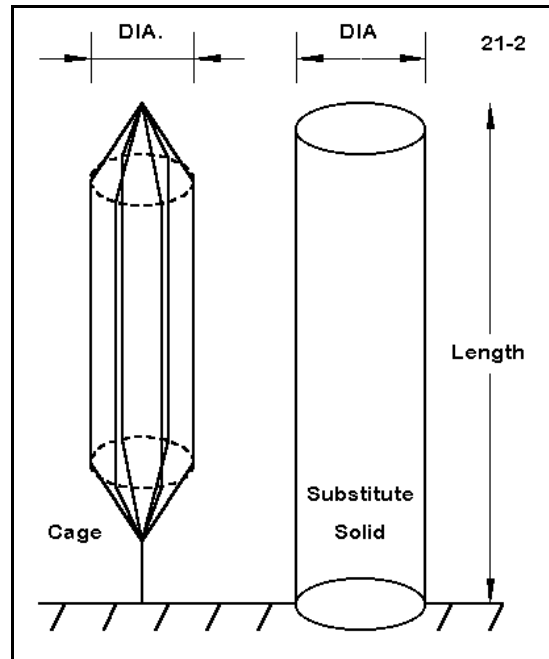
The merits of a helical dipole or Yagi are secondary in this exercise to appreciating the technique by which one can create helices. Although the helical elements of these antennas were produced casually, many UHF circularly polarized antennas require extreme rigor in helix dimensions. Moreover, in UHF helical antennas, the first turn may require a transitional or variable pitch rate to establish one or more operating parameters. Hence, the first turn may have different values for each step along its length. For this order of precision, the antennas are ordinarily modeled with many more than 6 wires per turn.

21-2.NEC: Cage antennas for 3.7 MHz

A common practice in the lower HF and the full MF region is to use "cage" elements. A cage element is composed of many wires forming a cylinder, with spacers to maintain a constant diameter to the collection. The free end is brought to a common point, as is the feedpoint. It is common to see cage construction for the legs of a dipole; more rarely we see the technique used with monopole antennas.

Figure 21-2 shows a cage monopole of the sort we shall construct in this exercise. Since the cage is likely to have a fairly complex structure, we shall initially model half of a dipole against perfect ground. When we achieve a desired result, we may move the antenna to free space and complete the other side.

For the main cylinder of the cage, construction techniques involve the same geometric relations we used in creating a helix. However, each of the points we calculate will mark 2 of the coordinates for a single wire. Let us use #12 AWG copper wire and create a 6-wire cage. For the monopole version, we can use the relations apt to the hexagon to set the X and Y coordinates. Let the diameter of the cage be 12" long. The coordinates for each of the wires about a common center of 0,0 will be 6,0; 3,5.196; 3,-5.196; -6,0; -3,-5.196; and -3;5.196.



```

CM Cage element/perfect ground
CE
GW 1 1 0 0 745 6 0 730 4.04133858267717E-02
GW 2 1 0 0 745 3 5.196 730 4.04133858267717E-02
GW 3 1 0 0 745 3 -5.196 730 4.04133858267717E-02
GW 4 1 0 0 745 6 0 730 4.04133858267717E-02
GW 5 1 0 0 745 -3 -5.196 730 4.04133858267717E-02
GW 6 1 0 0 745 -3 5.196 730 4.04133858267717E-02
GW 7 50 6 0 730 6 0 30 4.04133858267717E-02
GW 8 50 3 5.196 730 3 5.196 30 4.04133858267717E-02
GW 9 50 3 -5.196 730 3 -5.196 30 4.04133858267717E-02
GW 10 50 -6 0 730 -6 0 30 4.04133858267717E-02
GW 11 50 -3 -5.196 730 -3 -5.196 30 4.04133858267717E-02
GW 12 50 -3 5.196 730 -3 5.196 30 4.04133858267717E-02
GW 13 1 6 0 30 0 0 15 4.04133858267717E-02
GW 14 1 3 5.196 30 0 0 15 4.04133858267717E-02
GW 15 1 3 -5.196 30 0 0 15 4.04133858267717E-02
GW 16 1 -6 0 30 0 0 15 4.04133858267717E-02
GW 17 1 -3 -5.196 30 0 0 15 4.04133858267717E-02
GW 18 1 -3 5.196 30 0 0 15 4.04133858267717E-02
GW 19 1 0 0 15 0 0 0 4.04133858267717E-02
GS 0 0 .02540
GE 1
GN 1
EX 0 19 1 0 1 0
  
```

21-2-1

The length should be an estimate of the length needed for resonance, minus some inches need to bring the cage wires together and to establish a single-wire source. The exact lengths necessary for these modeling tasks depend upon the segmentation density, since the segment lengths for the end sections should be roughly equal. If we give each wire in this 3.7 MHz cage about 50 segments, then the tapered sections can each be about 15" long, and the

source segment a similar length.

Open model 21-2-1.NEC, shown partially on the preceding page. The monopole is constructed from the top down, beginning with 6 wires from a point in a cone that is 15" long to 6 cage-cylinder end points. Each of these cage wires is 730" long, ending 30" above perfect ground. A second 15" cone brings the 6 wires to a single point. The 15" source segment terminates at ground. The resulting construction contains 19 wires and 313 segments.

For simplicity of modeling, we may attempt a substitute element composed of a single wire roughly equal in diameter to the diameter of the cage cylinder. The 12" copper wire can be highly segmented and still result in a much smaller model than the cage, as shown in model 21-2-2.NEC. This model reflects the substitute solid element shown on the right side of **Figure 21-2**. Run both this substitute model and the cage version, recording the gain and source impedance of each antenna.

```

CM Cage element/perfect ground
CM Substitute element
CE
GW 1 53 0 0 745 0 0 0 6
GS 0 0 .02540
GE 1
GN 1
EX 0 1 53 0 1 0
LD 5 1 1 53 5.8001E7
FR 0 1 0 0 3.7 0
RP 0 181 1 1000 -90 0 1 1
EN
21-2-2

```

```

CM Cage element: free space
CE
GW 1 1 -745 0 0 -730 6 0 4.04133858267717E-02
GW 2 1 -745 0 0 -730 3 5.196 4.04133858267717E-02
GW 3 1 -745 0 0 -730 3 -5.196 4.04133858267717E-02
GW 4 1 -745 0 0 -730 -6 0 4.04133858267717E-02
GW 5 1 -745 0 0 -730 -3 -5.196 4.04133858267717E-02
GW 6 1 -745 0 0 -730 -3 5.196 4.04133858267717E-02
GW 7 50 -730 6 0 -30 6 0 4.04133858267717E-02
GW 8 50 -730 3 5.196 -30 3 5.196 4.04133858267717E-02
GW 9 50 -730 3 -5.196 -30 3 -5.196 4.04133858267717E-02
GW 10 50 -730 -6 0 -30 -6 0 4.04133858267717E-02
GW 11 50 -730 -3 -5.196 -30 -3 -5.196 4.04133858267717E-02
GW 12 50 -730 -3 5.196 -30 -3 5.196 4.04133858267717E-02
GW 13 1 -30 6 0 -15 0 0 4.04133858267717E-02
GW 14 1 -30 3 5.196 -15 0 0 4.04133858267717E-02
GW 15 1 -30 3 -5.196 -15 0 0 4.04133858267717E-02
GW 16 1 -30 -6 0 -15 0 0 4.04133858267717E-02
GW 17 1 -30 -3 -5.196 -15 0 0 4.04133858267717E-02
GW 18 1 -30 -3 5.196 -15 0 0 4.04133858267717E-02
GW 19 3 -15 0 0 15 0 0 4.04133858267717E-02
GW 20 1 15 0 0 30 6 0 4.04133858267717E-02
GW 21 1 15 0 0 30 3 5.196 4.04133858267717E-02
GW 22 1 15 0 0 30 3 -5.196 4.04133858267717E-02
GW 23 1 15 0 0 30 -6 0 4.04133858267717E-02
GW 24 1 15 0 0 30 -3 -5.196 4.04133858267717E-02
GW 25 1 15 0 0 30 -3 5.196 4.04133858267717E-02
GW 26 50 30 6 0 730 6 0 4.04133858267717E-02
GW 27 50 30 3 5.196 730 3 5.196 4.04133858267717E-02
GW 28 50 30 3 -5.196 730 3 -5.196 4.04133858267717E-02
GW 29 50 30 -6 0 730 -6 0 4.04133858267717E-02
GW 30 50 30 -3 -5.196 730 -3 -5.196 4.04133858267717E-02
GW 31 50 30 -3 5.196 730 -3 5.196 4.04133858267717E-02
GW 32 1 730 6 0 745 0 0 4.04133858267717E-02
GW 33 1 730 3 5.196 745 0 0 4.04133858267717E-02
GW 34 1 730 3 -5.196 745 0 0 4.04133858267717E-02
GW 35 1 730 -6 0 745 0 0 4.04133858267717E-02

```

Before commenting on the results of the modeling run, let's create the corresponding free space dipoles for both the cage and solid monopoles. A portion of the cage model (21-2-3.NEC) appears at the left. Note that the antenna length has been transferred to the X-axis, while the wire coordinates appear as values of Y and Z. Even the partial view of the model description reveals that this is a large model for what is essentially electrically simple: a dipole. The complete model contains 37 wires and 647 segments. The size may prevent the model from running on programs with a 500-segment limit. However, you may slight the cage cylinder wires a few segments each (13 or more, to be more precise), so

long as every cylinder wire is equally reduced in the total number of segments. The result

will bring the total model size under 500 segments and permit you to run it. As usual, record the gain and the source impedance on the table that appears on the next page.

Model 21-2-4.NEC shows the simplicity of a substitute model using a single 12" diameter wire for the entire 1490" length of the dipole. This 103-segment model has the same diameter as the cage cylinders of the preceding model. Unlike the cage model, which required cones each side of center to produce a 1-wire source point, the source of this model may be placed at the wire's center. Run this model and add its gain and source data information to the table below.

```

CM Cage element--free space
CM Substitute element
CE
GW 1 103 -745 0 0 745 0 0 6
GS 0 0 .02540
GE 0
EX 0 1 52 0 1 0
LD 5 1 1 103 5.8001E7
FR 0 1 0 0 3.7 0
RP 0 1 360 1000 90 0 1 1
EN
21-2-4

```

21-2 Test Data				
Antenna	Cage Gain dBi	Source Z R ± jX Ω	Substitute Gain dBi	Source Z R ± jX Ω
Monopole				
Dipole				

Comments: The gain and source impedance values for the substitute solid wire monopole and dipole are quite normal within the perfect-ground and free-space environments, respectively. The element lengths (slightly over 62' for the monopole and 124' for the dipole) are well within the shortening one might expect from such a fat element. However, the model cage structures appear to tell a different story, perhaps suggesting that the more complex form of the antennas provides additional gain (about 1.7 dB for the monopole and 1.3 dB for the dipole). The cage structures also appear to present lower source impedances than their solid substitutes.

21-2 Reference Data				
Antenna	Cage Gain dBi	Source Z R ± jX Ω	Substitute Gain dBi	Source Z R ± jX Ω
Monopole *	6.85 (5.39)	22.6 + j 3.7 (31.6 - j 1.1)	5.14 (5.14)	35.6 - j 1.5 (35.6 - j 1.5)
Dipole *	3.44 (2.28)	49.5 + j 6.2 (64.4 + j 1.4)	2.13 (2.13)	71.1 - j 3.6 (71.1 - j 3.5)

(* Figures in parentheses are NEC-4.1 output values for the same models.)

Appearances can be deceiving. Despite the small size of the wire, the spacing between wires in the cage is below the threshold beyond which NEC-2 can yield accurate results. The unaccountable rise in reported gain combined with the equally unaccountable decrease in source impedance together form the warning that the threshold has been passed, as we noted in some of the models in Chapter 10. (Although NEC-4 is superior in this regard, it still yields gains that are systematically high and source impedances that are systematical low, but to a much lesser degree.)

An alternative structure with greater accuracy is possible. The chief source of inaccuracy in the original models is the tapered sections that join the wires. Although they reflect actual construction, they also pass farthest beyond the geometric limitations of NEC-2. Hence, one may build a model with butt ends, as in the monopole in model 21-2-5.NEC, shown in part to the right. A run of this model should yield a gain of 5.23 dBi and a source impedance of $33.9 + j 5.1 \Omega$, figures much closer to the substitute model.

```

CM Cage element/perfect ground
CM No tapered ends
CE
GW 1 1 6 0 745 3 5.196 745 4.04133858267717E-02
GW 2 1 3 5.196 745 -3 5.196 745 4.04133858267717E-02
GW 3 1 -3 5.196 745 -6 0 745 4.04133858267717E-02
GW 4 1 -6 0 745 -3 -5.196 745 4.04133858267717E-02
GW 5 1 -3 -5.196 745 3 -5.196 745 4.04133858267717E-02
GW 6 1 3 -5.196 745 6 0 745 4.04133858267717E-02
GW 7 50 6 0 745 6 0 15 4.04133858267717E-02
GW 8 50 3 5.196 745 3 5.196 15 4.04133858267717E-02
GW 9 50 3 -5.196 745 3 -5.196 15 4.04133858267717E-02
GW 10 50 -6 0 745 -6 0 15 4.04133858267717E-02
GW 11 50 -3 -5.196 745 -3 -5.196 15 4.04133858267717E-02
GW 12 50 -3 5.196 745 -3 5.196 15 4.04133858267717E-02
GW 13 1 6 0 15 3 5.196 15 4.04133858267717E-02
GW 14 1 3 5.196 15 -3 5.196 15 4.04133858267717E-02
GW 15 1 -3 5.196 15 -6 0 15 4.04133858267717E-02
GW 16 1 -6 0 15 -3 -5.196 15 4.04133858267717E-02
GW 17 1 -3 -5.196 15 3 -5.196 15 4.04133858267717E-02
GW 18 1 3 -5.196 15 6 0 15 4.04133858267717E-02
GW 19 1 6 0 15 0 0 0 4.04133858267717E-02
GS 0 0 .02540
GE 1
GN 1
LEX 0 19 1 0 1 0

```

21-2-5

(NEC-4 reports a gain of 5.14 and a source impedance of $34.6 + j 4.9 \Omega$, closer still to the substitute. However, the divergence from NEC-2 values and the progression toward the substitute suggest that the solid-wire substitute may be the most reasonable model of the cage.)

Thus, the substitute model serves two purposes. First, it forewarns of the possibility that the close-spaced structure may exceed the geometry limitations of NEC-2. Second, it provides the primary means by which one can model the behavior of the cage structure. Although only a comparison with an actual cage antenna can confirm the accuracy of the substitute model, it can pass an additional test for reasonableness: frequency sweeping the cage and solid models for ± 250 kHz of the very close resonant frequencies yields similar curves for changes in both source resistance and source reactance.

21-3.NEC: A triangular tower structure

Isolating the largest source of modeling error for the cage antenna structure in the tapered cones that brought the wires together opens an avenue for modeling an additional structure of great interest to antenna work: the typical triangular support tower.

Triangular tower structures with elements no larger than 30 mm in diameter and at least 0.5 m spacing between longitudinal elements can be modeled effectively down to at least

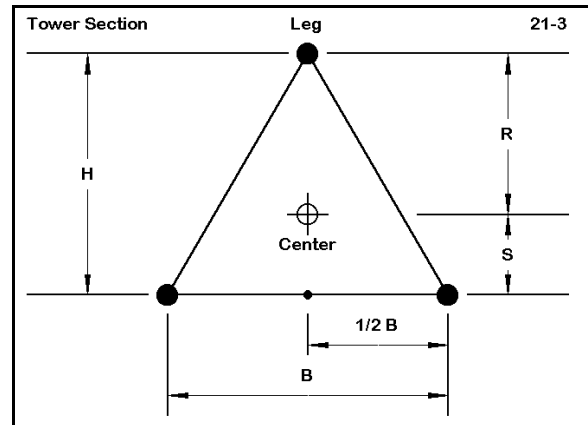
3 MHz. Wide spacing increases accuracies at lower frequencies, while larger element diameters may decrease accuracy.

In this exercise, we shall explore the construction of models of towers, but we shall not investigate them as antennas. Although a source has been placed in each model, it is there only to complete the model formally, not to test the tower's use as an antenna.

The key cross-section dimensions of a tower appear in **Figure 21-3**. For an equilateral triangle, $H = 0.866 B$, while $R = 0.67 H$ and $S = H - R$. Therefore, for a vertical tower structure, the following X and Y coordinates would apply, based on a known value of B:

Leg #	X	Y
1	R	0.0
2	-S	0.5 B
3	-S	-0.5 B

First, let's build some tower sections. Since towers are usually composed of relatively identical sections which are stacked on top of each other, developing a basic stock of "reusable" sections can be handy. The section in this exercise will use 30 mm steel legs (assigned a conductivity of $1.0E6$ s/m) with a face width of 0.5 m. It is tempting to catch each horizontal and angular cross member in the model, but we shall simplify the design for this exercise. To avoid any possible difficulties with angular junctions of wires having dissimilar diameters, we shall add at the top of each section three horizontal cross members to connect the vertical legs, and each cross member will have the same diameter as the leg.



```

CM Tower: 1 m section
CE
GW 1 5 .29 0 0 .29 0 1 .015
GW 2 5 -.14 .25 0 -.14 .25 1 .015
GW 3 5 -.14 -.25 0 -.14 -.25 1 .015
GW 4 2 .29 0 1 -.14 .25 1 .015
GW 5 2 -.14 .25 1 -.14 -.25 1 .015
GW 6 2 -.14 -.25 1 .29 0 1 .015
GS 0 0 1
GE 1
GN 1
EX 0 3 1 0 1 0
LD 5 1 1 5 1e6
LD 5 2 1 5 1e6
LD 5 3 1 5 1e6
LD 5 4 1 2 1e6
LD 5 5 1 2 1e6
LD 5 6 1 2 1e6
FR 0 1 0 0 3.7 0
RP 0 181 1 1000 -90 0 1 1
EN

```

21-3-1

Open model 21-3-1.NEC, a model of a 1-m long tower section. For a face width (B) of 0.5 m, the values of R, S, and 0.5B are 0.29, 0.14, and 0.25, respectively. View the model from all perspectives on NEC-Vu.

From this model, you can create longer towers simply by repeating the model elements, but changing the Z coordinates to join to the next lower section. A second section atop this one shown at left would have Z values of 1 for the open ended legs and 2 for the top part with the cross members. In this manner, or with suitable variations, you can simulate with small model sections any required level of cross-membering of

towers, even if the termination points of model sections do not coincide with the divisions of actual steel structures.

Open models 21-3-2.NEC and 23-3-3.NEC. View each on NEC-Vu. These models are in principle identical to the first one, except that legs are longer: 2 m and 4 m, respectively. Note the proportionally larger number of segments per leg for these longer tower sections.

Using model 21-3-2 as a basis, construct an 18-m tall tower over the standardized perfect ground of this exercise by copying and revising the basic section. Your resulting model should have 9 sections and 54 wires, as shown (partially) in the check model 23-3-4.NEC to the right. Use a careful scan of your wire table and NEC-Vu to ensure that every element in the model is correctly placed.

The construction of tower models usually serves as a check to see if the structure is influencing the performance of antennas placed at the top or to the sides of the tower. Hence, the source position in use would be within additional antenna structures added to this model. Use of the tower as an antenna element would normally involve additional physical structures on which the source would be located. However, you may wish to run the 18-m tower and ascertain the reported gain and source impedance.

CM Tower: 18 m, 2-m sections		21-3-4	
CE			
GW	1 10 .29 0 0 .29 0 2 .015		
GW	2 10 -.14 .25 0 -.14 .25 2 .015		
GW	3 10 -.14 -.25 0 -.14 -.25 2 .015		
GW	4 2 .29 0 2 -.14 .25 2 .015		
GW	5 2 -.14 .25 2 -.14 -.25 2 .015		
GW	6 2 -.14 -.25 2 .29 0 2 .015		
GW	7 10 .29 0 2 .29 0 4 .015		
GW	8 10 -.14 .25 2 -.14 .25 4 .015		
GW	9 10 -.14 -.25 2 -.14 -.25 4 .015		
GW	10 2 .29 0 4 -.14 .25 4 .015		
GW	11 2 -.14 .25 4 -.14 -.25 4 .015		
GW	12 2 -.14 -.25 4 .29 0 4 .015		
GW	13 10 .29 0 4 .29 0 6 .015		
GW	14 10 -.14 .25 4 -.14 .25 6 .015		
GW	15 10 -.14 -.25 4 -.14 -.25 6 .015		
GW	16 2 .29 0 6 -.14 .25 6 .015		
GW	17 2 -.14 .25 6 -.14 -.25 6 .015		
GW	18 2 -.14 -.25 6 .29 0 6 .015		
GW	19 10 .29 0 6 .29 0 8 .015		
GW	20 10 -.14 .25 6 -.14 .25 8 .015		
GW	21 10 -.14 -.25 6 -.14 -.25 8 .015		
GW	22 2 .29 0 8 -.14 .25 8 .015		
GW	23 2 -.14 .25 8 -.14 -.25 8 .015		
GW	24 2 -.14 -.25 8 .29 0 8 .015		
GW	25 10 .29 0 8 .29 0 10 .015		
GW	26 10 -.14 .25 8 -.14 .25 10 .015		
GW	27 10 -.14 -.25 8 -.14 -.25 10 .015		
GW	28 2 .29 0 10 -.14 .25 10 .015		
GW	29 2 -.14 .25 10 -.14 -.25 10 .015		
GW	30 2 -.14 -.25 10 .29 0 10 .015		
GW	31 10 .29 0 10 .29 0 12 .015		
GW	32 10 -.14 .25 10 -.14 .25 12 .015		
GW	33 10 -.14 -.25 10 -.14 -.25 12 .015		
GW	34 2 .29 0 12 -.14 .25 12 .015		
GW	35 2 -.14 .25 12 -.14 -.25 12 .015		

The modeled tower represents no known tower section currently in production. The reason for using a hypothetical tower section is simple: determining the adequacy of a tower section model--or even a model of a total tower--requires empirical testing of the tower itself. Rather than trying to create a model that catches every detail of the actual construction of a given tower section, it is usually easier to adjust the length of the basic model tower section used until it replicates at full length the actual tower's electrical characteristics. Since the cross-members are symmetrically placed on the structure, their diameter can be changed to smaller values with little introduction of error. The process of modification to meet the requirements of an actual tower may also involve changing the conductivity value for the tower material. Our exercise value of 1.0E6 s/m is slightly lower than the value of type 302 stainless steel. An actual tower's RF conductivity value may vary considerably, depending upon both the basic material (steel or aluminum) and any surface coating (galvanizing or metallic paint).

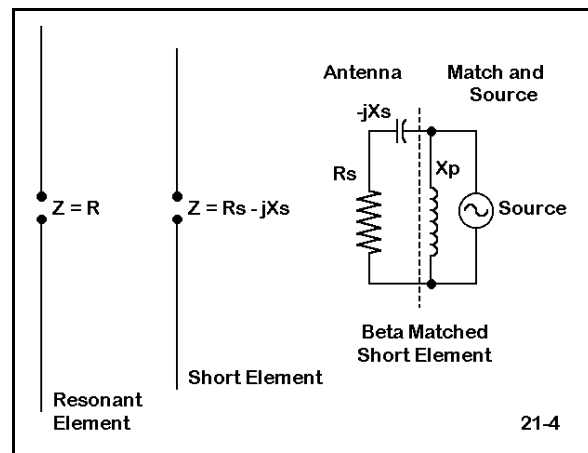
Unlike exercises involving antennas, tower modeling in the abstract does not present an accurate set of expectations about the electrical performance of an actual object. At most, it provides a collection of techniques that can be applied to real cases to simplify the modeling aspect of a more complex task that involves gathering carefully measured data. However, you may often use a variety of hypothetical towers made from sections having variable lengths, such as our basic models in this exercise, to determine whether a

tower structure is likely to affect the performance of an attached antenna. While the answer will not be definitive for reality, it may indicate lines of further work.

As a supplementary exercise, you may wish to validate the tower models used in this exercise at the design frequency and at other frequencies. Place one of the tower sections in free space. Add a second set of cross members on the initially open end of the structure. Place the source at the center of one of the legs. Lengthen the legs to resonance (for each frequency tested), increasing the number of segments per leg to a suitable value. The result is a complex form of the "folded dipole" which will have at resonance a free space gain of about 2.21 dBi. If the legs remain extended in the Z-axis, the azimuth pattern will be circular. Departures from these parameters tend to indicate that the model either has errors or is not usable at the test frequency as a tower model.

21-4.NEC: A beta-match for a 3-element 14.175 MHz Yagi

Not all special structures are large compared to the antenna of which they are a part or to which they join. Consider the beta match, a method of matching a lower impedance antenna to a higher impedance feedline system. If the antenna driven element can be shortened without otherwise jeopardizing the desired characteristics of the antenna, then it forms a series impedance, with a capacitive reactance. To match a higher resistive impedance to a lower resistive impedance, as viewed from the source or feedline, a simple L-circuit consisting of a shunt inductive reactance in parallel with the source and a capacitive reactance in series with the load will suffice. The shortened antenna element contains 2 of the system elements: the load and series capacitive reactance. A simply calculated inductor shunted across the antenna terminals and the feedline provides the remaining items. The question for this exercise is whether a beta match can be effectively modeled.



Since loads are in series with the source, the beta inductor cannot be modeled as an LD card. Since at least one major purpose of modeling a beta coil as part of the antenna would be to take frequency sweeps to check the operating bandwidth, modeling a value of inductance would be more accurate than modeling a simple shunt reactance. Hence, physical modeling is the most direct route.

Open model 21-4.NEC, a three element Yagi for 14.175 MHz. Run the model and determine its source impedance at the design frequency, which is at the center of the 20 meter amateur radio band allocation. Record the gain, front-to-back ratio, and source impedance in the table on the next page.

```

CM 3-el Yagi: 14.175 MHz
CE
GW 1 101 -5.292 0 0 5.292 0 0 .0125
GW 2 101 -4.947 3.024 0 4.947 3.024 0 .0125
GW 3 101 -4.786 6.049 0 4.786 6.049 0 .0125
GS 0 0 1
GE 0
EX 0 2 51 0 1 0
LD 5 1 1 101 2.4938E7
LD 5 2 1 101 2.4938E7
LD 5 3 1 101 2.4938E7
FR 0 1 0 0 14.175 0
RP 0 1 360 1000 90 0 1 1
EN

```

21-4

A source impedance of about 25Ω requires a series capacitive reactance of about 25Ω and a shunt inductive reactance of about 50Ω to effect a match to a $50\text{-}\Omega$ source or system feedline. See standard references for L-circuit equations. The modeled source impedance is close to the required resistance and capacitive reactance values. A $0.56 \mu\text{H}$ inductor across the antenna terminals would complete the match.

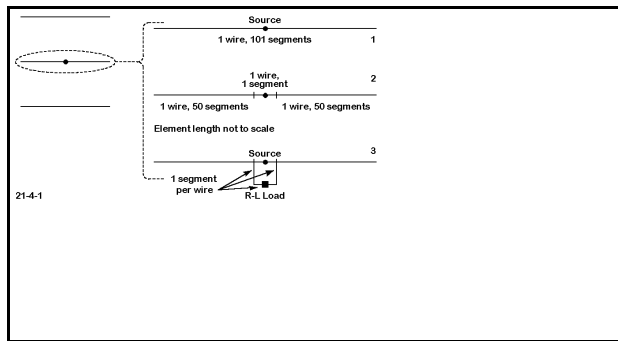


Figure 21-4-1 shows the steps involved in modeling a beta match. First ensure that the initial values derive from a model using sufficiently short segments (but within program limits) to permit element subdivision into very small parts. The 101 segments on the model driven element yields segments about 0.098 m long. Subdivide the driver into 3 wires, as indicated by the sketch, with the center 1-

segment wire exactly centered and equal in length to the individual segments of the outer wires.

Open model 21-4-1.NEC, the same Yagi with the driver subdivided. Note that the center segment is exactly centered and is 0.098 m long. Run this model and add its data to the table. In this procedure, it is essential that you check each modification of the model to ensure that no modification makes a significant difference in the operating characteristics of the antenna.

```

CM 3-el Yagi: 14.175 MHz
CE
GW 1 101 -5.292 0 0 5.292 0 0 .0125
GW 2 50 -4.947 3.024 0 -.049 3.024 0 .0125
GW 3 1 -.049 3.024 0 .049 3.024 0 .0125
GW 4 50 .049 3.024 0 4.947 3.024 0 .0125
GW 5 101 -4.786 6.049 0 4.786 6.049 0 .0125
GS 0 0 1
GE 0
EX 0 3 1 0 1 0
LD 5 1 1 101 2.4938E7
LD 5 2 1 50 2.4938E7
LD 5 3 1 1 2.4938E7
LD 5 4 1 50 2.4938E7
LD 5 5 1 101 2.4938E7
FR 0 1 0 0 14.175 0
RP 0 1 360 1000 90 0 1 1
EN

```

21-4-1

The third step of the procedure is to create a square of three wires, all identical in length to the center wire and connecting to its ends. There are two directions in which the wires can go: vertical with respect to the plane of the antenna and within the plane itself. We shall model the square both ways, as shown in models 21-4-2.NEC and 21-4-3.NEC. The purpose in creating both models is to select the one which has the lesser impact on the

performance characteristics of the antenna.

```

CM 3-el Yagi with beta match
CM vertical placement
CE
GW 1 101 -5.292 0 0 5.292 0 0 .0125
GW 2 50 -4.947 3.024 0 -.049 3.024 0 .0125
GW 3 1 -.049 3.024 0 .049 3.024 0 .0125
GW 4 1 -.049 3.024 0 -.049 3.024 .098 .0125
GW 5 1 -.049 3.024 .098 .049 3.024 .098 .0125
GW 6 1 .049 3.024 .098 .049 3.024 0 .0125
GW 7 50 .049 3.024 0 4.947 3.024 0 .0125
GW 8 101 -4.786 6.049 0 4.786 6.049 0 .0125
GS 0 0 1
GE 0
EX 0 3 1 0 1 0
LD 0 5 1 1 .25 .56e-6 0
LD 5 1 1 101 2.4938E7
LD 5 2 1 50 2.4938E7
LD 5 3 1 1 2.4938E7
LD 5 4 1 1 2.4938E7
LD 5 5 1 1 2.4938E7
LD 5 6 1 1 2.4938E7
LD 5 7 1 50 2.4938E7
LD 5 8 1 101 2.4938E7
FR 0 1 0 0 14.175 0
RP 0 1 360 1000 90 0 1 1
EN

```

21-4-2

Do not run either model without first inserting a load in the wire parallel to the antenna element, in these models, wire 5. If you wish to check the exact degree of affect created by the small structure, you may insert a resistive load of 1.0E10, essentially creating an open circuit. However, we shall go directly to a type 1 series R-L-C load consisting of an inductance of 0.56 μH ($X = 50 \Omega$ at 14.175 MHz) and a resistance of 0.25 Ω (which assumes a Q of about 200 for the inductor).

Run both models 21-4-2.NEC and 21-4-3.NEC, and record the gain, front-to-back, and source impedance values on the table on the next page.

If you discover relatively insignificant differences in antenna performance (except for the source impedance), revise one of the two new models. Change the frequency entry to start at 14.0 MHz and use 6 0.07 MHz steps to frequency sweep the antenna through 14.35 MHz. Use model 21-4-4.NEC as a check on your modifications. Record the results on the next page.

```

CM 3-el Yagi with beta match
CM horizontal placement
CE
GW 1 101 -5.292 0 0 5.292 0 0 .0125
GW 2 50 -4.947 3.024 0 -.049 3.024 0 .0125
GW 3 1 -.049 3.024 0 .049 3.024 0 .0125
GW 4 1 -.049 3.024 0 -.049 2.926 0 .0125
GW 5 1 -.049 2.926 0 .049 2.926 0 .0125
GW 6 1 .049 2.926 0 .049 3.024 0 .0125
GW 7 50 .049 3.024 0 4.947 3.024 0 .0125
GW 8 101 -4.786 6.049 0 4.786 6.049 0 .0125
GS 0 0 1
GE 0
EX 0 3 1 0 1 0
LD 0 5 1 1 .25 .56e-6 0
LD 5 1 1 101 2.4938E7
LD 5 2 1 50 2.4938E7
LD 5 3 1 1 2.4938E7
LD 5 4 1 1 2.4938E7
LD 5 5 1 1 2.4938E7
LD 5 6 1 1 2.4938E7
LD 5 7 1 50 2.4938E7
LD 5 8 1 101 2.4938E7
FR 0 1 0 0 14.175 0
RP 0 1 360 1000 90 0 1 1
EN

```

21-4-3

```

CM 3-el Yagi with beta match
CM "hairpin" (600-Ohm stub)
CE
GW 1 101 -5.292 0 0 5.292 0 0 .0125
GW 2 50 -4.947 3.024 0 -.049 3.024 0 .0125
GW 3 1 -.049 3.024 0 .049 3.024 0 .0125
GW 4 1 -.049 3.024 0 -.049 2.926 0 .0125
GW 5 1 -.049 2.926 0 .049 2.926 0 .0125
GW 6 1 .049 2.926 0 .049 3.024 0 .0125
GW 7 50 .049 3.024 0 4.947 3.024 0 .0125
GW 8 101 -4.786 6.049 0 4.786 6.049 0 .0125
GW 9 1 2114.938 2114.938 2114.938 2114.96 2114.96 .00211
GS 0 0 1
GE 0
EX 0 3 1 0 1 0
LD 5 1 1 101 2.4938E7
LD 5 2 1 50 2.4938E7
LD 5 3 1 1 2.4938E7
LD 5 4 1 1 2.4938E7
LD 5 5 1 1 2.4938E7
LD 5 6 1 1 2.4938E7
LD 5 7 1 50 2.4938E7
LD 5 8 1 101 2.4938E7
TL 5 1 9 1 600 .28 0 0 10000000000 10000000000
FR 0 1 0 0 14.175 0
RP 0 1 360 1000 90 0 1 1
EN

```

21-4-5

Before we survey the work we have done, open model 21-4-5.NEC. A beta match may be implemented not only with an inductor, but as well with a "hairpin," a shorted transmission line stub having the same design inductive reactance as the inductor. This model changes the LD0 entry to a TL entry for a 600- Ω shorted transmission line 0.28 m long, the calculated length to achieve 50 Ω at 14.175 MHz. (Note: since transmission lines are in parallel with sources, you may delete the added wires and place the TL "hairpin"

directly on the source segment.) Run model 21-4-5.NEC along with the others, and then modify it to make a frequency sweep. Use the same specifications: start at 14.0 MHz and use 6 steps, each 0.07 MHz, to end the sweep at 14.35 MHz. Record the results in the appropriate tables.

21-4 Test Data			
Version	Gain dBi	F-B dB	Source Z $R \pm jX \Omega$
Basic			
Subdivided Driver			
Vertical Load			
Horizontal Load			
600- Ω hairpin			

Comments: By constructing the extra beta match antenna structure as small as feasible and by carefully tracking the steps to ensure that no significant change in antenna performance occurred, we have developed a reasonably trustworthy model of the antenna plus its matching element. (Maximum changes of 0.03 dB gain and 0.03 dB front-to-back ratio are not significant and could not be measured in a real antenna.) Had the antenna showed significant changes of performance with the extra wires, the model would not have been usable. Likewise, had one version of the load structure affected performance figures more than the other, we would have had cause to eliminate that version from our task.

21-4 Reference Data			
Version	Gain dBi	F-B dB	Source Z $R \pm jX \Omega$
Basic	7.84	29.79	23.4 - j 24.6
Subdivided Driver	7.84	29.79	23.4 - j 24.6
Vertical Load	7.86	29.80	57.1 - j 2.0
Horizontal Load	7.86	29.81	57.1 - j 2.1
600- Ω hairpin	7.88	29.82	57.4 - j 2.3

The slightly high resultant source impedance stems from at least two factors. First, the

original antenna source resistance value is below the rough load resistance figure (25Ω) used to casually calculate the beta match, resulting in a higher figure at the network source terminals. Second, the added structure is also part of the shunt load and exhibits parallel transmission line effects on the results. In order to sort the two error sources, you may calculate a more precise beta inductor value, taking into account as well the slight variance of the series capacitive reactance. Any remaining difference between the model results and calculations belongs to the added structural wires.

21-4-4/5		Test Data			
Frequency MHz		Gain dBi	F-B dB	Source Z $R \pm jX \Omega$	50- Ω VSWR
14.00	L TL				
14.07	L TL				
14.14	L TL				
14.21	L TL				
14.28	L TL				
14.35	L TL				

Note: "L" indicates model 21-4-4.NEC, using the inductor as the shunt element, while "TL" indicates the modified model, 21-4-5.NEC, using the transmission line stub shunt element.

For any practical purpose, there is no difference in the performance of the two methods of effecting a beta match across the range of the frequency sweep. The model transmission line, of course, is lossless, while an actual transmission line under 1' in length and constructed in all likelihood of heavy parallel aluminum wires will have a finite loss. However, that loss, while calculable in principle, would not be measurable in the field during adjustment of the antenna. Likewise, the coil Q of 200 (series resistance: 0.25Ω for a reactance of 50Ω) is a reasonable value to use.

As a supplemental exercise, you may experiment with physical and TL hairpin structures, using wires of various diameters and setting them at various spacings. Calculate the

resultant characteristic impedance and then calculate the required length of a shorted stub to achieve the desired inductive reactance. Perform frequency sweeps of the prescribed range to see what difference, if any, the alternative hairpin designs make in the VSWR curve.

Likewise, assume a range of Q values for the beta coil ranging from the indefinitely large (series resistance: 0Ω) to about 50, the lowest value that a poorly designed and well-weathered inductor might reach. Again, perform frequency sweeps across the 14.0 to 14.35 MHz range to test the effects of Q on VSWR.

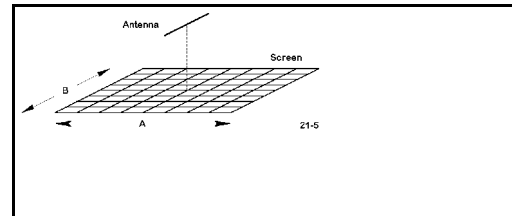
21-4-4/5		Test Data			
Frequency MHz		Gain dBi	F-B dB	Source Z $R \pm jX \Omega$	50- Ω VSWR
14.00	L	7.67	22.38	81.8 + j 18.3	1.76
	TL	7.70	22.38	82.5 + j 18.2	1.77
14.07	L	7.73	28.00	73.6 + j 8.2	1.51
	TL	7.76	28.00	74.1 + j 8.0	1.51
14.14	L	7.81	33.33	63.0 + j 0.5	1.26
	TL	7.83	33.33	63.3 + j 0.3	1.27
14.21	L	7.90	26.15	51.1 - j 3.8	1.08
	TL	7.92	26.15	51.2 - j 4.0	1.09
14.28	L	8.01	21.07	39.3 - j 4.5	1.30
	TL	8.03	21.07	39.4 - j 4.6	1.30
14.35	L	8.13	17.61	29.1 - j 2.4	1.72
	TL	8.14	17.60	29.2 - j 2.4	1.72

21-5.NEC: An elevated dipole with screen for 145.5 MHz

Most structures with flat or gently curved surfaces call for wire-grid modeling, since NEC-2 uses straight wires for all purposes. A wire grid is simply a grid of short wires arranged so that the overall outline traces the general outline of the metallic object being modeled. Each wire is short--as short as feasible within the segment limits of the program. Often, wires are 1 segment long, with connections to other wires in the grid at each end. Since the wire grid is modeling a solid surface, a maximum of interconnections prevents any one wire from being independently resonant and thus potentially throwing off the actual antenna performance over or beside the object modeled.

We shall sample the use of a wire grid to model a very simple but often used object: a screen placed beneath a VHF antenna to increase its gain.

Figure 21-5 shows the general properties of the total model. We shall use a common horizontal dipole and compare its performance in free space, 10 meters over average S-N ground, and 1λ above



two sizes of wire grid screens. The grids will be squares, alternately 1λ and 2λ per side (about 2.05 and 4.1 m per side). To properly model the close-spaced screening (like window screening) actually used in such installations would require more segments than we have to use. However, we at least may see some trends that will be useful.

Open model 21-5.NEC. This common free space 6061-T6 dipole with a 1.5 mm diameter is the basic antenna for our efforts. The design frequency is 145.5 MHz.

```
CM Dipole: 145.5 MHz
CM 10 m up
CE
GW 1 21 -.494 0 10 .494 0 10 .00075
GS 0 0 1
GE 1
GN 2 0 0 0 13 .005 0 0 0 0
EX 0 1 11 0 1 0
LD 5 1 1 21 2.4938E7
FR 0 1 0 0 145.5 0
RP 0 181 1 1000 -90 90 1 1
EN
21-5-1
```

```
CM Dipole: 145.5 MHz
CM Free Space
CE
GW 1 21 -.494 0 0 .494 0 0 .00075
GS 0 0 1
GE 0
EX 0 1 11 0 1 0
LD 5 1 1 21 2.4938E7
FR 0 1 0 0 145.5 0
RP 0 1 360 1000 90 0 1 1
EN
21-5
```

Open model 21-5-1.NEC, which is the same unit 10 m over S-N ground (cond. = 0.005 s/m; perm. = 13). For both this antenna and the free space model, record the gain, take-off angle (if relevant), and source impedance.

Now comes the more tedious part. At 8 meters above ground, create a wire grid of 1 mm diameter 6061-T6 wire that is 1λ on a side, with the center of the dipole centered in the grid, roughly as shown in **Figure 21-5**. Place the wires on 0.1λ centers. For economy, use 1 segment per wire. You should at least plot this grid on graphing paper before opening model 21-5-2.NEC. Note that each element of the grid between intersections consists of a single wire and that every intersection represents a junction that terminates the wires touching it. Wires may NOT pass through other wires. Hence, every square within a grid consist of 4 separate wires.

Inspect model 21-5-2.NEC, shown partially at right. The model has 221 wires, only one of which is the antenna. The wires are systematically arranged 0.206 m apart. If you examine the grid on NEC-Vu, you will see that **no connection is left open within the grid**. Although the segmentation density is less than optimal, the grid will suffice to indicate its affect on the dipole 1λ above it. Record the data for this antenna model on the table on the next page.

Now open model 21-5-3.NEC. This model also has a screen, which for economy has been limited to 220 wires (in addition to the single dipole wire). As you inspect that model, notes its similarity to the preceding model, except for the dimensions. The grid is now about 2.06 m per side, and the spacing between wires has been increased to about 0.412 m. The consequence of choosing these dimensions is that wire spacing is now about 0.2λ . However, to create a grid of this new size with 0.1λ spacing would have required about 840 wires, which would not run on a program limited to 500 segments. However, the model is still useful if not fully accurate. Record its data on the table.

```

CM Dipole: 145.5 MHz                21-5-2
CM 10 m up, 1 wl screen 8 m
CE
GW 1 21 -.494 0 10 .494 0 10 .00075
GW 2 1 -1.03 -1.03 8 -1.03 -.824 8 .0005
GW 3 1 -1.03 -.824 8 -1.03 -.618 8 .0005
GW 4 1 -1.03 -.618 8 -1.03 -.412 8 .0005
GW 5 1 -1.03 -.412 8 -1.03 -.206 8 .0005
GW 6 1 -1.03 -.206 8 -1.03 0 8 .0005
GW 7 1 -1.03 0 8 -1.03 .206 8 .0005
GW 8 1 -1.03 .206 8 -1.03 .412 8 .0005
GW 9 1 -1.03 .412 8 -1.03 .618 8 .0005
GW 10 1 -1.03 .618 8 -1.03 .824 8 .0005
GW 11 1 -1.03 .824 8 -1.03 1.03 8 .0005
GW 12 1 -.824 -1.03 8 -.824 -.824 8 .0005
GW 13 1 -.824 -.824 8 -.824 -.618 8 .0005
GW 14 1 -.824 -.618 8 -.824 -.412 8 .0005
GW 15 1 -.824 -.412 8 -.824 -.206 8 .0005
GW 16 1 -.824 -.206 8 -.824 0 8 .0005
GW 17 1 -.824 0 8 -.824 .206 8 .0005
GW 18 1 -.824 .206 8 -.824 .412 8 .0005
GW 19 1 -.824 .412 8 -.824 .618 8 .0005
GW 20 1 -.824 .618 8 -.824 .824 8 .0005
GW 21 1 -.824 .824 8 -.824 1.03 8 .0005
GW 22 1 -.618 -1.03 8 -.618 -.824 8 .0005
GW 23 1 -.618 -.824 8 -.618 -.618 8 .0005
GW 24 1 -.618 -.618 8 -.618 -.412 8 .0005
GW 25 1 -.618 -.412 8 -.618 -.206 8 .0005
GW 26 1 -.618 -.206 8 -.618 0 8 .0005
GW 27 1 -.618 0 8 -.618 .206 8 .0005
GW 28 1 -.618 .206 8 -.618 .412 8 .0005
GW 29 1 -.618 .412 8 -.618 .618 8 .0005
GW 30 1 -.618 .618 8 -.618 .824 8 .0005
GW 31 1 -.618 .824 8 -.618 1.03 8 .0005

```

21-5 Test Data			
Model	Gain dBi	T-O angle degrees	Source Z $R \pm jX \Omega$
free space		-----	
10 m, no screen			
1λ screen			
2λ screen			

Comments: The potential benefits from placing a screen 1λ below a dipole appear dramatically in the table. Although the take-off angle does not change, the addition of a 2λ screen increases gain by over 1.3 dB. In fact, screens with more closely spaced wires show even higher gain (to over 10 dBi). Note that the placement of the screen 1λ below the antenna does alter the source impedance to a discernible degree.

Nevertheless, a number of questions remain open. First, will the improvement in gain still appear with truly close-spaced wires, such as those found in conductive window screening? Further modeling with implementations of NEC that have no segment limitations may answer such questions, although the run times may be quite long. Second, is it necessary to extend the screen equally both broadside to and off the ends of the dipole? Further modeling might disclose a shape that yielded the desired performance but which saved on screening (and modeling) material.

21-5 Reference Data			
Model	Gain dBi	T-O angle degrees	Source Z $R \pm jX \Omega$
free space	2.10	-----	72.4 + j 0.3
10 m, no screen	7.93	3°	73.5 + j 0.5
1 λ screen	8.29	3°	73.0 - j 9.3
2 λ screen	9.29	3°	70.3 - j 1.4

Third, how far may the screen be extended and still produce usable amounts of additional gain? The sizes of screening chosen for this exercise were arbitrary. Hence, further modeling is in order to determine the point at which further size increases (in either or both dimensions) yield insufficient increments of added gain to justify the construction. Fourth, is 1 λ the optimum height for spacing from the screen to the antenna? Adding this question to the mix creates the possibility of a matrix of planar dimensions vs. separation from the antenna in terms of optimal screen construction and maximum antenna gain at the lowest angles.

These questions do not exhaust the inquiries we might relevantly make of the wire-grid construction and its relationship to the dipole. However, useful questions exist in other directions. As a supplementary exercise, you may wish to replace the dipole with other types of antennas, both horizontally and vertically polarized, to determine if the benefits of the screen extend to them. Initially, models of a vertical dipole and of a 3-element Yagi--extracted from earlier chapters of this guide--form good candidates for further studies of VHF screens.

The questions we have posed of the wire-grid screen are typical of those which might be asked about any object created in antenna fields. Wire grids may form any number of passive but conductive constructs, ranging from sappy trees to automobiles and other transportation media; from house wiring to tall buildings, water towers, and similar structures. In some cases, we may be searching for maximum effect upon the antenna;

in others, we may be seeking the conditions that yield the minimum effect. The utility of wire grids is limited only by the imagination.

Summing Up

Summarizing a potpourri of modeling possibilities would do little more than repeat what has already been said throughout the chapter. If the diverse exercises in this set have convinced you that there are potentials and limitations of the process well beyond what we have introduced in these pages, then these structural workouts have done their job.

Instead, let's summarize some of the possibilities in NEC-2 that lie beyond this basic hands-on tutorial--some techniques and functions that might appear in a more advanced volume.

On the output side of the ledger, far field analysis is only one of NEC's available field outputs. The program is capable of near field analysis, which is important both in local interference studies and in the arena of radiation hazard analysis. NEC also offers the possibility for a combined field output calculation (the RP1 option). When more than performance-at-a-distance is at stake, these alternative outputs can be very useful.

On the input side, we have not come close to exhausting NEC's potentials. It is possible to implement additional ground conditions, whereas we have used uniform ground conditions throughout our work. We may change soil types at a specified distance from the geometric center of the model, as well as stepping downward at that point. Of course, nothing requires us to place the antenna at the center of this ground geometry.

Transmission lines, which we examined in detail, are a special case of network creation between two wires. NEC has a more general admittance network input for the creation of complex networks. We sampled this provision every time we called for a current source. We have also by-passed a number of advanced source provisions within NEC, including incident plane waves of both linear and elliptic polarization.

Although we hand-calculated a basic helix, NEC offers an automated helix creation input, as well as a cylindrical structure generation function. For work at UHF and above, one can also specify surface patches. (NEC-4 also offers automated catenary wire creation.) When complex constructs may be used in many models--perhaps environmental objects associated with a potential range of antennas--the advanced modeler may create them and use the numerical Green's function option to incorporate the results of the object analysis without recalculating the entire object matrix with each model run.

Also available are various techniques involving antenna symmetry that may reduce the size of the matrix calculations. These reductions can shorten run times and hold models

within any program segment limitations imposed by the implementation. The actual model and matrix reduction size will depend upon the number of degrees of symmetry available in the model.

In addition to improving the handling of tapered-diameter linear elements, NEC-4 offers additional capabilities of use in advanced modeling. Whereas NEC-2 uses only bare wire, NEC-4 offers the potential for modeling insulated wires having a velocity factor of less than 1.0 in antenna element use. Additionally, NEC-4 offers the ability to place wires beneath the ground surface, a feature useful in the evaluation of ground planes and subterranean antenna structures.

Lest we leave you with the impression that this volume has omitted more than it has included, let's close with a caution: none of the advanced features can be implemented in a trustworthy fashion without a thorough mastery of the basic functions of NEC-2 and a good bit of experience in using these functions to create a wide variety of models of real antennas. Without these two factors, the modeler would lack the ability to know when the results made sense. Even experienced professional antenna modelers are occasionally guilty of missteps. One goal of all of the exercises in this guide is to reduce the missteps you will take to an absolute minimum.

The other goal of the guide is to give you the confidence in your modeling abilities as a foundation for new and creative antenna modeling endeavors. There is much yet to learn about antennas--and method-of-moments antenna modeling software packages, such as NEC-2 and the NECWin Plus implementation, provide us with important tools to uncover some of what we do not yet know and have not yet created.

User Notes

Appendix

Some Useful Data for Antenna Modelers

The following pages contain a potpourri of information useful to antenna modelers. You should perhaps clip or key this appendix, since you are likely to refer often to the data on these pages.

1. Conductivity and Permittivity of Common Ground Conditions
2. Conductivity and Resistivity of Common Materials Used in Antenna Construction
3. Common Wire Gauges and Associated Diameters in Inches and in Millimeters
4. Some Common Frequency-Wavelength Relationships
5. Frequency Domains
6. Some Common Transmission Lines Values
7. Metric-English Conversion
8. List of Models in Order of Appearance

1. Conductivity and Permittivity of Common Ground Conditions

The following soil descriptions are commonly used in antenna modeling. Always substitute more precise values wherever known. The table represents an adaptation of values found in *The ARRL Antenna Book* (p. 3-6), which are themselves an adaptation of the table presented by Terman in *Radio Engineer's Handbook* (p. 709), taken from "Standards of Good Engineering Practice Concerning Standard Broadcast Stations," *Federal Register* (July 8, 1939), p. 2862. Terman's value for the conductivity of the worst soil listed is an order of magnitude lower than the value shown here.

Soil Description	Conductivity in S/m σ	Permittivity (Dielectric Constant) ϵ	Relative Quality
Fresh water	0.001	80	
Salt water	5.0	81	
Pastoral, low hills, rich soil, typical from Dallas, TX, to Lincoln, NE	0.0303	20	Very Good
Pastoral, low hills, rich soil, typical of OH and IL	0.01	14	Good
Flat country, marshy, densely wooded, typical of LA near the Mississippi River	0.0075	12	
Pastoral, medium hills, and forestation, typical of MD, PA, NY (exclusive of mountains and coastline)	0.006	13	
Pastoral, medium hills, and forestation, heavy clay soils, typical of central VA	0.005	13	Average
Rocky soil, steep hills, typically mountainous	0.002	12-14	Poor
Sandy, dry, flat, coastal	0.002	10	
Cities, industrial areas	0.001	5	Very Poor
Cities, heavy industrial areas, high buildings	0.001	3	Extremely Poor

3. Common Wire Gauges and Associated Diameters in Inches and in Millimeters

Common AWG wire size diameters in inches and in millimeters. Although program input pages may permit the entry of wire diameters (or AWG gauge numbers), direct entry on the GW wire card require the radius (1/2 the listed diameter).

AWG Gauge #	Diameter Inches	Diameter Millimeters	AWG Gauge #	Diameter Inches	Diameter Millimeters
1	0.2893	7.348	21	0.0285	0.723
2	0.2576	6.544	22	0.0253	0.644
3	0.2294	5.827	23	0.0226	0.573
4	0.2043	5.189	24	0.0201	0.511
5	0.1819	4.621	25	0.0179	0.455
6	0.1620	4.115	26	0.0159	0.405
7	0.1443	3.665	27	0.0142	0.361
8	0.1285	3.264	28	0.0126	0.321
9	0.1144	2.906	29	0.0113	0.286
10	0.1019	2.588	30	0.0100	0.255
11	0.0907	2.305	31	0.0089	0.227
12	0.0808	2.053	32	0.0080	0.202
13	0.0720	1.828	33	0.0071	0.180
14	0.0641	1.628	34	0.0063	0.160
15	0.0571	1.450	35	0.0056	0.143
16	0.0508	1.291	36	0.0050	0.127
17	0.0453	1.150	37	0.0045	0.113
18	0.0403	1.024	38	0.0040	0.101
19	0.0359	0.912	39	0.0035	0.090
20	0.0320	0.812	40	0.0031	0.080

Common BSWG wire size diameters in inches and in millimeters.

BSWG Gauge #	Diameter Inches	Diameter Millimeters	BSWG Gauge #	Diameter Inches	Diameter Millimeters
1	0.3000	7.620	21	0.0320	0.813
2	0.2760	7.010	22	0.0280	0.711
3	0.2520	6.401	23	0.0240	0.610
4	0.2320	5.893	24	0.0220	0.559
5	0.2120	5.385	25	0.0200	0.508
6	0.1920	4.877	26	0.0180	0.457
7	0.1760	4.470	27	0.0164	0.417
8	0.1600	4.064	28	0.0148	0.376
9	0.1440	3.658	29	0.0136	0.345
10	0.1280	3.251	30	0.0124	0.315
11	0.1160	2.946	31	0.0116	0.295
12	0.1040	2.642	32	0.0108	0.274
13	0.0920	2.337	33	0.0100	0.254
14	0.0800	2.032	34	0.0092	0.234
15	0.0720	1.829	35	0.0084	0.213
16	0.0640	1.626	36	0.0076	0.193
17	0.0560	1.422	37	0.0068	0.173
18	0.0480	1.219	38	0.0060	0.152
19	0.0400	1.016	39	0.0052	0.132
20	0.0360	0.914	40	0.0048	0.122

Depending upon the selected units of measure for the input interface, diameters in millimeters may require multiplication by 0.001 for entry in meters and by 0.1 for entry in centimeters. Diameters in inches may require multiplication by 0.0833 (1/12) for entry in feet.

4. Some Common Frequency-Wavelength Relationships

Because the speed of electromagnetic radiation in free space is not exactly 300E6 m/s, and because sometimes more exact measures of wavelength are required, the following tables present the length of a free space wave (λ) in both feet and meters for frequencies from 1 to 10 MHz and for the amateur bands between 160 meters and 23 centimeters. Band center points are the geometric mean frequency within the band. You may interpolate other values from the ones given. Or you may divide 299.7925 by the frequency in MHz to obtain the wavelength in meters or divide 983.5712 by the frequency in MHz to obtain the wavelength in feet.

Frequency MHz	λ feet	λ meters	Frequency MHz	λ feet	λ meters
1.000	983.5712	299.7925	8.000	122.9464	37.4741
160 m			9.000	109.2857	33.3103
1.800	546.4285	166.5514	10.000	98.3571	29.9793
1.897	518.4877	158.0351	30 m		
2.000	491.7856	149.8963	10.100	97.3833	29.6824
3.000	327.8571	99.9308	10.125	97.1428	29.6091
80 m			10.150	96.9036	29.5362
3.500	281.0204	85.6550	20 m		
3.742	262.8464	80.1156	14.000	70.2551	21.4138
4.000	245.8928	74.9481	14.174	69.3926	21.1509
5.000	196.7142	59.959	14.350	68.5416	20.8915
6.000	163.9285	49.9654	17 m		
40 m			18.068	54.4372	16.5925
7.000	140.5102	42.8275	18.118	54.2870	16.5467
7.148	137.6009	41.9408	18.168	54.1376	16.5011
7.300	134.7358	41.0675			

Frequency MHz	λ feet	λ meters	Frequency MHz	λ feet	λ meters
15 m			1.25 m		
21.000	46.8367	14.2758	222.000	4.4305	1.3504
21.224	46.3424	14.1252	223.495	4.4009	1.3414
21.450	45.8541	13.9763	225.000	4.3714	1.3324
12 m			70 cm		
24.890	39.5167	12.045	420.000	2.3418	0.7138
24.940	39.4375	12.0206	434.740	2.2624	0.6896
24.990	39.3586	11.9965	450.000	2.1857	0.6662
10 m			33 cm		
28.000	35.1275	10.7069	902.000	1.0904	0.3324
28.837	34.1080	10.3961	914.910	1.0750	0.3277
29.700	33.1169	10.0940	928.000	1.0599	0.3231
6 m			23 cm		
50.000	19.6714	5.9959	1240.00	0.7932	0.2418
51.962	18.9289	5.7695	1269.60	0.7747	0.2361
54.000	18.2143	5.5517	1300.00	0.7566	0.2306
2 m					
144.000	6.8304	2.0819			
145.990	6.7373	2.0535			
148.000	6.6458	2.0256			

5. Frequency Domains

Abbrev.	Classification	Frequency Range
VLF	Very low frequencies	10 to 30 kHz
LF	Low frequencies	30 to 300 kHz
MF	Medium frequencies	300 to 3000 kHz
HF	High frequencies	3 to 30 MHz
VHF	Very high frequencies	30 to 300 MHz
UHF	Ultra-high frequencies	300 to 3000 MHz
SHF	Super-high frequencies	3 to 30 GHz
EHF	Extremely high frequencies	30 to 300 GHz

6. Some Common Transmission Lines Values

Modeling transmission lines requires a knowledge of both the characteristic impedance (Z_0) of the line and the Velocity Factor (VF). NEC does not make use of other parameters of transmission lines, such as conductor size and spacing, capacitance per foot, remnant inductive reactance within the characteristic impedance, or line loss values.

The values shown are representative. For more precise values, consult manufacturer specification sheets.

The listings on the left are for common "RG-" coaxial cables. The listing is necessarily incomplete. In addition, other types with improved loss, flexibility, or jacket properties are available under specific manufacturer numbers. The listing to the right contains representative figures for "hard lines" and common parallel transmission lines.

RG-#	Z_0 (Ω)	VF	Type	Z_0 (Ω)	VF
RG-6	75.0	0.75	Alum. jacket; foam diel.		
RG-8	52.0	0.66	1/2; 3/4; or 7/8"	50.0	0.81
RG-8 foam	50.0	0.78	1/2; 3/4; or 7/8"	75.0	0.81
RG-8A	52.0	0.66			
RG-8X	50.0	0.78	Twin leads		
RG-11	75.0	0.66	75- Ω transmitting	75.0	0.67
RG-11 foam	75.0	0.78	300- Ω flat	300.0	0.82
RG-11A	75.0	0.66	300- Ω tubular	300.0	0.80
RG-58	53.5	0.66			
RG-58A	50.0	0.66	"Window"		
RG-58A foam	50.0	0.78	1/2"	300.0	0.95
RG-58C	50.0	0.66	1"	450.0	0.95
RG-59	75.0	0.66			
RG-59 foam	75.0	0.79			
RG-213	50.0	0.66			

7. Metric-English Conversion

As a convenience, the following table provides handy conversion factors for changing the units of measure for antenna model dimensions.

From	To	Conversion
Millimeters	Inches	0.03937 x mm
Centimeters	Inches	0.3937 x cm
Meters	Inches	39.3701 x m
Millimeters	Feet	0.00328 x mm
Centimeters	Feet	0.03281 x cm
Meters	Feet	3.28084 x m
Millimeters	Yards	0.001094 x mm
Centimeters	Yards	0.01094 x cm
Meters	Yard	1.0936 x m
Inches	Millimeters	25.4 x in.
Inches	Centimeters	2.54 x in.
Inches	Meters	0.0254 x in.
Feet	Millimeters	304.8 x ft.
Feet	Centimeters	30.48 x ft.
Feet	Meters	0.3048 x ft.
Yards	Millimeters	914.4 x Yd.
Yards	Centimeters	91.44 x Yd.
Yards	Meters	0.9144 x Yd.

8. List of Models in Order of Appearance

Filename (x-x.NEC)	Antenna Type	Frequency in MHz	Material, Diameter	Ground Type, Cond. / Diel. Const.
1-1	Dipole	7.05	#12 copper	S-N, .005/13
2-1	Dipole	28.5	6063-T832 al., 5/16" + 3/16"	F. S.
2-2	Yagi, 2-el.	28.5	6061-T6 al., 1/2" + 3/8"	S-N, .005/13
2-3	1/4 λ vertical, gp	14.1	3 mm copper	S-N, .005/13
2-4	Quad loop	21.15	#14 copper	F. S.
2-5	Delta loop, VO-VP	7.15	#12 copper	S-N, .005/13
2-6	Half square VP	146.0	6061-T6 al., 3 mm	S-N, .005/13
3-1	Dipole	14.0	5 mm lossless	F. S.
3-2	Dipole	14.0	5 mm copper	S-N, .005/13
3-3	1/2 λ vertical dipole	24.95	6061-T6 al., 1/2"	S-N, .005/13
3-4	Yagi, 3-el.	50.2	6061-T6 al., 1/2"	F. S.
3-5	Yagi, 3-el.	50.1	6061-T6 al., 1/2"	F. S.
4-1	Dipole	7.05	#14 copper	fast, .005/13
4-2	Yagi, 3-el.	146.0	6061-T6 al., 1/4"	S-N, .005/13
4-3	Yagi, 3-el VO-VP	146.0	6061-T6 al., 1/4"	S-N, .005/13
4-4	Half square, 2-el., VP	146.0	6061-T6 al., 1/4"	S-N, .005/13
4-5	Dipole	3.6	#12 copper	S-N, .005/13
4-6	Rectangle VO-VP	3.6	#12 copper	S-N, .005/13
4-7	Right-angle delta, VO-VP	7.15 (18.118)	#12 copper	S-N, .005/13
4-8	Extended double Zepp	10.125	#14 copper	S-N, .005/13
4-9	Moxon rect- angle, 2-el.	10.125	#14 copper	F. S.
4-10	Yagi, 3-el.	144.5	6061-T6 al., 5 mm	S-N, .005/13

Filename (x-x.NEC)	Antenna Type	Frequency in MHz	Material, Diameter	Ground Type, Cond. / Diel. Const.
5-1	134' doublet	3.5- 29.7	#14 copper	fast, .005/14
5-2	Folded dipole	28.48	#14 copper	F. S.
5-3	Quad loops (2 nested)	24.95 28.5	#14 copper	F. S.
5-4	Folded X-beam, 2-el.	28.5	6061-T6 al., 12.5 mm	F. S.
5-5	Capacity-hat 1/4 λ vertical	7.2	6061-T6 al., 25 mm	Perfect
6-1	Dipole	14.0	#12 copper	S-N, .005/13
6-2	1 λ center-fed	28.0	#12 copper	S-N, .005/13
6-3	Yagi, 2-el.	28.05	6061-T6 al., 1/2"	S-N, .005/13
6-4	Yagi, 2-el.	28.05	6061-T6 al., 1" + 7/8"	S-N, .005/13
6-5	Yagi, 2-el.	7.1	6061-T6 al., 2.25" to 0.5"	S-N, .005/13
6-6	Folded X-beam	28.5	6061-T6 al., 1/2" #18 copper	S-N, .005/13
6-7	Right-triangle, VO	7.1	#12 copper	S-N, .005/13
7-1	Open-sleeve dipoles	10.125 18.118	6061-T6 al., 12.5 mm	S-N, .005/13
7-2	Quad beam, 2-el.	14.175 28.5	#14 copper	F. S.
7-3	1/4 λ vertical, sloping gp	51.0	6061-T6 al., 5 mm	F. S.
7-4	Quad loop VO	51.0	6061-T6 al., 5 mm	F. S.
7-5	Yagi, 2-el.	14.175	6061-T6 al., 1"	F. S.
7-6	Yagi, 3-el.	14.175	6061-T6 al., 1"	F. S.
7-7	Dipole	1.0	25 mm copper	F. S.
7-8	Yagi, 3-el.	144.5	6061-T6 al., 3/16"	F. S.
8-1	Dipole	299.7925	1 mm lossless	F. S.
8-2	1 λ , center-fed	299.7925	1 mm lossless	F. S.
8-3	Dipole	299.7925	1 mm lossless	F. S.
8-4	Inverted-Vee	14.0	#14 copper	F. S.
8-5	Crossed dipoles	14.0 21.0	#12 copper	F. S.
8-6	1/2 λ off-	7.15	#14 copper	S-N, .005/13center-fed

Filename (x-x.NEC)	Antenna Type	Frequency in MHz	Material, Diameter	Ground Type, Cond. / Diel. Const.
8-7	2-element phased horizontal array	28.5	6061-T6 al., 1"	F. S.
9-1	Monotapered dipole	14.0	6061-T6 al., 1"	F. S.
9-2	TDE dipole	14.0	6061-T6 al., 1"	F. S.
9-3	Substitute TDE dipole	14.0	6061-T6 al., 1"	F. S.
9-4	TDE dipole	7.1	6061-T6 al., 1"	F. S.
9-5	3-element Yagi	21.22	6061-T6 al., 1"	F. S.
9-6	Short vertical, capacity hat	10.0	6061-T6 al., 1"	Perfect
10-1	Folded dipoles	28.5	0.5" & #12 lossless	F. S.
10-2	Quad loops	28.5	0.5" & #12 lossless	F. S.
10-3	Elongated quad loop	146.0	0.75" 6061-T6; #14 copper	F. S.
10-4	Capacity-hat vertical	3.75	1" 6061-T6 al; #12 copper	Perfect
10-5	Dipoles, close- spaced	14.0 21.0	1" 6061-T6 al.	F. S.
11-1	16-element Yagi	432.0	5 mm 6061-T6	F. S.
11-2	2-element Yagi	7.15	#12 copper	F. S.
11-3	2-element Moxon	7.15	#12 copper	F. S.
11-4	Capacity-hat vertical	14.175	1" 6061-T6 al; #12 copper	Perfect
11-5	Capacity-hat dipole	14.174	1"6061-T6al; #12 copper	Perfect
11-6	Dipole	1.9	#14 copper	S-N, .005/13
11-7	6-element Yagi	21.2	25 mm 6061-T6 al	Fast and S-N, .005/13
11-8	Vertical dipole	7.15	50 mm 6061-T6 al	S-N, various
12-1	Dipole	7.0	#14 copper	F. S.
12-2	Dipole	4.0	various copper	F. S.
12-3	3-element Yagi	225.0	3 mm various	F. S.
12-4	Elongated quad loop	50.0	3/8" 6061-T6 al; #14 copper	F. S.
12-5	Rhombic	14-28	#12 copper	S-N, .005/13
12-6	Dipole, resistive loading	7.0	#14 copper	F. S.

Filename (x-x.NEC)	Antenna Type	Frequency in MHz	Material, Diameter	Ground Type, Cond. / Diel. Const.
12-7	Transmission line: parallel	14.0	#12 copper	F. S.
13-1	Shortened dipole	14.175	25 mm 6061-T6 al	F. S.
13-2	Loaded short dipole	14.175	25 mm 6061-T6 al	F. S.
13-3	2-element Yagi center-loaded	28.5	1" 6061-T6 al	F. S.
13-4	2-element Yagi mid-el.-loaded	28.5	1" 6061-T6 al	F. S.
13-5	2-element Yagi	28.5	1" 6061-T6 al	F. S.
13-6	Extended double Zepp	7.15	#12 copper	S-N, .005/13
13-7	Modified extended double Zepp	7.15	#12 copper	S-N, .005/13
13-8	2-element quad	21.22	#14 copper	F. S.
13-9	Trap dipole	14.175, 28.5	.5" 6061-T6 al	F. S.
14-1	Dipole with transmission line	21.2	#14 copper	S-N, .005/13
14-2	Phased $1/4\lambda$ verticals	7.1	1.5" 6061-T6 al	Perfect
14-3	Phased 2-el. array horizontal	28.5	12 mm 6061-T6 al	F. S.
14-4	Dipole, TL broad-banded	7.15	#14 copper	F. S.
14-5	Dipole, stub-loaded	14.175	#14copper	F.S.
14-6	Ex. dbl. Zepp, stub-matched	28.5	#14copper	F.S.
15-1	$1/4\lambda$ monopole	3.0	25.4 mm 6061-T6	Perfect
15-2	Short monopole hat loaded	3.0	25.4 mm 6061-T6	Perfect
15-3	Elevated monopole w/g.p.	7.05	50 mm 6061-T6	F. S. & S-N, .005/13
15-4	Monopole w/ sloping g.p.	7.05	50 mm 6061-T6	S-N, .005/13
15-5	Monopole w/ g.p. close to ground	7.05	50 mm 6061-T6	S-N, .005/13
15-6	$1/4$ & $5/8\lambda$ monopoles w/ g.p.	7.05	50 mm 6061-T6	S-N, .005/13

Filename (x-x.NEC)	Antenna Type	Frequency in MHz	Material, Diameter	Ground Type, Cond. / Diel. Const.
16-1	Dipoles, vert. & horiz.	10.0	1" 6061-T6 al.	F. S.
16-2	Vertical dipole	7.05	2" 6061-T6 al.	S-N, various
16-3	3-el. vert. Yagi	7.05	2" 6061-T6 al.	S-N, .005/13
16-4	Triangular vert. dipole array	7.05	2" 6061-T6 al.	S-N, .005/13
16-5	1/4 λ vert. mono- pole phased array	10.0	7.25 mm copper	Perfect
16-6-1	Delta SCV	7.15	#12 copper	S-N, .005/13
16-6-2	Rectangle SCV	7.15	#12 copper	S-N, .005/13
16-6-3	Half square SCV	7.15	#12 copper	S-N, .005/13
16-7	Parasitic half square array	7.15	#12 copper	S-N, .005/13
17-1	1 λ collinear	14.175	#12 AWG copper	S-N, .005/13
17-2	8JK end-fire	14.175	#12 AWG copper	S-N, .005/13
17-3	Lazy-H broadside	14.175	#12 AWG copper	S-N, .005/13
17-4	Extended double Zepp	28.5	#12 AWG copper	S-N, .005/13
17-5	Collinear EDZ	21.225	#12 AWG copper	S-N, .005/13
17-6	EDZ Lazy-H	28.5	#12 AWG copper	S-N, .005/13
17-7	Sterba curtain	3.6/7.2	#12 AWG copper	S-N, .005/13
17-8	Vee-Beam	14.175	#12 AWG copper	S-N, .005/13
18-1	2-el. Yagi; dr-refl	28.5	3/4" 6061-T6 al	F. S.
18-2	2-el. Yagi; dr-dir	28.5	3/4" 6061-T6 al	F. S.
18-3	2-el. Yagi; reversible	10.125	#12 copper	F. S.
18-4	3-el Yagi; high-gain	14.175	1" 6061-T6 al	F. S.
18-5	3-el Yagi; wide-band	14.175	1" 6061-T6 al	F. S.
18-6	5-el Yagi	14.175	tapered-dia; 6061-T6	F. S.
18-7	6-el Yagi	14.175	tapered-dia; 6061-T6	F. S.
18-8	4-el Yagis; (2 stacked)	14.175	1" 6061-T6 al	S-N, .005/13
18-9	4-el Yagi; 2-band	18.2; 24.95	tapered-dia; 6061-T6	F. S.

Filename (x-x.NEC)	Antenna Type	Frequency in MHz	Material, Diameter	Ground Type, Cond. / Diel. Const.
18-10	6-el Yagi; 2-band	14.175; 21.2	16 and 12.5 mm; 6061-T6	F. S.
19-1	2-el quad beam	21.22	#14 copper	F. S.
19-2	5 2-el quads	14-28	#14 copper	F. S.
19-3	2-el EDZ	28.5	#12 copper	F. S.
19-4	2-el phased array folded dipoles	28.5	0.375" copper	S-N, .005/13
19-5	2-el phased array linear dipoles	28.5	1" 6061-T6	S-N, .005/13
19-6	3-el phased array with director	24.94	0.75" 6061-T6	F. S.
19-6-2	3-el Yagi	24.94	0.625" 6061-T6	F. S.
19-6-3	4-el Yagi	24.94	0.75" 6061-T6	F. S.
19-7	5-el LPDA	19-29	20 mm 6061-T6	F. S.
20-1	6-el Yagi	51	6.25 mm 6061-T6	F. S.
20-2	26-el Yagi	432	4 mm 6061-T6	F. S.
20-3-1	8-el Yagi	432	#14 copper	F. S.
20-3-2	8-el quagi	432	#12 copper	F. S.
20-4	8-el Yagi	144.2	4.76 mm 6061-T6	F. S.
20-5-2	2-el half square	146	0.5" 6061-T6	S-N, .005/13
20-5-3	3-el half square	146	0.5" 6061-T6	S-N, .005/13
20-5-5	2-el bobtail	146	0.5" 6061-T6	S-N, .005/13
20-6-3	J-pole	146	0.5" 6061-T6	S-N, .005/13
20-7	Corner reflector array	432	10 mm 6061-T6	F. S.
20-8-2	Turnstile	300	1 mm 6061-T6	F. S.
20-8-3	Lindenblad variant	300	1 mm 6061-T6	F. S.
21-1-1	Helical dipole	28.5	#12 copper	F. S.
21-1-2	Helical 2-el Yagi	28.5	#12 copper	F. S.
21-2-1	Cage monopole	3.7	#12 copper	Perfect
21-2-3	Cage dipole	3.7	#12 copper	F. S.
21-3	Triangular tower sections	----	Steel	----
21-4-4	3-el Yagi; beta- match inductor	14.175	1" 6061-T6	F. S.
21-4-5	3-el Yagi; beta- match TL stub	14.175	1" 6061-T6	F. S.
21-5	Dipole above wire-grid screen	144.5	1.5 mm 6061-T6	S-N, .005/13

Explanation of miscellaneous abbreviations and units of measure:**Antenna Type:**

Certain geometries may be laid out vertically or horizontally relative to the ground. **VO** means the antenna is vertically oriented with respect to the ground; **HO** means the antenna is horizontal relative to the earth.

Certain antenna types may be changed from mostly horizontally polarized radiation to mostly vertically polarized radiation, depending upon where along the wire the antenna one places the source. The distinction is noted by **VP** and **HP**.

Ground plane antennas are indicated by **gp** or **monopole w/g.p.**

Material:

Wire diameters listed as gauges (for example, #12) are AWG unless otherwise indicated.

Ground Type:

Conductivity (σ) is measured in Siemens per meter. Permittivity or the dielectric constant (ϵ) has no unit of measure.

Special Note on Antenna Operating Frequencies: Most of the antenna models used in this guide have been intentionally placed within the U.S. amateur bands from MF through UHF. Amateur radio operations involve both wide-band and narrow-band antenna requirements for directional and non-directional communications that may be surface wave, point-to-point, or skip, with vertical or horizontal polarization. Moreover, an amateur radio license of General Class or better permits the holder to operate experimentally with any of the antenna designs in this guide with no further action necessary to approve test transmissions. Therefore, wherever empirical work seems wise as a cross check upon any modeling exercise, the holder of an amateur radio license may build and test the antenna in question within the frequencies authorized by the class of license held.

User Notes

Index

The following brief index uses the following two conventions. 1. Only the beginning page for a topic is listed. 2. Major treatments are highlighted.

Antenna Types (omnidirectional, bi-directional, directional)	4-11	Folded X-Beam	5-8, 6-11
Antenna Element	1-4	Moxon Rectangle, 2-el	4-12, 11-5
Antenna Height	3-7, 3-14	Quad Beam, 2-el	7-4, 13-17, 19-3
Antenna Model Wire	1-4	Quad Beam, 2-el, 5-band	19-5
Antennas (listed by related types)		Double Extended Zepp, parasitic beam	19-8
HF: Horizontal Single Wire		Collinear Double Extended Zepp Array	17-11
Dipole	2-4, 3-2, 3-6, 4-3, 4-8, 6-3, 9-3, 9-5, 9-7, 10-13, 11-10, 12-3, 12-5, 14-3, 16-2	Horizontal Phased Array, 2-el	8-12, 14-8
Dipole, loaded	12-12, 13-3, 14-14	Rhombic	12-10
Dipole with "capacity hat"	11-7	Collinear Array	17-4
Dipole, broadbanded	14-12	8JK End-Fire Array	17-5
Folded Dipole	5-5, 10-3	Lazy-H Broadside Array	17-7, 17-13
Inverted Vee	8-7	Sterba Curtain	17-15
Off-Center-Fed $1/2\lambda$ Wire	8-11	Vee-Beam	17-17
Helical Dipole	21-2	ZL-Special (phased array)	19-10
Cage Dipole	21-6	Phased/Parasitic Array, 3-el	19-14
1λ Doublet	6-4	Log-Periodic Dipole Array	19-18
Double Extended Zepp	4-11, 13-15, 17-9	HF: Vertical	
Multi-band Doublet	5-3, 7-12	Vertical Dipole	3-10, 16-2, 16-4
Delta Loop	2-15, 4-7	Vertical Loops, 1λ	16-14
Right Triangle	6-12	Vertical Monopoles, phased	14-6, 16-10
Quad Loop	2-14, 5-7, 10-6	Vertical Monopole with ground plane	2-13, 15-3, 15-10, 15-13, 15-15, 15-17
HF: Horizontal Multi-Wire		Vertical Monopole, center-loaded	11-12
Coupled Dipoles	7-3	Vertical Monopole with "capacity" hat	5-11, 9-12, 10-11, 11-7, 15-6
Crossed Dipoles	8-9	Vertical Yagi, 3-el	16-7
Yagi, 2-el	2-10, 6-5, 6-7, 6-9, 11-5, 18-3, 18-4, 18-8	Vertical Array, 3-el	16-9
Yagi, 2-el, dual band, non-interlaced	18-19	Half Squares, parasitic	16-17
Yagi, 3-el	3-15, 3-16, 7-10, 9-9, 13-9, 18-11	VHF	
Yagi, 3-el, loaded	13-9	Quad Loop	7-7, 12-9
Yagi, 3-el, dual band, interlaced	18-21	Elongated Quad Loop	10-10
Yagi, 4-el, stacked	18-17	Yagi, 3-el	4-5, 4-15, 7-13, 12-7
Yagi, 5-el	18-14	Yagi, 6-el	20-3
Yagi, 6-el	11-11, 18-14	Yagi Array,	20-9
Helical Yagi, 2-el	21-2	Half Square	2-16
		Half-Square Array	4-6, 20-11
		Bobtail Curtain Array	20-11

Vertical monopole with ground plane	7-6, 20-15	Elevated	15-10
Vertical Dipole	20-15	Ground-Level	15-15
Vertical J-Pole	20-15	Sloping	15-13
UHF		Ground Planes	15-1 , 16-6
Dipole	8-3	Elevated Ground Planes	15-10
Yagi, 8-el	20-7	Ground Level Planes	15-15
Yagi, 16-el	11-3	Sloping Ground Planes	15-13
Yagi, 26-el	20-5	Ground: Minimum Height Above	11-1, 11-2
Quagi, 8-el	20-7	H-Plane	16-2
Corner Reflector	20-18	Helical Dipoles and Yagis	21-2
Turnstile	20-20	HF vs. VHF/UHF Modeling Differences	20-1
Lindenblad	20-21	Junction Limitations	1-9
Azimuth Patterns (far field)	3-15, 4-6	List of Models	App-11
Forward Lobe	4-12	Loads	1-5, 12-1 , 13-1
Main and Side Lobes	4-11	Beta Matches	21-12
Bi-Directional Wire Arrays	17-1	Resistive Loads, Spot	12-2, 12-10
Broadside Arrays	17-2, 17-7, 17-13	Resistive Loads, Distributed	12-1
Collinear Arrays	17-1, 17-4, 17-11	Type 4	13-1
End-Fire Arrays	17-1, 17-5	Type 1	13-2, 13-20
Cage Antennas	21-6	Type 0	13-2, 13-14
"Capacity" Hats as Loads	15-6	Load Placement	13-8
Convergence Testing	6-1	Load Q	13-4
E-Plane	16-2	Metric-English Conversion	App-10
Element ends	5-12	Modeling Forms (paper)	2-4
Elevation Patterns (far field)	4-6	NEC Output File	4-2
Far Fields	4-1	NEC Input File "Cards"	
Frequency Scaling	7-13	CM-Comments	2-2
Frequency Sweep	7-8	GW-Antenna Geometry	2-2
Frequency Specification	7-1	GN-Ground	2-3, 11-1
Frequency Domains	App-8	EX-Excitation	2-3, 8-1
Frequency-Wavelength Relationships	App-6	LD-Load	2-3, 12-1, 13-1
Front-to-Back Ratio		FR-Frequency Request	2-3, 7-1
180-degree	4-13	RP-Pattern request	2-3, 4-1
Front-to-Rear	4-13	NEC Control Cards	4-1
Worst-Case	4-13	NEC Input File Structure	2-1
Front-to-Side Ratio	4-12	NECWin Plus	1-10
Gain Averaging Test	10-17	Files	1-11
Geometry Limitations	10-1	Inputs	1-13
Close-Spaced wires	10-13	Outputs	1-14
Folded Dipole	10-3	Numerical Electromagnetics Code (NEC)	1-2, 1-10,
Quad Loop	10-6	Parasitic Antenna Concepts	18-1
Ground	1-7, 11-1	Phased Arrays, Horizontal	19-1
Free Space	3-2, 11-1	LPDAs	19-18
Perfectly Conducting Ground	11-1	Phased and Parasitic Combinations	19-14
Reflection Coefficient Ground	1-7, 11-2	ZL-Special	19-10
Sommerfeld-Norton Ground	1-7, 3-6, 11-2	Radiation Pattern Angles	5-4
Ground Description	3-9, 3-13, 16-6, App-2	Radiation Polarization	4-4, 16-2
Conductivity	App-2	Segments/Segmentation	1-4, 1-5, 5-4, 5-7, 6-3
Permittivity (Dielectric Constant)	App-2	"Self-Contained" Vertical Antennas	16-14
Ground Plane Radials	15-2		

Source	1-5
Source Types	
Current Sources	8-12
Multiple Sources	8-12
Split Sources	8-3
Voltage Sources	8-1
Source Placement	5-4, 8-1
Source Impedance Data	6-14, 7-9, 7-11, 7-12
Stub Loading	14-14, 18-8
Stub Matching	14-17
Take-Off Angle (elevation)	4-7
Tapered-Diameter Elements	1-9, 6-9, 9-1
Leeson Corrections (for tapered-diameter elements)	9-1
Substitute Elements	9-6, 9-12
Tower Structures	21-9
Transmission Lines	1-8, 14-1
Transmission Line Values	App-9
Transmission Line, Stub Loading	14-14
Transmission Line, Parallel (Model)	12-15
Transmission Line (TL) Requirements	14-1
Transmission Line, Element Phasing	14-6
Traps (as loads)	13-20
Vertical Monopoles	15-1
Vertical Dipoles	16-2
Vertical Angle Resolution	4-14
Vertical Antennas, "Self-Contained"	16-14
Vertical Monopoles with Capacity Hats	15-6
Vertical Arrays, Parasitic	16-7
Vertical Arrays, Phased	14-6, 16-10
VHF/UHF Omnidirectional Antennas	20-14, 20-20
VHF/UHF Wide-Band Antennas	20-18
VHF/UHF Vertical Arrays	20-11
VHF/UHF Yagis	20-3
VHF/UHF Yagi Arrays	20-9
VSWR	3-5
Wire Diameter	3-4, App-4 , App-5
Wire Materials	3-3
Wire Grid Screens	21-17
Wire Conductivity	3-3, App-3
Yagis	18-1
2-Element	18-3
3-Element	18-11
Interlacing	18-19
Long-Boom	18-14
Stacking	18-17

User Notes